PB-235 829

PROCEEDINGS OF A SYMPOSIUM ON CONTROL OF FINE-PARTICULATE EMISSIONS FROM INDUSTRIAL SOURCES, HELD JANUARY 15-18, 1974, SAN FRANCISCO, CALIFORNIA

U.S. - U.S.S.R. Working Group on Stationary Source
Air Pollution Control Technology

PREPARED FOR
Environmental Protection Agency
Office of Water Resources Research

1974

DISTRIBUTED BY:
NTIS
National Technical Information Service
U. S. DEPARTMENT OF COMMERCE

SELECTED WATER RESOURCES ABSTRACTS

INPUT TRANSACTION FORM

PB 235 829

W74-12208

PROCEEDINGS, SYMPOSIUM ON CONTROL OF FINE PARTICULATE EMISSIONS FROM INDUSTRIAL SOURCES,

--Held January 15-18, 1974, San Francisco, California, Sponsored by US/USSR Working Group, Stationary Source Air Pollution Control Technology. Environmental Protection Agency, Report EPA-600/2-74-008, (1974), 775 p.

Proceedings of the symposium contain papers from US and USSR on the application of conventional technologies for control of fine particles (3 microns and less), new concepts for fine particulate control, advances in measurement techniques, and chemical composition of fine particulates. The theory behind and the application of electrostatic precipitators, wet scrubbers, and fabric filters for removal of fine particulates from stationary sources are covered. New concepts covered include sonic agglomeration, electrically induced agglomeration, coagulation and condensation with utilization of electrophoresis, thermophoresis, and diffissiophoresis. The presently applied particulate mass measurement methods, plume opacity measurement, instruments measuring efficiency of particulate control equipment, sampling from high-temperature, reactive, and corrosive gases, measurement of particle size distribution at emission sources are covered in papers on measurement techniques. (EPA)

*Air Pollution, *Control, Technology, *Particle size, Particle shape, *Measurement, Filters, *Industrial wastes, *Conferences, Instrumentation, Coagulation, Condensation, *Pollutant identification, Electrophoresis, Waste treatment

--Fabric filters, *Fine particulates, Electrostatic precipitators, Wet scrubbers, Sonic agglomeration, Emissions, Air pollution sources,

Reproduced by
NATIONAL TECHNICAL
INFORMATION SERVICE
U S Department of Commerce
Springfield VA 22151

05A, 05G, 02K

2.25

716

13.00

i

Send To:

WATER RESOURCES SCIENTIFIC INFORMATION CENTER
U.S. DEPARTMENT OF THE INTERIOR
WASHINGTON, D.C. 20240

PROCEEDINGS

SYMPOSIUM ON CONTROL OF FINE-PARTICULATE EMISSIONS FROM INDUSTRIAL SOURCES

January 15-18, 1974

San Francisco, California

Sponsored by the
U.S. - U.S.S.R. WORKING GROUP
STATIONARY SOURCE AIR POLLUTION CONTROL TECHNOLOGY

FOREWORD

The Symposium on Control of Fine-Particulate Emissions from Industrial Sources was conducted by the Particulate Technical Sub-Group of the U.S. - U.S.S.R. Working Group on Stationary Source Air Pollution Control Technology. Paul W. Spaite, Chairman of the Sub-Group, also served as Chairman of the Symposium. The Symposium had the support of the U. S. Environmental Protection Agency, under the guidance of Richard E. Harrington, Director of the Air Pollution Control Division. Arrangements for the Symposium were made by Southern Research Institute.

TABLE OF CONTENTS

Paper No.		Page No.
1	Keynote Address, by Stanley M. Greenfield, U. S. Environmental Protection Agency..........	3
2	Overview of the Fine Particulate Problem, by Alfred B. Craig, U. S. Environmental Protection Agency....................................	17
3	Electrostatic Precipitators—Major Fields of Application, Technology, and Problem Areas, by Harry J. White................................	55
4	Design Features of the Modern Flue Gas Electrostatic Precipitators, by M. A. Alperovich and Ildus K. Reshidov, State Research Institute of Industrial and Sanitary Gas Cleaning...........	79
5	Theoretical Basis for Design of Modern High-Efficiency Electrostatic Precipitators, by V. I. Levitov, Ildus K. Reshidov, and V. M. Tkachenko, State Research Institute of Industrial and Sanitary Gas Cleaning...........	97
6	Removal of Ash from Flue Gases of Power Stations with Electrostatic Precipitators, by I. A. Kizim, Ildus K. Reshidov, and V. M. Tkachenko, State Research Institute of Industrial and Sanitary Gas Cleaning....................................	119
7	Theoretical and Practical Aspects of Fine Particle Collection by Electrostatic Precipitators, by Grady B. Nichols, Southern Research Institute...	137
8	Operating Experience with Gas Conditioned Electrostatic Precipitators, by George P. Green and W. S. Landers, Public Service Company of Colorado....	169
9	Scrubber Performance for Particle Collection, by Seymour Calvert, A.P.T., Inc.................	189
10	Use of Venturi Scrubbers for Removal of Highly Dispersive Particulates, by Georgy K. Lebedyuk, State Research Institute of Industrial and Sanitary Gas Cleaning.........................	213

Preceding page blank

TABLE OF CONTENTS
(Continued)

Paper No.		Page No.
11	Wet Gas Cleaning in Iron and Steel Industry, by Georgy K. Lebedyuk, A. Yu. Valdberg, and F. Ye. Dubinskaya, State Research Institute of Industrial and Sanitary Gas Cleaning.........	221
12	Effect of Water Vapor Condensation on Particle Collection by Scrubbers, by Leslie E. Sparks, U. S. Environmental Protection Agency...........	239
13	Use of Scrubbers for Control of Emissions from Power Boilers—U. S., by Irwin A. Raben, Combustion Equipment Associates, Inc............	267
14	High Velocity Synthetic Fiber Mist Eliminators, by Georgy K. Lebedyuk, B. I. Myagkov, I. G. Kamenshchikov, and V. V. Malikov, State Research Institute of Industrial and Sanitary Gas Cleaning......................................	317
15	Major Applications of Fabric Filters and Associated Problems, by Charles E. Billings, Environmental Engineering Science and John E. Wilder, GCA Corporation........................	329
16	Bases of Gas Filtration Through Porous Media Theory, by Valery P. Kurkin, State Research Institute of Industrial and Sanitary Gas Cleaning	373
17	Factors in the Collection of Fine Particulate Matter with Fabric Filters, by Richard Dennis and John E. Wilder, GCA Corporation............	385
18	The State of the Art of High Temperature Filtration and Current Technology Developments, by Dean C. Draemel, U. S. Environmental Protection Agency......................................	425

TABLE OF CONTENTS
(Continued)

Paper No. Page No.

19 Atomization and Cloud Behavior in Wet Scrubbers, by Howard E. Hesketh, Southern Illinois University.............................. 455

20 Removal of Carbon Black from Industrial Gases, by Valery P. Kurkin, State Research Institute of Industrial and Sanitary Gas Cleaning.. 479

21 The Application of Wet Electrostatic Precipitators for Control of Fine Particulate Matter, by Even Bakke, United States Filter Corporation..................................... 489

22 The Influence of Ash Chemistry on the Volume Conduction in Fly Ash, by Roy E. Bickelhaupt, Southern Research Institute..................... 521

23 Basic Processes in Fine Particle Control, by James R. Brock, University of Texas............. 545

24 Systems of Charged Particles and Electric Fields for Removing Sub-micron Particles, by James R. Melcher and K. S. Sachar, Massachusetts Institute of Technology......................... 563

25 Advances in the Sonic Agglomeration of Industrial Aerosol Emissions, by David S. Scott, University of Toronto.................................... 597

26 The Present Status of Particulate Mass Measurements, by J. A. Dorsey and D. B. Harris, U. S. Environmental Protection Agency........... 625

27 Plume Opacity Measurement, by David S. Ensor, Meteorology Research, Inc...................... 641

28 Instrumentation for Dispersion Analysis of Particulates in Industry, by S. S. Yankovskiy and Valery P. Kurkin, State Research Institute of Industrial and Sanitary Gas Cleaning......... 673

29 Technology of Particulate Sampling from Reactive, Damp and High-Temperature Gases, by V. A. Anikeyev, V. P. Bugayev, V. A. Limanskiy, Ye. N. Andrusenko, and V. Yu. Padva (presented by Valery P. Kurkin, State Research Institute of Industrial and Sanitary Gas Cleaning)........ 695

TABLE OF CONTENTS
(Continued)

Paper No.		Page No.
30	Measurement of Particle Size Distributions at Emission Sources with Cascade Impactors, by Michael J. Pilat, University of Washington	709
31	The Chemical Composition of Fly Ash, by David F. S. Natusch, University of Illinois	731

SESSION 1

Paper No.

1	Keynote Address
	Stanley M. Greenfield U. S. Environmental Protection Agency Washington, D. C.
2	Overview of the Fine Particulate Problem
	Alfred B. Craig U. S. Environmental Protection Agency Research Triangle Park, N. C. 27711

Preceding page blank

Paper No. 1

KEYNOTE ADDRESS

by

Stanley M. Greenfield

U. S. ENVIRONMENTAL PROTECTION AGENCY

Washington, D. C.

KEYNOTE ADDRESS

By

Stanley M. Greenfield, Ph. D.
Assistant Administrator
for Research and Development

U.S. Environmental Protection Agency

The surge of concern for the environment in the mid-60's proved to be more than a fad. We have come a long way since that first public recognition that "planet earth" was faced with a grave problem, pollution that is growing at a dismaying rate. With the passage of the National Environmental Protection Act, in early 1970, a concern for and recognition of man's impact on the environment became national policy. The Environmental Protection Agency was established later in 1970 to carry out a program of enforcement of environmental sanctions.

Symposium on Control of Fine-Particulate Emissions from Industrial Sources - San Francisco, California - January 15, 1974

A Federal environmental research and development program can provide incentives to the private sector to engage in research; it can furnish direction and seed money, and it can try to identify gaps in our knowledge, and it can serve as a liaison point for research on an international scale, as we are coming to understand more and more the enormous global implications of modern man's thoughtless and ignorant misuse and abuse of his own planet. EPA's research organization cannot alone provide an understanding of the ecological processes and effects of pollutants, of the means to monitor the pollutants, and of the technology and practices necessary to control them.

We are making some progress in that understanding of our impact on the ecosphere, and this symposium is witness to an effort to identify and plan an attack on one particular kind of pollutant affecting primarily one medium.

Fine particulates, defined as solid or liquid airborne aerosols less than three microns in diameter, are one of the major air pollutants, and thus are one of the Environmental Protection Agency's major targets for control. The size is critical in this determination. First, coarser particulates either settle quickly upon release or are easily collected by conventional control equipment, and hence are a more temporary air pollutant, but the finer particulates remain airborne for extended periods. Secondly, their greater ability to obstruct light causes the limited visibility typical of air pollution haze and smog. Thirdly, fine particulates are a health hazard, since in contrast to coarser particles, they can bypass the body's respiratory filters and penetrate deeply into the lungs. Further, these particles have been identified as transport vehicles for gaseous pollutants, both adsorbed and reacted, and hence can produce synergistic effects deleterious to human health. The problem of fine particulates is intensified by the tendency of metallic materials, some of which are chemically and catalytically highly active, to condense as fine particulates from high temperature processes, such as combustion and pyrometallurgical processes.

Fine particulate air pollutants may be classified into two major classes based on their origin. These are (1) primary fine particulates which are emitted or immediately condensed as fine particulates from a specified source and (2) secondary fine particulates which are the products of atmospheric reactions. Water is excepted as an air pollutant except as it may occur as man-made ice fog.

Primary particulates typically result from physical or chemical processes, which may include condensation of gaseous products or products of chemical reactions. High temperature processes such as metallurgical operations and combustion of fossil fuels are major sources. Metallurgical operations, the former, represent major sources of metal fumes unique to the process, such as lead, zinc, copper or iron oxide fumes. Combustion processes produce a spectrum of materials found as ash components of the fuels. Combustion of residual oil, for example, produces quantities of vanadium, chromium, nickel, iron, copper and other highly reactive and catalytic metals. Primary sources of fine particulates represent the principle source of these metallic constituents in the air. It has been theorized that these highly active and catalytic materials play a key role in the formation of secondary particulates by acting as catalysts in chemical and photochemical smog-forming processes.

Some processes emit solid and liquid hydrocarbon emissions such as organic condensibles, tars and carbon particles capable of sorption of more volatile constituents. These emissions constitute another type of primary fine particulates. The processes from which these emissions come include pyrolysis, incomplete combustion, vaporization of lubricating or process oils, and many chemical processes such as textile, refinery, petrochemical and plastics production operations. Forest fires as well as controlled agricultural and slash burning also are sources of this category of fine particulates.

Secondary particulates result from atmospheric reactions between gaseous pollutants. Photochemical reactions requiring sunlight as a stimulous have been long known and studied for several years and are generally found to be complex and difficult to model. Some of these reactions result in condensible, solid or liquid state components or products that react readily with water to produce particulates. Since these secondary particulates are usually the product of gaseous reactions, they are seldom if ever the source of metallic particulates. Being arionic in nature, they can and probably frequently combine with metallic particulates to form salts.

There are no good data on the relative amounts of primary and secondary fine particulates in the atmosphere. Since both are almost exclusively the product of manmade pollution, they would be expected to vary significantly from site to site depending upon such factors as industry composition, fuel-use patterns, and climate and weather. It seems clear, however, that since both primary and secondary particulates are the results of emissions from human activity, the key to their control is to prevent their release or the release of their precursers to the atmosphere.

Basis of Concern for Fine Particulates

As is frequently the case with non-infectuous pollutants and toxicants, the health effects case against fine particulates is not clear cut. First it must be remembered that fine particulates are not a single pollutant but a large category of pollutants with a common set of size, transport and behavioral characteristics. Once dispersed, fine particulates behave, depending upon their size, like something between a coarse particle and a gas. They remain suspended, diffuse, are subject to brownian motion, exhibit little inertial characteristic, follow fluid flow around obstacles, and like gas molecules, can penetrate deeply into the respiratory system.

The moderate amount of information that is available concerning the deposition of particles in man and lower animals is based upon mathematical models and to a limited extent, experimental data obtained from man. Particles larger than 5 microns are deposited in the nasal cavity or nasopharynx. Increasing numbers of smaller particles are deposited in the lungs. Over 50% of the number of particles between 0.01 and 0.1 microns that penetrate into the pulmonary will be deposited. This ability of particulates to penetrate into the respiratory system and be captured is principally a function of their geometry and is almost completely independent of the chemical properties of the particle.

The health effects of fine particulates that have penetrated the respiratory system and been captured, on the other hand, is almost completely dependent on their chemical or toxic nature. It is, therefore, not possible to generalize on health effects; rather the health effects of specific materials must be considered. Here the data become sparce and it becomes necessary to draw on our knowledge of toxic characteristics of specific substances gained through other information sources and our understanding of physiological mechanisms that work to dispose of collected materials.

The principal means through which air pollutants exert an effect on health is through inhalation and direct effects on the respiratory system. This may result in short term irritant effects or longer term damage such as silicosis or asbestoses. In either case the respiratory system is directly impaired.

A second mechanism involves the respiratory system indirectly as a significant route of entry for non-respiratory toxicants. In this case, substances which are deposited in the respiratory system are translocated to the gastro-intestinal system by muco-ciliary transport and swallowed. They may then exert a primary toxic effect or be absorbed and translocated to other tissues where an adverse health effect might be elicited.

In addition to the chemical and toxic nature of the particulate, they have potential for causing adverse health effects dependent upon the solubility of the particle in the transport mucus; if highly soluble, particulates may cause toxic inflammation.

Particles deposited deep in the lungs may be cleared very slowly. In this case, the clearing is dependent upon particle solubility.

The preponderance of evidence indicates that non-soluble particles remain deep in the lungs for long periods -- weeks, months, even years. Thus the carcinogenic hazard of long-lived radioactive metals and airborne chemicals; hydrocarbons are of special concern.

Because certain metals may be soluble in respiratory secretion, the toxic properties of these substances may be manifested in the lung or airways or may be translocated to other organs. Vanadium is one example of such a metal. Unfortunately, however, the minimum time concentration exposure of vanadium and other metals is not adequately known. Needless to say, the combined effects of multiple pollutants is also not adequately known.

Because of the present paucity of knowledge concerning the health effects of specific pollutants and combinations of pollutants, many years will be required to develop a data base to quantify the health effects problem of fine particulates. This quantitative understanding will come as our data base is enlarged through continued and expanded programs such as the EPA Community Health Environmental Surveillance Study (CHESS) program and studies of selected cities in the United States.

Sufficient information does exist, however, to conclude that fine particulates must be controlled if public health is to be protected. It is therefore essential that the research strategies for fine particulate control include a program of control technology development that will assure the ability of industry to prevent the release of primary particulates and the gaseous precursers of secondary fine particulates.

Role of Symposium

I would like to talk for a minute about the particular purpose and role of this symposium within the context of international concern. In May, 1972, President Nixon and President Podgorny signed an agreement calling for cooperation between the United States and the Soviet Union in the solution of common problems. This agreement, implemented by the specific Environmental Agreement signed by Mr. Train of EPA and Academician Fedorov, of the Soviet Union, and by the efforts of individual working groups such as this group recognize major common problems that are too complex and too expensive and too pressing to be solved by one Nation alone. It called for the combined technical expertise of both Nations to be brought to bear in developing solutions in the most cost effective manner possible. Control of fine particulates is one of these problems.

The need for control of this pollutant has only recently been recognized. We do not adequately understand its importance or effect on public health and welfare. We do not know what pollutants are most important or insidious or to what extent they should be controlled. We do recognize, however, that control is necessary.

Since this is a new problem, the technology requirements for measurement and control are unassessed and undeveloped. It is essential that we learn what level of control can be achieved with existing control technology, where existing systems can be applied, and what new technologies are needed. New, advanced, more economic methods are needed to fill the technological gaps. These technology gaps provide an excellent opportunity for experts from both Nations to work cooperatively to find solutions.

I have chosen not to address the issue of the status of control technology in my keynote address, even though this is the topic of this symposium. It should be our purpose in these three days to objectively and without bias address the questions of the adequacy of existing technology, the potential of new approaches and probable future needs. It will serve no purpose for me to speculate about the outcome of these assessments. Rather, I have chosen to focus on the nature of the problem and the urgent need for control of this pollutant.

I urge you therefore to take maximum advantage of this forum of technical experts to identify and pursue areas and activities for cooperation that will yield the tools needed to solve the fine particulate control problem.

# # #

Paper No. 2

OVERVIEW OF THE FINE PARTICULATE PROBLEM

by

Alfred B. Craig

U. S. ENVIRONMENTAL PROTECTION AGENCY

Research Triangle Park, N. C.

OVERVIEW OF THE FINE PARTICULATE PROBLEM

The vehicle for control of air pollution in the United States is the Clean Air Act of 1970. The stated purposes of the Act are:

"(1) to protect and enhance the quality of the Nation's air resources so as to promote the public health and welfare and the productive capacity of its population;

"(2) to initiate and accelerate a national research and development program to achieve the prevention and control of air pollution;

"(3) to provide technical and financial assistance to State and local governments in connection with the development and execution of their air pollution prevention and control programs; and

"(4) to encourage and assist the development and operation of regional air pollution control programs."

The Clean Air Act of 1970 called for specific federal action in the control of air pollution. Automobile emission control levels were mandated for 1975, national ambient air quality standards to protect health and welfare were authorized, air quality control regions covering the whole country were to be designated in 90 days, and strict timetables for state and federal actions were established for the development and evaluation of state implementation plans that would cover the nation with regulations for air pollution control. Also included for the first time was authority to promulgate national emission standards for major new sources and for new and existing sources of hazardous pollutants.

The Act provides three different methods for mandating air pollution control for stationary sources: 1) setting of primary and secondary ambient air quality standards; 2) setting standards for hazardous air pollutants; and 3) setting new source performance standards.

National primary ambient air quality standards are defined by the Act as "standards, the attainment and maintenance of which ... are a requisite to protect the public health."

The Act states that "any national secondary ambient air quality standard ... shall specify a level of air quality, the attainment and maintenance of which ... is requisite to protect the public welfare from any known or anticipated adverse effects associated with the presence of such air pollutant in the ambient air."

Hazardous air pollutant is defined as "an air pollutant to which no ambient air quality standard is applicable and which in the judgement of the Administrator may cause, or contribute to, an increase in mortality or an increase in serious irreversible, or incapacitating reversible, illness."

The term, New Source, is defined as "any stationary source the construction or modification of which is commenced after the publication of regulations prescribing a standard of performance ... applicable to such source."

The federal government through EPA (Environmental Protection Agency) has the responsibility for proposing, reviewing, promulgating, and where necessary, revising all three types of air pollution control regulations. The states have the primary responsibility for assuring air quality within their boundaries and are responsible for developing adequate plans for implementation, maintenance, and enforcement of all standards promulgated by EPA. If a state defaults on this responsibility, the federal government is mandated to assume it. All state implementation plans must be approved by EPA. The states may set more stringent controls than the federal ones, but not less stringent ones.

On April 30, 1971, EPA promulgated National Primary and Secondary Ambient Air Quality Standards for six pollutants -- sulfur dioxide, particulate matter, carbon monoxide, photochemical oxidants, hydrocarbons, and nitrogen dioxide. These are frequently referred to as the criteria pollutants. No other pollutants have been added to this list, to date.

Standards have been promulgated for three hazardous pollutants -- mercury, beryllium, and asbestos.

To date, five New Source Performance Standards have been promulgated, as listed in Table 1. Of these, four had particulate standards (both total emissions and opacity). Large steam generators are limited to 0.18 gram per million calorie input, maximum 2-hour average. Large incinerators are limited to 0.18 gram per cubic meter, corrected to 12% carbon dioxide, maximum 2-hour average. Portland cement plants are limited to 0.15 kilogram from a kiln per metric ton of feed to the kiln plus 0.05 kilogram from a clinker cooler per metric ton of feed to the kiln, maximum 2-hour average. Sulfuric acid plants are limited to 0.075 kilogram of acid mist per metric ton of acid produced, maximum 2-hour average, expressed as H_2SO_4. The fifth source covered by these initial New Source Performance Standards was nitric acid plants which do not have a particulate standard. Table 2 lists the second group of New Source Performance Standards to be promulgated in the near future. These include asphalt concrete plants, petroleum refineries, storage vessels for petroleum liquids, secondary lead smelters, secondary brass and bronze ingot production plants, iron and steel plants, sewage treatment plants, copper smelters, lead smelters, and zinc smelters. All of these, with the exception of vessels for petroleum liquids storage, have particulate standards proposed. Table 3 lists Group III of proposed New Source Performance Standards. This group includes aluminum reduction plants, ferro-alloy plants, coal cleaning plants, Kraft pulp mills, iron and steel mills, phosphate fertilizer plants, and gas turbines. Four out of seven types of plants in Group III will have particulate standards.

Summarizing the data reported in Tables 1 through 3 shows that 17 out of 22 proposed New Source Performance Standards will contain a particulate standard. This is indicative of the importance which EPA places on particulate standards.

Under a study carried out for EPA, MRI (Midwest Research Institute) published on May 1, 1971, Volume I of Particulate Pollutant System Study covering mass emissions of particulates from U. S. Industry. This study estimated that gross particulate emissions in the U. S. in 1968 totaled 16 million metric tons per year broken down by major industries as shown in Table 4.

A second major facet of MRI's Particulate Pollutant System Study had as its primary objective the estimation of the mass and number of fine particles emitted from particulate sources. This area is covered in Volume II of the study. Analysis of the particle size distribution data then available (1969-70) indicated that more than 95% had been obtained using sampling and sizing procedures that are not suitable for the particle size range below 2 microns. Accurate data on the fractional efficiency of commercial control systems were also lacking and usually generalized in nature.

Since particle size distributions for uncontrolled sources and fractional efficiency curves were not available in the 0.01-2 micron range, it was necessary to extrapolate available data for larger particles to this size range. A linear extrapolation was performed by plotting data on log-probability coordinates. Figures 1 and 2 show how this was done for uncontrolled pulverized coal-fired boilers and for pulp mill recovery furnaces. The extrapolated fractional efficiency of typical control devices used in this study is shown in Figure 3.

Based on this type of extrapolation, fine particulate emission data from major industrial sources was estimated at the levels shown in Table 5. You will note a major reshifting of order based on particulate size of less than 3 microns, as compared to the data for mass emissions shown in Table 4. This order is also different if 1 micron is used as the upper limit of "fine particulate" rather than 3 microns. Inadequacy of data made it impossible to extrapolate fine particulates from agricultural operations, forest products, clay products, and primary non-ferrous metals -- four of the ten largest particulate emitters on a mass basis -- and consequently, these important sources of particulate are not included in Table 5.

MRI also estimated fine particulate emissions by the number of particles generated as compared to mass. Again this resulted in a major reordering.

Midwest originally published a priority list of fine particulate sources based on total mass emissions in this particle size range. More recently, they have revised the priority list based not only on the mass of fine particulate but also on the amount and type of potentially hazardous pollutants emitted, and the normal plant location (whether urban or rural). Weighing these four variables equally, Midwest has prepared the priority listing for sources of fine particle emissions shown in Table 6.

The Table 6 priority listing has not been adopted by EPA but is shown here as representative of the type of prioritizing necessary to our fine particulate control program. This type of priority listing is tenuous since many variables are really not adequately known and consequently, such lists are reordered as pertinent new data becomes available.

At the time of the MRI study, it became obvious that the severe lack of particle size data below 2 microns was partially the result of not having adequate sampling, sizing, and particle measurement techniques in the fine particle size range. As a result, CSL (Control Systems Laboratory) of EPA set out to sponsor the further development of particulate sampling and measurement capability in this range. Emphasis was placed on inertial impactors as the most practical approach since they had been used by various researchers since 1945. They also appeared most readily applicable to in-stack measurements of particulates. This study culminated in a recent comparison of available inertial impactors in a series of 192 individual measurements on a single utility boiler. This study showed that, when properly used, inertial impactors can give reproducible particle size distribution and mass fractional efficiency data down to about 0.1 micron. These impactors are now being used routinely by EPA personnel and their contractors and upwards of 100 sets of particle size distribution data have been generated in the last few months. Using these data, the MRI report on fine particulates is being updated so that the results down to 0.1 micron will be based on actual data rather than extrapolated data.

In an effort to push our measurement capabilities to an even lower level, Southern Research Institute under EPA sponsorship has recently been using a series of diffusion batteries coupled with condensation nuclei counters to provide concentration and size distributions by number over the size range from about 0.01 to 0.3 micron.

Typical findings of some of these most recent impactor and diffusion battery analyses will be presented later in this paper.

Although secondary particulates, per se, are not controllable by techniques under discussion at this symposium, an overview of the fine particulate problem is not complete without at least a cursory discussion of them.

Secondary fine particulate is defined as fine particulate that is formed or modified by atmospheric transformation processes. Photochemically generated particulates (including organic materials), sulfates, and nitrates are examples of secondary particulates.

Recent studies have shown that sulfate is the most abundant secondary fine particulate making up more than 50% of all particulate below 1 micron in ambient air samples from some locations.

Most sulfate found in the ambient atmosphere is formed by oxidation of SO_2. At least four mechanisms are known to play a part in this transformation. One of these involves direct oxidation catalyzed by trace quantities of metallic oxides found in the air. These oxides are almost solely a result of emissions from stationary sources. Because of their very large surface area, they may also serve as a site for the oxidation step.

The amount of sulfate formed in ambient air does not appear to be very dependent on the SO_2 concentration, once it is above a certain level (80 mg/m^3), but appears to be dependent upon other factors, such as type and intensity of photochemical smog, concentration of ammonia, or concentration of catalysts. Therefore, reduction in SO_2 will not necessarily produce a proportional reduction in sulfate. This result has been observed in several cities in the U. S. in the past year, where SO_2 levels have decreased significantly but sulfate levels have remained constant.

This finding has an important bearing on our fine particulate control program. Emissions of fine particulates containing metal ions or metal oxides may have to be rigorously controlled in order to eliminate their catalytic effect on the formation of sulfates.

Table 7 shows our current best judgement of the short term thresholds for adverse effects of particulate sulfate as compared to total suspended particulate and sulfur dioxide. Table 8 shows the long term thresholds. Data in these two tables indicate that particulate sulfate has a threshold health effect level about 1 order of magnitude lower than total suspended particulate. These data are a pretty good indication that sulfate will have to be controlled in any fine particulate control strategy. The only obvious way to control these is through the control of their precursors, both the raw material (SO_2) and catalyst (metallic oxides and ammonia).

EPA is actively studying the chemical composition of fine particulates, both primary and secondary. CSL has a program underway to characterize extensively the chemical composition and toxicology of particulates as a function of particle size and industrial source. As would be expected, chemical composition varies dramatically depending on source. For example, particulate emissions from an open-hearth furnace were found to be about 90% iron oxide with the remainder being other metallic oxides and compounds depending on source of ore and fluxes used. In contrast, particulate from a cement plant was 40% CaO, 20% SiO_2, 10% Fe_2O_3, and the remainder primarily other metallic oxides.

In fossil fuel burning, flyash varies tremendously in composition depending on source of coal and degree and type of combustion. All contain substantial quantities of oxides of silicon, aluminum, iron, and calcium. As many as 30 to 40 additional elements are identifiable in trace to significant quantities. Most are present at roughly constant levels in all particle sizes. However, some of the more toxic elements appear in increasing concentrations with decreasing particle size. Determination of toxicology versus particle size is underway.

Now, let us turn our attention to a brief discussion of the health effects problem. The Clean Air Act requires that primary ambient air standards be set to protect the public health with an adequate margin of safety. Thus, a no-effects threshold for any adverse effect is assumed. Both specifically susceptible subgroups and the population as a whole must be fully protected. Excluded are persons who require an artificial environment; that is, those who are not free living. Adverse effects include both aggravation of preexisting diseases and increased frequency of disorders. Evidence of an increased risk of future disease is an adverse effect also. Table 9 shows the spectrum of biological responses to pollutant exposures. Table 10 lists the variety of diseases attributable to air pollution.

Locus of deposition and time of retention in the respiratory system are both dependent on particle size. Figure 4 shows the effect of aerodynamic particle size on the amount of deposition in the three compartments of the respiratory system -- nasopharynx, trachea and bronchial tree, and pulmonary. This model was developed in 1965 by the Task Group on Lung Dynamics for Committee II of the International Radiological Protection Commission. The same type of data is shown in the drawing of the respiratory system in Figure 5 where a particle size scale has been placed in proportion to the depth penetration of the particles under normal breathing conditions.

Figure 6 shows the actual deposition versus particle size of inhaled particles in the upper respiratory tract and the lungs of the guinea pig and monkey compared to that of man. The upper respiratory deposition is shown in the left graph indicating that particles larger than 3 microns are deposited in this region. The right graph shows that lung deposition is primarily limited to particle size below about 3 microns.

Figure 7 shows that post exposure retention is also highly dependent upon particle size, with fine particles retained for much longer periods of time.

Earlier I mentioned the use of impactors and diffusion batteries for the measurement of fine particulates in the 0.01 to 3 micron range. I want to report to you a few examples of what we have recently found in using these techniques to measure fractional efficiencies of high efficiency control devices installed on several types of fine particulate sources. Some of these results will be discussed in more detail by other speakers later in the week.

Table 11 shows results obtained on high efficiency ESP's (Electrostatic precipitators) operating on four sources. The first ESP is installed on the CSL

Cat-Ox demonstration project for the control of sulfur dioxide by conversion to sulfuric acid. This ESP has been studied under a sub-test program of the Cat-Ox demonstration. Data obtained show that this ESP removes 98% of all particulate down to 0.05 micron.

The second ESP is installed on a utility boiler in south Alabama. Our tests made during standard operation of the utility boiler and the ESP showed removal of greater than 90% of all particulate down to less than 0.1 micron.

The third ESP is a large pilot installation on a utility boiler burning a western coal and removed greater than 95% of all particulate except that in the range of 0.5 micron. The significance of this dip in efficiency of ESP's at this particle size will be discussed by Grady Nichols in the session on electrostatic precipitators.

The fourth ESP in installed on a Kraft recovery boiler at a CSL demonstration at the Missoula, Montana, plant of Hoerner-Waldorf. Although this source is very high in fines, the ESP is removing 99% of the particulate down to 0.1 micron.

Table 12 shows the results of testing two baghouses with reverse air cleaning installed on coal-burning combustion sources. The first is installed on a utility boiler burning a mixture of anthracite coal tailings and metallurgical coke. Tests made under standard operating conditions showed greater than 99% removal of all particulate down to 0.1 micron even during the cleaning cycle. The baghouse has operated efficiently and relatively trouble-free for 1 year with no bag failures. CSL has scheduled an extensive test program on this unit beginning in May. The use of diffusion batteries in these tests will make possible number fractional efficiency measurements down to 0.01 micron.

The second unit is a pilot scale baghouse with reverse air cleaning installed on a slip stream of an industrial boiler burning bituminous coal and operated at a high gas to cloth ratio. Initial testing showed greater than 99% efficiency down to 0.1 micron. This unit is also to be tested further under an expanded test program.

Table 13 shows recent results of testing of three types of scrubbers. The first is a three-stage turbulent contact absorber operating on a 30,000 cfm slip stream of a utility boiler at the Shawnee power plant of the Tennessee Valley Authority. This joint EPA-TVA project is directed primarily at controlling sulfur dioxide using the wet limestone process. Tests to determine the particulate fractional efficiency of this unit have shown that it is 98% efficient at 1 micron 96% at 0.5 micron, and 94% at 0.1 micron. These results were much better than expected but have been verified in recent repeat tests.

The second scrubber tested is a high energy two-phase venturi scrubber installed on a ferro-alloy plant. The energy is supplied by superheated water. The tests showed that fractional efficiency dropped off below 1 micron.

The third scrubber, developed by Lone Star Steel Company, is probably the most efficient fine particulate control device we have ever tested. These tests were made in December after more than 2 years of negotiations with the company. Energy is supplied to this unit by high temperature, high pressure steam which also serves as the aspirating pump for the dirty gas stream. The unit tested was installed on an open hearth furnace producing a very fine particulate. Greater than 99% of all particulate was removed down to 0.05 micron. Lone Star claims similar results for a unit installed on one of their basic oxygen furnaces. In both installations the high pressure steam is generated using waste heat from the steel making process. This scrubber has reasonable economics under these conditions but probably not on processes without waste heat availability.

The results shown in Tables 11 through 13 show that we have made substantial progress in developing technology to control fine particulate emissions from the high priority sources shown in Table 6. However, complexity of types of sources of fine particulate emissions and the physical and chemical composition of these emissions as well as the off-gas streams bearing them presents a complicated problem of almost staggering proportions. This is true even before we know all the species of fine particulates requiring control and the level of control necessary.

In addition to work on upgrading conventional control devices, CSL started a small program about 3 years ago, to identify and develop novel devices and entirely new concepts to control fine particulate. This program has been greatly expanded during the past year and now makes up slightly more than 50% of our particulate program. We have either completed or scheduled field tests on five novel devices and have four under technical evaluation. We are supporting research on five new concepts and have two additional concepts under technical evaluation. We have an active "bush beating" program and are making every effort to encourage, identify, and support research on new particulate control technology at the earliest possible stage. Many of the subjects to be covered this week by the outstanding array of speakers assembled here are represented by tasks in our current program. However, we hope to gain new insight in these areas and to uncover entirely new concepts during the week's discussions. Consequently, those of us within EPA working in the fine particulate field are looking forward to a stimulating and exciting week.

TABLE 1. NEW SOURCE PERFORMANCE STANDARDS -- GROUP I

Source Category	Particulate Standard
Steam generators	(1) 0.18 g/10^6 cal. (2 hr. av.) heat input (2) < 20% opacity
Incinerators	(1) 0.18 g/Nm^3 corrected to 12% CO_2
Portland cement plants	(1) 0.15 Kg from kiln per metric ton of feed to kiln (2) 0.05 Kg from klinker cooler per metric ton of feed to kiln (3) < 10% opacity from kiln and cooler (4) < 10% opacity from all other sources in plant
Sulfuric acid plants	(1) 0.075 Kg of acid mist per metric ton of acid produced (2) < 10% opacity
Nitric acid plants	None

TABLE 2. PROPOSED NEW SOURCE PERFORMANCE STANDARDS — GROUPS II & IIA

SOURCE	POLLUTANT
ASPHALT CONCRETE PLANTS	PARTICULATES
PETROLEUM REFINERIES	SULFUR DIOXIDE PARTICULATES CARBON MONOXIDE
STORAGE VESSELS FOR PETROLEUM LIQUIDS	HYDROCARBONS
SECONDARY LEAD SMELTERS	PARTICULATES
SECONDARY BRASS AND BRONZE INGOT PRODUCTION PLANTS	PARTICULATES
IRON AND STEEL PLANTS	PARTICULATES
SEWAGE TREATMENT PLANTS	PARTICULATES
COPPER SMELTERS	PARTICULATES SULFUR DIOXIDE
LEAD SMELTERS	PARTICULATES SULFUR DIOXIDE
ZINC SMELTERS	PARTICULATES SULFUR DIOXIDE

TABLE 3. PROPOSED NEW SOURCE PERFORMANCE STANDARDS -- GROUP III

Source	Pollutant
Aluminum reduction plants	Fluorides
Ferro-alloy plants	Particulates
Coal cleaning plants	Particulates
Kraft pulp mills	Total reduced sulfur
Iron and steel mills	Particulates Carbon monoxide
Phosphate fertilizer plants	Fluorides
Gas turbines	Particulates Nitrogen oxides Sulfur oxides

TABLE 4. MAJOR INDUSTRIAL SOURCES OF PARTICULATE EMISSIONS (1968)

SOURCE	PARTICULATE EMISSIONS (METRIC TONS/YEAR)
FUEL COMBUSTION	5,400,000
CRUSHED STONE, SAND, AND GRAVEL	4,170,000
AGRICULTURAL OPERATIONS	1,650,000
IRON AND STEEL	1,300,000
CEMENT	840,000
FOREST PRODUCTS	530,000
LIME	520,000
CLAY	430,000
PRIMARY NONFERROUS	430,000
FERTILIZER AND PHOSPHATE ROCK	300,000
OTHER MISCELLANEOUS	800,000
TOTAL	16,370,000

TABLE 5. MAJOR INDUSTRIAL SOURCES OF FINE PARTICULATE EMISSIONS (1968)

SOURCE	PARTICULATE EMISSIONS (METRIC TONS/YR <3 μM)	PARTICULATE EMISSIONS (METRIC TONS/YR <1 μM)
FUEL COMBUSTION	1,180,000	300,000
CRUSHED STONE	787,000	116,000
IRON AND STEEL	396,000	325,000
KRAFT PULP MILLS	289,000	157,000
CEMENT PLANTS	161,000	42,000
ASPHALT PLANTS	154,000	54,000
FERRO-ALLOYS	139,000	122,000
LIME KILNS	103,000	9,000
MUNICIPAL INCINERATORS	33,000	24,000
OTHER MISCELLANEOUS	327,000	10,000
TOTALS	3,569,000	1,159,000

TABLE 6. PRIORITY LIST FOR SOURCES OF FINE PARTICLE EMISSIONS

Group I (High priority)
1. Stationary combustion (all fuel types)
   A. Electric utility
   B. Industrial
2. Iron and steel plants
   A. Open hearth furnaces
   B. BOF furnaces
   C. Electric arc furnaces
   D. Metallurgical coke ovens
3. Municipal incinerators
4. Ferroalloy plants
   A. Electric furnace
   B. Blast furnace
5. Primary nonferrous metallurgy
   A. Zinc roasting, sintering and distillation
   B. Copper roasting and converting
   C. Aluminum reduction cells

Group II (Medium priority)
1. Hot-mix asphalt plant
2. Iron foundry cupolas
3. Asphalt roofing materials
   A. Asphalt blowing
4. Secondary copper, lead and zinc

Group III (Low friority)
1. Iron ore pellet plants
2. Structural clay products
3. Cement and lime plants
4. Kraft pulp mills
5. Crushed stone

TABLE 7

BEST JUDGMENT EXPOSURE THRESHOLDS FOR ADVERSE EFFECTS

(SHORT TERM)

EFFECTS	24-HOUR THRESHOLD, $\mu g/m^3$		
	SULFUR DIOXIDE	TOTAL SUSPENDED PARTICULATES	PARTICULATE SULFATE
MORTALITY HARVEST	300 TO 400	250 TO 300	NO DATA
AGGRAVATION OF SYMPTOMS IN ELDERLY	365	80 TO 100	8 TO 10
AGGRAVATION OF ASTHMA	180 TO 250	100	8 TO 10
ACUTE IRRITATION SYMPTOMS	340	170	NO DATA
PRESENT STANDARD	365	260	NO STANDARD

TABLE 8

BEST JUDGMENT EXPOSURE THRESHOLDS FOR ADVERSE EFFECTS

(LONG TERM)

EFFECT	ANNUAL THRESHOLD, $\mu g/m^3$		
	SULFUR DIOXIDE	TOTAL SUSPENDED PARTICULATES	PARTICULATE SULFATE
DECREASED LUNG FUNCTION OF CHILDREN	200	100	11
INCREASED ACUTE LOWER RESPIRATORY DISEASE IN FAMILIES	90 TO 100	80 TO 100	9
INCREASED PREVALENCE OF CHRONIC BRONCHITIS	95	100	14
PRESENT STANDARD	80	75 (GEOMETRIC)	NO STANDARD

TABLE 9

SPECTRUM OF BIOLOGICAL RESPONSE TO POLLUTANT EXPOSURE

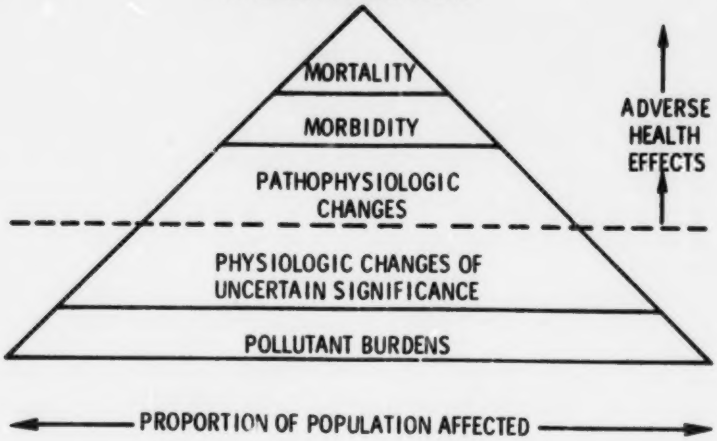
MORTALITY
MORBIDITY
PATHOPHYSIOLOGIC CHANGES
PHYSIOLOGIC CHANGES OF UNCERTAIN SIGNIFICANCE
POLLUTANT BURDENS
ADVERSE HEALTH EFFECTS
PROPORTION OF POPULATION AFFECTED

TABLE 10. VARIETY OF DISEASES ATTRIBUTABLE TO POLLUTION

I. ACUTE DISEASES:

COMMON RESPIRATORY ILLNESSES

AGGRAVATION OF PRE-EXISTING DISEASES

- ASTHMA
- HEART DISEASE
- LUNG DISEASE

IRRITATION SYMPTOMS: EYE, NOSE, THROAT, CHEST

II. CHRONIC DISEASES:

CHRONIC BRONCHITIS AND EMPHYSEMA

RESPIRATORY (AND OTHER) CANCER

CORONARY HEART DISEASE

CONGENITAL ABNORMALITIES

IMPAIRMENT OF DEFENSE MECHANISMS, RESULTING IN HIGHER RISK OF MULTIPLE DISEASES

TABLE 11. HIGH EFFICIENCY ELECTROSTATIC PRECIPITATORS

SOURCE	PARTICULATE PRESENT, %		MASS EFFICIENCY	FRACTIONAL EFFICIENCY, % AT			
	<3 μM	<1 μM		1 μM	0.5μ M	0.1 μM	0.05μM
UTILITY BOILER (BITUMINOUS COAL)	25	10	99.6	99+	98	98	99+
UTILITY BOILER (BITUMINOUS COAL)	5	2	99.6	95	92	98	
UTILITY BOILER (WESTERN COAL)	15	3	98	96	91	98	99+
KRAFT RECOVERY BOILER	90	60	99+	99	99	99	

TABLE 12. HIGH EFFICIENCY BAGHOUSES

SOURCE	PARTICULATE PRESSENT, %		MASS EFFICIENCY	FRACTIONAL EFFICIENCY, % AT		
	<3 μM	<1 μM		1μM	0.5μM	0.1μM
UTILITY BOILER (ANTHRACITE COAL-COKE)	35	20	99+	99+	99+	99+
INDUSTRIAL BOILER (BITUMINOUS COAL)	25	10	99+	99+	99+	99

TABLE 13. HIGH EFFICIENCY SCRUBBERS

SOURCE	SCRUBBER TYPE	PARTICULATE PRESENT % <3 µM	PARTICULATE PRESENT % <1 µM	MASS EFFICIENCY	FRACTIONAL EFFICIENCY, % 1µM	FRACTIONAL EFFICIENCY, % 0.5µM	FRACTIONAL EFFICIENCY, % 0.1µM	FRACTIONAL EFFICIENCY, % 0.05µM
UTILITY BOILER (BITUMINOUS COAL)	3-STAGE TURBULENT CONTACT ABSORBER	60	20	99+	98	96	94	—
FERRO-ALLOY FURNACE	2-PHASE VENTURI	60	15	93	95	90	80	—
OPEN HEARTH STEEL FURNACE	STEAM EJECTOR VENTURI	95	70	99.9	99+	99+	99+	99+

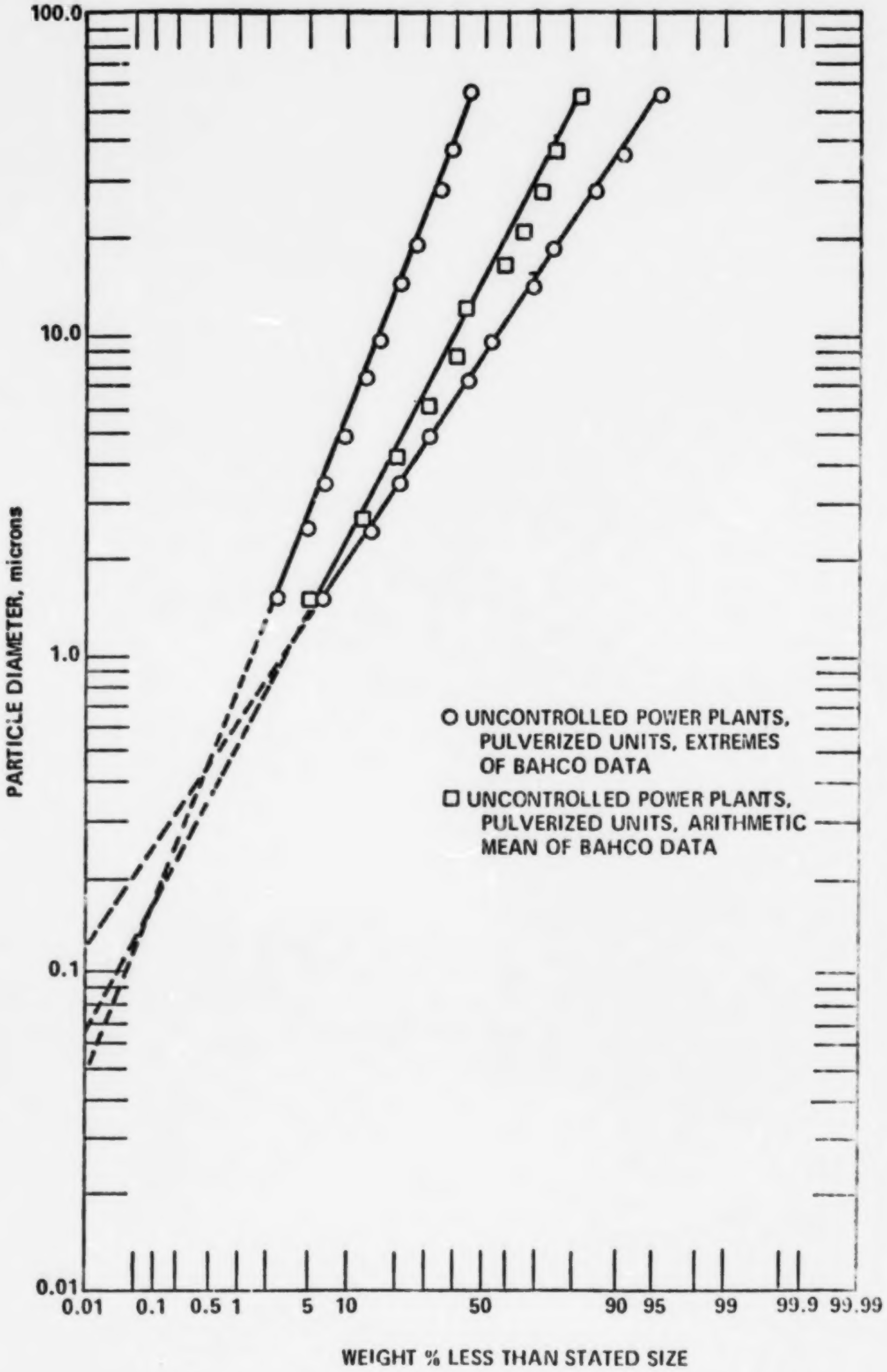

Figure 1. Pulverized coal-fired boiler emissions.

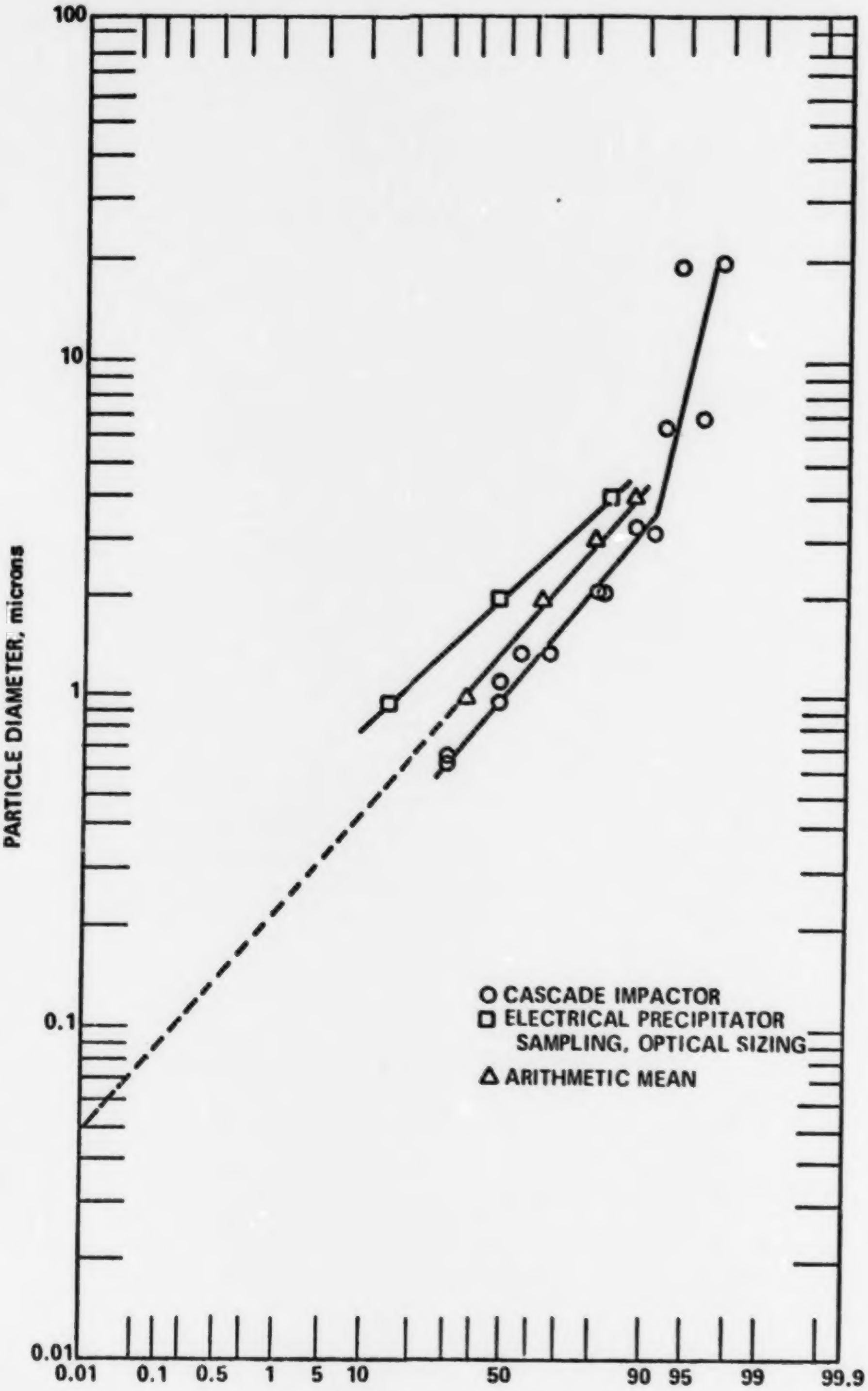

Figure 2. Pulp mill recovery furnace emissions.

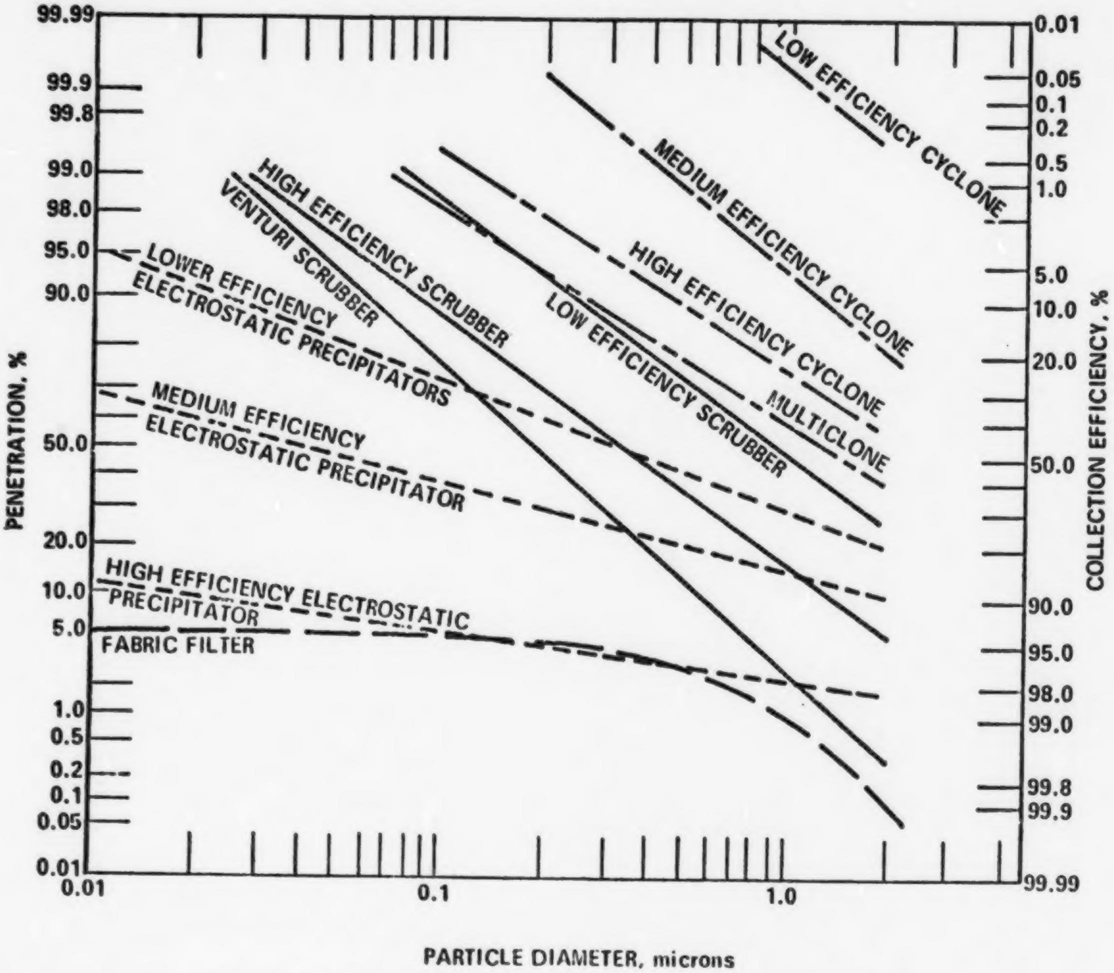

PARTICLE DIAMETER, microns

Figure 3. Extrapolated fractional efficiency of control devices.

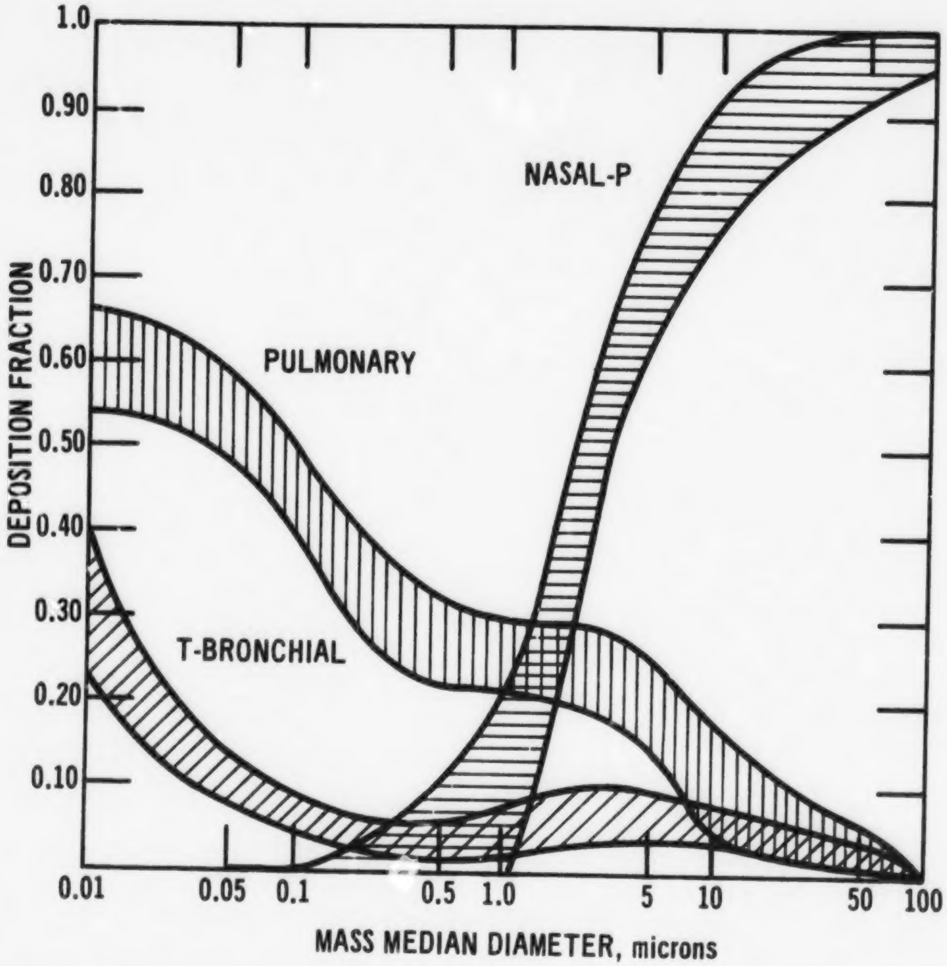

Figure 4. Fraction of particles deposited in the three respiratory tract compartments as a function of particle diameter.

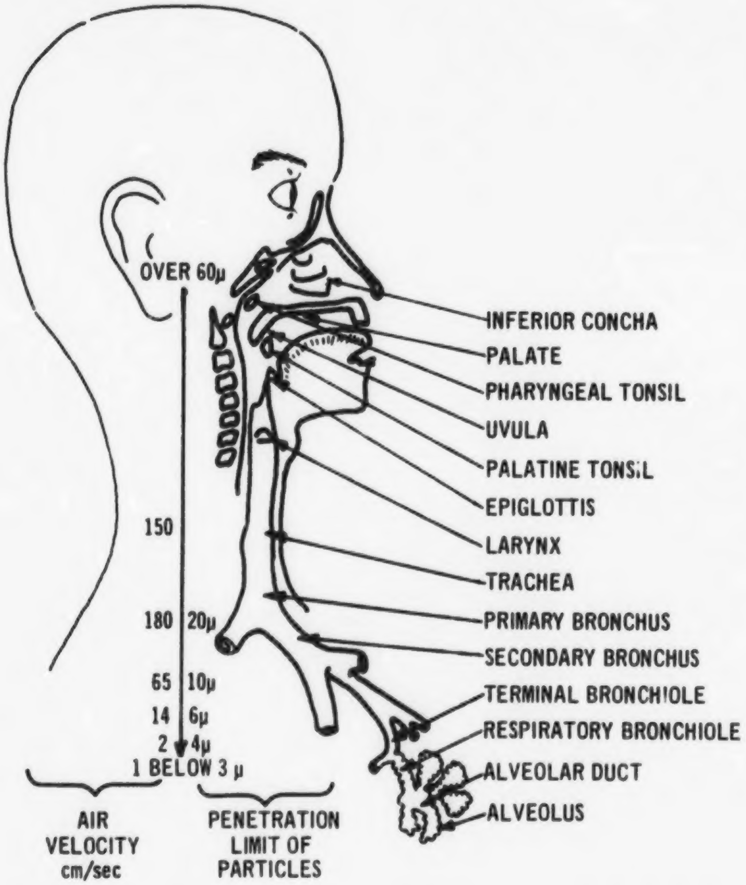
OVER 60μ
150
180
20μ
65
10μ
14
6μ
2
4μ
1 BELOW 3 μ
AIR VELOCITY cm/sec
PENETRATION LIMIT OF PARTICLES
INFERIOR CONCHA
PALATE
PHARYNGEAL TONSIL
UVULA
PALATINE TONSIL
EPIGLOTTIS
LARYNX
TRACHEA
PRIMARY BRONCHUS
SECONDARY BRONCHUS
TERMINAL BRONCHIOLE
RESPIRATORY BRONCHIOLE
ALVEOLAR DUCT
ALVEOLUS

Figure 5. Depth penetration of particles under normal breathing conditions.

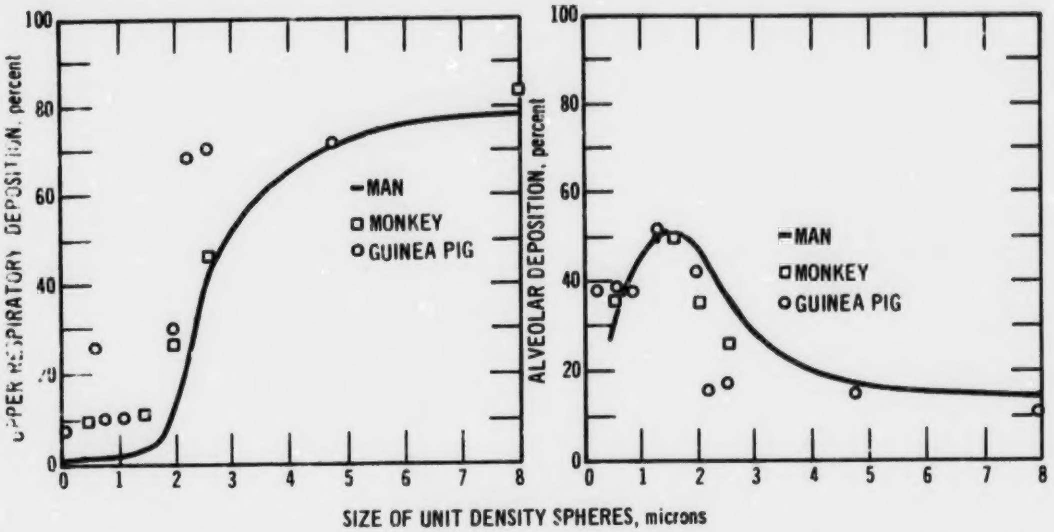

Figure 6. Deposition versus particle size of inhaled particles in the upper respiratory tract and in the lungs of the guinea pig and monkey compared with man.

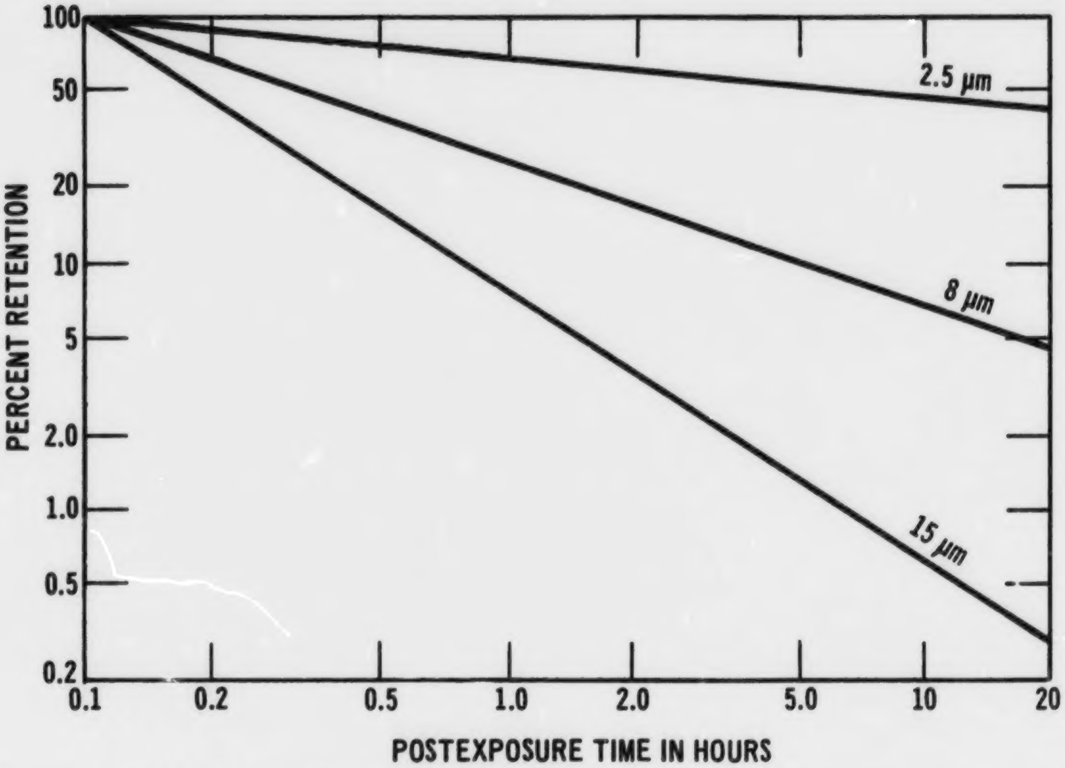

Figure 7. Effect of particle size on rate of clearance from tracheobronchial tree after oral exposure of five minutes duration. (Representative curves.)

SESSION 2

CONVENTIONAL TECHNOLOGY, ELECTROSTATIC PRECIPITATORS

Chairman: Sabert Oglesby, Jr.
Southern Research Institute
Birmingham, Alabama

Paper No.

3 Electrostatic Precipitators—Major Fields of Application, Technology, and Problem Areas

Harry J. White, Consultant
Carmel, California

4 Design Features of the Modern Flue Gas Electrostatic Precipitators

M. A. Alperovich and
Ildus K. Reshidov
State Research Institute of
Industrial and Sanitary Gas Cleaning
Moscow
U.S.S.R.

5 Theoretical Basis for Design of Modern High-Efficiency Electrostatic Precipitators

V. I. Levitov,
Ildus K. Reshidov, and
V. M. Tkachenko
State Research Institute of
Industrial and Sanitary Gas Cleaning
Moscow
U.S.S.R.

6 Removal of Ash from Flue Gases of Power Stations with Electrostatic Precipitators

I. A. Kizim,
Ildus K. Reshidov, and
V. M. Tkachenko
State Research Institute of
Industrial and Sanitary Gas Cleaning
Moscow
U.S.S.R.

SESSION 2 - Continued

Paper No.

7 Theoretical and Practical Aspects of Fine Particle Collection by Electrostatic Precipitators

Grady B. Nichols
Southern Research Institute
Birmingham, Alabama

8 Operating Experience with Gas Conditioned Electrostatic Precipitators

George P. Green and
W. S. Landers
Public Service Company of Colorado
Denver, Colorado

Paper No. 3

ELECTROSTATIC PRECIPITATORS--MAJOR FIELDS OF APPLICATION, TECHNOLOGY, AND PROBLEM AREAS

by

Harry J. White

Carmel, California

ABSTRACT

The important role of electrostatic precipitation in the high-efficiency collection of fine particles from industrial gases is discussed and assessed. Growth in applications and the trends toward higher collection efficiencies are shown. Broader aspects and highlights of precipitator technology are considered, together with some of the more prominent recent developments and advances in the field. Precipitator problems and strategies for correction are covered as an important phase of the technology.

ELECTROSTATIC PRECIPITATORS -

MAJOR FIELDS OF APPLICATION, TECHNOLOGY, AND PROBLEM AREAS

Control of particulate emissions from industrial sources has long been a matter of concern in the industrialized countries of the world. A new dimension has recently been added to the problem in the United States in the form of stringent air pollution control legislation that, in effect, requires particulate emissions from stacks to be reduced practically below the level of visibility. Particle removal efficiencies exceeding 99 percent are usually necessary to meet these stringent standards. High collection efficiencies of submicron particles are especially important because these particles usually account for most of the visibility of stack emissions, and may also be injurious to health. The collection problem is multiplied because these fine particles are also the most difficult to separate from gases, regardless of the method used.

Experience over many years shows that cleaning of industrial gases presents complex problems arising from the fineness of the particles, their high concentration in the gases, and the huge volumes of hot and frequently corrosive gases that must be treated. The gas cleaning systems used must be highly reliable, must provide consistently high performance, and be relatively insensitive to process conditions. These factors, coupled with the increasing size and complexity of modern industrial plants, require fullest use of known technology, as well as attainment of new levels of technology, if air pollution goals are to be met.

Despite the obvious need, there are no easy methods for the efficient collection of fine particles from large-scale industrial processes. The variety and complexity of industrial operations usually precludes routine application of even long-established particle collection methods. Most gas cleaning problems require their own analyses and equipment designs if desired performances are to be achieved.

The choice of basic processes for the effective removal of fine particles from gases is essentially limited to electrostatic precipitation, filtration, and high-energy scrubbing. Of these, electrostatic precipitation has the largest application in terms of volume of gas cleaned and mass of particles collected. Electrostatic precipitation also differs fundamentally from the other two processes in that the separation forces are electrical and are applied directly to the particles themselves, rather than indirectly through the gas stream. The electrical process has the inherent capability of capturing submicron particles at high efficiency with relatively low energy consumption and small pressure drop through the gas cleaning system.

This marked capability of removing fine suspended particles from gases at high efficiency is the major reason for the extensive use of precipitators, which are relatively expensive devices, in industrial gas cleaning. Much cheaper mechanical methods can be used for particle sizes above a few microns diameter.

While both theory and experience show that the particle collection rate for electrostatic precipitators decreases somewhat with decreasing particle size, it is also found to reach a minimum for particles of a few-tenths micron diameter and then to increase substantially for the superfine particles of less than a few-tenths micron diameter.

Field experience over many years has shown that there have been many highly successful precipitator installations, but also many cases where precipitators have failed to meet performance goals, sometimes by large margins. These deficiencies are, in this author's view, usually attributable to neglecting to take a sufficiently broad systems view of air pollution and environmental problems in plant design and operation, with resultant underestimates of requirements, inattention to engineering design and construction of the gas cleaning equipment, and to what should be the obligation of precipitator vendors to provide adequate equipment. Also, the level of attention to environmental problems by some industrial companies has been minimal.

Major Fields of Application

Electrostatic precipitation was developed in the United States in the early years of this century as an effective method for meeting public demand for control of air pollution caused by smelters and other industries. Although the industrial smoke and dust problem was by no means new, existing control methods of the era had proved to be incapable of coping with the complexities of treating huge volumes of hot, dirty, and often corrosive gases. To Cottrell goes the credit for developing and demonstrating the practicability of large-scale electrostatic precipitation. His largest commercial unit was for 250000 cfm for collection of lead and zinc oxides, and was built in 1910. This was followed shortly thereafter by the successful application of the process by Schmidt to the cleaning of cement kiln gases. The Schmidt precipitator treated over one million cfm of gas, collecting 100 tons of dust per day.

Major growth and development of electrostatic precipitation since these pioneer efforts came initially from applications to other existing industrial air pollution problems, and later from technological advances in various industrial fields which gave rise to new gas cleaning problems. Increasingly stringent air pollution control legislation, especially in recent years, has not only expanded the fields of application, but has also required new levels of efficiency and performance. Examples of developing technology leading to large new fields of precipitator application are the introduction of powdered-coal-fired boilers in electric power generation, the fluidized catalyst process in gasoline production, and basic oxygen furnaces in the steel industry. Economic recovery of valuable materials has also played a role, as for example the recovery of soda ash in kraft paper mills, and recovery of expensive catalyst dust in the fluidized catalyst process.

The first comprehensive survey of the major applications of precipitators in the United States was made about fifteen years ago by the author (1), and has been updated several times since then, most recently in 1969-70 (2,3,4). Such surveys are becoming more difficult to make with confidence, because of uncertainties in air pollution control requirements, changing plans of precipitator users, the proliferation of precipitator vendors, and most recently the confusions of the energy crisis. Projections of future demands for precipitators are especially difficult and uncertain, but increased application seems unquestionable.

Major applications of precipitators in the United States are summarized in Table 1. Fly ash collection is seen to be by far the most important field, comprising some 75 percent of the total in terms of volume of gas treated. This is followed by metallurgical, cement, and paper mill applications, each in the five to 10 percent range. All other fields combined account for less than five percent, although individually they may be of great importance and some, such as municipal incinerators, are growing areas of application. Precipitator application as a whole has historically grown at a rather rapid pace, as illustrated in Fig. 1. It is also evident that fly ash precipitation has been the dominant field for many years. Although only rough estimates of the particulates collected by precipitation are possible, calculations based on the gas volumes treated and particle concentrations for the various fields show a total of the order of 90 million tons per year for all applications, of which fly ash amounts to about 40 million tons per year.

Precipitator collection efficiency trends are of basic interest in reflecting levels of air pollution control and the cleanliness of industrial gas emissions. These trends are shown in Fig. 2 for fly ash precipitators, and in Fig. 3 for cement kiln and paper mill recovery furnace precipitators. Trends for maximum and average efficiencies are given for fly ash and average efficiencies for cement and paper mills. The averages are weighted in accord with the gas volumes represented. The rapid increases in efficiencies are especially evident for the past five to 10 years, coinciding with greater public awareness and increasingly stringent air pollution control legislation. Currently, virtually all precipitators are being designed for 99 percent or better collection efficiency. Efficiencies at these levels are sufficient in many cases to provide virtually clean stacks as observed by eye.

The over-all growth of electrostatic precipitator applications in the United States is remarkable when both the increases in cfm capacity and in collection efficiency are taken into account. A precipitator designed for 99 percent efficiency, for example, will be at least two to three times larger than one for 90 percent efficiency. On this basis, the per annum rate of growth of new precipitator capacity is of the order of 20 times greater for the 1965-1970 era as compared with the 1945-1950 era.

Newer trends in precipitator applications which may be mentioned include the following:

1. Use of precipitators ahead of the air preheaters in power plants to collect fly ash at high temperatures of 600 to 800°F as a means of avoiding high resistivity problems in plants burning low sulfur coals. This precipitator arrangement has become known colloquially as a "hot" precipitator.

2. Changing from wet-bottom to dry-bottom precipitators in paper mills using odor-free recovery boilers. The dry-bottom designs require relatively large hoppers and are usually equipped with scraper mechanisms to effectively remove the very low-density collected dust characteristic of the process. Relatively low precipitation gas velocities, good gas distribution, and larger hopper capacities are necessary to avoid the "snowing" problem.

3. Changes in steel-making technology from open-hearth to basic oxygen furnaces (BOF) involve cooling and humidifying the gas ahead of the precipitator. High resistivity can be a problem for part of the BOF cycle. Very high collection efficiencies of 99.5 percent or higher are also required because of the high concentrations and fineness of the particles.

4. Use of wet precipitators in aluminum reduction plants to reduce particle emissions from the reduction furnaces to the level of invisibility and to collect mist carry-over from scrubbers preceding the precipitators. Outlet

concentrations of particulates as low as 0.002 grain per ft^3 have been reported with this arrangement (5).

5. The increasing use of municipal incinerators in the United States has resulted in a growing new field of precipitator application in this country, although incinerator precipitators have been used in Europe for some time.
6. Development work has been conducted over the past several years to meet the demand for precipitators to clean gases at high temperatures and pressures, up to 1700°F and 100 lbs. per in^2 respectively (6), for application to newer industrial processes such as MHD (magneto-hydrodynamic) power generation and coal gasfication.

A remark regarding the impact of the present energy crisis on industrial air pollution control and efforts may be in order at this point. The uncertainties of fossil fuel resources and availability, the growing dependence on coal for electric power production, and panic reactions, have led to an attitude in some quarters of jettisoning hard-won air pollution control legislation and enforcement. Questions are raised about technical and economic feasibility under these circumstances. Without attempting to make sweeping judgment, this author believes that sacrificing particulate controls is entirely unjustified because of the proved technical ability which we now possess to deal with most of these problems, including high-efficiency cleaning of flue gases from power plants burning so-called "dirty" coal.

Technology and Problems

Precipitation technology is far from an exact and unified field. It has long presented a peculiar dichotomy of theory and practice, with several schools of thought in existence ranging from pure empiricism to a high degree of reliance on scientific methods. The theory and principles underlying the field have been largely codified and are available in the technical and scientific literature.

On the other hand, the documentation of the practice, as represented by records of the large body of accumulated field experience, has been for the most part fragmented in the files of precipitator vendors and individual engineers, and therefore has been unavailable to the public. These files are often regarded as containing trade secrets, even though their actual value may be highly questionable. Considerable efforts have, however, been made in the past few years toward codifying and making the field experience generally available (see reference 3, for example) as a strategic means of improving air pollution control.

The advantages of a recognized scientifically based precipitation technology are readily apparent in terms of sound engineering design, development of performance standards, equipment evaluation, and as a basis for major improvements through systematic research and development. Some efforts toward unification and development of technical standards are being made through an industry trade group (7) but most of the investigative work in this country is being carried on by contract research institutes under Environmental Protection Agency sponsorship (8), to a lesser extent by universities, and in a few instances by precipitator users.

It is impossible within the confines of this paper to do more than touch on some of the broader aspects and highlights of precipitator technology, and to mention the more prominent recent developments and advances in the field.

Precipitator design

A fundamental task in precipitation technology is the design of optimum precipitators for given applications. These should take into account relevant technical, economic, legal, and public relations factors, but this is seldom done, and precipitator designs are usually based only on technical and cost criteria. For example, the broad over-all evaluation of collector equipment should include the large costs which can be incurred as a result of being forced to curtail production because of excessive particulate emissions from deficient collector equipment, yet this is seldom done even though for the case of a large power plant, for example, these costs can run into tens of thousands of dollars per day. Clearly these broader issues are the province of the precipitator user, but precipitator manufacturers should be conversant with them.

Under current competitive bidding conditions, the precipitator design problem most often reduces to developing a design to meet a set of equipment performance specifications and requirements at presumably the lowest cost to the customer. There have been attempts to standardize precipitator bidding and evaluation practices in the United States (9). However, actual purchase specifications may range from elementary statements covering hardly more than gas flow and required collection efficiency to comprehensive documents specifying basic design parameters, details of construction, and the like. The latter practice is the outgrowth of users' attempts to insure satisfactory performance and to protect themselves against deficient equipment. Unfortunately, some of the most essential physical and chemical properties of the particles and gases which influence precipitator performance are seldom specified, and frequently are not known. The most conspicuous example is the resistivity of the particles. Even in those cases where these properties can be measured in existing plants these measurements may never be made, nor even requested by either purchaser or seller, for equipment design purposes.

In practice, several different approaches are used for the basic design of precipitators. These range from simple extrapolations of previous field experience, and design by analogy, to more sophisticated methods derived from theory and underlying principles. For some applications, such as collection of sulfuric acid mist where the particle and gas properties are well established, design by analogy can be applied with a high degree of success. On the other hand, for fields such as fly ash collection where particle properties tend to be highly variable, design by analogy is a hazardous process. There are many examples of fly ash precipitators which have been designed to operate at 95 to 99+ percent collection efficiency but actually perform at only 50 to 80 percent.

Pilot precipitators are often used in the case of existing plants, or where new processes are being developed, as a means of determining design of full-scale precipitators. The main problem here is the scale-up factor to be used, since it is well known that pilot units operate much better per unit size than do those of commercial size. The scale effect is chiefly attributable to differences in electrical energization and gas flow, with the former being the most important factor. In general, pilot precipitator data should be supplemented as fully as possible by basic data on the particle and gas properties, and especially by resistivity information.

Precipitator designs might, in principle, be deduced from theory alone if all the significant variables were known. But this is not the case in practice, and it is necessary to specify some of the basic design parameters primarily from field experience. Recently, theoretical techniques have been advanced by the development of a computer model for precipitator design and performance analysis (10). Although still in the developmental stage, this approach shows much promise for future practical engineering use.

Basic parameters used in precipitator design, together with the numerical values used for fly ash, are summarized in Table 2. It is to be noted that the values of these parameters will vary with fly ash and flue gas properties, with gas flow, and with required collection efficiency. The highly important precipitation rate parameter w found in actual operation depends strongly on such factors as accuracy of precipitator electrode alignment, uniformity and smoothness of gas flow through the precipitator, rapping of the electrodes, and the size and electrical stability of the rectifier sets. These factors have to do with the mechanical and electrical quality of the precipitator, and experience shows that deficiencies in quality often exist in these areas. Therefore allowance needs to be made for them in the design process.

Precipitator problems

Experience has shown that problems of some magnitude are encountered in a significant percentage of precipitators. It is not uncommon to find that several years and much expense are required to correct the problems. Under these circumstances, it is advisable to approach precipitator problems in a systematic way. For this purpose, it is helpful to classify the problems into three major categories: fundamental, mechanical, and operational. In practice it is not uncommon for all three types of problems to be present, which obviously can complicate matters. Scientific and engineering procedures exist for diagnosing and correcting most of the problems. Attempts to correct them on the basis of offhand judgments and random guesses usually prove costly, time-consuming, and unproductive.

Examples of fundamental problems are high resistivity particles, poor gas flow, and deficient electrical energization. Mechanical problems include, for example, poor alignment of the electrodes, breakage of corona wires by fatigue or by electrical burning, and air inleakage to the hoppers. Operational problems commonly encountered include poor electrical set adjustments, shorted corona sections (caused by broken wires, for example), overloading the precipitator by excessive gas flow, and failure to empty hoppers of collected dust.

High resistivity

Although high resistivity has been a troublesome problem from the earliest years of electrostatic precipitation, the incidence of the problem has been greatly increased in recent years because of the wider use of low-sulfur coals in the electric power industry.

Methods for dealing with the high resistivity problem in the precipitation of fly ash include: conditioning with SO_3, collection at high temperatures of 600° to 800°F, collection at low temperatures of the order of 200° or 230°F, use of very large precipitators, and, quite recently, the possibility of conditioning the ash by addition of small quantities of sodium compounds such as Na_2CO_3 to the coal being burned.

The role of sodium in increasing the conductivity of fly ash is an interesting one and the subject of considerable recent and on-going research (11,12). The effect of sodium content on fly ash resistivity in some typical cases is shown in Table 3. It is observed that high sodium content results in low resistivity ash, and vice versa. Research shows that the increased conductivity is due to sodium ion migration through the fly ash particles, and is effective at gas temperatures above about 350°F.

List of References

1. H. J. White, "Fifty Years of Electrostatic Precipitation," paper presented at the Golden Jubilee Meeting of the Air Pollution Control Association, June 1957

2. H. J. White, Industrial Electrostatic Precipitation, pp. 24-26. Reading, Mass: Addison-Wesley, 1963.

3. S. Oglesby, Jr. and G. B. Nichols, "A Manual of Electrostatic Precipitator Technology," sponsored by National Air Pollution Control Administration, August 1970.

4. A. B. Walker and R. E. Brown, "Statistics on Utilization, Performance and Economics of Electrostatic Precipitators for Control of Particulate Air Pollution." Paper presented at Second International Clean Air Congress, Washington, D.C., December 1970.

5. J. L. Byrne, "Fume Control at Harvey Aluminum." Paper presented at Air Pollution Control Association at Spokane, Washington, Nov. 1o70.

6. R. F. Brown and A. B. Walker, "Feasibility Demonstration of Electrostatic Precipitation at 1700°F." Journal of the Air Pollution Control Association 21 617 (Oct. 1971).

7. The reference here is to the Industrial Gas Cleaning Institute.

8. Most of the R/D/I work referred to is being done at Southern Research Institute.

9. Industrial Gas Cleaning Institute, Publications E-P-4 and E-P-5, 1968.

10. Southern Research Institute, "An Electrostatic Precipitator Performance Model." Report to the Environmental Protection Agency. Sept. 1971

11. W. E. Bucher, "A Study of the Bulk Electrical Resistivity Characteristics of Fly Ash from Lignite and Other Western Coals." M. S. Thesis, University of North Dakota, December 1970

12. Southern Research Institute, "Investigation of the Volume Resistivity of Fly Ash from the Sundance and Wabamun Power Stations." Final Report to Calgary Power, Ltd. June 1972.

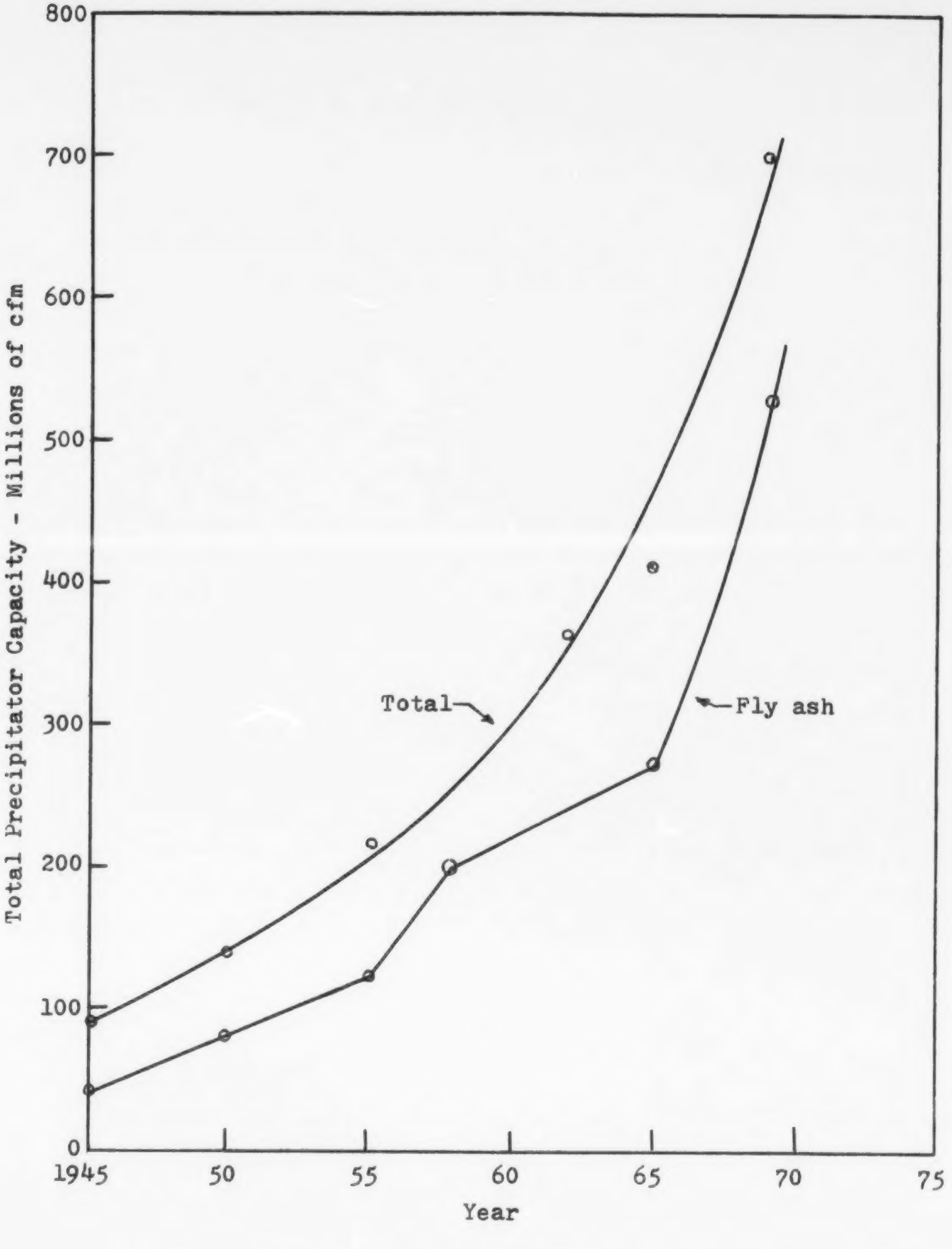

Figure 1. Growth in total and fly ash precipitation cfm capacity in the United States since 1945.

H. J. White
Jan. 1974

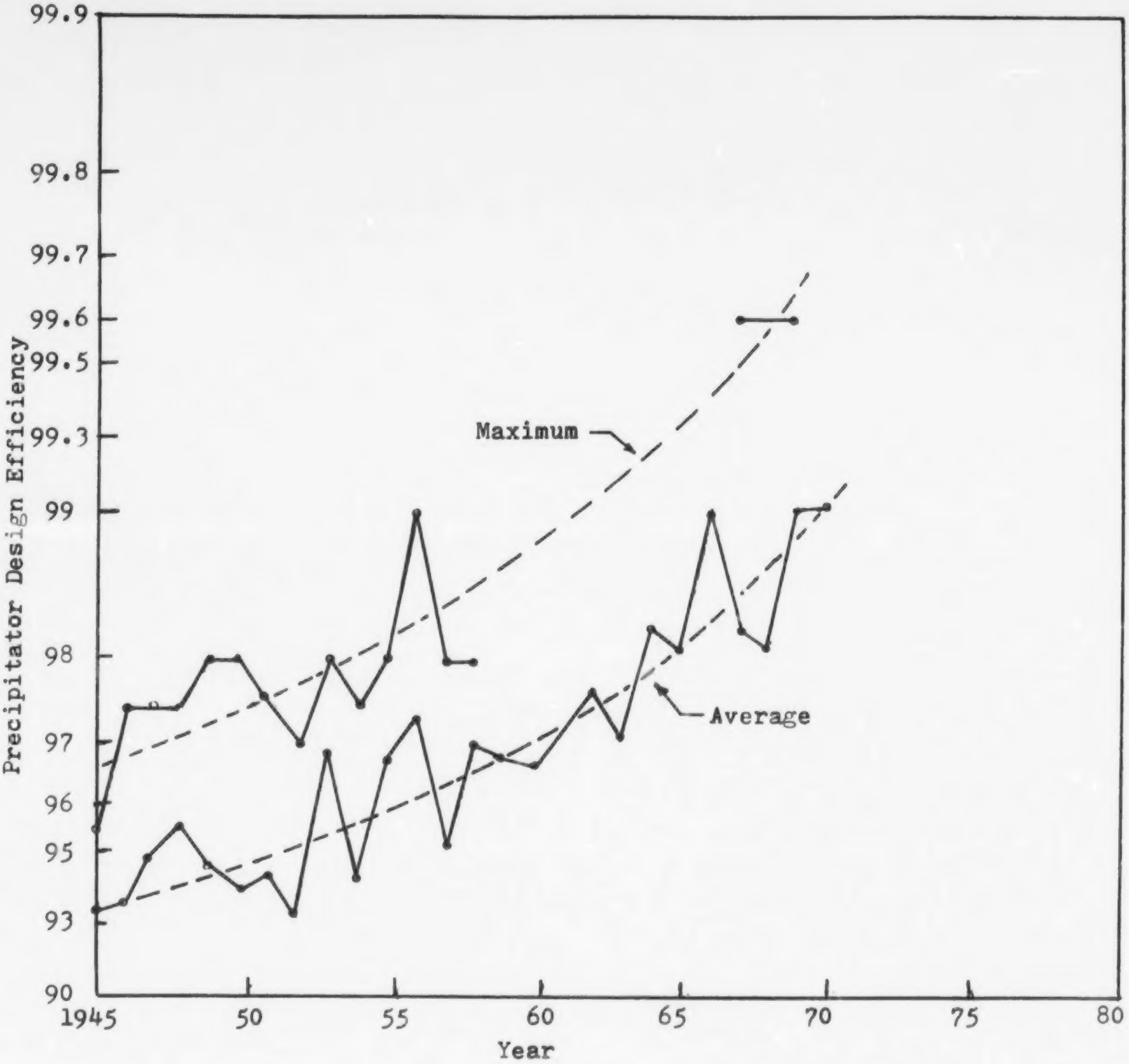

Figure 2. Fly ash precipitator efficiency trends.

H.J. White
Jan. 1974

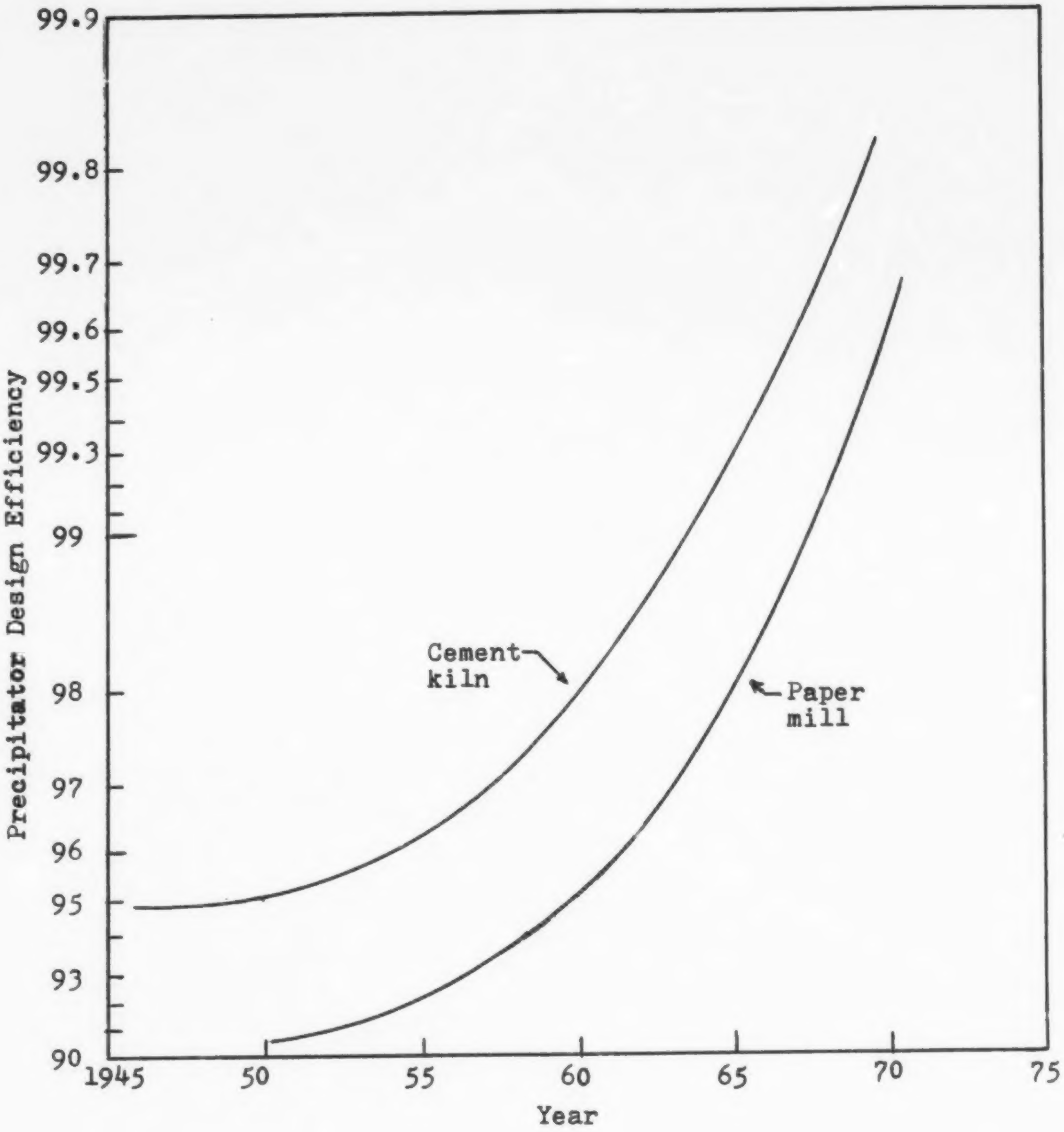

Figure 3. Efficiency design trends for cement kiln and paper mill precipitators.

H.J. White
Jan. 1974

Table 1

Summary of United States Precipitator Installations in Major Fields of Application, 1907-1970

Application	First installation	Total number precipitators	Total gas flow, million cfm	Percent of total gas flow
Electric power industry (fly ash)	1923	1330	530	75.3
Metallurgical:				
Copper, lead, & zinc	1910	250	18	
Iron & steel	1919	340	40	
Aluminum	1949	80	6	
		670	64	9.1
Cement	1911	300	42	6.0
Gypsum	~1930	70	2	0.3
Paper Mills	1916	230	35	5.0
Chemical Industry	1907	~700	~14	2.0
Detarring of fuel gases	1915	700	6	0.8
Municipal incinerators	~1965	~10	~2	0.3
Petroleum fluidized catalyst	1942	42	4	0.6
Carbon black	1926	90	3	0.6
Totals		4142	702	100.0

H. J. White
January 1974

Table 2

Range of Basic Design Parameters Encountered in Practice for Fly Ash Precipitators

Parameter	Symbol	Range of values
precipitation rate	w	0.1 - 0.6 ft/sec
$\frac{\text{collection surface}}{\text{1000 cfm}}$	$\frac{A}{V}$	100 - 500 ft^2/1000 cfm
gas velocity	v	4 - 8 ft/sec
aspect ratio	$\frac{L}{H}$	0.5 - 1.5 $\frac{\text{length of ducts}}{\text{height of ducts}}$
$\frac{\text{corona power}}{\text{1000 cfm}}$	$\frac{P_c}{V}$	50 - 500 watts/1000 cfm
$\frac{\text{corona current}}{\text{sq ft plate area}}$	$\frac{I_c}{A}$	5 - 70 microamps/ft^2
plate area per electrical set	A_s	5000 - 80000 ft^2/el. set
no. of H.T. sections in gas flow direction	N_s	2 - 8
degree of H.T. sectionalization	$\frac{N}{V}$	0.4 - 4 $\frac{\text{H.T. bus sections}}{\text{100000 cfm}}$

H. J. White
January 1974

Table 3

Effect of Sodium Content on Resistivity of Fly Ash

Power Plant	Coal Analysis		Flue Gas	Fly Ash	
	S %	Na_2O %	Temp. °F	Na_2O %	Resist. ohm-cm
1	0.25	0.01	350	0.3	2×10^{12}
2	0.25	0.40	350	2.4	5×10^{10}
3	0.54		330	5.6	3×10^{9}

Preceding page blank

Paper No. 4

DESIGN FEATURES OF THE MODERN FLUE GAS ELECTROSTATIC PRECIPITATORS

by

M. A. Alperovich
and
I. K. Reshidov

STATE RESEARCH INSTITUTE OF
INDUSTRIAL AND SANITARY GAS CLEANING

Moscow

Design Features of the Modern Flue Gas Electrostatic Precipitators

Alperovich M. A., Reshidov I. K.

The modern flue gas electrostatic precipitators are used in various branches of industry. They are used effectively when compared to other types of collectors used for dry cleaning large gas volumes from non-reactive and inflammable dusts containing fine particulates.

Usually horizontal multi-field electrostatic precipitators are used allowing 99% or higher level of cleaning.

Two types of such electrostatic precipitators are made in the USSR: UG type - for gases with T up to 250°C, and UGT - up to 400°C.

When the conditions do not allow the use of UG type or when the necessary cleaning does not need to exceed 98%, vertical electrostatic precipitators can be used. Those are one field DVPN type ESPs. When they are used, the initial dust concentration should not exceed 20g/nm^3. At the present time in place of the DVPN new UV type vertical electrostatic precipitators are used.

For the collection of flammable dusts, from coal or lignite, with flue gas temperature up to 130°C or air temperature up to 90°C, vertical, one section UVP electrostatic precipitators are used. The cleaned gases are emitted directly into the atmosphere through the roof of the ESP body. No outlet pipes or smoke stacks are used. Such installations assure minimum resistance to the gas flow and prevent breakdown of the apparatus in case of trouble with the emergency drying system. The explosive valves are located on the roof of the electrostatic precipitator and serve that purpose. The new UVV electrostatic precipitators are used to replace the UVP type.

In all of the above electrostatic precipitators flow of the dust laden gas is perpendicular to the electric field. The collector electrodes are located parallel to the axis of gas inlet and make transverse cross-section of the ESP to the gas inlet. In this way necessary surfaces for the dust collection are formed.

Three types of the "Uniform Horizontal" electrostatic precipitator exist. Those are single section with no internal partitions.

UG1 - with electrodes 4.5 m high and fields 2.5 m long, two and three field, with functional cross-section area 10 and 15 m^2;

UG2 - electrode height 7.5 m, field length 2.5 m each, three and four field, with areas of functional cross-section 26, 37, 53, and 74 m^2;

UG3 - electrode height 12 m, field length 4 m each, three and four field, with areas of functional cross-section 88, 115, 177, 230, 265 m^2.

Interelectrode spacing (width of the gas passage) - 275 mm.

In the ESPs "UG2" (functional cross-section area 53 and 74 m^2) and in all "UG3" ESPs the fields are sectioned to allow the autonomic electric supply of sections from the separate rectifier units. In two largest "UG3" ESPs each field is divided into four sections.

The electrostatic precipitator sizes were determined by the body dimensions. It was found appropriate to use base supports with module spacings (multiple 1.5 m) and structural elements of uniform size. The summated functional length of the field should not be shorter than the functional height of the electrode.

1.1 Collector electrodes (Fig. 1) are made of the rolled steel sheets with thickness up to 1.5 mm. Each electrode is made of uniform C-formation elements, 350 mm wide. The number of the electrodes depends on the field length.

The elements of each collector electrode are bolted to one beam on the ceiling with two horizontal beams leaning on the support structures of the ESP body.

The rapping beam of two steel rails is fastened to the lower end of the element. The anvil is welded to one side of the beam.

The rapping of collector electrodes is done by striking the hammer over the anvil through the intermediate rod. (Fig. 2)

The hammers (one for each electrode) are secured with some angular displacement on the axis to the shaft inside of the ESP. The hammers fall alternately thus securing rapping of individual ESP electrodes.

Rotation of the hammer shaft with velocity h=0.6 turns/min. originates from the driving gear--standard motor-decelerator, installed inside of the ESP body. The shaft with hammers rotates in special dust bearings.

The maximum weight of the striking parts is determined by the properties of the collected dust. In the "UG3" electrostatic precipitator it is 13 kg.

The rapping applied secures proper acceleration on the collector electrode and removal of dust.

For easier installation and transport, collector electrodes rapping mechanism is set up as a separate unit.

1.2 Corona electrodes - frame, with corona elements mounted on piping frames. (Fig. 3).

To simplify transportation the corona electrodes are made of two or four parts, depending on the size of the electrostatic precipitator.

Two types of corona elements are used: belt-needle and belt-tooth.

The belt-needle element is made of a steel belt 1mm thick. In this element, 16 mm wide, the needles are stamped out perpendicular to the belt surface. The needles are 6 or 12 mm long with spacings 80 to 40 mm between the needles on each side of the element.

The belt-tooth element is made of steel 1.5 mm thick, 15 mm wide. The teeth are 5 mm high and are stamped out on both sides of the belt steel.

The corona elements are secured in the frame with nuts. A pin is welded on one end of the corona electrode element and on the other end cylinder is stamped out.

The corona elements are fastened to the frame in 180 mm intervals. The surface of the belt-needle element with its needles can be parallel or perpendicular and in the case of the belt-tooth element can only be perpendicular to the frame surface.

The corona electrodes of each field or field section are fastened to two frames on the ceiling, each of which is suspended on the piping to the quartz support-bushing. The latter are installed in the top part of the electrostatic precipitator in special insulation casings.

The driving gear of the corona electrode rapping is analogous to the driving gear of the collector electrodes and is located over the insulation casing on the cover of the ESP.

The rapping of the corona electrodes in each field is done on one side in the "UG1" and UG2" ESPs on one level, in UG3 on two levels of height.

The rapping mechanism consists of shafts with hammers, bobbin mechanism with transfer relationship i = 1:3 and rods opposite the anvils of the corona electrodes.

Figure 4 shows kinematic scheme of rapping mechanism for the corona electrodes.

Velocity of hammer shaft rotation is 0.2 turns/min.

Maximum weight of the striking part of the hammer is 6.5 kg.

Each insulator is supplied with electric heaters containing Screens to protect from surface condensation.

The insulated casings have hermetically sealed doors and blocking mechanism which grounds the high voltage system.

Before the gas enters the ESP the insulators preliminarily are heated to the dew point temperature of the gases, which is then maintained with help of the thermal relay.

1.3 Gas distribution grating is installed at the gas inlet to each electrostatic precipitator. It is made of individual held together steel bars 3 mm thick with flanged edges and stamped out openings 60 mm diameter. Active cross-section of grating is 45%.

Rapping of the gas distribution grating if necessary is done with hammers mounted on shafts. The latter are installed in special bearings behind the grating.

The driving gear for rapping of the grating is installed outside the apparatus and is analogous to the rapping of the electrodes.

Additional gas distribution grating is installed in the mixing chambers and diffusers. The design of the grating is based on the aerodynamic modeling of gas distribution for gas cleaning installation under consideration.

1.4 Electrostatic precipitator body is steel, welded, calculated for the internal rarefaction 400 kg/m^2 and internal pressure 50 kg/m^2. With special ordering the electrostatic precipitator body can be designed for rarefaction up to 1000 kg/m^2. The design of the body is prepared for outside installation with calculated minimum temperature of the surroundings down to -40°C.

The body of the electrostatic precipitator is insulated from the exterior.

The hermetic seal of the body is checked during the operation. The supply of the outside air should not exceed 2% of the volume of gases to be cleaned.

For servicing and inspection of the electrostatic precipitators interior and exterior stairs are mounted on the body. The openings are through the hermetically sealed iron doors in the walls and in hood of the body.

On top of the ESPs "UG1" and "UG2" cabins are set up for the rapping driving gear and for the servicing personnel.

On the roofs of the large "UG3" electrostatic precipitators, in the intermediate space above the insulating casings along the entire width of the body corridors are constructed for the corona electrodes rapping driving gear and for the servicing personnel. The openings to the insulated casings are through the hermetically sealed doors located on the front walls of the body and through the doors of the above described corridors.

1.5 High voltage current is supplied either by a cable from the step-up rectifying unit located behind the limits of the electrostatic precipitator bodies or directly from the body roof by way of a rail current feeder through a quartz bushing.

1.6 Installation of the interior equipment is possible from the "side" with the side walls of the body removed. The major interior equipment is installed in units (collector and corona electrodes). The design of the ESP also allows installations through the open top of the body.

Only quality installation of the equipment and the body assures normal highly efficient performance of the electrostatic precipitator.

The electrostatic precipitator cannot be used without heat insulation as that averts sagging of the beams and in turn nonalignment of the electrodes.

2. Electrostatic precipitators "UGT"

The Uniform Horizontal Temperature Stable ESPs for the cleaning of stack gases are serially prepared, three field, with functional field height 7.5 m, and lenght 2.5 m and with the interelectrode space 260 mm.

The "UGT" is known for the high level of assembly unification and equipment detail.

The "UGT" and also "UG" sizes are determined by the necessity of the base support system with modular spacing of 1.5 m.

The electrostatic precipitators used have following dimensions:

1.	Type	UGTI-30	UGTI-40	UGTI-60	UGTI-80
2.	Functional cross-section surface, m^2	30	40	60	80
3.	Number of gas inlets	16	22	33	44
4.	Body width, mm	4500	6060	8920	11780
5.	Distance between the extreme base supports by width,mm	4500	6000	9000	12000

Longitudinally the length of all these is the same with 12 m distance between the extreme supports.

2.1 Collector electrodes - plate-like, rod-shaped.

The electrode is made of two plates each of which is composed of 8mm steel rods in 15 mm spacings inserted at the top and bottom into the steel bar guides fastened with two connecting rods.

The two plates are connected through the guides forming one rapping beam 7.5 m high in the center of the electrode.

The collector electrode is suspended from the ceiling with two connecting rods. In the top, middle and lower part the electrode is fixed with remote supports fastened to the cross structures of the body.

The rapping of the electrodes is done with hammer mechanism located in the interfield spaces. Usually the hammers for each field are fastened to the shaft at the height corresponding to the middle of the electrode. In design the hammer rapping is analogous to the one used in "UG" ESPs.

The "UGT" electrostatic precipitators are made also with uniform collector electrodes of C-formation belt elements, 7.5 m high, like in "UG" precipitators. The stipulation for the use of such collector electrodes is the guaranteed stability of gas temperature excluding even a short time increase above 400°C.

2.2 Corona electrodes - wire, nichrome wire of 2.5 mm diameter or belt-tooth. The latter are made of a belt 1mm thick, 20 mm wide with 5 mm teeth stamped out on both sides with 40 mm spacings. Depending on the type of the gas the steel used might be stainless steel.

The rectilinearity and tension of the electrodes is secured by the weights attached to each wire.

The corona electrodes are suspended from the top of frames made of bar steel. The electrodes are centered at the lower frames which are fastened to the top with connecting rods. This also prevents loosening of the corona electrodes.

All of the electrostatic precipitators use frames of the same size. The bars of top frames often are made of low-alloy steel.

The system of the corona electrodes for each field or section is suspended by way of two gas pipes to the support structure located on the ceiling of the ESP body. The current carrying parts are insulated from the body of the apparatus by means of quartz piping and porcelain bracket insulators.

The rapping driving gear is located on the top of the insulator casing.

The driving gear is the same as for the collector electrodes.

2.3 Body of the electrostatic precipitator "UGT" - steel, calculated for the indoor and outdoor installation. The top cabins, servicing stairs can rest only against the face of the ESP body.

The body design is calculated for rarefaction up to 400 kg/m^2 with outside temperature down to -30°C. In horizontal cross-section the body is composed of TT-formation frames, carrying the major elements of equipment and bracing of rolled horizontal beams. The side walls of the body are continuous, made of 5 mm sheet with horizontal and vertical ribs made of rolled corner steel or bar steel.

The horizontal covers of the body have openings for the equipment installation. These are closed with blind trap doors following the installation completion.

The insulator casings are mounted above the openings.

The general cross-sectional stability of the body is secured by the installation of low-alloy steel cross ties of 48 m diameter in the end planes of the body.

In the design calculations the assumptions were made: 1.8 t/m^3 weight of collected dust, 60° angle of rest, 100% of the volume emergency filling capacity of the hoppers, 10 mm thickness of dust layer on the surface of the collector electrodes.

The body of the ESP should be covered with thermal insulation. The temperature drop should not be more than 30°-40°C in the ribs of the body and support beams. The thickness of the rib insulation should not be lower than for the body walls.

The body of the electrostatic precipitator should lean on the base support across the balance beams.

Gas distribution grating is analogous to "UG" ESP type.

Unification of assemblies and details of the "UGT" ESP equipment secures block supply of

a) insulator casings with corona electrode rapping mechanism and with equipment for their suspension;

b) rapping driving gear and section of hammer rapping of the collector electrodes;

c) collector electrode plates.

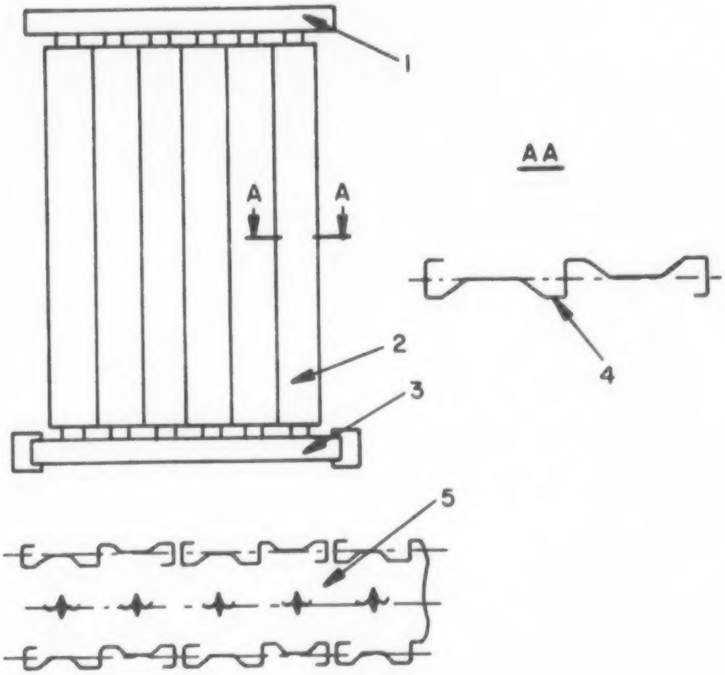

Figure 1. Collector electrode

1. Support beam
2. Rapping rail
3. Element
4. Element profile
5. Scheme of the location relationship between the elements of the corona and the collector electrodes

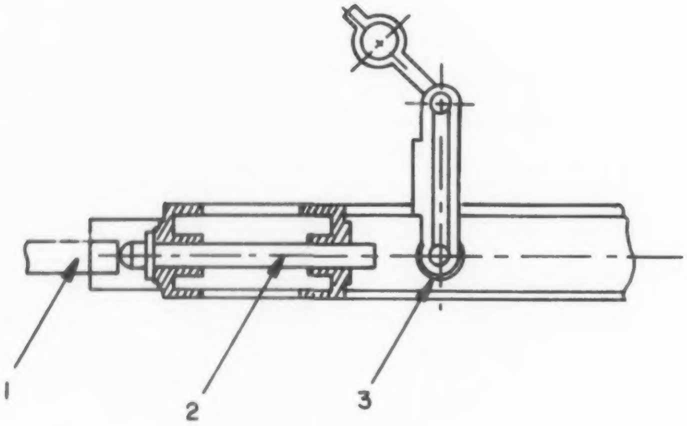

Figure 2. Rapping mechanism of the collector electrode

1. Rapping rail
2. Rod
3. Hammer

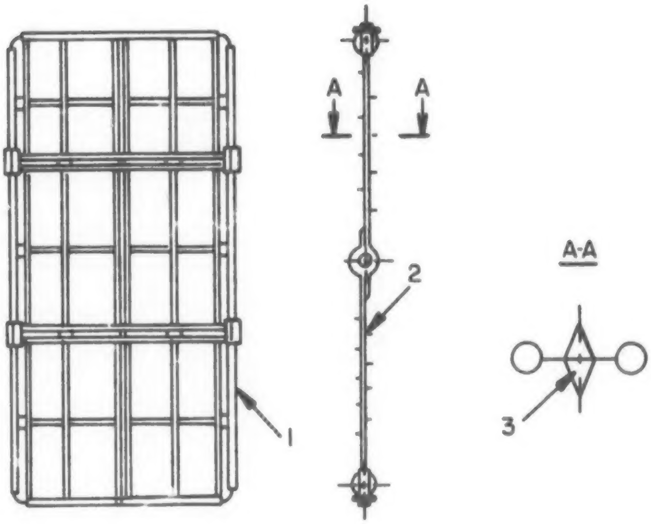

Figure 3. Corona electrode

1. Frame of the corona electrode
2. Needle element
3. Element profile

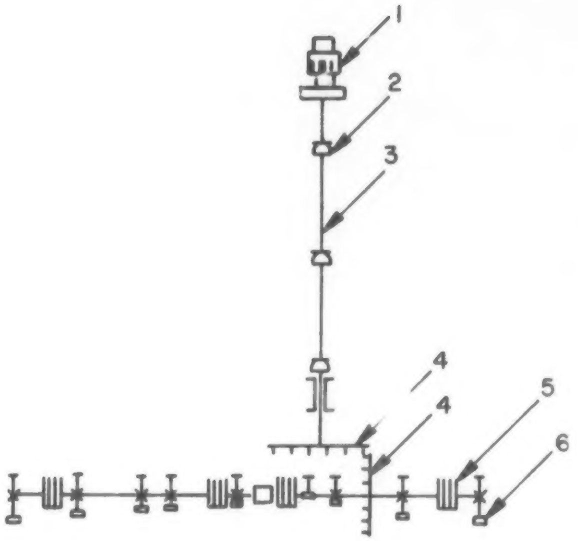

Figure 4. Kinematic scheme of corona electrode rapping

1. Vertical motor-reducer
2. Connecting joint
3. Shaft-insulator
4. Two bobbins
5. Dust bearing
6. Hammer

Paper No. 5

THEORETICAL BASIS FOR DESIGN OF MODERN HIGH-EFFICIENCY ELECTROSTATIC PRECIPITATORS

by

V. I. Levitov,
I. K. Reshidov,
and
V. M. Tkachenko

STATE RESEARCH INSTITUTE OF
INDUSTRIAL AND SANITARY GAS CLEANING

Moscow

Theoretical Basis for Design of Modern High-Efficiency Electrostatic Precipitators

Levitov V. I., Reshidov I. K., Tkachenko V. M.

Highly efficient methods of particulate removal from the stack gases are beneficial not only from the sanitary standpoint but also because in many cases valuable raw materials can be recovered.

The use of electrostatic precipitators is one of the ways to remove highly dispersive particulates efficiently. The exact level of efficiency depends on the physical and the chemical properties of the collected dusts.

The NIIOGAZ and its Semibratovsk branch conducted studies of the phenomena during the reverse corona formation in the dust layer. Based on these studies, recommendations were made to increase the efficiency of the ESP. It is obvious that in order to accomplish the above set of goals a detailed study of the electric field had to be undertaken.

The theoretical explanation of the corona discharge field is quite complicated even for the unipolar case and was found only for the comparatively simple electrode system.

At the present time, there are no serious theoretical explanations of the reverse corona formation, especially for the complex electrostatic precipitators used in the industrial installations.

The only applicable method for the study of the electrical fields at the present time is an experimental one.

The method of probe characteristics was used for the experimental study of the unipolar and bipolar corona field.

The essence of the probing measurements methodology is based on the following. Potential from the extraneous source is applied to the probe located in investigated point of outside zone of the corona field. The current is measured depending on the size of the applied potential. The influence of ion mobility on their density and field potential in the investigated point is determined by such voltage - current probe characterization.

Figure 1 shows a picture of electric fields for the electrode systems characteristic of the widely used plate electrostatic precipitators: a number of cylindrical wires (3 mm) between parallel plates and a number of needle electrodes between parallel plates. With the needle electrodes measurements were taken with voltages of 28 kv, 50 kv, 65 kv, when the specific currents were similar to the currents of smooth wires measurements were taken with voltages 50 kv, 65 kv, 80 kv respectively.

The comparison of the obtained pictures of the field shows the true difference between needle and wire electrodes in configuration as well as in the intensity size.

It is apparent that with the growth of the voltage applied to the electrodes not only the field intensity increases but also the uniformity of the field distribution longitudinally to the electrostatic precipitator. However for the needle electrodes the field is less uniform than for the cylindrical wire electrodes.

Table 1 shows the experimental values for field intensity.

Table 1

Electrode System	Y_{pr}, kV	i, mA/m	E_{EkV}, kV/cm	$E_{EkV}/\sqrt{r}$
Number of wires between parallel plates	50	0.075	1.7	6.2
	65	0.318	3.06	5.45
	80	0.672	4.4	5.4
Number of needle electrodes between parallel plates	28	0.06	1.33	5.5
	50	0.345	3.16	5.38
	65	0.66	4.28	5.3

It is apparent that, independently of the corona electrode design and the size of the applied voltage, the size of the field intensity with similar values of the individual corona current does not differ significantly and the expression $E_{EkV}/\sqrt{i}$ remains practically constant.

Figure 2 shows equipotential lines of the electric field for the industrial system of electrodes. The complex field configuration is specified by the configuration of the collector electrodes and also by their lack of symmetry. The conditional neutral line of force (that is the line of force with smallest field intensity) does not coincide with the neutral surface passing through the joints of the adjacent electrodes. The field intensity is significantly higher than for the plate collector electrodes which is the result of the increase in the specific corona current brought about by the reduction in the center distance from 300 to 275 mm.

Table 2 gives a quantitative comparison of electrical field characteristics for two different collector electrodes.

Table 2

Type of Corona Electrode	Type of Collector Electrode	У_{pr}, kV	i, mA/m	E_{EkV}, kV/cm	$E_{EkV}/\sqrt{i}$
Needle with 20 mm space between the needles	C-formation	50	0.63	3.2	4.05
		65	1.18	4.53	4.14
	broad-banded C-formation	50	0.665	3.2	3.97
		65	1.26	4.69	4.16

The comparison of the values in Table 2 shows them to be identical for all practical purposes in the field characteristics. Because of this, when the design advantages of the broad-banded collector electrodes for the uniform horizontal ESP are considered only these are manufactured.

It was also shown that current was more evenly distributed on the surface of the C-formation collector electrodes than on the plate electrodes. The chances for the reverse corona formation decreased as well.

The empirical expressions were found for the calculation of the equivalent field intensity for the different electrode systems. The expressions were found with the stipulation of $\bar{E}_{ekv}/\sqrt{r_i}$ constancy.

The optimal relation H/d (H-discharge space) was studied to secure maximum field intensity. The obtained results indicate that an increase in the expression from 0.65 - 0.85 to 1 - 1.25 would be appropriate.

The electrical field and the nature of the dust mobility under the conditions of the reverse corona were experimentally studied to decrease or eliminate the influence of the reverse corona on the level of gas cleaning with ESP.

During the first stage of the investigations the field of the concentric cylinders with dust layer on the collector electrode was studied. The level of the discharge current and the field intensity reduction in the external zone of the corona was found as it depended on the change of the collected dust layer.

At the same time, the possibility of the layer potential calculation with the volt-ampere corona characteristics was shown, as well as the relationship between the layer potential and the corona current density was found. These relationships show that the layer potential does not increase proportionally to the current density but reaches a certain critical value. Once this value is exceeded, reverse corona develops. During the studies of ash from the near-Moscow coal the critical value of the field gradient in the layer was found to be 15-20 kv/cm.

The reverse corona formed on the ash layer is non-uniform. For that reason, probing field studies with bipolar space charge were conducted on the synthetic surface (nylon fabric).

The reduction of the average intensity in the investigated portion of the field was calculated to be 30-35% in comparison to the unipolar case. It was also determined that the relationship between the space charge and mobility of the ions is a function of the field coordinate, unlikely to what is presented in the literature. The sizes of this relationship in different points of the field and the level of reduction of the limiting particle charge are expressed in the formula:

$$\xi = \frac{q_m'}{q_m} = \frac{1-\Re}{1+\Re} \qquad (3)$$

where q_m', q_m - limiting particle charge with and without reverse corona

$$\Re = \sqrt{\frac{\rho + k +}{\rho - k -}}$$

ρ - space charge density

κ - ion mobility

The values are presented in Table 3.

Table 3

U_{pr}, kV	i, mA/m	$\rho\kappa$, $K \times 10^{-9}$ V×M×sec \ r, mm	60	70	80	90	100	110	120
65	1.0	$\rho + \kappa +$	1.2	1.1	0.7	0.75	0.85	0.95	2.5
		$\rho - \kappa -$	9.9	8.2	6.7	5.4	4.3	3.5	3.0
		$\Re$	0.346	0.367	0.325	0.386	0.443	0.52	0.915
		ξ	0.485	0.465	0.51	0.44	0.386	0.316	0.045

U_{pr} - voltage applied

i - specific corona current

r - field coordinate

The data indicates that under the conditions of the reverse corona reduction of the limiting particle charge occures as the distance to the collector electrode is decreased.

The next series of the experiments were conducted for several needle corona electrodes between parallel plates. The reverse corona developed on the layer of powder forming teflon reinforced with tar epoxide.

The pictures of the electric field are shown in figure 3. The significant deformation of the field is noted, characterized by the field concentration in the central force line.

Table 4 shows equivalent field intensity showing its reduction with reverse corona.

Table 4

Electrode System	U_{pr}, kV	Without reverse corona		With reverse corona	
		i, mA/m	E_{EKV}, kV/cm	i, mA/m	E_{EKV}, kV/cm
Number of needle electrodes between parallel plates	50	0.345	3.16	0.67	2.15
	65	0.66	4.28	1.85	3.32

The experimental data shown in figure 4 is important to the understanding of collection under the conditions of the reverse corona. The figure shows data on the distribution of the space charges of different signs, which allow for the possibility of full particle overcharging.

The studies have shown that the area of exceeding the positive (reverse) space charge above the negative increases with the increase of the applied voltage. This is indicative of the inappropriateness of the voltage increase to the maximum possible level for the electrostatic precipitators, performing under the conditions of the reverse corona.

From the analysis of the results, it follows that even in the field areas where the space charge of the fundamental sign is greater than the reverse charge, the limiting charge of the particles is significantly reduced. Under the experimental conditions it does not exceed the unipolar case by 5%. which means practically lack of collection.

With the reverse corona in contrast to the unipolar case, there is no ordered particle movement in the direction of the collector electrode. This was confirmed by the study of the particle trajectories using the method of photoregistration in the light beam.

Not only were the differential characteristics of the field of the reverse corona studied but also the integral voltage current characteristics were measured (figure 5). It was also concluded that part of the voltage-current characteristics obtained with the increase of voltage and with its reduction do not coincide and the descending part runs above the ascending one.

The hysterisis character of the voltage current characteristics with current increase of the descending part is the result of the reverse corona and under the conditions of the unipolar corona is not observed. That phenomenon is the criteria for the presence of reverse corona in the ESP. This method of exposure of the reverse corona is widely used at the present time for the study of the ESP efficiency.

One of the ways with which the reverse corona can be eliminated or at least decreased in its intensity is to lower the current density of the corona, flowing through the layer of the deposited dust by evenly distributing the current on the surface of the collector electrode. However, the question of corona electrodes form which satisfies the described requirements is left unexplained. To help in the explanation, one of the plates was sectioned into squares of "mosaic" type and detailed current distribution with various corona electrodes was mapped.

The oscillographs of the current of separate "mosaic" elements show that for the needle electrodes corona without impulse occurs unlike from the electrodes with cylindrical and bar crossection. In addition, when the corona is focused on the needles, the current distribution is stationary in time and stable in space.

For the bar and the cylindrical wires the character of the current distribution is much more complicated. Unequal introduction of the space charge into the charging space caused by the movement of corona foci on the wire surface causes rather unequal current distribution on the plate surface.

Table 5 shows maximum current sizes in the separate "mosaic" elements for different corona electrodes.

It is apparent from the table that for equal specific corona currents the density of the current and the coefficients of non-uniformity for the needle electrodes are 5 to 7 times smaller than for the wires of the cylindrical and bar crossection. Even with equal voltage when the specific current of the needle electrodes significantly exceeds current of the wires density of the current is lowered more than two times. It is also apparent that the decrease in spacing between the needles aids to a more equal current distribution.

It is of advantage, therefore, to use needle electrodes with small spacings (20-40 mm) in electrostatic precipitators collecting weekly conductive particulates. Figure 6 presents data which confirms the appropriateness of the use of small spaces between the electrode needles. With the needle electrodes an area of the unipolar charge existed on the layer of high-resistivity ash of ekibastuzskiy coal at the time when for the bar wire reverse corona occurred with the voltage practically equal to the initial voltage of the primary corona.

Besides the use of the small spacings between the needles proper regulation of the ESP electric system can increase the level of high resistivity dust removal from gases.

The optimal voltage for the electrodes in a certain field of a multi-field ESP can be determined with the known relationship between the dust concentration in the gas stream and the corona discharge current of the next filter field. Naturally, with higher dust concentration in the gas stream the discharge current will be lower in the second ESP field than in the first one. under the conditions with which appearance and existence of the reverse corona is possible can be made using the known relationship between the corona discharge current of the next (second) filler field and the dust concentration in the gas stream. Naturally, with higher dust concentration in the gas stream the discharge current will be lower in the second ESP field. On the other hand, dust concentration flowing into the second field is determined by the collection efficiency of the first one which depends on the electrical system of that field. In this way a relationship exists between the voltage or the current in the first field and the size of the same characteristics in the second field, which is determined by the dust concentration in the gas stream flowing into that field. In other words, the second field can serve as an indicator characterizing efficiency of the first field. It follows then that the characteristics of the electrical system of the second field (voltage or current) can be used as the initial parameters for the regulation of the electrical system performance in the preceding field.

The analysis of the external characteristics of the serial loading aggregate of AFAS type together with the volt-ampere characteristics of the separate fields in the industrial scale ESP show that the relationship between the voltage of the second field and the current of the first one is U-shaped (figure 7). The minimum of this U curve corresponds to the highest level of gas cleaning in the first field with the pre-determined conditions. The minimum in U-curve determines the optimal performance of the first field electrical system. In this way the problem for the regulation is brought down to finding the extreme point in the above relationship.

Table 5

Type of corona electrode		U, kV	i, mA/m	j max, mA/m^2	$k = \frac{j\ max}{j\ cp}$
Conductor	Cylindrical 3 mm	50	0.052	2.5	17.3
		60	0.296	8.0	9.75
		80	0.663	13.0	7.05
	Bar 4 x 4	50	0.066	3.3	20.7
		65	0.31	9.6	11.2
		80	0.673	15.4	8.24
Needle Electrodes with spacings h	h = 40 mm	26.5	0.052	0.42	2.00
		50	0.392	1.86	1.71
		65	0.74	3.35	1.63
		80	1.17	5.2	1.6
	h = 80 mm	30.72	0.052	0.48	3.32
		50	0.301	2.05	2.45
		65	0.592	3.78	2.3
		80	0.96	5.75	2.05
	h = 120 mm	29.8	0.053	0.52	3.6
		50	0.261	2.35	3.24
		65	0.5	3.96	2.85
		80	0.81	5.65	2.52

One of the possible schemes, which solves the problem of regulation works in the following way: signal proportional to the voltage or the current of the proceeding field is given from the indicator to the extreme regulator. The regulator through the power amplifier with the help of the magnetic amplifier (or other control instrument) supports the electrical system of the field under consideration on the level corresponding to the minimum voltage or maximum current on the electrodes of the next field.

The described system is patented and used in "Aktyubrentgen" plant as one of the variations for the regulation of voltage for the serial supply unit of AUF type.

The efficiency of the practical recommendations based on the conducted studies was checked for ESPs in various industries.

The studies were conducted in those industrial installations where the efficient dust removal with ESPs was complicated by low conductivity of the dust. Some results of these studies are shown in table 6.

In the plant Novorostsement for the collection of high-resistivity dust from flue gases electrostatic precipitator is used. The plant uses wet method of cement production with sea water for slurry preparation. The electrostatic precipitators were redesigned to change the bar conductors to the needle electrodes with 80mm spacings and the channeled collector electrodes were changed to C-formation wide band electrodes with reinforced shakers. The level of gas cleaning increased from 86% to 98.4% and assured meeting of not only the sanitary norms but also allowed for the recovery of valuable raw material.

In the Slantsevskiy cement plant with collection of clincker particulates from the dry methods of cement preparation the level of cleaning was raised from 92% to 95.6% only by the use of the developed method for voltage regulation.

Table 6

No. Plp.	Parameters	Novorostsemkombinat Before redesign	Novorostsemkombinat After redesign	Slantsevyi cem. plant Before redesign	Slantsevyi cem. plant After redesign
1.	Aggregate	AFAP-80-225	ARS-250	AFAS-80-250	AFAS-80-250
2.	Collector Electrodes	pocket	C-formation	C-formation	C-formation
3.	Corona Electrodes	bar	needle	needle	needle
4.	Rapping	striking	hammer	hammer	hammer
5.	Gas T °C	208	210	258-305	296-305
6.	Gas velocity m/Sec.	1.2	1.28	0.9	0.99
7.	Particulates concentration g/nm^3				
	a) before ESP	5.3	5.1	20.6	24.4
	b) after ESP	0.54	0.05	1.56	1.03
8.	Time in the Electrical Field Sec.	81	7.6	10.0	9.76

Table 6 Cont'd.

No. Plp.	Parameters	Novorostsemkombinat		Slantsevyi cem. plant	
		Before redesign	After redesign	Before redesign	After redesign
9.	Average electrical indicators				
	voltage kV	50.3-51.2	52.0-55.5	19.2-35.2	23.3-37.0
	current mA/m	0.02-0.11	0.17-0.19	0.056-0.12	0.03-0.067
10.	Effective drift velocity cm/sec	3.2	6.7	3.18	4.04
11.	Collection efficiency %	86	98.4	91.88	95.8

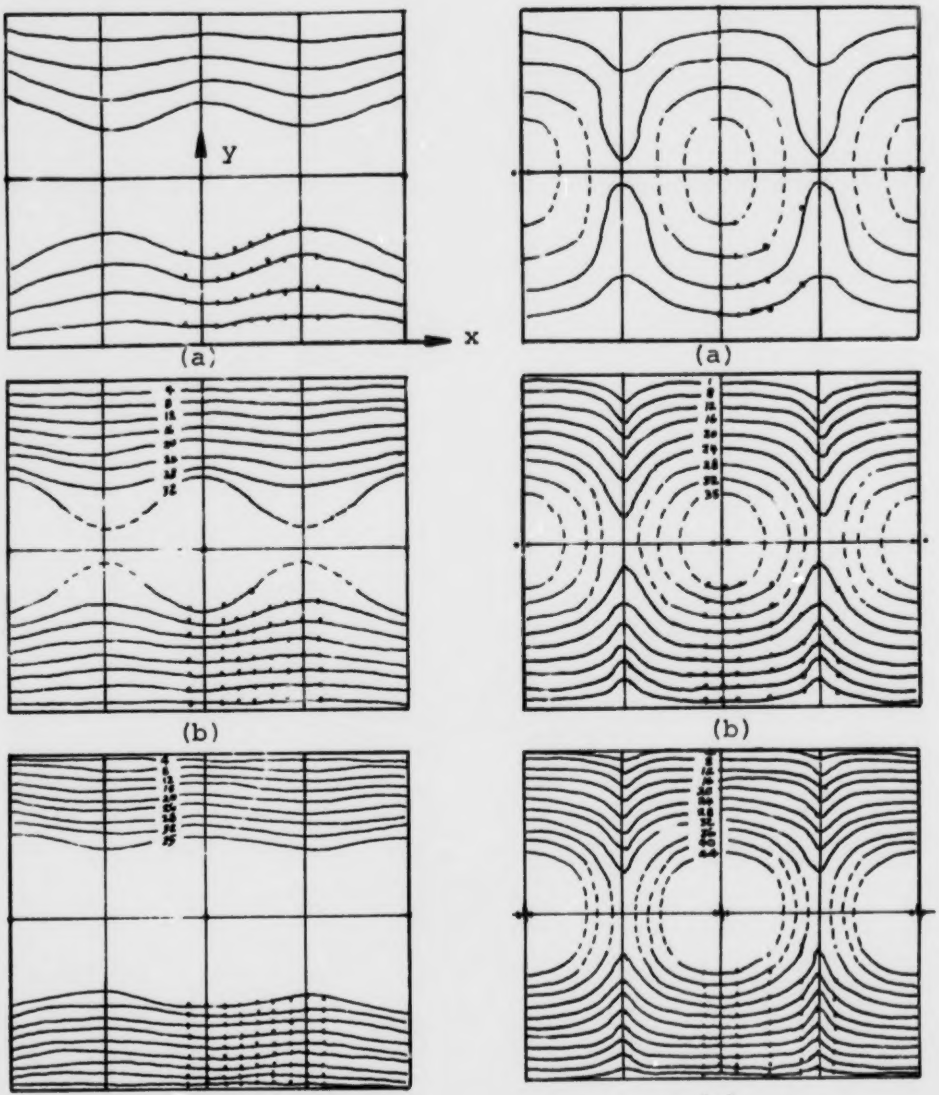

(a) (a)

(b) (b)

(c) (c)

I II

Figure 1. Equipotential surfaces of the electrical field.

4, 8, 12... - field potentials (kV)

I. Series of Conductors between plates
a) Jpr = 50 kV i = 0.075 mA/m
b) Jpr = 65 kV i = 0.318 mA/m
c) Jpr = 80 kV i = 0.672 mA/m

II. Series of needle electrodes between plates
a) Jpr = 28 kV i = 0.06 mA/m
b) Jpr = 50 kV i = 0.345 mA/m
c) Jpr = 65 kV i = 0.66 mA/m

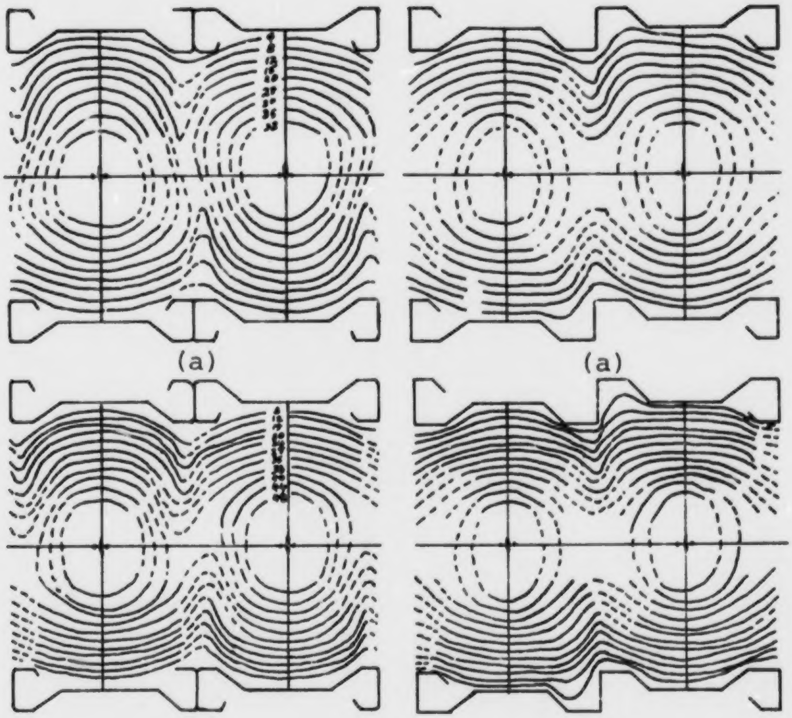

(a) (a)

(b) (b)

I II

Figure 2. Equipotential surfaces of the electrical field

4, 8, 12... - field potentials (kV)
I. Industrial electrode system
a) J pr = 50 kV i = 0.63 mA/m
b) J pr = 65 kV i = 1.18 mA/m
II. Wide band collector electrodes
a) J pr = 50 kV i = 0.665 mA/m
b) J pr = 65 kV i = 1.26 mA/m

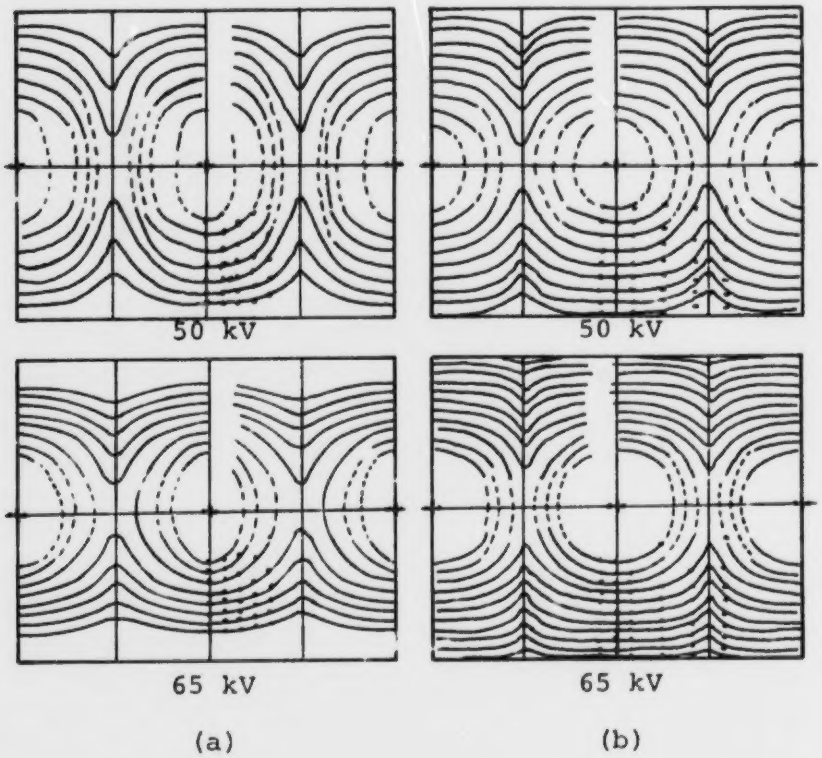

Figure 3. Equipotential surfaces of the electrical field

Series of needle electrodes between plates
a) $\mathcal{U}_{pr}$ = 50 kV   i = 0.67 mA/m with presence
$\mathcal{U}_{pr}$ = 65 kV   i = 1.85 mA/m of reverse corona
b) $\mathcal{U}_{pr}$ = 50 kV   i = 0.34 mA/m without reverse
$\mathcal{U}_{pr}$ = 65 kV   i = 0.66 mA/m corona

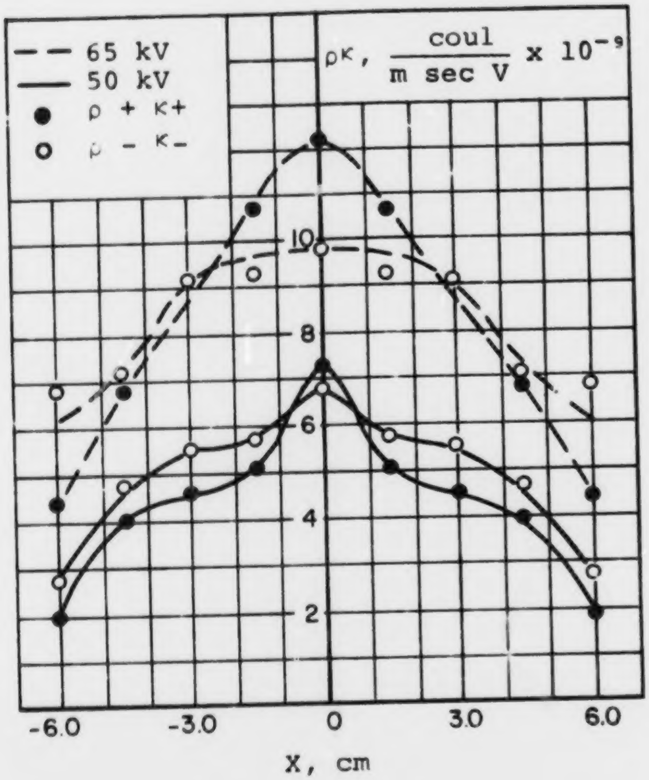

Figure 4. Distribution of ρκ 35 mm from the surface with reverse corona.

Series of needle electrodes between plates

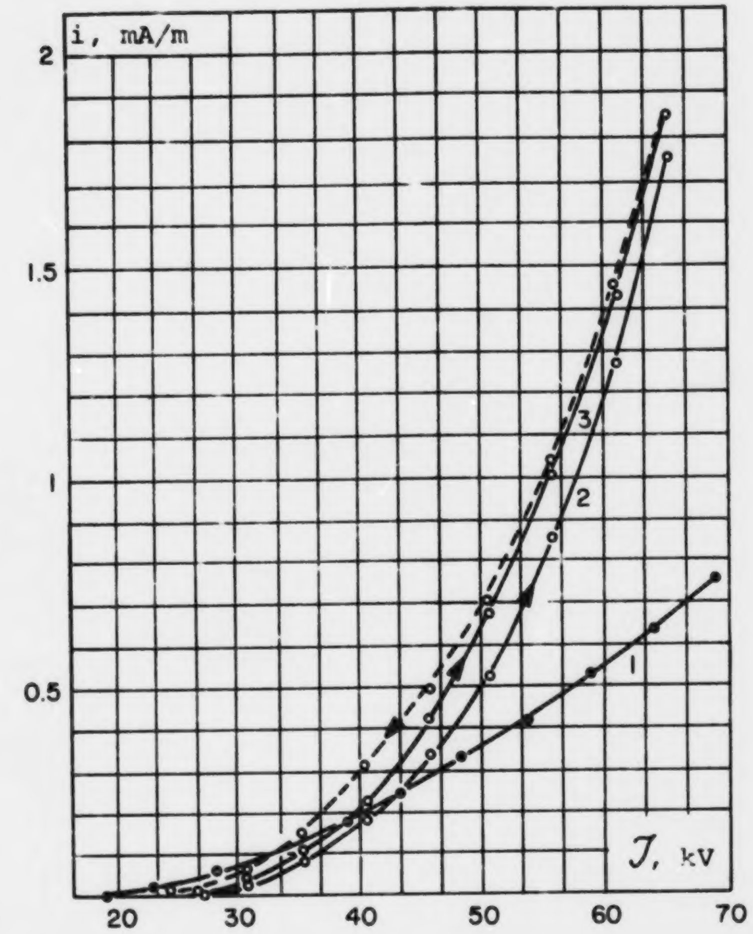

Figure 5. Volt-ampere characteristics

Series of needle electrodes between plates
1. with unipolar corona
2. with reverse corona
(first characterization)
3. with reverse corona (following the reverse corona point formation on the layer)

——— ascending
----- descending

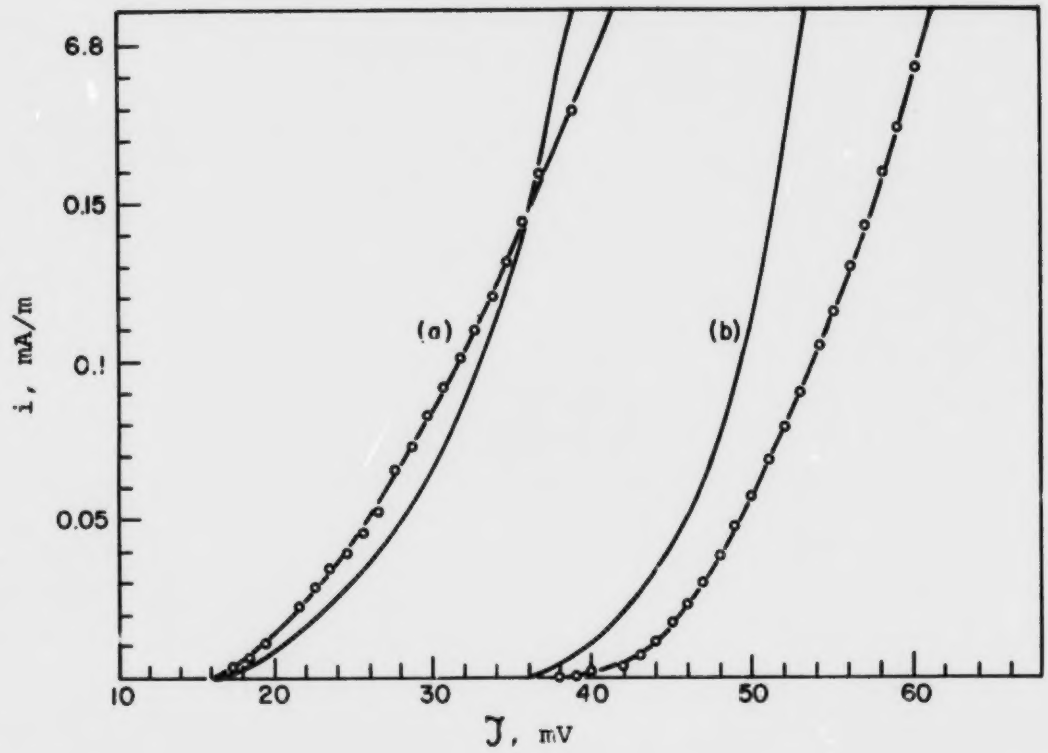

Figure 6. Volt-ampere characteristics of the corona in the wire plate system of electrodes with ash layer present on the surface (______) and with no ash layer (o———o)

a) needle electrode
b) bar wire

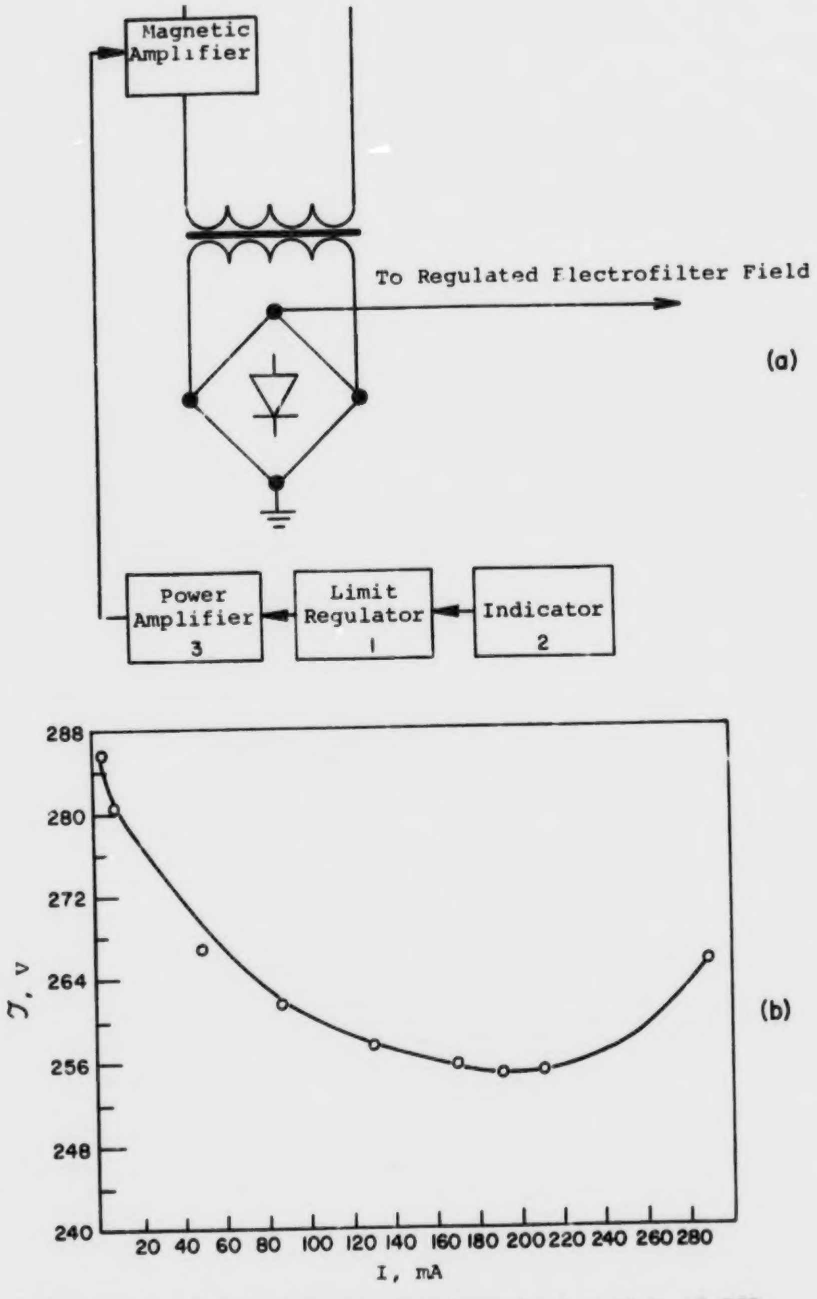
Magnetic Amplifier
To Regulated Electrofilter Field
(a)
Power Amplifier 3
Limit Regulator 1
Indicator 2
288
280
272
264
256
248
240
𝒯, v
20 40 60 80 100 120 140 160 180 200 220 240 260 280
I, mA
(b)

Figure 7. Regulation of the electrical system of ESP

a) Structural scheme for voltage regulation in the next field of the ESP
b) Relationship between the voltage of the 2nd field of ESP and the corona current of the 1st field

$\mathcal{J}_{pr}$ = constant

Paper No. 6

REMOVAL OF ASH FROM FLUE GASES OF POWER STATIONS WITH ELECTROSTATIC PRECIPITATORS

by

I. A. Kizim,
I. K. Reshidov,
and
V. M. Tkachenko

STATE RESEARCH INSTITUTE OF
INDUSTRIAL AND SANITARY GAS CLEANING

Moscow

Removal of Ash from Flue Gases of Power Stations with Electrostatic Precipitators

Kizim I. A., Reshidov I. K., Tkachenko V. M.

Today's power stations contain 300 MW units and larger and use multi-field electrostatic precipitators with 12 m. high electrodes. To assure the necessary level of gas cleaning, gas velocity in the apparatus is somewhere around 1.5 m/sec.

The leading examples of the electrostatic precipitators with 12 m high electrodes are located in the 300 MW Ladyzhinskiy power station which uses GSSh fuel. These are three field installations with 177 m^2 cross-section with the length of each field equal to 4 m. (Fig. 1)

Following the repair, modernization and finishing of the separate units of the installation interdepartmental studies of these electrostatic precipitators were conducted.

In spite of the disparity between the actual parameters of the dust laden gas and the design (higher fuel ash content) electrostatic precipitators EG7-3-177 assure 98.0-98.7% efficiency of dust removal. The dust emissions do not exceed 0.5 g/nm^3. The ESPs were recommended for serial production.

The studies conducted in NIIOGAZ are used not only in construction of modern electrostatic precipitators but also for improvement of older ESPs used in various branches of industry.

The Cherepetskiy (150 MW unit) power station uses two-field electrostatic precipitators of DGP-55-2 type. The study of these electrostatic precipitators conducted by Yuzh ORGES and Semibratovsk branch of NIIOGAZ have shown that with gas velocity about 2 m/sec and inlet dust concentration ranging from

35 to 50 g/nm^3 the efficiency was 80%.

The most important reasons for the unsatisfactory performance of the EP were: the occurrence of the reverse corona related to the high specific resistivity of the ash from the near-Moscow coal, (10^{12} ohm cm) highly adhesive ash, and inefficiency of the rapping mechanism.

After SF NIIOGAZ recommendation the DGP-55-2 electrostatic precipitator was redesigned to the PGDS type with C-formation collector electrodes, belt-needle corona electrodes with 80 mm spacings between the needles, needle length 12 mm, hammer rapping. The ARS-400 units were substituted for the AFA-90-200 units with mechanical rectifiers.

The redesign allowed for an increase of efficiency to 97.8% and a ten fold decrease of dust emissions. The reverse corona did not form because of the use of the needle electrodes and more intense rapping of electrodes. (Fig. 2, Table 1).

The Cherepetsk power station, 300 MW unit uses electrostatic precipitators, DGPP-55-3, with pocket collector and wire corona electrodes with bar cross-section. The study of the system showed that with 2m/sec. gas velocity level of gas cleaning ranged from 87.8 to 92.1% and dust emissions into the atmosphere were three times higher than in the original design specifications.

One of the main reasons for the low efficiency was the low specific current load related to the use of wire corona electrodes. To eliminate occlusion of the corona, wire electrodes of bar corss-section were substituted with belt-needle electrodes with 80 mm space between the needles. The use of such modified electrostatic precipitators showed that the level of cleaning

BASIC PARAMETERS OF REDESIGNED ESPs TABLE 1

Parameters	Units	Cherepetsk before redesign	GRES after red.	Troyitsk before	GRES after	Pribaltiysk before	GRES after
1. Type used		AFA-90-200	ARS-400	AFAS-80-250	ARS-400	AFAS-80-250	ARS-400
2. Collector electrodes		pocket	C-formation	wire	C-formation	pocket	pocket
3. Corona electrodes		bar	needle	bar	needle	bar	needle
4. Rapping		strike	hammer	strike	hammer	strike	hammer
5. Gas T °C	°C	150	153	150	143	153	150
6. Gas velocity in inactive part of ESP	m/sec.	1.94	1.72	2.45	2.47	1.53	1.51
7. Dust concentration							
a. before ESP	g/nm^3	42	43	48.4	41.5	21.3	19.3
b. after ESP	g/nm^3	14.6	0.8	6.6	1.26	0.92	0.53
8. Time in the ESP active zone	sec.	3.85	3.8	3.06	4.05	6.47	6.56
9. Aver. electrical indicators							
a. first field of ESP	KV	45.2	70.1	34.0	35.7	46.5	36.1
	mA/m	0.065	0.082	0.01	0.07	0.03	0.14
b. second field of ESP	KV	40.1	68.8	35.4	35.3	46.8	37.6
	mA/m	0.07	0.08	0.03	0.06	0.05	0.13
c. third field of ESP	KV	=	=	32.8	36.0	44.8	40.2
	mA/m	=	=	0.04	0.08	0.06	0.20
d. fourth field of ESP	KV	=	=	=	36.7	=	=
	mA/m	=	=	=	0.06		
10. Effective drift velocity	cm/sec	4.9	12.5	7.6	10.6	7.32	8.32
11. Collection efficiency	%	68	97.8	87.5	96.8	95-62	97.21

increased to 95.5% (design value 95%).

Installation of the needle electrodes allowed for an increase in the specific corona current and allowed for a three fold increase in the corona discharge output.

In the Troyitsk power station, 300 MW unit, which uses ekibastuzsk coal IGO-3-38 PBTs electrostatic precipitators were installed. The level of gas cleaning in these ESPs, as was shown by S[illegible] NIIOGAZ, VTI and Uo ORGRES, on the average reached 87.5% when inlet dust concentration was 50g/nm^3 and gas velocity 2.5-2.7 m/sec.

The unsatisfactory performance is due to an increase of gas velocity over the design value, intensive reverse corona, inefficient rapping of the electrodes, and the low efficiency of the preliminary direct flow battery cyclones.

It is a known fact that with the high resistivity dust, the specific resistivity (UES) $\rho_v > 10^{10}$ ohmcm, reverse corona can occur lowering the level of dust cleaning. When the current passes through the electrode covered by the dust layer with high UES, voltage drops. The drop size depends on the size of UES, current density j, and layer thickness B:

$$U_{layer} = \rho_v j B$$

$$E_{layer} = \rho_v j$$

There are two ways to decrease the critical intensity of the layer and to decrease the intensity of the reverse corona. These are to decrease ρ_v or j.

The decrease of ρ_v is accomplished usually by gas conditioning with water or with chemical reagents. To decrease the corona current density on the unit of the surface layer needle corona electrodes with small spacings can be used. Such design allows for a decrease in the coefficient of the current non-uniformity (k) equal to the relationship between the maximum current and the average value. Table 2 shows the experimental data (SF NIIOGAZ studies) for different types of the corona current.

Table 2

Type of Corona Electrode	Voltage	Corona Current		Coefficient of Current non-uniformity K
	KV	m^A/m	m^A/m^2	
1. Wire of bar cross-section 4 x $4mm^2$	50.0	0.052	2.5	17.3
	65.0	0.296	5.6	9.75
2. Belt-needle electrode with needle spacing 40mm	26.5	0.052	0.42	2.0
	50.0	0.392	1.86	1.71
	65.0	0.74	3.35	1.63
3. Belt-needle electrode with needle spacing 80mm	30.7	0.052	0.48	3.32
	50.0	0.301	2.05	2.45
	65.0	0.592	3.78	2.30

With the equal specific corona currents, maximum current densities on the surface layer of the collection electrode and the coefficients of current non-uniformity for the needle electrodes are six times lower than for the bar cross-section wires. Even with equal voltage, when the specific corona current of the needle electrodes exceeds corona current in the wires significantly, the current density remains lower by a factor of 2. In addition, the decrease in the space between the needles promotes more uniform current distribution (Fig. 3)

However, under the conditions of the reverse corona maximum intensification of the corona discharge is not always appropriate. In some cases, therefore, it is necessary to limit the average current of the needle electrodes. The experiments showed that this can be accomplished by reduction of the needle length or their parallel orientation to the surface of the collector electrodes.

Probe measurements showed that parallel location of the belt-needle and the belt-tooth electrodes to the collector electrodes surface significantly equalizes the field in the interelectrode space and lowers the corona current by 1.4 to 1.6 times (Fig. 4) in comparison to the normal design of these electrodes. In addition, the maximum current density is reduced almost by a factor of two, which appears to be useful for the reduction of the reverse corona.

Based on the results of these studies one of the electrostatic precipitators, PGDZ-38 PBTs, in Troiytsk power station, 300 MW unit was redesigned. One of the main reasons for a decrease in the efficiency of ash removal was the formation of the reverse corona. The reverse corona formation resulted from the high-resistivity of ekibastuzskiy coal ash related to low dampness and low sulfur concentration in the flue gases. ($Sp < 1\%$) In redesign the bar wires were changed to belt-needle electrodes with 80 mm spacings. The wire collector electrodes were changed to C-formation wide-band shaped electrodes. The electrode rapping was intensified. Also, the preliminary cyclon battery was dismounted and in its place an additional electrostatic precipitator field was installed.

To equalize the corona currents in the ESP fields, needle electrodes with decreased needle length (6mm instead of 12 nm) were used in the last two fields.

The level of gas cleaning increased on the average from 87.5 to 96.8% and the outlet dust concentration decreased more than five fold.

Because of the supression of the reverse corona in the first two ESP fields and the reduction of its intensity in the subsequent fields the effective drift velocity of the dust particles to the collector electrode increased by 30% and reached 10 cm/sec. with gas velocity equal to 2.47 m/sec.

Because the minimum coefficient of non-uniformity for the current in the needle electrodes occurs when the space between the needles is 40 mm such electrodes were installed in the place of the electrodes with 80 mm spacing in the experimental ESP with 12 m high electrodes. The ESP was installed parallel to the functioning PGDZ-38 PBTs electrostatic precipitators of unit No. 7, 300 MW of Troiytsk power station. The experimental ESP is a four field apparatus with the functional cross-section equal to $60m^2$ and the length of each field equal to 2.5 m. The C-formation collector shaped electrodes and belt-needle corona electrodes were used in the ESP.

To decrease the average current in the last two ESP fields with the most intensive reverse corona the belt-needle elements were turned 90°.

The modernization of the experimental ESP corona system allowed a 30% reduction in the dust concentration and allowed for an increase in the level of gas cleaning to 96.5%. These data were obtained with continuous rapping of the electrodes.

The analogous results were obtained with the electrostatic precipitators of Lurgi and Luk firms where electrodes were 12m high. These ESPs were installed at Reftinsk and Yermakovsk power stations (Table 3). Because of the extremely high resistivity of the ekibastuzsk coal the reverse corona cannot be completely supressed and further increase in the efficiency can be accomplished with gas conditioning.

Table 3

No. P/P	Parameters	Measurement Results Lurgi ESP		Luk ESP	
1.	Boiler capacity t/hr	475	482	440	456
2.	Fuel parameters:				
	A^P,o/o	40.3	40.0	38.2	38.2
	W^P,o/o	5.9	6.5	5.2	5.2
	Q_n^P, kcal/Kg	3940	3964	4120	4120
3.	Gas T before ESP, °C	135	135	145	147
4.	Dust concentration before ESP, g/m^3	56.0	55.0	41.3	40.9
5.	Same after ESP, g/m^3	2.70	1.94	2.82	0.99
6.	Level of gas clearing,o/o	95	96.5	92.7	97.5
7.	Gas velocity in ESP, m/sec	1.18	1.19	1.17	1.19
8.	Effective drift velocity,cm/sec.	3.7	4.2	2.7	3.9
9.	Time in the active ESP zone, sec.	11.5	11.4	14.4	14.1
10.	Electrical indicators:				
	First field Voltage,k^V	32.9	33.0	40.0	40.8
	First field Corona current,mA/m	0.18	0.18	0.15	0.16
	Second field Voltage,kV	31.2	31.8	39.0	38.6
	Second field Corona current mA/m	0.18	0.18	0.14	0.12
	Third field Voltage,kV	29.3	30.6	37.0	35.7
	Third field Corona field,mA/m	0.18	0.18	0.16	0.18
	Fourth field Voltage,kV	-	-	36.0	34.7
	Fourth field corona field mA/m	-	-	0.19	0.19
11.	Rapping System	cont.	periodical	cont.	periodical

The Pribaltiyskaya power station uses shale with high ash content (45 to 50%) as the fuel. The necessity existed to use two step ash removal scheme made up of cyclons and electrostatic precipitators. Even though 30% of the ash is removed in the boiler, the dust concentration before the cyclon reaches 60 g/nm^3.

The composition and the properties of the shale ash make it a valuable raw material. The efficient dust collection is therefore necessary not only for air pollution control, proper stack functioning but also for obtaining material which is used as an additive in the cement production and in the agriculture for the alkalization of the acid soils.

The installed DGPN electrostatic precipitators did not assure the necessary level of gas cleaning. Based on the suggestion from the NIIOGAZ VTI and Leningrad branch of Giprogazoochistka the ESPs were redesigned. The bar cross-section corona electrodes were changed to needle electrodes 12m high and with spacing of 80 mm. The automatized aggregates of ARS supply were introduced and also the periodic system of the electrode rapping. These measures allowed to reduce the final dust concentration from 2 to 0.3-0.4 g/nm^3, which for the Pribaltiyskaya power station is below the sanitary norms.

By only introducing the needle corona electrodes in place of the bar electrodes, all other conditions remaining unchanged (Table 1) the emission of the ash was decreased by a factor of two.

POWER STATION FUEL PARAMETERS TABLE 4

No. P/P	Power Station	Fuel Type	ash content A^P,o/o	FULL PARAMETERS dampers W^P o/o	FULL PARAMETERS Q_h^P $\frac{\text{kcal}}{\text{kg}}$	S^P,o/o	C^{T}_{y}n,o/o
1.	Ladyzhinskiy 300 MW unit	mixture of fuels GSSH, GR, GO, DSSH	30	12.3	4300	3.5	1.7
2.	Cherepeyiskiy, 150 MW unit	near-Moscow coal	23.5	30.0	2500	2.9	-
3.	Cherepeyiskiy, 300 MW unit	Donetsk, Ash	21.0	6.0	5780	-	10-22
4.	Iroyitskiy, 300 MW unit	Ekibastuzskiy coal, SS	39.0	5-7	4250	0.8	3.0
5.	Rejtinskiy 300 MW unit	"	40.3	6.0	3950	0.8	3-10
6.	Pribaltiyskiy 200 MW unit	Estonia Shale	50.0	15.0	2400	-	-
7.	Yermakovskiy 300 MW unit	Ekibastuzskiy coal, SS	38.2	5.2	4120	0.8	3.6

RESULTS OF THE EXPERIMENTAL NH_3 CONDITIONING AT INLET TO THE EXPERIMENTAL ESP OF IROYITSK POWER STATION

			Results	
No. P/P	ESP Parameters		Without Conditioning	With Conditioning
1.	Gas T at inlet to ESP, °C		156	156
2.	Same at outlet from ESP, °C		1.47	1.49
3.	Gas velocity in ESP, m/sec.		1.5	1.51
4.	Gas quantity at inlet to ESP, $\frac{10^3\ m^3}{hr}$		324	326
5.	NH_3 used, m.o.d.		-	25.0
6.	Dust concentration at inlet to ESP, g/nm^3		49.9	47.7
7.	Same at the outlet from ESP g/nm^3		5.45	0.757
8.	Level of gas cleaning		88.6	98.3
9.	Effective drift velocity, cm/sec.		4.06	7.62
10.	Electrical indicators			
	a) first field	kV	31.6	32.0
		mA	349	226
	b) second field	kV	25.2	34.4
		mA	430	295
	c) third field	kV	21.0	32.0
		mA	153	176
	d) fourth field	kV	21.0	31.5
		mA	229	319
11.	Specific ash resistivity			
	ohm cm		0.8×10^{13}	0.6×10^{10}

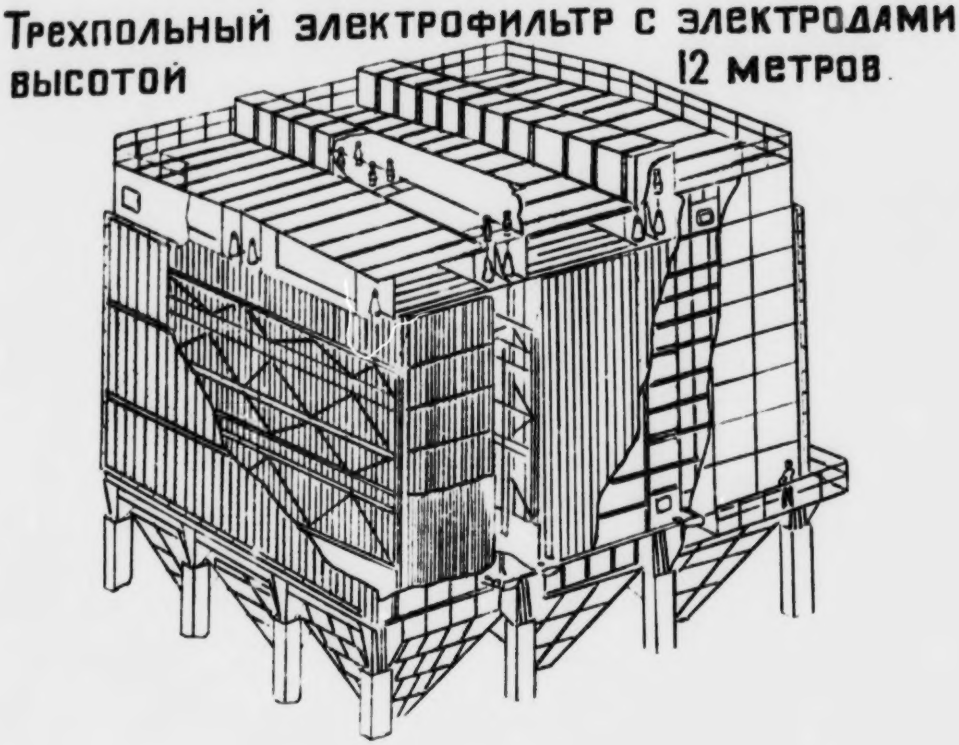
Трехпольный электрофильтр с электродами
высотой 12 метров

Figure 1. Three-field electrostatic precipitator with 12m high electrodes.

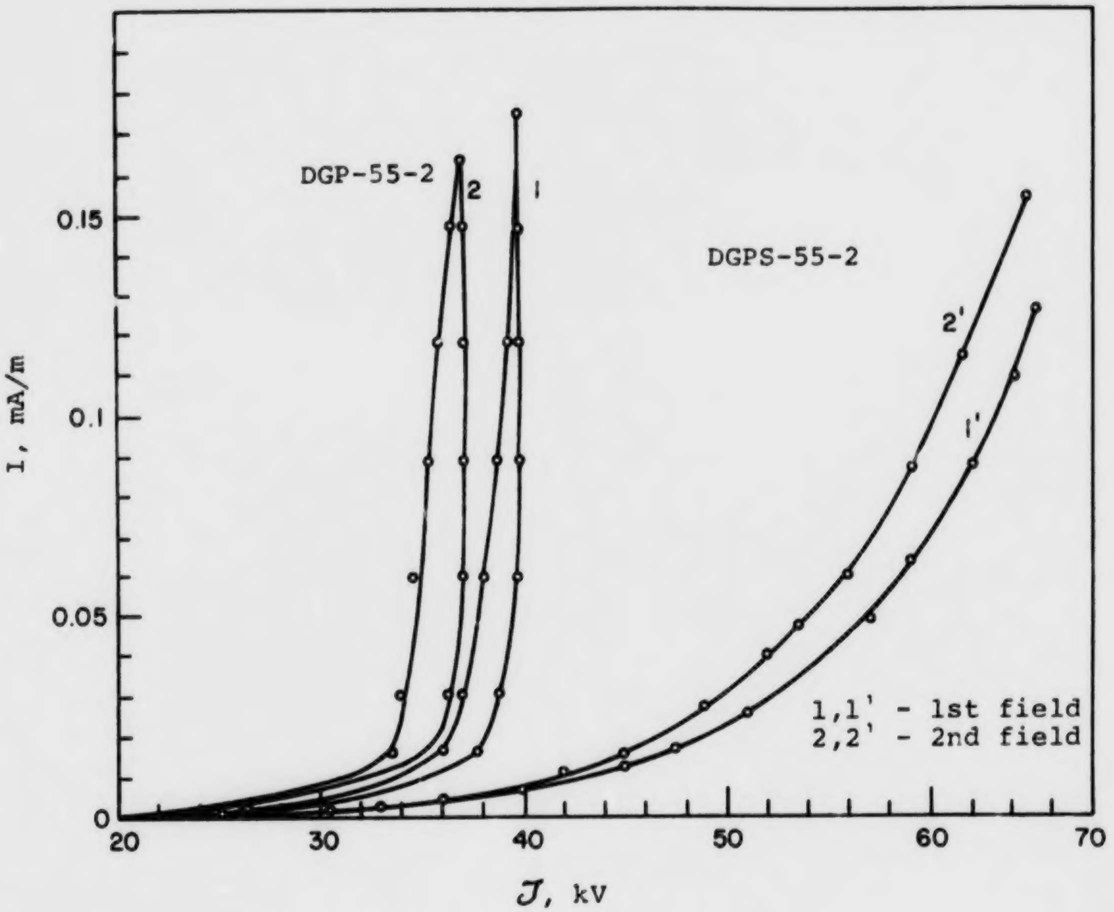

Figure 2. Voltage-current characteristics. Electrostatic precipitators of Cherepetsk power station.

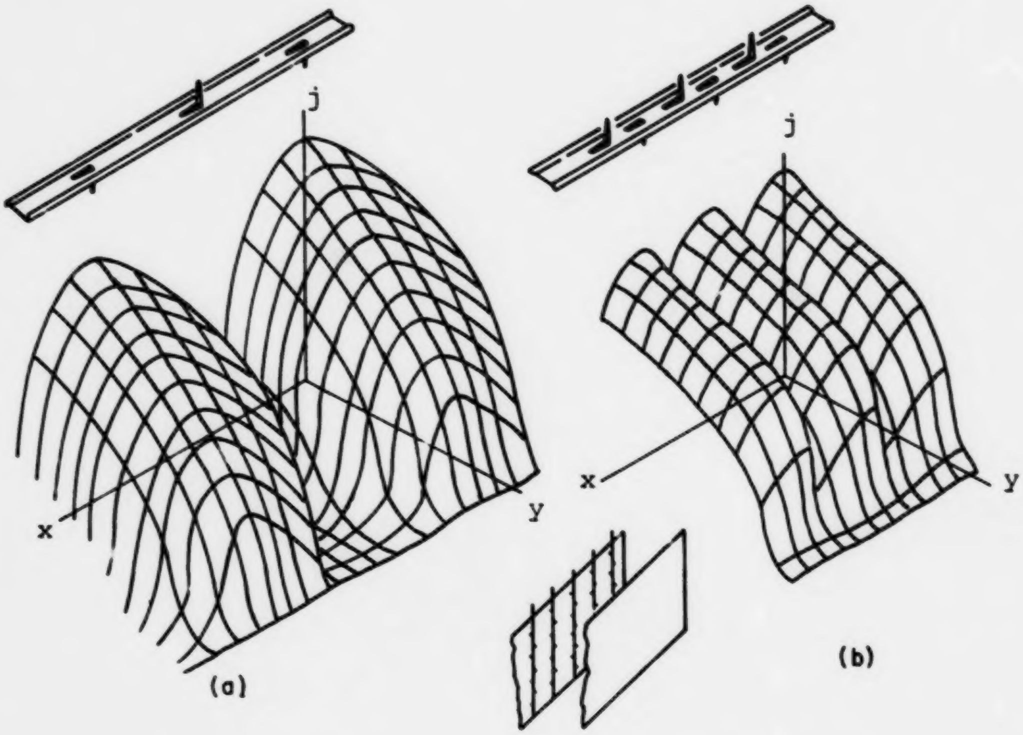

Figure 3. Current distribution on the surface of non-corona electrode.

Corona electrodes - needle with spacing:

a) h = 120 mm
b) h = 40 mm

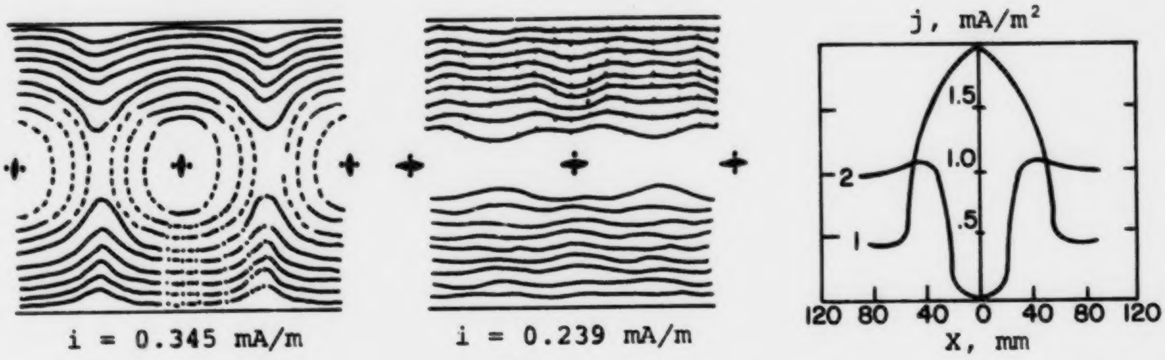

i = 0.345 mA/m

$\mathcal{J}_{pr} = 50$ kV

i = 0.239 mA/m

$\mathcal{J}_{pr} = 50$ kV

1 - without elements turned

2 - turned 90°

Figure 4. Distribution of the electric field and current density.

Preceding page blank

Paper No. 7

THEORETICAL AND PRACTICAL ASPECTS OF FINE PARTICLE COLLECTION BY ELECTROSTATIC PRECIPITATORS

by

Grady B. Nichols

SOUTHERN RESEARCH INSTITUTE

Birmingham, Alabama

ABSTRACT

This paper reviews the theory pertinent to the electrostatic collection of particles in effluent gas streams with emphasis on those particles smaller than 2 μm diameter. Measurements verifying the theoretical relationships are included with a short discussion of the measurement techniques. Some of the basic limitations on electrostatic precipitator performance are also discussed. The data reported are for the emissions from coal-fired electrical power generation boilers.

THEORETICAL AND PRACTICAL ASPECTS OF FINE PARTICLE COLLECTION BY ELECTROSTATIC PRECIPITATORS

Introduction

The need to collect the fine size fraction (2 μm or smaller) of the particulate emissions from industrial processes has been emphasized by the National Academy of Engineering (United States) in a recent report.[1] This emphasis is caused by the consensus of opinion that particle sizes smaller than about 2 μm have a greater impact on visibility, health effects, and water droplet nucleation than larger particles even though the total mass represented by the larger particles is greater; in addition, they have longer retention times in the atmosphere. These factors point to the need for effectively controlling the emissions to the atmosphere of particles in the smaller size range.

Electrostatic Precipitation Theory Review

The electrostatic precipitator is one of the conventional particulate control devices that shows promise to effectively control the emissions of the particles in this critical range. The collection mechanism is dependent upon the electrical force that results from the action of an electric field on an electrically charged particle. This force acts to remove the particulate matter from the effluent gas stream. The motion of a charged particle is governed by the dynamics of the force system acting on the particle. The forces that combine to govern this motion are:

1. electrostatic
2. viscous drag
3. gravitational
4. inertia

A free body diagram for the force system is shown in Figure 1. In commercial electrostatic precipitators, the gravitational and inertial forces are negligible in comparison to the electrostatic and viscous ones. Thus, the motion of the particles is governed by these two remaining forces. The electrical force is related to the magnitude of the electrical charge and field ($F = qE$*) while the viscous drag force is related to the velocity, dimensions of the particle, and the viscosity of the gas medium ($F = 6\pi a\mu w$). These two forces will act in opposition to each other. The resultant motion defined by the application of these two forces is a particle moving at a "terminal" velocity where the viscous drag force balances the applied electrical forces. This velocity is termed the migration velocity of the particle, and is described mathematically as $w = qE/6\pi a\mu$.

Both the electrical charge on the dust particle and the viscous drag force from the gas stream are related to the particle size. The electrical charging of particles has been the subject of considerable research; this research is continuing today. Existing electrostatic theory describes particle charging in terms of electrical charge driven by an electric field (field charging) as well as those driven by the thermal motion of the molecules in the gas stream (diffusion charging). Field charging is thought to be negligible for particles smaller than perhaps 0.1 μm while diffusion charging is insignificant for particles

---

* See list of symbols.

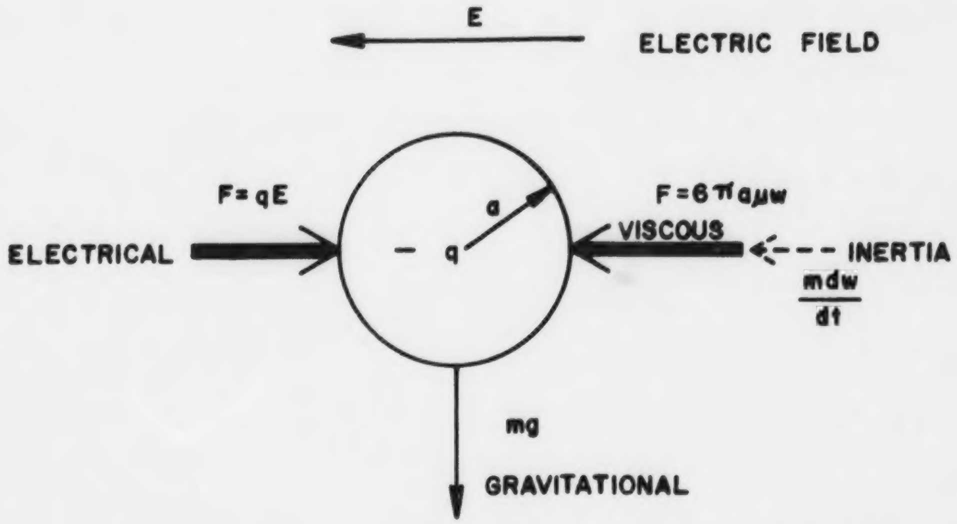
E
ELECTRIC FIELD
F=qE
ELECTRICAL
a
– q
F=6πaμw
VISCOUS
INERTIA
mdw/dt
mg
GRAVITATIONAL

Figure 1. Free Body Diagram of a Charged Particle Under the Influence of Electric and Gravitational Fields.

greater than about 1-2 μm. Utilizing the theory of diffusion charging by ions as reported by Liu and Yeh[2] - together with the field charging as described by White[3] yields an electrical charge as a function of particle size approximately as shown in Figure 2. The conditions selected for this example are typical for a full scale electrostatic precipitator collecting fly ash from a pulverized fuel fired power station boiler. These power station precipitator conditions are given below in Table I.

TABLE I

Precipitator Design and Operating Parameters for the Efficiency Versus Size Plot as Shown in Figure 5

Item	
Collection Area to Volume Ratio	300 ft^2/1000 cfm
Current Density	20 μamps/ft^2
Plate Spacing	9 in.
Applied Voltage	31,000 volts
Corona Wire Size	0.109 in.
Gas Velocity	5.3 ft/sec

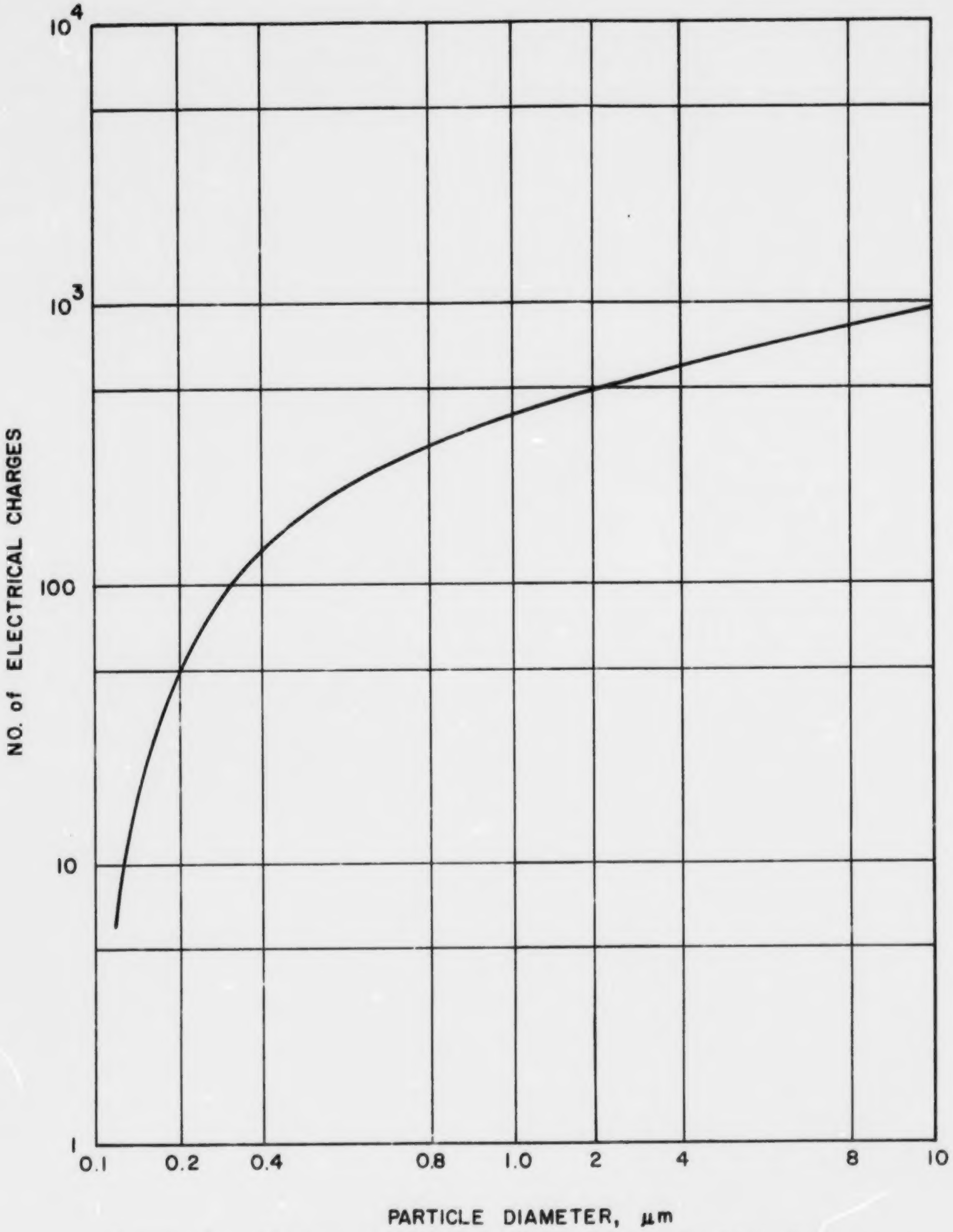

Figure 2. Charge as a Function of Particle Size for Conditions Representative of a Full-Scale Power Station Electrostatic Precipitator.

The viscous drag force from the gas stream also exhibits a variation with particle size. The viscous flow conditions are dependent upon the viscosity of the fluid medium and the size of the particle being driven (Stokes Law). The viscous drag force must be further reduced for particle sizes that approach the mean free path of the molecules in the gas stream. This reduction, described as the slip correction factor to Stokes Law, is associated with the reduction in molecular collisions per unit time for the small particles. This slip correction factor as a function of particle size is shown in Figure 3, for particle sizes ranging from 0.05-2 μm.

The gas flow conditions within the precipitator are highly turbulent resulting in an exponential collection efficiency relationship that is commonly referred to as the Deutsch equation

$$\eta = 1 - \exp[-(Aw/v)]$$

By performing an incremental calculation of the quantity w and determining the resulting incremental collection efficiency for the particle sizes of interest, the collection efficiency as a function of particle size can be computed. The results of such a calculation are given in Figures 4 and 5, where the migration velocity and the collection efficiency respectively are given as a function of particle size for the conditions existing in a well designed normally operating electrostatic precipitator treating an effluent gas stream from a coal fired electric power station boiler as described previously in Table I. (Note - these calculations do not consider reentrainment.)

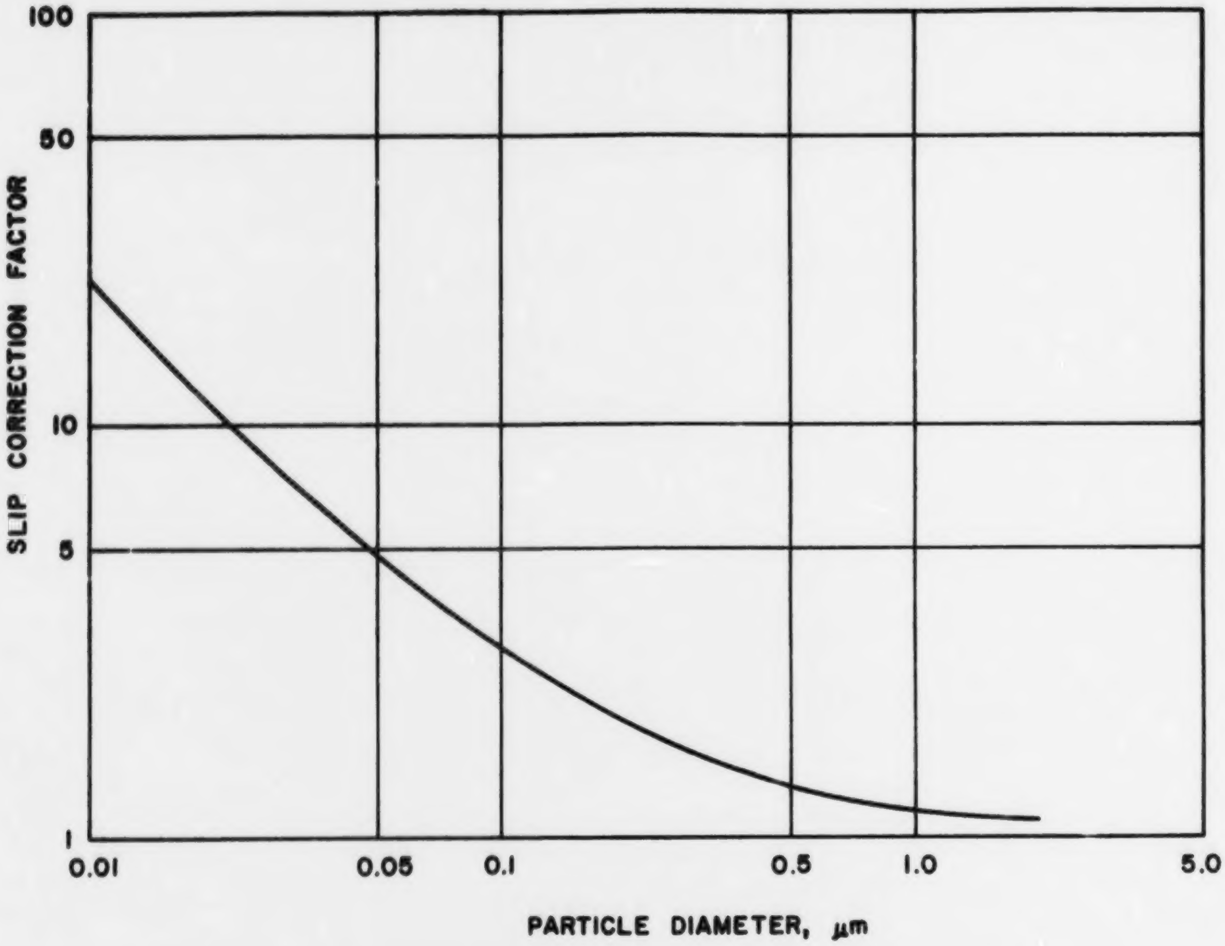

Figure 3. Slip Correction Factor to Stokes Law Settling as a Function of Particle Size.

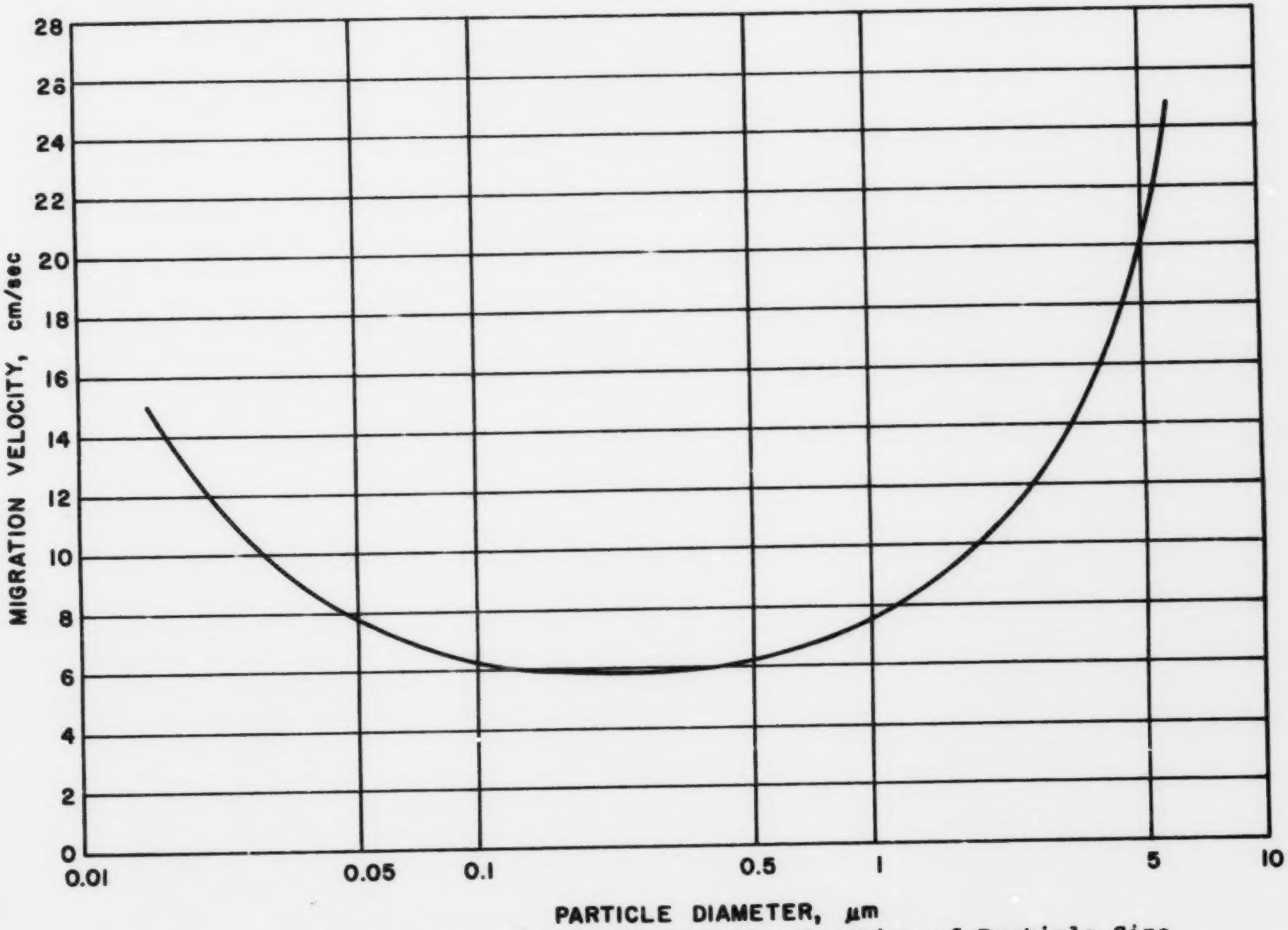

Figure 4. Theoretical Migration Velocity as a Function of Particle Size for Typical Precipitator Conditions.

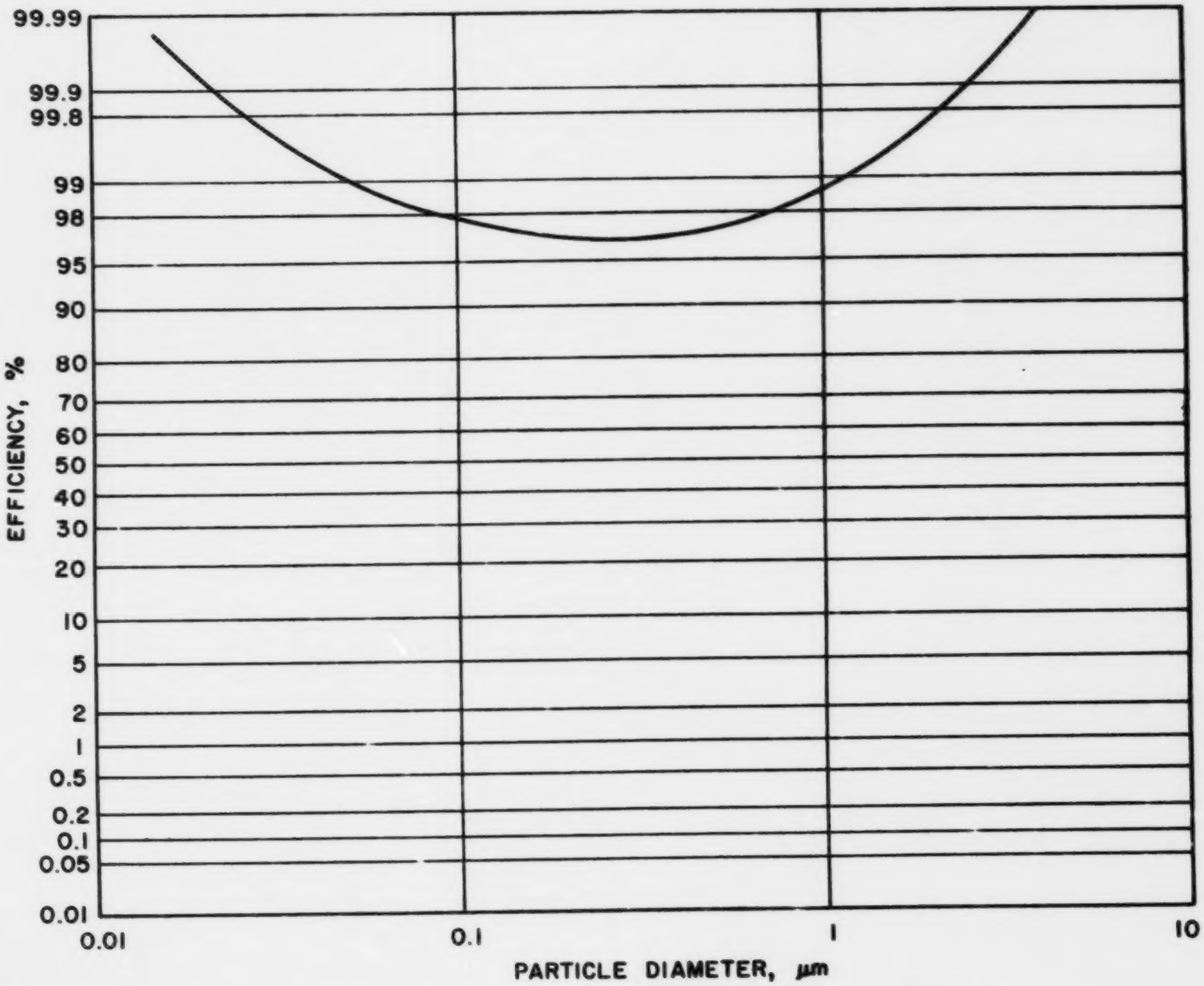

Figure 5. Theoretical Collection Efficiency as a Function of Particle Size.

Thus we see that the conventional electrostatic precipitator theory predicts that the device is an efficient collector of particulate matter from the larger particles down through the ultra-fine ones.

Experimental Measurement Techniques Utilized for Verification of the Theory

The fractional collection efficiencies of three electrostatic precipitators were measured in order to compare theoretical values with those achieved in practice. Two tests conducted on full-scale precipitators and one test on a pilot-scale unit are included. Fractional collection efficiencies were obtained by determining particle concentration (number/m^3) or mass loading (grams/m^3), or both, at the precipitator inlet and outlet. The variety of conditions that were encountered in these measurements required the use of several types of sampling and measuring equipment.

Cascade impactors (inertial devices) were used to measure particle size in the range from 0.3 to 10 μm, diffusional sizing was used for 0.01-0.2 μm particles, and optical sizing was used for 0.3-2.0 μm particles.

The cascade impactor measurement technique was described by Bird, et al,[4] with data reduction by a computer, as suggested by Brink, et al.[5]

The optical and diffusional sizing techniques are illustrated schematically in Figure 6. The sample is introduced at the apex of a perforated cone and clean dilution air is pumped through the perforations. Calibrated orifices are used to measure the

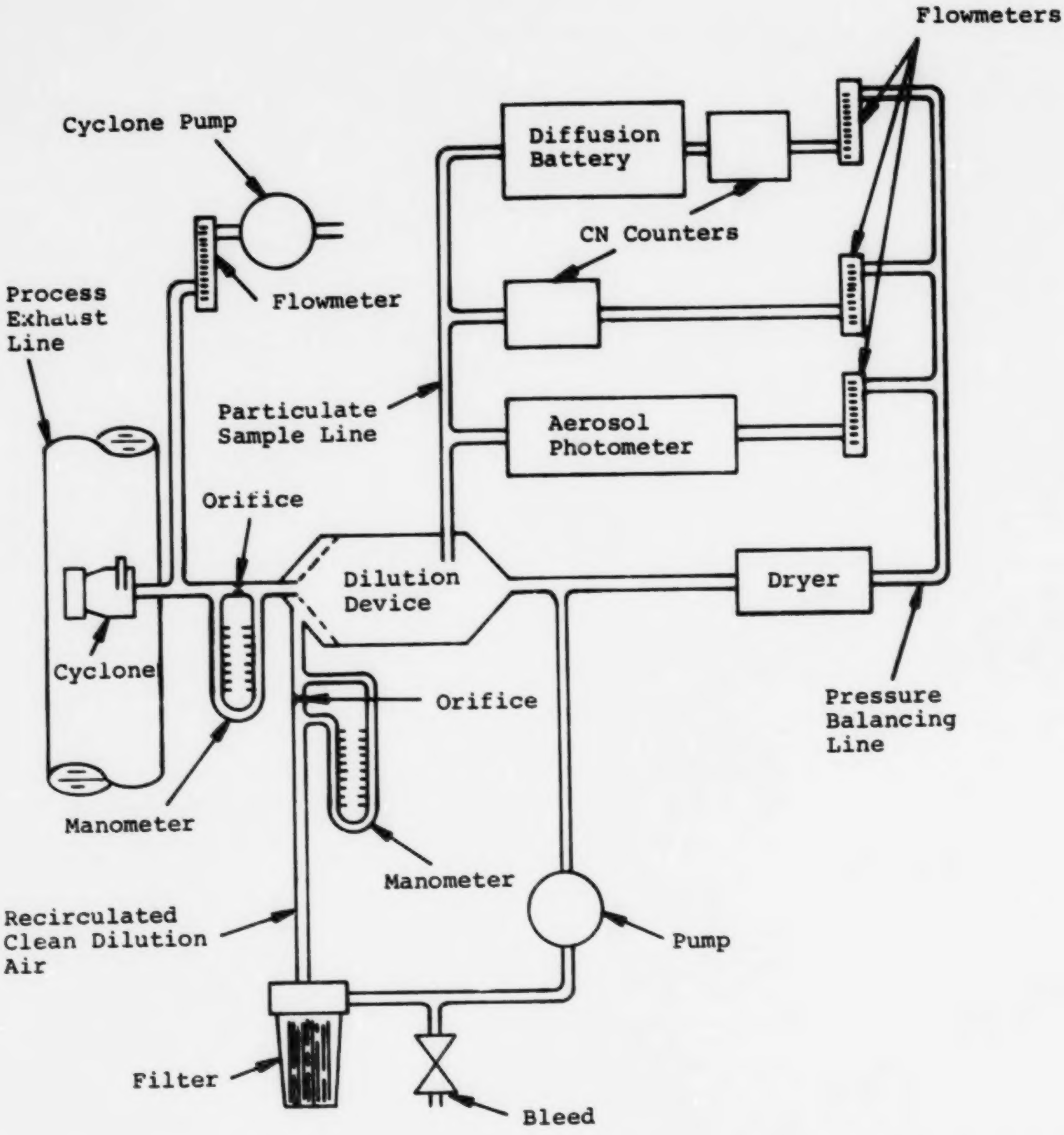
Flowmeters
Cyclone Pump
Diffusion Battery
CN Counters
Flowmeter
Process Exhaust Line
Particulate Sample Line
Aerosol Photometer
Orifice
Dilution Device
Dryer
Cyclone
Orifice
Pressure Balancing Line
Manometer
Manometer
Recirculated Clean Dilution Air
Pump
Filter
Bleed

Figure 6. Optical and Diffusional Sizing System.

sample and dilution air flow rates from which the dilution factor is calculated. The upper size limit for particle sizing is determined by the cyclone precollector, which is used to prevent large particles from entering the system and perhaps clogging the sampling orifice.

The sample is dried simultaneously with dilution by recirculating the filtered dilution air through condensers and drying tubes. In this way the concentrations of moisture and other condensable vapors in the sample are reduced by approximately the same fraction as the particle concentration. Dilution factors of 50-500 are required to reduce the concentration of 0.3 μm and larger particles in typical flue gas to about $300/\text{cm}^3$.

Although line losses can be a problem in out-of-stack sampling, they are not serious for particles having sizes between 0.01 and 2 μm and with sampling lines of reasonable length.[6]

The optical (or photoelectric) sizing device used was a Climet Aerosol Analyzer equipped with a scanning pulse height discriminator and a digital rate meter. This analyzer was calibrated in our laboratory by the use of polystyrene latex beads.

Results and Analysis

Figure 7 shows an "inlet" particle-size distribution (obtained at the precipitator outlet with the power supplies deenergized) and the corresponding outlet particle-size distribution for one of the full-scale precipitators (designated full-scale precipitator A) reported on a cumulative count basis (number per cm^3). These data were obtained with the diffusional and optical techniques discussed above. Figure 8 presents an inlet and an outlet distribution in terms of cumulative mass loading from impactor measurements on full-scale precipitator A. Similar measurements were made on a pilot-scale precipitator. Optical and diffusional measurements were also made on another full-scale precipitator (designated full-scale precipitator B). Actual inlet concentrations were obtained for both the pilot-scale unit and precipitator B. Efficiencies as a function of particle size were obtained from the particle-size distribution data on all three units and are presented in Figures 9, 10, and 11.

Overall efficiencies were determined simultaneously with the fractional efficiency measurements at precipitator A and at the pilot plant location; the efficiencies obtained were 99.59% and 99.69% at precipitator A, and 98.32% at the pilot precipitator.

The precipitators designated A and B were installed on power stations utilizing coal supplies with medium levels of sulfur at a flue gas temperature such that the electrical

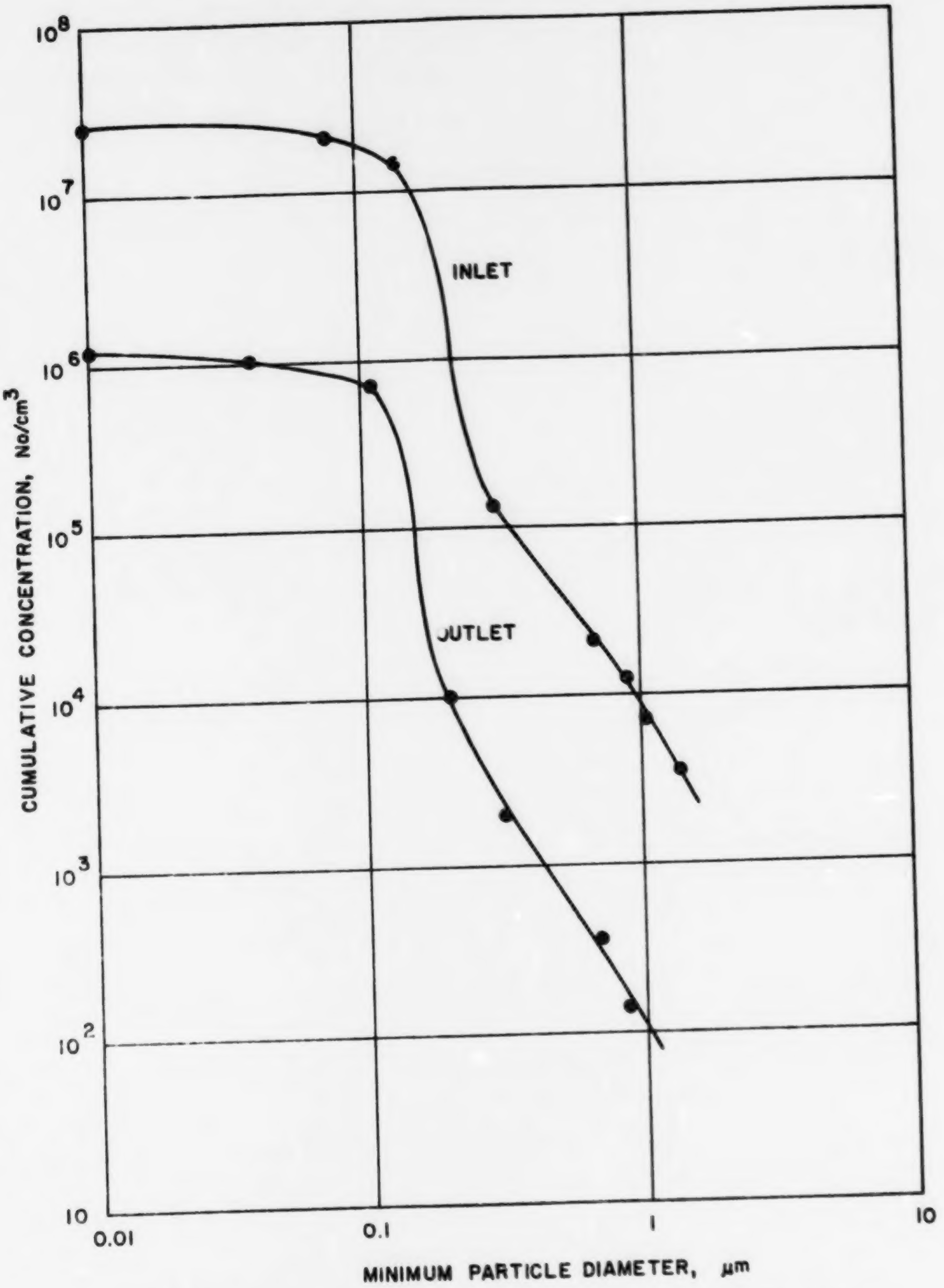

Figure 7. Cumulative Particulate Concentrations for the Inlet and Outlet of Precipitator B.

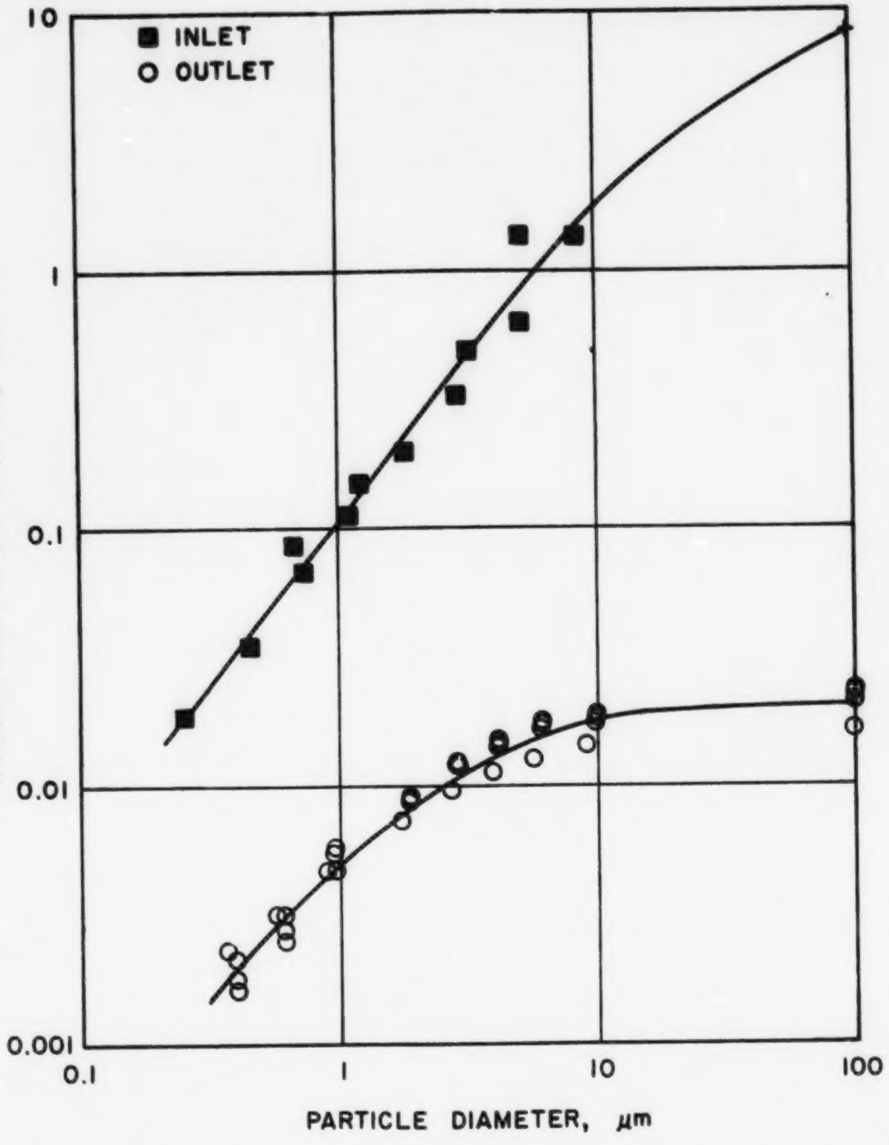

Figure 8. Inlet and Outlet Cumulative Mass Loading at Precipitator A.

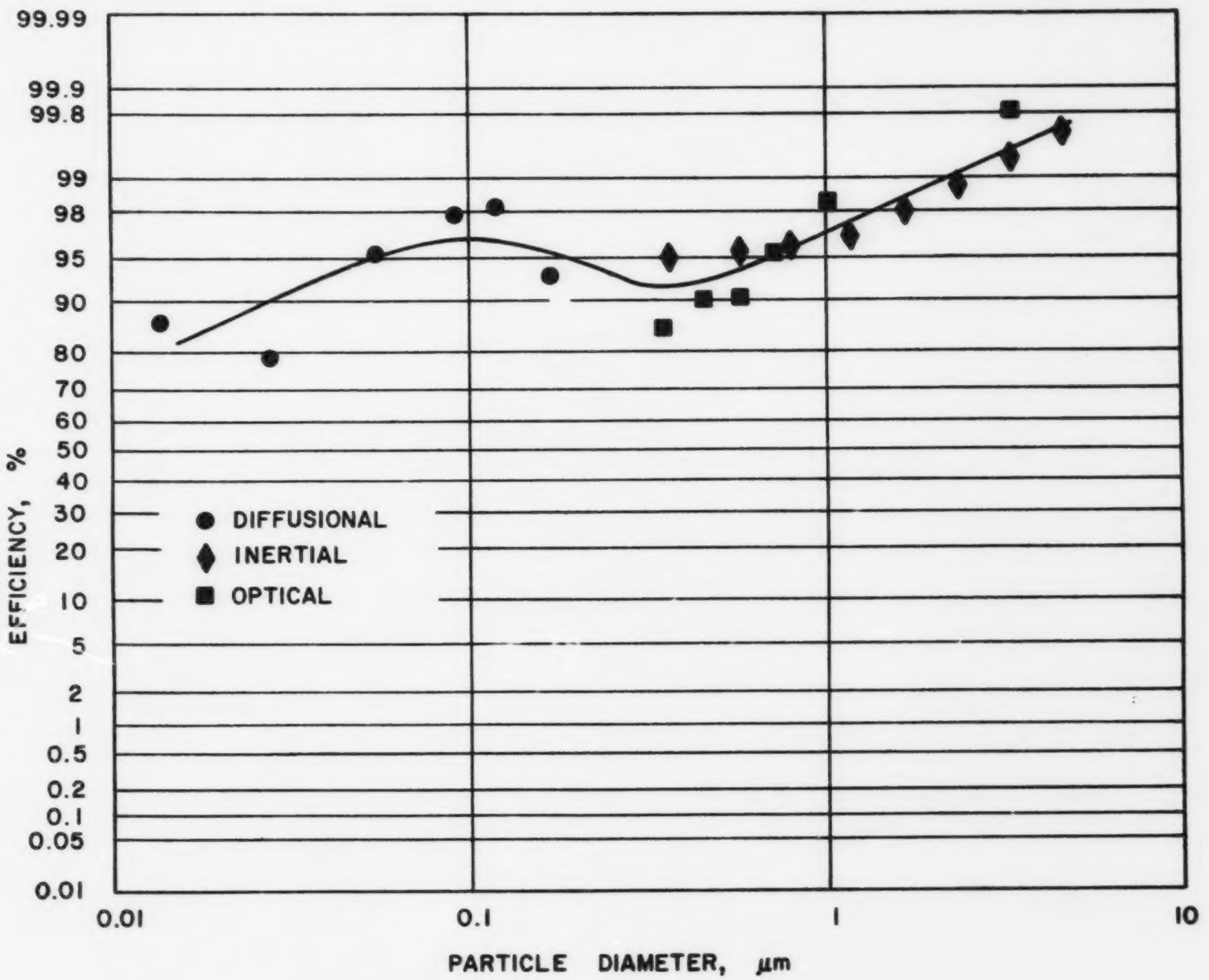

Figure 9. Fractional Efficiencies Obtained at Precipitator A.

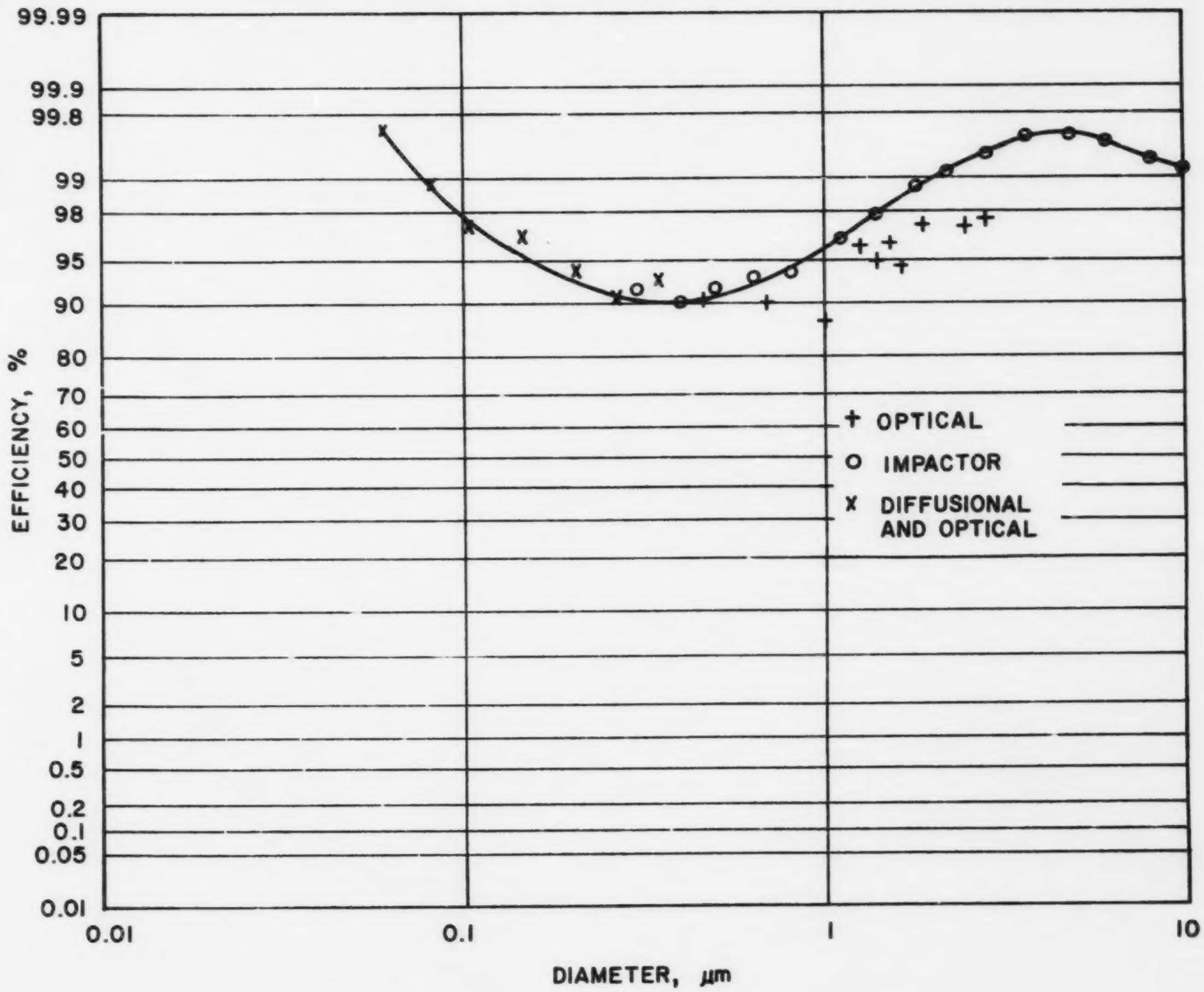

Figure 10. Fractional Efficiencies Obtained at Pilot Precipitator Location.

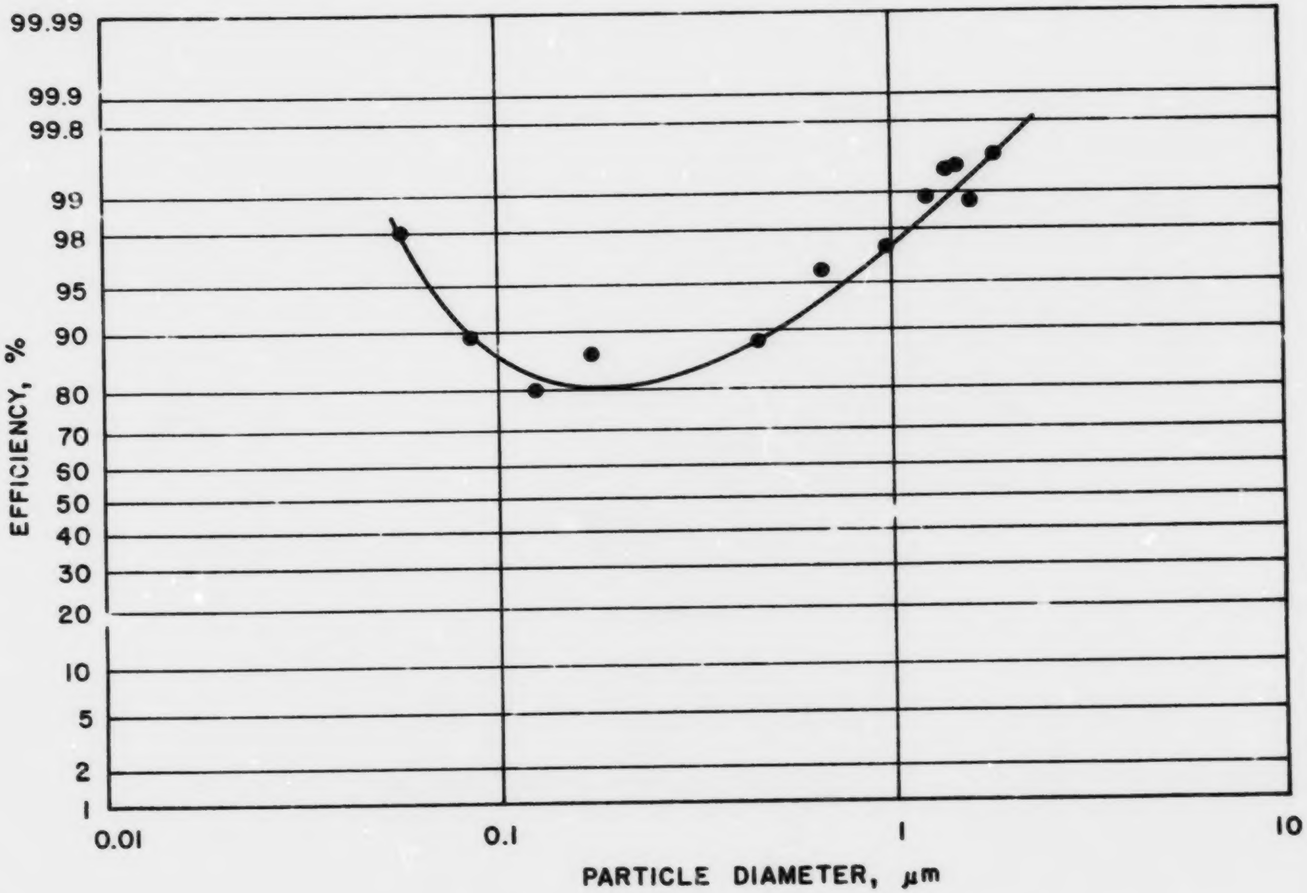

Figure 11. Fractional Efficiencies Obtained at Precipitator B.

resistivity of the fly ash did not limit the allowable current density in the collector. The pilot precipitator, however, was treating gases resulting from the combustion of a low-sulfur coal, and current density was held to a value of about 15 Na/cm^2, which is reasonably low and corresponds to the current density which can be expected when collecting high resistivity dusts. The full-scale precipitators operated at an average current density of around 20-25 Na/cm^2, with some of the outlet fields at installation A operating at values as high as 40 Na/cm^2.

The particle-size distributions shown in Figures 7 and 8 are fairly typical of those obtained at coal-fired utility boilers. Due to the operating characteristics of the impactor used for inlet measurements, it was not practical to obtain size data for particles larger than about 10 μm in diameter. Therefore, the particle-size distribution curve in Figure 8 was arbitrarily extended to 100 μm by using an overall average of inlet mass loading obtained from an inlet traverse with what is termed an Environmental Protection Agency sampling train. For the case of the outlet mass distribution, the total mass loading obtained from the impactors is plotted at 100 μm. These impactor measurements were obtained by conducting a traverse across the duct system rather than a one-point determination as is sometimes used. The overall mass loadings obtained with the impactor measurements at the outlet were on the average about 30% lower than mass loadings obtained with an EPA train, which is considered to be fair agreement.

Figures 12, 13, and 14 present the efficiency data for these three installations converted to effective migration velocity, calculated by using the Deutsch equation for particle sizes up to 1 μm. Also shown are projections of effective migration velocity obtained using a computer program developed by Southern Research Institute under contract with the Environmental Protection Agency.

This computer program is a mathematical model which calculates migration velocity as a function of particle size and conditions existing in the precipitator. Collection efficiency as a function of particle size is computed by an incremental application of the Deutsch equation. The important input parameters are current density, applied voltage, particle size distribution, and precipitator geometry. Note that in the particle size range 0.1-1 μm, the poorest agreement between the computer projections and the values obtained from the field measurements is exhibited by the pilot precipitator installation. Referring to Figure 10, the efficiency curve for the pilot precipitator for sizes larger than 1 μm deviates drastically from the theoretically expected functional form, possibly as the result of reentrainment. Therefore, reentrainment may be the cause of the disagreement indicated in Figure 13.

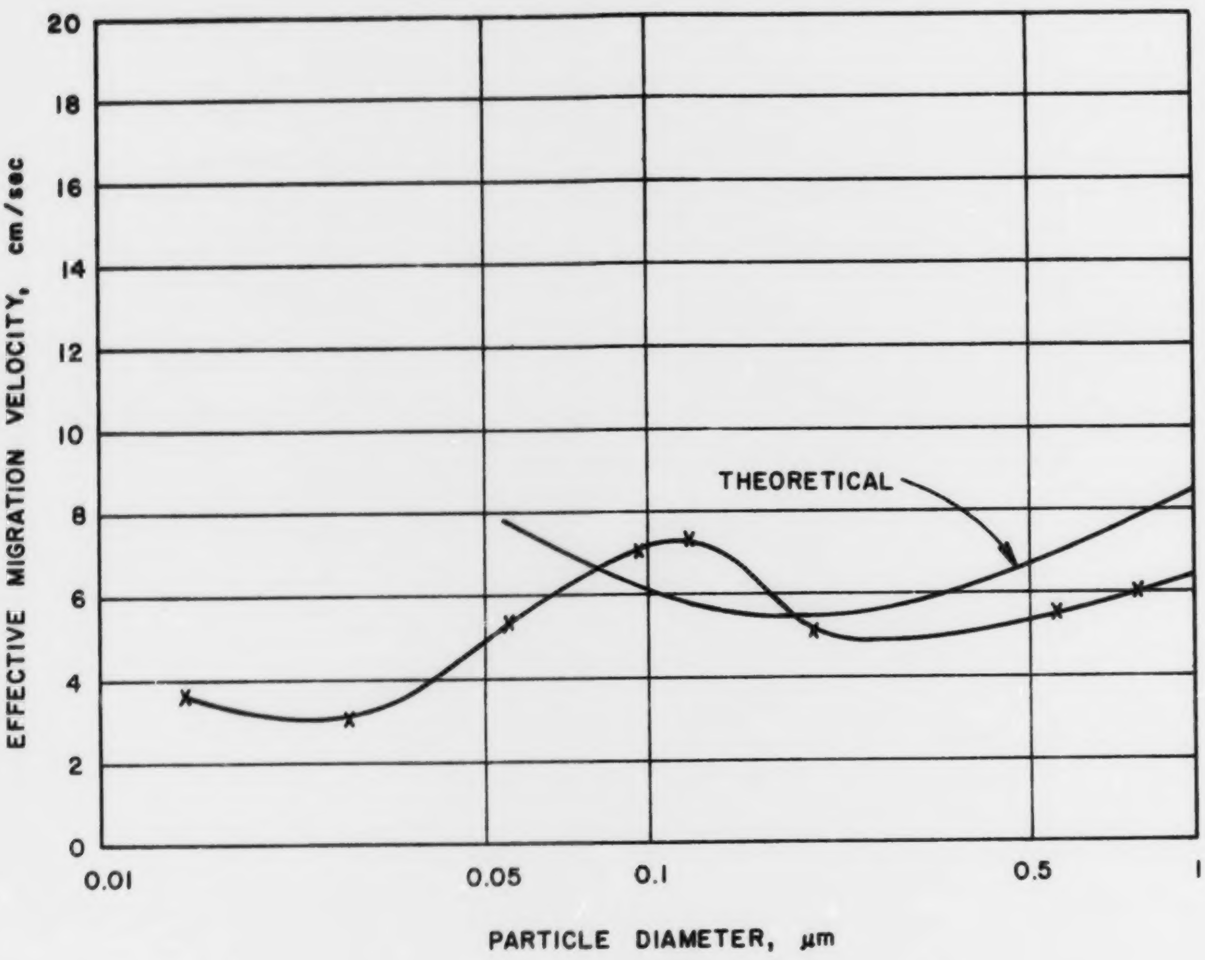

Figure 12. Effective Migration Velocities at Precipitator A.

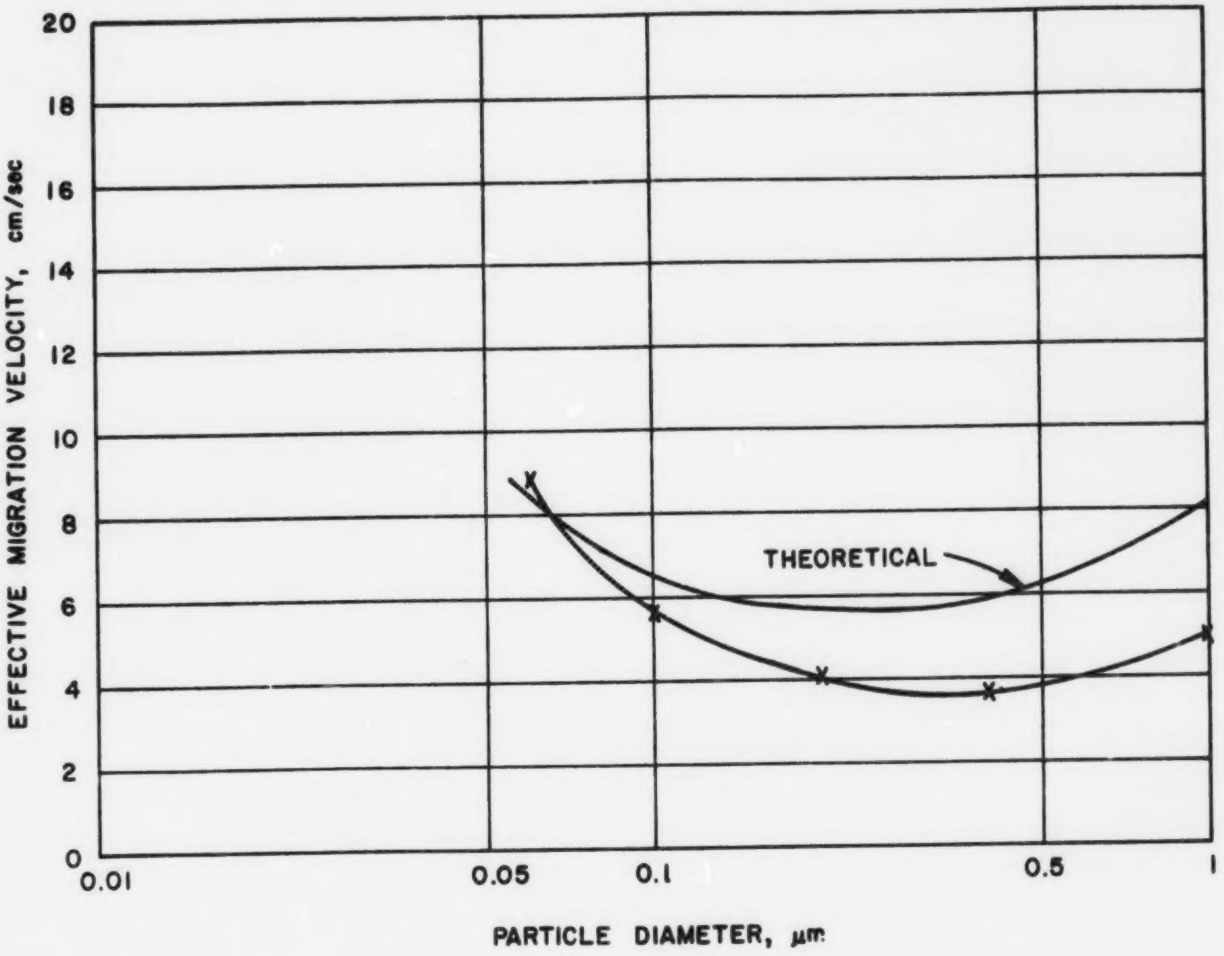

Figure 13. Effective Migration Velocities at Pilot Precipitator.

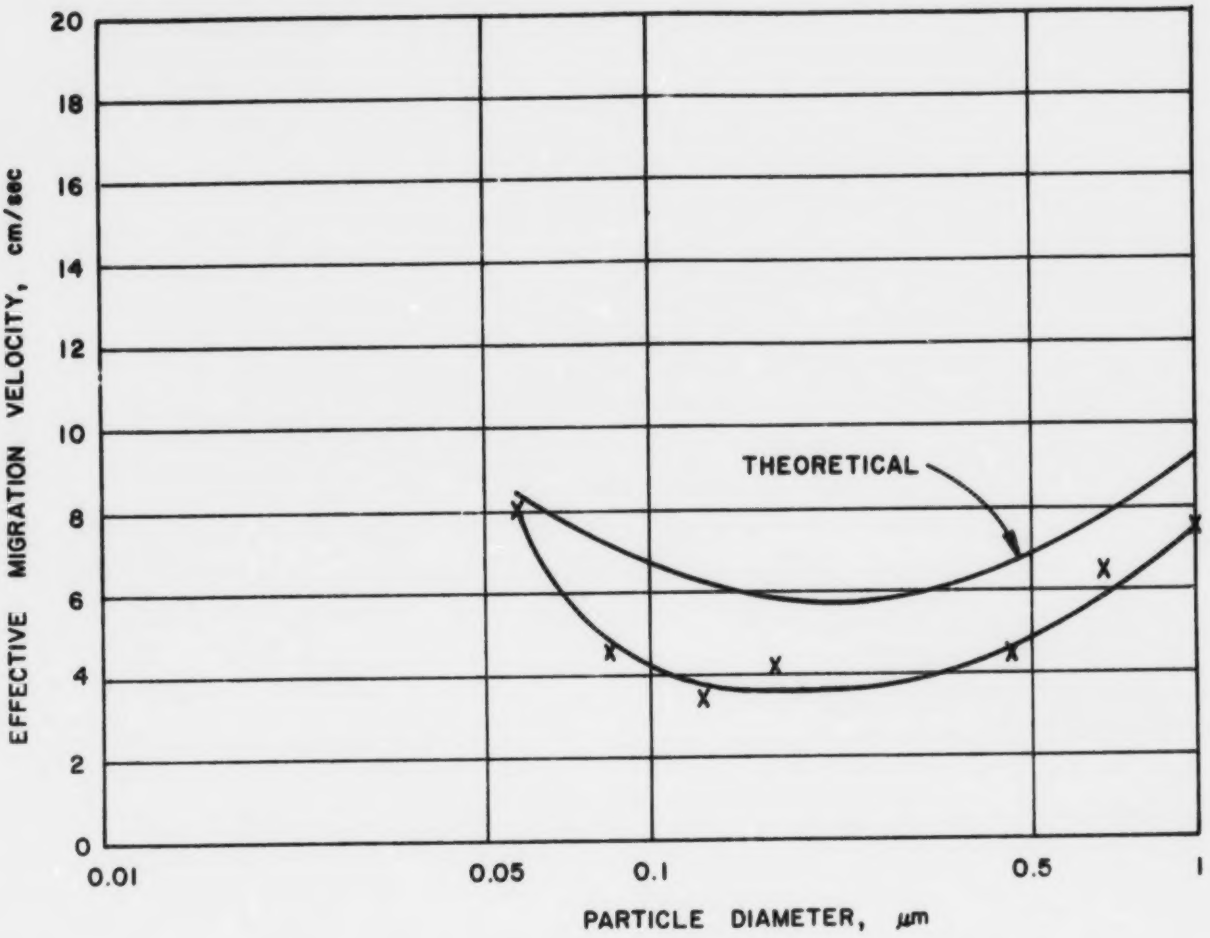

Figure 14. Effective Migration Velocities at Precipitator B.

Discussion of the Limitations on the Precipitation Process

Several basic or fundamental relationships are thought to limit the operation of an electrostatic precipitator. The limits are primarily associated with the limitations on the electrical charge on the particle. The first limitation is associated with the finer size fraction of the material where the number density of the particles approaches the number density of the ions in the precipitators (~$10^{[illegible]}$ ions $m^{[illegible]}$). When this condition occurs the charging relationships become probabilistic rather than deterministic. This condition may exist for particles in the 0.01 μm size range where a single charge constitutes a sufficient charge for efficient collection.

A second fundamental limitation exists when the electric field in the vicinity of the particle due to the charge on that particle approaches a value sufficiently high to achieve field emissions of an electron (typically $10^{[illegible]}$ volts/meter). This condition is not of practical interest because fields of this magnitude do not exist in the conventional precipitator.

Another limitation that is sometimes suggested is when the electric field in the vicinity of a charged particle approaches the breakdown strength of the gas (~$2.0\times10^{[illegible]}$ v/m). The idea is that an electron avalanche would occur leaving behind positively charged ions. These ions would drift to and neutralize the charge on the particle.

This condition almost surely cannot exist in that free electrons are required to act as initiating electrons for the avalanche process and the electric field must exceed the breakdown strength of the gas medium for at least one or two mean free paths of the gas. The free electron concentration is only on the order of 10-20 per cubic centimeter, and the electric field from a charged sphere decreases in proportion to the reciprocal of the radial distance squared. These conditions will not be met in conventional electrostatic precipitators.

Summary

The electrostatic precipitator is an effective device for collecting the fine size fractions of the particulate emissions from industrial installations. This performance is predicted by theory and verified by the measured fractional collection efficiencies of 3 precipitators, two full-scale and one pilot-scale, as shown previously. The collection efficiencies ranged from a minimum of about 80% at about 1.2 μm to a maximum of about 99.8% at 0.06 μm in precipitators of moderate size operating at relatively low current density. Measured collection efficiencies for particles larger than 1.0 μm in diameter were considerably lower than predicted from theory, presumably because of reentrainment.

It can be seen that at the minimum values of effective migration velocities that were found, relatively high collection efficiency of fine particulate can be achieved under favorable operating conditions at reasonable ratios of plate area to volume flow.

Birmingham, Alabama
January 4, 1974   jf

REFERENCES

1. "Abatement of Particulate Emissions from Stationary Sources", National Research Council - National Academy of Engineering, EPA-R2-72-042, July, 1972.

2. B. Y. H. Liu and H. C. Yeh, "On the theory of charging of aerosol particles in an electric field", J. Appl. Phys. 39, 1396 (1968).

3. H. J. White, Industrial Electrostatic Precipitation, Addison-Wesley, Reading, Mass. (1963).

4. A. N. Bird, Jr., J. D. McCain, and D. B. Harris, "Particulate sizing techniques for control device evaluation", Paper 73-282, presented at the Annual Meeting of the Air Pollution Control Association (June 1973).

5. J. A. Brink, Jr., E. D. Kennedy, and H. S. Yu, "Particle size measurements with cascade impactors", paper presented at the 65th Annual Meeting of American Institute of Chemical Engineers (November 1972).

6. L. Ström, Transmission efficiency of aerosol sampling lines", Atmos. Environ. 6, 133 (1972).

LIST OF SYMBOLS

a = particle radius, m

q = electrical charge, coulombs

w = migration velocity, m/sec

A = collection electrode area, m^2

E = electric field, volts/meter

F = force, Newtons

V = volume flow rate, m^3/sec

η = efficiency, %

μ = gas viscosity (kg/meter-sec)

Paper No. 8

OPERATING EXPERIENCE WITH GAS CONDITIONED ELECTROSTATIC PRECIPITATORS

by

George P. Green
and
W. S. Landers

PUBLIC SERVICE COMPANY OF COLORADO

Denver, Colorado

ABSTRACT

For over three years Public Service Company of Colorado has used SO_3 gas conditioning to improve the operation of electrostatic precipitators installed at its steam electric generating plants that burn low sulfur Western United States coals. Three methods of generating and adding SO_3 are in use on eight precipitators installed on pulverized coal burning units. Addition of 15-20 ppm of SO_3 has significantly improved collection efficiency on all units. The resistivity of the untreated ash is about 10^{13} ohm/cm and the precipitatiors operate at 260-300°F. Gas conditioning did not compensate for design deficiencies other than the resistivity problem.

The Public Service Company of Colorado (PSCo) began burning western, sub-bituminous, low-sulfur coal in its first fossil fired unit in 1926. All of the coal burned in the Company's existing and proposed conventional steam generating stations is mined in Colorado and Wyoming. The principal source of coal purchased in Colorado is Routt County with minor purchases from Weld, Moffat, Gunnison, and Delta Counties. Most of the Wyoming coal comes from the Gillete, Wyoming area.

Typical analysis of the principal Colorado and Wyoming coals used are shown in Table 1. For comparison, the analysis of an important steam coal used in mid-western utilities is shown. When considering the problems peculiar to Public Service Company's particulate control programs, the sulfur content of the coals is a major factor. The coals we use contain less than 1.0 percent sulfur, compared to the about 2.5 percent contained in average eastern and mid-western utility coals. Because of the wide difference in heating value of the coals, a more significant comparison is that our coals contain about 0.7 pounds of sulfur per million Btu's while an eastern steam coal of 2.5 percent sulfur will contain nearly 2 pounds of sulfur per million Btu's.

In 1948, the Company installed its first mechanical cyclone collector. Mechanical separators were subsequently installed on all of the major generating units on the Company's system, with the exception of the new units recently completed or under construction. These mechanical collectors have performed satisfactorily over the years maintaining a collection efficiency in the range of 75-85 percent, and requiring only minimal maintenance.

TABLE NO. 1

TYPICAL COAL AND ASH ANALYSIS

	Colorado Coal	Wyoming Coal	Midwestern Steam Coal[1]
Proximate Analysis as Received:			
Moisture	9.8%	29.0%	2.2%
Volatile Matter	35.3%	33.4%	35.6%
Fixed Carbon	45.5%	32.4%	53.3%
Ash	9.4%	5.2%	8.9%
Sulfur	0.7%	0.6%	2.2%
HHV, BTU/lb.	11,010	8,250	13,280
Hardgrove Grindability	44	55	-
Pounds of Sulfur/million BTU's	0.64	0.73	1.66
Ash Fusion Temperatures:			
Initial Deformation	2560°F.	2010°F.	2090°F.
Softening (H=W)	2665°F.	2150°F.	2210°F.
Fluid	2690°F.	2210°F.	2330°F.
Ash Composition:			
Silica (SiO_2)	54.1%	34.5%	47.2%
Alumina (AL_2O_3)	28.3%	20.6%	23.2%
Iron Oxide (Fe_2O_3)	3.0%	6.8%	21.9%
Phosphorus Pentoxide (P_2O_5)	1.1%	0.2%	.2%
Titanium Oxide (TiO_2)	0.7%	Trace	1.0%
Calcium Oxide (CaO)	5.0%	20.0%	2.4%
Magnesium Oxide (MgO)	1.5%	2.7%	.6%
Sodium Oxide (Na_2O)	0.6%	0.2%	.4%
Potassium Oxide (K_2O)	1.0%	4.3%	1.6%
Sulfur Trioxide (SO_3)	1.8%	10.7%	1.6%

[1] Pittsburgh No. 8 steam coal from Jefferson County, Ohio.

Starting in 1962, and continuing thru 1968, electrostatic precipitators were installed on all major generating units. During this period, a total of 10 precipitators purchased from five manufacturers were installed. Table No. 2 lists the station, year, and basic design data of each precipitator. Our trend during these six years was toward larger plate area, lower velocity, and higher guaranteed efficiency.

During this same period, the State of Colorado was also making the following changes in the regulations:

	1962	1969	1971	1975
Particulate	.85 lbs/1,000 lbs. flue gas	.4 lbs/1,000 lbs. flue gas	.1 lb/1,000 lbs. flue gas*	.1 lb/1,000 lbs. flue gas
Visual	40% Opacity	20% Opacity	20% Opacity	20% Opacity
SO_x	2,000 ppm	2,000 ppm	500 ppm	150 ppm**

*The actual law reads .1 lb. per million BTU input to furnace which is approximately equivalent to .1 lb/1,000 lbs. of flue gas.

**The SO_x regulation of 150 ppm by 1975 has been extended until 1978 on existing units; however, all new units constructed after 1975 will still be required to meet 150 ppm.

The major operating problems encountered with electrostatic precipitators were excessive electrode wire breakage, insulator failures, and rapper failures. Experience to date indicates that the majority of wire breakage can be alleviated by the use of shrouds at the lower end of the wire near the bottom of the collecting plate. Also, particular care must be taken to prevent ash buildup in the hoppers so that ash does not hamper the movement of or lift the wire weights. The excessive insulator failures appear to be mainly a design problem and have been corrected by installing a proper gasket material between the insulator and top of the precipitator. We have also found that

TABLE NO. 2

ELECTROSTATIC PRECIPITATOR COMPARISON DATA

Unit	Year Purchased	Gas Volume CFM	Gas Temp. °F.	Collecting Surface Ft^2/1000 CFM	Gas Velocity FPS	Guaranteed Efficiency
Valmont #5	1962	746,000	271°	88.8	7.52	87.0
Zuni #2	1962	297,000	341°	117	4.17	87.0
Cherokee #3	1963	545,000	272°	108	7.44	87.0
Cameo #2	1964	221,300	280°	116	6.83	87.0
Arapahoe #4	1964	545,000	305°	128	6.6	87.0
Cherokee #4	1965	1,390,000	267°	135	5.94	87.0
Arapahoe #3	1965	250,000	350°	121	6.6	90.0
Cherokee #1	1965	471,000	285°	123	6.47	90.0
Cherokee #2	1967	495,000	290°	159	4.95	94.2
Arapahoe #2	1968	258,000	306°	215	4.35	97.5

special care must be taken to insure that the rapper rods remain vertical so that the full intensity of the rapper rod is transmitted to the rappers. Maintenance inspections on some of the units have revealed that the rods have become bound in the sleeves and the rapping force is then transmitted to the entire precipitator frame.

It goes without saying that continuing good maintenance and alignment is definitely required in order to maintain precipitator performances; this also includes maintenance of the ash handling system.

None of the precipitators met the guaranteed efficiency. After research and study by Public Service Company engineers, the Denver Research Institute, and the Southern Research Institute, it was determined that the major cause of the non-performance of the precipitators was the high resistivity of the fly ash. The resistivity of the fly ash from low sulfur western coals are typically in the 10^{13} ohm/cm range. As a result of this high resistivity, the negatively charged ash particle does not lose its negative charge as rapidly or as completely as it should when it migrates to the positive plate. A layer of negatively charged ash remains on the plate even when it is periodically rapped. This layer repels subsequent ash particles, thus allowing portions of the ash to pass thru the precipitator uncollected.

In early 1970, the Company decided to install gas conditioning equipment to artifically reduce the ash resistivity. Gas conditioning, although not [redacted] original, was locally researched and adapted to the Company system. As mentioned earlier, the coal burned in the Company's boilers is very low in sulfur content (less than 1%). It was determined that if sulfur trioxide (SO_3) could be injected into the flue gas stream and absorbed or adsorbed on the fly ash, the electrostatic precipitators would function more efficiently. When the sulfur in coal is burned, it produces 99 parts of sulfur dioxide (SO_2) to one part of sulfur trioxide, and for every million parts of flue gas, PSCo coal produces about five parts of SO_3. It was found that if the concentration of SO_3 could be increased to 20 parts per million, the electrostatic precipitators would work more efficiently and sulfur oxide emissions from the stacks would not be increased.

The objective then, was to increase the SO_3 by 15 parts per million without increasing the SO_2. The SO_3 layer on the ash particles, or more probably the H_2SO_4 layer, lowers the resistivity allowing the particles to become neutralized on the plate. The use of this process has considerably increased precipitator efficiency and quantity of fly ash that is captured.

The SO_3 is injected directly into the flue gas stream before it enters the electrostatic precipitators. The necessary SO_3 is produced externally, picked up by the stream of flue gases, and carried into the electrostatic precipitators. The additional sulfur trioxide is captured by the ash particles, allowing them to be more easily collected.

The injection rate varies between 18 and 25 parts of sulfur trioxide per million parts of flue gas. Numerous tests have been conducted in the last two years to determine if additional amounts of SO_3 can be detected in the flue gas effluent from the precipitators at the above injection ratio. To date, we have not found any carry-over of SO_3. One way of determining the most effective injection rate is to raise SO_3 injection until increased SO_3 is detected in the stack gases. Precipitator efficiency falls off with excessive SO_3 injection, and the optimum injection level must be determined for each installation. This loss of efficiency is probably caused by reentrainment of small ash particles that have lost their charge too rapidly to permit agglomeration on the plates.

We presently have three different SO_3 injection systems in operation on eight different boilers. The most successful system to date has been the vaporized sulfuric acid system which is installed on four boilers. This system basically vaporizes a 92° Baume sulfuric acid at 550°F into a stream of electrically heated air and injects it into the flue gas stream in the vapor state. A second system utilized on only one boiler installation takes a commercial grade sulfuric acid and with the use of a gas fired boiler heats the acid to 1000°F, disassociating the sulfuric acid to SO_3 and water. The products of combustion, SO_3, and water are then injected into the flue gas stream. The third system that is in operation on the remaining three boilers uses stabilized liquified SO_3, which can be vaporized at approximately 150°F for injection into the flue gas stream in an air sweep.

Approximately a year was required to complete the development and debugging of all of these systems. At present, all of the systems are in operation, and in some cases have proved to be very successful in bringing the precipitators into compliance with the State regulations.

Figure 1 shows the flow diagram used on four boilers for the vaporization of sulfuric acid at 550°F using electrically heated air to vaporize, decompose, and sweep the acid into the duct. All of the heat needed is supplied in the sweep air. The temperature of the air is maintained constant, and the quantity of sulfuric acid metered to the vaporizer is controlled by the air flow to the boiler. The volume of the gas sweep to the vaporizer is controlled by the vaporizer exit temperature.

Figure 2 shows a similar unit used on one boiler. In this case, hot gases at 1000°F are produced in a pressurized gas burner and sweep the vaporizer.

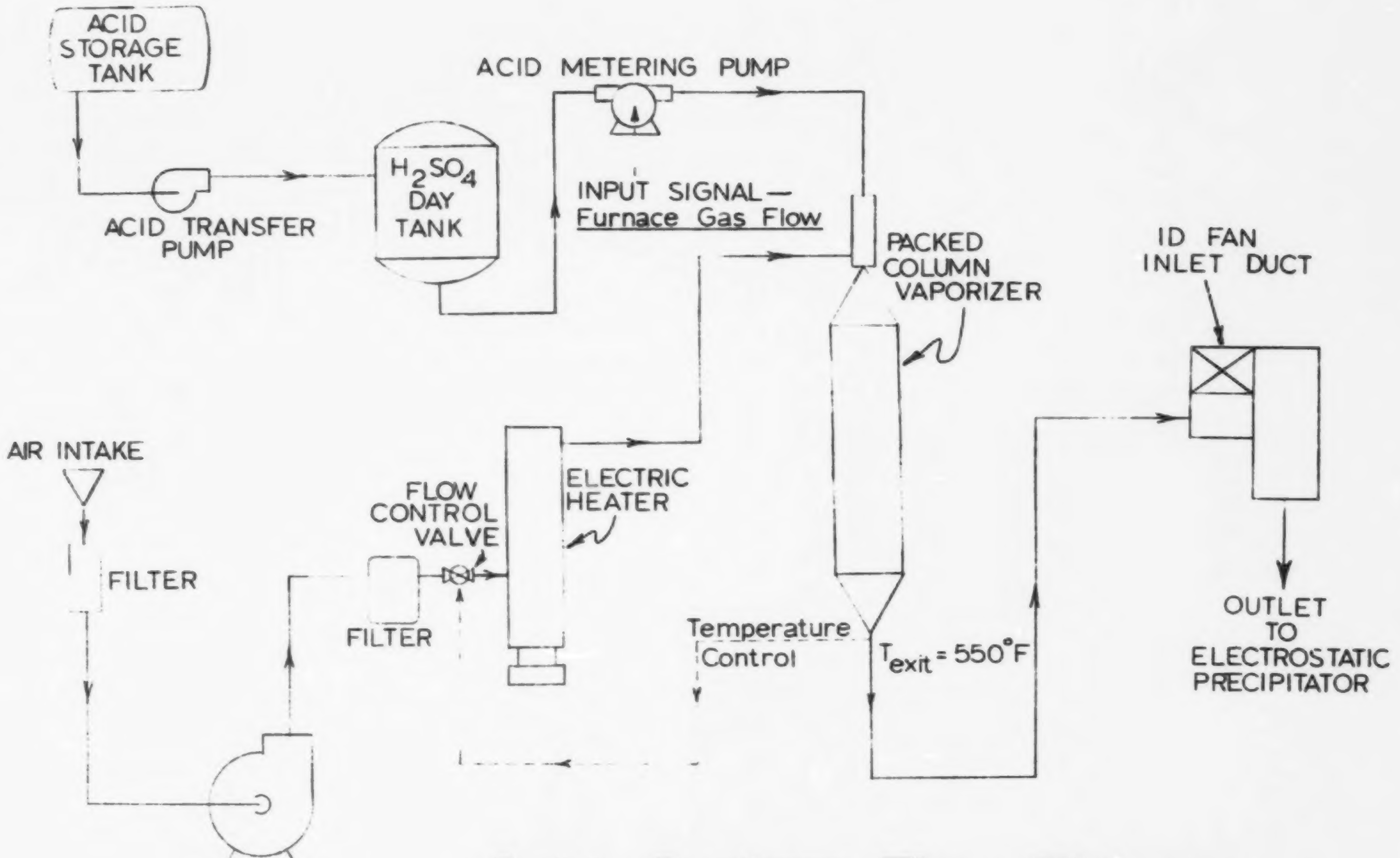
ACID STORAGE TANK
ACID TRANSFER PUMP
H_2SO_4 DAY TANK
ACID METERING PUMP
INPUT SIGNAL—Furnace Gas Flow
PACKED COLUMN VAPORIZER
ID FAN INLET DUCT
AIR INTAKE
FILTER
FLOW CONTROL VALVE
ELECTRIC HEATER
FILTER
Temperature Control
$T_{exit} = 550°F$
OUTLET TO ELECTROSTATIC PRECIPITATOR
AIR BLOWER

Acid System Flow Diagram
Electrically Heated Air Sweep

Figure 1

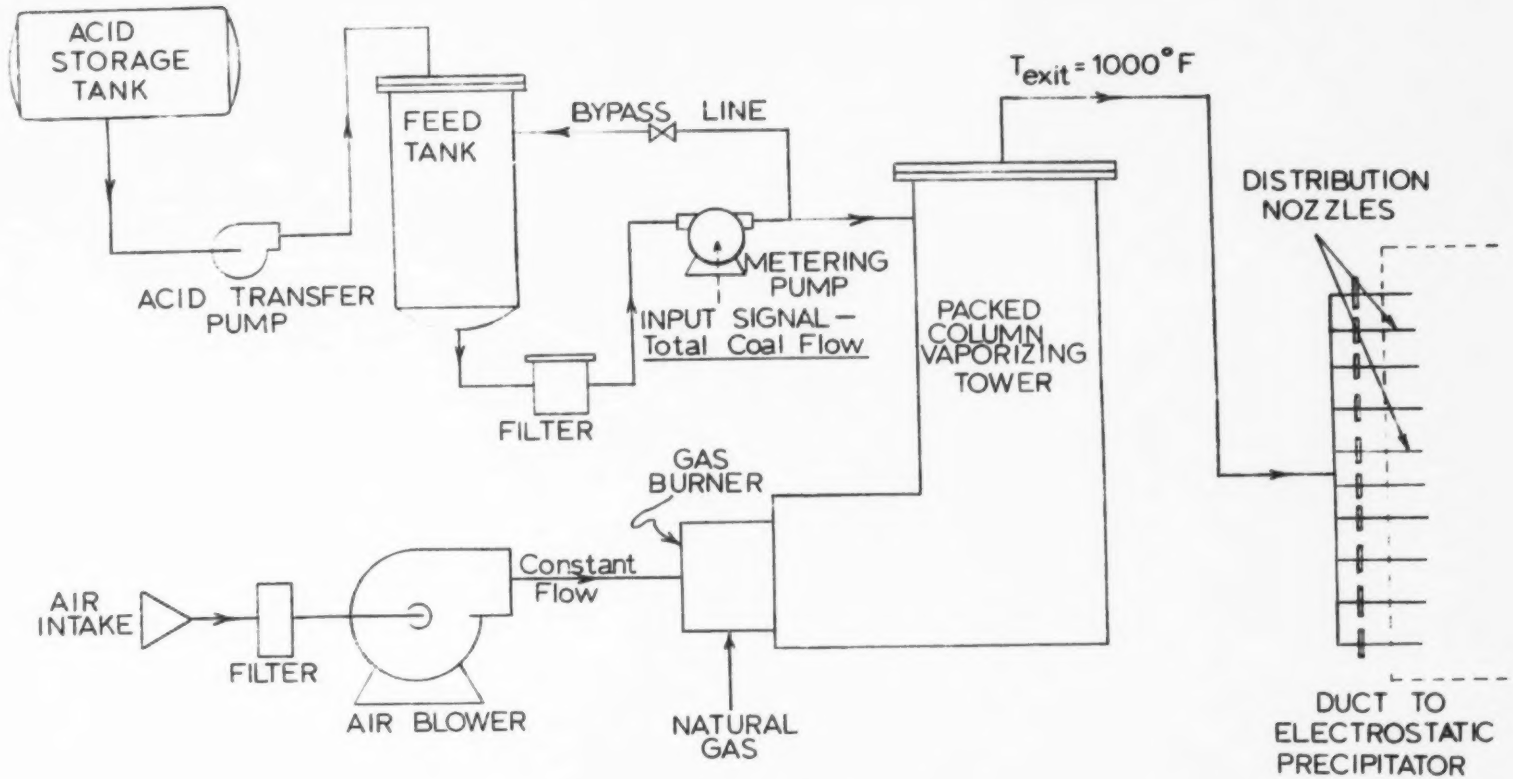
ACID STORAGE TANK
ACID TRANSFER PUMP
FEED TANK
BYPASS LINE
METERING PUMP
INPUT SIGNAL – Total Coal Flow
FILTER
T_{exit} = 1000°F
PACKED COLUMN VAPORIZING TOWER
DISTRIBUTION NOZZLES
DUCT TO ELECTROSTATIC PRECIPITATOR
GAS BURNER
AIR INTAKE
FILTER
AIR BLOWER
Constant Flow
NATURAL GAS

Acid System Flow Diagram
Gas~Air POC Sweep

Figure 2

Acid feed to the vaporizer is controlled by boiler fuel supply. Sweep air is constant.

Figure 3 shows the liquid SO_3 unit used on three boilers. Stabilized SO_3 is metered into the steam heated vaporizer. The resultant SO_3 vapor is picked up and transported to the ductwork by electrically heated air at 290°F. The stabilizer does not vaporize and is reclaimed from the base of the vaporizer. Reagent rate is manually set and sweep air volume and temperature are maintained constant.

Operating problems encountered on all gas conditioning systems fall into two classes:

1. Condensation.
2. Ash buildup.

The high SO_3 concentration and the high moisture (from acid decomposition and carrier gas) in the two acid systems result in a high dew point. The immediate affect is accelerated corrosion. The solution has been additional insulation and electric strip heaters to maintain temperature.

The ash buildup occurs on the injection nozzles in the ducts. Air or gas flow must be maintained in these nozzles even if the acid system is not in use. This is not always possible while maintaining and repairing the acid system, and plugging usually occurs under this condition.

Corrosion is a continuing problem. We use aluminum clad pipe and replace it as needed. The main points of corrosion are at welds. Since the injection systems are pressurized, leaks are easily located.

Table No. 3 summarizes the tests run on each of the precipitators with gas conditioning. Tests are performed on a continuing basis and are fairly representative of efficiency values maintained over the past three years.

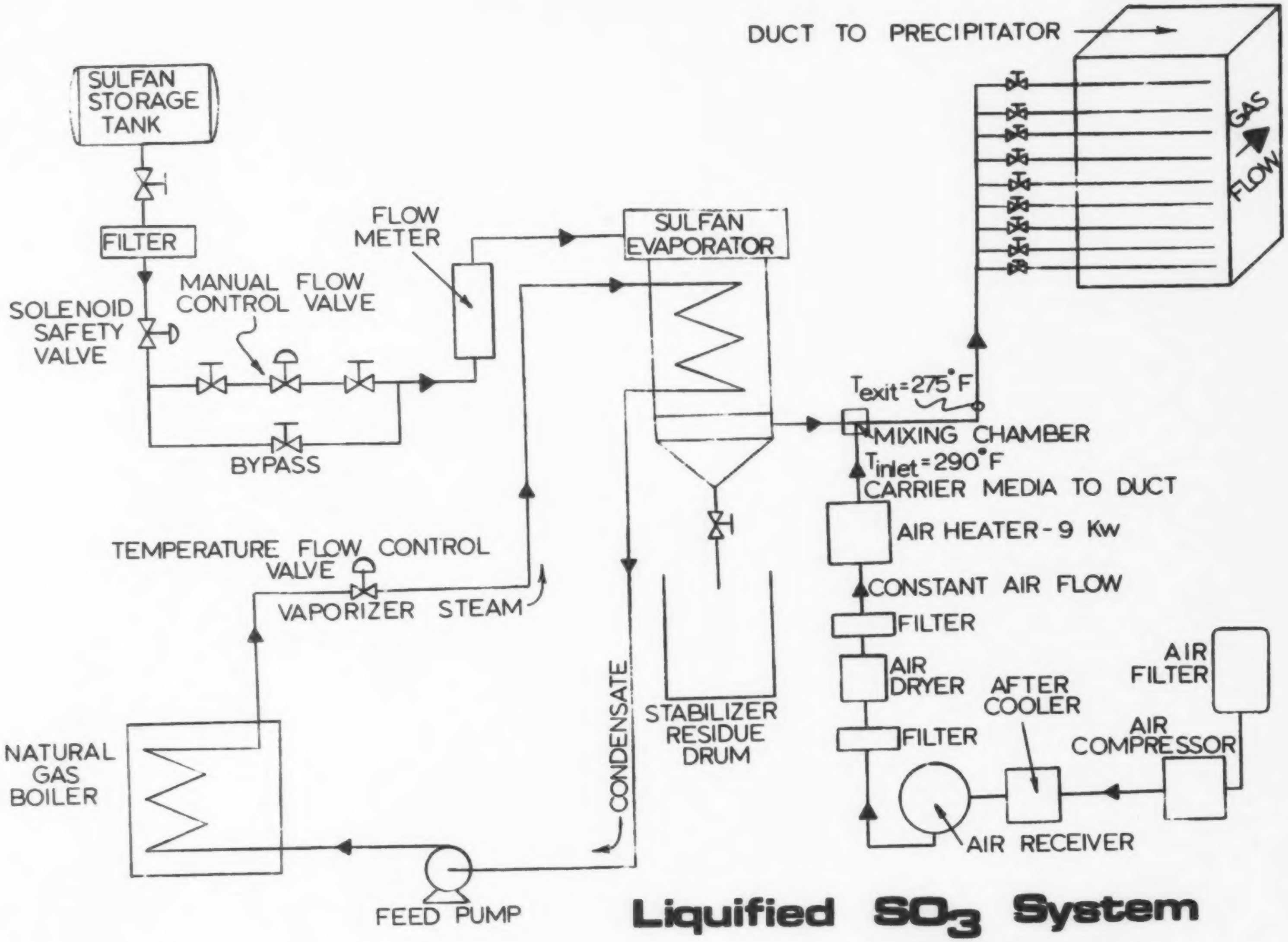
DUCT TO PRECIPITATOR
GAS FLOW
SULFAN STORAGE TANK
FILTER
SOLENOID SAFETY VALVE
MANUAL FLOW CONTROL VALVE
BYPASS
FLOW METER
SULFAN EVAPORATOR
TEMPERATURE FLOW CONTROL VALVE
VAPORIZER STEAM
NATURAL GAS BOILER
FEED PUMP
CONDENSATE
STABILIZER RESIDUE DRUM
T_{exit}=275°F
MIXING CHAMBER
T_{inlet}=290°F
CARRIER MEDIA TO DUCT
AIR HEATER - 9 Kw
CONSTANT AIR FLOW
FILTER
AIR DRYER
AFTER COOLER
AIR FILTER
AIR COMPRESSOR
FILTER
AIR RECEIVER

Liquified SO_3 System

Figure 3

TABLE NO. 3

Unit	Name-plate Rating	Guaranteed Efficiency %	Without Gas Conditioning		With Gas Conditioning	
			Obs. Eff. %	#/M^2 BTU	Obs. Eff. %	#/M^2 BTU
Cherokee #1	100 MW	90.0	57.9	0.49	72.6	0.44
Cherokee #2	110 MW	94.2	94.0	.08	95.2	.08
Cherokee #3	150 MW	87.0	37.5	.44	51.4	.33
Cherokee #4*	350 MW	98.05*	86.0*	.58	90.7*	.35
Arapahoe #2	44 MW	97.5	77.5	.61	96.2	.08
Arapahoe #3	44 MW	90.0	81.0	.32	94.5	.10
Arapahoe #4	100 MW	87.0	67.3	.24	77.3	.19
Cameo #2	44 MW	87.0	54.1	.72	95.0	.11

*All test reports on Cherokee #4 are based on a combined efficiency of both mechanical collector and electrostatic precipitator. This was necessary because of the location of the test ports. All other efficiencies shown are for the precipitators only.

It is important to note that in every case there was an improvement in precipitator performance; however, in some cases the improvement was not sufficient to bring the unit into compliance.

CONCLUSION:

The use of gas conditioning has certainly proved to be successful when applied to electrostatic precipitators whose performance was relatively marginal to begin with. For precipitators with extensive design deficiencies, the use of gas conditioning may not prove to be the answer. We certainly would not recommend that gas conditioning be considered for use in a new installation as a means of meeting initial particulate emission compliance. New installations should consider hot precipitators and/or scrubbers. We also recommend that gas conditioning not be installed until laboratory tests demonstrate its efficacy on the ash in question.

SESSION 3

CONVENTIONAL TECHNOLOGY, WET SCRUBBERS

Chairman: C. E. Lapple
Stanford Research Institute
Menlo Park, California

Paper No.

9	Scrubber Performance for Particle Collection Seymour Calvert A.P.T., Inc. Riverside, California
10	Use of Venturi Scrubbers for Removal of Highly Dispersive Particulates Georgy K. Lebedyuk State Research Institute of Industrial and Sanitary Gas Cleaning Moscow U.S.S.R.
11	Wet Gas Cleaning in Iron and Steel Industry Georgy K. Lebedyuk, A. Yu. Valdberg, and F. Ye. Dubinskaya State Research Institute of Industrial and Sanitary Gas Cleaning Moscow U.S.SR.
12	Effect of Water Vapor Condensation on Particle Collection by Scrubbers Leslie E. Sparks U. S. Environmental Protection Agency Research Triangle Park, N. C.

SESSION 3 - Continued

Paper No.

13 Use of Scrubbers for Control of Emissions from Power Boilers—U.S.

Irwin A. Raben
Combustion Equipment Associates, Inc.
San Francisco, California

14 High Velocity Synthetic Fiber Mist Eliminators

Georgy K. Lebedyuk,
B. I. Myagkov,
I. G. Kamenshchikov, and
V. V. Malikov
State Research Institute of
Industrial and Sanitary Gas Cleaning
Moscow
U.S.S.R.

Paper No. 9

SCRUBBER PERFORMANCE FOR PARTICLE COLLECTION

by

Seymour Calvert
A.P.T., INC.
Riverside, California

Preceding page blank

ABSTRACT

Scrubbers utilize liquid for the collection of particles and/or the clearance of particles from the collecting surface. The effectiveness of a scrubber can be related to the basic mechanism(s) of particle collection and is to a great extent, predictable. Major scrubber types are discussed and relationships which may be used to predict scrubber efficiency are presented.

"Scrubber Performance for Particle Collection"

by Dr. Seymour Calvert,
President, A. P. T., Inc.

Wet scrubbers of appropriate type have the ability to collect fine particles (i.e., those smaller than 2.0 µm diameter) with high efficiency under the right conditions. This paper is a brief outline of the general capabilities of scrubbers and the circumstances under which they will perform at various levels of efficiency on fine particle collection. We will begin by noting the general types of scrubbers and the basic mechanisms by which particles can be separated from the gas phase.

Scrubbers may be classified according to their geometry, or their "unit mechanisms", or other characteristics. We prefer the first two, as given in the "Scrubber Handbook" and as summarized in Table I. Note that the unit mechanisms are the simple particle collection elements which account for the scrubber's capability.

Within any of the unit mechanisms the particles may be separated from the gas by one or more of the following particle deposition phenomena:

1. Inertial impaction
2. Interception
3. Brownian diffusion
4. Turbulent diffusion
5. Gravitational force
6. Electrostatic flux force
7. Diffusiophoretic flux force
8. Thermophoretic flux force
9. Magnetic flux force
10. Photophoretic flux force

TABLE I

Scrubber Classifications

Geometric Type	Unit Mechanism for Particle Collection
Plate	Jet impingement, bubbles
Massive packing	Sheets (curved or plane), jet impingement
Fibrous Packing	Cylinders
Pre-Formed Spray	Drops
Gas Atomized Spray	Drops, cylinders, sheets
Centrifugal	Sheets
Baffle and Secondary Flow	Sheets
Impingement and Entrainment	Sheets, drops; cylinders, jets
Mechanically Aided	Drops, cylinders, sheets
Moving Bed	Bubbles, sheets
Combinations	-

The understanding and analysis of any scrubber can be reached by determining which combination(s) of unit mechanism and particle deposition phenomenon are involved. Once the basic elements of the scrubber are determined and their performance capabilities defined by mathematical equations or charts, the performance of the scrubber can be predicted. We will now turn to the discussion of the capabilities of scrubbers in present use; but first we must explain the way in which we will describe scrubber performance.

Difficulty of separation

The "cut diameter" method, first described in the "Scrubber Handbook" and further discussed in a forthcoming edition of the A.I.Ch.E. Symposium Series (for 1972), will be used. This method is based on the idea that the most significant single parameter to define both the difficulty of separating particles from gas and the performance of a scrubber is the particle diameter for which collection efficiency is 0.5 (50%).

For inertial impaction, the most common particle separation process in presently used scrubbers, aerodynamic diameter defines the particle properties of importance.

$$d_{pa} = d_p\ (\rho_p\ C')^{1/2} (\text{common units} = \mu m(g/cm^3)^{1/2} \equiv \mu mA) \qquad (1)$$

When other separation mechanisms are important, other particle properties may be more significant but this will occur generally when "d_p" is less than a micron.

When a range of sizes is involved, the overall collection efficiency will depend on the amount of each size present and on the efficiency of collection for that size. We can take these into account if the difficulty of separation is defined as the aerodynamic diameter at which collection efficiency (or penetration) must be 50%, in order that the necessary overall efficiency for the entire size distribution be attained. This particle size is the required "separation cut diameter", "d_{RC}" and it is related to the required overall penetration, $\overline{Pt}$, and the size distribution parameters.

Materials whose dispersion is attained by comminution (milling, grinding, crushing) have a size distribution which is generally log-normal. The number and weight size distribution data for most industrial particulate emissions follow the log probability law. Hence, the two well established parameters of the log-normal law adequately describe the size distributions of particulate matter. They are the geometric mean weight diameter "d_{pg}" and the geometric standard deviation "σ_g".

Penetration for many types of inertial collection equipment can be expressed as:

$$Pt = \exp\left(-A_a \, d_{pa}{}^{B}\right) \qquad (2)$$

We use the simplifying assumption that this relationship can be based on actual diameter, d_p. This will not introduce much error and it will conservatively utilize too low an efficiency for particles smaller than a micron or so. Thus:

$$Pt = \exp\left(-Ad_p{}^{B}\right) \qquad (3)$$

Packed towers, centrifugal scrubbers, and sieve plate columns follow the above relationship. For the packed tower and sieve plate column "B" has a value of 2. For centrifugal scrubbers "B" is about 0.67. Venturi scrubbers also follow the above relationship and B ≈ 2 when the throat impaction parameter is between 1 and 10.

The overall (integrated) penetration, $\overline{Pt}$, of any device on a dust of any type of size distribution will be:

$$\overline{Pt} = \int_0^W \left(\frac{dw}{W}\right) Pt \qquad (4)$$

The right-hand side of the above equation is the integral of the product of each weight fraction of dust times the penetration on that fraction. If equation (4) is solved for a log-normal size distribution and collection as given by equation (3), the resulting equation can be solved to yield Figures 1 and 2.

Figure 1 is a plot of "$\overline{Pt}$" vs. $(d_{p50}/d_{pg})^B$ with B ln (σ_g) as a parameter. For a required "$\overline{Pt}$" one can find the value of d_{RC} when "d_{pg}", "σ_g", and "B" are given. For convenience, Figure 2 is presented as a plot of "$\overline{Pt}$" vs. (d_{p50}/d_{pg}) with σ_g as the parameter when B = 2.

To illustrate the use of the separation cut diameter, assume that 2% penetration is needed for dust with d_{pg} = 10 μm, ρ_p = 3g/cm³ and σ_g = 3. If a scrubber such as a packed bed, sieve plate, or venturi is to be used, Figure 2 shows that the cut diameter, d_{p50}, must be 0.09 x (d_{pg}) = 0.9 μm. The corresponding aerodynamic diameter is d_{RC} = 1.7 μm (g/cm³)$^{1/2}$ = 1.7 μmA. Of course if the scrubber is capable of a smaller cut diameter, that is good; so "d_{RC}" is the maximum cut diameter acceptable. Some scrubbers, such as venturis, are only approximately fitted by relating penetration to exp (d_p^2) and more accurate plots can be prepared by using more representative performance equations. To avoid confusion these will not be given here, although they are presented in the Scrubber Handbook (5).

Collection efficiencies have been reported in the form of "grade efficiency" curves, which are plots of particle collection efficiency versus particle diameter for "typical" scrubbers. Unfortunately, there can be great variation in performance, depending on operating conditions and scrubber geometry so that one would need a grade efficiency curve for each important set of parameters.

The cut diameter approach proves to be a much more compact way to characterize scrubber performance. We have applied it to a number of the important types of scrubbers and present performance graphs for them. It has the great virtue of being a single-number criterion with a wide range of quantitive validity. Capability is defined by "performance cut diameter", "d_{PC}", which is the aerodynamic particle diameter at which the scrubber gives 50% collection efficiency.

Once a scrubber type, size, and operating conditions are chosen by matching the "separation" and "performance" cut diameters, (i.e., $d_{RC} = d_{PC}$) a more accurate efficiency diameter relationship can be developed and a more accurate computation of overall penetration can be made. The reason this step is necessary is that the relationship between overall penetration and separation cut diameter as shown in Figures 1 and 2 is only correct for packed beds and similar devices and is an approximation for others.

Spray Chamber Performance

A spray chamber consists essentially of a round or rectangular chamber into which water is introduced through one or more sprays. Drop size depends upon liquid pressure drop and the type of nozzle used. Water pressure drop varies from 1.4 to 7.3 atm (20 to 100 psi) and water consumption is usually in the range of 0.067-0.268 l/m^3 (0.5 - 2 gal/MCF). In practice a gas velocity of 0.6 to 1.2 m/sec (2 to 4 ft/sec) is used and the gas pressure drop is about 2 cm of water.

Vertical Countercurrent Flow-Inertial Impaction

Some solutions of the equations for inertial collection in a counter-current spray chamber are plotted in Figures 3a, b, c, and d as "d_{PC}", vs. column height, with drop diameter, air velocity and water to air ratio as parameters. Standard air and water properties have been used, so the figures can only be applied to cases where the gas and liquid properties approximate those.

Cross-Flow - Inertial Impaction

In the cross-flow case the water is sprayed at the top of the spray chamber while the gas flows horizontally. The equations for inertial collection in a cross-current spray chamber are plotted in Figures 4a and b.

The lack of uniformity in liquid distribution and the fraction of liquid hitting the walls will vary from one spray chamber to another and will introduce empirical correction factor. For small scrubbers the correction factor might be on the order of 0.2 to account for spray running down the walls, (i.e., use 0.2 x Q_L/Q_G actual).

Venturi

Venturi scrubbers employ gradually converging, then diverging sections, although geometry does not seem to have an important effect on performance. Usually liquid enters the venturi upstream of the throat through nozzles. Alternately, the liquid may flow along the converging section walls until reaching the throat. At the throat, the liquid is shattered into droplets by the high velocity gas.

Venturi performance is shown in terms of its predicted aerodynamic cut size against gas velocity, with liquid to gas ratio as parameter, and with constant pressure drop lines indicated in Figure 5, based on mean drop diameter. A value of 0.25 for the empirical factor, f, has been used; as is appropriate for hydrophobic particles and medium to high liquid to gas ratios.

Once one has computed the required separation cut diameter for a given application, he can find the approximate operating region from Figure 5. This does not tell the whole story however, because the penetration depends not only on the collection efficiency of a single drop but also on the extent to which the gas is swept by drops. In other words, the drop holdup (volume fraction drops) in the throat is a significant factor in determining particle penetration and it cannot be accounted for by a simple power relationship with particle diameter.

Figures 6 and 7, plots of penetration as a function of aerodynamic diameter and the liquid to gas flow rate, show this effect. Note that penetration reaches a limiting value as particle size increases; showing that even though the collection efficiency of one drop for that size particle approaches 100%, there are not enough drops to completely sweep the gas stream.

Plate and Packed Columns

Particle separation in sieve (perforated) and impingement (Peabody type) plates can be defined mathematically by starting from the basic mechanisms of particle collection in bubbles, on drops and jet impaction. Experimental data on performance were used in both cases to evaluate empirical constants in the mathematical relationships. For impingement plates the efficiency is predicted based on the impingement of round jets on plane surfaces.

Some examples of the performance predictions, based as much as possible on experimental data (which are very few for the impingement plate), are given in Figures 8 and 9. Figure 8 is a plot of aerodynamic cut diameter for a sieve plate as a function of air velocity through the holes, u_h, the froth density, F, and hole diameter, d_h. Predictions are given for froth densities of 0.4 and 0.65 and for standard air and water properties. Froth density must be predicted from relationships for sieve plate behavior.

Figure 9 is also a plot of predicted aerodynamic cut diameter for an impingement plate as a function of hole velocity and hole diameter (froth density is not a factor). As in all of the performance figures presented here, the only mechanism considered was inertial impaction.

Packings

Particle collection in packed columns can be described in terms of gas flow through curved passages and performance for a variety of packing shapes can be correlated simply by the packing diameter. Aerodynamic cut diameter is predicted (for inertial impaction) as a function of packing diameter, d_c; bed depth, Z, and bed porosity, ε for three different superficial air velocities and plotted in Figures 10a, and b. Any effect or liquid rate is neglected; this is on the conservative side since the available data indicate that efficiency increases with "Q_L".

Scrubber Energy

The energy required for particle scrubbing is mainly a function of the gas pressure drop, except for pre-formed sprays and mechanically aided scrubbers. Previously we have been shown that there is an empirical relationship between particle penetration and power input to the scrubber for a given scrubber and a specific particle size distribution (Lapple and Kamack (1955) and Semerau (1960)). However, this "power law" did not provide a way to predict performance vs. power input for any size dust.

A new relationship, between d_{PC} and scrubber pressure drop, has been developed by the author and is presented here. Figure 11 is a plot of performance cut diameter (d_{PC}) versus gas pressure drop for sieve plates, venturi (and similar), impingement plates, and packed columns. The basis for the four lines are as follows:

1. Sieve plate particle collection and pressure drop data by Taheri and Calvert (1968) were the source of line #1 in Figure 11. Note that the line and its extensions apply to one or more plates in series because the slope corresponds to $\Delta P \propto d_{PC}^{-2}$. Perforation diameter and spacing will

influence foam density and, therefore, particle penetration so line #1 should be recognized to represent typical (but not all) designs.

2. Venturi penetration and pressure drop data are taken from correlations, such as Figure 5, given in the "Scrubber Handbook". The points used in line #2 are for $Q_L/Q_G \approx 1\ \ell/m^3$, corresponding to about the minimum pressure drop for a given penetration.

3. Impingement plate data used for line #3 were predicted, as described earlier, because no reliable experimental data were available. Cut diameters for 2 and 3 plates in series are 88% and 83% of those shown in line #3, which is for 1 plate.

4. Packed column penetration and pressure drop data were taken from the correlations given in the Scrubber Handbook. Line #1 is representative of columns from 1 to 3 meters high and packing of 2.5 cm nominal diameter.

It is interesting to observe that the four lines are quite close together, despite the differences in slopes. The sieve plate and venturi lines are identical with slopes such that $\Delta P \propto d_{PC}^{-2}$. Thus, a reduction of cut diameter by a factor of 1/2 would result in a pressure drop 1/4 the original.

To estimate the penetration for particle diameters other than the cut size, under a given set of operating conditions, one can use the approximation of equation (3) with $B = 2.0$. Alternatively, one could use more precise data or predictions for a given scrubber. Figure 12 is a plot of the ratio of particle aerodynamic diameter to cut diameter versus penetration for that size particle (d_{pa}), on log-probability paper. One line is for equation (3) and the other is based on Figure (6) for a venturi scrubber.

Performance Limit for Inertial Impaction

The limit of what one can expect of a scrubber utilizing inertial impaction is clearly indicated by Figure 11. From line #2, for a venturi, and its extrapolation we can pick some illustrative points as shown in Table II, below. Particle sizes for penetrations of 0.1 and 0.9 (i.e., collection efficiencies of 90% and 10%, respectively) were computed from d_{PC} by means of Figure 12.

TABLE II

Particle Diameters for Several Penetrations and Pressure Drops

ΔP (cm W.C.)	d_{PC} (μmA)	d_{pa} (μmA) Pt $\overset{@}{=}$ 0.1	d_{pa} (μmA) Pt $\overset{@}{=}$ 0.9	ΔP (in W.C.)
50	1.0	1.8	0.4	19.6
100	0.72	1.3	0.29	39.4
200	0.52	0.93	0.21	79.0
400	0.37	0.67	0.15	157.0

If a cut diameter of 1.0 μmA, or smaller is required, the necessary pressure drop is in the medium to high energy range. High efficiency on particles smaller than 0.5 μmA diameter would require extremely high pressure drop if inertial impaction were the only mechanism active.

High efficiency scrubbing of sub-micron particles at moderate pressure drop is possible, but it requires either the application of some particle separation force which is not dependent on gas velocity or the growth of particles so that they can be collected easily. Particle separation phenomena which offer promise and have been proven to some extent are the "flux forces" due to diffusiophoresis, thermophoresis, and electrophoresis. Brownian diffusion is also useful when particles are smaller than about 0.1 μm diameter.

Particle growth can be accomplished through:

1. Coagulation (agglomeration)
2. Chemical reaction
3. Condensation on particles
4. Ultrasonic vibrations
5. Electrostatic attraction

Summary and Conclusions

Wet scrubbers can collect fine particles with high efficiency under the proper circumstances. When particle collection is due to inertial impaction only, high efficiency on sub-micron particles requires the expenditure of high pressure drop. Other particle separation phenomena such as Brownian diffusion, diffusiophoresis, thermophoresis, and electrophoresis can give high efficiency at low pressure drop. Particle growth by any of several mechanisms can provide the means for subsequent high efficiency collection by inertial impaction.

In view of the other presentations to be made at this Symposium, this paper emphasizes the inertial impaction collection mode, which is most characteristic of present scrubber operation. Charts for the estimation of scrubber performance and energy requirement are presented.

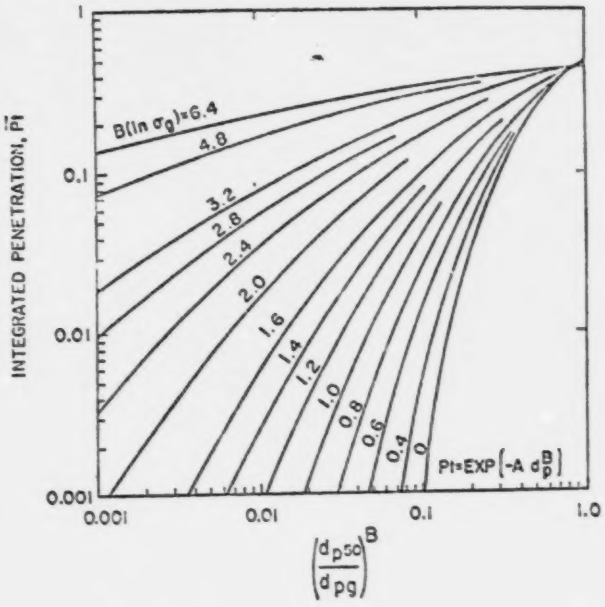

Figure 1
Integrated (overall) penetration as a function of cut diameter, particle parameters and collector characteristic.

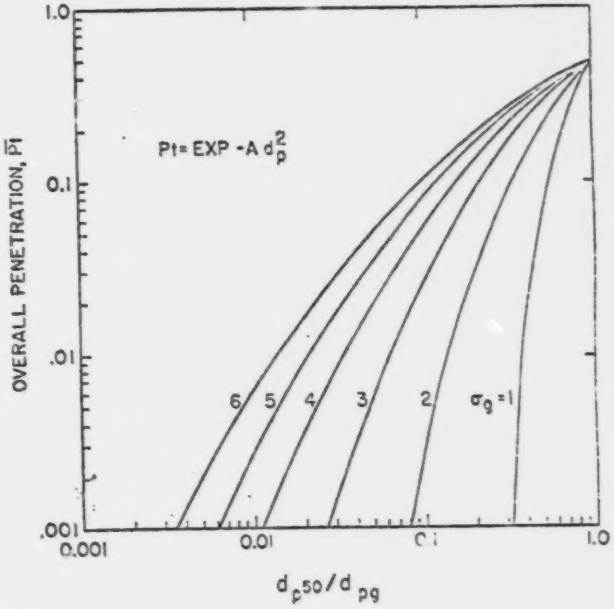

Figure 2
Overall penetration as a function of cut diameter and particle parameters for common scrubber characteristic, B = 2.

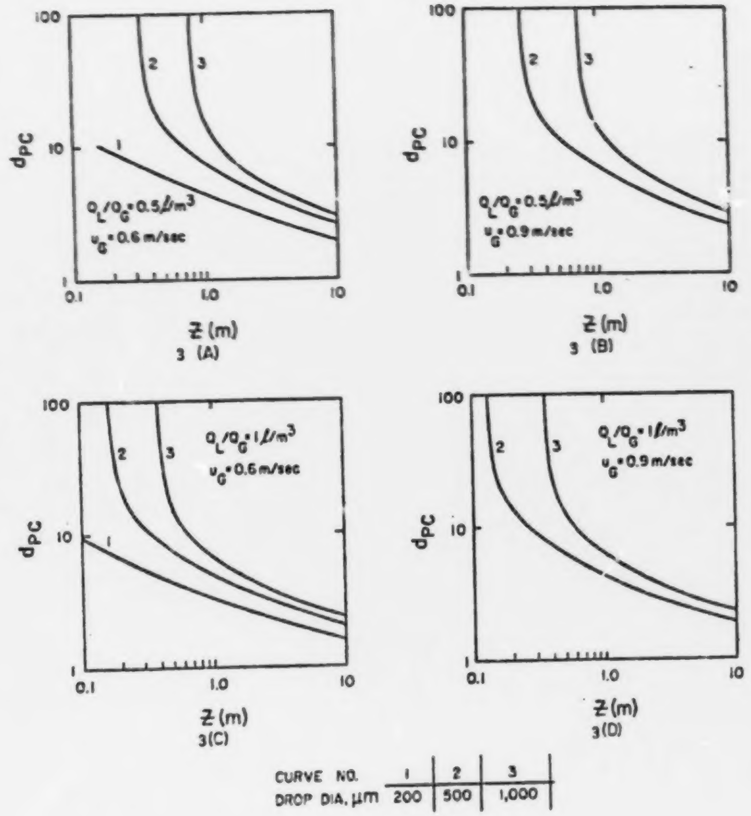

Figure 3
Performance cut diameter predictions for typical vertical countercurrent spray.

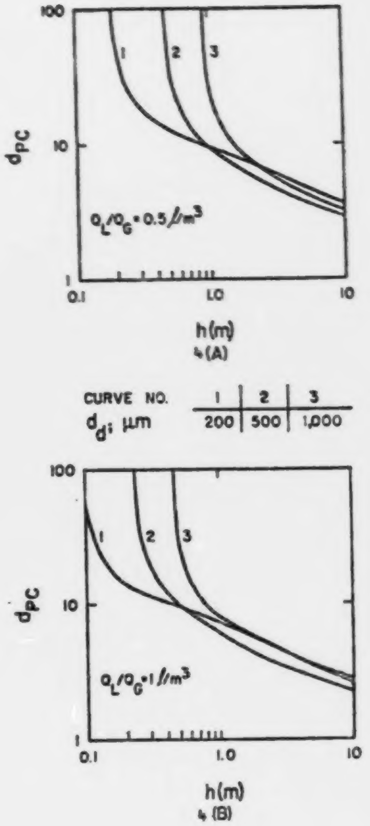

Figure 4
Performance cut diameter predictions for typical cross-current spray.

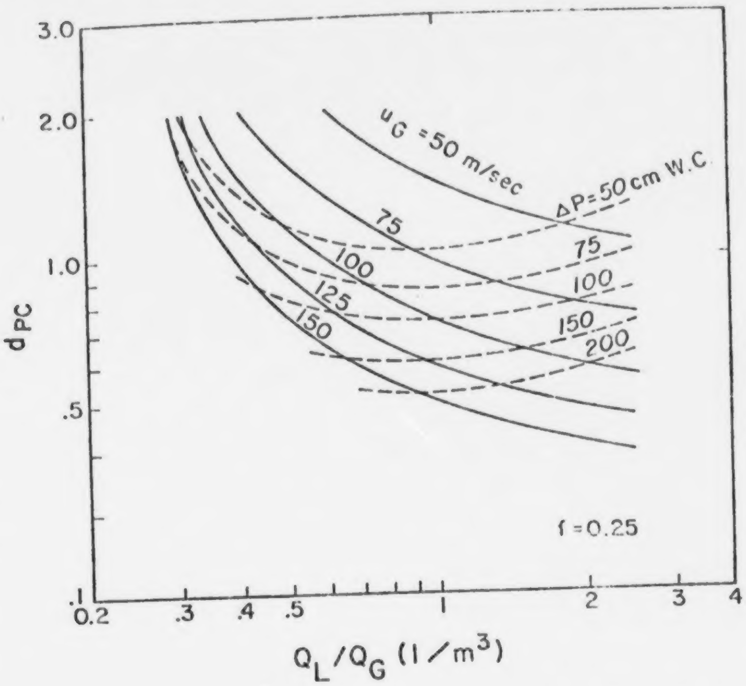

Figure 5
Performance cut diameter predictions for
venturi scrubber.

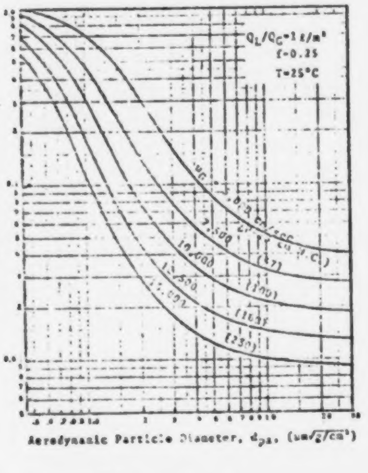

Figure 6
Venturi scrubber penetration
vs. aerodynamic particle
diameter with gas velocity
as parameter.

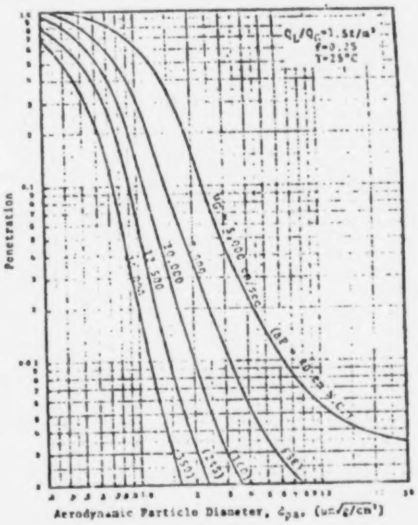

Figure 7
Venturi scrubber penetration
vs. aerodynamic particle
diameter with gas velocity
as parameter.

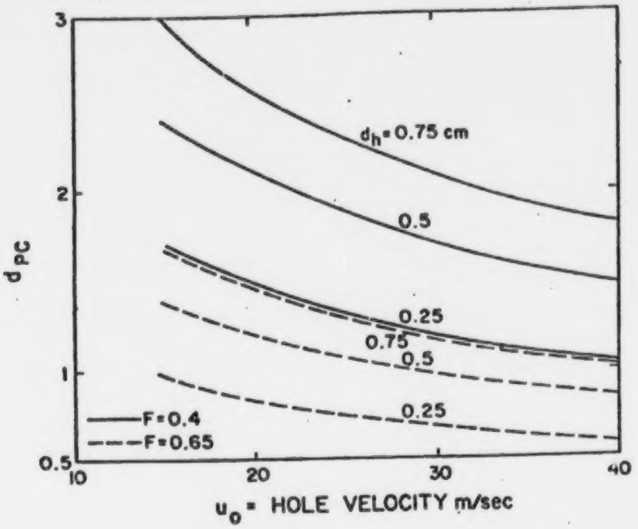

Figure 8
Performance cut diameter prediction for typical sieve plate conditions.

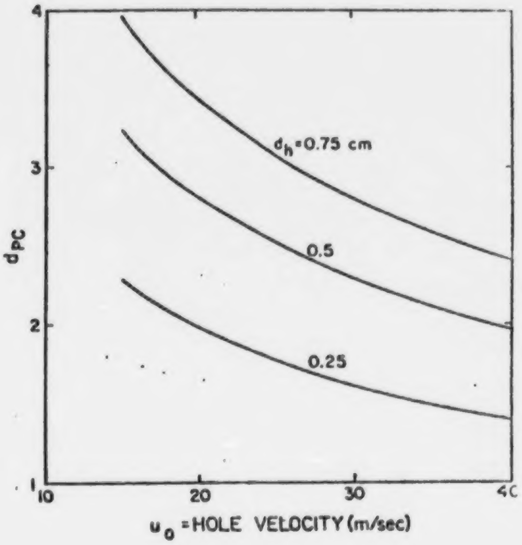

Figure 9
Performance cut diameter predictions for typical impingement plate conditions.

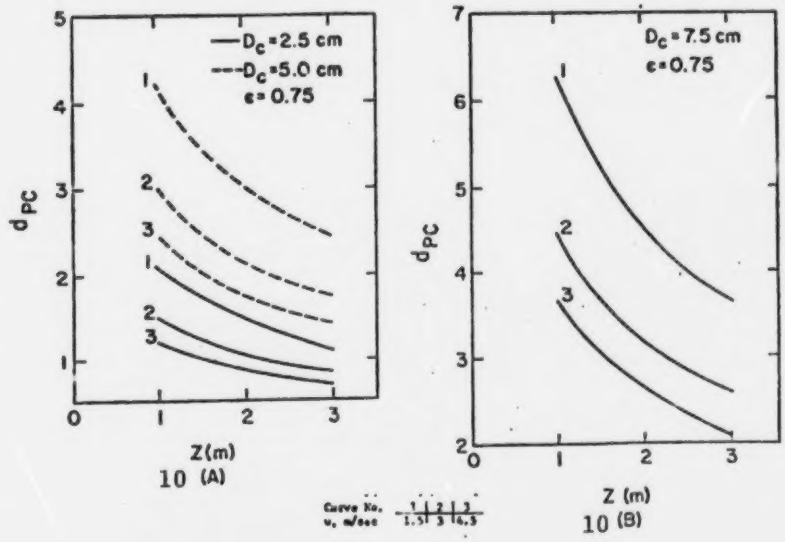

Curve No.	1	2	3
u_o m/sec	1.5	3	4.5

Figure 10
Performance cut diameter predictions for typical packed bed conditions.

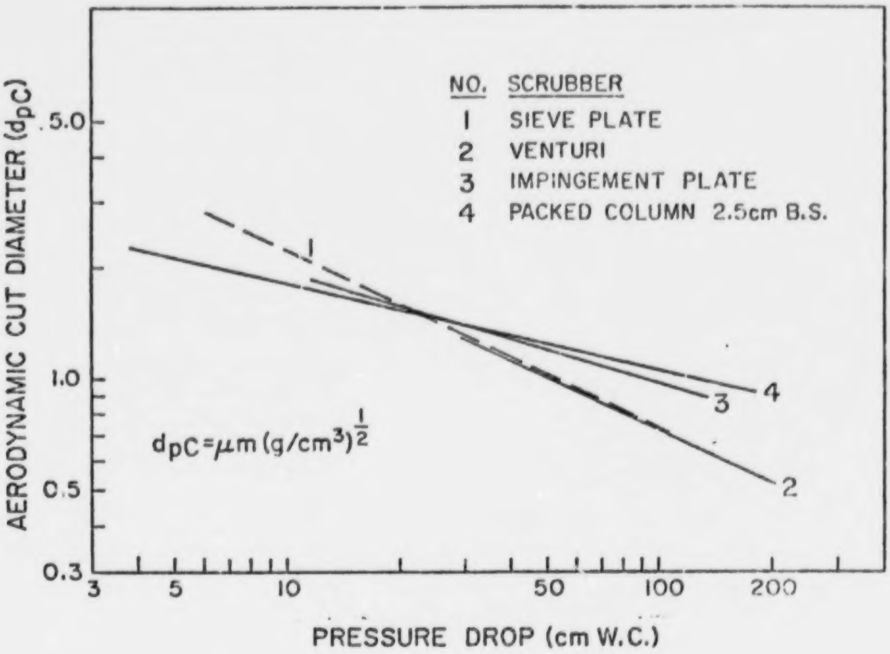

Figure 11
Representative cut diameters as a function of pressure drop for several scrubber types.

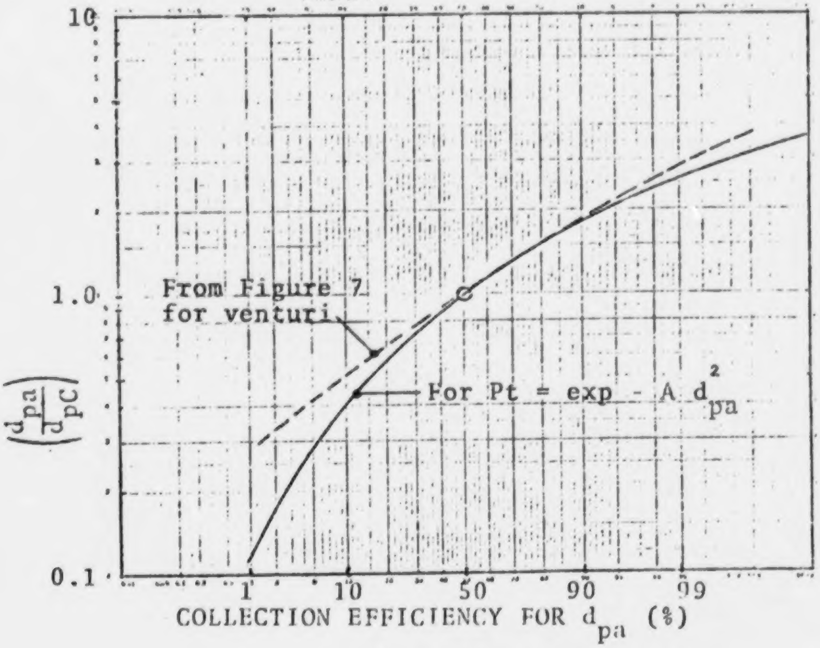

Figure 12
Ratio of particle diameter to cut diameter as a function of collection efficiency.

NOMENCLATURE

Latin

A = a constant in eq. (3)
A_d = total outside surface area of drops in scrubber cm^2
B = a constant in eq. (3)
C' = Cunningham correction factor
d_b = bubble diameter, cm
d_c = packing diameter (nominal), cm
d_d = drop diameter, cm
d_h = sieve plate hole diameter, cm
d_p = particle diameter μm or cm
d_{p50} = diameter of particle collected with 50% efficiency μm
d_{pa} = aerodynamic particle diameter μmA
d_{PC} = performance cut diameter (aerodynamic), μmA
d_{pg} = geometric mean particle diameter, μm
d_{RC} = required separation cut diameter (aerodynamic), μmA
E = efficiency, fraction or %
f = empirical constant for sprays
F = foam density, g/cm^3
h = height of scrubber, cm
Pt = penetration = 1 - E, fraction or %
$\overline{Pt}$ = average (integrated over particle size distribution) penetration, fraction or %
ΔP = pressure drop, cm W.C. or atm.
Q_G = gas volumetric flow rate, m^3/sec
Q_L = liquid volume flow, m^3/sec or l/sec
r_c = collector radius, cm
r_d = radius of drop, cm
u_d = drop velocity relative to duct, cm/sec
u_G = gas velocity relative to duct, cm/sec
u_h = gas velocity through sieve plate hole, cm/sec

w = weight of particles, g

W = width of rectangular jet or diameter of round jet, cm

W.C. = water column = pressure as measured by water manometer, cm

Z = height of packing or column, m or cm

Greek

ϵ = fraction void volume space

ρ_L = liquid density, g/cm^3

ρ_p = particle density, g/cm^3

σ_g = geometric standard deviation of particle size distribution

REFERENCES

Calvert, S., J. Goldshmid, D. Leith, and D. Mehta. Scrubber Handbook. A.P.T., Inc. Riverside, California. EPA Contract No. CPA-70-95. August 1972. PB-213-016.

Lapple, C. W., and H. J. Kamack. Performance of Wet Dust Scrubbers. Chem Eng Prog. 51(3):110-121, March 1955.

Semrau, K. T. J Air Pollution Control Assoc. 10, 200 (1960).

Taheri, M., and S. Calvert. Removal of Small Particles From Air by Foam in a Sieve-Plate Column. J Air Poll Control Assoc. 18:240-245, 1968.

Paper No. 10

USE OF VENTURI SCRUBBERS FOR REMOVAL OF HIGHLY DISPERSIVE PARTICULATES

by

Georgy K. Lebedyuk

STATE RESEARCH INSTITUTE
OF INDUSTRIAL AND SANITARY GAS CLEANING

Moscow

Use of Venturi Scrubbers for Removal of Highly Dispersive Particulates

G. K. Lebedyuk

Venturi scrubbers appear to be most universal of scrubbers used because of wide range of their applicability and their efficiency in removal of particulates. Their special value lies in very successful removal of highly dispersive particulates. This successful removal can be accomplished because high energies in contact zone can be applied in venturi scrubbers efficiently. 1500-30,000 n/m^2 is the range of hydraulic resistance which can be used in venturi scrubbers. Scrubbers which use pressure drops 10,000-30,000 n/m^3 are used in removal of micron and submicron particulates.

Simplicity in design and use of venturi scrubbers also explain their wide use.

Venturi scrubbers can be divided into three groups based on their energy supply. Energy necessary for scrubbing can be carried by:

1. Gas and scrubbing liquid
2. Gas
3. Scrubbing liquid

In the first case, scrubber works with a fan and pump, in the second case, only with a fan (self-induced spray venturi scrubbers), and in the third case, only with a pump (ejector venturi scrubbers).

At the present time, many varied designs for venturi gas atomized spray scrubbers exist. This multiplicity is a result of insufficient knowledge of aerosol collection mechanism in scrubbers and also is a result of patent plan considerations.

In actual design scrubber installations often differ significantly from a classical venturi scrubber.

Differences exist in configuration of transverse cross-section of contact zone, in longitudinal geometry of contactor, in ways of supplying spray liquid, in entrainment separators and in combinations of the above.

In transverse cross-section, contact zone is either round or rectangular or ring-shaped slit.

Longitudinal geometry is also varied but most often it approximates venturi profiles. Such longitudinal geometry assures minimal aerodynamic losses.

Following, is the list of ways in which spray liquid is applied to contact zone of a scrubber.

1. Central supply through nozzle.
2. Central supply with help of atomizer.
3. Peripheral supply.
4. Film supply.
5. Supply with preliminary atomization of liquid with obstructions.
6. Combination supply.

Almost all known entrainment separators can be used in venturi scrubbers. Following is the list of most widely used ones:

1. Cyclon separators with director and reverse gas flow.
2. Separators with twisted elements.

3. Column separators.

4. Separating capacities (settling chambers).

Form of transverse cross-section, longitudinal geometry of contact zone, supply of liquid to the contact zone assuring even distribution to the entire cross-section do not affect the efficiency of venturi scrubbers. It is the type of the entrainment separator that has great influence on efficiency of venturi scrubbers.(1) At the present time, more frequently two-step schemes of separation are used.

In combinations, venturi scrubbers have significance individually as well as in groups.

Under normal conditions, use of sequentially set-up venturi scrubbers do not raise general level of cleaning in comparison to a single level scrubber which has the same energy expenditures. This was shown in experimental studies and in practical applications. However, with wide range of gas temperatures before cleaning it becomes advantageous to use a two-level scrubber scheme. In the first level small energy expenditures are calculated. Sufficient amount of liquid is used in the first level to cool and stabilize gas volumes. In this way, conditions are set up for efficient scrubbing in the second level.

Figure 1 shows the relationship between collecting efficiencies of different types of scrubbers (including venturi scrubber) and amount of energy losses for those scrubbers. Data comes from numerous experimental and industrial scale installations.

Nomogram shows the efficiency and energy expenditure relationship for only four particle fractions. For other values, relationship can be obtained with parametric scale.

Relationship between collection efficiency and energy losses is presented on the nomogram as shaded areas rather than as lines. This is because removal of particulates from gas depends on their physical-chemical properties, gas characteristics, temperatures, humidity, etc. With an increase in expended energy in scrubbers, influence of those factors decreases.

Nomogram shown in Figure 1 concerns itself only with effective energy expenditures in scrubbers' contact zone. Energy expenditures in overcoming aerodynamic resistance in the gas stream and coefficients of effective performance for induction of gas and liquid flow are not accounted for in the nomogram. This means that actual energy expenditures for gas cleaning with scrubbers are twice as high.

Besides three basic scales (energy expenditures in kilowatt/m^3 of cleaned gas, suspended particles removal efficiency, particle dispersion expressed in % and in microns) nomogram has scale which shows by how much outlet concentration of particles is lower than inlet concentration. Another scale on the nomogram shows pressure drops in the scrubber with the assumption that all energy for contact is supplied only by gas. Nomogram qualitatively and quantitatively allows for evaluation of the need for an increase in energy expenditures with a decrease in sizes of collected particles. It also allows for evaluation of the need to increase requirements to standard gas scrubbing.

References

1. Lebedyuk, G. K. Evaluation of Wet Gas Scrubbing including Entrainment Separators "Khimicheskaya promyshlennost", 1968, No. 5, 368-369.

2. Lebedyuk, G. K. Applicability of Use of Wet-Scrubbing Methods for Particulate Removal from Gases and Choices of Scrubber Installations. Collection of papers presented at inter-regional seminar on gas cleaning, Yaroslavl, 1972, 104-109.

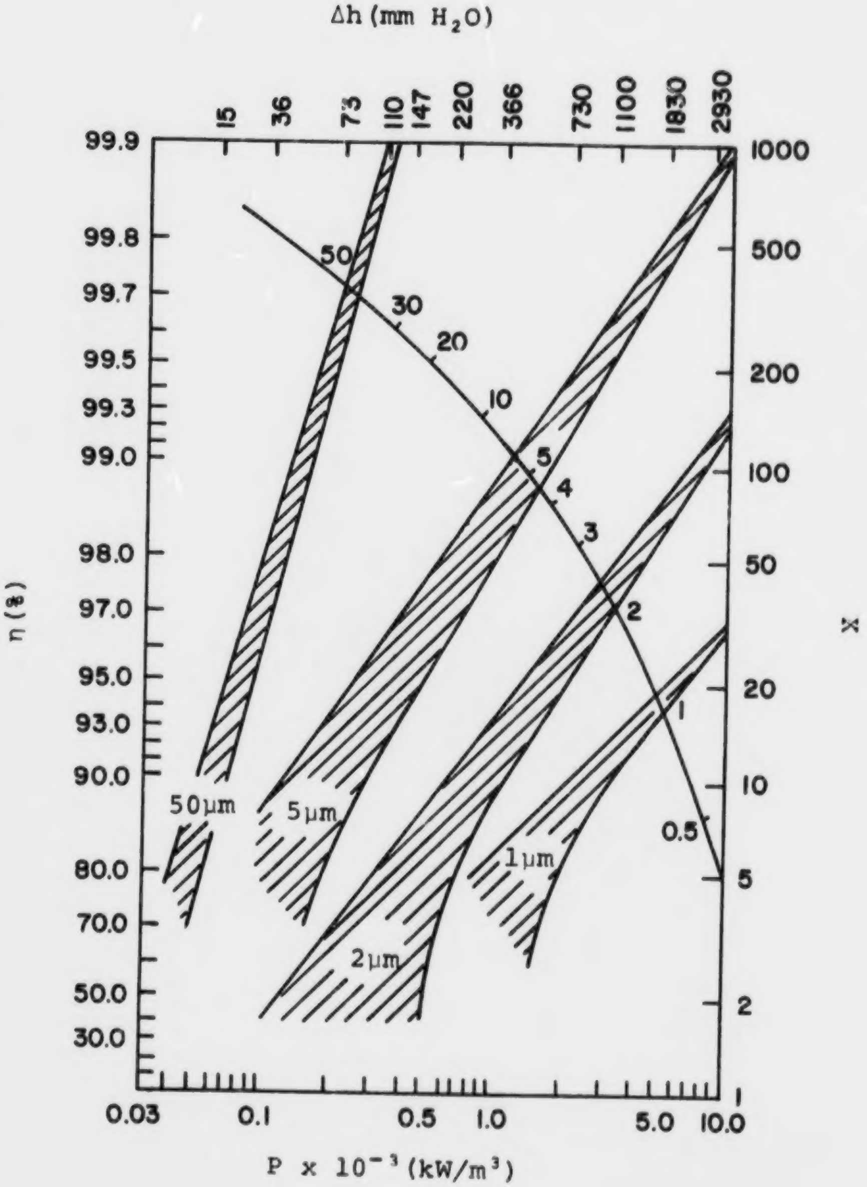

Figure 1. Relationship of the collection of suspended particles from a gas stream to energy consumption in the contact zone of a wet scrubber.

Paper No. 11

WET GAS CLEANING IN IRON AND STEEL INDUSTRY

by

Georgy K. Lebedyuk,
A. Yu. Valdberg,
and
F. Ye. Dubinskaya

STATE RESEARCH INSTITUTE
OF INDUSTRIAL AND SANITARY GAS CLEANING

Moscow

Wet Gas Cleaning in Iron and Steel Industry

G. K. Lebedyuk, A. Yu. Valdberg, F. Ye. Dubinskaya

It is necessary to use highly efficient methods to remove particulates from gases originating in different metallurgical processes. With absolute growth of metallurgical production, their intensification as a result of oxygen furnace application, change to a system of gas removal without complete combustion of CO , concentration of emitted particulates has increased.

Figure 1 shows data on particulate dispersion composition at inlet to gas cleaning equipment in a number of metallurgical processes. Data is presented in form of integral curves of distribution.

In principle, particulates can be removed from gases using dry methods (electrostatic precipitators, bag filters) as well as using high-pressure wet scrubbers.

High initial gas temperature, explosiveness, flamability of particulates, significant temperature fluctuations, and significant fluctuations in gas volumes influence the choice of gas cleaning methods.

Electrostatic precipitators are used in cleaning gas from blast furnaces and especially from open-hearth furnaces. Introduction of bag filters on an industrial scale to clean gases from electric furnaces is being considered.

Wet scrubbing is the only method used to remove particulates from gases of converters and closed melting furnaces. Wet scrubbing is also used in some metallurgical plants in cleaning of gases from open-hearth and electric furnaces.

In cleaning gas from metallurgical plants, basically, two types of wet scrubbers are used: Open spray scrubbers and Venturi scrubbers. The former is used as a conditioning step which cools, humidifies the gas and removes large particles. Open scrubbers are also used in conditioning of gas which is cleaned with dry methods. (blast, open-hearth, and electric furnaces)

Use of open spray scrubbers as conditioners to dry gas cleaning systems is more difficult than their use in systems of wet scrubbing. In wet scrubbing systems, where gases can be cooled to saturation, it is possible to apply coarse sp ray which works effectively with recycled water. When open spray scrubbers are used as conditioners to electrostatic precipitators and bag filters, it is necessary to keep temperature of removed gases above dew point. For this reason, it is necessary to use atomizers which assure a very fine spray. The atomizers have to work under high-pressure and with small nozzle diameter. Recycled water supplied to the scrubber has to be cleaned extremely well for that reason.

Efficiency of gas cleaning with open spray scrubber can be increased with the use of condensation effect. This takes place during cooling of gas to low temperatures in wet scrubbing systems.

Using as an example work of open spray scrubbers in closed melting furnaces, Figure 2 shows an effect of the level of gas cooling (in other words extent of condensation of water vapor) on particulate concentration at outlet of apparatus.

In all cases gases were practically completely saturated with water vapor (gas dew point 60-70°C) at inlet to the scrubber. Outlet concentration of particulates decreased with an increase in cooling level. Maximum efficiency of collection was reached with highest condensation. This was true regardless of the type of open scrubber and regardless of the type of spray system used.

Fine cleaning of gases in USSR metallurgic plants is done in high-pressure venturi scrubbers. Their use allows to bring final concentration of particulates in gas down to practically any desired level.

Efficiency of particulate collection in venturi scrubbers can be calculated on the basis of energy expenditures according to which level of particulate removal from gas is determined by specific energy consumption and does not depend on sizes and design features of scrubbers. Design of wet scrubbers and its use should be optimal to aerodynamics of gas stream and to good supply of spray liquid.

In that case, all energy losses for wet scrubbing of gas are calculated from following expression:

$$N_4 = A \; K_4^{x} \qquad (1)$$

where: N_4 - number of transport units, determined from relationship

$N_4 = n \frac{Z_1}{Z_2}$, Z_1, Z_2 - concentration of particulates in gas before and after scrubbing, Kg/m^3.

K_4 - energy expenditures for cleaning 1000 m^3 of gas.

A,x - constants, determined by dispersion composition of dust.

Value of K_4 for venturi scrubber is found from the formula:

$$K_4 = \Delta P_p + \Delta P_{es} + m P_{\ell}$$

where: ΔP_p - hydraulic resistivity of venturi pipe, n/m^2;

Δ Pes - hydraulic resistivity of entrainment separator, n/m^2;

m - specific discharge of spray liquid, m^3/m^3;

P_{ℓ} - pressure of sprayed liquid, n/m^2.

Values of coefficients A and X for a number of metallurgic processes are shown in Table 1.

It is not difficult to calculate necessary energy expenditures for wet scrubbing of gas and to choose gas cleaning equipment knowing concentration of particulates at inlet and requirements for final concentration, (sanitary norms as set by Ministry of Health in USSR.)

Figure 3 shows data on final concentration of particulates in converter gases as it depends on hydraulic resistivity of venturi scrubbers. Data represents different industrial plants in USSR.

Studies conducted in NIIOGAZ and analysis of wet scrubber performance abroad have shown that efficiency of particulate collection to a large degree depends on chemical composition of particulates.

Table 2 shows chemical composition of particulates from several metallurgic operations.

As an example, presence of SiO_2 in ferroalloy particulates (above 70% in melting of siliceous alloys and 20-30% in melting of silicomanganese) is acknowledged with an exceptionally low allowable breathing zone concentration: 1 mg/nm^3 with melting of siliceous alloys and 2mg/nm^3 with melting of silicomanganese. Because of this in combustion of gases final particulate concentration should not exceed 30mg/nm^3. The same applies to melting of quality steel.

Low concentration of Mn and SiO_2 in particulates from converters and open-hearth furnaces makes them practically non-toxic. This allows for emission of gases with final particulate concentration up to 100mg/nm^3.

Venturi scrubbers used in metallurgic plants do not differ in design from those used in other industries. However, depending on the quantity

TABLE 1

Parameters A and X For Some Furnaces in Metallurgic Industries

Type of Particulate	A	X
Converter particulates (oxygen furnace)	9.88×10^{-2}	0.466
Particulates from basic Bessemer converter	0.268	0.26
Particulates from open-hearth furnace	1.915×10^{-2}	0.57
Particulates from open-hearth furnace	1.74×10^{-6}	1.59
Particulates from open-hearth furnace which uses oxygen enriched blowing torch	1.565×10^{-6}	1.62
Cupcla furnace	1.355×10^{-2}	0.62
Particulates from blast furnaces	0.1925	0.325
Particulates from closed melting furnaces: 45% ferrosilicon	2.42×10^{-5}	1.26
Silicomanganese	6.9×10^{-3}	0.67
Carbon Ferrochrome	6.49×10^{-5}	1.1

TABLE 2

Chemical Composition of Particulates
(% by weight)

Type of Particulate	Type of Alloy	Fe_{total}	SiO_2	MnO	CaO	MgO	FeO	C	S	V
particulates from melting furnaces	Si -18	-	65.7- 78.4	0.6- 0.9	1.0	0.1- 0.4	6.0- 9.6	6.8- 8.7	2.9- 4.65	-
	Si -25	-	68.2- 76.8	0.17- 0.25	0.3- 0.5	0.19- 0.2	3.7- 7.5	6.6- 9.0	2.25- 3.6	-
	Si -45	-	77.8- 91.25	0.35- 0.6	0.24- 6.8	1.52- 6.8	3.22- 6.48	-	2.95- 12.35	-
	commodity silicomanganese	-	18.9- 26.6	23.5- 29.2	2.4- 3.7	6.9- 11.8	0.3- 0.5	2.6- 3.8	2.1- 3.1	-
	cast silicomanganese	-	37.0	30.3	2.5	1.2	1.22	9.61	3.2	-
particulates from converter	steel from cast iron	67.2	2.1	1.83	4.45	0.45	13.3	-	-	-
	steel from phosphorous iron	60.3	0.44	-	8.14	2.0	-	-	-	-
	steel from vanadium iron	68.4	1.62	1.2	2.0	tr	-	-	-	0.12
open-hearth particulates	steel from Oxygen-fed torch	49.5- 58.3	1.0- 5.45	2.30- 3.70	0.65- 9.16	0.75- 4.34	-	-	-	-
	steel from Oxygen-fed tank	52.7- 66.0	1.2- 4.2	1.97- 2.78	1.98- 6.24	0.34- 1.85	-	-	-	-
electric furnaces	high-quality steel	13.3- 14.0	14 - 22	4.0	17-22	30-38	-	2.3	0.25	-
particulates from between bell space of blast furnace	--	38.2	12.6	-	10.6	9.0	8.5	8.5	0.23	-

of gas for cleaning, two types of set ups are used. One venturi pipe is used with small gas volumes. (closed melting furnaces, electric furnaces with up to 20t capacity). When the volume of gas is large battery Venturi scrubber or a group consisting of a few venturi pipes is used. Battery venturi scrubber used for cleaning convertor gases (Fig. 4) is composed of a large number of venturi pipes with sprayers of nozzle diameter 90mm (opening angle 63°, of diffuser - 7°). This scrubber has two modifications. In first modification, two plates with perforations of 6mm diameter and free cross-section 0.24 m^2/m^2 are used. In the second modification, battery of direct flow cyclons with diameter 500mm and height 3.5 m is used.

Insufficiently treated water used for spraying causes plugging up of sprayers. Significant decrease in efficiency of cleaning is caused by even a small number of sprayers not functioning. Because of this individual supply of spray to each venturi pipe is lately being substituted with spray (coarse spray, large nozzle diameter) supplied from top of the apparatus designed (above pipes) to cover scrubber's entire cross-section.

Use of a group of venturi scrubbers assures better exposure of clogged up sprayers than the battery arrangement. Group of venturi scrubbers has been used for cleaning of gases from large capacity electric furnaces.

An advantage of group and battery scrubbers is the possibility to disconnect some pipes with changeable gas volumes. However, the question of regulation can also be solved by use of pipes with changeable nozzle cross-section, bypassing part of the gas and changing specific amount of spray. Studies have shown that the last method can be used only with small fluctuations of gas volume. Usually specific amount of spray used in venturi pipes is 0.5 to 1.5 ℓ/m^3.

For fine cleaning of gases, two step venturi scrubber system is used. In the first step, venturi works in a low-pressure system. It cools and humidifies the gas. In the second step, venturi works in a high-pressure system.

Low-pressure venturi scrubber is also used in cleaning of gas from blast furnace before wet electrostatic precipitator. Combined use of venturi scrubber and electrostatic precipitator assures high collection efficiency when volume of gas from blast furnace fluctuates. With lowered volume of blast furnace gas efficiency of venturi scrubber decreases and that of ESP increases. Just the opposite is true with an increase in gas volume although hydraulic resistance in venturi scrubber also increases slightly.

Successful work is being conducted in the Soviet Union on application of ejector scrubbers for cleaning metallurgic plant gases. This type of scrubber is advantageous because it guarantees necessary levels of gas cleaning and allows for elimination of mechanical inducers of gas flow from gas cleaning scheme. One more advantage to the use of ejector scrubbers is the possibility of creating gas cleaning schemes which work under pressure. That is, with ejector scrubbers reliable and safe schemes can be developed for cleaning of gas which has higher and unstable CO content. Such cleaning is advantageous for metallurgical processes without complete CO combustion and for the use of chemically bound heat of removed gases in regenerators.

Two types of ejector scrubbers are used to clean gases from iron and steel melting processes. Those are scrubbers working with high liquid pressures (up to hundreds of atmospheres) with small specific discharge ot liquid (up to 1 ℓ/m^3) and scrubbers which use liquid pressures up to 15 atm. with specific discharge of liquid up to 10 ℓ/m^3.

Ejector scrubbers are used for cleaning of gases from cupola, open-hearth and arc furnaces.

In metallurgic plants wet scrubbing is almost always a closed cycle spraying. Water used is recycled. Therefore, for reliable operation of the system quality of spraying liquid is important for gas cleaning especially in venturi scrubbers used for final cleaning.

Cooling and chemical cleaning of regenerated water is just as important as its treatment to assure not only stable efficiency but also high operational reliability of the entire system. Figure 5 shows a system of cleaning gas from melting furnaces which includes recycling of water. Every twenty-four hours, quantity of fresh water is added which does not exceed 1 to 1.5% of entire water volume.

Table 3 shows characteristics of a number of wet scrubbers from melting operations of USSR.

Table 3

Characteristics of Wet Scrubbers Used on Closed Melting Furnaces in U.S.S.R.

Alloy	45% Ferrosilicon	75% Ferrosilicon	Silico-Manganese	Carbon Ferrochrome
Furnace Type	RKZ - 16.5	RKZ - 16.5	RPZ - 48	OKB - 539
available capacity	12.3-14.65	12.5-13.3	35.8-42.3	9.5-10.5
number of simultaneously working gas outlets	1	2	3	1
volume of gas for cleaning nm^3/hr.	2000-2500	2700	7500-8400	2200-2500
gas temp. °C:				
°before level 1	850	-	274-345	150-360
°before level 2	49-58	-	38-45	30-34
°at outlet from gas cleaning system	47-55	-	35-40	28-30
particulate concentration g/mm^3:				
°at inlet	29-30	46-74	25.6-31.3	6-11
°following 1st level	6-13	5-8	6-12	2-4
°at outlet	0.02-0.07	0.008-0.007	0.02-0.06	0.08-0.07
specific volume of regenerated water, l/nm^3:				
°for 1st level	22-35	12-15	35	9.0-9.6
°for 2nd level	3.4-4.6	1.85-2.2	0.6-2.0	2.9-7.6
hydraulic resistance of scrubber Kn/m^2	19-21	-	20-26	18-23

REFERENCES

1. Dubinskaya F. Ye., Zaytsev M.M. "Cleaning of Gases from Small Oxygen Converters", Nllinformatyazhmash, 1966, 48-51.

2. Goltsman M.I., Karmyshev V.V., Belokon S.M. "Removal and Cleaning of Gas from Melting of Ferrosilicon 51-75 in Closed Electric Furnaces", Collection of papers VN1P1 Chermetenergoochistka, publisher: Metallurgiya, ed. 14, 1974.

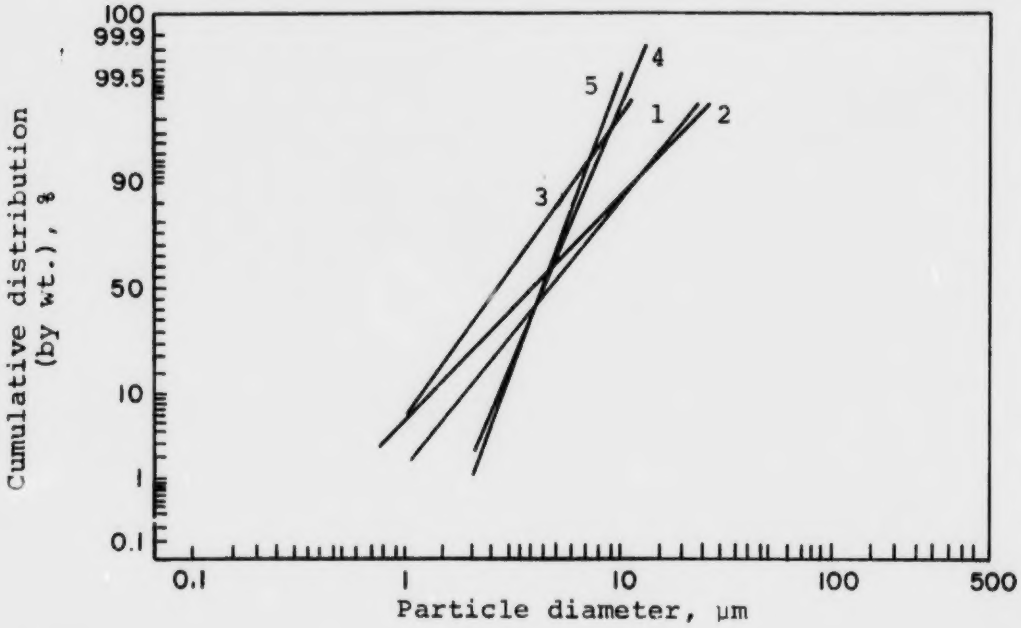

Figure 1. Particle size distribution, particles from metallurgic furnaces:

1. electric furnace; 2. oxygen converter; 3. preparation of silicomanganese in closed furnace; 4. preparation of 75% ferrosilicon in closed furnace; 5. preparation of 45% ferrosilicon in closed furnace.

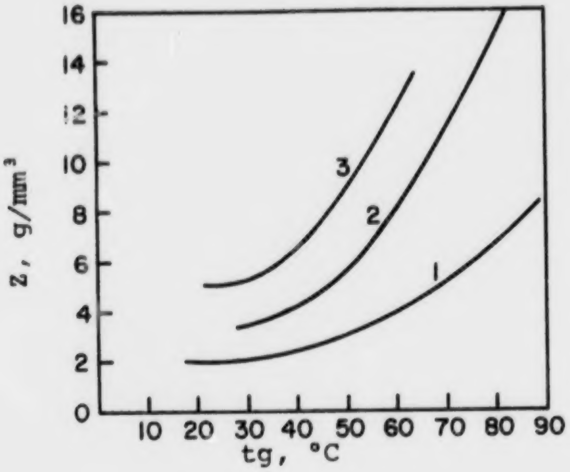

Figure 2. Relationship between particulate concentration at outlet of scrubber and gas temperature:

1. Preparation of 45% ferrosilicon, initial concentration of particulates 10-20 g/nm³.

2. Preparation of silicomanganese, initial concentration of particulates 10-20 g/nm³.

3. Preparation of 45% ferrosilicon, initial concentration of particulates 20-30 g/nm³.

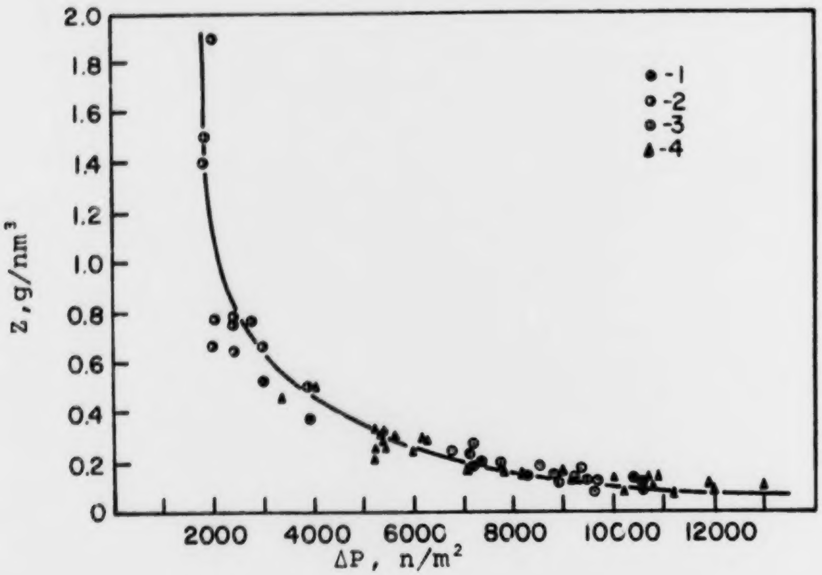

Figure 3. Relationship between final particulate concentration in converter gases and hydraulic resistance of Venturi scrubber:

1. converter of 10t capacity, battery Venturi scrubber (30 pipes),

2. converter of 27t capacity. Venturi scrubber with 400 mm nozzle diameter,

3. converter of 130t capacity, battery Venturi scrubber (96 pipes),

4. converter of 50t capacity, Venturi scrubber with 500 mm nozzle diameter.

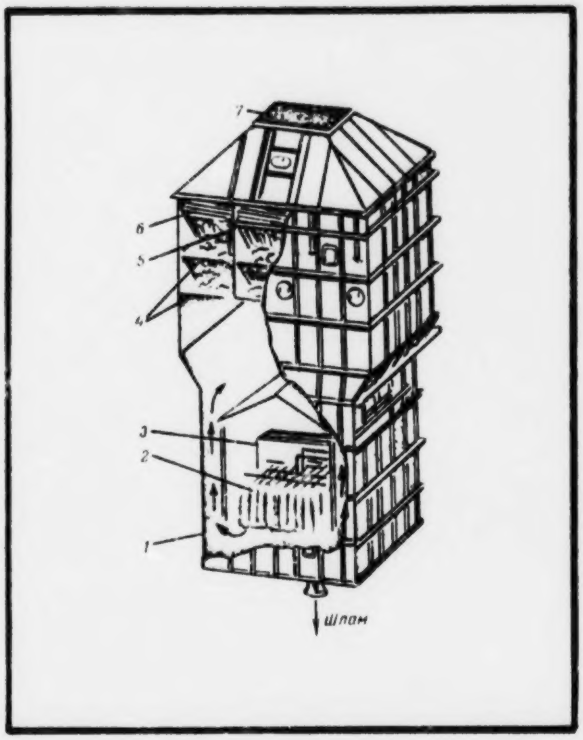

Figure 4. Battery Venturi scrubber:

1. body; 2. Venturi pipe, 3. supply of liquid,
4. plates, 5. supply of liquid to plates, 6. entrainment separator, and 7. gas outlet.

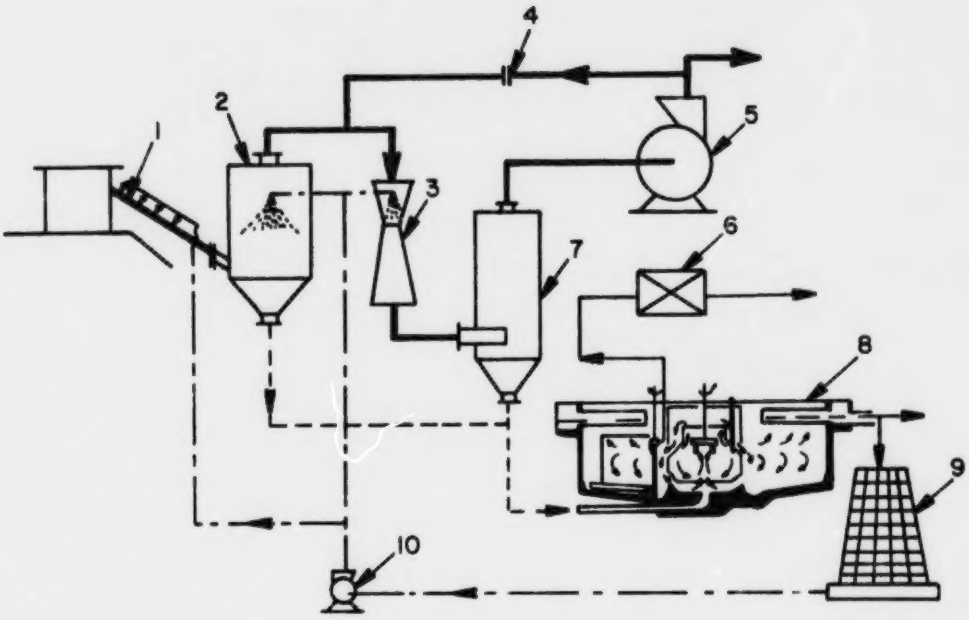

Figure 5. System of cleaning gases from closed melting furnaces:

1. inclined spray gas stream;
2. open spray scrubber;
3. Venturi pipe;
4. valve regulating bypassing of cleaned gases;
5. fan
6. filter-press;
7. cyclon - entrainment separator;
8. settling tank for water treatment;
9. water-cooling system;
10. pump

Paper No. 12

EFFECT OF WATER VAPOR CONDENSATION ON PARTICLE COLLECTION BY SCRUBBERS

by

Leslie E. Sparks

U. S. ENVIRONMENTAL PROTECTION AGENCY

Research Triangle Park, N. C.

Preceding page blank

ABSTRACT

Water vapor condensation can be used to improve particulate collection by scrubbers. The improved particulate collection is due to diffusiophoresis and/or particle growth. Scrubbers which utilize condensation are defined as condensation scrubbers. The literature on condensation scrubbing is reviewed. The results of recent EPA sponsored research on condensation scrubbing are presented. These results show that the particle collection efficiency of a condensation scrubber is a function of the amount of water vapor condensed. The costs of condensation scrubbing are compared with the costs of high energy scrubbing. The comparison indicates that condensation scrubbing is economically feasible for many applications.

EFFECT OF WATER VAPOR CONDENSATION ON PARTICLE COLLECTION BY SCRUBBERS

by

L. E. Sparks

I. Introduction

It is generally recognized that large energy expenditures are required to achieve high particle collection efficiencies by wet scrubbers. This fact led Semrau et al (1955) to propose the power law correlation. Calvert et al (1973) refined the power law to include the effects of particle size. In most cases this modified power law fits the experimental data very well. The major deviation from the power law occurs when conditions favorable to water vapor condensation occur in the scrubber, Semrau (1963). These deviations from the power law have led many researchers to believe the efficient utilization of condensation effects is the key to collecting fine particles by wet scrubbers without excessive energy consumption, e.g. Calvert et al (1972). The evidence that condensation affects scrubber performance; the possible mechanisms active when condensation occurs; and the economics of utilizing condensation effects are discussed below.

II. Reports of Condensation Effects

One of the earliest demonstrations of the effects of condensation on particle collection is the work done by Schauer in the late 1940's. The dust laden gases were passed through special types of steam ejectors where condensation was achieved by adiabatic expansion. The gases were then passed through a cooling chamber where the condensation was stabilized and then through a Pease Anthony scrubber. Very high collection efficiencies were obtained when wet steam was used, Yellott and Bralove (1950) and Schauer (1951). The major disadvantage of Schauer's system was that very large energy inputs were required. Yellott and Bralove (1950) and Bralove (1951) presented a lucid discussion of the application of condensation phenomena to fine particle collection and of the various methods of inducing condensation. Lapple and Kamack (1955) reported that the addition of steam (2-3 times that necessary to saturate the air at room temperature) produced a fivefold reduction in dust loss at a given air pressure drop for several types of laboratory scale scrubbers. The improved performance was attributed to particle growth, Stefan-flow effects,and to changes in the wetting characteristics of the dust. Semrau et al (1955) and Semrau (1960, 1963) reported that the particle collection efficiency at a given pressure drop was higher when black-liquor recovery furnace fume was scrubbed using cold water than when hot liquors were used. They attributed the improved performance to Stefan-flow effects.

Although the studies discussed above demonstrated the improvement in scrubber performance under condensing conditions, there was little interest in the subject until the later 1960's. By then it was obvious that high efficiency collection of fine particles was required to meet the public's demands for reduced air pollution. Several investigators then became active in studying condensation effects in scrubbers.

Coy (1969), for example, reported that the particle collection efficiency of a laboratory scale cyclonic scrubber increased when the air was humidifed prior to entering the scrubber. Litvinov (1967, 1972) studied venturi scrubbers followed by cyclone or sieve tray entrainment separators. He concluded that: (1) condensation of water vapor in a venturi and a sieve tray scrubber increases the particle collection efficiency. (2) Particle growth and phoretic forces do not affect collection of particles larger than 0.1 μm in diameter. (3) Tray columns with condensation are more efficient than venturi scrubbers with condensation in energy consumption. Rozen and Kostin (1967) studied the collection of a fine oil mist in a sieve plate scrubber with alternate hot and cold plates. They concluded that: (1) collection efficiency increased with the quantity of steam condensed; (2) collection in each pair of plates is higher than in the preceding pair. (They attributed this to particle growth).

Lancaster and Strauss (1971) and Prakash and Murray (1973) conducted experiments of steam injection using redispersed dusts. They concluded that particle growth was the major mechanism responsible for improved scrubber performance when steam was injected.

The most extensive study of condensation effects is that of Calvert et al (1973). They reviewed the literature on condensation effects, developed mathematical models to predict the influence of condensation, and conducted laboratory scale experiments to verify the mathematical models. Their summary of the results of selected references is presented in Table I.

An analysis of the available data shows that the particle penetration, Pt, (one minus the efficiency) is a function of the condensation ratio defined as the amount of water vapor condensed per unit mass of dry air. The data from the studies listed in Table II are plotted against the condensation ratio. The data shown in Table II and Figure 1 show that:

1. Particle penetration depends heavily on the amount of water vapor condensed per unit, mass of dry gas (q').

2. Particle penetration also depends significantly on particle concentration. By referring to the concentration data given in Table II, one can see that there is a clear trend of penetration decreasing as particle number concentration decreases. This effect can be shown theoretically to accompany condensation on particles and their growth at the expense of the water vapor concentration in the gas. The fewer the particles which share a given quantity of condensation, the larger they will grow and the easier they are to collect.

3. The data for references 4 and 6 are the only ones in Figure 1 for penetration versus steam injection ratio rather than condensation ratio. The exceptionally low penetration shown for soluble hygroscopic materials such as Na_2CO_3 and Na_2SO_4 is due to their being able to grow by condensing water vapor when the relative humidity is less than 100%.

4. The effects of scrubber design, while not too apparent from Figure 1, are shown by theoretical and experimental studies by Calvert et al (1973) to include the following:

a. Multiple-stage or continuous contact type equipment is superior to single-stage condensation because it provides more opportunity for the collection of particles after they have grown.

b. Distribution of the condensation over several stages is preferable because of the enhanced growth which can occur after the particle concentration has been reduced.

TABLE I - Selected References on FF/C Applications

AUTHORS	YEAR	HIGH POINTS OF STUDY	REFERENCE
Semrau K., Marynowski C., Lande K., Lapple C.	1958	Attributed increase in collection efficiency to scrubbing liquid temperature.	Ind. Eng. Chem. 50, 1615 (1958
Lapple C., Kamack H.J.	1955	Addition of steam reduced dust loss at a given air pressure drop.	Chem. Eng. Prog. 51, 110, (1955)
Schauer P.J.	1951	Addition of steam into a venturi scrubber increase removal of DOP smoke.	Ind. Eng. Chem. 43, 1532, (1951)
Rozen A.M., Kostin V.M.	1967	Studied experimentally the collection of fine oil mist in a plate column. They found that: 1. Collection efficiency increased with the quantity of steam condensed and proposed the empirical correlation $Pt = 12.5\, q^{-0.56}$ "Pt" is penetration and "q" = g steam condensed to g inlet particles. 2. Collection in each pair of plates is higher than in the preceding pair. (They attributed the increase in collection efficiency to particle growth.)	Intern. Chem. Eng., 7, 464 (1967)

AUTHORS	YEAR	HIGH POINTS OF STUDY	REFERENCE
Litvinov A.T.	1964A 1964B 1965 1967 1972	His studies concentrated on venturi scrubbers followed by cyclone or sieve tray for entrainment separation. In his 1967 and 1972 papers he reaches the following conclusions: 1. Phoretic forces are not important for particles larger than 0.1 μm in diameter. 2. Condensation of water vapor in a venturi and a sieve tray column increases particle removal efficiency. 3. He gives a design equation for the venturi based on an experimental optimum liquid film thickness, which permits calculation of the "optimum" quantity of condensed steam. 4. He gives the equation $N_{Nu}=0.78\ N_{Re}^{0.65}$ for the heat transfer coefficient from the gas to the liquid drops. 5. Particle growth does not affect collection efficiency. 6. Tray columns with condensation are more efficient than venturi with condensation in energy consumption.	Khim. prom. 8, (1964) Vestn. tekhn, i ekonom. inform. 5, (1964) Stal', 7, (1965) Zhurn, Priklad, Khim, 40, 353 (1967)

AUTHORS	YEAR	HIGH POINTS OF STUDY	REFERENCE
Terebenin A.N., Bykov, A.P.	1972	Analyzed the collection of particles 0.128 μm in diameter in cluster of wetted wall rectangular ducts. They concluded that in the presence of steam particle removal is attributed to growth and flux forces. They give reference to particle growth equation, the results of which do not agree with their experimental findings of particle diameter. No attempt to calculate penetration was made.	Zh. prikl. khim. 45, 1012, (1972)
Lancaster B.W., Strauss W.	1971	Studied the collection of ZnO agglomerates with a mean diameter of 1 μm in a 5 cm x 10 cm rectangular duct 1.85 m long. In different experiments steam was injected upstream or downstream of the aerosol injection port, and it was assumed that when steam was injected upstream of the aerosol it condensed on the aerosol particles. They concluded: 1. Particle build-up was the major mechanism responsible for improved scrubber performance. 2. Flux forces were not important. 3. For their system the dust penetration could be correlated with the rate of steam injection by: $Q = 0.2 \frac{1-\eta}{1-\eta_o} -1$ where η and η_o are	Ind. Eng. Chem. Fund., 10, 362 (1971)

AUTHORS	YEAR	HIGH POINTS OF STUDY	REFERENCE
		the scrubber collection efficiency with and without steam addition and "Q" is the steam injection rate lb steam/lb air. 4. Steam was used inefficiently in this particular scrubber.	
Lohs W.	1969	Fine particle removal efficiency was studied in a spray column. Na_2SO_4 and polystyrene aerosol with median particle diameter varying from 0.43 to 0.8 µm and from 0.4 to 1.3 µm respectively. Collection efficiency was improved by steam addition for both aerosols. The increase in collection efficiency was higher for the soluble Na_2SO_4 aerosol. (0.3 - 0.5 µm particles can be removed at 60% efficiency) The separation of hydrophobic fine dust is also increased particularly if the particle surface is rendered hydrophilic by means of a wetting agent. Increased efficiency is attributed to particle growth only though Stefan flow is mentioned. No equations, correlations or design method are attempted.	Staub 29, 43, (1969)

AUTHORS	YEAR	HIGH POINTS OF STUDY	REFERENCE
Horst T.W. Hales J.M., Horst T.W., Schwendiman Hales J.M., Schwendiman L.C. Horst T.W.	1968 1970 1971	This series of studies carried out at Battelle Northwest was concerned with the transport and deposition of a radioactive aerosol expected to be generated by fuel overheating following an accident. Their solutions to the case of aerosol deposition through laminar naturally-convected boundry layer are more rigorous than for the parallel turbulent case. Their conclusions were: 1. In a laminar boundry layer the dominant mechanism is diffusiophoresis. In the turbulent case turbulent deposition may rival diffusiophoresis. 2. Relationships can be derived between steam consumption and particle deposition. 3. The rate of deposition of particles 0.5 - 2 μm in diameter in a laminar boundry layer is independent on particle diameter and depends only on the operating conditions within the air steam boundry layer. 4. When particle deposition is assumed at the mass average velocity of the fluid, values 20-60% lower than in the case of flux forces are calculated for a laminar boundry layer.	Battelle Northwest reports No. BNWL 848 (1968), BNWL 1125 (1970) BNWL SA-3592 (1971) BNBL-SA-3734 (1971)

AUTHORS	YEAR	HIGH POINTS OF STUDY	REFERENCE
Goldsmith P., Delafield H.J., Cox L.C.	1963	Experiments with radioactively tagged nickel-chromium aerosol (particles 0.02 to 0.2 μm in diameter) gave deposition velocities close to those predicted from the Waldman and Bakanov et al. equations.	Quart. J. of the Reg. Meteor. Soc. 89, 43, (1963)
Goldsmith P., May F.G.	1966	Comparison of thermophoretic velocities with theoretical predictions shows that for $r_p > \lambda$(r_p the particle radius, λ - the mean free path under the given conditions) they vary over a wider range. Derjaguin equation predicted a velocity 16% lower and Brock equation 40% higher than measured. Diffusiophoretic and thermophoretic forces are additive. Experiments of particle deposition efficiency were run in a Liebig condenser. The results show that collection efficiency could be plotted vs. the rate of steam condensation g/min.	Chapt. VII in Aerosol Science, C.N. Davies ed (1966)
Sparks, L.E. Pilat M.J.	1970	Single droplet target efficiencies for particle collection by the combined mechanism of inertial impaction and diffusiophoresis were calculated. These values were used to calculate overall collection efficiency in a spray tower. It was found that condensation can greatly improve particle collection.	Atmos. Env. 4, 1, (1970)

AUTHORS	YEAR	HIGH POINTS OF STUDY	REFERENCE
Davis R.J. Truitt J.	1972	They concluded that diffusio and thermophoresis would be too expensive for use in scrubbers. Particle growth due to condensation followed by turbulent agglomeration is the best way to increase scrubber efficiency.	Instrum. and Control Systems pp. 68-70, (Nov 1972)
Matsuzaki K.	1970	The invention describes a venturi scrubber where steam is added tangentially upstream of the throat.	Japanese patent No. Sho 41-41184
Mashita T.	1971	Describes the Solivore scrubber which is composed of venturis with water sprays upstream and downstream of the throat. Several operating conditions are described.	Indus. Public Nuisance 7, 573, (1971)

TABLE II

CONDENSATION SCRUBBING PERFORMANCE DATA SOURCES

Ref. No.					
1	Investigator(s)	Scrubber Type	d_{pg} (μm)	Particle Material	n_p #/cm^3
2	Calvert, Jhaveri, and Goldshmid (1973)	(A) Sieve plate (1 cold plate) (B) Sieve plate (1 to 3 cold plates)	0.7 0.75	D.B.P. Ferric Oxide	5×10^5 2×10^5
3	Fahnoe, Lindroos, and Abelson (1951)	(A) Cyclone, or (B) Peabody (1 plate)	<2.0	NaCl	10^3
4	Goldsmith and May (1966)	Tubular Condenser	?	Nichrome & Others	?
5	Lancaster and Strauss (1971)	Steam Nozzle + Spray + Cyclone	1.0	ZnO	10^5 -10^6
6	Litvinov (1967)	Venturi + 2 sieve plates	1.7	Apatite	$\sim10^5$
7	Prakash and Murray (1973)	Steam nozzle + Dry Duct		ZnO, $CaCO_3$, Na_2CO_3, + Na_2SO_4	
8	Rozen + Kostin (1967	Sieve plate with alternate hot and cold plates	0.3	Oil	10^5 -10^8
9	Schauer (1952)	Steam nozzle + Peabody (5 plates)	0.3	D.O.P.	2×10^7
10	Stinchombe and Goldsmith (1966)	Tubular Condenser	0.1	Iodine	10^3 -10^4
11	Terebenin and Bykov (1972)	Vertical Wetted Planes	0.05	Tin Fume	5×10^7

Note: d_{pg} = Mass median diameter, μm
n_p = Number concentration of particles, #/cm^3

III. Mechanisms Contribution to Improved Particle Collection

Calvert et al (1973) have shown both theoretically and experimentally that diffusiophoresis (defined here to include Stefan-flow) and particle growth are the major mechanisms contributing to improved particle collection in a condensation scrubber. Thermophoresis, which several investigators have suggested may be important, was shown to be insignificant under conditions existing in scrubbers.

The effect of diffusiophoresis on particle collection by scrubbers was reported by Sparks and Pilat (1970), Calvert et al (1972), and Calvert et al (1973). They showed that particle deposition due to diffusiophoresis can significantly increase scrubber performance. Calvert et al (1973) showed the particle penetration is a function of the condensation ratio and is independent of particle concentration when diffusiophoresis is the only condensation effect contributing to particle collection i.e. when there is no particle growth due to condensation. (For a review of the theory of diffusiophoresis see Bakanov and Dergaguin (1957, 1960), Goldsmith and May (1966) and Dergaguin et al (1960).)

The effects of particle growth on scrubber performance were reported by Calvert et al (1973). They showed that the amount of particle growth is a function of both the condensation ratio and the particle concentration. Maximum growth occurs with low particle concentrations and high saturation ratios. The relation between particle growth and condensation ratio is shown in Figure 2. Note that the final particle diameter is a weak function of the initial particle diameter. It should be noted that particle growth can result in improved particle collection only if the grown particles are in the active region of the scrubber. Otherwise the scrubber will not "see" the grown particles.

Which of the above two mechanisms is most important is a function of factors such as particle concentration, particle surface properties and scrubber design. Diffusiophoresis is dominant in single stage devices or on the first stage of multistage devices. Diffusiophoresis is also probably dominant when the particle concentration is high and when the particles are nonwettable. Particle growth is probably most important when the particle concentration is low and the particles are wettable. Particle growth can be very significant when the particles are hygrosocpic or deliquescent.

IV. Economics of Condensation Scrubbing

The following analysis is from Calvert (1973).

Costs for condensation scrubbing are highly dependent on the amount of steam which is condensed, especially if steam (or the fuel to evaporate water) has to be purchased. In order to provide some general guides as to economically attractive operating conditions, the major operating costs for condensation scrubbers have been compared to those for high-energy scrubbers. Depreciation costs are not included in these comprisons because they will be roughly in the same cost range and they will usually be overshadowed by power and utility costs. Likewise, any costs for waste treatment would be nearly the same.

A base case of 1,420 m^3/minute (50,000 C.F.M.) of dry gas was chosen for illustration. Fan power costs for 200 cm W.C. (80" W.C.), 400 cm W.C., and 500 cm W.C. pressure drop scrubbers were computed for an overall fan and motor efficiency of 50% and power costs of 1¢/KWH. Hourly costs for these conditions are plotted (dashed lines) on Figure 2, a graph of hourly operating cost vs. the condensation ratio. Since no steam is condensed in the high energy scrubber, the dashed lines are horizontal.

If steam has to be purchased or generated from purchased fuel, it might cost somewhere around \$1.32/MKg (\$0.60/1,000 lb.) One line is shown on Figure 3 for costs due to steam alone. Cooling water is also required to condense the steam and will cost anywhere from 0.26¢/MKg (1¢/M gal) to 4¢/MKg (15¢/M gal). Recirculating cooling tower water might be had for around 0.8¢/MKg, based on quoted costs and on cooling tower depreciation plus pumping costs.

The amount of cooling water needed will depend on the temperature rise of the water in the scrubbing system. If one assumes a 28°C (50°F) temperature rise, about 20 g of cooling water will be required to condense 1.0 g of steam. Based on this assumption, the lines for hourly cost due to steam plus cooling water and for cooling water alone (at two prices) were plotted on Figure 3.

One may make the following observations based on the illustrations in Figure 3:

1. The most favorable set of circumstances will be approximately as shown by the line for 0.8¢/MKg water and 25 cm W.C. fan costs; corresponding to scrubbing a hot gas which does not require any purchased steam. Depending upon the particle penetration required, this system could compete with a wide range of conventional scrubbers. For example, if 58% penetration of particles with an aerodynamic diameter, d_{pa}, of 0.5 μm $(g/cm^3)^{1/2}$ were required, a conventional venturi scrubber would have to be operated at about 200 cm W.C. pressure drop. Figure 1 shows that condensation scrubbing would require around 0.05 g condensed/g dry gas. The hourly operating cost ratio for conventional to condensation scrubbing would, therefore, be about (\$9.50/\$2.50) = 3.8 .
2. Cooling water costs as high as 2.64¢/MKg (10¢/M gal) or even 4¢/MKg (15¢/M gal) can be economically acceptable where low penetration is required.

3. Purchased steam plus cooling water can be economically competitive where low penetration is required. For example, a 400 cm W. C. pressure drop venturi would be required to give 27% penetration @ $d_{pa} = 0.5\ \mu m\ (g/cm^3)^{1/2}$. Figure 1 shows that a condensation ratio of 0.07 to 0.17 g/g might be required in a condensation scrubber, depending on the number concentration of particles, their nucleation characteristics, and the scrubber configuration. Inspection of Figure 3 shows that the cost comparison would be close and the final resolution of which system is cheaper would require additional experimental testing and design computations.

V. Commercial Application of Condensation Scrubbers

There is limited information on commercial scrubber system where condensation is claimed to be an active mechanism for particle collection. Teller (1970) described a cross flow packed scrubber utilizing condensation for fine particle collection. Grain loadings as low as 10^{-4} gr/ft^3 are claimed for commercial installations.

Mashita (1971) described the Solivore scrubber which is composed of several venturis. High particle collection for particles as small as 0.04 μm are claimed.

Matsuzaki (1970) in a Japanese Patent describes a venturi scrubber where steam is injected before the throat.

Strauss (1966) describes a condensation scrubber for which high efficiency is claimed.

VI. Conclusions

The results summarized in this paper clearly show that condensation improves the fine particle collection of scrubbers. The degree of improvement depends on factors relating to scrubber design and the nature of the particulate. The economics of using condensation to improve fine particle collection appear to be favorable for many sources, if the scrubber system is properly designed. The question of what is the proper scrubber design has not been fully answered.

The Control Systems Laboratory (CSL) has sponsored research to define the proper scrubber system. The results of this work are reported by Calvert et al (1973). CSL is continuing to sponsor work to develop new scrubber systems, called Flux Force/Condensation scrubbers, to take maximum advantage of water vapor condensation. In closing it must be pointed out that Flux Force/Condensation (FF/C) scrubbers are not a "cure all". There are many industrial sources of fine particulate where FF/C scrubbers are technically and economically attractive. However, there are many other sources where FF/C scrubbing is not attractive. Thus, sound engineering judgement is still needed to determine what type of particulate control system is best for each source.

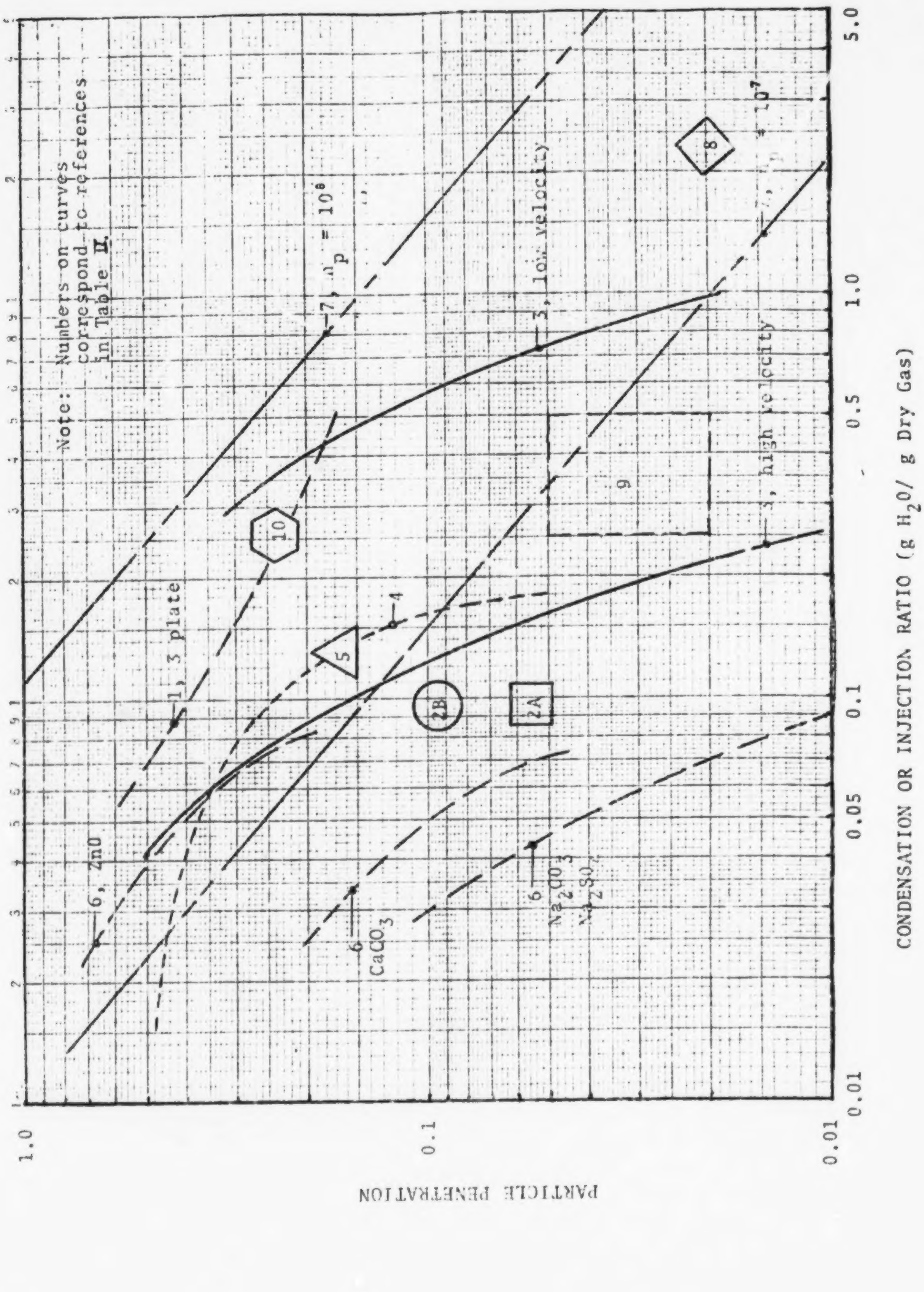
Note: Numbers on curves correspond to references in Table II
PARTICLE PENETRATION
CONDENSATION OR INJECTION RATIO (g H_2O/ g Dry Gas)
1.0
0.1
0.01
0.01
0.05
0.1
0.5
1.0
5.0
6, ZnO
1, 3 plate
7, $n_p = 10^8$
3, low velocity
3, high velocity
$n_p = 10^7$
4
5
10
2B
2A
8
9
6 CaCO$_3$
6 Na_2CO_3
Na_2SO_4

Figure 1

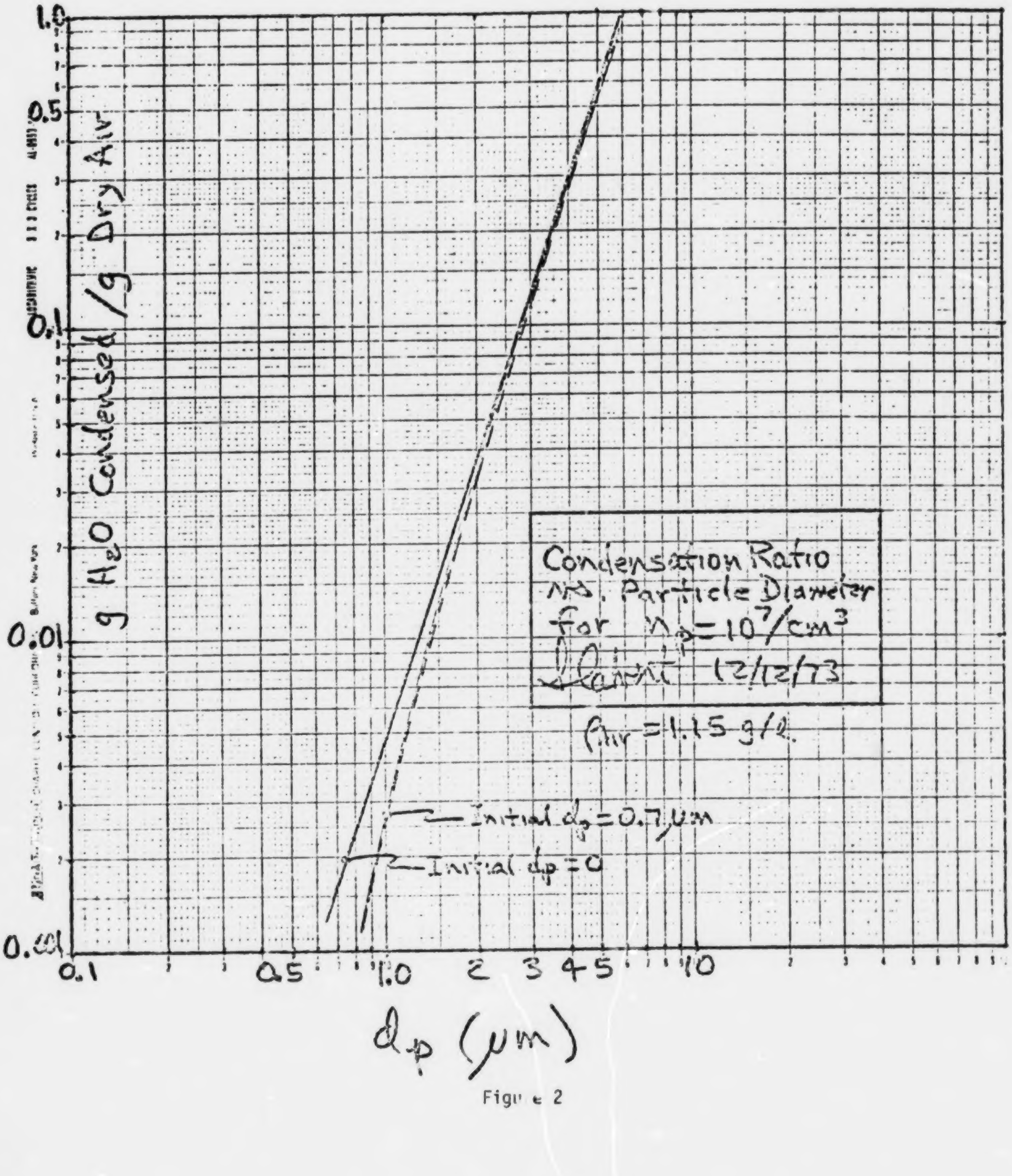
g H₂O Condensed /g Dry Air
1.0
0.5
0.1
0.01
0.001
0.1
0.5
1.0
2
3
4
5
10
d_p (μm)
Condensation Ratio
vs. Particle Diameter
for n_p = 10⁷/cm³
12/12/73
ρ_air = 1.15 g/l
Initial d_p = 0.7 μm
Initial d_p = 0

Figure 2

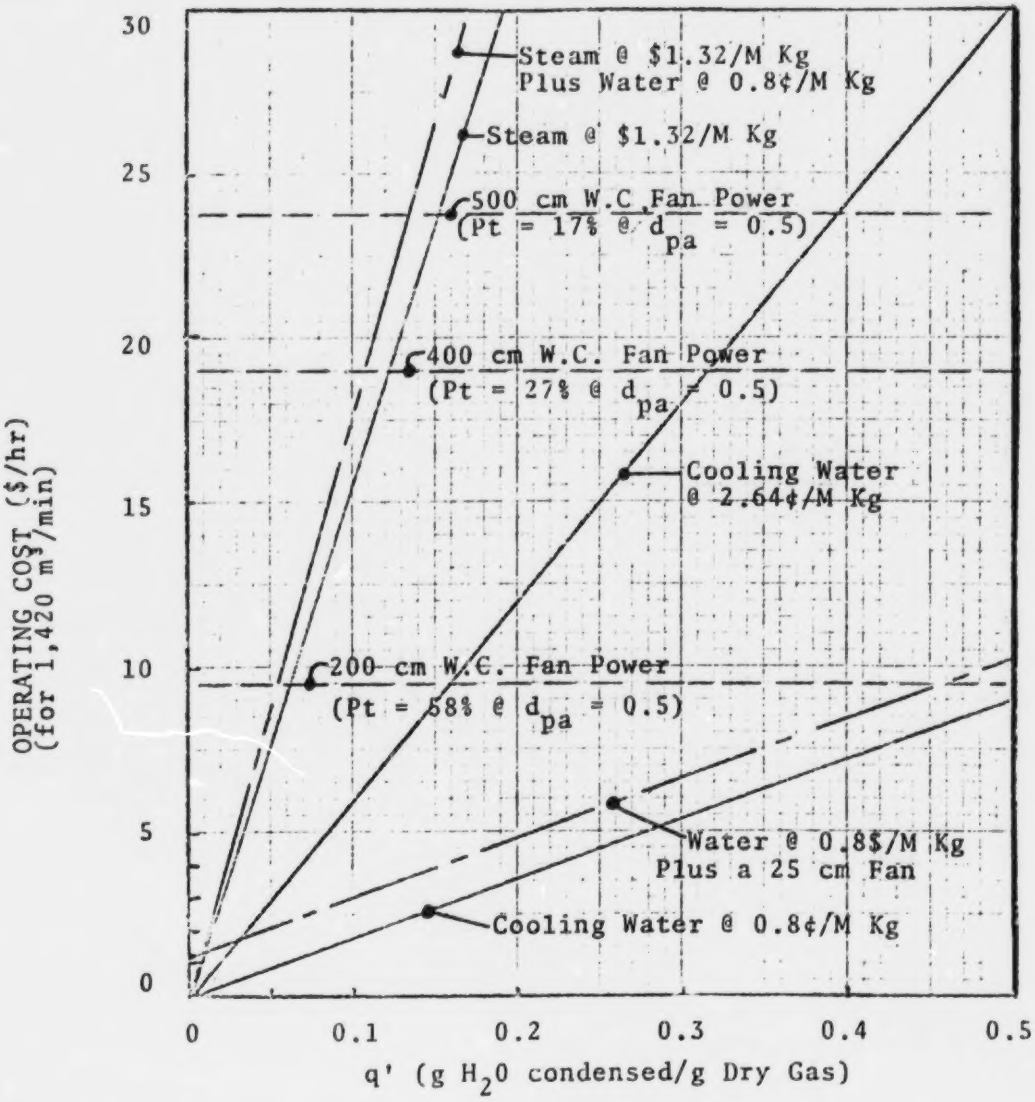

NOTES:

1) Costs are for a 1,420 m^3/min (50,000 CFM) scrubber
2) Particle diameter, d_{pa}, is aerodynamic (μm $(g/cm^3)^{1/2}$)
3) Power cost is 1¢/KWH
4) Fan plus motor efficiency is 50%

Figure 3 - Operating Costs Comparison.

REFERENCES

Bakanov, S.P., and Dergaguin, B.V. (1957 A theory of the interaction between evaporating or growing droplets at large distances. Sov. Phys. Dokl. 2, 41 (in English).

Bakanov, S.P. and Dergaguin, B. V. (1960) The motion of a small particle in a non-uniform gas mixture. Discuss. Faraday Soc. 30, 130.

Bralove, A. (1951) Radioactive Dust Separation Equipment. Nucleonics, 8 37.

Calvert, S., Goldshmid, J., Leith, D. and Mehta (1972). Scrubber Handbook. A.P.T., Inc. Riverside, California. EPA Contract No. CPA-70-95. NTIS #PB 213 016.

Calvert, S., Goldshmid, J;Leith, D.,and Jhaveri, N. Feasibility of Flux Force/Condensation Scrubbing for Fine Particulate Collection, A.P.T., Inc., Riverside, California, EPA Contract 68-02-0256.

Calvert, S (1973) Personal Communication.

Coy, D. W. (1969) "Comparison of Wet Scrubber Efficiency Using Humidified and Non-humidified Gas Streams" M. S. Thesis West Virginia University, Morgantown, West Virginia.

Dergaguin, B.V., Yalamov, Y.I. and Storozhilova (1966) Diffusiophoresis of large particles. J. Colloid Sci. 22, 117.

Fahnoe, F., A. E. Lindroos, and R. J. Abelson (1951). Aerosol Build-Up Techniques. Ind. Eng. Chem. 43, 1336.

Goldsmith, P., and F. G. May (1966). Diffusiophoresis and Thermophoresis in Water Vapor Systems. In: Aerosol Science, Davies, C.N. (ed.). New York, Academic Press, p. 163-194.

Lancaster, B. W., and W. Strauss (1971). A study of Steam Injection Into Wet Scrubbers. Ind Eng Chem Fundamentals. 10(3): 362-369.

Lapple, C. W., and H. J. Kamack (1955). Performance of Wet Dust Scrubbers. Chem. Eng Prog. 51(3):110-121.

Litvinov, A. T. (1967). Influence of Condensation on the Effectiveness of Capture of Fine Particles During Cleaning of Gases by the Wet Method. Zhurnal Prikladnoi Khimii. 40(2): 353-361.

_______(1972). Fine Gas Scrubbing to Remove Highly "Dispersed Hydrophopic Particles Using Condensation Effect" stal 2, 184.

Mashita, T. (1971). Industrial Public Nuisance. 7:573.

Matsuzaki (1970). Japanese Patent Number Sho 41-41184.

Prakash, C. B. and F. E. Murray (1973). Particle Conditioning by Steam Condensation. Preprint of paper.

Rozen, A.M., and V. M. Kostin (1967). Colelction of Finely Dispersed Aerosols in Plate Columns by Condensation Enlargement. Inter Chem Eng. 7:464-467.

Schauer, P. J. (1951) Removal of submicron aerosol particles from moving gas streams. Ind. Engng Chem. 43, 1532.

Semrau, K., Marynowski, C., Lande, K. and Lapple, C. (1958) Influence of power input on efficiency of dust scrubbers. Ind. Engng Chem. 50, 1615.

Semrau, K. T. (1960) "Correlation of Dust Efficiency" J.Air Poll. Control Assoc. 10, 200.

_______(1963) "Dust Scrubber Design -- A Critique of the State of the Art" J. Air Poll. Control Assoc. 13 587.

Sparks, L.E. and Pilat, M. J. (1970) "Effect of Diffusiophoresis on Particle Collection by Scrubbers", Atmos. Environ. 4, 651.

Stinchcome, R. A. and P. Goldsmith (1966). Removal of Iodine from the Atmosphere by Condensing Steam. J. Nuc Energy, 20, 261.

Strauss, W. (1966) Industrial Gas Cleaning, Pergamon Press, New York, N.Y.

Teller, A. J. (1970) "New Concepts of Pollution Control" Trans. New York Acad. of Science, 32, 837.

Terebenin, A. N. and A. P. Bykov. Aerosol Sedimentation Mechanisms in Water Vapor Diffusion Fields. Zhurn Priklad Khim. 45, 1012, 1972.

J. I. Yellott and A. Bralove (1952) "Condensation Techniques for Dust Detection & Collection" Chapt. 40 of Air Pollution Proceeding of the United States Technical Conference on Air Pollution 1950, L.C. McCabe, Chairman, McGraw-Hill Book Company, N.Y.

Paper No. 13

USE OF SCRUBBERS FOR CONTROL OF EMISSIONS FROM POWER BOILERS -U. S.

by

Irwin A. Raben

COMBUSTION EQUIPMENT ASSOCIATES, INC.

San Francisco, California

SUMMARY

The use of scrubbers for control of particulate emissions from coal fired power boilers has been described with respect to pilot plant programs, commercial system design criteria and the status of full size installations.

There are presently 23 full size scrubbing systems which are being engineered, constructed or operated in the United States for particulate control. Scrubbers most frequently installed are the venturi, turbulent contact absorber and marble-bed unit.

Scrubber technology for particulate control has been on a learning curve with the present location being at the 90% point. Experience has shown that particulate control with water scrubbing must consider SO_2 removal because it effects liquor chemistry, scaling and reliability.

New systems are being designed for higher liquid to gas ratios, higher percent solids in the circulating liquid, longer residence time in the recirculating tank and pH control to provide greater reliability.

INTRODUCTION

In 1970, the U.S. Clean Act became law with its main objective to protect the health of the citizens. The U.S. Environmental Protection Agency was created and in 1971 performance standards for new stationary sources were issued. These standards included maximum emissions for both particulate and sulfur dioxide from coal fired power plants.

Scrubbers have been used many years in the control of particulate emissions from steel plants. Therefore, their use in power plants appeared to be a good application, since scrubber operation is independent of particulate resistivity, a critical factor in electrostatic precipitator design. As of December 1973, there are twenty-three scrubber installations in the United States, which are being engineered, constructed or operated (6000 MW) primarily for the control of particulate emissions from coal fired power plants.

It is the object of this paper to describe the advances in application of scrubbers for the control of emissions from power boilers. Design and operating data for pilot plants, prototype and full size units will be presented. Certain design criteria will be discussed. It must also be emphasized that scrubber systems designed for particulate control must also consider sulfur dioxide absorption. SO_2 absorption effects the pH of the scrubber liquor and without pH control will cause corrosion and scaling which reduces system reliability.

U.S. PILOT PLANT PROGRAM

When the first scrubbing systems were designed in 1970-1971, limited data based on coal fired power boiler emissions were available. Therefore, short term pilot plant test programs were established to determine required liquid to gas ratios (L/G) and gas pressure drops to obtain outlet particulate concentrations of 0.03 gr/SCFD. This value was established to satisfy both quantative and opacity requirements. These pilot units were installed on existing coal fired boilers and generally had a capacity 3000 ACFM gas at 300°F. The most common scrubbers tested were the Venturi, Turbulent Contact Absorber (TCA), and the marble-bed scrubber. At that time, test programs generally were 6-8 weeks in duration to verify design criteria.

The Venturi pilot plant consisted of a Venturi scrubber followed by a liquid-gas separator. In addition, recirculating pumps and tanks, and instrumentation for measuring gas and liquid rates and pH were provided. Liquid to Gas ratios tested varied from 10 to 40 gal/1000 ft^3. Gas pressure drop was varied from 10 to 30 inches H_2O.

The TCA pilot plant was similar to the Venturi with the following exceptions. The TCA is a counter current absorber with three stages of grids with plastic spheres in turbulent motion between the grids. Higher liquid circulation rates are required to establish optimum conditions. The demister is located in the top of the absorber, L/G tested varied from 30-80 gal/1000 ft^3 gas. Gas pressure drops were varied from 6"-12" H_2O.

The marble-bed scrubber utilized a similar pilot plant system. It contains one or two beds of marbles or glass spheres which move about. This scrubber has cocurrent flow of gas and liquid which enter the bed at the bottom and flow upward through the marbles. L/G as tested were generally between 10-30 gal/1000 CF; gas pressure drop varied between 6"-12" H_2O.

Experiments were generally carried out at inlet particulate grain loadings at 2-5 gr/SCFD. Data from these tests generally indicated that Venturi scrubbers required L/G's of 10-20 gal/1000 ft^3 and gas pressure drops of 10"-20" H_2O to achieve outlet particulate loadings of .02-.04 gr/SCFD.

TCA scrubbers generally required liquid to gas ratios of 30-60 gal/1000 ft^3 with two to three stages and gas pressure drops of 6"-10" H_2O to achieve outlet loadings of .02-.04 gr/SCFD.

Marble bed scrubbers generally required L/G is of 20-40, pressure drops of 7"-12" H_2O to obtain outlet grain loadings of .03-.04 gr/SCFD.

In addition, particle size distributions were obtained using a Brink impactor to determine the effect of inlet particle size on removal efficiency. An EPA mass sampling train was used to measure total inlet and outlet particulate grain loading.

The data from these pilot plant test programs were then used to design full size systems.

As the state of the art advanced, greater attention was given to system chemistry and long term reliability. In addition, disposal of wet solids was studied.

In order to understand system chemistry, it must be noted that as particulate removal occurs, SO_2 is also absorbed with the pH of the water solution decreaseing to as low as 2. If a solution of this pH is recirculated, corrosion can result. In addition, fly ash contains varying amounts of available lime as CaO, which can react with the dissolved SO_2 in water and create insoluble $CaSO_3$, causing scaling within the system. Therefore, pilot plant programs began to study not only liquid to gas ratio and gas pressure drop, but also liquor pH, percent solids in the circulating liquid and residence time in the recirculating tank.

There have been many Pilot Plant programs which have been conducted over the past three years. This paper will discuss three typical test programs: Montana Power Co's, TVA and The EPA test Facility.

Montana Pilot Plant Program

The main objectives of Montana Power Co's pilot plant program were to demonstrate the particulate and sulfur dioxide removals that could be achieved over a range of liquid-to-gas ratios and gas pressure drops studied and to optimize these variables as they influence system performance. Other objectives were to demonstrate that operating conditions produce no scaling and long term reliability. The pilot plant results verified the performance requirements for the full size units. (Ref. 1).

The 3000 ACFM pilot plant system (Fig. 1) consisted of a Venturi scrubber with an SO_2 spray/de-entrainment section, flue gas reheater and induced draft fan.

Based on 75 tests, particulate removal was found to vary as follows with gas pressure drop. A inlet grain loading of 2 gr/SCFD was observed and liquid-to-gas ratios of 10-20 gal/1000 ft^3 saturated gas were maintained in the venturi during these tests.

VENTURI ΔP	PARTICULATE LOADING GR/SCFD	
INCHES H_2O	SCRUBBER INLET	SCRUBBER OUTLET
12	2.15	0.0276
17	1.99	0.0178
22	1.89	0.0156

A plot of venturi ΔP vs. outlet particulate loading in Figure 2 shows little effect of venturi L/G (10-20) on outlet grain loading. Venturi particulate removal efficiency, within the ranges of venturi gas velocity and venturi ΔP examined in the pilot plant is primarily a function of Venturi ΔP. The linear gas velocity was approximately 200 ft/sec. The ΔP across the venturi is a function of gas velocity (throat diameter) and L/G. Figure 3 presents scrubber average collection efficiency versus venturi ΔP for all test series.

Table 1 presents data obtained with a Brink impactor and shows the particulate distribution from greater than 7 microns to less than 0.5 microns. Percent removal by particle size and pressure drop is reported.

The scrubber outlet dust loading in the smaller particle size was considerably less for the 17 in. venturi ΔP than for the 12 in. ΔP, while there was less difference in the outlet loading of fine particulate between the venturi ΔP's of 17 in. and 24 in.

Scrubber fractional collection efficiency is plotted in Figure 4 at a venturi ΔP of 17 inches H_2O. Data for ΔP's of 12 in. and 24 in. H_2O are also shown.

Montana coal has a sulfur content which varies from 0.5-1.0% and sulfur dioxide removal has been provided as part of the scrubbing system. The fly ash produced by burning this coal has a high degree of alkalinity as CaO, which can be utilized to remove sulfur dioxide. The pilot plant program, therefore, also studied the effect of liquid to gas ratio, recirculating tank residence time, percent solids in liquor and pH on SO_2 removal. Pilot plant results

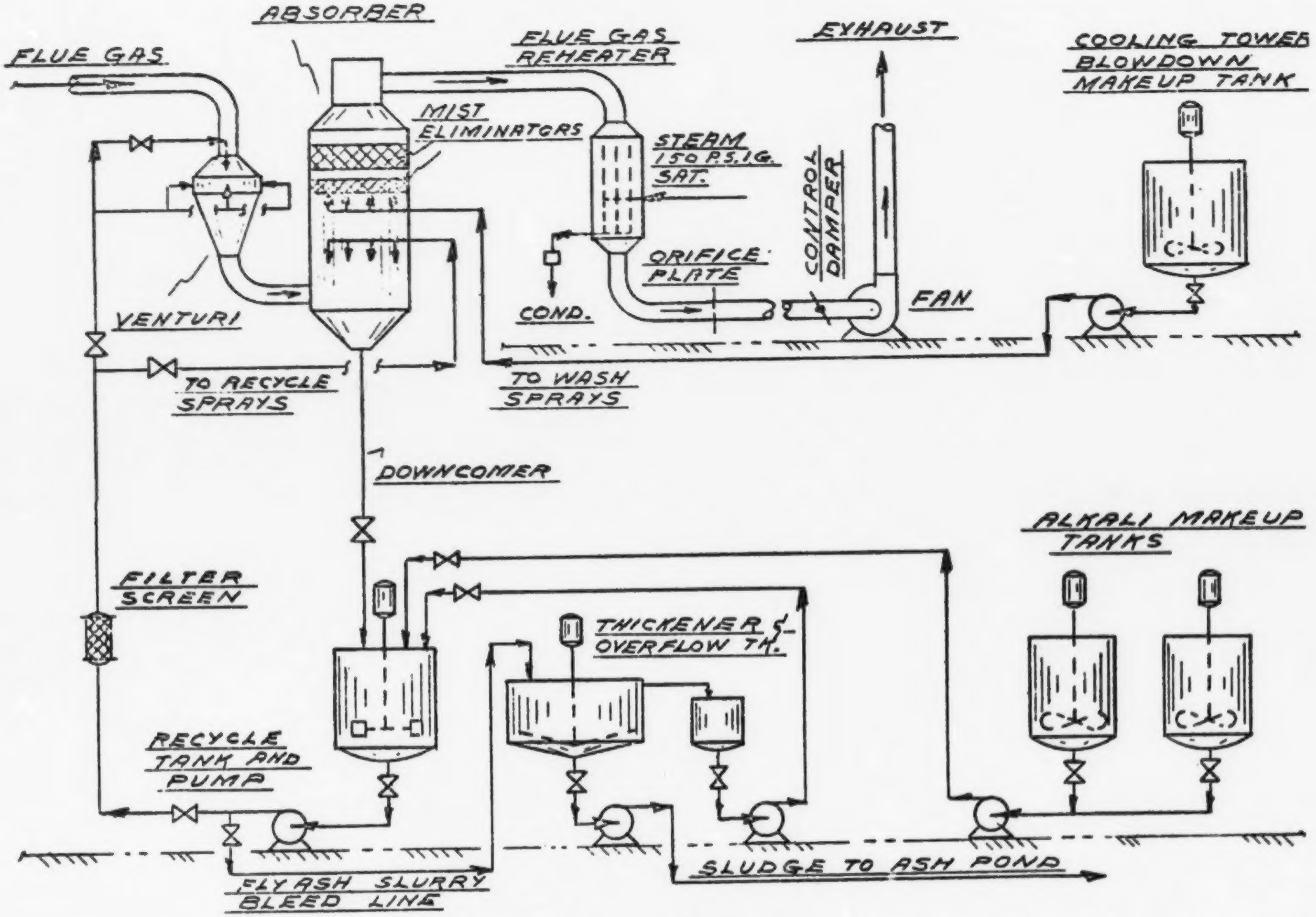
FLUE GAS
ABSORBER
FLUE GAS REHEATER
EYHAUST
COOLING TOWER BLOWDOWN MAKEUP TANK
MIST ELIMINATORS
STEAM 150 P.S.I.G. SAT.
CONTROL DAMPER
ORIFICE PLATE
FAN
COND.
VENTURI
TO RECYCLE SPRAYS
TO WASH SPRAYS
DOWNCOMER
ALKALI MAKEUP TANKS
FILTER SCREEN
THICKENER & OVERFLOW TK.
RECYCLE TANK AND PUMP
SLUDGE TO ASH POND
FLY ASH SLURRY BLEED LINE

FIGURE 1
MONTANA POWER CO.
PILOT PLANT SCRUBBING SYSTEM.
January-June 1973

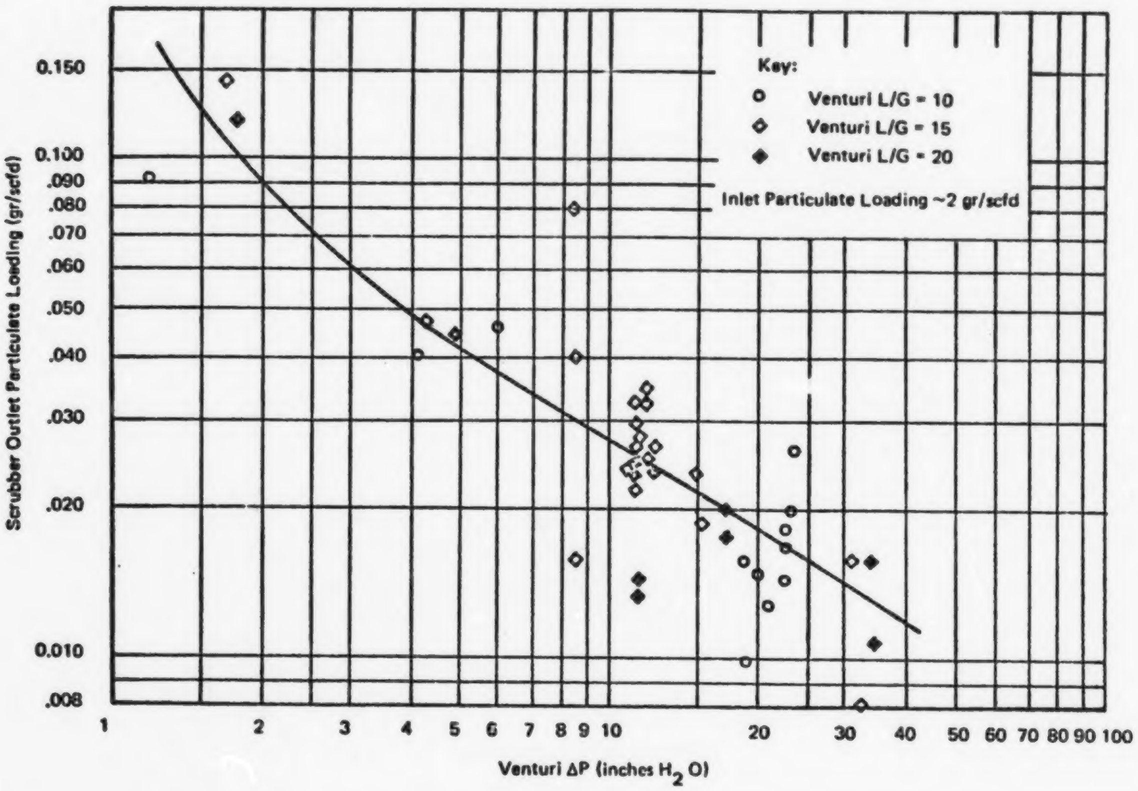

FIGURE 2 . OUTLET PARTICULATE LOADING VERSUS PRESSURE DROP AND L/G – TEST SERIES 200 AND 300

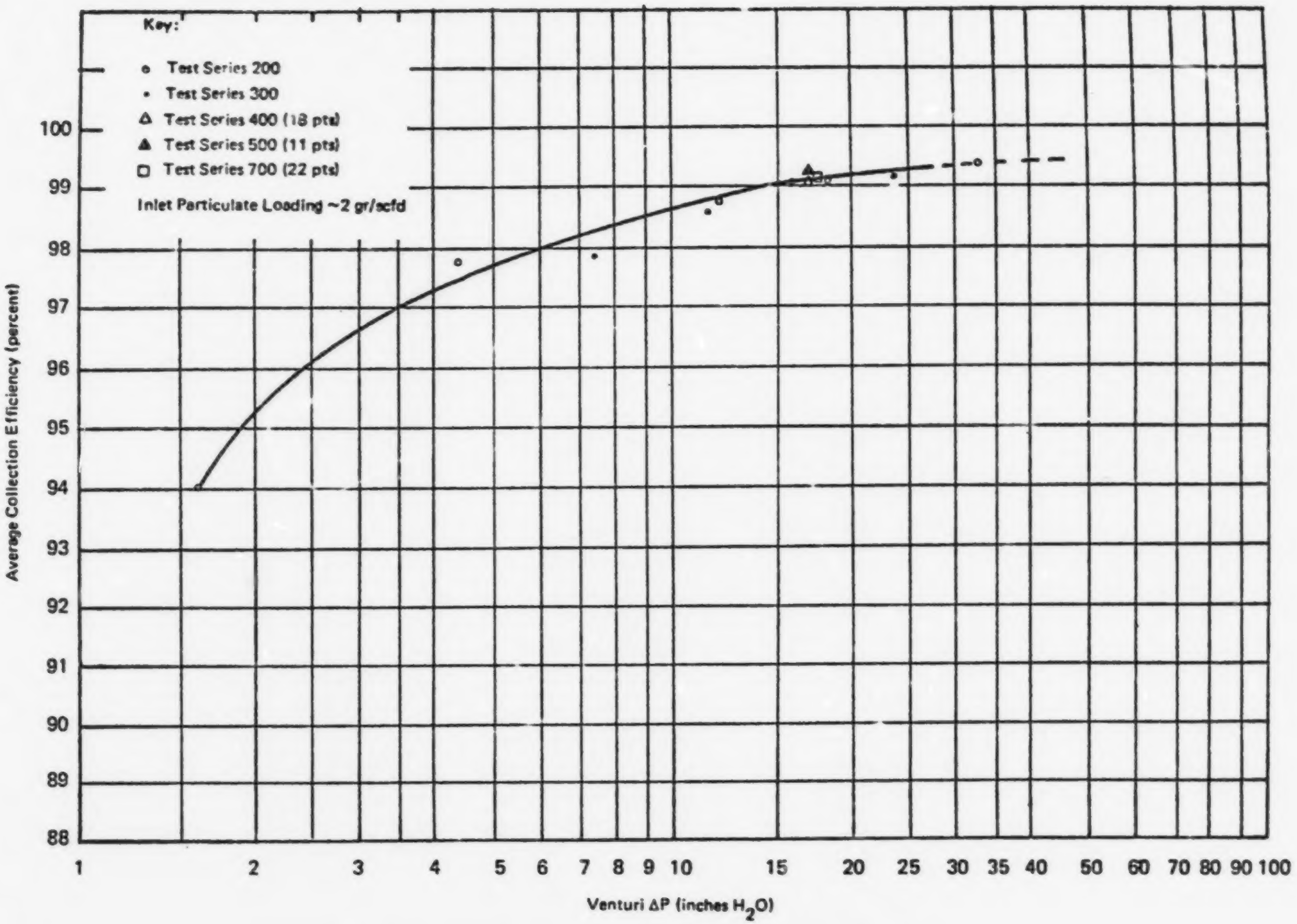

FIGURE 3 SCRUBBER AVERAGE COLLECTION EFFICIENCY VERSUS VENTURI ΔP FOR ALL TEST SERIES

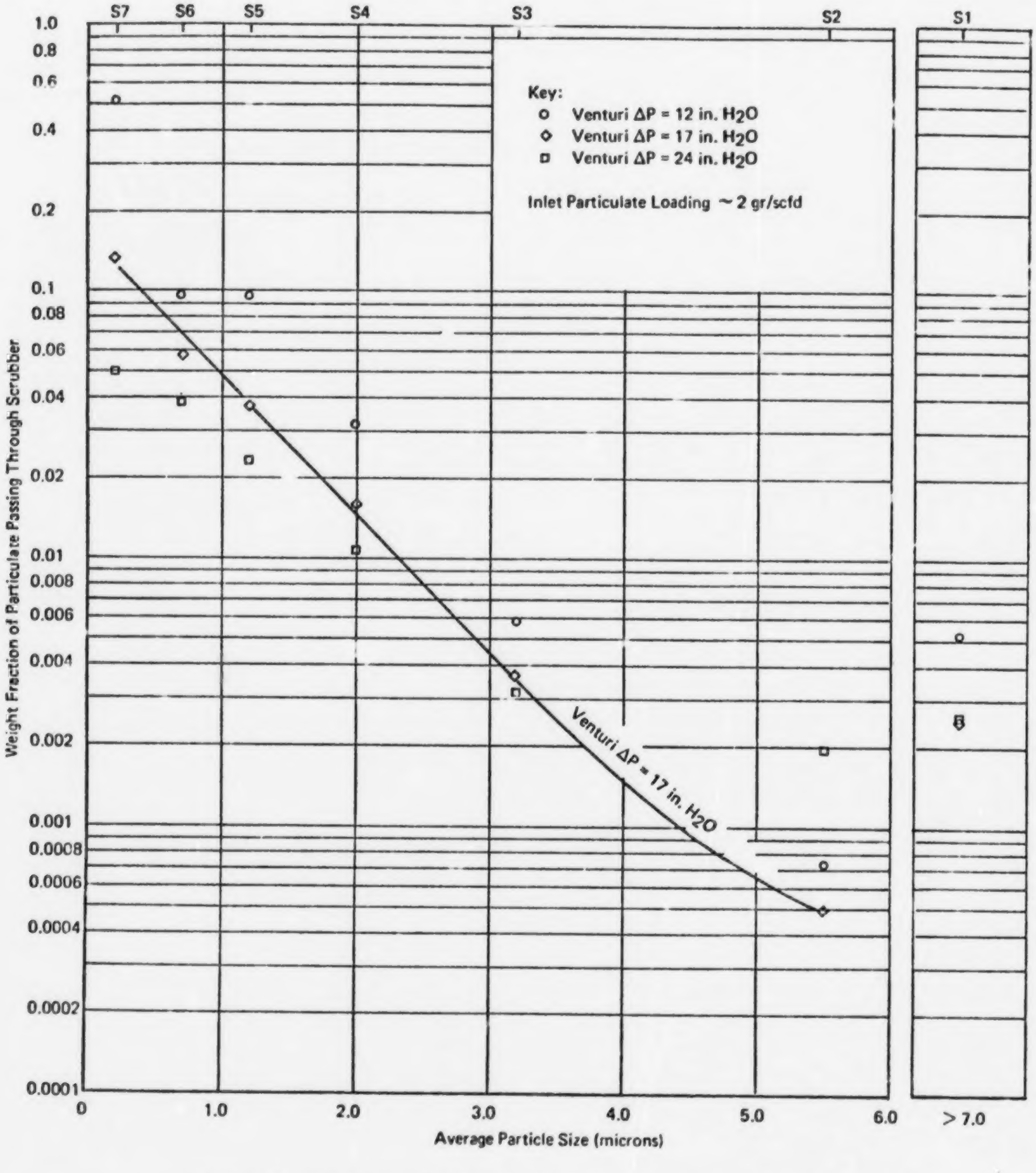

FIGURE 4 SCRUBBER FRACTIONAL COLLECTION EFFICIENCY – TEST SERIES 300

TABLE 1

AVERAGE PARTICULATE SIZE DISTRIBUTION IN AND OUT OF SCRUBBER SYSTEM

		Particulate Loading (gr/scfd)															
		Stage 1 >7μ		Stage 2 <7μ		Stage 3 <4μ		Stage 4 <2.4μ		Stage 5 <1.6μ		Stage 6 <0.85μ		Stage 7 <0.5μ		Total	
	Test	In	Out	In	Out	In	Out	In	Out	In	Out	In	Out	In	Out	In	Out
VenturiΔP=12in	324	1.325	.0071	0.502	.0003	0.151	.0006	0.040	.0011	0.019	.0029	0.011	.0026	0.023	.0071		
	326	0.998	.0053	0.313	.0003	0.091	.0008	0.032	.0014	0.061	.0048	0.043	.0025	0.007	.0084		
	Avg.	1.161	.0062	0.408	.0003	0.121	.0007	0.036	.0012	0.040	.0038	0.027	.0026	0.015	.0078	1.808	.0226
	Efficiency	99.5%		99.9%		99.4%		96.7%		90.5%		90.4%		48.0%		98.8%	
VenturiΔP=17in	306	1.415	.0050	0.362	.0000	0.090	.0000	0.040	.0000	0.094	.0014	0.048	.0020	0.069	.0062		
	321	1.489	.0000	0.466	.0000	0.135	.0006	0.047	.0009	0.040	.0032	0.028	.0020	0.017	.0073		
	322	-	.0061	-	.0006	-	.0006	-	.0012	-	.0029	-	.0026	-	.0035		
	Avg.	1.452	.0037	0.414	.0002	0.112	.0004	0.044	.0007	0.067	.0025	0.038	.0022	0.043	.0057	2.170	.0154
	Efficiency	99.7%		99.9%		99.6%		98.4%		96.3%		94.2%		86.7%		99.3%	
VenturiΔP=24in.	309	2.238	.0030	0.362	.0008	0.088	.0000	0.037	.0008	0.092	.0008	0.052	.0014	0.070	.0000		
	311	1.848	.0053	0.324	.0008	0.074	.0006	0.059	.0003	0.072	.0011	0.042	.0031	0.009	.0000		
	318	0.984	.0045	0.385	.0006	0.124	.0003	0.046	.0003	0.044	.0028	0.022	.0001	0.042	.0059		
	Avg.	1.690	.0043	0.357	.0007	0.095	.0003	0.047	.0005	0.069	.0016	0.039	.0015	0.040	.0020	2.337	.0109
	Efficiency	99.7%		99.8%		99.7%		98.9%		97.7%		96.1%		95.0%		99.5%	

TABLE 1 (continued)

Venturi ΔP = 17 in.

Test	Stage 1		Stage 2		Stage 3		Stage 4		Stage 5		Stage 6		Stage 7		Total	
	In	Out	In	Out	In	Out	In	Out	In	Out	In	Out	In	Out	In	Out
713	-	.0083	-	.0010	-	.0008	-	.0008	-	.0029	-	.0044	-	.0000	-	
717	-	.0000	-	.0000	-	.0003	-	.0005	-	.0021	-	.0021	-	.0097	-	
726	-	.0047	-	.0000	-	.0008	-	.0010	-	.0029	-	.0021	-	.0115	-	
730	-	.0060	-	.0000	-	.0005	-	.0005	-	.0029	-	.0026	-	.0120	-	
741	-	.0086	-	.0000	-	.0000	-	.0003	-	.0003	-	.0010	-	.0044	-	
756	-	.0055	-	.0003	-	.0000	-	.0000	-	.0029	-	.0026	-	.0068	-	
761	-	.0084	-	.0000	-	.0000	-	.0003	-	.0029	-	.0026	-	.0136	-	
Avg.	-	.0059	-	.0002	-	.0003	-	.0005	-	.0024	-	.0025	-	.0083	-	.0201

Note: Tests 314, 315, 317 were omitted from this table due to fan vibration and tests 301 and 303 omitted due to inadequate heating of sample probe during the test sampling procedure indicated 40-50% removal of sulfur dioxide without supplimental alkali addition. In addition, the influence of these variables on reliability (no scaling or plugging) was evaluated. Phase I of the pilot plant testing was conducted during the period of January 18 to June 6, 1973. Phase II, which is presently in operation, is being conducted to train operating personnel, assess the long term reliability of the system and to analyze the sludge generated in the scrubber system to provide information for the design of the disposal system.

TVA Pilot Plant Program

A test program (Ref: 2) was initiated by TVA to study particulate removal at power plants which burn coal containing 2-4% sulfur. Three methods for removal of dust (particulate) were evaluated using a high-efficiency sampling train. Based on this study, a predictive equation for dust removal, when sulfur dioxide is also a major concern, was developed.

Three methods were evaluated:

(1) Dust Difficulty Determinator (DDD) to determine pressure drop required for dust removal. (Fig. 5).

(2) Turbulent Contact Absorber (3 stages) using water to determine dust removal efficiency. (Fig. 6).

(3) Ventri-rod/spray tower SO_2 pilot plant to determine particulate removal efficiency. (Fig. 7).

Dust Difficulty Determinator (DDD)

A total of 45 tests were completed at the Widows Creek Station using the DDD. Table II summarizes the data collected.

Turbulent Contact Absorber (TCA)

The pilot unit was a three-stage turbulent contact absorber with cross-section area of one square foot. The purpose of this test series was to determine the dust removal capability of the TCA. The test plan consisted of 20 tests in which liquor flow and gas velocities were varied. The data collected are summarized in Table III.

Ventri-Rod Spray Tower Scrubber

TVA used a Ventri-Rod spray tower pilot unit to study SO_2 removal and particulate removal. The test plan consisted of 21 tests. Dust data collected are summarized in Table IV.

Analysis of Experimental Results

A. Dust Difficulty Determinator

The data collected with the DDD were analyzed and a model constructed. Tests numbers used in the analysis were 16-22, 24-42, and 45. Tests 1-15 were not used since these data were obtained during shake down testing.

The following equation was developed which relates outlet grain loading to $\frac{L}{G}$ and Δ P.

$$Y = .12 \left(\frac{L}{G} . \Delta P\right)^{-.54}$$ where

Y = outlet grain loading = gr/ft^3
L - Liquid circulated = gal/min.
G - gas rate = 1000 ft^3/min.
Δ P - pressure drop = inches H_2O

Figure 8 is a plot of equation (1) and with actual data points indicated by X. Data from Western Precipetator Co. using venturi scrubbers, which tested plants burning Western U.S. coal is also shown in Fig. 8.

Turbulent Contact Absorber (TCA)

The test data as shown in Table 3 indicated the majority of the data gave an outlet loading of .01-.04 gr/SEFD at L/G of 40-70 and ΔP of 6.5-10 inches H_2O.

Venturi-Rod Spray Tower Scrubber

The test data was correlated so that a comparison could be made between this data and the model generated with the DDD data. The comparison of the indicated outlet grain loading vs. the observed as shown in Table 4.

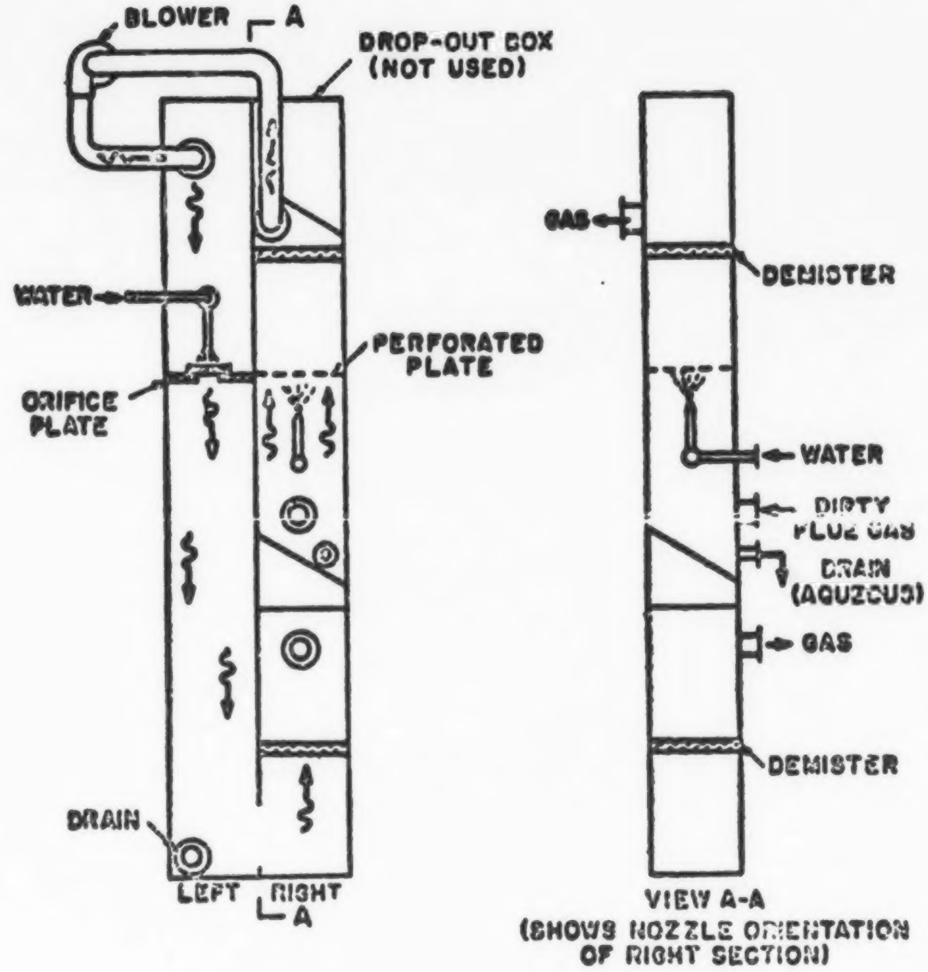
BLOWER
A
DROP-OUT BOX
(NOT USED)
GAS
DEMISTER
WATER
PERFORATED
PLATE
ORIFICE
PLATE
WATER
DIRTY
FLUE GAS
DRAIN
(AQUEOUS)
GAS
DEMISTER
DRAIN
LEFT
RIGHT
A
VIEW A-A
(SHOWS NOZZLE ORIENTATION
OF RIGHT SECTION)

FIGURE 5

Schematic - Dust Difficulty Determinator

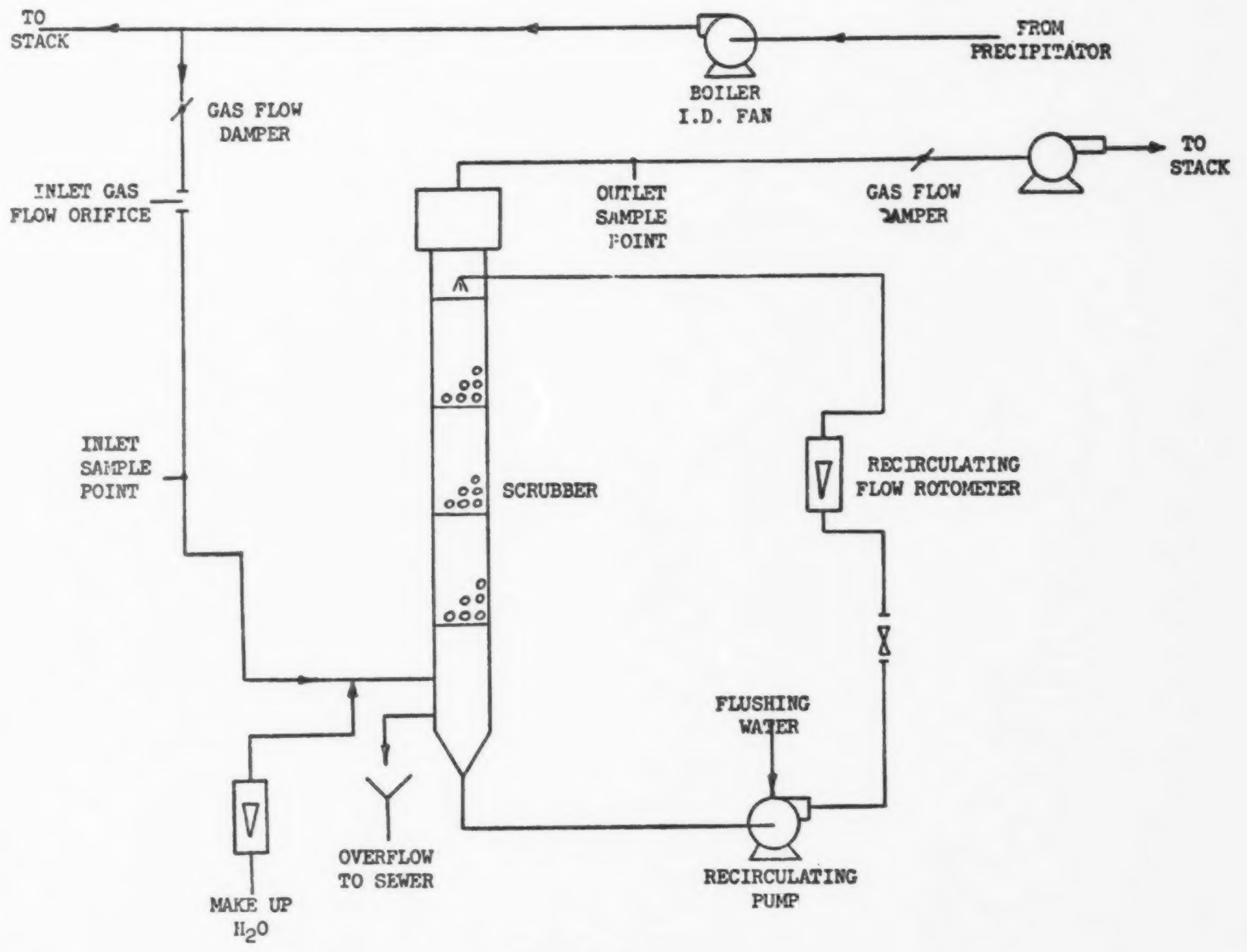
TO STACK
FROM PRECIPITATOR
BOILER I.D. FAN
GAS FLOW DAMPER
TO STACK
INLET GAS FLOW ORIFICE
OUTLET SAMPLE POINT
GAS FLOW DAMPER
INLET SAMPLE POINT
SCRUBBER
RECIRCULATING FLOW ROTOMETER
FLUSHING WATER
MAKE UP H_2O
OVERFLOW TO SEWER
RECIRCULATING PUMP

FIGURE 6

Schematic - Universal Oil Products Scrubber System

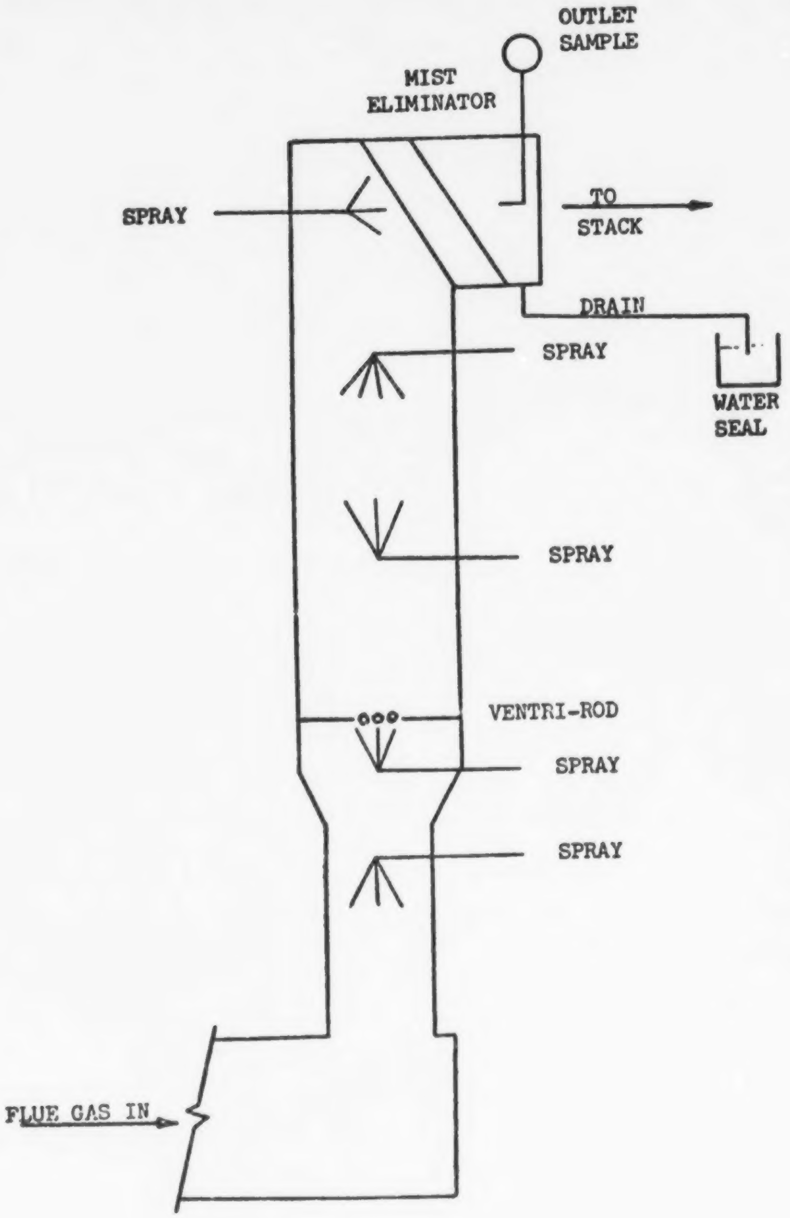
OUTLET SAMPLE
MIST ELIMINATOR
SPRAY
TO STACK
DRAIN
SPRAY
WATER SEAL
SPRAY
VENTRI-ROD
SPRAY
SPRAY
FLUE GAS IN

FIGURE 7

Schematic - Ventri-Rod Spray Tower System

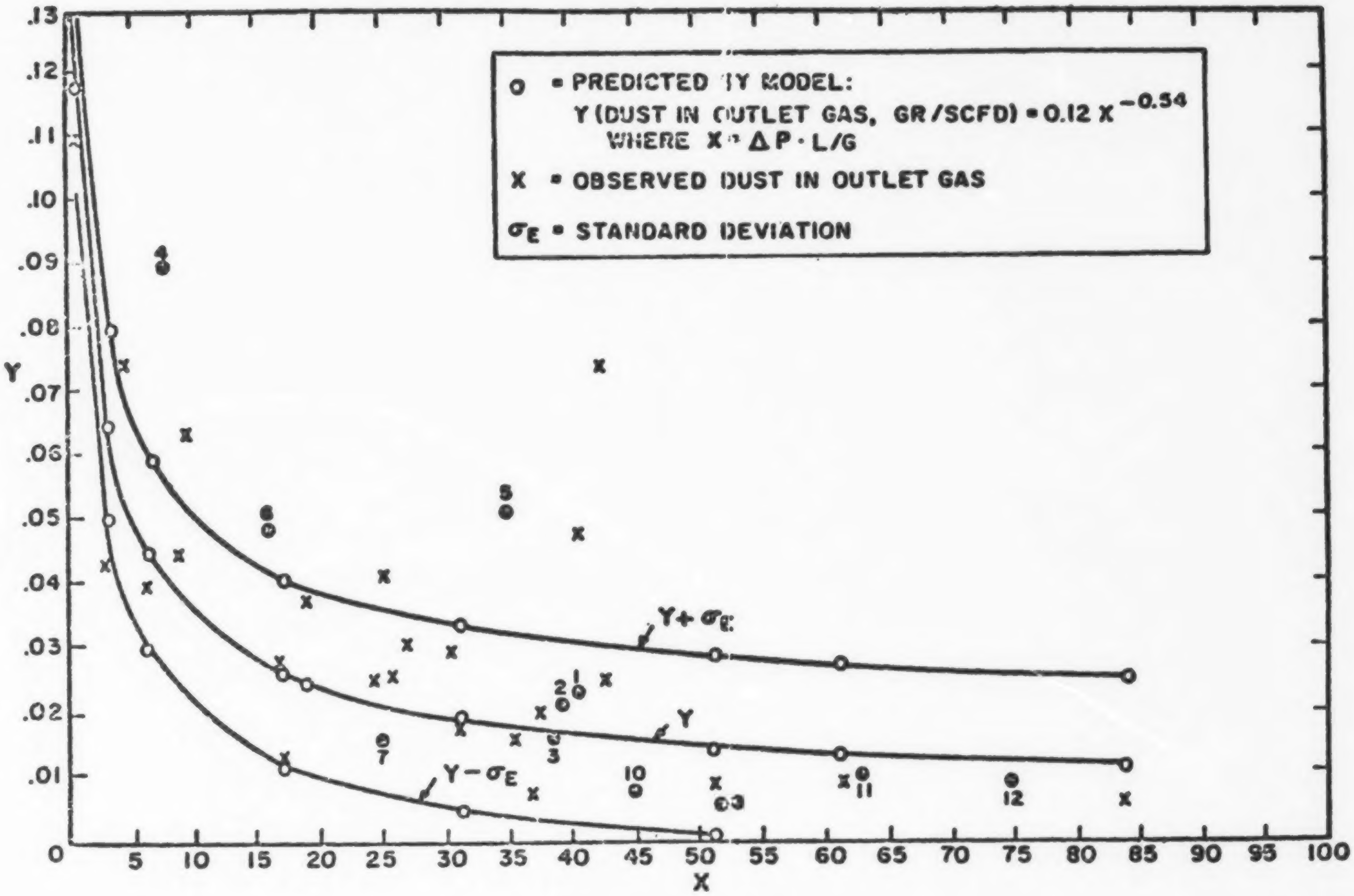

FIGURE 8

Correlation of Observed and Predicted Dust Removal Data from Widows Creek Tests

Data from the Western Precipitation Corporation have been added (denoted by No. 1-12)

TABLE 2

TEST DATA - DUST DIFFICULTY DETERMINATOR

Run	$\triangle$P-inches H_2O	L/G $\frac{\text{gal}}{1000\ \text{ft}^3}$	Inlet Loading gr/SCFD	Outlet Loading gr/SCFD
1-15	Check out			
16	4.0	27	5.9	.011
17	2.2	27.7	3.2	.009
18	1.8	28.3	2.9	.009
19	2.1	20.2	2.7	.025
20	2.1	17.5	2.9	.007
21	2.1	12.8	3.0	.031
22	5.5	15.2	1.9	.006
24	4.9	7.2	5.9	.016
25	3.4	5.0	6.01	.013
26	4.3	7.2	4.53	.018
29	0.2	3.9	2.2	0.11
30	0.2	5.2	3.9	0.09
31	1.2	5.2	6.6	0.04
32	0.8	3.9	4.0	0.044
33	0.4	2.6	3.7	0.13
34	1.7	2.6	3.4	.075
35	3.2	5.2	3.5	.028
36	3.2	7.8	2.7	.042
37	2	4.7	2.4	.064
38	2	9.4	3.7	.038
39	2	13	3.3	.026
40	4.9	2.6	2.2	.02
41	4.5	5.4	-	.0246
42	4.2	2.1	5.2	.0843

TABLE 3

TEST DATA FROM WIDOWS CREEK USING UOP SCRUBBER (THREE-BED TCA PILOT UNIT)

Run No.	ΔP	L/G	Gas Flow CFM	Liquid Rec. Rate Gal/Min/Ft^2	Inlet UOP Thimble Gr/SCFD	Outlet UOP Thimble Gr/SCFD	Outlet With DDD Sampling Train Gr/SCFD
1	6.5	40	750	30	2.37	0.081	0.0467;0.0338
2	6.5	40	750	30	0.998	0.052	
3	7.0	40	750	30	2.52	0.050	
4	6.0	27	750	20	1.56	0.043	
5	6.0	27	750	20	0.315	0.018	} ESP's on
6	7.0	73	550	40	0.54	0.010	
7	7.0	73	550	40	5.15	0.037	
8	7.0	49	675	33	6.45	0.036	
9	6.8	49	675	33	3.65	0.0295	0.0259
10	7.8	70	675	47	2.50	0.013	0.012
11	7.8	70	675	47	2.49	0.015	0.0234
12	7.5	54	750	40	5.35	0.0172	0.030
13	8.8	67	750	50	4.70	0.013	0.0174
14	7.5	54	750	40	-	-	0.0081
15	7.0	40	825	33	5.34	0.0043	0.0337
16	5.3	60	500	30	5.22	0.0393	0.0217
17	7.0	54	750	40	2.98	0.044	0.0086
18	7.0	40	825	33	1.21	-	0.0123
19	5.5	27	750	20	3.05	0.066	0.0142
20	7.5	54	750	40	2.44	0.0296	0.0111
21	8.4	67	750	50	1.42	0.028	0.0101
22	6.5	40	750	30	2.15	0.0341	0.0135
23	5.8	27	750	20	2.22	0.0362	0.0133
24	10.8	57	825	47	2.26	0.0308	0.0108
25	8.4	42	950	40	2.34	0.0236	0.0098
26	7.6	48	825	40	2.20	0.026	
27	6.8	40	825	33	1.49	0.0222	
28	5.8	24	825	20	1.27	0.0329	
29	7.6	69	680	47	1.64	0.0243	

TABLE 4

Ventri-Rod - Spray Tower

Run	Δ P V-R	Total L/G	Flyash Observed	$Y=0.12(x)^{-0.54}$ Predicted
1	6.5	56	0.0104	0.0050
2	6.0	38	0.0093	0.0063
3	14.5	28	0.0063	0.0047
4	15.0	48	0.0040	0.0034
5	10.0	46	0.0047	0.0044
6	13.2	36	0.0033	0.0043
7	13.9	66	0.0037	0.0030
8	15.6	58	0.0138	0.0031
9	7.2	68	0.0048	0.0042
10	11.1	46	0.0031	0.0041
11	7.4	46	0.0041	0.0051
12	15.2	58	0.0059	0.0031
13	15.0	36	0.0030	0.0040
14	7.4	48	0.0027	0.0050
15	11.3	46	0.0042	0.0041
16	7.0	26	0.0028	0.0072
17	7.0	38	0.0032	0.0059
18	15.0	46	0.0023	0.0035
19	7.2	56	0.0027	0.0047
20	11.6	46	0.0012	0.0041
21	14.9	66	-	-
21	15.1	68	0.0016	0.0028

EPA Shawnee Test Facility

The EPA Shawnee Test Facility consists of three parallel scrubber systems (Ref. 3).

(1) a Venturi followed by a spray tower (Fig. 9).
(2) a Turbulent Contact Absorber (TCA) (Fig. 10).
(3) a Marble-Bed absorber (Fig. 11).

Each system is capable of treating approximately 10 MW equivalent (30,000 ACFM at 300°F) of flue gas containing 1800- 4000 ppm sulfur dioxide and 2-5 grains/SCF of particulates.

Particulate removal studies were conducted by EPA during factorial testing and other limited test series.

The inlet and outlet aerodynamic size distributions were obtained using a Brink Impactor. In order to use the impactor at scrubber inlet mass loading conditions, a modified EPA mass sampling train was used. The train is of 316 ss construction and consists of a heated sample probe (6 ft. x 1/2 inch OD), a cyclone and the Brink Impactor with a 144 mm glass fiber filter. The impactor draws a sample from the gas stream exiting the cyclone.

At the scrubber outlet, the Brink Impactor was used directly in the flue gas duct (without sample probe and cyclone).

Overall Removal Efficiencies

The overall particulate removal efficiencies for the three scrubbers, obtained during the limestone short-term factorial testing are presented in Tables 5, 6 and 7. Only those data which were taken at close-to-isokinetic sampling conditions have been included in the Tables.

From Table 5, it is seen that overall particulate removal efficiencies at 99.4 to 99.8 percent were obtained for the Chemico venturi at a gas flow rate of 30,000 acfm (330°F) and liquid-to-gas ratios from 13 to 27 gal/mcf (300-600 gpm), with venturi plug pressure drops from 6 to 12 inches H_2O. For the spray tower, the removal efficiency was about 98.5 percent at a gas velocity of 4 ft/sec. and a liquid-to-gas ratio of 40 gal/mcf (15,0000 acfm and 450 gpm).

Table 6 shows that, for the TCA scrubber with 5 grids and no spheres, the overall removal efficiencies were 98.6 to 99.8 percent at a gas velocity of 7.5 ft/sec. and a liquid-to-gas ratio of 50 gal/mcf (19,300 acfm and 730 gpm), with total pressure drops (includes Koch tray, demister and inlet duct) from 4-7 inches H_2O.

The Marble-Bed scrubber (see Table 7) gave an overall particulate removal efficiency range of 98.8 to 99.6 percent, at a gas velocity of 5 ft/sec. and a liquid-to-gas ratio of 54 gal/mcf (20,000 acfm and 810 gpm), with 12 inches H_2O total pressure drop.

During the limestone realiability verification testing, a series of particulate removal testa with the TCA scrubber (3 stages, 5 inches of spheres/stage) were conducted by EPA. Results from these tests are presented in Table 3-12. The overall removal efficiencies of 98.7 to 99.9 percent were achieved at gas velocities from 8 to 10 ft/sec. (20,000-25,000 acfm), liquid-to gas ratios from 40-80 gal/mcf (600-1200 gpm), and total pressure drops from 5.5 to 10 inches H_2O. The higher pressure drops generally gave higher overall removal efficiencies.

The overall particulate removal efficiencies shown in Tables 5 through 8 appear to be higher than the efficiencies predicted from the "Impaction Theory." These improved efficiencies could be due to (1) the condensation of water vapor in the flue gas on the solid particles* and (2) solids accumulations upon the demisters or underneath the TCA Koch tray during the duration of particulate testing.

Particulate Size Distribution in the TCA

For the runs listed in Table 8, the particle size distributions of the particulates at the TCA inlet and outlet were also determined. The results are shown in Figure 12.

As shown in Figure 13, the mass mean diameter of the inlet solids is approximately 23 microns, which is slightly greater than the "normal" range of from 10-20 microns. The data for the outlet size distribuiton shows some scatter. The mass mean diameter ranges from about 0.5 to 0.75 micron, for a total pressure drop range of 5.5-10.0 inches H_2O. Generally, the higher pressure drops give smaller outlet mass mean diameters.

---

*The condensation of water vapor per unit mass of inlet solids has been estimated to be from 1-5 grains water/grain inlet particulates.

Particulate Removal Efficiency in the TCA as a Function of Particle Size

The particulate removal efficiency as a function of particle size was determined by EPA for the TCA runs shown in Table 8. In Figure 13 the percent penetration (100-percent removal) is plotted vs. particle diameter in microns, for different ranges of total pressure drop.

From Figure 13, it is seen that for the submicron particles (0.11 to 0.99 micron), the removal efficiency drops rapidly with decreasing particle size, especially at low total pressure drop. The efficiencies were 95 to 99 percent at 9.8 inches H_2O total pressure drop, 93 to 95 percent at 7.6 inches H_2O, and 71 to 90 percent at 5.6 inches H_2O.

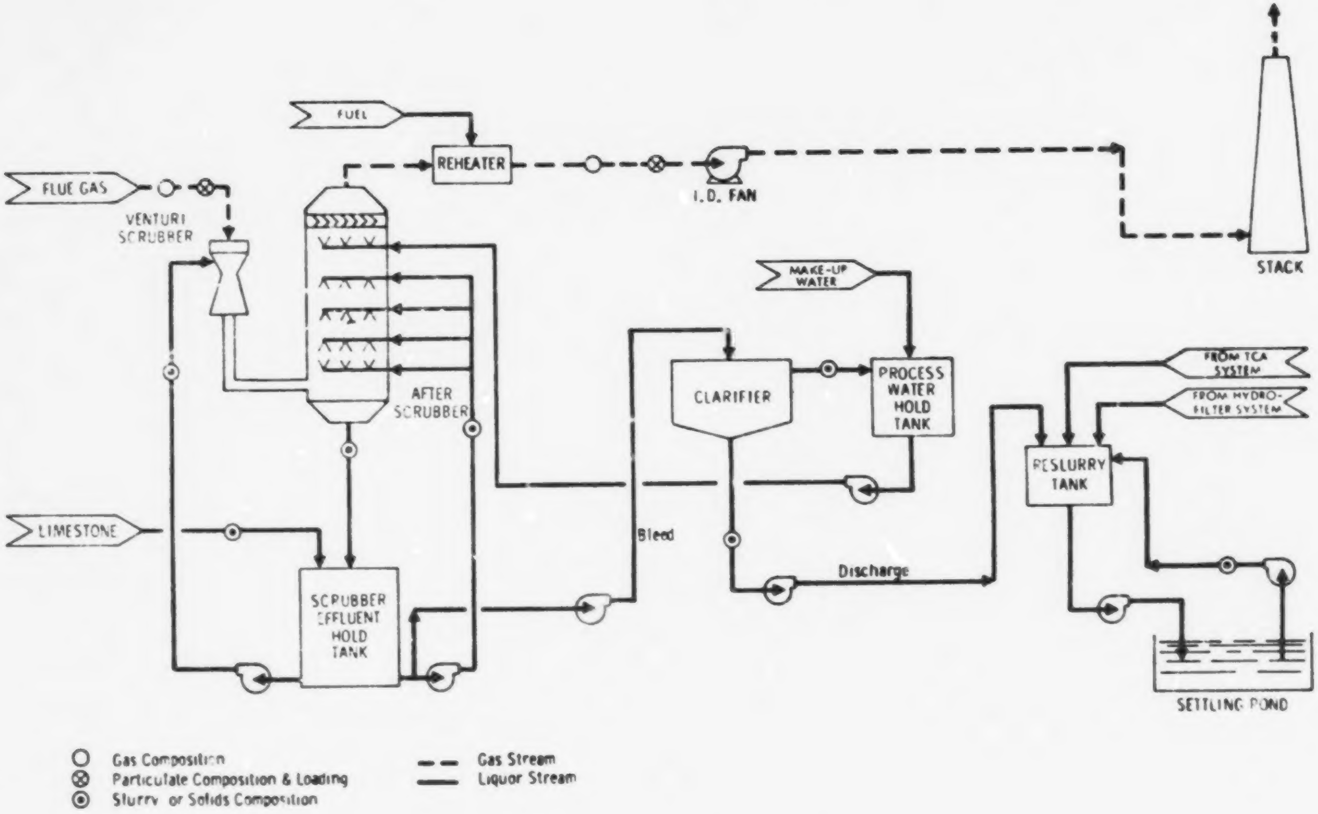
FUEL
FLUE GAS
VENTURI SCRUBBER
REHEATER
I. D. FAN
STACK
AFTER SCRUBBER
MAKE-UP WATER
CLARIFIER
PROCESS WATER HOLD TANK
FROM TCA SYSTEM
FROM HYDRO-FILTER SYSTEM
RESLURRY TANK
LIMESTONE
Bleed
Discharge
SCRUBBER EFFLUENT HOLD TANK
SETTLING POND
○ Gas Composition
⊗ Particulate Composition & Loading
⊙ Slurry or Solids Composition
Gas Stream
Liquor Stream

Figure 9 Typical Process Flow Diagram For Venturi System

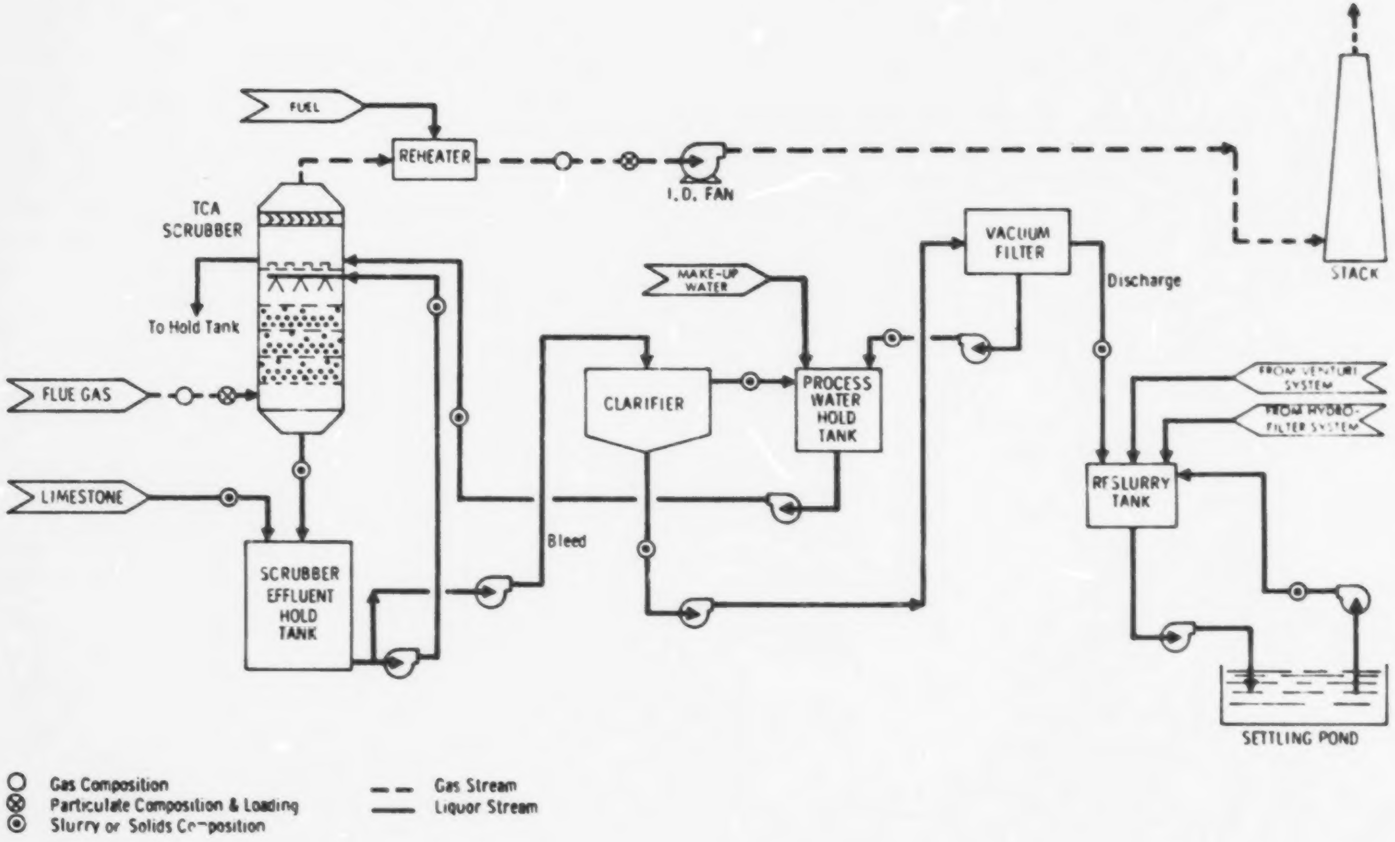
FUEL
REHEATER
I.D. FAN
STACK
TCA SCRUBBER
To Hold Tank
FLUE GAS
LIMESTONE
SCRUBBER EFFLUENT HOLD TANK
Bleed
CLARIFIER
MAKE-UP WATER
PROCESS WATER HOLD TANK
VACUUM FILTER
Discharge
FROM VENTURI SYSTEM
FROM HYDRO-FILTER SYSTEM
RESLURRY TANK
SETTLING POND
○ Gas Composition
⊗ Particulate Composition & Loading
⊙ Slurry or Solids Composition
– – Gas Stream
— Liquor Stream

Figure 10 Typical Process Flow Diagram For TCA System

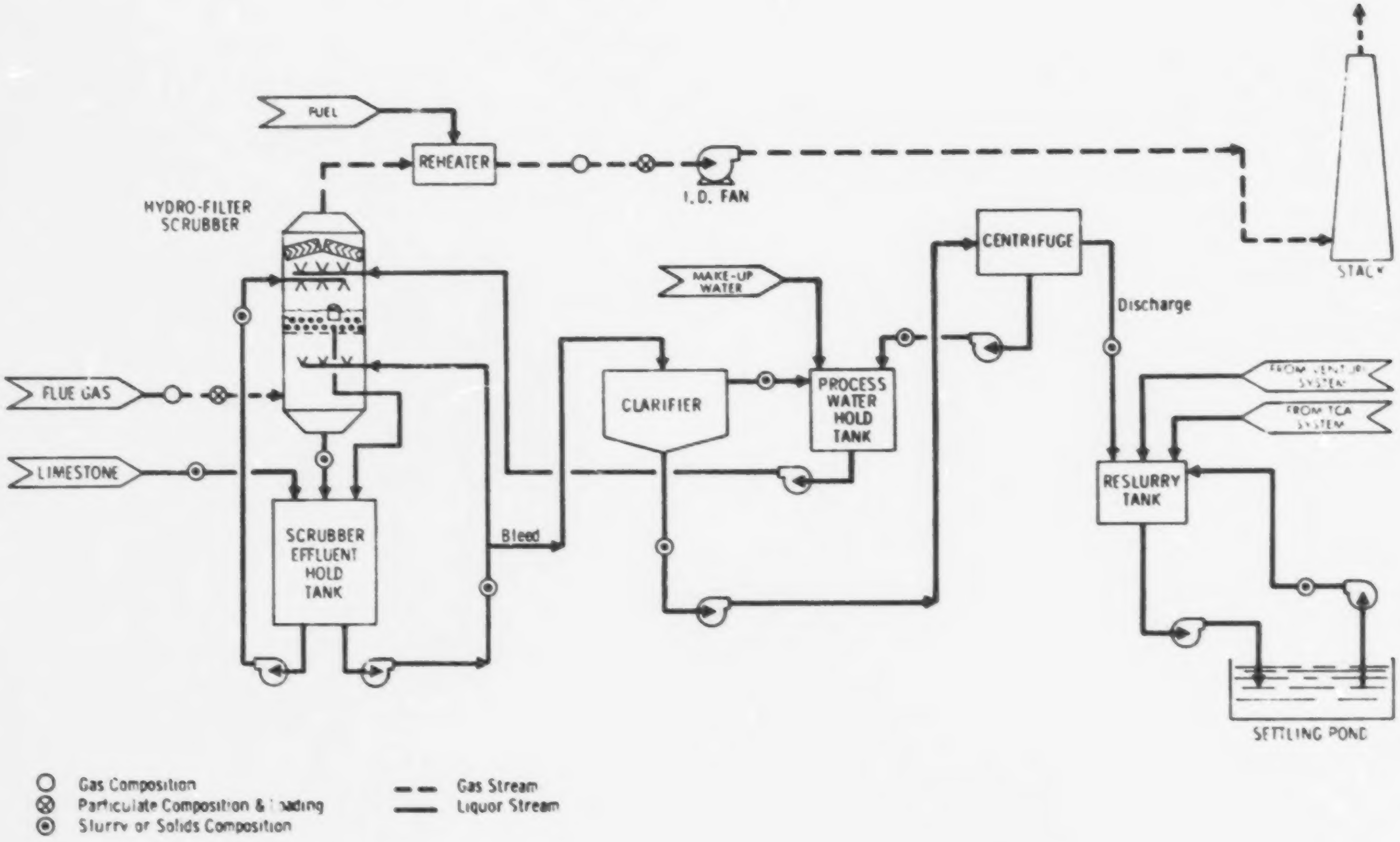
FUEL
REHEATER
I. D. FAN
STACK
HYDRO-FILTER SCRUBBER
FLUE GAS
LIMESTONE
SCRUBBER EFFLUENT HOLD TANK
Bleed
CLARIFIER
MAKE-UP WATER
PROCESS WATER HOLD TANK
CENTRIFUGE
Discharge
FROM VENTURI SYSTEM
FROM TCA SYSTEM
RESLURRY TANK
SETTLING POND
○ Gas Composition
⊗ Particulate Composition & Loading
⊙ Slurry or Solids Composition
Gas Stream
Liquor Stream

Figure 11 Typical Process Flow Diagram For Hydro-Filter System

Table 5

PARTICULATE REMOVAL IN VENTURI AND SPRAY TOWER SCRUBBER DURING FACTORIAL TESTS

Run No.	Date	Gas Rate, acfm @ 330°F	Liquor Rate, gpm		Pressure Drop, in. H_2O		Grain Loading, g/scf		Percent Removal
			Venturi	Spray Tower	Venturi	Spray Tower	Inlet	Outlet	
415-1A	11-09-72	30,000	305	0	9.0	1.1	4.38	0.012	99.7
414-1D	11-12-72	30,000	305	0	9.0	1.0	2.1	0.010	99.5
414-1D	11-14-72	29,900	305	0	9.0	1.0	3.32	0.013	99.6
414-1C	11-15-72	29,900	305	0	6.4	1.0	3.40	0.02	99.4
417-1A	12-22-72	30,000	605	0	9.5	1.0	3.38	0.012	99.6
414-1E	12-25-72	30,000	300	0	12.0	1.0	4.17	0.009	99.8
418-1C	12-27-72	14,900	600	0	12.5	0.2	6.39	0.114	98.2
453-1B*	12-31-72	14,900	12	460	2.5	0.25	2.6	0.004**	99.8
454-1B*	1-04-73	14,900	12	450	0.75	0.25	4.62	0.07	98.5
456-1A*	1-05-73	14,900	12	450	0.70	0.25	3.38	0.056	98.3

*Spray tower only.

**Data point questionable.

Table 6

PARTICULATE REMOVAL IN TCA SCRUBBER WITH NO SPHERES DURING FACTORIAL TESTS

Run No.	Date	Gas Rate, acfm @ 330°F	Liquor Rate, gpm	Pressure Drop, in. H_2O	Grain Loading, g/scf		Percent Removal
					Inlet	Outlet	
WC-5	12-21-72	19,200	730	1.5	1.70	0.004	99.8
WC-5A	1-06-73	19,300	730	1.5	4.16	0.029	99.3
WC-5A	1-09-73	19,300	730	1.5*	1.32	0.019	98.6
WC-11	1-12-73	19,400	745	1.5*	3.29	0.017	99.5
WC-12	1-14-73	19,300	375	1.0*	3.65	0.022	99.4

*These listed values are the assumed pressure drops across the scrubber. Increases in total pressure drop for these runs were most likely due to pluggage of the inlet gas duct during testing.

Table 7

PARTICULATE REMOVAL IN HYDRO-FILTER SCRUBBER DURING FACTORIAL TESTS

Run No.	Date	Gas Rate. acfm @ 330°F	Liquor Rate, gpm	Pressure Drop, in. H_2O	Grain Loading, g/scf		Percent Removal
					Inlet	Outlet	
427-3A	11-13-72	20,000	810	12.0	2.6	0.030	98.8
427-3A	11-16-72	20,000	810	12.0	3.32	0.035	98.9
426-3B	11-28-72	20.000	810	10.0	4.43	0.032	99.3
427-3C	12-02-72	20.000	800	12.5	4.24	0.033	99.2
427-3B	12-24-72	20.000	805	11.0	2.19	0.027	98.8
428-3A	12-28-72	20,000	810	11.5	3.78	0.025	99.3
428-3A	12-29-72	20.000	810	11.5	4.12	0.016	99.6
428-3A	12-30-72	20,000	810	11.5	3.63	0.035	99.0
438-3A	1-07-73	19,900	400	7.0	4.20	0.020	99.5
440-3A	1-11-73	12,500	600	6.8	3.82	0.042	98.9
440-3A	1-13-73	12,500	600	6.8	3.59	0.066	98.2

Table 8

OVERALL PARTICULATE REMOVAL IN TCA SCRUBBER DURING LIMESTONE RELIABILITY VERIFICATION TESTS

Run No.	Date	Gas Rate, acfm @ 300°F	Liquor Rate, gpm	Pressure Drop, in. H_2O	Grain Loading, grains/scf		Percent Removal
					Inlet	Outlet	
503-2A	5/22-23	25,000	1200	9.8	3.16	0.00852	99.7
					3.00	0.00375	99.9
506-2A	5/24	20,000	1200	7.5	2.89	0.0143	99.5
					2.13	0.0152	99.3
505-2A	5/23	20,000	600	5.6	2.34	0.031	98.7
					2.61	0.020	99.2
					2.28	0.010	99.6

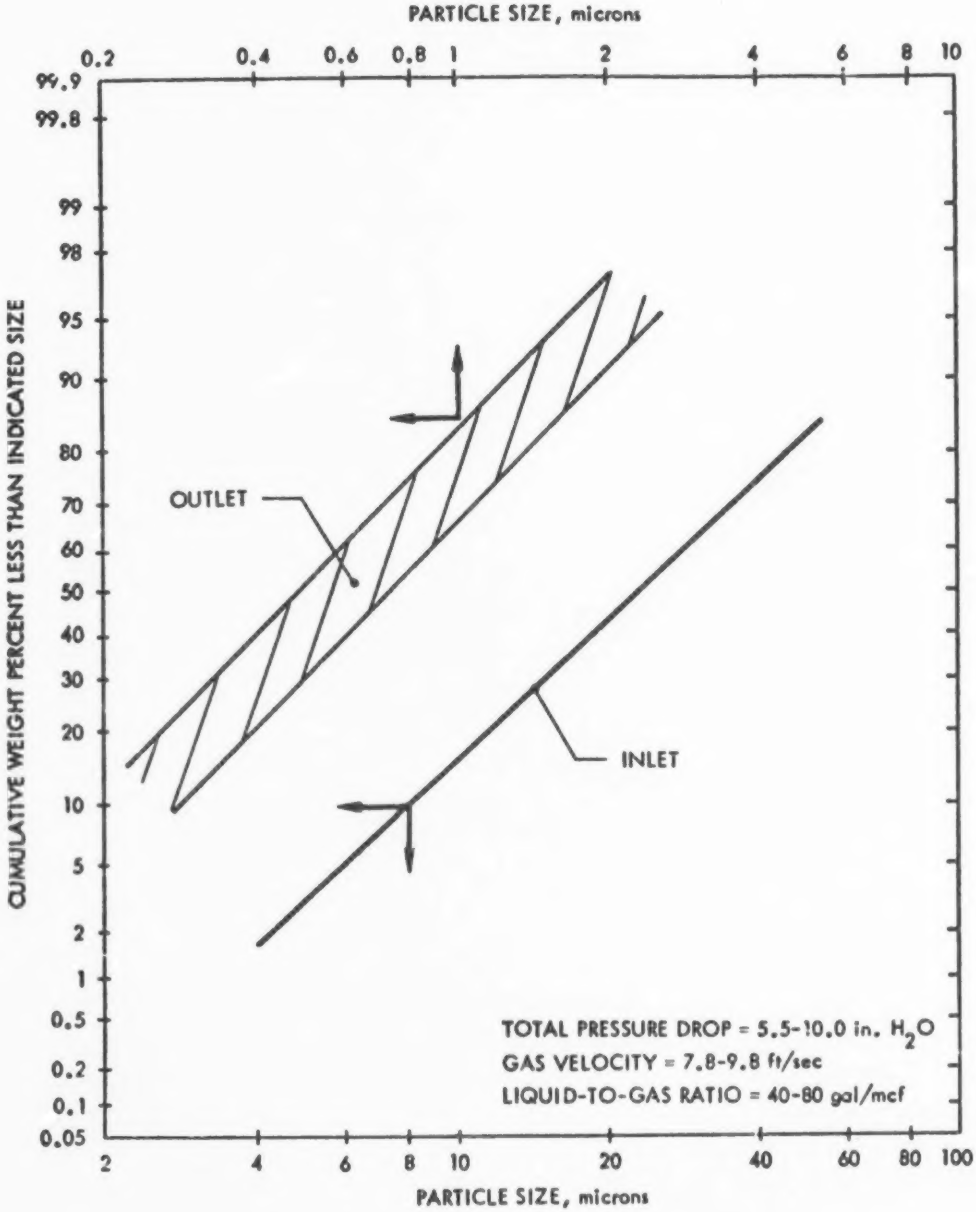

Figure 12 Particle Size Distributions at TCA Inlet and Outlet

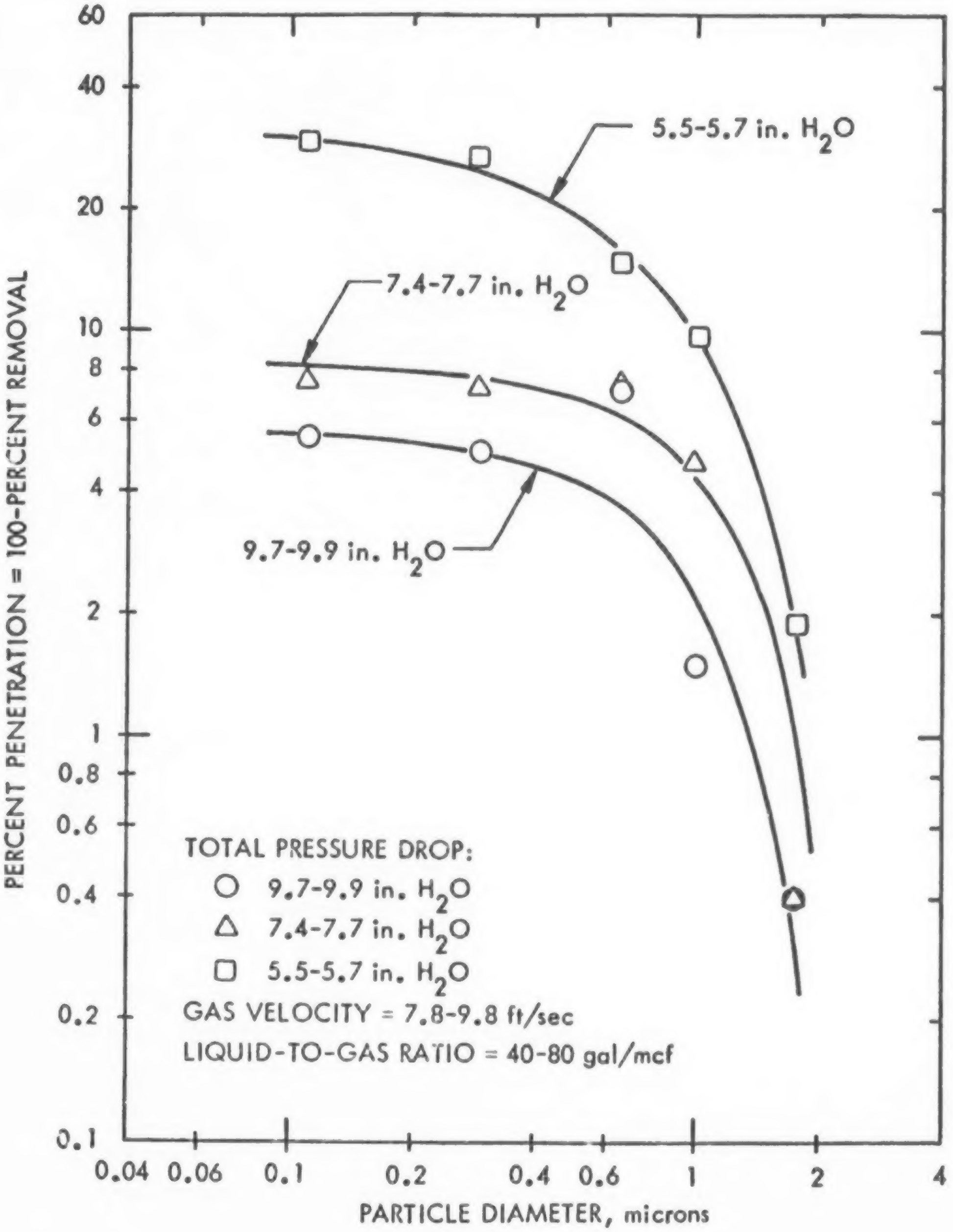

Figure 13 TCA Particulate Removal Efficiency as a Function of Particle Size

Commercial System Design

The design of wet scrubbing systems for particulate control should consider the following main design criteria:

- Scrubber type
- System pressure drop
- Scrubber size and spare capacity
- Liquid to gas ratio
- Demister design and wash cycle
- Gas reheater design and materials of construction
- Fan design
- Materials of construction
- Percent solids and pH of circulating liquid
- Residence time in recirculing tank
- Waste disposal

The principle types of scrubbers used in full size systems are venturi, turbulent contact absorbers and marble-bed scrubbers.

Venturi scrubbers have demonstrated particulate removal efficiencies required to obtain .03 gr/SCFD at liquid to gas ratios of 15-20 gal/1000 ft^3 at the venturi throat and a pressure drop of 10-20 inches H_2O. Sprays have been added in the separator section for additional SO_2 removal.

Turbulent Contact Absorber (TCA) is a counter current multistage scrubber consisting of screens that both support and restrain the plastic spheres. The spheres move in turbulent fashion providing good gas-liquid contacts. The number of stages generally vary between two and four and pressure drop is 2-3 inches H_2O per stage. Liquid to gas ratios vary between 30-60 gal/1000ft^3 to achieve 99. +% particulate removal.

Marble-Bed Absorber. The marble-bed absorber utilizes one or two 4 inch beds of glass speres (marbles) that are in slight vibratory motion. A turbulent layer of liquid and gas above the glass spheres increases mass transfer and particulate removal. Pressure drop is generally 6-8 inches H_2O. Liquid to gas ratios of 20-30 have been used.

System Pressure Drop. Scrubber System pressure drop consists of scrubber, demister, reheater and duct losses. Typical losses are as follows:

Scrubber System	Gas ΔP inch H_2O	Fan losses percent station capacity	L/G	percent loss
Venturi	20	2.0	30	0.5
TCA	16	1.7	50	0.7
Marble-Bed	14	1.5	30	0.5

Scrubber Size and Spare Capacity

In order to keep particulate removal system investment as low as possible, scrubber size of 500,000 to 600,000 CFM have been designed. This design is desirable due to the large quantities of flue gas treated, 3000 ACFM/MW. An additional design consideration is scrubber turndown due to changes in boiler load. Some scrubbers can be turned down to 50% of design and others require compartmentalization.

In order to insure greater system reliability and boiler availability, spare modules are being constructed, so that with one unit down, maximum boiler availability will be possible.

Liquid to Gas Ratio, percent Solids and pH control of circulating liquor

Particulate removal systems are presently being designed with higher liquid to gas ratios (gal/1000 ft^3 gas), higher percent solids in the circulating liquor and control of the pH at 5 or above of the recycle liquor. These design considerations are necessary to achieve greater system reliability and to prevent scaling in the scrubbing systems. Liquid to gas ratios have been increased to 30-50 gal/1000 ft^3 gas. The percent solids in the circulating liquor have been increased to 5-10% total solids which contain 1-2% $Ca(SO)_4$ as seeding material.

Earlier scrubber systems designed primarily for particulate removal did not incorporate pH control. This resulted in scaling throughout the system. Systems presently being designed have lime addition systems for pH control of the recycle liquor. Desirable pH range is 5-6.

Residence time in the recirculatory tank has been increased from 1-2 minutes to ten minutes to accomplish desupersaturation and pH control.

Demister Design and Wash Cycle

Demisters have been developed in various designs and are typically of open construction and have a low pressure drop. Demisters are designed to have one to four passes or stages to prevent mist carry over to the reheater and the fan. Demisters are designed using stainless steel or plastic.

The principle problem concerning demisters is the prevention of solids accumulation on the demister which causes plugging, high pressure drop and eventual shut down of the scrubbing system.

New design approaches to eliminate demister problem being used are:

- -Reducing gas velocity to demisters to 6-8 ft/sec.
- -Better washing of the demister, particulary on the upstream side. This includes washing more frequently with maximum available fresh water. Top washing is also used on a less frequent cycle.
- -Simpler demister design-two pass versus four pass.
- -Installation of wash tray to decrease solids entering demister.

Gas Reheater Design and Materials of Construction

In order to achieve plume buoyancy and dispersion, it is generally agreed that the saturated and cooled gas should be reheated. There is no generally acceptable degree of reheat but 50°F reheat appears to be the most widely practiced.

Methods of stack gas reheat can be direct or indirect heating. Direct heating has the advantage of greater reliability because there is no heat transfer surface on which fouling can occur. The methods of direct reheating that have been used are: direct fired with low sulfur oil or gas, depending on availability; flue gas by passing, and hot air injection.

Indirect reheating of the flue gas requires an exchanger to transfer heat from the heating medium to the gas. This design is subject to fouling and provision for soot blowers should be considered to keep exchanger surface clean. The two alternative indirect reheating methods are: (1) reheat with steam and (2) recuperative reheat, in which a heat exchanger may be used for direct transfer of heat from scrubber inlet gas to the exit gas.

Reheater materials of construction have been 316 stainless steel, corten but corrosion has been experienced during operation using these materials. Recent corrosion studies indicate Inconel 625 and Incoloy 825 are preferred materials.

Fan Design

Two types of fan design have been used in particulate control scrubbing systems. The dry fan, which follows a reheater, forces a dry gas at 175-200°F out through the stack. The fan is generally constructed of carbon stee.

The second type is a wet fan, which pumps wet gas (no reheat) after the demister to a wet stack. Problems both of a corrosive nature and mechanical stress have been reported. The wet fan must be washed continuously to prevent deposits and the rotor should be fabricated from Inconel material.

Materials of Construction

The scrubbing system internals which are in contact with wet SO_2 gases or acidic liquor should be constructed of acid resistant material. Because of the presence of solids in the system, abrasion resistant material should be used. Materials specified should withstand the highest temperature encountered during normal or upset conditions.

Stainless steel 316 L has been used for scrubber construction. If chlorides are present stress corrosion will be a problem.

Soft rubber or neoprene lined carbon steel has been found satisfactory under abrasive conditions as at a maximum temperature of 175°F. A further advantage of these linings is the low maintenance costs in descaling.

Slurry piping and pumps should be rubber lined. Experience to date has shown little or no deterioration of the linings.

An acid-proof gunite is now being offered by Pennwalt for areas which are exposed to high temperature. The gunite is bonded directly by the steel with thickness from 0.5 to 1.5 inches and can withstand temperatures to 750°F.

Another material which has been used in scrubbing systems is glass flake reinforced polyester resin such as Cealcote

100 and 200 series. The material is trowel applied at 40-80 mills thickness on to the steel.

Dry fans have generally been constructed of carbon steel. Wet fans have been manufactured of 316 ss and Incoloy 825.

Ash and Sulfur content of Fuel

The ash content and characteristics of the ash effect the design of the scrubbing system. Some ashes are more errosive and require careful attention to materials of construction. Certain ash have greater alkalinity and this effects the chemistry of the system and scale control.

The sulfur content of the fuel effects the process chemistry, particularly when SO_2 and fly ash are remove simultaneously. Waste solids disposal requirements are greater and require more careful design considerations.

Waste Disposal

The nature of waste solids, which are a mixture of fly ash and calcium sulfite and sulfate, leaving the system has created a design consideration which requires careful study to resolve a particular design. The preferred disposal site is an on site pond. Available data indicated the solids settled to an ultimate concentration of 50 WT percent. Location and preparation of the disposal pond are important to prevent water pollution.

Status of Full Size Scrubbing Systems for Particulate Removal

U.S. Industry is engineering, constructing or operating 23 full size scrubbing units for particulate control from coal fired boilers. Fifteen systems are retrofit units; eight are on new boilers. Total announced capacity, which will be in operation by the middle of 1976, is 6000 MW. Eight units treat stack gases from high sulfur coal, fifteen units are planned for boilers using low sulfur coal.

Table 9 summarizes the scrubber installations for particulate control in the U.S. Venturi scrubbers are installed on 14 units; TCA has been used on five systems and the Marble-bed scrubber, four.

Commonwealth Edison Co. (Ref: 4) installed the Babcock and Wilcox scrubbing system on a 180 MW cyclone boiler at its Will County Station. The system was designed to remove both particulate (fly ash) and sulfur dioxide. It consists of a Venturi scrubber followed in series by Turbulent contact absorber (TCA). A flow diagram for the process is shown in Fig. 14. Typical test data are presented in Table 10. Operating problems encountered were keeping the demisters clean and mechanical equipment problems. The demister problem is reported solved. Further testing is being continued.

Pacific Power & Light Co. (Ref: 5) presented a description of its Dave Johnston, Unit 4, scrubber installation. The scrubber system is installed on a 330 MW pulverized coal fired steam generating unit. Unit 4 is equipped with three wet Venturi scrubbers, which were placed in operation in July, 1972 for particulate emission control (Fig. 15.)

Fuel for the Dave Johnston system is Western Sub-butumenous coal with a sulfur composition of 0.5 WT percent, Ash 12.0 percent and a heat value of 7400 BTU/lb.

The Chemico wet Venturi scrubber system includes three scrubbing vessels, 34 ft. in diameter by 44 feet high, three Wet ID fans, and a single 250 ft. tall steel chimney. The scrubbing vessels, ducts and chimney are lined with a coating of field applied polyester material. The fan housings and piping are rubber lined. The fan wheels are unlined Inconel.

The scrubbing unit was designed for a inlet dust loading of 12 gr/SCF dry and an outlet dust loading of 0.04 gr/SCF dry at a gas pressure drop of 10 inches water and a liquid-to-gas ratio of 20 gal/1000 ft^3 gas. Test data indicate the outlet dust loading obtained varies between 0.02-0.04 gr/SCFD at an inlet loading of 3-5 gr/SCFD. In addition, due to the high alkalinity of ash (20% CaO), operating data indicate 40% SO_2 removal.

Operating experience reveals principal difficulties associated with internal deposits of two types, semi-hard ash deposits and hard scale deposits.

The primary problem areas have been (1) semi-hard ash and hard scale calcium deposits inside the vessel and pipe lines, (2) pluggage of bleed and recycle lines, (3) deposits on ID fan rotors and (4) pluggage of sensing lines and pressure taps. The most serious problem has been the ash and gypsum build-up within the scrubber vessels.

The ash deposits on the tangential shelf and roof areas were thought to be due to a wet-dry interface condition. A 30 degree conical skirt was added to the gas inlet duct plus a lip was installed at the end of the extension. These modifications reduced the ash deposits considerably. Further tests with sprays to completely remove these ash deposits are being evaluated.

All three wet ID Fans have experienced vibrations due to scale deposits on the rotor. The original water wash system has been redesigned and increased quantities of water sprayed into the gas. Those changes have significantly reduced this problem.

In order to control the scrubbing liquor chemistry, a lime addition system has been installed. The lime slurry is fed to the clear pond, just ahead of the suction of returned water pumps. Conclusive evidence assessing the effectiveness at this approach is not yet available. In addition, a water wash system (1000 gpm) is operated once a week for a period of two hours to flush ash and scale deposits from the vessels.

The development work described above has reduced scrubber system outages. Additional engineering studies are continuing to improve the system liability.

Public Service Co. of Colorado (Ref: 6) has installed five scrubber systems for particulate control. These systems used Turbulent Contact Absorbers (TCA) with two stages of plastic spheres. The units consist of a pressure fan, TCA, Demister and reheater. The following table summarizes design operating data:

Station	Gas Flow ACFM 260°F	L/G	△ P inch water	Inlet gr/SCF	Outlet gr/SCF
Valmont 5	463,000	60	12	0.80	0.02
Cherokee 1	520,000	60	12	0.80	0.02
Cherokee 3	610,000	55	12	0.40	0.02
Cherokee 4	1,520,000	56	12	0.70	0.02
Arapahue 4	520,000	56	12	0.80	0.02

The TCA scrubbers are approximately 50 ft. high x 40 ft. wide x 14 ft. deep. The demister section is expanded to 20 ft. deep. Materials of Construction are carbon steel with 1/4" thick rubber lining. Power consumption per scrubber system is approximately 4 percent.

Operating data indicate outlet particulate loadings of .01-.03 gr/SCF are obtained.

Operating problems reported were grid support cracks due to vibration, plastic ball erosion, demister and reheater deposits. The grids have been modified and this problem has been eliminated.

Demister water wash has been installed and demister solids have been largely eliminated. Soot blowers have been installed between reheater bundles and fouling of the heat excharger surface largely eliminated.

Arizona Public Service Co. (Ref. 7) has reported the following operating data for the Four Corner's wet scrubbers on Units 1, 2 and 3:

Venturi pressure drop - 21 inches water ACF
Liquid to gas ratios - 20 gal/1000 ACF
Inlet grain loading - 6.5 gr/SCFD
Outlet grain loading - 0.02 gr/SCFD

Full size scrubber technology for particulate removal (and SO_2 removal) has been on a learning curve over the past 2-3 years with the present location on the curve at the 90% point. We now know that scrubbers can remove particulate to outlet grain loadings of 0.02 gr/SCFD. We also know that in order to provide system reliability, we must control liquor chemistry. New systems, such as the Colstrip Station of Montana Power Co., are being designed for higher liquor to gas ratios (30-40), higher percent solids in circulating liquid (6-12%), increased residence time in the recirculating tank (5-10 minutes) and pH control (5-6) Long term pilot plant tests have demonstrated little or no scale within the scrubber and piping. It is anticipated that this improved operation will soon be seen in full size units.

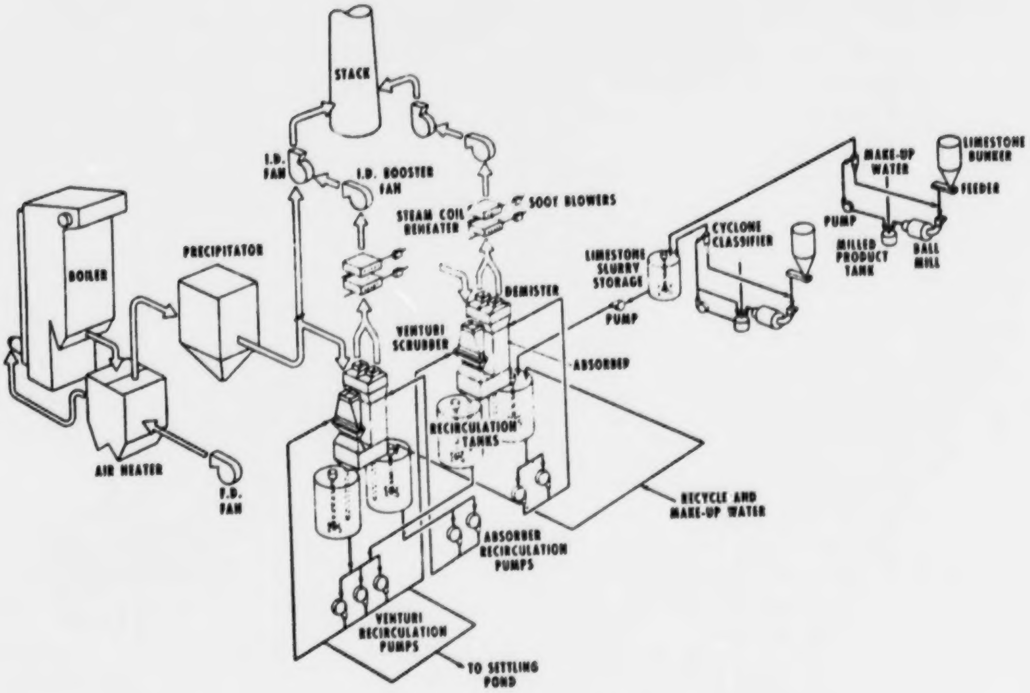
STACK
I.D. FAN
I.D. BOOSTER FAN
SOOT BLOWERS
STEAM COIL REHEATER
LIMESTONE BUNKER
MAKE-UP WATER
FEEDER
PUMP
CYCLONE CLASSIFIER
MILLED PRODUCT TANK
BALL MILL
LIMESTONE SLURRY STORAGE
BOILER
PRECIPITATOR
DEMISTER
PUMP
VENTURI SCRUBBER
ABSORBER
RECIRCULATION TANKS
AIR HEATER
F.D. FAN
RECYCLE AND MAKE-UP WATER
ABSORBER RECIRCULATION PUMPS
VENTURI RECIRCULATION PUMPS
TO SETTLING POND

Figure 14 Will County Station Unit No. 1

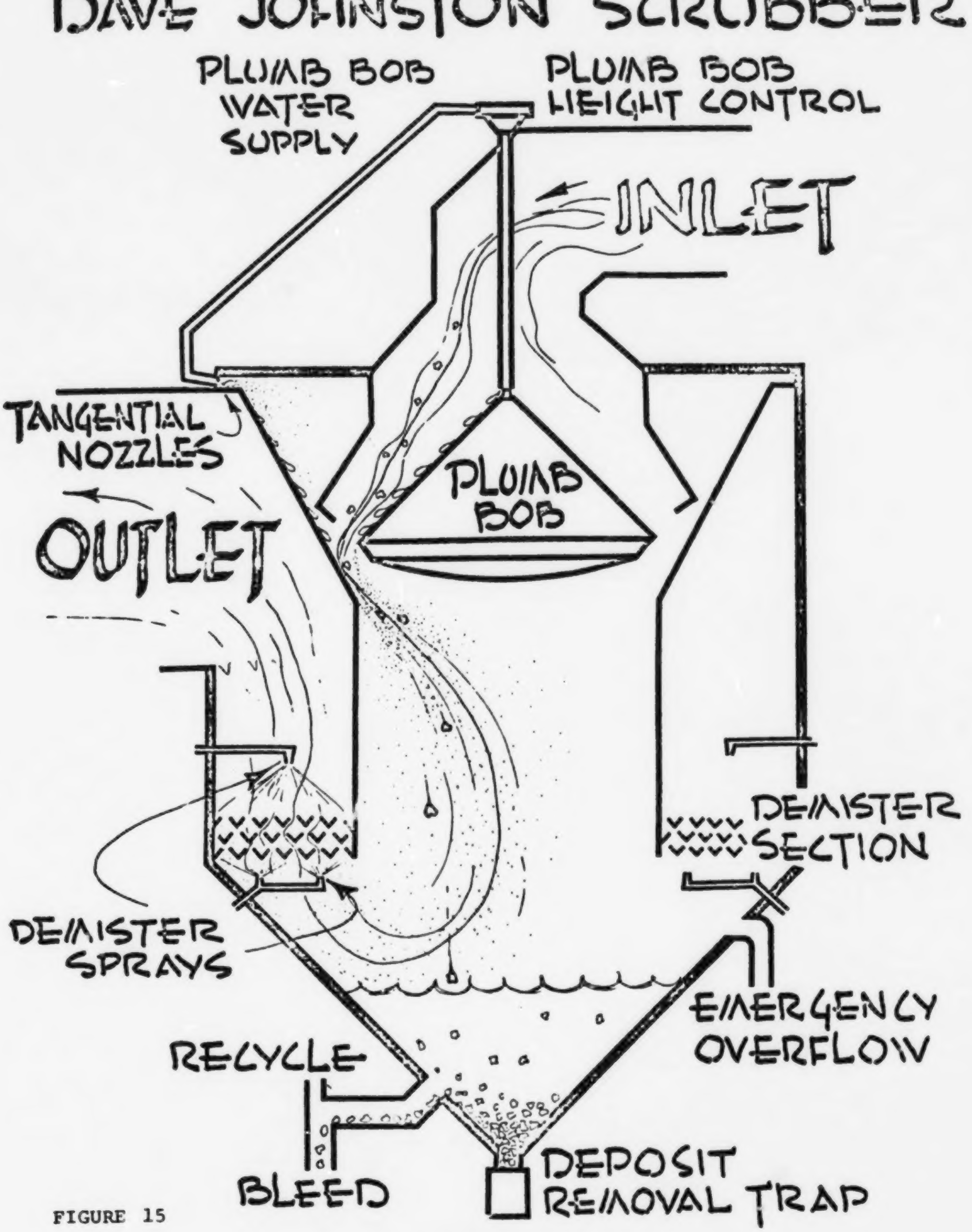
DAVE JOHNSTON SCRUBBER
PLUMB BOB WATER SUPPLY
PLUMB BOB HEIGHT CONTROL
INLET
TANGENTIAL NOZZLES
PLUMB BOB
OUTLET
DEMISTER SECTION
DEMISTER SPRAYS
EMERGENCY OVERFLOW
RECYCLE
BLEED
DEPOSIT REMOVAL TRAP

FIGURE 15

TABLE 9

U.S. SCRUBBER INSTALLATIONS FOR PARTICULATE CONTROL

UTILITY	SIZE MW	STARTUP	SCRUBBER TYPE
Pennsylvania Power Holtwood	80	5/70	Venturi
Kansas Power & Light Co. Lawrence Station			
Unit 4	125	12/68	Marble-Bed
Unit 5	430	12/71	Marble-Bed
Arizona Public Service Four Corner 1, 2, 3	575	12/71	Venturi
Commonwealth Edison Will County No. 1	175	2/72	Venturi/TCA
Pacific Power & Light Dave Johnston #4	360	3/72	Venturi
Public Service of Colorado			
Valmont	180	9/71	TCA
Cherokee 3	150	9/72	TCA
Cherokee 4	350	8/74	TCA
Arapahoe 4	110	11/73	TCA
Cherokee 1	110	9/73	TCA
Kansas City Power & Light La Cyne Station	840	4/73	Venturi
Duquesne Light Co.			
Phillips Station	400	5/73	Venturi
El Rama Station	600	1/74	Venturi
Nevada Power Co. Reid Gardner Station		1/74	Venturi
Units 1 & 2	250	1974	Venturi
Unit 3	125	1976	Venturi
Detroit Edison Co. St. Clair No. 6	180	3/74	Venturi
Montana Power Co. Colstrip Units 1 & 2	720	5/75	Venturi
Northern States Power Co. Sherburne County #1 & 2	1360	5/76	Marble-Bed
Philadelphia Electric Co. Eddystone Station	100	11/73	Venturi

TABLE 10
WET SCRUBBER TEST DATA
COMMONWEALTH EDISON CO.
WILL COUNTY UNIT 1

Load, MW	113	114	115	111	110	111
Gas Flow, 10^3 CFM	335	335	340	335	315	335
Scrubber Pressure Drop* inches H_2O	29	21	25	24	23	23
Dust Inlet gr/SCFD	.0944	.1440	.1470	.1105	.3060	.2580
Dust Outlet gr/SCFD	.0079	.0073	.0298	.0261	.0205	.0334
SO_2 Inlet, ppm	1145	890	930	1130	1000	545
SO_2 Outlet, ppm	67	294	35	285	223	180

*Total system pressure drop includes pressure drop across Venturi, TCA, Demister, reheater and ducts. Typical pressure drop across Venturi was 9 inches H_2O and TCA absorber 6 inches.

REFERENCES

1. Particulate and Sulfur Dioxide Pilot Plant Test Program Report for the Colstrip Generation Station, Montana Power Co, Combustion Equipment Associates, Inc., Arthur D. Little, Inc. and York Research Corp., August, 1973.

2. TVA Pilot Plant Reports, 1972, Particulate Removal, B.G. McKinney and N.D. Moore.

3. Preliminary Report of Test Results from EPA Test Facilities at the TVA Shawnee Power Plant and Research Triangle Park, Bechtel Corp., Environmental Protection Agency, and Tennessee Valley Authority, December, 1973.

4. Will County, Unit 1, Limestone Wet Scrubber, D.C. Gifford, Proceedings Electrical World Conference-Sulfur In Utility Fuels, Chicago, Illinois, October 1972.

5. Operating Experience Report, Flue Gas Scrubbing System, Pacific Power & Light Co., Dave Johnston, Unit 4, T.M. Ashton, ASME National Symposium, April 1973, Philadelphia, Pa.

6. Private Communication, G. Green, Public Service Co. of Colorado, Operation and Design Information on TCA Particulate Removal Systems, December 1973.

7. Private Communication, L.K. Mundth, Arizona Public Service Co., Four Corners' Wet Scrubbers Operating Data, January, 1974.

Preceding page blank

Paper No. 14

HIGH VELOCITY SYNTHETIC FIBER MIST ELIMINATORS

by

Georgy K. Lebedyuk,
B. I. Myagkov,
I. G. Kamenshchikov,
and
V. V. Malikov

STATE RESEARCH INSTITUTE OF
INDUSTRIAL AND SANITARY GAS CLEANING

Moscow

High Velocity Synthetic Fiber Mist Eliminators

G. K. Lebedyuk, B. I. Myagkov,
I. G. Kamenshchikov, V. V. Malikov

Rapid development of chemical industry with the use of new, high capacity and output units as well as the ever increasing need for controlling air pollution brought out a real problem of developing new methods and instruments for acid mist elimination. The new methods have to be more economical and efficient than the most widely used today electrostatic precipitators and venturi scrubbers.

During the last 10-15 years in USSR as well as in other countries, fiber and mesh mist and spray eliminators have come to use. Their use has become especially widespread in the manufacture of sulfuric and phosphoric acids. Fiber and mesh mist eliminators are characterized by high efficiency high reliability, simplicity of design and use and by small size.

Self-cleaning fiber and mesh mist eliminators capture liquid particles on fibers. They coalesce on the fiber surface and form film of liquid. The liquid is removed from filtering material in large drops and streams.

The drops are removed from the filtering material by the force of gravity, cappilary forces, and by entrainment of drops in the gas stream.

Analysis of work with fiber mist eliminators (1-3) shows that structure of the filtering surface is most important.

Use of glass fiber heat insulating felts and packing layers as filters rarely allows reliable, efficient and economic performance. Therefore, materials used for mist elimination must be developed especially for that purpose.

Studies performed in NIIOGAZ have shown that needle punching method of fiber layer formation gives filtering felts of very favorable textures for mist eliminators.

Liquid is moved with capillary forces mainly in places of needle punching. In places of needle punching funnels are formed which fill up with fibers. Material thickness varies from 4 to 12 mm weight 400-1000g for 1 m^2. Felts are prepared from materials of different diameters - from 20-110 microns.

Because these materials are used with large velocities and large pressure drops, (100-500 mm of water column) fibers should be firmly braced in all areas in this way maintaining high porosity and uniformity. Structure and chemical stability usually are the limiting factors for reliable performance of polymer fibers. Most important and complex problem is a guarantee of high structural stability of materials to condensing loads. It was shown that structure stability depends on polymer elastic properties, diameter, length and especially on the degree of fiber twisting. Besides this, number of fibers, perpendicular to the surface in punched places, is important to filter performance. To assure necessary permeability optimal number of needle punches is from 30-60/cm^2. (4) To increase filter life and its efficiency three layers of material are used. Middle layer is made up of thin fibers with 91-94% porosity. Other two layers are made up of coarse fibers with 94-97% porosity.

Polypropylene materials were shown to be most adequate because of their chemical stability and mechanical strength. These properties make them useful in elimination of acid mists (H_2SO_4, HCl, HF, M_3PO_4, HNO_3) and strong alkali.

The study of fractional filter efficiency showed that collection of 0.1 to 0.5 micron particles in coarse fiber layers does not depend on velocity to any significant degree. But for particles 0.5 micron and larger, collection sharply increases with velocity. Pressure drop and Stokes criterion are important factors for collection efficiency on all types of materials. (Fig. 1) Equal collection efficiency can be obtained with different materials with same values of resistivity by varying filtration velocity. Agglomeration of collected liquid in the layer does not have significant influence on efficiency.

When spray is carried away from the layer, which happens usually with filtration velocity higher than 1.7-2.5 m/sec. it is necessary to install mesh packets-spray collectors or polypropylene felts behind the filters. Fiber filter diameter required under those conditions is 70-100 microns. When filtration velocity is between 1.5 and 2.5 m/sec, filters of 3-5 mm thickness are used. Packets of bound mesh are also used.

Polypropylene filters are used as mist eliminators for sulfuric acid with concentrations up to 95% and in manufacture of phosphoric acid. Felts with fibers of 50-80 micron diameter are used with filtration velocity from 5-9.5 m/sec. and pressure drops from 120-750 mm water column.

Polypropylene filters were also successfully used as mist eliminators in the process of dilute sulfuric acid concentration for the preparation of pigmented titanium dioxide. Because the mist contained large quantities of solid components (soot, tar, iron sulfate) filters were fitted for periodic cleaning of material.

With filtration velocity 4.5-7 m/sec. efficiency of mist elimination reaches 95.4% hydraulic resistivity changes from 140-650 mm water column. Long use of this system has shown it to be reliable.

Few types of filters equipped with polypropylene needle punched materials exist. Figure 2 shows a filter with a cylindrical element mounted into the layer of collected acid on a connecting pipe which fits inside of the body. Mist collecting element with a large diameter is braced on the meshed cylinder. It is made up of screens or layered coarse fiber felt with 3-5 mm thickness.

Variations of mist eliminators have been developed with bottom and top gas supply and also with elements for periodic cleaning of filters when contaminated mists are being removed.

Eighteen types (by size) of installations were developed with filtration area of from 0.55 to 1.5 m^2 which corresponds to gas volumes of from 1500 to 30,000 m^3/hr. with filtration velocities from 1-5 m/sec. Nominal volumes were 10,300 - 22,100 m^3/hr. with average filtration velocity, 3m/sec.

In mist eliminators with removable flat cassettes (Fig. 3) felt is braced with clamp frames of "pyalets" type. This allows easy exchange of filtering material with disconnecting of only one part from the gas stream. For elimination of contaminated mists roll (spool) filters were designed. They are made with adjusting filtering material.

At the present time, NIIOGAZ is working on the design of high temperature mist eliminators made of teflon and other thermally stable fibers and also on the design of filters for mists containing large amounts of solid particles.

REFERENCES

1. G. L. Fairs, Trans. Inst. Chem. Eng., London, 1958, 36, 475.
2. J. A. Brink, W. F. Burggrade, J. A. Greenwell, Chem. Ind., 1970, 22, No. 7, 439.
3. U. S. Pat. No. 3,540,190 (1970).
4. B. I. Myagkov, *et al*, Avt. Svid. U.S.S.R. No. 291,547 (1969).

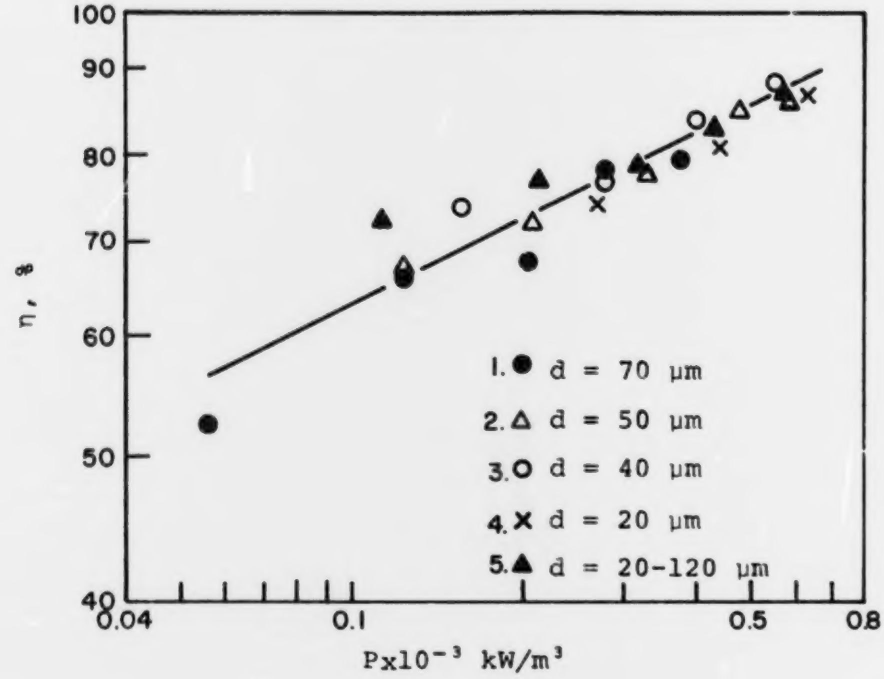

Figure 1. Relationship between collection efficiency and pressure drop for filters with different fiber diameter: 1-70 microns, 2-50 microns, 3-40 microns, 4-20 microns, 5-mixture of fibers 20-120 microns.

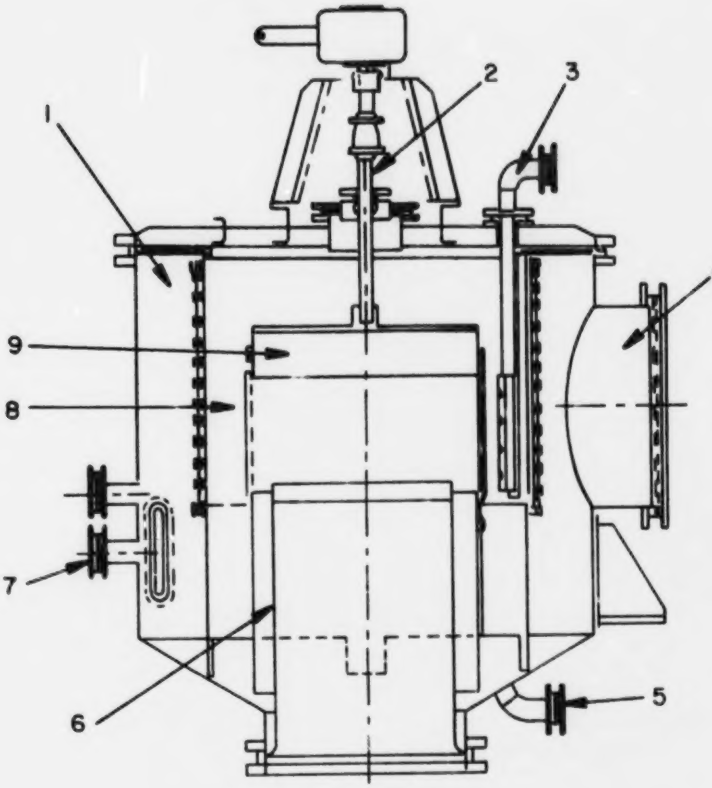

Figure 2. Cylindrical fiber mist eliminator with rising (TVTs P):

1. Body
2. Device for pulling filtering element
3. Flat-torch spray washer
4. Connecting pipe for gas outlet
5. Connecting pipe for water removal
6. Nozzle
7. Connecting pipe for acid outlet
8. Mist eliminator
9. Filtering element

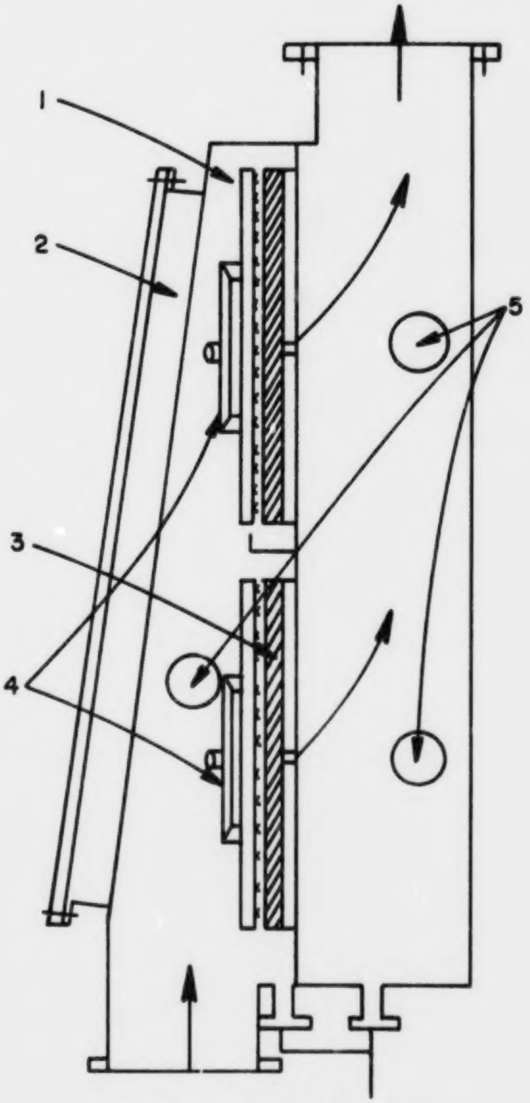

Acid Outlet

Figure 3. Mist eliminator with horizontal elements.

1. Body
2. Door
3. Felt
4. Jet horizontal washers
5. Windows

SESSION 4

CONVENTIONAL TECHNOLOGY, FABRIC FILTERS

Chairman: George Rodgers
Louisville, Kentucky

Paper No.

15 Major Applications of Fabric Filters and Associated Problems

Charles E. Billings
Environmental Engineering Science
Chestnut Hill, Massachusetts

and

John E. Wilder
GCA Corporation
Bedford, Massachusetts

16 Bases of Gas Filtration Through Porous Media Theory

Valery P. Kurkin
State Research Institute of
Industrial and Sanitary Gas Cleaning
Moscow
U.S.S.R.

17 Factors in the Collection of Fine Particulate Matter with Fabric Filters

Richard Dennis and
John E. Wilder
GCA Corporation
Bedford, Massachusetts

18 The State of the Art of High Temperature Filtration and Current Technology Developments

Dean C. Draemel
U. S. Environmental Protection Agency
Research Triangle Park, N. C.
(now at Chemical Engineering Department, University of California, Berkeley)

Preceding page blank

Paper No. 15

MAJOR APPLICATIONS OF FABRIC FILTERS AND ASSOCIATED PROBLEMS

by

Charles E. Billings

ENVIRONMENTAL ENGINEERING SCIENCE

Chestnut Hill, Massachusetts

and

John E. Wilder

GCA CORPORATION

Bedford, Massachusetts

Preceding page blank

Abstract

Fabric filters are widely used in industrial dust and fume control systems designed for air pollution control, production processing, or product recovery. This paper presents results of a survey of a number of operating fabric filter systems in each of ten industrial categories.

Estimates of fabric filter applications are reviewed with respect to sales distribution, size distribution, and quantities by application. From these data and proposed new source performance standards, projections of increased utilization of fabric filters are derived with respect to growth of traditional markets, displacement of other collector types, and new markets. Data are presented on major engineering variables affecting design and use (filtering velocity, dust concentration, specific dust-fabric filter resistance coefficient); on economic factors related to capital, operating, and maintenance costs; and on the types of operating problems or failure modes associated with bag life, repair, and maintenance. These findings are compared to similar data reported in various literature sources.

Size surveyed ranged from 10^2 to 10^5 sq. ft. Specific dust-fabric filter resistance coefficients were found to range from 1 to 10^3, depending upon parameters such as particle size, application, fabric construction, etc. Capital costs ranged from 1 to $>$ 20 \$/cfm depending principally on severity of service requirements. Maintenance costs ranged from 0.10 to 1.0 \$/cfm/year. Reported bag life ranged from a few months to greater than ten years. In general, most applications surveyed indicated one or more of several bag failure modes or other problem areas associated with continued satisfactory performance.

INTRODUCTION

A fabric filter consists of a porous flexible layer of woven or felted textile material through which a dusty gas is passed to separate the particles. As particles accumulate, resistance to gas flow increases. Deposits are removed periodically by vigorous cleaning of the cloth to reduce the resistance and maintain the pressure drop within practical operating limits. Provision of methods for cleaning the fabric in place is a distinguishing characteristic of this class of gas filter. Fabric filters are commonly used for control of dust concentrations in the range of 10^2 $\mu g/m^3$ (urban atmospheric dust) to 10^3 g/m^{3}* (pneumatic conveying). They provide effective removal of particles whose sizes range from submicron fumes to >200 micron (μm) powders. Fabrics are available to permit operation at gas temperatures up to about 500°F and to provide chemical resistance against specific acid or alkaline chemical constituents of the gas or particulate. Fabric filters are also used to provide a substrate for support of granular reactants or adsorbents, to recover gaseous components.

This paper presents the results of a study of a number of operating fabric filter systems in several industries. The study is part of a comprehensive sponsored investigation of current application practices in particulate air pollution control technology. Data are presented on engineering design parameters, economic factors, and reported operating problems, and are compared to similar published information.

---

*One gram per cubic meter = 0.435 grains per cubic foot.

FABRIC FILTER SYSTEMS SURVEY

A broad survey of U. S. fabric filter manufacturers and users has been completed. Information and data have been obtained from a sample of 50 users of operating fabric filters, several fabric and filter manufacturers, and by review of several hundred technical papers, reports and other documents. The structure of the user survey is shown in Table 1, columns 1, 2 and 3. Industrial applications were classified by each of 10 major categories as shown in column 1, including all or part of the Standard Industrial Classifications indicated. Columns 2 and 3 indicate the number and percent of user installations surveyed in each of the categories indicated. A fabric filter user questionnaire was prepared containing 128 specific items related to plant, product, process and operation, and to collector design, operation, and performance, as outlined in Table 2. In most cases, questionnaires were completed during an interview with plant operating personnel, and in conjunction with an inspection of the installation, by members of the survey task group. Data from the questionnaires were collated, appropriate calculations were performed and summary findings analyzed as discussed below.

Table 3 indicates the general level of data recoverability using the interview-questionnaire technique modified as required by follow-up contacts. Two characteristic findings are exhibited by these data. About 2/3rds of user technical personnel seem to have adequate data on engineering details of operating flow rate, pressure drop, inlet dust loading and cleaning mechanisms, but collection efficiency was largely unknown, indicating a need for effluent monitors. In addition, the large majority of users had or could estimate fabric failure rate and associated maintenance costs, but only a small number (5%) were able to provide details on the design of fabrics in use, a factor which affects fabric life and associated operating costs.

Forty-nine U.S. manufacturers of fabric filters were identified and requested to provide product information on their individual models.

TABLE 1

FABRIC FILTER SURVEY SAMPLE STRUCTURE AND SUMMARY OF 1967 SALES BY INDUSTRIAL APPLICATION CATEGORY

Application Category No. Title SIC No.*	Installations Surveyed Number	Installations Surveyed %	% of Fabric Filter Sales $ of Total Particulate Control Eq. Sales $ **	% of Fabric Filter Sales by Category,** : Number	% of Fabric Filter Sales by Category,** : Dollar Value
1. Combustion STC 010,020,49	4	9	1	0.3	1.1
2. Food & Feed SIC 20	1	2	60	5.3	4.8
3. Pulp & Paper SIC 26,27	0	0	6	1.0	0.8
4. Inorganic Chemicals SIC 28/	3	7	24	2.5	3.4
5. Organic Chemicals SIC 28/30	4	9	70	12.8	17.7
6. Petrol Refining SIC 29	0	0	8	0.5	1.3
7. Non-Metallic Minerals Industry, SIC 14,32	12	25	56	5.4	19.5
8. Iron & Steel, Foundry SIC 10/33/	13	30	42	12.3	29.4
9. Non-Ferrous Metallurgy SIC 10/33/	5	13	35	2.0	5.2
10. Miscellaneous, NEC SIC 00,22,23,24, 25,31,34,35,36 37,38,39	1	2	55	57.9	16.8
Total:	43	100%	Average: 27%	Total: 100%	100%

* Standard Industrial Classification Number

** This data is based on a table titled "Summary of the Manufacturers' Report of Air Pollution Control Equipment Sales (Particulate)" reported for the years 1966 and 67 by the Industrial Gas Cleaning Institute and based on a computation of control equipment sales prepared on Contract CPA 22-69-5 for the U.S. Dept. of Health, Education and Welfare.

TABLE 2

FABRIC FILTER USER QUESTIONNAIRE

Section	Information and Data Requested	No. of Questions
1.	General Information Company name, plant location Person to contact Principal products	4
2.	Process Application Name of process, operations served Process capacity and rate Gas flow and conditions to filter Particulate rate and properties to filter Timing of filter on process	19
3.	Collector Design Date, manufacturer, costs Filter element dimensions, arrangement Fabric material supplier Sketch of collector with dimensions	30
4.	Operational performance Pressure drops through cycle Air/cloth ratios through cycle Collection efficiency Operating costs, maintenance costs Fan design, manufacturer Alternate fabrics tried	28
5.	Removal of dust deposit Cleaning method Cleaning timing Cleaning intensity and effectiveness Disposal of collected dust and appearance	23
6.	System Aspects Gas pretreatment, quality Fabric seepage, blinding Difficulties with system Suggestions for design improvements Research requirements	12
7.	Additional details Fabric design, surface treatments Application extentions	12
	Total	128

TABLE 3

TYPICAL DATA OBTAINED FROM FABRIC FILTER USER PERSONNEL

Details Requested	% of Interviews where requested data was obtainable
Engineering Parameters	
Inlet dust loading	65
Flow rate	60
Pressure drop	60
Cleaning mechanism details	60
Efficiency	15
Fabric details	5
Economic Factors	
Installation costs	35
Maintenance costs	70
Operating Problems	
Rate of fabric failure	90

Information obtained from producers is summarized in Table 4. Column 1 indicates the manufacturer and column 2 the product model identification. Column 3 indicates those manufacturers who make an envelope fabric geometry. All other models contain tubes, bags, or modifications of a basic cylindirical geometry. Columns 4 and 5 indicate whether dust deposits on the outside (O) or inside(I) of the cylinder, and whether dusty gas flow is directed primarily up (U) or down (D) the cylinder. Cleaning methods are summarized in columns 6 through 12, and include pulse-jet, reverse-jet, reverse flow, collapse, shaking, rapping or vibrating, and manual. Sizes are indicated in columns 13 and 14. Compartment configuration options and ability to provide intermittent or continuous on-line cleaning are summarized in columns 15 through 18 Column 19 indicates those designs which have features allowing fabric access for maintenance while the rest of the collector remains in operation.

Collectors are readily available in sizes from a few square feet of cloth up to several hundred thousand square feet as modular configurations. Total gas flows handled by individual units range from < 100 cfm to $>10^6$ cfm. Units up to a few hundred square feet of cloth are fabricated and shipped assembled in relatively large quantities. Larger units are usually designed to meet the requirements of specific applications and are frequently erected at the installation site. The average collector size produced (1969) is about 3000 ft^2. A typical industrial manufacturing plant may have from one to over a hundred individual units in use on a variety of product recovery and air pollution control applications.

Annual sales of fabric filters in the U.S. (1969) have been estimated conservatively at $25 million for approximately 8000 units. Sales of filter fabric are estimated conservatively at $15 million or 10^8 ft^2 of fabric, including new and replacement uses, per year (1969). The total number of fabric filters in use is estimated at 100,000 units. (These estimates may be low by a factor near 2.) Table 1, columns 4,5, and 6 indicates the approximate distribution of sales and numbers of fabric filters produced in each of ten industrial categories for 1967. The largest numbers of

TABLE 4

FABRIC FILTER EQUIPMENT SUMMARY

MANUFACTURER		Configuration E	Configuration O	Configuration I	Cleaning Method Pulse	Cleaning Method RJet	Cleaning Method Revflo	Cleaning Method Clpse	Cleaning Method Shake	Cleaning Method Vib rap	Cleaning Method Manual	Size, ft^2 Min	Size, ft^2 Max	Modular	Compartmented	Intermittent	Continuous	Contin. Access	Comment
Ace-Sycamore	1-Bag			x							x		100			x			
Aerodyne Machinery	VS		U				x			x		625	and up	x	x		x		
	RAS		U				x					625	and up	x	x		x		
	SJ		U		x							8	800				x		Cylindrical
	HPE		U		x							1400	and up	x	x			x	
	RSI			U	x		x					2000	and up				x		
Aget Mfg. Co.	FH		U						x			700	2800	x		x			
"	FT		U	D					x			120	383			x			
"	1-Bag										x	(20)	(300)			x			
Air Preheater	Ray Jet		U		x							450	3600				x		
AAF	Amerjet			D		x						310	2390				x		Cylindrical
	Amerpulse		D		x							61	4400				x		Bottom plenum
	Amer Therm			U				x				1320	9660				x		
	Amer Tube			U			x		x			1339	11675			x	x		
	Arrester	x								x		80;150	and up	x		x			
	Arrestall	x							x		x	30	180			x			
Bahnson				■					x		x	-	(1000)						
Buell-Norblo	Automatic			U			x		x			960	and up	x				x	Vertical shake
	Intermittent			U					x			360	and up	x		x			
	Portable			U					x		x	36	135			x			
	Atmos-Fltr			U					x			392	and up			x			Ultrafiltration
	Shakerless			C				x				---	---	x	x				
Buffalo Forge	Aeroturn B			D		x						90	and up	x				x	
	Aeroturn S			U					x			628	and up	x		x		x	

TABLE 4 (continued)

MANUFACTURER		Configuration E	Configuration O	Configuration I	Cleaning Method: Pulse	Cleaning Method: RJet	Cleaning Method: Rev flow	Cleaning Method: Clpse	Cleaning Method: Shake	Cleaning Method: Vib rap	Cleaning Method: Manual	Size, ft^2 Min	Size, ft^2 Max	Modular	Compartmented	Intermittent	Continuous	Cont. Access	Comment
California Blowpipe,	No data obtained																		
Carter-Day	Daynamic DF				x		x					--	--				x		
	CS	x	U		x		x					58	1530				x		Cylindrical
	RJ	x	U				x					58	1530				x		Cylindrical
	RT,RTR			U					x			50	660			x			
	AC		D			x						50	1217				x		
Cincinnati Fan	Dust Master			x							x	(6)	---						With Cyclone
Cox Assoc.	---			U					x			300	and up			x			
Dracco/Fuller	Plenum Pulse		U		x							(500)	and up	x	x		x		Cylindrical or regular
	Uni-Filter			U					x			100	600			x			
	Mark II			U					x			720	and up	x	x				
	Glass Cloth			UD				x				80	and up	x	x		x		
	Retro Pulse			U				x				1000	and up	x	x		x		
	Atmos-Filter			U															Ultra-filtration
Ducon Co.	UVB			U					x			20	200			x			
	UFS			U					x			40	200			x			
	Uniflow			D			x					880	and up	x			x		
	FD			U							x	50	400			x			
Dustex/Am Prec.	Inductaire			U	x		x					800	and up	x			x		
	RA		U				x					225	8500				x		
Dusty Dustless	(4 Models)			U					x		x	12	6000			x			
Environ.Res.Corp.	HI, HA			U					x			784	and up	x	x	x	x		
	HC			U					x			125	1300			x			Cylindrical

TABLE 4 (continued)

MANUFACTURER		Configuration E	Configuration O	Configuration I	Cleaning Method: Pulse	Cleaning Method: R.Jet	Cleaning Method: Rev flo	Cleaning Method: +Clpse	Cleaning Method: Shake	Cleaning Method: Vib,rap	Cleaning Method: Manual	Size, ft^2 Min	Size, ft^2 Max	Modular	Compartmented	Intermittent	Continuous	Cont.Access	Comment
Flex-Kleen	BV,RA,UD		U		x							17	and up	x			x		
	FK,CT		U		x							15	2000				x		Cylindrical
Fluidizer	---		U		x		x										x		
Halliburton, No data obtained																			
Hoffman	Dustuctor			U					x			---	---			x			
	Hoffcovac			U					x			30	63			x			Portable
Hydromation				D?	x							100	1000				x		
Johnson-March	MB			U			x		x			250	1250			x	x		
	1000			U			x		x			1750	and up	x				x	
Kice	Dyna-Jet C,S,M		U		x							10	and up	x			x		
	R		U		x							75	891				x		Cylindrical
Kindt Collins	Master			U					x		x	20	---			x			Single Bag
Lamson	Exidust			U					x			38	727			x			
Macleod	SV	x							x			880	and up			x	x		
	Unit	x							x			80	1500			x			
	Tube			U					x			880	and up						
Mahon	---	U			x							265	and up				x		
				U					x			--	--		x				
Meyer	Roto-flo				x							85	930				x		
Pangborn	CH-3	x					x					400	and up				x		
	CM,CN,CT			U					x			200	and up	x		x			Multi-Tube Filter Element
	CH-2,CD	x								x	x	180	and up			x	x		
	CO			U	x		x					1000	and up		x		x		
	Poisi-pulse			U	x		x					11	and up	x			x		Cylindrical or regular
	Totalaire								x			--	---						Ultrafiltration

TABLE 4 (continued)

MANUFACTURER		Configuration E	Configuration O	Configuration I	Cleaning Method Pulse	Cleaning Method RJet	Cleaning Method Rev flo	Cleaning Method +Cplse	Cleaning Method Shake	Cleaning Method Vib,rap	Cleaning Method Manual	Size, ft^2 Min	Size, ft^2 Max	Modular	Compartmented	Intermittent	Continuous	Cont. Access	Comment
Parsons, No data obtained																			
Perlite Corp.	H			D			x								x		x		Multiple Reverse Fans
Precipitair	---			D			x												
Pulverizing M/C	Mikro-pulsaire		U		x							25	and up	x			x		
	Mikro-cyl.		U		x							42	900				x		Cylindrical
	Mikro-collector			D		x						25	and up				x		
	Mikro-Custom			U				x				3,300	and up		x				
Rees Blow Pipe	Standard			U					x			1400	22,000			x			
	AE			U					x			700	22,000		x		x		
	ANS			U			x		x			1500	24,000		x		x		
	Unit								x		x	380	860			x			
Research Cottrell	Air-shake			U					x			3927	and up			x	x		Horizontal air Shake
	Shake-kleen			U					x			1600	and up			x	x		
	Uni-kleen			U					x			295	1860			x			
Also Flex-kleen(see)																			
Ruemelin	Unit			U					x			53	755			x			Portable
	Standard			U					x			1000	9155		x	x	x		
Smico	Suction Filter				x														
Systems (Semco)	DC,DCV		U		x							8	3112				x		Cylindrical/Rectangular
Setco	7AR,7GAR,A B1	x									x	50	---						
Seversky	---			U				x	x			200	and up	x					

TABLE 4 (continued)

MANUFACTURER		Configuration E	Configuration O	Configuration I	Cleaning Method: Pulse	R Jet	Rev Flo	"±Clpse	Shake	Vib,rap	Manual	Size, ft^2 Min	Size, ft^2 Max	Modular	Compartmented	Intermittent	Continuous	Cont. Access	Comment
W.W. Sly	Pactecon-PC	x			x							88	1065				x		
	Pactecon-PS	x			x				x		x	88	1065			x			
	Dynaclone	x					x					748	and up				x		
	Intermittent	x					x		x			242	and up			x			
	Economy	x							x		x	176	352			x			
Smico	Suction Filter				x														
Sprout-Waldron	Multi-Tube			U					x			74	100			x			
	BV,Series			U							x	12	453			x			
Sterling	R			U						x		111	552			x			
Sternvent	Cabinet		x						x			32	1200			x			
	Filter Tube			U					x			426	1800			x			
Tailor	Controlled Cycle			U	x				x			400	and up	x				x	Controlled Start-up
Torit Corp.	Cabinet	x							x		x	30	1200			x			
United McGill	RF,VAV	x						x			x							x	
	MHS,High Temp			U				x		x							x		
U.O.P.	Aeropulse		U			x						4200	22K	x		x		x	
Western Ptpn	Thermo-flex			U					x	x				x		x		x	
	Pulsejet -C8		U			x						75	1135					x	Cylindrical
	Pulsejet -M8		U			x						1130	and up	x				x	
Wheelabrator	Ultra-Jet		U			x						--	---					x	
	Dustube			U						x		273	and up				x	x	
	Dustube			U						x		(10K)						x	Also Ultrafiltration
Young M/C	Uni-Cage		U			x						39	and up	x				x	Cylindrical/Regular
	Uni-Horiz.		H			x						27	368					x	Horizontal Tubes
	Shaker			U						x		94	631				x		

Table 4 (continued)

PRINCIPLE MANUFACTURERS OF FABRIC FILTER DUST AND FUME COLLECTORS

Ace-Sycamore, Inc.
448 DeKalb Avenue
Sycamore, Illinois 60178

Aerodyne Machinery Corporation
6330 Industrial Drive
Hopkins, Minnesota 55343

Aget Manufacturing Company
1408 E. Church Street
Adrian, Michigan 49221

Air Preheater Company
A Subsidiary of Combustion Engineering
Wellsville, New York 14895

American Air Filter Company, Inc.
215 Central Avenue
Louisville, Kentucky 40208

Bahnson Company
1001 South Marshall Street
Winston-Salem, N. Carolina 27108

Buell Engineering Company, Inc.
Northern Blower Division
6409 Barberton Avenue
Cleveland, Ohio 44102

Buffalo Forge Company
490 Broadway
Buffalo, New York 14204

Carter-Day Company
655 19th Avenue, N.E.
Minneapolis, Minn. 55418

Cincinnati Fan & Ventilator Company
6521 Wiche Road
Cincinnati, Ohio 45237

R. F. Cox Associates
Essex, Mass.

Dracco Division
Fuller Company
124 Bridge Street
Catasauqua, Pennsylvania 18032

Ducon Company, Inc.
157 East Second Street
Mineola, Long Island, New York 11500

Dustex Division
American Precision Industries
2777 Walden Avenue
Buffalo, New York 14225

Dusty Dustless
2914 E. Genesee Street
P.O. Box 86
Baldwinsville, New York 13027

Flex-Kleen Corporation(Div.Research-Cottrel
407 South Dearborn Street
Chicago, Illinois 60605

Fluidizer, Inc.
Hopkins, Minnesota

Hoffman Air & Filtration Division
Clarkson Industries, Inc.
P.O. Box 214
Eastwood Station
Syracuse, New York 13206

Hydromation Engineering Company
39201 Amrhein Road
Livonia, Michigan 48150

Johnson-March Corporation
3018 Market Street
Philadelphia, Pennsylvania 19104

Kice Metal Producst Company
2040 South Mead Avenue
Wichita, Kansas 67211

Kindt-Collins Company
12631 Elmwood Avenue
Cleveland, Ohio 44111

Lamson Division
Diebold, Inc.
306 Lamson Street
Syracuse, New York 13201

Table 4 (continued)

Macleod Company
125 Mosteller Road, P.O. Box 452
Cincinnati, Ohio 45421

Mahon Industrial Division
R.C. Mahon Co.
P.O. Box 808
Warren, Michigan 48090

Wm. W. Meyer and Sons, Inc.
8262 Elmwood Avenue
Skokie, Illinois 60076

Pangborn Corporation
P.O. Box 380
Hagerstown, Maryland 21740

Perlite Corporation
200 E. Duttonmill Rd.
Chester, Pennsylvania 19014

Precipitair Pollution Control, Inc.
Chimney Rock Road
Bound Brook, New Jersey 08805

Pulverizing Machinery Div.
The Slick Corporation
10 Chatham Road
Summit, New Jersey 07901

Rees Blow Pipe Manufacturing Co.
2929 Fifth Street
Berkeley, California 94710

Research Cottrell, Inc.
P.O. Box 750
Bound Brook, New Jersey 08805

Ruemelin Manufacturing Company
3860 North Palmer Street
Milwaukee, Wisconsin 53212

Systems Engineering & Manufacturing Co.
6330 Washington Avenue
P.O. Box 7634
Houston, Texas 77007

Setco Industries, Inc.
5880 Hillside Avenue
Cincinnati, Ohio 45233

Seversky Electronatom Corp.
30 Rockefeller Plaza
New York, N.Y., 10020

W.W. Sly Manufacturing Company
P.O. Box 5939
Cleveland, Ohio 44101

Smico, Inc.
500 N. MacArthur Blvd.
Oklahoma City, Oklahoma

Sprout-Waldron & Co., Inc.
Muncy, Pennsylvania 17756

Sterling Blower Company
771 Windsor Street
Hartford, Connecticut

Sternvent Company, Inc.
12 Van Dyke Street
Brooklyn, New York 11231

Tailor and Company, Inc.
2403 State Street
Bettendorf, Iowa 52722

Torit Corporation
1133 Rankin Street
St. Paul, Minnesota 55116

United McGill Corporation
Dust Collector Division
883 North Cassady Avenue
Columbus, Ohio 43219

UOP Air Correction Division
P.O. Box 1107
Darien, Connecticut 06820

Western Precipitation Division
P.O. Box 2744 Terminal Annex
Los Angeles, California 90054

Wheelabrator Corporation
Air Pollution Control Division
400 South Byrkit Street
Mishawaka, Indiana 46544

Young Machinery Company
Painter Street and Schuyler Avenue
Muncy, Pennsylvania 17756

fabric filters (57.9%) were applied to miscellaneous dust sources (category 10, column 5), but the largest fraction of sales (48.9%) were associated with metallurgical industry applications (categories 7 and 8, column 6). Fabric problems associated with high temperatures, condensibles, and acids have historically limited the sales of filters for control of particulates from combustion processes (category 1).

DATA ANALYSIS - ENGINEERING PARAMETERS

The quantity of air or process gas, dust concentration, and the specific flow-resistance properties of the particulate deposit determine the amount of cloth area required for any selected value of operating pressure drop. Cloth area is generally selected to provide an operating pressure drop in the range of 3 to 4 inches of water, but some designs can operate substantially in excess of 10 inches of water. Average filtration velocity (total air volume filtered/total cloth area), commonly called air-to-cloth ratio, is often 2 to 3 and generally in the range of 1 to 15 cfm/ft^2 (i.e., 1 to 15 ft/min). However, values in excess of 50 ft/min can be achieved at moderate pressure drop with certain cleaning devices on coarse dusts.

The resistance of clean fabric prior to filtration of dust is determined by fabric design and construction, and is reported by fabric manufacturers as permeability (air flow in cfm/ft^2 at 1/2 inch water pressure drop). In normal operation the fabric immediately after cleaning will still contain some residual dust. In general, gas flow through the residual fabric-dust combination is viscous at low velocities, and the pressure drop across the combination is directly proportional to flow,

$$\Delta p_1 = K_1 V$$

where Δp_1 = pressure drop across fabric, inches of water,

K_1 = resistance of the fabric, inches of water per ft/min,

V = gas flow velocity, ft/min.

During filtration, a layer of dust deposits on the fabric and produces an additional resistance to flow $\Delta p(t)$ proportional to the properties of the granular layer. This additional resistance is the same order of magnitude as the residual resistance. Arguing from considerations of Kozeny Carman flow through granular media, Williams, et al[1] described the change in pressure drop as a consequence of deposit build-up as

$$\Delta p(t) = \left[\frac{k}{g} \cdot \frac{\mu_f}{\rho_f} \cdot S^2 \, \frac{1-\epsilon}{\epsilon^3} \cdot \frac{1}{\rho_p}\right] \frac{V^2 L t}{7000}$$

where V = gas flow velocity, ft/min

L = inlet dust concentration, grains/cu ft.

t = time, min

and k = a dimensionless constant ≈ 5 for a wide variety of fibrous and granular meterials up to porosity $\epsilon \approx 0.8$.

g = gravitational acceleration, ft/sec^2

μ_f/ρ_f = gas viscosity/gas density, ft^2/sec

ρ_p = true density of particulate material, lbs/ft^3

S = specific surface area per unit volume of solids in the dust layer, ft^{-1}

ϵ = porosity or fraction void volume in dust layer, dimensionless

$\Delta p(t)$ = the change in pressure drop in feet of fluid flowing, over the time interval t.

The equation above is typically presented as

$$\Delta p(t) = K_2 \, V^2 L t/7000$$

where K_2 is called the specific dust-fabric filter resistance coefficient defined by the term in brackets above. K_2' can be derived from observations on an operating fabric filter.

However, for design purposes in a new fabric filter installation, an estimate of the specific dust-fabric filter resistance coefficient is required to predict the relationship between operating pressure drop, filtering velocity, and time between cleaning cycles on which the operational and maintenance costs depend. Resistance coefficients have been calculated from the bracketed term above, and are compared with values computed from collectors observed in the field survey, and with reported values from several studies. It is evident from these analyses that the effects of fabric structure and deposition velocity are probably not adequately represented in the coefficient in its present form.

Values of the theoretical area per unit volume of dust are shown in columns 1 and 2 of Table 5 under the assumption that particles are spherical. Experimental values of S can be estimated for a specific dust of interest from gas adsorption data obtained with commercially available equipment (cm^2 area/gram) and the true density of the material ($grams/cm^3$). Porosity or void volume will have a range approximately as indicated in column 3 of Table 5, so that the term $(1-\epsilon)/\epsilon^3$ varies from about 0.4 to 48 as shown in column 4. Void volume is partly dependent on the range of particle sizes present in the dust. It is also affected by the forces acting on the deposit producing consolidation, mainly the drag caused by the gas flow through the layer. Typical experimental values of void volume as a function of particle size for sized powders are shown in Figure 1. They are also readily obtainable experimentally from the weight of a known dust volume, in conjunction with a particle size analysis.

Letting $k = 5$, $\gamma = \mu_f/\rho_f = 0.15\ cm^2/sec$, $g = 980$, and for $\Delta p = 10\ \mu$, $\epsilon = 0.5$, and assuming $\rho_p = 2$, $(S)^2 = 3.6 \times 10^7\ cm^{-2}$, $(1-\epsilon)\ \epsilon^3 = 4$, K_2 is calculated as 6.5, or

$$\Delta p(t) = 6.5\ LV^2t/7000\ \text{(inches of water)}$$

The calculated value can be compared to K_2' derived from the field data shown in Table 6. For lime kiln dust with a stated particle size of 10 μ, (line 19) the computed K_2' value was 8.8. The estimated value for this system is of the proper order of magnitude. Data in Table 6 indicate a wide variation in the dust resistance coefficient only partly associated with particle size. Variations in the values of K_2' computed from field-furnished data undoubtably relate to crude estimates of particle size and dust loading

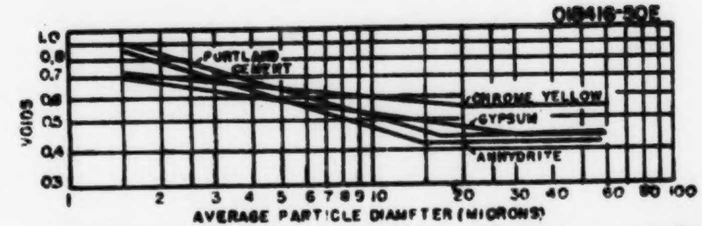

Figure 1. Bulking properties of various powders
(from Dallavalle, Ref. 2)

TABLE 5

CALCULATED VALUES OF SPECIFIC AREA PER UNIT VOLUME AND POROSITY VARIATIONS FOR DUST RESISTANCE COEFFICIENTS

Particle Size, μm D_p	$(S)^2$ cm^{-2}	Porosity ϵ	$\frac{1 - \epsilon}{\epsilon^3}$
500	1.44×10^4	0.8	0.39
200	0×10^4	0.75	0.595
100	3.6×10^5	0.7	0.878
50	1.4×10^6	0.65	1.27
20	9×10^6	0.6	1.85
10	3.6×10^7	0.55	2.70
5	1.4×10^8	0.5	4.0
2	9×10^8	0.45	6.04
1	3.6×10^9	0.4	9.38
2.5	1.4×10^{10}	0.3	15.1
0.2	9×10^{10}	0.3	25.9
0.1	3.6×10^{11}	0.25	48.0

Note: $S = 6\pi D_p^2 / \pi D_p^3 = 6/D_p$, $cm.^{-1}$

TABLE 6

SPECIFIC DUST-FABRIC-FILTER RESISTANCE COEFFICIENTS FOR OPERATING COLLECTORS SURVEYED IN FABRIC FILTER SYSTEM STUDY (1969)

Dust	Operation	Dust Loading gr/cu.ft.	Filtering Velocity fpm	Operating Drag In H_2O/fpm		K_2'*	Particle Size** µm	Fabric Characteristics Material, Remarks	Cleaning Method	Temp. °F
				Residual ↓	Maximum ↓					
Carbon black	Oil-furnace	14	1.6	4.4	5.0	56	< 1	Glass, Silicone	Reverse Flow	425
Carbon black	Oil-furnace	26	1.1	4.0	6.2	38	< 1	Glass, -	Rev. flow & sh.	375
Fe_2O_3	Elec. furnace	(1.5)	3.3	1.4	1.6	(3)	< 1	Dacr.^{R}-Orl.^{R}, 2.2tw., 12.5 oz.	Sh. & rev. flow	215
Fe_2O_3	Elec. furnace	1.5	3.0	-	-	(10)	< 1	Orlon^R, -	Shake	330
Fe_2O_3	Elec. furnace	0.8	3.0	1.0	2.6	45	< 1	Orlon^R, -	Shake	110
Fe_2O_3	Elec. furnace	0.3	1.4	3.5	4.9	715	< 1	Dacron^R, -	Rev. flow	225
ZnO	Brass smelter	8.1	0.6	0.9	5.4	40	< 1	Glass, -	Sh.& rev. flow	600
ZnO, PbCℓ	Blast furnace	1.2	1.2	7.2	7.3	18.5	< 1	Glass, tw., 9 oz.	Shake	375
Fly Ash	Oil-fired fce.	0.01	6	1.0	1.1	127	< 1	Glass, 10 oz.	Rev. flow, collapse	260
PbO	Smelter	2.3	1.0	2	3	57	0.5-10	Dacron^R, 10 oz.	Sh.& rev. flow	275
Fe_2O_3	Cupola	(< 1)	12.5	-	0.7	(10)	0.5-50	Nomex^R, -	Pulse jet	240
Fe_2O_3	Cupola	0.7	2.1	2.9	4.3	121	0.5-50	Glass, -	Shake	450

TABLE 6 (Continued)

Dust	Operation	Dust Loading gr/cu.ft.	Filtering Velocity fpm	Operating Drag In H_2O/fpm		K_2'*	Particle Size** µm	Fabric Characteristics, Material, Remarks	Cleaning Method	Temp °F
				Residual ↓	Maximum ↓					
Fly Ash	Mun. incin.	0.3	2.5	1.3	1.7	180	3	Glass, plain	Collapse	480
Fly Ash	Mun. incin.	0.5	4.5	0.9	1.1	50	(10)	Glass, -	Pulsed rev. flow	425
PVA	Matl. handling	0.05	10.4	0.1	(0.1^+)	25	3	Wool, felt	Pulsed rev. flow	70
$CaSO_4$	Dryer	( )	7.5	( )	( )	0.4	5	Dacron®, felt	Pulse jet	220
Cement	Bagging	(10)	2.5	(4)	(6)	(350)	10	Cotton	Rev. flow	70
Cement	Kiln	0.5	1.5	2.0	3.3	12	15	Glass, tw., 9 oz.	Collapse	525
Lime	Kiln	7.5	2.3	(2)	(2^+)	8.8	10	Glass, 14 oz.	Rev. flow & for. pulse	500
Fe_2O_3, ZnO	Elec. furnace	0.5	1.9	2,8	3.1	66	10	Glass, -	Collapse	195
Gypsum wallbd	Trim saw	0.7	3.4	( )	( )	9.2	> 10	Cotton, tw.	Shake	140
Flour	Milling	14	8.6	0.2	0.6	(4.3)	1-30	Wool, felt	Rev. jet	110
Resin, fiber	Matl. Handl.	2.9	2.7	(1)	(1^+)	(8)	1-100	Cotton, flannel	Shake	70
Cement	Milling	5	1.8	1.0	1.6	70	20	Cotton, 17oz.	Shake	325
Dolomite	Kiln	7	3.3	2.9	5.0	670	40	Dacron®, -	Collapse	150
Cement	Clinker cooler	4	2.5	1.8	2.6	9	50	Glass, 3x1 tw., 54x56	Collapse	500

TABLE 6 (Continued)

Dust	Operation	Dust Loading gr/cu.ft.	Filtering Velocity fpm	Operating Drag In H_2O/fpm		K_2' *	Particle Size ** μm	Fabric Characteristics Material, Remarks	Cleaning Method	Temp ^oF
				Residual ↓	Maximum ↓					
Kish	HM pour	0.4	2.5	2.4	4.2	230	80	Dacron^R, silicone, monofil	Shake	200
Hypochlorite	Matl. Handl.	2.3	3.3	0.8	1.0	15	(50)	Dynel^R, -	Shake	70
Alum. hydrate	Matl. Handl.	$>10^3$	1.0	0.8	1.1	0.2	100	Dacron^R, felt, 18 oz.	Pulse jet	70
Sinter dust	Sinter disch. crusher	1.9	2.3	1.5	2.9	12.5	(100)	Glass, -	Collapse	287
Sand, iron scale	Casting clng	6.7	5.0	0.8	1.6	3	<200	Cotton, -	Rev jet	70

* $K_2' = 7000\ \Delta p/LV^2t$, inches of water per pound of dust per square foot of fabric, per foot per minute filtering velocity.

** Particle size as stated by user or estimated from process characteristics.

during observation of the pressure drop, and to effects associated with fabric, temperature, etc.

Other data on values of K_2' found in experimental studies are shown in Table 7A and 7B. Effects of particle size are illustrated by data in Table 7A. Finer sizes produce a larger value of $(S)^2$ (higher K_2) which outweigh any corresponding additional change in the porosity term. Reduction in particle size of a given dust from 100 μm to 40 μm would be expected to produce an increase in $(S)^2$ and K_2 of about 6, with probably little or no shift in ϵ (Figure 1). The change in K_2 reported in Table 7A over this particle size range is of the same order. Cloth characteristics were not reported in this original study.

Effects of fabric variables on the value of K_2 with a single test dust are reported in the studies of Durham, Stevens, Snyder and Pring, and Kohn, as shown in Table 7B. Data of Durham indicate that tightly woven fabrics (low permeability) yield higher values of K_2 when compared to more open weaves. Bulkier yarns, napped fabrics, or felts with larger number of projecting interstitial fibers tending to produce a more open deposit would also be expected to yield lower values for K_2. These effects can be observed in a general way in these data. Effects of filtration velocity on K_2, have been observed in several studies probably related to bed compaction and reduction in ϵ. Typical results are presented in the Stevens data taken at 5 and 15 or 20 fpm. In general, higher filtering velocity appears to cause an increase in K_2 as anticipated. Analyses of these data are continuing in an attempt to provide a general index or guide to the probable effects on K_2 of fabric structure, yarn, processing, particle characteristics, and filtering velocity.

Data presented in Table 7 taken from the literature can be compared to K_2 values obtained from the field survey in Table 6. The general conclusions one draws from these comparisons are that the specific dust-fabric resistance coefficient is related to particle size and filtering velocity; its values range from about 1 to $>10^2$, and fabric parameters tend to produce modifications in the coefficient that have not been satisfactorily

TABLE 7 A

SPECIFIC DUST FABRIC FILTER RESISTANCE COEFFICIENTS (K_2') FOR CERTAIN INDUSTRIAL DUSTS[a,b]

(Industrial Cloth-type Air Filters)

	Particle Size						
	Coarse			Medium[d]		Fine[d]	
	800 µm	100 µm	40 µm	< 90 µm	< 45 µm	< 20 µm	< 2 µm
Granite	1.58	2.20				19.8	
Foundry	0.62	1.58	3.78				
Gypsum			6.30			18.9	
Feldspar			6.30			27.3	
Stone	0.96			6.30			
Lamp Black							47.2
Zinc Oxide							15.7[c]
Wood				6.30			
Resin (cold)		0.62				25.2	
Oats	1.58			9.60	11.0		
Corn	0.62		1.58	3.78	8.80		

[a] Inches water gage, per pound dust per square foot cloth per foot per minute filtering velocity

[b] Williams, et al(1)

[c] Flocculated material, not dispersed, size actually larger.

[d] Theoretical size of silica, no correction made for materials having other values of ρ'. (Size estimated from elutriation velocity)

TABLE 7B

FILTER RESISTANCE COEFFICIENTS, K_2'

Reference	Dust	Cloth	K_2'	A/C Ratio	Dust Char.	Perm.	Cloth Char. Wt.	Cloth Char. Yarn	Ave. Thread Count
Borgwardt, et al (3)	Fly ash	Glass	7.0	2.3	20 μ, ave.				
	" "	"	12.0	3.5					
	" "	Cotton	4.3	2.3					
	" "	"	7.8	3.5					
	Stone dusts		2-13						
	"		4-6						
Robinson et al (4)	Cement dust	?	6.1	3.0	Coarse			?	
	"		7.6	"	Fine				
	Limestone		9.7	"	Coarse			?	
	"		14.1	"	Fine				
Durham (5)	Fly ash	Nomex Fil.	11.5	4.0	10μ,ave.	17.5	4.5	Cont.Fil.	87
	"	Polypro.	6.2	"		15	4.3	Cont.Fil.	73
	"	Nomex®	7.8	"		22.5	5.4	Fil. Spun	76
	"	Teflon®	8.7	"		30	8.5	Cont.Fil.	69
	"	Cotton Sateen	5.8	"		17.5	9.5	Spun	80
	"	Dacron®	7.7	"		25	5.77	Fil.Spun	79
	"	Spun Orlon®	5.8	"		20	5.7	Spun	81
	"	Spun Acrylic	5.8	"		60	9.8	Spun	37
Stevens Co. (6)	AC Test Dust	Nomex	2.0/2.6	5/20	5-10μ,ave.	18	4.6		
	"	Acrylic	0/3.4	"		31	4.4		
	"	"	2.9/2.3	"		24	4.4		
	"	"	2.1/9/2	"		19	3.8		
	"	"	16.5/13.5	5/15		10	3.9		
	"	"	1.0/1.3	5/20		29	5.7		

TABLE 7B (continued)

Reference	Dust	Cloth	K_2'	A/C Ratio	Dust. Char.	Perm.	Cloth Char. Wt.	Cloth Char. Yarn	Ave. Thread Count
Stevens (6)	AC Test Dust	Olefin	1.5/5.2	5/20		13	4.3		
	"	Nylon	5.0/14.5	5/20		26	3.4		
	"	Polyester	1.2/2.1	5/20		26	6.0		
	"	"	1.5/1.9	5/20		37	3.1		
	"	"	22.6/?	5/-		1.6	3.3		
	"	"	0.1/1	5/20		75.5	4.25		
	"	"	3.1/5.0	"		24.5	4.50		
	"	"	2.0/2.1	"		17	5.85		
	"	"	0.6/1.9	"		70	4.51		
Snyder & (7)	Petroleum Coke	Orlon®	17.1	~3.4±	(Med.Surface cloth)	35/10	3.9		
		"	12.5	"		85/58	7.6	Napped filament,	3/1 twill
	"	"	15.0	"		60/33	7.5	Knit, napped	
	"	"	7.4	"	(Hi Surface)	100/50	9.0	Spun staple	
	"	"	13.0	"		110/62	4.9	Spun staple, napped 2s	
	"	Fiberglas	29.8	3.6	(Low Surface)			Spun fiberstock	3/2 twill
	Fresh MgO	Orlon®	234.0	?	Napped side	35?/4.2	4 oz.	Napped filament,	74 3/1 twill
	"	"	254.0	?	Unnapped side	35?/8.1	"	"	" " "
	Steel paint drums, abrasive blasted	Orlon	29.2	3.60	"Very fine dust"			Hi twist-unnapped	
		"	14.8	3.55	"			Fiberstock-unnapped	
	Silica Gel	"std"cotton Sateen Cloth	57.4	3.82	43% < 10μ				
	Gnd limestone	"	0.43	2.90	32% - 325 mesh (-50μ±)				
	Steel paint Drums etc.	μ	5.3	3.78	2% < 10μ				

TABLE B (continued)

Reference	Dust	Cloth	K'_2	A/C ratio	Dust. Char.	Perm.	Cloth Char. Wt.	Cloth Char. Yarn	Ave. Thread Count
Egorova et al (8)	Aℓ pwdr	Glass	0.74	2.96	5μ, Ave.	12.0	8.5	---	0.28 mm thick
Kohn (9)	Quartz pwdr	"Nettle"	0.85	120 fpm	72% < 10μ 100% < 25μ	61.0	5.4		0.61 mm
		Cotton smooth	2.36	"	"	14.0	13.8		1.64 mm
		Cotton rough	1.50	"	"	23 0	13.8		2.48 mm
	Quartz pwdr	Wool 510	1.55	120 pfm	72% < 10μ,	61	11.4		2.52 mm
		" 410	0.97	"	100% < 25μ	68	13.3		2.76
		" 610	1.50	"	"	22	14.5		3.14
		" 650	1.89	"	"	28	15.2		2.81
		Polyacrylinitrile 360S	3.8	"	"	40	8.0		0.98
		" 380R	3.8	"	"	42	8.1		1.18
		" 410S	4.1	"	"	60	9.1		1.15
		" 410R	1.6	"	"	55	9.2		1.55
		" 376S	3.4	"	"	36	10.3		1.38
		" 376R	1.6	"	"	38	10.3		1.53
		Glass	7.1	"	"	9.7	10.3		0.3
		Mesh	14.0	"	"	64			0.3
Kohn (10)	Quartz pwdr	Nessel 1	0.50	"		62	5.4		0.4
		" 9S	2.0	"		14.5	13.7		1.2
		" 9R	1.2	"		23	13.7		1.6
		Wool 51	1.2	"		59	11.7		1.6
		" 65	1.8	"		41	14.9		1.9
		PAN 36S	2.0	"		53	7.7		0.6
		" 76S	2.1	"		38	10.0		0.9
		" 36R	0.3	"		45	8.2		0.75
		" 76R	1.3	"		35	10.5		1.25
		"Lace"30	1.3	"		65	45		0.3

qualified. Further studies of these effects are continuing.

Data on fabric filter collection efficiency was practically unobtainable from users, most of whom stated subjective observations of stack discharge clarity as evidence of high efficiency. High efficiency at modest cost is an inherent characteristic of the separation process utilized in fabric filters. If properly designed, installed, operated and properly maintained, fabric filters will generally collect more than 99.9% of the incoming dust. Annual operating costs relative to weight removal efficiency for fabric filters and other types of gas cleaning equipment on a single test dust are shown in Figure 2 adapted from Stairmand.(11) Fabric filters are seen to yield lower penetration (higher efficiency) at costs less than those which are predicted from the guideline shown. This favors fabric filters in those situations where their use is not precluded by other factors, and where very high collection efficiency is required on fine particles.

In many industrial applications, the discharge from the fabric filter can be returned to the interior of the plant, and will be respirably acceptable if the conveying gas is respirable, thus effecting a saving on heating or cooling of make-up air. The collector discharge dust concentration will frequently be found to be less than 100 $\mu g/m^3$ which is of the order of the ambient atmospheric dust concentration found in many major U.S. cities. In general, increased outlet concentrations are frequently associated with higher inlet concentrations, more cleaning energy, and higher filtering velocity. Figure 3 illustrates typical values of inlet and outlet concentrations for screen and tube type collectors (intermittently cleaned, woven fabric, field data), reverse jet collectors (continuously cleaned felts, field data) and a pulse jet collector (continuously cleaned felt, laboratory results). Low efficiencies reported appear to be characteristic of low inlet concentrations with continuous cleaning, usually accompanied by poor maintenance or seeping dusts (for which fabric treatments are furnished).

DATA ANALYSIS - ECONOMIC FACTORS

Costs of using a fabric filter may be viewed in two parts, those

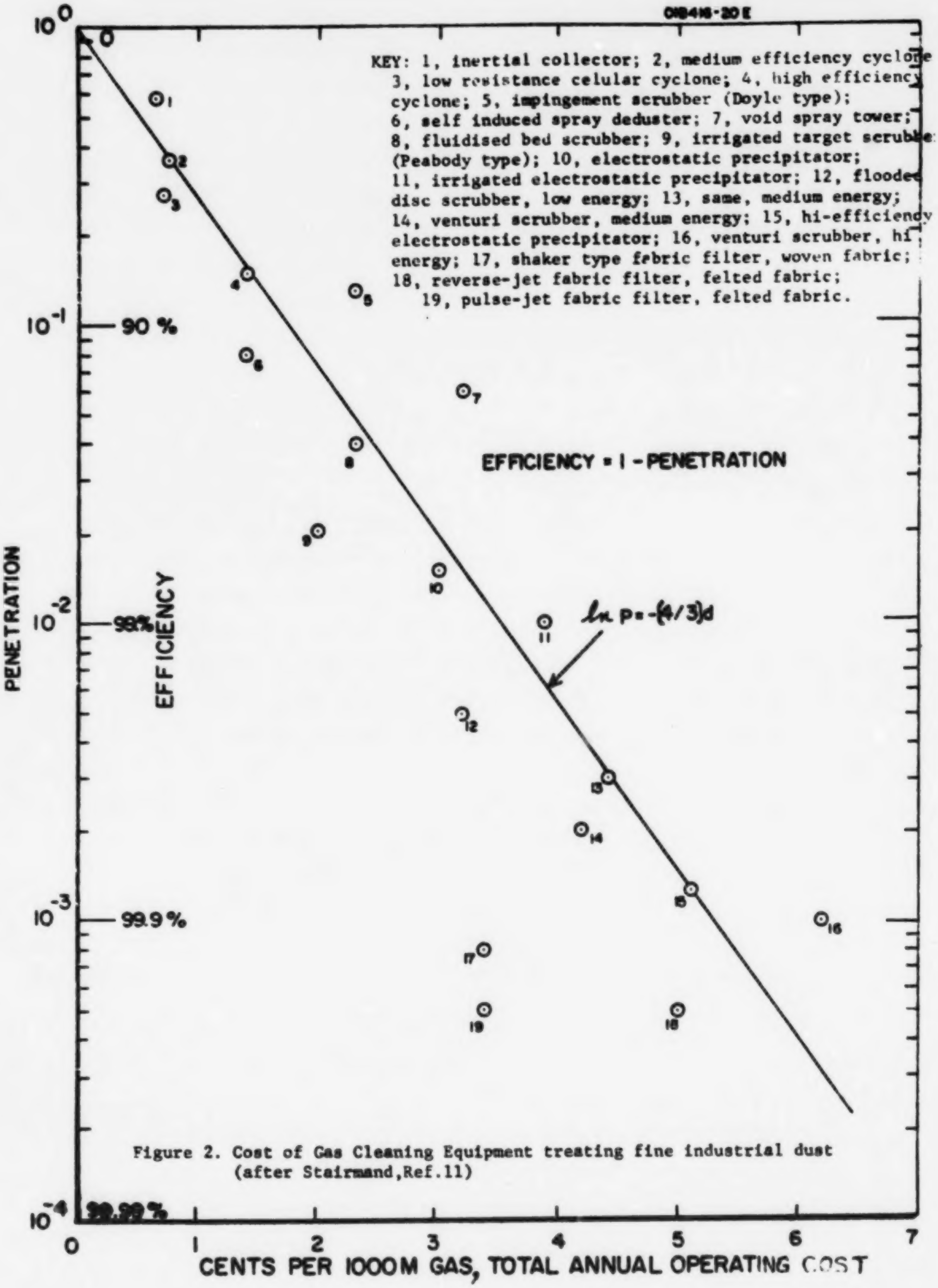

Figure 2. Cost of Gas Cleaning Equipment treating fine industrial dust (after Stairmand, Ref. 11)

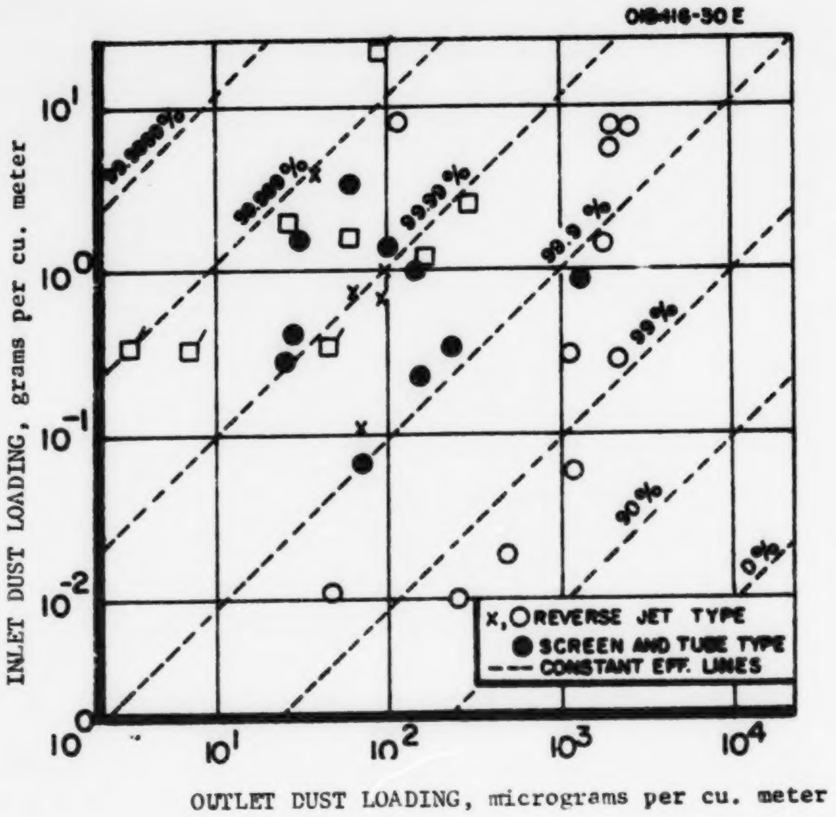

○ ● Dennis, Johnson, First & Silverman, field tests, USAEC Report No. NYO-1588(1953) (13)

x Caplan & Mason field tests, USAEC Report No. WASH-149 (1954) (14)

□ Pulse-jet laboratory data; USAEC Report No. NYO-4816(1962), resuspended vaporized amorphous silica powder (15)

□⁄ Same; resuspended fly ash

Figure 3. Fabric filter efficiency.

connected with providing the equipment with initial start-up operations, and the subsequent costs related to operation and maintenance. Table 8 indicates that the initial and annual costs for a typical collector system are of the same order of magnitude and combine to a few dollars per CFM per year or on the order of \$8 per ft^2 of fabric per year. Although Stairmand (Figure 2) in comparing these costs to other means of collection has estimated slightly smaller costs, costs vary depending on collector quality and size, the particle and gas properties, plant overhead costs, etc.

Table 8 lists the principle costs of a typical new fabric filter from the planning stage through start-up. Most items are self-explanatory and most can vary by a factor of two or more depending on the specific application. Any prospective installation must be separately analyzed especially with regard to the larger portions of the installed cost.

The range of costs for the collector itself varies between \$1 and \$10 per ft^2 of fabric depending on type; on-line cleaned equipment may cost two to three times more than simple intermittently cleaned designs. On the basis of dollars per CFM filtered, collector types are more competitive. For the typical air/cloth ratio of 3 fpm, the initial cost F.O.B. may be \$.80 per CFM. The cost of the fan and ducting may be a similar amount, and the various costs connected with purchasing, installing, and learning how to get the equipment into satisfactory operation may be again a similar amount. Thus the range \$1. to \$4. per CFM for the total installed cost takes in a large number of the fabric filter systems now in use. Figure 4 indicates the distribution of total installed costs encountered in the present survey. Attempts to generally explain the installed cost on the basis of collector size, temperature of application, or particle size have been only partially successful; generally the high temperature fume collectors and the small filters (below 100 ft^2 of fabric) seem to have the highest first costs per cfm.

Elements of the annual cost are also listed in Table 8. The largest annual item is the cost of plant overhead. Cost of space in a typical industrial building has been estimated at \$2.75 per ft^2 of floor annually.

TABLE 8

TYPICAL* FABRIC FILTER COSTS

(8,000 CFM, SHAKER TYPE)

1. Installed Cost - $2.38 per CFM

F.O.B. Fabric Filter	$ .80
Freight	.05
Fan and motor	.25
Ducting	.65
Disposal equipment	.10
Instrumentation	.05
Planning and design	.10
Foundation and installation labor	.28
Start-up	.10
Total:	$ 2.38

II. Annual Cost - $1.26 per CFM per year

Electric power	$ .12
Cloth purchases	.10
Labor	.29
Plant overhead	.75
Total:	$ 1.26

III. Total Cost of Operation - $1.62 per CFM per year

Annual cost	$ 1.26
Amortization of the installed cost, at 10%	.24
Interest on the unamortized portion of Installed cost, at 10%	.12
Total:	$ 1.62

---

* 8,000 hour year

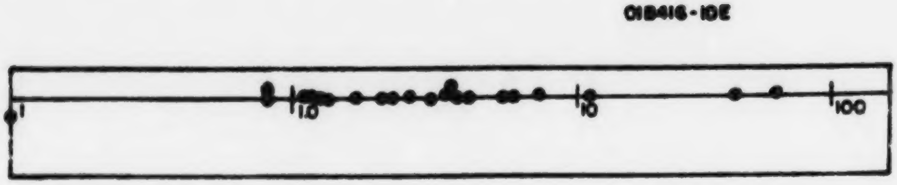

Figure 4. Total installed cost, $/CFM, field reports.

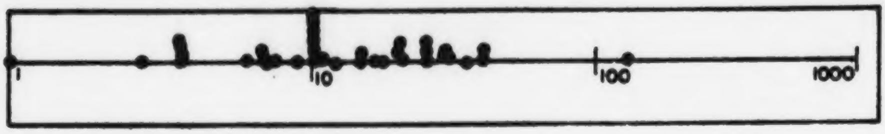

Figure 5. Fabric life,Months field reports.

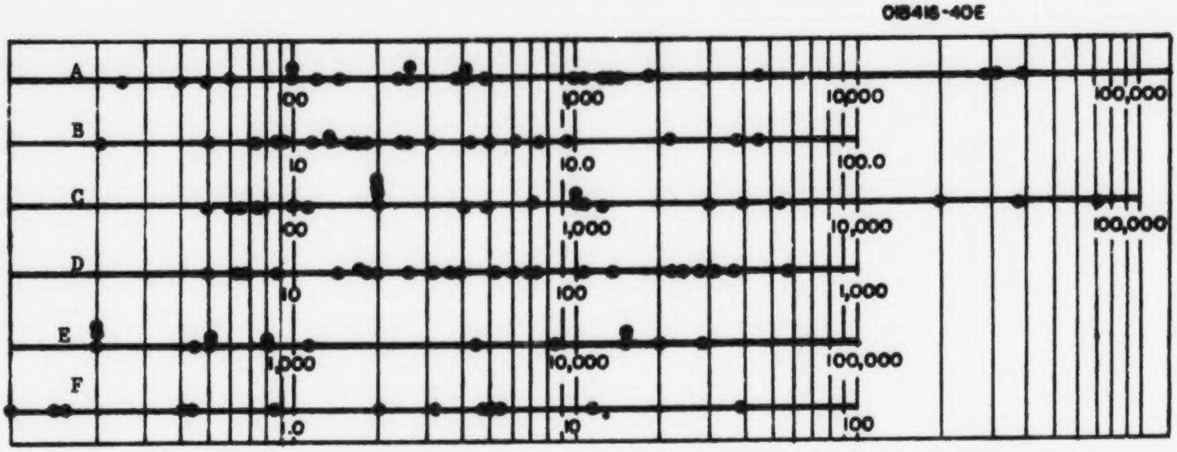

Figure 6. Reported Labor Costs:
A. Replacement Labor, $/year
B. Replacement Labor, $/bag
C. Other Maintenance Labor, $/year
D. Other Maintenance Labor, $/KCFM-year
E. Disposal Costs, $/year
F Disposal Costs, $/ton

The annual cost of the heat carried out of the building by air not recirculated through the collector depends on geographical location. In the northern half of the U.S. fuel costs average to around $.40 per exhausted CFM over one year; an average for the overall country may be $.15 per CFM-year. Insurance, property taxes and lighting can also be considerable.

Summary of Overhead Costs per CFM-Year

Space	$.55	(at 5 CFM per ft^2 of floor)
Heat	.15	
Ins. etc.	.05	
Total	$ .75	

The cost of electric power depends on the location and type of company, but is usually less than 10 mils per kilowatt hour. Power is used both in providing airflow and in fabric cleaning, and ranges from 1 to 5 HP per 1000 CFM treated. Primary flow is normally kept to the minimum allowed by ventilation requirements. From one half to nearly all of the static pressure at the fan may be associated with the fabric-dust deposit, and hence the dust deposit absorbs a large part of the filtering power. Additional power is consumed in cleaning, particularly by reverse pulse and reverse jet equipment in which high pressure or high velocity air is necessary for effective cleaning. For reverse pulse equipment, the pulse power cost is similar to the cost of filtering power, per cubic foot filtered. Cleaning power is generally less for reverse jet equipment, but lower power costs are partially offset by more mechanical elements and greater maintenance costs.

Median fabric life reported in the survey was 18 months with a range from 1 month to 13 years as indicated in Figure 5. The item "cloth purchases" in Table 8 refers to the purchase price of the fabric divided by the life, while the labor associated with replacing and maintaining the fabric is included under "labor". Cloth purchase costs range anywhere from $1 to $100 per filter element (bag, tube, or panel) depending on fabric material, element size, and fabrication costs. Typical purchase prices of filter bags are indicated by the following approximate costs:

Glass bag, 11.5" dia. x 25' long	$15 to 25
Orlon^{R} bag, 6" dia. x 10' long	$ 5
Cotton bag, 5" dia. x 5' long	$ 1.50

Fabric costs depend on fabric life. There are many possible reasons for fabric failure, including heat and moisture (which causes plugging or blinding), abrasion between bags or between bag and particles, holes from tension or tearing, and seam failure. The reasons for necessity of fabric replacement encountered in this survey are given in Table 9 together with the frequency of report. Blinding due either to excessively sticky particulate or to inadequate cleaning was the most common problem reported.

The item in the list of annual costs called labor at $.29 per CFM per year is based on the assumption that labor overhead is about the same amount as wages. Wages were reported by the collector users as from $4 to $5 per hour, and the $.29 figure is based on a total rate of $8 per hour. This average includes both supervisory and skilled categories as well as labor for such work as dust disposal. Figure 6 shows the labor costs before overhead, reported by about 30 of the collector installations surveyed. From the figure one might select the following as being typical:

Bag replacing (excludes bag cost)	$400/yr	or $2. per bag (~1/2 hour)
Other maintenance	$1000/yr	or $50. per yr-KCFM
Dust disposal	$1000/yr	or $1. per ton

(Bag cleaning and repairing could be an additional cost of around $1. per bag, but this was rarely reported as being practiced.) Using the above figures for a 10,000 ft^2 collector filtering 0.5 gr/CF at 2 CFM/ft^2 and having 800 filter bags with life of one year, the maintenance wages would be estimated as:

Bag replacing	$1600. per year
Other maintenance	1000. "
Dust disposal	360. "
Total	$2960. per year

TABLE 9

FABRIC RELATED OPERATING PROBLEMS REPORTED

	Freq.
1. Fabric - dust deposit interactions	
a. interstitial deposit-related abrasion, wear	8
b. flexure wear failure	10
c. seeper	4
d. blinding	14
e. burning, heat	6
f. holes, pinholes, shot holes	6
g. hygroscopic	4
h. condensation	5
i. deposited dust hardens, cake tears, cracks bag	3
Subtotal	60
2. Fabrication failures not particularly related to dust interaction, mechanical	
a. seams, sewing	2
b. tears at top	4
Subtotal	6
3. Design or maintenance failures related to tensioning, supports, rings, collars, or cleaning device interactions	
a. chafe on housing or other bags	3
b. tensioning, bags too loose	1
c. cage, wire, ring abrasion, wear (also dust related), support mechanism interact	5
d. cleaning carriage bag wear	1
e. seals around cloth-metal collars	2
Subtotal	12

This is approximately equivalent to 750 hrs, \$.148/yr-CFM, .029 ¢/KCF \$.29/yr-ft^2 for wages alone, and double these costs including overhead. There are of course many reasons for the variations in labor indicated in Figure 6. Generally one expects relatively more maintenance for smaller collectors, higher filtration temperature, higher dust concentration and smaller particles.

Table 8 indicates how the overall cost of owning and operating the collector may be estimated. The simplest method is to distribute the initial costs over some reasonable life of the collector, probably between 10 and 30 years, and to estimate the capital cost of the investment at some reasonable interest rate. Distributed cost, interest cost, plus annual operating and maintenance cost combine to give the total yearly cost of collector operation. Table 8 indicates a net cost believed to be the right order of magnitude, although this is an estimate as the collector users were not specifically asked for this figure.

DATA ANALYSIS - OPERATING PROBLEMS

Table 9 presents a summary of reported user problems associated with fabric filter operation. Analysis of these reports with respect to fabric material and abrasiveness of dust being filtered has indicated little or no correlation. Further analysis of reported problems with regard to collector cleaning method will be attempted. Very few fabric filter users reported no problems. The majority of users expressed a desire for longer fabric life. Very little quantitative information on fabric life was found in literature reports, beyond a statement of how long a given set of bags had been in successful use. For normal applications conservative design should result in fabric life of several years. The parameters that enter such an optimization have not been generalized as yet.

Fabric filter users commented frequently on poor quality of equipment. For example in some instances it appeared that too many filter bags were packed into too small a space, causing abrasion of the bags on each other or on the walls or other parts of the collector. It was not always possible to distinguish between poor design and improper application or use.

Table 10 indicates the fabrics reported to be in use in the surveyed collectors, and the collector manufacturers whose products were represented. It is estimated that cotton fabrics are used in over half the fabric filter collectors in service, most of the remainder being man-made fiber. Shaking is used for cleaning in about half of the present fabric filters. Data are not available relating the distribution of fabrics to application or industrial category, nor the relative distribution of fabric filter designs or cleaning mechanisms.

CONCLUSIONS

1. The Fabric Filter Systems Study has indicated that there are approximately 50 U.S. manufacturers of a wide variety of devices. Annual sales are in excess of $25 million for approximately 8000 fabric filters. There are estimated to be more than 10^5 fabric filters in use, ranging in size from 10^2 to 10^6 cfm. A national registry, or census, of applications with appropriate supporting data is required for cost-effectiveness modelling.

2. A survey of 40 fabric filters in service has indicated that most users report satisfactory overall operation. The majority of operating problems reported were associated with the fabric, particularly inadequate life in service. Median fabric life was reported to be approximately 18 months with a range from 1 month to over 10 years. The elements of fabric design, fabric life, and filter device parameters require further correlation to provide users with data on fabric life and associated economics in specific applications.

3. Study of engineering parameters required in the design of fabric filters indicates that present technology is inadequate to provide analytical generalizations useful for optimization modelling and reduced total cost.

4. Efficiency of fabric filters in service is largely unknown and indicates the need for inexpensive effluent dust monitors to indicate satisfactory performance or incipient failure. Visual criteria reported

TABLE 10

SUMMARY OF OBSERVATIONS

Fabric	Frequency	%frequency
Cotton	13	32.5
Dacron^R	6	15.0
Dynel^R	1	2.5
Glass	13	32.5
Nomex^R	2	5.0
Orlon^R	2	5.0
Polyprop. felt	1	2.5
Wool	2	5.0
	Total	100.0

Collector Manufacturer	Freq.
AAF	4
Carter-Day	3
Dustex	1
Flex-Kleen	2
Fuller-Dracco	1
Hydromation	1
Kleissler	1
Norblo	3
Own Design	5
Pangborn	5
Research Cottrell	1
Sly	3
Wheelabrator	9
Western Pptn	1
Total	40

generally relate to concentrations of the order of 0.02 grains/cu ft (0.04 grams/m^3) which may be higher than tolerable for air quality standards in the years immediately ahead.

5. Total installed cost for most fabric filters in service ranged from \$1 to \$10 per cfm, depending upon severity of service. There appears to be a clear requirement for cost reduction studies associated with higher filtering velocity, more adequate cleaning, and mechanically more durable filter media.

6. Power required for flow and for fabric cleaning ranges from 1 to 5 HP per 1000 cfm of gas treated, for intermittently cleaned compartmented designs and reverse or pulse-jet designs, respectively. Operating cost reductions could be achieved by application of cleaning technology with attainment of lower pressure drop at higher filtering velocity. Only limited data are available on velocities >100 fpm. These developments require a broader understanding of the role of cake and fabric mechanics in the specific dust-fabric resistance coefficient, in order to develop configurations having better dust-holding capacity per unit of pressure drop.

ACKNOWLEDGMENTS

This study has been made possible through the kind cooperation of a large number of individual manufacturing firms utilizing fabric filters for the control of industrial dusts and fumes. Several fabric filter manufacturers and their voluntary association, the Industrial Gas Cleaning Institute, provided valuable insights and helpful data. Fabric and fiber manufacturers have also supplied basic information on these aspects of the fabric filtration industry.

We acknowledge with thanks the many contributions and cooperative participation of these groups.

The work upon which this publication is based was performed pursuant to Contract No. CPA 22-69-38 with the National Air Pollution Control Administration, Public Health Service, U.S. Department of Health, Education, and Welfare.

REFERENCES

1. Williams, C.E., Hatch, T., and Greenberg, L. Determination of Cloth Area for Industrial Air Filters, *Heating, Piping, and Air Conditioning*. 259, April (1940).

2. Dallavalle, J.M., *Micromeritics, The Technology of Fine Particles*, 2nd Ed., Pitman Publishing Co., New York, pg. 144, (1948).

3. Borgwardt, R.H., Harrington, R.E., and Spaite, P.W. Filter Characteristics of Fly Ash from a Pulverized Coal-Fired Powerplant, APCA annual Meeting, #67-35 (1967).

4. Robinson, J.W., Harrington, R.E., and Spaite, P.W., A New Method for Analysis of Multicompartmented Fabric Filtration, *Atmospheric Environment*, *1*, 499 July (1967).

5. Durham, J.F., Filtration Characteristics of Fabric Filters,National Air Pollution Control Administration, Cincinnati, Feb. (1969). Unpublished.

6. J.P. Stevens & Co.,Inc.,*Selecting Fabrics for Filtration and Dust Collection, Plus supplement N*, J.P. Stevens & Co., New York, N.Y.(1969)

7. Snyder, C.A. and Pring, R.I., Design Considerations in Filtration of Hot Gases, *Ind. Engg. Chem 47*, 960, May (1955).

8. Egorova, L.G., Sakhiev, A.S., Bassel, A. B. and Kosareva, N.S., Use of Bag Filters for Removing Fine Metal Particles from Air Suspension, *Soviet Powder Metallurgy and Metal Ceramics 33*, 774, Sept.(1965).

9. Kohn, H., Dust Elimination by Fabric Filtn (German), *Tonindustrie-Zeitung 89,* 1516, 97 (1965)

10. Kohn, H., Theory and Practice of Dust Elimination Through Fabric Filters, *Staub* (English Translation) *21* 9, Sept.(1961).

11. Stairmand, C.J., Selection of Gas Cleaning Equipment, A study of Basic Concepts, Filtration Soc. Conf. on Dust Control, Olympia, London, Sept. 22-25, (1969)

12. First, M. and Silverman, L., Predicting the Performance of Cleanable Industrial Fabric Filters, *J^{nl} A.P.C.A. 13*, 581, Dec.(1963).

13. Dennis, R., Johnson, G.A., First, M.W., and Silverman, L., Performance of Commercial Dust Collectors, U.S. Gov't Printing Office, Wash., D.C., Report No. NYO-1588 (Nov., 1953).

14. Caplan, K.J., and Mason, M.G., Efficiency of Reverse-jet Filters on Uranium Refining Operations, USAEC Air Cleaning Seminar, Ames Laboratory, Sept. 15-17, 1952; U.S. Technical Information Service, Wash-149, (Mar. 1954).

15. Dennis, R., Kristal, E., Peters, G.A., and Silverman, L., Laboratory Performance of the Mikro-Pulsaire Collector, USAEC Report No. NYO-4816, Harvard University School of Public Health,(15 June 1962).

Paper No. 16

BASES OF GAS FILTRATION THROUGH POROUS MEDIA THEORY

by

Valery P. Kurkin

STATE RESEARCH INSTITUTE
OF INDUSTRIAL AND SANITARY GAS CLEANING

Moscow

Bases of Gas Filtration Through Porous Media Theory

V. P. Kurkin

1. Characteristics of filtration processes in non-stationary systems.

The following characteristics of gas filtration through porous media are important: efficiency of aerosol collection, hydraulic resistance, life of filtrating material before change or regeneration is required.

Theoretical and experimental studies of the filtration process are directed to establish the relationship between the above indicators and the structural properties of porous media, properties of collected aerosols and properties of gas flow system.

The filtration theory has been worked out most completely for the fiber filters. According to this theory, aerosol particles settle on the fiber filter under the influence of hydrodynamic and molecular forces. In addition to this, deposition efficiency is determined by one of the important factors, namely;

a) effect of contact;

b) inertial collision;

c) diffusion effect, caused by Brownian or thermal motion of highly dispersive particles;

d) deposition due to gravitational force (sedimentation effect);

e) electrostatic effect.

Usually the filtration process is divided into two stages.

The sedimentation of the particles in the filtration process initially occurs on the elements composing porous structure of the media. (fibers, granules). The sedimentation of particles occurs by means of the same processes as in fiber aerosol filters. At this stage which is called stationary filtering, collection efficiency and hydraulic resistance do not change with time and their sizes are determined only by the structure of the filtering media and by the parameters of the gas stream.

The efficiency and resistance of the filters change with time. As a result, besides primary filtration stage, a concept of secondary stage is introduced in which change of all parameters of the filtration process depends on time-non-stationary system. A complex process occurs when pores of the filtering surface become filled with aerosol particles. In a short period of time "secondary" porous structure is formed which plays a role in the collection of particles from gases. The filtering medium at that time consists not only of the porous material but also of particle layer which forms on the surface.

The first stage in industrial conditions is short lasting. The second stage of filtration process is of greater importance.

With the layer formation the pores between the particles are usually of the same size or smaller than the particles themselves. Consequently the layer of the deposited particles will collect aerosols from gas stream as if sifting them, that is, practically all particles will be collected. The greater portion of these dust particles does not penetrate inside of the medium but settles on the surface layer thus causing an increase in its t thickness.

As it was shown through specially designed measurements, aerosols do not pass through the media. The particles already deposited collapse. The experiment was conducted in which an evenly distributed layer of cement particulates was collected on a glass fiber filter and was followed by filtration of ash which was not gray like cement but red in color. However, even though the type of filtered dust was changed only gray cement particulates were collected on the control paper filter which was placed behind the glass fiber filter. This indicates that initially formed dust layer fully entraps subsequent aerosol particles. As a result of this phenomenon efficiency of particulate collection increases with time. The experiment reflected most descriptively on the features of non-stationary filtering of particulates with the formation of particle layer on the media.

The layer of particles not only increases the efficiency of collection in comparison to that accomplished with the clean medium but also increases the hydraulic resistance of the medium which often becomes greater than the resistance of the clean medium.

The industrial filtration then, depends mainly on hydrodynamic processes in the particulate layer. It is that layer formation which determines efficiency for the cleaning of gases.

The process of dust deposition on the filtering media during the gas filtration is of practical interest as it specifies high efficiency for gas cleaning.

2. Non-stationary functions of particulate collection.

The wide application of non-stationary processes of solid dispersive aerosol phase deposition on the collection surfaces makes these processes interesting scientifically and practically. These processes occur during filtration of gas containing particulates through porous media.

To identify general principles of the deposition of the solid dispersive aerosol phase in the non-stationary system we shall look at the process of particulate deposition on the deposition surface.

The most characteristic feature of that process is the accumulation of solid dispersive aerosol phase on the deposition surface which results in an increase of filter's hydraulic resistance.

We shall write the function of particulates deposition on the porous media as a relationship between particulate mass deposited on the unit of surface in the time interval t, and general mass deposited on that surface.

$$Z^* = \frac{z_i\, w_i\, \Delta t}{z_i\, w\, t}, \qquad (1)$$

where Z^* - function of particulates deposition in relative units,

z - average concentration of particulates in gas for filtration in the time t,

w - average velocity of filtration in time t;

t - maximal amount of time to regeneration,

Δt - interval of time for particulates deposition,

i - index which characterizes particulates deposition system in Δt.

Usually, $z = z_i$ and $w = w_i$ and particulates deposition function becomes simply:

$$Z^* = \frac{\Delta t}{t} \qquad (2)$$

Obviously, particulates deposition function written in a different form expresses filtration efficiency.

$$\eta = 1 - \frac{zi \; \Delta t}{zi \; \Delta t} \qquad (3)$$

where η - efficiency

zi, Δzi - initial and final concentration of particulates in gas during time interval Δt.

The limiting value of these functions will determine the type of solution of the appropriate differential equations. In particular, as follows from calculation of particulates deposition function that limit is confined in the interval 0-1. At the same time corresponding interval for efficiency change is written in the interval $0 - \eta/\eta_{max}$ (maxium value of efficiency). The indicated limits are established by the change in the thickness of particulates layer. The assumption is made that functions (1) and (3) in the considered interval of changes are continuous and non-stationary, that is, they change with time.

3. Equation of continuity.

Let's consider solid dispersive aerosol phase mass in an arbitrary element of particulate layer volume V limited by the deposition surface d_s. In the infinitely small interval of time dt mass influx to the surface of particulates deposition is entered as the surface integral from normal component of v_n vector in the closed surface:

$$- dt \int_s v_n \, ds, \qquad (4)$$

where

v_n - normal to the deposition surface composing the velocity of particulates' mass in the direction opposite to the flow of particulates in $\frac{m}{s}$.

Expression (4) correlates to an increase with velocity v_n of solid dispersive aerosol phase mass on the surface element d_s.

In conformity with Gauss theorem surface integral (4) may be transformed to a volume one from vector V_n divergency by volume, (volume of the surface under consideration) namely:

$$-dt \int_s v_n \, ds = -dt \int_s div(v_n) dv \qquad (5)$$

On the other hand, in the time interval dt, an increase in the mass of solid dispersive aerosol phase [$\varrho^*(1-E) \int_s dV$], which depends on particulates deposition function, specifies its increase in volume of the element of deposition surface.

$$\left(\frac{\partial}{\partial t} \int_v \varrho^* dV\right) dt = \left(\int_v \frac{\partial \varrho^*}{\partial t} dV\right) dt. \qquad (6)$$

$(1-E) \int_s$ is reduced under the integral of this equation.

Comparing equation (5) and (6) we get:

$$\int_v div(v_n) dv + \int_v \frac{\partial \varrho^*}{\partial t} dV = \int_v \left[div(v_n) + \frac{\partial \varrho^*}{\partial t}\right] dV = 0 \qquad (7)$$

and subsequently equation of continuity for the process of solid dispersive aerosol phase mass accumulation on the surface element is written as:

$$div(v_n) + \frac{\partial \varrho^*}{\partial t} = 0, \qquad (8)$$

which obviously does not depend on the direction of particulates deposition.

4. Potential system of deposition.

To obtain the closed system it is necessary to find functional relationship between the vector v_n and scalar ζ^*. Based on the general principles of hydrodynamics, vector v_n can be expressed through the gradient of scalar function which characterizes potential of velocity v_n. In so far as for each continuous function of ζ^* type its integral exists, the velocity potential can be expressed as:

$$v_n = - \text{grad}\, \zeta^* \qquad (9)$$

The negative sign in this equation describes the reverse direction of v_n vector and particulates containing gas stream. The obtained set of equations (8) and (9) can be solved analytically. Substituting v_n from equation (9) into equation (8) we have:

$$\text{div}\,(\text{grad}\, \zeta^*) - \frac{1}{a^2} \frac{\partial \zeta^*}{\partial t} = 0 \qquad (10)$$

This equation describes, in general, process of solid dispersive aerosol phase deposition in the non-stationary system. Proportionality coefficient a^2 in this equation with dimensions m^2/sec characterizes deposition mechanism for the solid aerosol phase in the layer.

It is obvious that an analogous equation describes filtration process efficiency. In that case ζ in equation (10) is expressed as the function. However, solution to these equations will be determined by different border and initial conditions of the filtration process.

5. Single measuring problem of non-stationary filtration.

We will look at the single measuring problem of particulates containing gas filtration process through porous media. Direction of the gas stream longitudinally to the x coordinate is the same as the direction of the particulates flow. Under those circumstances equation (10) should include single measuring function $\ell^*(x,t)$. With such inclusion equation (10) is written as a linear differential equation in individual derivatives which describe the solid dispersive aerosol phase accumulation process during filtration of particulates containing gas.

$$\frac{\partial^2 \ell^*}{\partial x^2} = \frac{1}{a^2} \frac{\partial \ell^*}{\partial t} \qquad (11)$$

The solution of this equation depends on the initial conditions which as it follows from particulates deposition function (1) are written as:

$$\ell^*/x,o/ = \begin{cases} 1 \\ 0 \end{cases} \text{when} \begin{matrix} x > \bar{x} \\ x < \bar{x} \end{matrix} \qquad (12)$$

This describes all cases for deposition of solid dispersive aerosol phase in non-stationary filtration.

To solve equation (11) similarity method is applied by transformation of variables x and t

$$\ell^*(x,t) = \ell^*(k_x, k^2 t), \qquad (13)$$

solution to equation (11) can be obtained as:

$$\ell^*(x,t) = \text{erf}\left(\frac{x}{2\sqrt{a^2 t}}\right), \qquad (14)$$

characterizing distribution of value x, which obeys normal law, symmetrically relating to dispersion center $\bar{x}$.

The solution to equation (11) in determination of efficiency for the filtration process is limited by initial conditions

$$(x,o) = \begin{cases} \ell_{MAX} & x > 0 \\ 0 & x < 0 \end{cases}$$

and becomes

$$\ell = \frac{\ell_{MAX}}{2}\left[1 + \text{erf}\left(\frac{x}{2\sqrt{a^2 t}}\right)\right] \qquad (15)$$

Equations (14) and (15) which characterize one and the same process of accumulation of the mass of solid dispersive aerosol phase allow to identify the most important feature of that process. The above equations on a probability coordinate scale are straight lines. The line of equation (14) starts at (o,o) and straight from (15) intersects the ordinate at $\frac{\ell_{max}}{2}$. The reciprocal arrangement of the straight lines which is characterized by tangents to the slope has fixed values, $\frac{\ell_{max}}{2}$.

One of the major derivations of non-stationary filtering theory appears to be the specified association between the efficiency and the deposition function.

Preceding page blank

Paper No. 17

FACTORS IN THE COLLECTION OF FINE PARTICULATE MATTER WITH FABRIC FILTERS

by

Richard Dennis
and
John E. Wilder

GCA CORPORATION

Bedford, Massachusetts

Preceding page blank

ABSTRACT

Field and laboratory measurements for several types of fabric filter systems are examined with respect to size and concentration properties of dust emissions. Cautions in the use of mass collection efficiency data and fractional particle size concepts are discussed. Significant changes in size distributions and particle concentrations are cited for typical shaken bag and pulse jet filtration cycles. Where possible, filter effluents are related to fabric and inlet dust characteristics, type and intensity of cleaning method, service life of the fabrics, and environmental factors such as temperature, humidity and electrostatic charge.

I. INTRODUCTION

The role of fine particles in the atmosphere with respect to physiological hazards and visibility problems and methods by which fine particle concentrations may be better measured and controlled are being examined with increasing concern by environmental scientists. As pointed out recently by Friedlander (1), about 70 percent of the aerosol particles in the Los Angeles atmosphere evolve from man-made activities. Half of this amount is discharged as particulate while the remainder is generated in the atmosphere from gas phase reactions.

The primary and secondary ambient air quality standards, 75 and 60 $\mu g/m^3$ respectively as annual geometric means, deal only with mass concentrations. No reference is made to particle size properties nor chemical composition although it can be deduced that the clean, suburban aerosol of 25 $\mu g/m^3$ is composed principally of submicron material. Conversely, the 200 to 500 $\mu g/m^3$ levels occasionally observed in heavily industrialized areas are probably associated with significant quantities of coarse particulates in the 5 to 10 μm diameter size range. In neither instance is it possible to identify nor predict the true extent of potential particulate problems without size information. Similarly, even when it is possible to estimate the weight fraction of processed material discharged to the atmosphere from industrial or power plant stacks, there are seldom any supporting data on particle size properties. Consequently, one cannot calculate the meteorological transport and dilution of these emissions, nor the available surface area for gas adsorption and chemical reactions.

Many evaluations of the principal particulate collection methods have indicated that the highest collection efficiencies are provided by fabric filter systems. At present, however, there are many high temperature and/or corrosive gas streams for which electrostatic precipitators or wet scrubbers are the only satisfactory cleaning devices. Amongst those operations where filtration furnishes 99 to 99.9% or greater collection efficiencies, the effluent size properties have often been ignored on the premise that the small amounts of material discharged would have negligible impact on the surrounding environment. Except for such uniquely toxic substances as asbestos, beryllium, or plutonium, the assessment of particulate emissions on a mass basis has been considered as the most practical approach. Because of the time and cost involved and the lack of appropriate instrumentation for routine field measurements, particle size data are quite limited. It is only recently that serious efforts have been made to extend the size measuring capabilities of field instruments below the nominal 0.5 μm level afforded by cascade impactors or in situ light scattering particle counters. Reference is made here to condensation nuclei counters and diffusion batteries that provide some indication of the size spectrum below 0.5 μm. This lower range (~ 0.01 to 0.5 μm) is now being examined with increased concern by physiologists.

In this paper, we have examined fabric filters with respect to the reduction of particulate emissions on the basis of mass and particle size properties. According to inquiries from several groups concerned with the prediction of present and future particulate emission levels, the data now available for modeling purposes are not only limited but also subject to serious misinterpretation by individuals not specialists in filtration.

The primary objectives of this discussion are a.) to review some earlier studies that bear upon the forecasting of filter effluent properties, and b.) to present some recent findings on filter performance. One reason for the general lack of sizing data for filtration systems has been the very high efficiencies attainable in many low temperature applications, 99.9 to 99.99% or greater. Therefore, the tendency has been to disregard the particulate fraction discharging to atmosphere. The fact is often overlooked, however, that a weight collection efficiency of 99.9% applied to inlet concentrations of 10 and 0.1 grains/ft.^{3}, respectively, represents a 100 times difference in outlet concentrations. Furthermore, although the percent difference in recovery is comparatively small (~ 1%) with respect to filters operating at 99 and 99.99%, respectively, one sees a 100 fold reduction in mass discharge on the basis of equal inlet concentrations. The above observations point out quite simply that accurate estimates of emission levels cannot derive from order of magnitude or worse estimates of filter efficiency.

The dependency of filter efficiency on inlet concentration levels for otherwise similar systems has often been neglected for filters operating at $<$1% penetration. According to Figure 1, however, field measurements suggest an inverse relationship between penetration and loading. On the premise that equal gas volumes were filtered, these measurements indicated that the mass emission rates were essentially constant for a given dust/fabric system irrespective of the inlet loading. The same test series also indicated that the effluent size properties as determined by light field microscopy were similar to those for low atmospheric dust concentrations and only slightly dependent on inlet dust size distributions. The above findings are qualitatively consistent with filtration theory, i.e., only those particle diameters of the order of 1 μm or less should exhibit any significant penetration.

From a practical point of view, it would be helpful if one could define simply the fractional particle size efficiency of a given filter system. This would automatically permit description of effluent mass concentration and size distribution in terms of the corresponding inlet dust parameters. In the case of many inertial dust collectors, the concept of fractional particle size efficiency represents a viable approach. When applied to filter systems, however, one can expect to predict the particle removal characteristics only when particle inlet concentrations are very low such that accumulation on the fibers does not alter filter collection properties. This is seldom the case in real systems.

Data published by Whitby et al (3) give fractional size efficiencies for very low (<atmospheric dust level) concentrations of organic dye particles when filtered through loaded and "just cleaned" sateen weave cotton fabrics. Although Whitby's original presentation recommended no generalized extrapolation of these tests, out-of-context interpretations of his data have given the impression that fractional particle size data are readily available or calculable parameters. The experienced individual will recognize that Whitby's values apply uniquely to the specified dye aerosols and the dust deposits (fly ash or A.C. dust) on the filters. Furthermore, the tests are not realistic since the inlet dust differs from that deposited previously on the filter and the inlet concentrations are several orders of magnitude lower than found for most industrial applications. Perhaps the most important conclusions to be drawn from Whitby's study are that a.) fractional particle efficiencies in the 0.05 to 0.5 μm range are not strongly size dependent, and b.) fractional particle size efficiencies may vary from 85 to 99.5% depending upon the weight and size distribution of

the dust deposited on the filter.

II. RECENT EXPERIMENTAL MEASUREMENTS

A. Test Procedures

As part of a fabric filter cleaning mechanisms study (4), weight collection efficiencies and particle number concentrations were determined for several dust/fabric combinations and three common fabric cleaning procedures. The detailed results of this study will be presented in a forthcoming report. Although the background data given here are sufficient to describe the test systems, they do not reflect the complexity of the measurements. Additionally, it is not recommended that the experimental findings be extrapolated to dust/fabric systems and operating conditions differing significantly from those reported here.

1. Test Fabrics

The filter bags evaluated in this study were readily available and commonly used commercial products. Bags used in mechanical shaking systems were sewn with a top loop for attachment to the shaker arm and a bottom cuff for connection with the thimble plate. Felted tubes used with the high pressure, pulse jet system were fabricated with a flat, closed bottom and a top cuff for attachment to the interior supporting cage. Basic bag specifications are given in Table 1.

2. Test Dusts

In this paper, test results are given for coal fly ash and commercial talc dust only. The size properties of the resuspended dusts as determined by Andersen impactor in the inlet air stream are given in Figure 3. According to microscopic sizing of the dry powders when well dispersed in immersion oil, the MMD value of the fly ash was lower, roughly

3 μm. It was concluded, therefore that the 90 psig compressed air used in the ejector-dispersor system was insufficient to break up all the agglomerates. Inlet dust concentrations, unless otherwise indicated, were usually in the range of 3.5 and 12 grains/ft.^{3}, respectively, for shaking and pulse jet systems.

3. Basic Testing Conditions

Air to cloth ratios for shaking and pulse jet tests as reported herein were maintained constant at 3.0 and 8.5 ft.^{3}/min. per ft.^{2} of fabric. Most measurements, except for woven fabric life tests, were performed with single bags and a total system gas flow ranging from 25 to 44 ft.^{3}/min. Gas temperature and relative humidity levels were held within the bounds of 70 ± 2°F and 40 to 50% R.H. Filter bags cleaned by mechanical shaking were operated for a 30 minute cycle with fly ash and a 20 minute cycle with talc to maintain similar resistance increases.

4. Cleaning Procedures

The mechanical shaking motion consisted of an essentially horizontal, harmonic displacement over a range of shaking amplitudes and frequencies of 1/2 to 2 in. and 4.3 to 11.4 cps. A 45 second shaking period was preceded and followed by a one minute settling interval while the filter flow was shut off. Pulse jet testing described here is limited to one basic cleaning system, i.e., 70 psig air pressure, a pulse frequency of one pulse per minute, and a pulse duration of 0.06 second. By means of a supplementary damping tank, the wave form of the pressure pulse was altered in some tests to reduce the rate of pressure increase.

5. Dust Concentration Measurements

Inlet dust concentrations were established by one or a combination of dust feeder delivery rate, hopper dust recovery, filter samples or Andersen impactor measurements. Effluent concentrations from shaken bag systems were usually determined by Bausch and Lomb (B&L) single particle light scattering counter because of the very low concentrations. When filter performance was less effective (99.9%) an RDM mass monitor was used to determine the integrated mass concentration. The effluent gas stream from pulse jet systems was sampled with the RDM and/or the B&L sampler depending upon the purpose of the test.

There were both advantages and limitations to the sampling equipment cited above. The Andersen impactor could be used for both up and downstream size and concentration measurements (different sampling periods) when filter efficiencies were of the order of 99.9 to 99.99%. On the other hand, the B&L device was confined to downstream testing since extensive dilutions, $\sim 10^4$ times, would have been required to use it for upstream sampling. Because of its high degree of sensitivity and rapid response time, the B&L was a very useful device to track changes in particle size properties and number concentrations during a filtration cycle. Although the computation of downstream mass concentrations from B&L measurements required somewhat tenuous assumptions with respect to particle density and light scattering properties, comparisons with parallel RDM measurements usually indicated agreement within a factor of 5. Although the B&L values were recognized to be low in many cases, their principal function was to indicate relative changes in concentration levels.

B. Test Results

A study of the factors that determine the overall effectiveness of various fabric cleaning methods has shown that filter effluent properties (concentration and size distribution) for a single dust/fabric system can undergo extreme changes. As pointed out previously such variations are sometimes overlooked when filter systems operate at 99.5% or higher weight collection efficiency. In view of prospects for more stringent emission standards, however, it is essential that the filter effluent be characterized along with those parameters defining operational and power requirements.

The data presented in this paper involve only a small fraction of the tests performed to identify and investigate the physical mechanisms responsible for dust removal in shaken bag and pulse jet cleaning systems. The results are considered to furnish a good index of single bag field performance under the stated cleaning conditions and for similar fabrics and dusts having the same basic properties of coal fly ash or industrial talc. It should be remembered, however, that most large filter units operate as multi-chamber systems with sequential compartment cleaning. In the case of single compartment pulse jet systems, the tubes (or other filter medium configurations) may be sequentially cleaned as individual or groups of tubes. The net result is that the integrated effect on filter drag, total gas velocity distribution, and particulate emissions for multi-chamber units must be developed in accordance with procedures suggested by Robinson et al (4), Walsh et al (5) and Spaite et al (6). Analyses of the above approaches and many other concepts by Billings and Wilder (7) indicate that the success of such predictions depends upon the availability of specific performance information for the dust/fabric combination of interest. In the absence of such base line data, the particle concentration and size results described in this section may be used to predict relative but not absolute changes for filter media and aerosols not included in the pilot study.

1. Mechanical Shaken Systems

Several experiments were performed with unnapped, cotton sateen bags (10 ft. x 6 in., Table 1) to determine filtration parameters for a fly ash aerosol. During these tests, filtration velocity and inlet dust concentrations were held constant at about 3 ft./min. and 3.5 grains/ft.^{3}, respectively. The bags have been described as new (N) since each had experienced less than 10^4 individual shakes. They were essentially at equilibrium, however, with respect to air flow/resistance data for repetitive filtration cycles. The main variables for the above tests were shaking amplitude and frequency as shown in Table 2. The filtration interval was 30 minutes and 360 shakes were used in all tests.

The effect of amplitude and frequency variations on outlet mass concentration (and % penetration) is shown in Figures 4 and 5. Emissions decreased by as much as 5 orders of magnitude over the first 5 minutes of filtration. The sensitivity limit of the B&L counter allowed for no estimates of number concentrations less than 150 particles/ft.^{3} nor computed mass concentrations less than 10^{-9} grains/ft.^{3}. Approximately 90% of the dust emission took place during the first minute of filtration and the average concentration for the 30 minute filtration period (10^{-6} to 10^{-5} grains/ft.^{3}) was about 30 times lower. Average dust emissions were shown to increase significantly (order of 30 times) for the amplitude range 1/2 to 2 in. but were essentially unchanged with respect to frequency variations.

The filtration of ambient air * showed a more pronounced increase in outlet concentration over the complete 30 minute cycle with 2 in. amplitude shaking, Figure 6. It is interesting to note that the average emission for 30 minutes, however, was the same as that for fly ash, (Figure 7). The latter finding appears to support field data presented in Figure 1 that show nearly constant outlet loadings for a fixed filter type regardless of inlet load levels.

Figure 8 shows how particle number concentrations varied with respect to filtration time based upon B&L measurements. Mass concentrations at specified times were computed from these data by assuming a specific gravity of one and using the arithmetic average of diameters for each size range.** Although one does not expect this calculation process to be very accurate, the outlet concentration and penetration values for the pilot plant fly ash/sateen weave cotton system fall on the Figure 1 regression line for foundry dust/sateen weave cotton measurements.

Inspection of Figure 8 indicates that the discharge of particles >1μm is restricted to the first few minutes of filtration accounting for

---

* Inlet loading defined as room air when dust feeder was turned off. In fact, some fly ash deposition from the inlet piping was probably resuspended when filtration was resumed.

** 0.3 μm refers to 0.3 to 0.5 μm range, $\overline{d} = 0.4$ μm

0.5 μm refers to 0.5 to 1.0 μm range, $\overline{d} = 0.75$ μm the very rapid decrease in outlet mass concentrations.

Accelerated shaking of cotton bags in conjunction with periodic fly ash dust loading and 30 minute filtration tests was carried out with sateen weave cotton bags to simulate probable performance changes over extended periods of use. After 20 x 10^6 shakes, it was postulated that a bag had seen the field equivalent of 3 to 5 years service. Average 1 and 30 minute outlet concentrations are shown in Table 3 for bags shaken at two tension levels, one fairly taut at 3.1 lbs. and the other installed at near slack conditions, 1.3 lbs. Surprisingly, the increases in average emission levels were relatively small, roughly a two fold increase after 20 x 10^6 shakes. At the same time, the bags shaken at the higher tension showed consistently higher (about 2 to 3 times) outlet concentrations for both abbreviated and extended shaking.

Size distribution curves were constructed from B&L data of the type shown in Figure 8. These data, Figure 9, show that the dust discharging from the filters is composed of relatively coarse material during the earlier phases of filtration. As the 3 minute time is approached, however, the outlet dust is approaching the size properties of atmospheric dust as determined by light field microscope.

The filtration characteristics of fly ash were also studied with napped sateen weave cotton, plain weave Dacron and crowfoot weave Dacron, Table 4. These comparisons were made at a 3.5 grains/ft.^{3} loading, 3 ft./min. filtration velocity, and a 30 minute filtering period. The cleaning cycle consisted of 360, 1 in. amplitude shakes at 8 cps. Changes in outlet concentration with time were again computed from B&L counter measurements. Reference to Figure 10 shows that measurable effluent concentrations for both

Dacron media persisted throughout the 30 minute filtration interval. In contrast to sateen weave cotton, the 1 minute and 30 minute concentrations were not appreciably different (2 to 5 times) and the average outlet concentrations over the full 30 minute filtering cycle were about 1000 times higher. In terms of weight collection efficiency, the average values for the Dacron bags were about 99.8%.

The total amount of dust emitted per sq. ft. of fabric per filter cycle was compared with the residual dust holding at the resumption of filtration. According to Figure 11, the amount of dust retained by the fabric matrix plays a significant role in determining dust retention. It may be inferred that the pore sealing process is nearly complete for cotton media and much less so for the Dacron weaves. It should also be noted that whereas the differences in filter resistance indicate that fan power requirements would only be about 25% higher for cotton fabrics, choice of the cotton would reduce particulate emissions by 1000 times. When emission data for similar talc filtration studies were adjusted for deposit bulk density (roughly 4.5 times that for fly ash) they too fell on the same regression line. Generally, the same relationship between dust holding and net dust penetration was indicated in recent tests by Draemel (8) for several dust/fabric combinations.

2. Pulse Jet Systems

The results of pulse jet cleaning studies cannot be extrapolated directly to field applications because measurements were made with a single tube system. As with any large compartmented units the resultant effluent from several tubes undergoing sequential cleaning should be cleaner than that from the most recently pulsed tube. A precise definition of the field effluent depends upon the fraction of tubes cleaned at any one time, the apportionment of gas flow among all the tubes in the system, and the effect of the pulse jet parameters on particulate emissions.

The pulse jet tests described in this section involved the following variations in cleaning parameters:

Pulse jet pressures - 40 to 100 psig (direct and damped)
Pulse duration - 0.06 second
Pulse interval - 1 minute

Direct pulses involved the direct venting of compressed air from the reservoir tank to the bag exit region. Damped pulses were produced by placing a dead end expansion tank in the line such that the same air volume was injected into the clean air side of the felt tube but at a less rapid rate.

All tests reported here were made with fly ash and wool or Dacron felt tubes at inlet dust loadings ~12 grains/ft.^{3} and an inlet velocity of 8.5 ft./min.

Average outlet concentrations for fly ash filtration are shown in Figure 12 for direct and damped pulses at 40 to 100 psig reservoir pressures. A six fold range in emission levels was noted for direct pulse systems in contrast to a 2.5 times change with damping. Absolute outlet concentrations were about 1000 greater than those determined for shaken cotton bags. Average operating resistance per 1 minute filtering cycle varied inversely with pulse jet pressure, Figure 13, and was approximately 20% higher with damped pulses. For this increase in resistance, however, a four fold reduction in effluent concentration was obtained at 100 psig reservoir pressure.

The changes in particle concentration on a number and weight basis over the 1 minute filtering period, Figure 14, showed the same trends exhibited by shaken Dacron bags. Although the highest number concentrations were noted during the first 20% of the cycle, the initial mass concentration was seldom more than 2 to 5 times the average outlet concentration. These results suggest that a brief, ~1 minute, filtering period is insufficient to permit any extensive pore blockage. Because of the much higher effluent concentrations, it was seldom possible to make B&L measurements for particle diameter 1 μm. Choking in the fine particle channels of the B&L leads to erroneously low estimates of number concentration. With a few exceptions, however, there appeared to be a constant ratio (~5/1) between B&L and RDM or Andersen impactor mass measurements.

Several comparisons were made between upstream cascade impactor samples and downstream B&L measurements. By plotting upstream measurements 4 orders of magnitude less than actual values, near superposition of fractional size concentration curves was obtained. Figure 15 indicates that the larger particles are more efficiently removed by both direct and damped pulse systems, irrespective of the type of felt. The data also suggest the liklihood of constant efficiency particle removal for sizes down to 0.3 μm.

A comparison of up and downstream Andersen impactor measurements in Figure 16 shows that the average effluent aerosol is actually slightly coarser than that entering the system. No rules of filtration are contradicted by these results. The downstream particulate is composed largely of agglomerated material loosened by the high energy pressure pulse and driven to the clean air side of the felt by a combination of fabric acceleration and normal air flow. It is postulated that the effluent from a multi-tube system would probably show a finer downstream particulate since the majority of the coarse particles are associated only with the most recently pulsed element.

References

1. Friedlander, S. K., "Small Particles in Air Pose a Big Control Problem" Environ. Sci. Technol., 7, 1115 (1973)

2. Dennis, R., Johnson, G. A., First, M. W., and Silverman, L. "How Dust Collectors Perform," Chem. Eng. 59 196 (1952)

3. Whitby, K. T. and Lundgren, D. A. "Fractional Efficiency Characteristics of a Torit Type Cloth Collector" Torit Manufacturing Co., St. Paul, Minnesota, August 1961.

4. Robinson, J. W., Harrington, R. E. and Spaite, P. W. "A New Method of Analysis for Multicompartmented Fabric Filtration, Atmos. Envir. 1, 495 (1967)

5. Walsh, G. W. and Spaite, P. W. "Characterization of Industrial Fabric Filters," ASME Annual Winter Meeting (December 1960)

6. Spaite, P. W. and Walsh, G. W. "Effect of Fabric Structure on Filter Performance" Am. Ind. Hyg. Assoc. J. 24, 357 (1963)

7. Billings, C. E. and Wilder, J. E. "Handbook of Fabric Filter Technology" Contract No. CPA-22-69-38, GCA Corporation, Bedford, Mass. (December 1970) Document PB 200-648, National Technical Information Service, U. S. Dept. of Commerce, Springfield, Va. 22151.

8. Draemel, D. C. "Relationship Between Fabric Structure and Filtration Performance in Dust Filtration." Control Systems Laboratory, U. S. Environmental Protection Agency, Research Triangle Park, EPA-R2-73-288 (July 1973)

TABLE 1

DESCRIPTION OF FABRICS USED IN PARTICULATE EMISSION STUDIES

Filter Fabric	Weight Oz./Yd.^{2}	Weave	Yarn Count	Permeability	Application
Cotton	10	Sateen	95 x 58	13	Shaking
Cotton (Napped)	10	Sateen	95 x 58	13	Shaking
Dacron^R	10	Plain	30 x 28 (Staple)	55	Shaking
Dacron^R	10	1/3 Crowfoot	71 x 51 (Filament)	33	Shaking or Reverse Flow
Dacron^R	18	Felt, Needled		35	Pulse Jet
Wool	16	Felted, No scrim (HCE Treatment)		30-40	Pulse Jet

Woven Fabrics - 10 ft. x 6 in., 10 ft. x 4 in. and 5 ft. x 6 in. bags
Felted Fabrics - 4 ft. x 4.5 in. tubes

TABLE 2

Collection Efficiency and Effluent Concentrations for Various Shaking Systems [a]

Shaking System cps	ampl. in.	Average Effluent Concentration - grains/ft^3 Fly Ash Filtration[b] First minute	30 minutes	Ambient Air Filtration[c] First minute	30 minutes	Shaking Tension lbs.	Fabric Dust Holding[d] grains/ft^2
7.5	2	3×10^{-4}	1×10^{-5}	2×10^{-4}	2×10^{-5}	10.7	200
7.5	1	3×10^{-5}	1×10^{-6}	2×10^{-5}	1×10^{-6}		300
7.5	1/2	1×10^{-6}	3×10^{-7}	1×10^{-5}	3×10^{-7}	3.5	410
4.3	1	1×10^{-4}	3×10^{-6}	2×10^{-4}	1×10^{-6}	4.8	420
7.15	1	5×10^{-5}	2×10^{-6}	2×10^{-5}	1×10^{-6}		290
11.3	1	5×10^{-5}	2×10^{-6}	2×10^{-5}	1×10^{-6}	7.5	200

---

a) 360 shakes per cleaning cycle, sateen weave, unnapped cotton

b) Fly ash, 3.5 grain/ft^3

c) Ambient air ~ 10^{-4} grains/ft^3

d) At resumption of filtration

TABLE 3

Fly Ash Effluent Concentrations vs. Number of Shaking Cycles for 1 and 30 Minute Averaging Periods, Unnapped Cotton Sateen 10 ft. x 6 in. Bags, 3.5 Grains/ft^3 Inlet Loading, 3 fpm Filter Velocity

Number of[b] Shaking Cycles	Average Effluent Concentration - grains/ft^3 x 10^6[a]			
	Taut Bag[c]		Loose Bag	
	First Minute	30 Minutes	First Minute	30 Minutes
6×10^6	750	25	250	8.7
10×10^6	750	25		8.3
15×10^6	500	17	350	12
20×10^6	900	30	450	15

[a] Measurements made after loading filter to ~700 grains/ft^2, and then cleaning.

[b] Shaking Cycle 8 cps, 1 in. ampl. 360 shakes

[c] Static Tension = 3.1 lbs., Shaking Tension 6.5 lbs.

[d] Static Tension = 1.3 lbs., Shaking Tension = 4.5 lbs.

TABLE 4

FLY ASH FILTRATION CHARACTERISTICS FOR NEW ($<10^4$ SHAKES) AND WELL-USED (2×10^7 SHAKES) BAGS

	FABRIC TYPE [a)]							
	Plain Weave Dacron		Crowfoot Dacron		Napped Cotton Sateen		Unnapped Cotton Sateen	
	N	U	N	U	N	U	N	U
Residual Drag in H_2O/fpm	0.17	-	(0.37)	(0.02)	(0.20)	(0.53)	0.47	(0.60)
Effective Residual Drag in H_2O/fpm	(0.35)	0.30	0.43	0.47	0.23	0.67	0.67	(0.73)
Terminal Drag in H_2O/fpm	(0.81)	0.73	1.12	1.11	0.82	1.17	1.24	1.41
Dust Collected [b)] per Cycle, Grains/ft^2	278	255	288	275	295	312	284	290
Residual Dust Grains/ft^2	207	113	92	73	449	336	413	375
% Dust Removed [c)] by Shaking	57	69	76	79	40	48	41	41

a) 10 ft. long x 6 in. diam. bags, N=New, U=Well Used

b) Inlet Loading -3.5 grains/ft.^{3}, Filter Velocity -3 fpm, 30 min. filter cycle

c) Cleaning Cycle -360 shakes, 1 in. amplitude, 8 cps

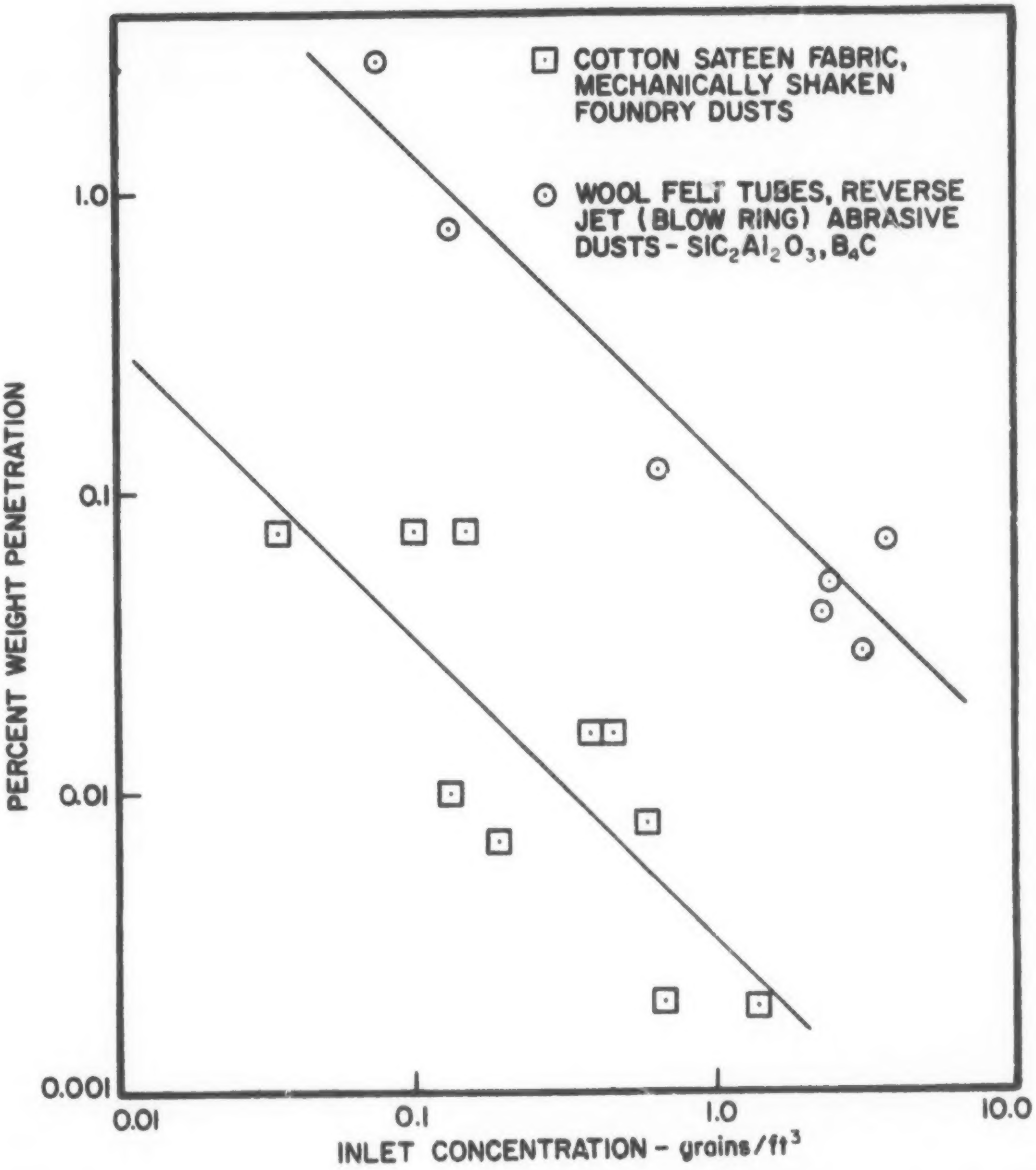

Figure 1. Inlet Concentration versus Percent Weight Penetration - Ambient Temperatures.

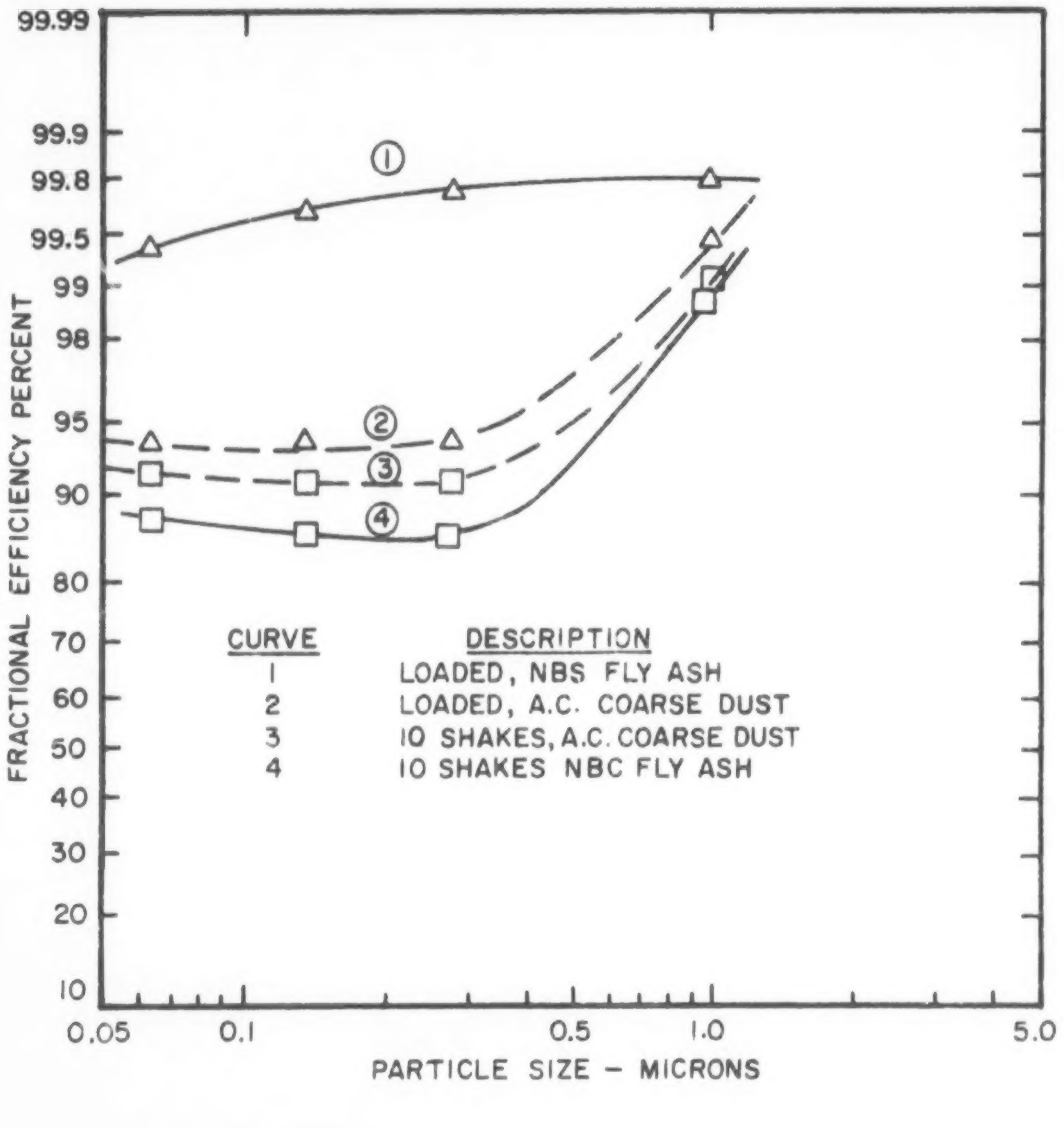

Figure 2. Fractional Efficiencies, Loaded and Shaken Sateen Weave Cotton Filter Media, A.C. Coarse Dust and NBS Fly Ash.

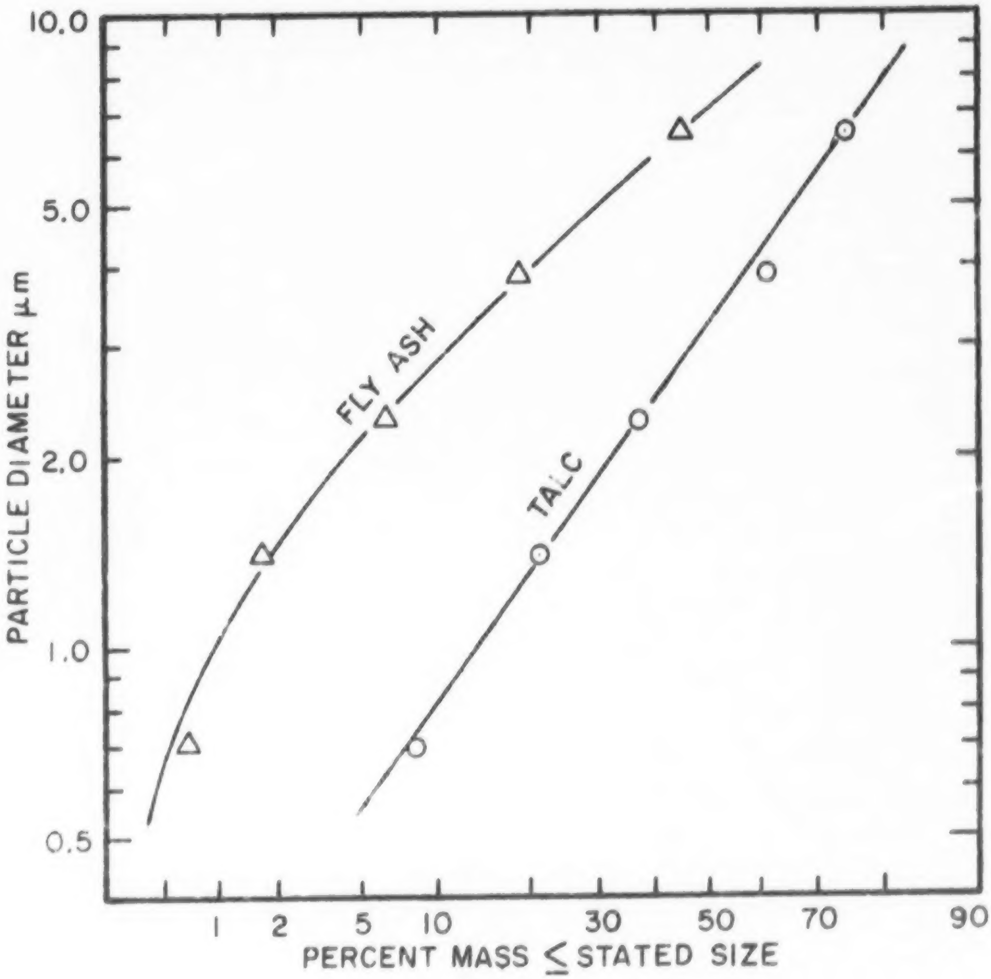

Figure 3. Comparative Size Properties for Resuspended Fly Ash (Coal) and Talc by Andersen Impactor. Inlet Aerosols.

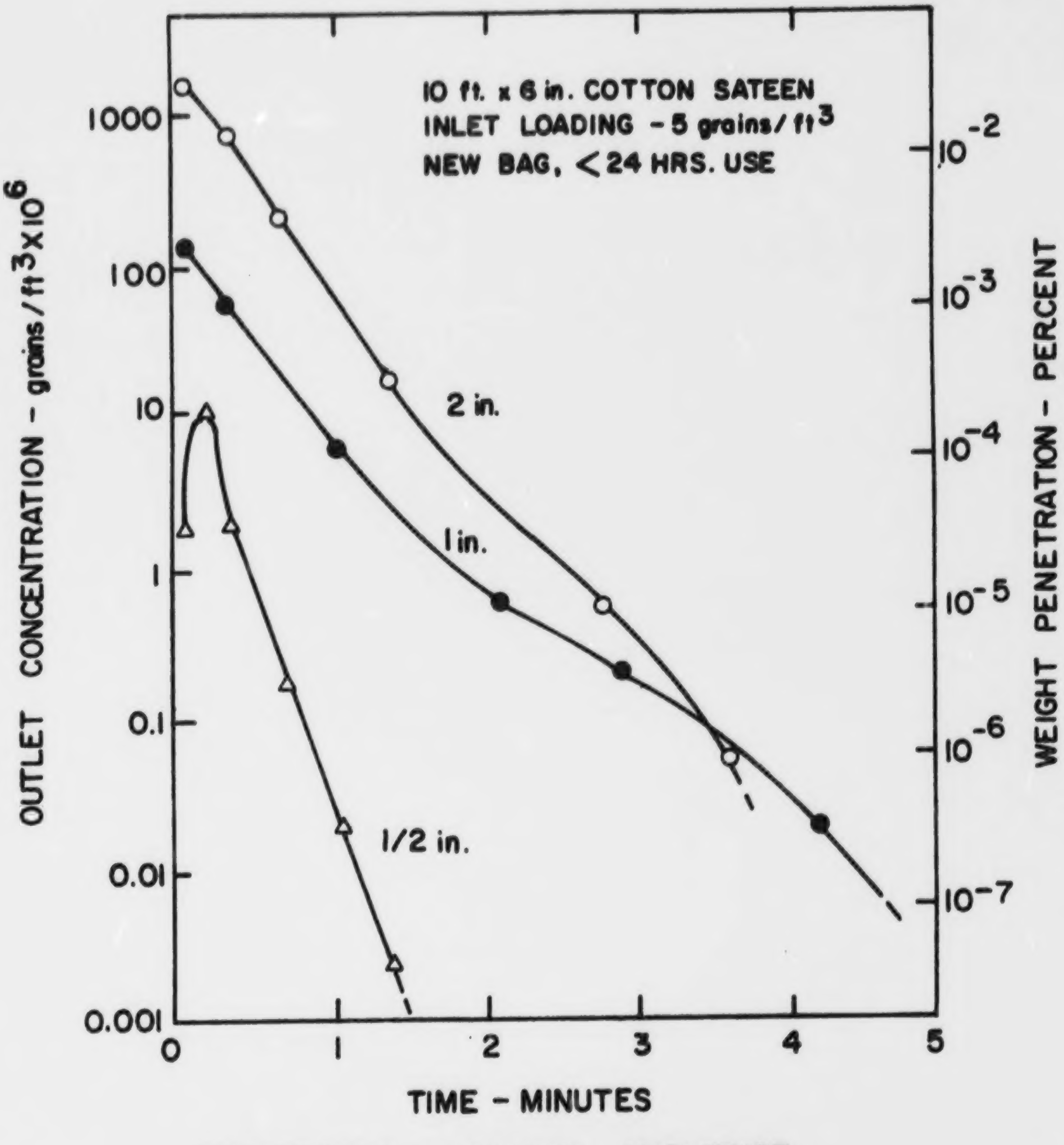

PENETRATION vs. SHAKING AMPLITUDE
CONSTANT FREQUENCY (7cps)

Figure 4.

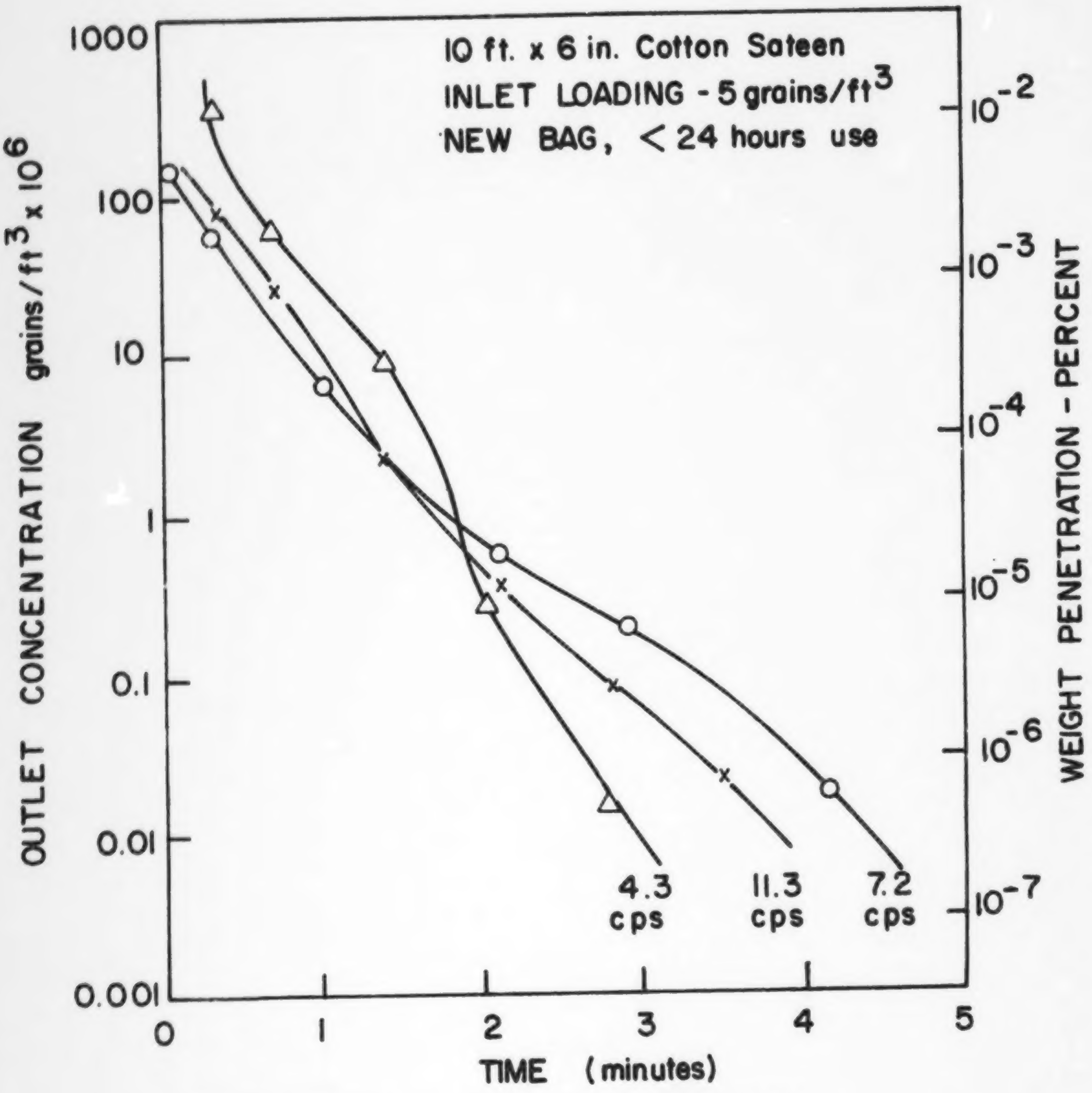

PENETRATION vs. SHAKING FREQUENCY, CONSTANT AMPLITUDE (1 in.)

Figure 5.

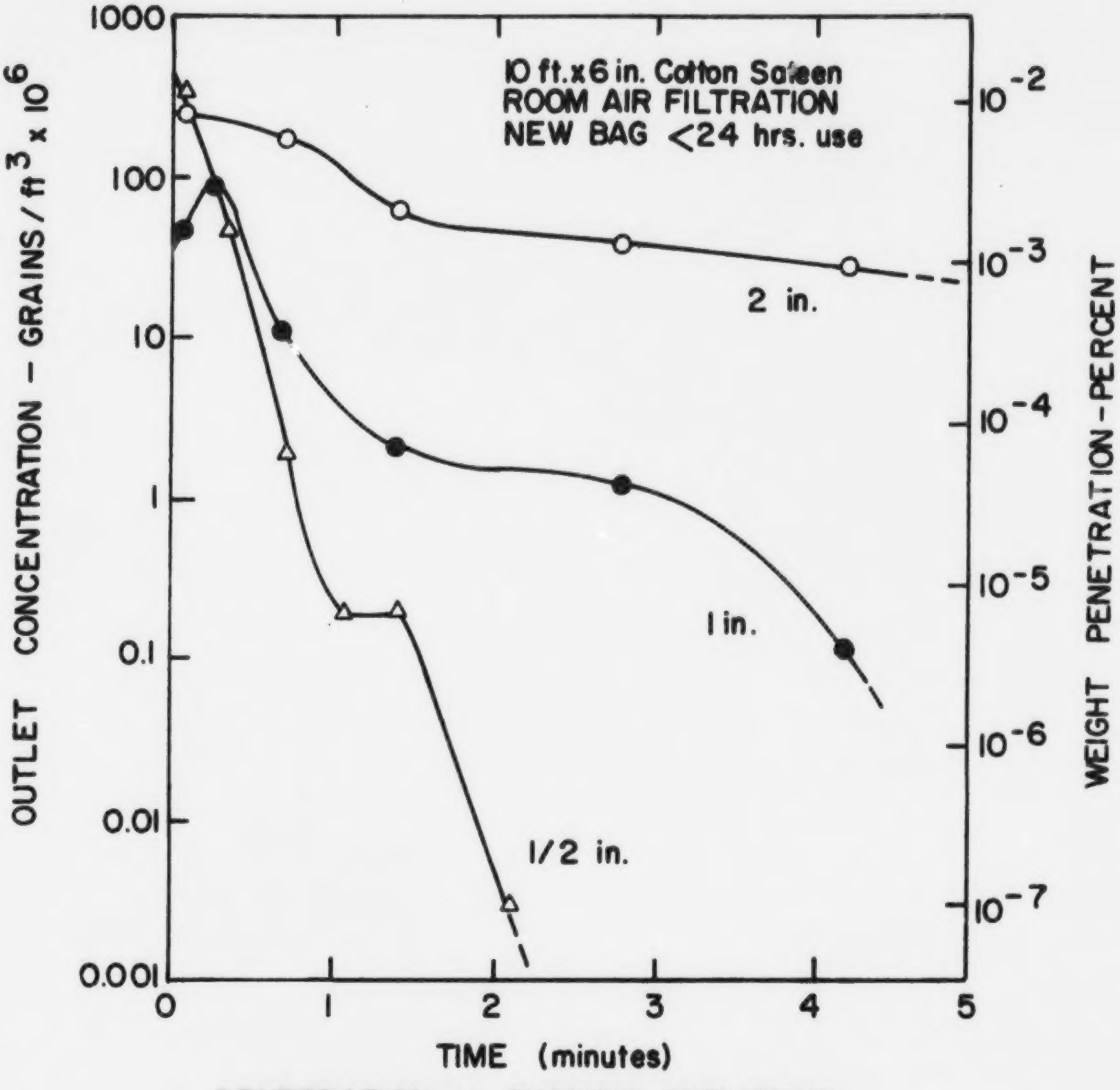

PENETRATION vs. SHAKING AMPLITUDE,
CONSTANT FREQUENCY, (7.5 cps)

Figure 6.

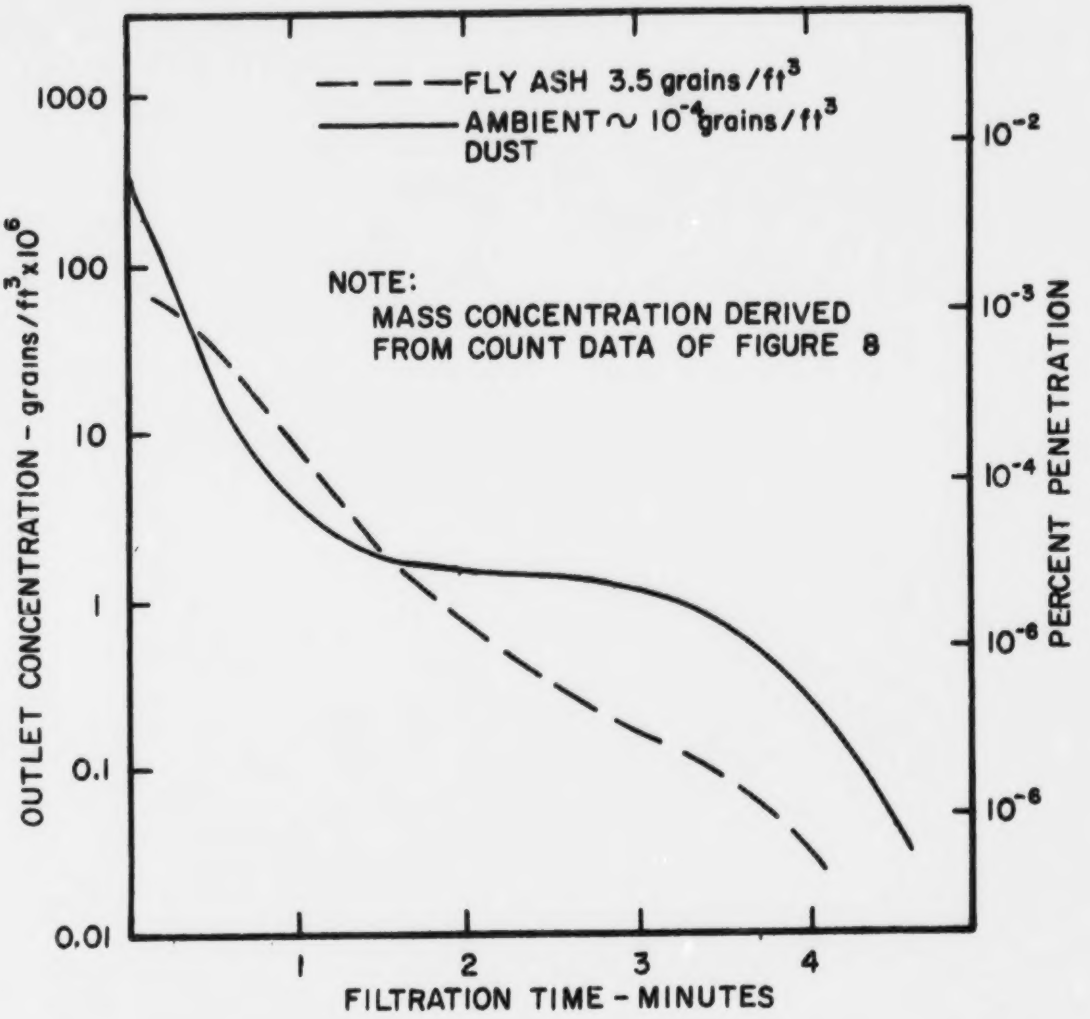

Figure 7. Decrease in Outlet Mass Loadings with Increased Filtration Time.

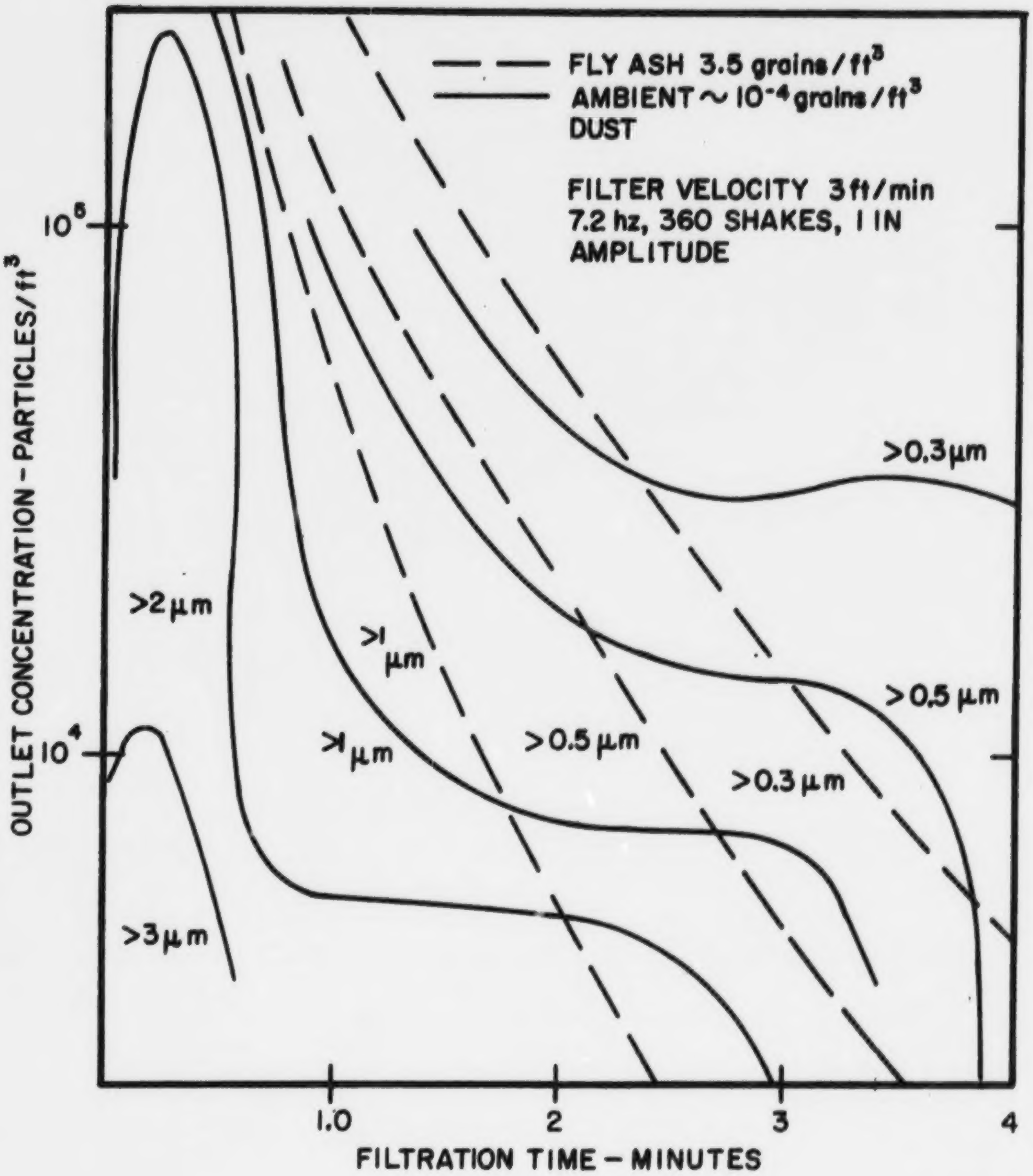

Figure 8. Variation in Outlet Loadings (Number and Size Basis) for Shaken Cotton Sateen Bags (No Nap). B&L Size Measurements.

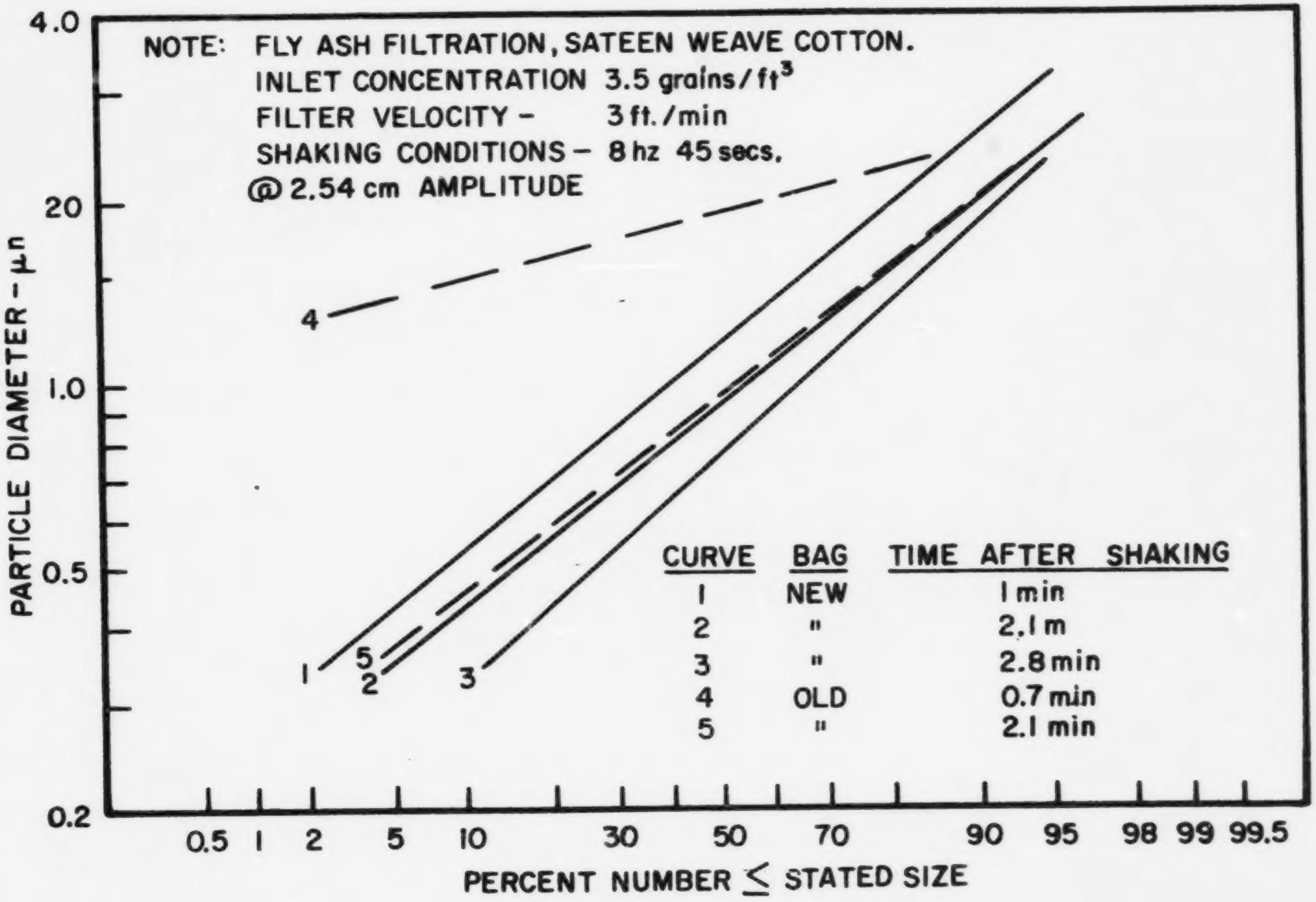

Figure 9. Changes in Effluent Size Properties with Filtering Time for New (< 10^4 Shakes) and Old (2 x 10^7 Shakes) Bags. (Sizing by Optical (B&L) Counter).

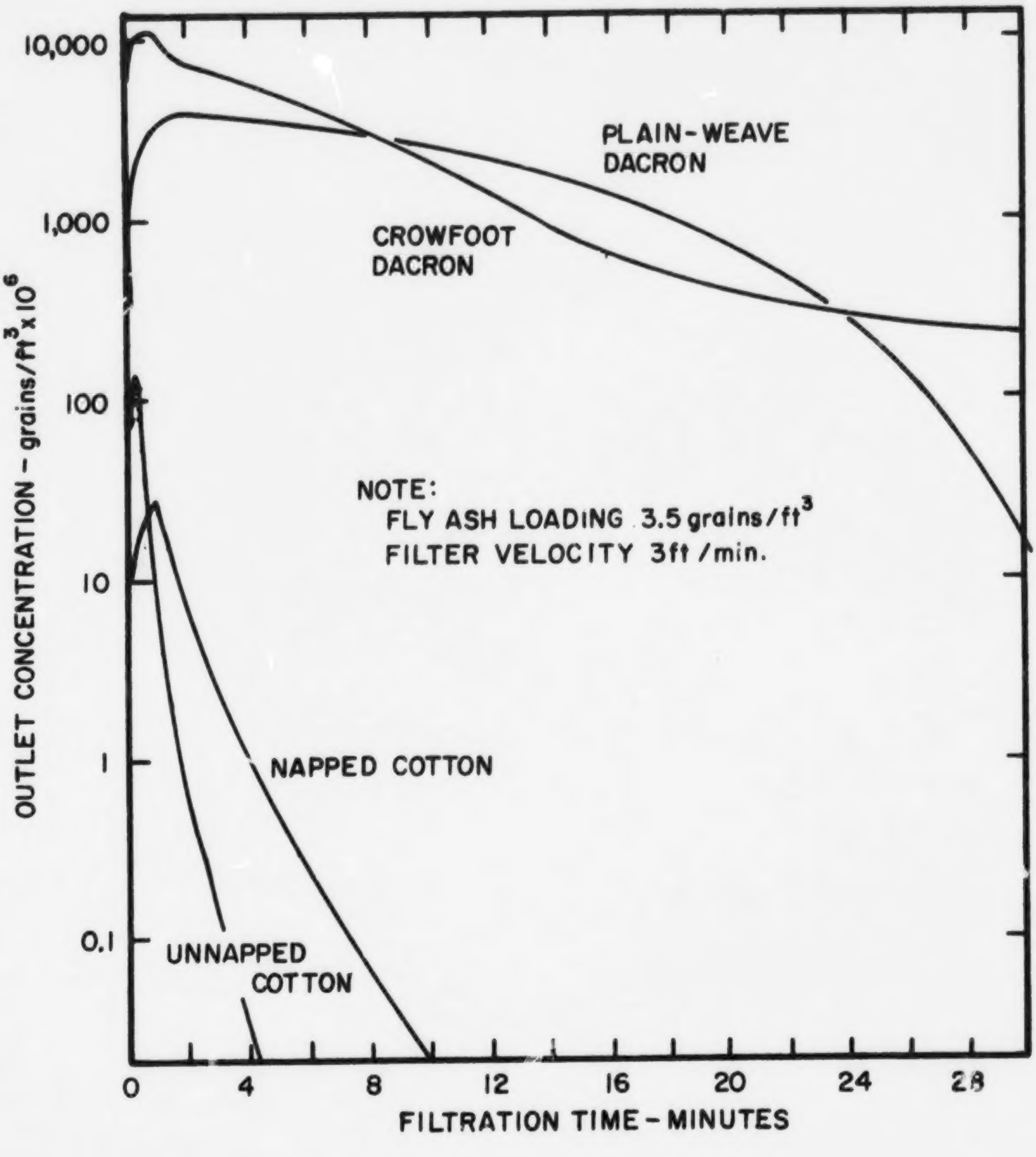

Figure 10. Fly Ash Emissions for Various Filter Media Cleaned by Mechanical Shaking; 30-Minute Filter Cycle, New Bags, Less Than 10^4 Shakes. (Based on Optical Counter Measurements).

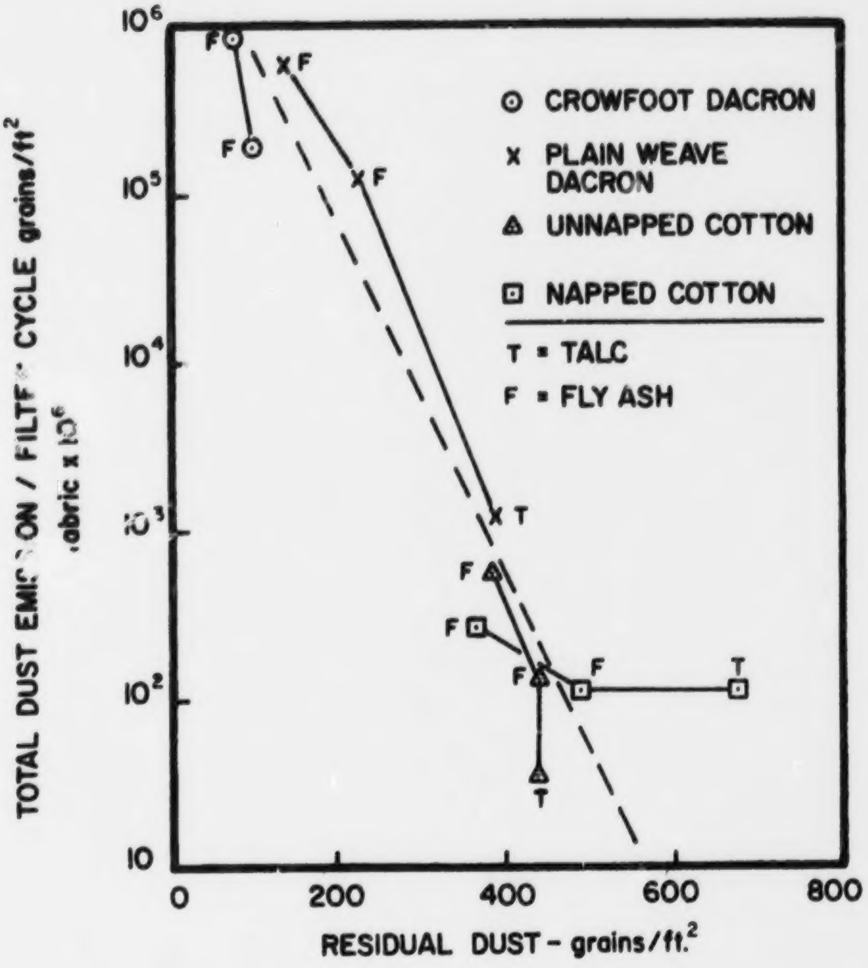

Figure 11. Total Dust Emitted per Filter Cycle versus Fabric Type and Residual Dust Holding.

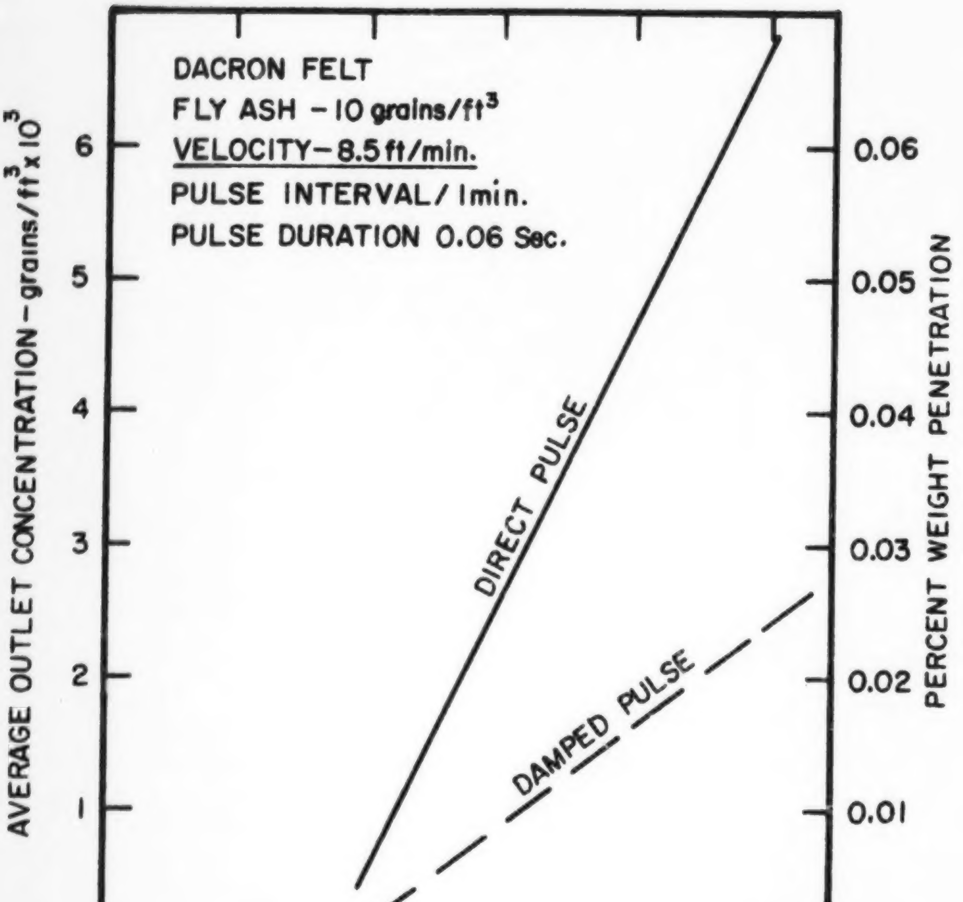

Figure 12. Dust Emissions for Fly Ash versus Pulse Intensity and Pulse Wave Form.

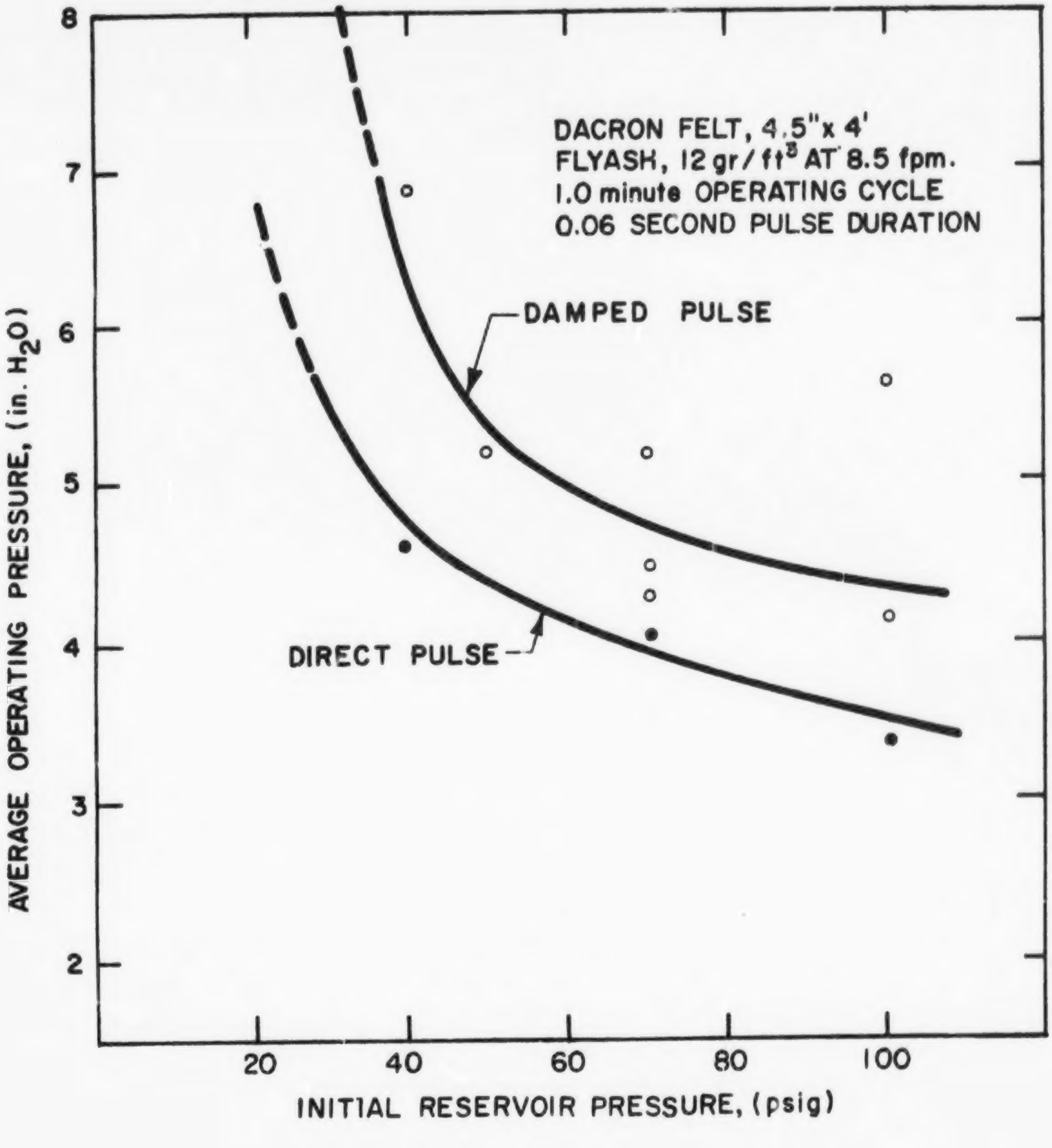

Figure 13 Pulse Jet Pressure vs. Average Bag Resistance for Direct and Damped Pulses

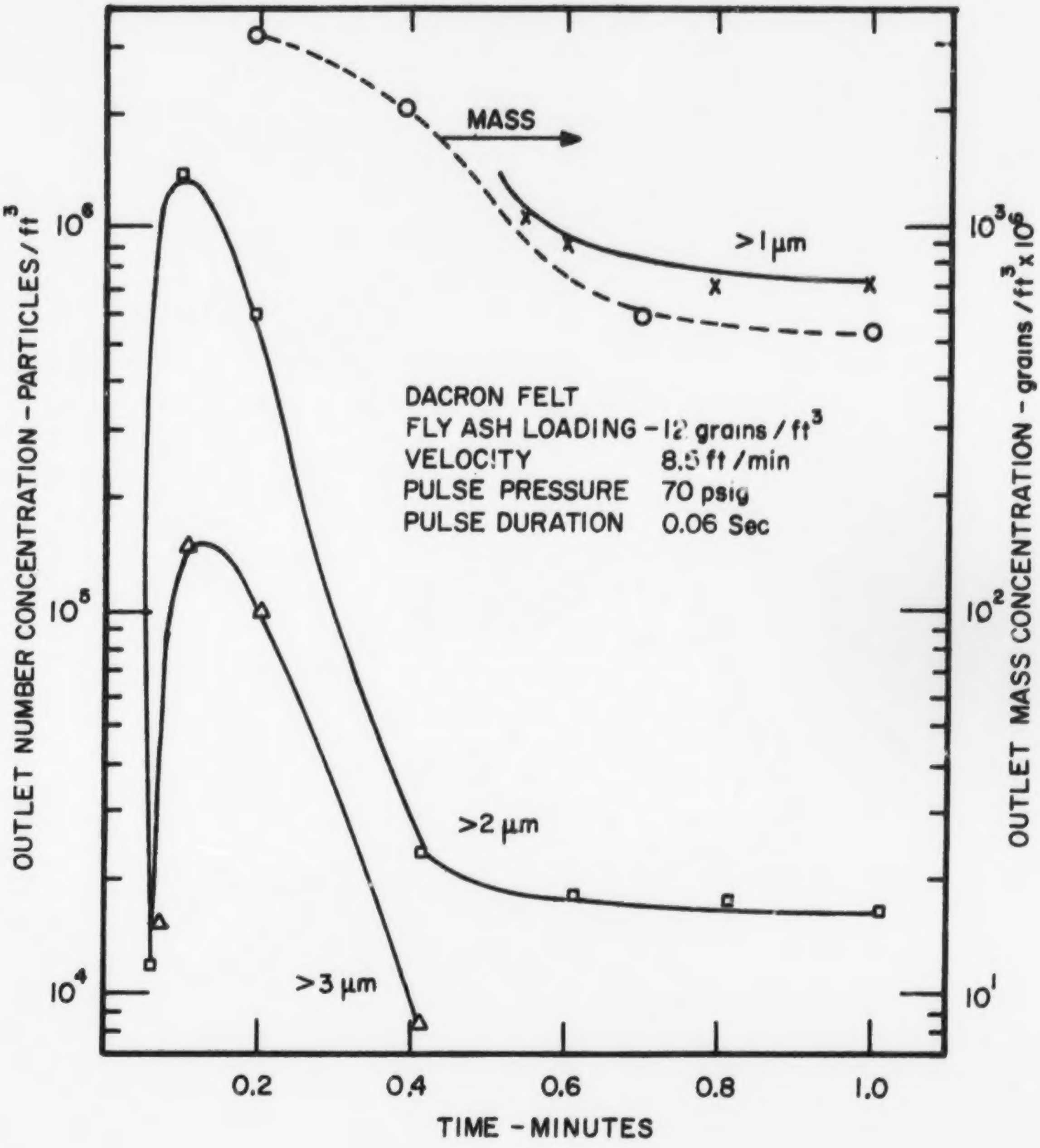

Figure 14. Variations in Particle Number and Mass Concentration versus Diameter and Time.

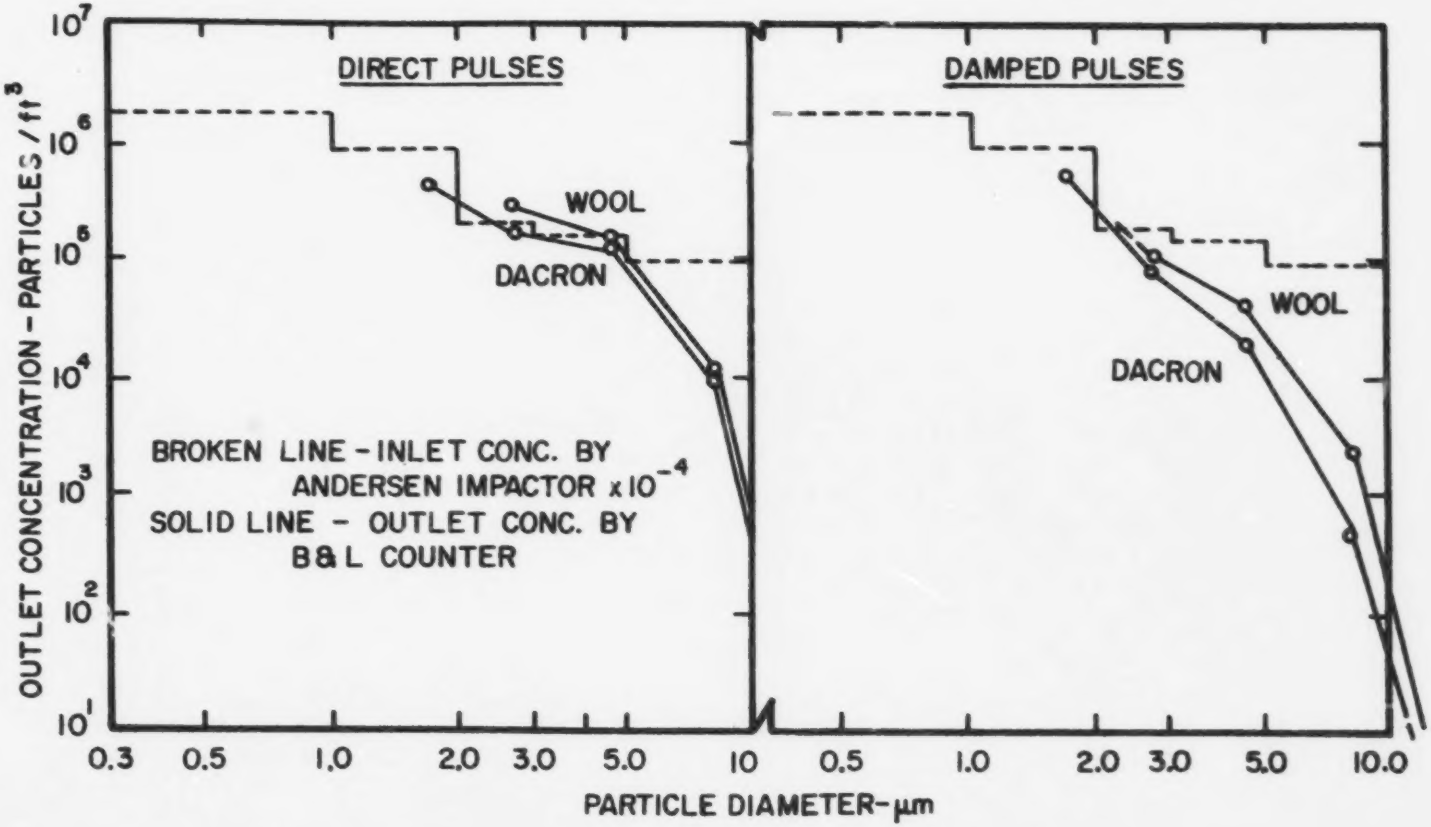

Figure 15. Average Outlet Number Concentrations for 1-Minute Pulse Intervals. Pulse Jetting at 70 psig for 0.06 sec.

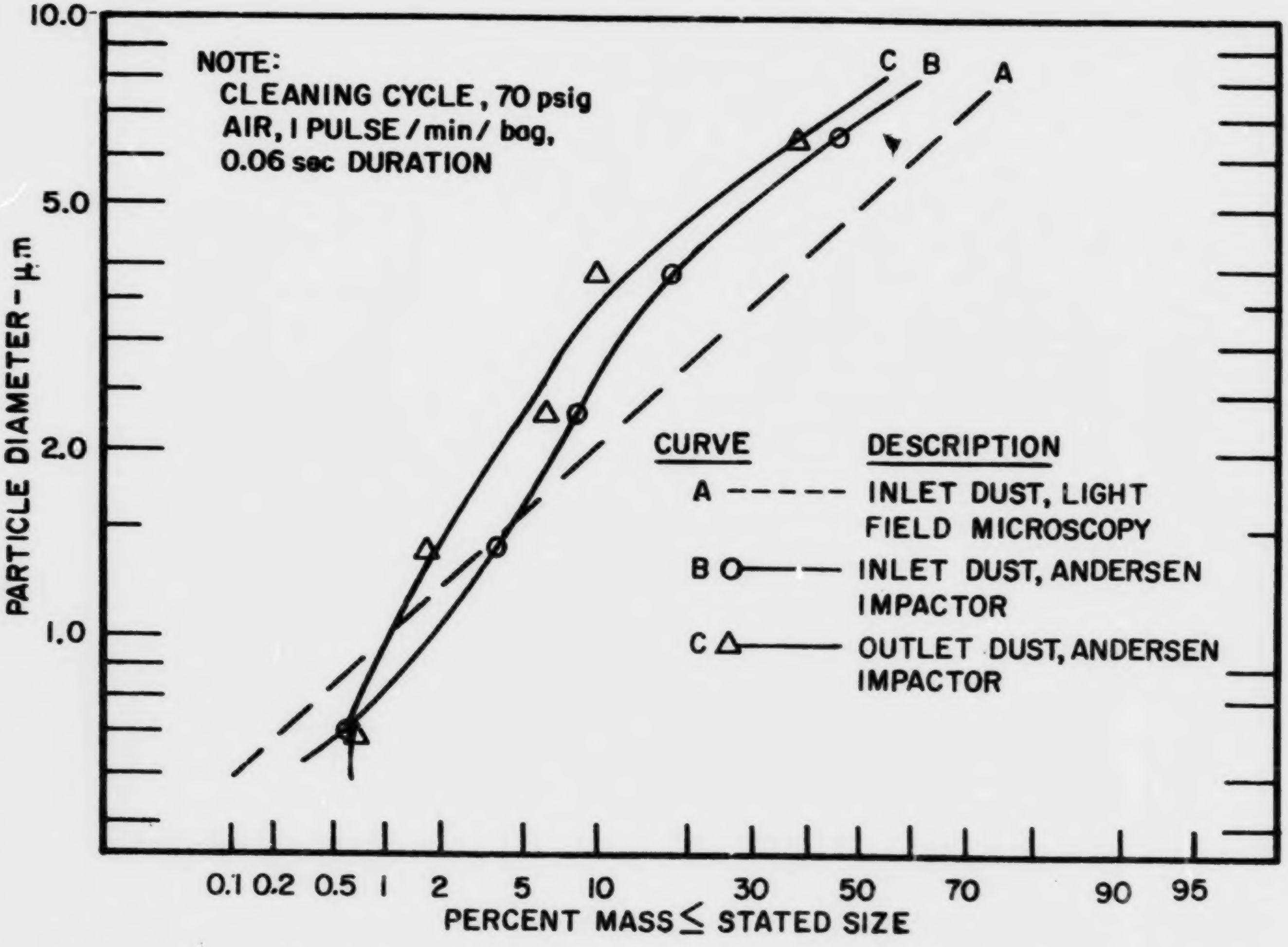

Figure 16. Fly Ash Filtration with Dacron Felt and Pulse Jet Cleaning. Size Distribution for Inlet and Outlet Dusts at Weight Collection Efficiency of 99.83%.

Paper No. 18

THE STATE OF THE ART OF HIGH TEMPERATURE FILTRATION AND CURRENT TECHNOLOGY DEVELOPMENTS

by

Dean C. Draemel

U. S. ENVIRONMENTAL PROTECTION AGENCY

Research Triangle Park, N. C.

Preceding page blank

ABSTRACT

This paper will deal with the state of the art of high temperature (+230°C) filtration technology and new applications or extensions of that technology. The discussion will generally discuss the state of the art by materials or media and will cover general markets, operating capabilities and development trends of each material or medium separately. Some broad generalizations and trends in high temperature filtration technology will be mentioned. High temperature filter materials which will be discussed are glass, mineral, carbon/graphite, teflon, organic and metal fibers and granular beds.

High Temp Fabric Filtration

Since the majority of high temperature filtration applications involve organic and inorganic fibers in woven or mat forms, a brief discussion of the fabric filtration industry follows.

General Filters(1)

There are on the order of 50 companies supplying fabric filter equipment with no one company having a major share of the market. Most of these companies have other products so that fabric filters represent only a fraction of sales. The result of these two factors is that fabric filter research is limited to small efforts by individual companies on the order of 1-2% of their fabric filter sales. The low level and the diversity of this research limits advances in high temperature filtration technology especially.

In 1969 the total market in fabric filter equipment sales was estimated to be about 7500 units per year with an average size of ~ 270 M^2. This resulted in equipment sales of $\sim 22 \times 10^6$ dollars per year with an annual growth rate of $\sim 7\%$. The new and replacement fabric market was estimated at $\sim 33 \times 10^6$ dollars per year with a similar growth rate giving a current replacement fabric market of $\sim 44 \times 10^6$ dollars per year. Total filters in use at the present time are thus estimated at $\sim 120{,}000$ units. These estimates of total sales are uncertain to within a factor of 2. Efforts to develop accurate market information have been hampered because of the diversity in manufacturers and their unwillingness to cooperate in surveys for fear of loosing a "competitive edge" on the market.

High temperature filtration on the order of +230°C is limited to a fraction of the total fabric filter market. Major market areas include carbon black, non metallic minerals, foundary cupolas, electric furnaces, sinter machines, small boilers, and brass refining, with cooling as required. An example of new applications which are foreseen for high temperature filtration would be on advanced power cycles utilizing turbine devices.

An article(2) entitled High Temperature Fabric Filtration of Industrial Gases by P. Spaite, D. Stephan and A. Rose, Jr., summarizes design considerations in high temperature filtration using conventional baghouse equipment. A maximum filtration temperature from a cost and materials standpoint, of roughly 400°C is practical for all but special fabric filtration applications. The rest of this paper will discuss filter media developments and applications for the relatively large 230-400°C market and the speciality +400°C market. Conventional high temperature fabric filters will find their main uses in the 230°-400°C range. Mechanical considerations generally lead to different medium physical configurations e.g., mats, sintered sheets or granular beds - for the +400°C range. The range of materials applicable to the +400°C range is thus more limited.

The goal of high temperature filtration technology development is essentially to provide dependable performance at higher temperatures. The problem of media development is one of materials science. Mechanical and thermal properties of a material must be adequate for the physical and chemical conditions of filter operation. Some advances in equipment design such as pulse jet or shock wave cleaning have reduced the mechanical abuse factor in filter failure but real advances in high temperature filtration technology rely on the development of improved media through material science. The main materials suitable for high temperature filtration applications are glass fibers, mineral fibers (SiO_2, aluminum silicate, BN), carbon or graphite fibers, Teflon, certain organics, metal fibers (stainless, etc.), granular beds, sintered metals and porous ceramics.

The following section will evaluate current performance, developments, and market status for the high temperature filter materials mentioned in the previous paragraph with emphasis on the fibrous materials and a brief discussion of closely related granular bed developments.

Glass

Glass fibers have a great advantage over most other potential high temperature filter media in their low cost and relatively high temperature limits. Glass yarns cost from 0.9 to 9.0 dollars per kilogram and the total glass fabric filtration market is roughly estimated at $\sim 7.5 \times 10^6$ dollars per year. The low temperature filtration fibers such as polyamides, polyesters, acrylics and polypropylene cost roughly the same for the yarns. High temperature filtration materials are generally much more costly. Using average figures for commercially available(3) yarns, fluorocarbon yarns cost roughly 50 dollars per kilogram, carbon or graphite yarns; 400 dollars per kilogram, high temperature polyamide; 18 dollars per kilogram, metal fibers; 150 dollars per kilogram and boron nitride; 550 dollars per kilogram.

Prior to 1960 silicon oil lubricants were used to protect glass against mechanical and chemical attack in filtration applications up to 230°C. Work sponsored by the U. S. Public Health Service in 1957-1959(4) showed improved bag filter flex life performance up to 290°C when colloidal graphite was applied to commercial silicone treated glass fabrics. Since that time, most commercial high temperature glass finishes have been a combination of silicone oils and graphite. With the development of Teflon in the 60's, new finishes were developed which included combinations of silicone oils, graphite and Teflon. Dupont Corporation supplies a fine colloidal form of Teflon which the glass fabric finishers apply in a variety of ways, most of which are considered proprietary.

Since 1970 most suppliers of glass fabrics for high temperature filtration have had at least one finish including Teflon in their line. The method of inclusion of Teflon in the finish affects the fabrics ability to resist mechanical and chemical attack. An "encapsulation" of glass fibers by a Teflon finish may provide excellent protection against chemical attack far superior to previous finishes. The temperature limits of these finishes are ∿300°C. In the last 15 years, finish technology alone has thus extended glass fabric filtration from 230°C to ∿300°C and provided significant improvements in bag life for many applications. Depending on application area, fabric life may be extended by a factor of two or more. Major application areas for more advanced Teflon based finishes are in the carbon black and small boiler areas. Massive bag failure from acid conditions and dew point excursions have been considerably reduced.

Glass fabrics are somewhat limited in their ability to withstand mechanical abuse and they also tend to bleed when structure, finish, dust and gas properties create difficult filtration conditions. As an alternative to heavier bulked glass fabrics for these applications, a new product has been developed and applied. This product is a napped glass fabric which has a basic all-filament construction. The continuous filament construction provides strength which is sacrificed in bulked yarns and allows lighter weight fabrics to be used. The fabric is supplied with a basically Teflon finish and is currently being used at Pennsylvania Power and Light's Sunbury Station. This development is felt to be significant in the application of high temperature glass fabric filtration to areas where bleeding and seepage of dust is a problem.

Standard "E" glass fibers are normally used to manufacture glass fabrics for filtration. In ~1968 Owens-Corning developed an "S" glass for filtration fabrics.(5) This S glass was claimed to have superior high temperature mechanical properties over standard E glass. Owens also developed a proprietary inorganic finish which would supposedly protect these S glass fabrics at operating temperatures of up to ~540°C. Owens was apparently unable to develop a market for this technology in the filtration industry and in ~1972 the technology was offered to major glass fabric producers and finishers for further development.(6) No organization has been involved in significant development of this technology since that time.

The high temperature glass filtration market is extremely wary of new developments and relatively unwilling to extend itself. Newer glass fibers are available with good mechanical properties for filtration applications up to ~540°C. Current finish technology is only applicable up to ~300°C and is probably limited to that without a breakthrough into competitive inorganic finishes. The producers have shown a reluctance to gamble on adequate investment in research and development is this area. The most probable cause is that equipment limitations at around 400°C do not offer vast market increases for the extension of finish technology over 300°C.

Numerous applications of conventional high temperature baghouse technology with glass fabrics have been made to utility boilers of various sizes. Perhaps the most thoroughly studied and well documented large scale application was at Southern California Edison's Los Alamitos Station.(7) This application was on a 320 MW oil fired unit. A great number of fabrics were tested and many operating problems for power plant applications were evaluated. Perhaps the major problem area identified and studied was the effect of acid operating conditions on bag life. Bag life was extended from less than 3 months for major failures to over 6 months and more minor failures. The unit was operated with oil under a variance from the Los Angeles County Air Pollution Control District for a limited time but the baghouse was shut down when the variance expired and the boiler was converted to low sulfur fuel. A number of applications to smaller coal fired power plants in the 10 MW range are known(8) with the largest current application being Pennsylvania Power and Light's Sunbury Station with two 47 MW units. The Sunbury Station burns a high ash and silt coal which is dredged from a river and petroleum coke. The effluent gases are filtered at ∼260°C.

In general, it is felt that there is a reluctance to specify high temperature filtration for particulate control in power plants. The excellent performance of fabric filters on fine particulates is well known. Unfortunately there are major problems which restrict applications. Aside from the obvious problems of large size, limited previous application data and uncertain costs, there is the additional problem of government regulations and pending court case results. If scrubbers are ultimately to be required for gaseous emission control, a separate particulate control device may be unnecessary. The possibility of using a baghouse as a chemical contactor for SO_x control with additive injection(5,9) has never shown competitive reactant utilizations as compared to wet scrubbing techniques. A small amount of additive injection mainly to control SO_3 emissions and reduce plume visibility is feasible but overall SO_x control is not. In addition, the uncertainty over fuels makes specification of control equipment very difficult. If low sulfur-high ash coals become widely available for power plant usage and if gaseous emission control regulations are relaxed then there is a good possibility of more high temperature baghouse applications to power plants.

Mineral Fibers

The mineral fibers which appear to offer promise for high temperature filtration applications are SiO_2, which is just a very pure form of glass, aluminum silicate, boron nitride and a new needled mineral structure which is being marketed for 360°C filtration with surges to 400°C.(10)

Silicon dioxide (SiO_2) fibers are produced by acid leaching of glass fibers to produce a modified glass containing ~96% SiO_2 or up to 99% SiO_2 for special applications.(11) These high purity glass fibers generally have excellent thermal shock characteristics although the yarn and fabric structures produced have slightly lower tenacity than standard E glass structures. These high purity glasses have higher softening points and highter theoretical operating temperatures (~1100°C vs ~540°C for regular glass) although the limitation on applying these fibers and fabrics to filtration applications is the technology of the surface treatments and protective agents. Costs for such fibers, yarns and fabrics are still comparable with glass. The Owens-Corning S glass mentioned previously is probably a high SiO_2 glass. Other high SiO_2 products are available(12) but filtration applications are very limited. A plate or sheet form of acid leached glass is available which might be used as a high temperature filter although no application of this material is known. In summary, no significant market for high temperature filtration using SiO_2 fibers has developed although the fibers and fiber structures are available.

Aluminum Silicate

This material is commercially produced in bulk, yarn, woven and non-woven forms.(12) As with most inorganic materials, mechanical properties restrict utilization in many filtration applications. Typical bag type filters are thus probably a poor configuration with this material. Thermal stability is excellent with continuous duty ratings up to ~1260°C. Again, although the fiber and structures are available, no significant market for high temperature filtration using aluminum silicate fibers is known.

Boron Nitride

The status of born nitride fiber developments was summarized in a paper entitled High Temperature Fabric Filtration Synthetics by Dr. J. Economy.(13) Boron nitride fibers appear to possess very desirable properties for high temperature fabric filters. The fibers have a relatively low modulus of $3\text{-}5\times10^6$ and a diameter of $\sim5\mu m$ while glass fibers have a modulus of $\sim10\times10^6$ and diameters of $\sim5\mu m$. The cost of BN fabrics may be reduced as low as $\$3.6/M^2$. The fibers and structures are resistant to corrosive attack when filtering air at ~810°C, steam at 590°C, molten Al at 1050°C and iron at 1500°C. Unfortunately, the fibers and structures do not appear to be particularly effective in filtering submicron particulates. The extremely high present costs and the present limited market for filtration at optimum conditions for BN result in no known major applications.

Carbon or Graphite

At the present time carbon or graphite fiber technology is not being applied to filtration applications. Approximately five major companies have been involved in efforts to produce carbon and graphite fibers in commercial quantities for other than specialty applications (brake lining, pressure vessels). All major attempts to produce these carbon or graphite fibers in quantities which could support fabric filter applications have led to large economic losses. Present technology can produce these fibers for about $55 per kg. and a reasonable estimate for a minimum price which may be reached with a larger volume of production is $22 per kg. Production is presently on a batch basis for lots of less than 1 kg. Tensile properties and many other mechanical properties are excellent at room temperatures but suffer from the same poor long term time/temperature behavior as all known organics because of high temperature oxidative instability of the C-C bond. This probably limits even potential filtration applications in air to ∿320°C. The use of carbon or graphite fibers is not foreseen for any significant filtration application in the next ten years.

Teflon

The stability of Teflon to chemical attack is well known. The cost of Teflon yarns and fabrics is a major disadvantage in their application as is their reduced strength in air at elevated temperatures (over ~100°C). Teflon yarns cost roughly 50 dollars per kilogram and roughly 50% of the fiber strength is lost in air at 100°C.(3) Teflon fabrics are also susceptable to bleeding and leaking of dusts because of the extremely smooth, slick surface of the basic material. Despite these disadvantages, Teflon is almost irreplaceable in some applications. In one case, dust abrasion was destroying the lower meter or so of glass filter bags in a short time (1-2 months). Bags were constructed with Teflon fabric for the bottom end and glass for the majority of the bag. This novel solution increased bag life tremendously without the increase in cost for all Teflon bags. In general, Teflon fabrics are ideally suited for smaller applications in the 100-300°C range where chemical conditions and/or mechanical abrasion are severe. The most significant application of Teflon to high temperature filtration is of course in glass fabric finish technology mentioned previously.

Organic Fibers

Aerospace technology development efforts attempted to produce organic fibers with maximum temperature stability. These fibers and fabrics were developed mainly for flame resistant suits or brief exposure situations and not filtration applications. The sophisticated new aromatic heterocyclic polymer fibers and fabrics such as poly benzoxazole imide (PBI) all show poor time-temperature mechanical response at temperatures over ~250°C. Other high temperature organics such as poly (amide-imide) and pyrrone are known but have not been suggested for filtration usage mainly because of cost. The one commercially available organic fiber (excluding carbon and graphite) which is in high temperature (230°C maximum) filtration use is Nomex, a form of nylon with good high temperature properties. For the purposes of this paper we shall discuss Nomex only briefly since it falls on the extreme lower limits of what we have chosen to call "high temperature" filtration usage.

Nomex

The performance of Nomex does have a significant effect on the high temperature (+230°C) filtration market since its use is often cost effective when balancing fabric life, temperature and fabric cost. Nomex probably represents close to the upper limit in the application of an organic fiber to high temperature filtration. The high temperature oxidative instability of the carbon-carbon bond and the increased costs of the more sophisticated organic fibers probably limit their share of the market and the mechanical and thermal limitations of the materials to roughly the present state. Nomex is finding wide application in areas previously dominated by polyester and is replacing glass in many installations. The use of Nomex with gas cooling in place of glass may represent a trend in some areas of the market.

The use of Nomex in place of glass may improve both bag life and baghouse performance. More advanced cleaning techniques such as pulse jet cleaning are ideally suited to Nomex felts. This allows baghouse operation at face velocities of 4 cm/sec. versus ∿1 cm/sec. with glass without significant increases in pressure drop. In addition, cases are cited in advertizing literature in which bag life was increased by a factor of 14 when replacing glass bags filtering dust from a copper converter furnace at ∿180°C.

Current market estimates place Nomex fabric sales for filtration use at $\sim 7.5\times10^6$ M^2/yr. Based on this relatively large sales volume it can be seen that although Nomex is rarely used at temperatures in excess of 200°C it may still affect the high temperature (+230°C) filtration market considerably. In general Nomex costs from 2 to 20 times as much as glass, Nomex may be operated with filter face velocities of from 2 to 4 times those with glass, and if temperatures are reduced to the Nomex range, bag lives may increase by a factor of from 2 to 10 with Nomex over glass.

Metal Fibers

Before discussing the application of metal filaments to filtration, a new development in the production of metal filaments will be discussed. Normally, metal filaments which could be used in filter media are drawn using the same technology as is used in the production of wire. The fine filaments which are most suitable for either woven fabrics or fiber mats are too costly to make wide application of these materials to filtration feasible. Recent developments in the production of metal filaments involving filament production from a melt will possibly lead to reduced prices for fine metal filaments and thus expand applications to high temperature filtration.

There are a number of processes under development for producing metal filaments by methods other than drawing of a single strand. These include slinging the melt from a disc or drum, drawing bundles of wire, melt spinning and the Taylor wire method using encapsulation of the melt in a drawn glass tube. These developments are generally being persued for the tire cord and electrical conductor markets and are not directed towards fabric filtration. Unfortunately, the filtration market is best served by 5-50μ filaments while the tire cord and electrical conductor markets do not require filaments smaller than 150μ and 75μ respectively. Even so, if commercial production of metal filaments by new techniques does become a reality, cost versus filament diameter conditions may lead to cheaper fine metal filaments which may be suitable for high temperature filtration applications.

Attempts may be made to operate high temperature, high velocity filters with metallic needled felts using presently available technology and materials. These felts may be used at filtration velocities of up to ~27 cm/sec. In addition to high temperature and high velocity capabilities, these metallic felts have excellent anti-static properties when compared to other mediums. This indicates a potential market in any condition where static sparking and explosion may be a problem. Metallic filaments are generally oxidatively reactive at elevated temperatures in the +450°C range. Finer filaments are more susceptable to attack because of surface area considerations so there may be practical limitations on filament diameter in high temperature situations. It is generally felt that this type of medium would be well suited to cupola or blast furnace applications where limited space, high temperature surges and possible sparks limit the application of more conventional filtration devices. One manufacturer predicts ~1 year life at 425°C with a cost for a low density metallic felt of between $160 and $540 per square meter.(15) Presently trends are to use evaporative cooling with lower temperature (120°C) application of conventional felts.

Granular Bed Devices

A NAPCA (an EPA predecessor organization) contract report(16) attempted to summarize the state of the art of granular bed filtration devices in June of 1969. Conclusions at that time were:

1. Granular bed devices might be effective in both SO_2 and particulate control using alkalized alumina beds.
2. Cost estimates indicated these devices would be competitive with other SO_2 removal systems or with electrostatic precipitators if used for particulate control only.
3. None of the units studied had been tested to the extent necessary to prove mechanical reliability.
4. Reliable values of filtration efficiencies for granular beds cannot be predicted from theory.

The uncertainties in costs, mechanical reliability and particulate collection efficiencies were responsible for the lack of application of granular bed devices to high temperature filtration in the late 1960's.

Granular bed devices offer some great advantages over fabric mediums in that the granular medium itself is capable of operation at temperatures of up to 550°C without difficulty. Recent developments and applications of granular bed devices indicate significant advances in this technology. Improved designs have reduced costs, increased mechanical reliability and data is being collected on particulate collection efficiencies. It should be noted that government control specifications may make collection efficiencies critical. Better cost data than previous estimates which were merely projections or conjectural should be available in the near future.

Application of granular bed devices to clinker coolers, an iron cupola, a refractory furnace and a lime kiln is in progress.(17) These applications range in size from 1550 M^3/minute to 4225 M^3/minute. Temperatures of operation of up to 480°C are possible with mild steel construction but high temperature alloys would allow application at higher temperatures. The granular medium itself is a quartz gravel of from .1-.5 cm diameter.

Some details of a granular bed device applied to a lime kiln are available. The filter system consists of eight granular beds in parallel. Total gas rate to the filters is 1700 actual M^3/minute at 370°C. Power is required for eight 7-1/2 horsepower motors and a 300 horsepower blower. The pressure drop is expected to be 35-40 cm of water when the system is completed. The mean size of the collected particulate is roughly 11 m. The filtration system removes 68 kg/hour of particulate matter from a unit processing 13,600 kg/hour.

It is significant that the application of granular bed filters to cement, refractory and cupola installations is in progress. Cement and refractories represent a significant application area for glass fabric filtration in the 180-280°C range.* Extension of fabric filtration to cupola applications is limited, but definitely a promising area of development.

---

*The author's personal estimate is that roughly 20-25% of the high temperature glass fabric filtration market may be in the area of the non-metallic minerals industry.

Successful operation of granular bed devices will possibly affect the high temperature filtration market significantly over the next five to ten years.

Sintered Metal and Ceramic Filters

The major uses of sintered metal and ceramic filters in high temperature filtration applications appear to be in catalyst recovery operations. These catalyst recovery operations are normally found in the chemical industry. Petroleum refining catalysts are generally cheaper, do not lend themselves to filtration by a solid porous medium and are used in systems where air entrainment is limited. A variety of materials and physical configurations are in use and are felt to represent an autonomous area of high temperature filtration technology.

REFERENCES

1. Handbook of Fabric Filter Technology, Dr. C. Billings and Dr. J. Wilder. Vols. 1-4, Final Report on Contract No. CPA 22-69-38, December 1970. National Technical Information Service # PB 200-648.

2. P. W. Spaite, D. G. Stephan and A. H. Rose, Jr., High Temperature Fabric Filtration of Industrial Gases, Journal of The Air Pollution Control Association, Vol. 11, No. 5, May 1961.

3. Industrial fibers profile, Fabric Research Laboratories, Inc.

4. Arthur D. Little, Inc., High Temperature Bag Filter Development, USDHEW Public Health Service. TR A61034, Taft Sanitary Engineering Center, Cincinnati, Ohio 1961.

5. Owens-Corning, Feasibility of Fabric Filter as Gas-Solid Contactor to Control Gaseous Pollutants, Final Report on Contract No. PH 22-68-64, August 1970, National Technical Information Service # PB 195-884.

6. Private Communication

7. F. A. Bagwell, L. F. Cox, and E. A. Pirsh, Design and Operating Experience with a Filterhouse Installed on an Oil-Fired Boiler, Presented to the Air Pollution Control Association, St. Paul, Minnesota, June 1968.

8. J. Turner, In-House report, Status of Fabric Filter Systems on Small Power Plants, Particulate and Chemical Processes Branch, Control Systems Laboratory, EPA, September 1973.

9. Air Preheater, Evaluation of Fabric Filter as Chemical Contactor for Control of SO_2 from Flue Gas, Final Report on Contract No. PH 22-68-21, December 1969. National Technical Information Service # PB 194-196.

10. Development reported at Air Pollution Control Association meeting, Buffalo, N. Y., October 15, 1973. No other details available.

11. R. Caroselli, High Temperature Characteristics of Inorganic Fibers, Annals New York Academy of Sciences.

12. A. A. Dunbeck, Guidebook to Man-Made Textile Fibers and Yarns of the World, 3rd ed., The United Piece Dye Works, New York, 1969.

13. J. Economy, High Temperature Fabric Filtration Synthetics, presented at Fabric Filter Symposium, Charleston, S. C. 3/16-18/71.

14. W. R. Jones, Jr., W. F. Hady and R. L. Johnson, Friction and Wear of Poly (Amide-Imide), Polyimide and Pyrrone Polymers At 260°C In Dry Air, NASA Technical Note, NASA TN D-6353, May 1971.

15. Private communication.

16. Avco Applied Technology Division, Evaluation of Granular Bed Devices, Final Report on Contract No. PH-86-67-51, June 1969, National Technical Information Service # PB 185-561.

17. R. Rovang, Trip Report, Engineering Services Branch, Emission Standards and Engineering Division, EPA, January 1973.

SESSION 5

ADVANCES IN APPLICATIONS

Chairman: Harold L. Falkenberry
Tennessee Valley Authority
Chattanooga, Tennessee

Paper No.

19 Atomization and Cloud Behavior in Wet Scrubbers

Howard E. Hesketh
Southern Illinois University
Carbondale, Illinois

20 Removal of Carbon Black from Industrial Gases

Valery P. Kurkin
State Research Institute of
Industrial and Sanitary Gas Cleaning
Moscow
U.S.S.R.

21 The Application of Wet Electrostatic Precipitators for Control of Fine Particulate Matter

Even Bakke
United States Filter Corporation
Summit, New Jersey

22 The Influence of Ash Chemistry on the Volume Conduction in Fly Ash

Roy E. Bickelhaupt
Southern Research Institute
Birmingham, Alabama

Paper No. 19

ATOMIZATION AND CLOUD BEHAVIOR IN WET SCRUBBERS

by

Howard E. Hesketh
SOUTHERN ILLINOIS UNIVERSITY
Carbondale, Illinois

Preceding page blank

ABSTRACT

The distinction between cloud and drop type atomization and theories to show why these systems can exist are presented. The methods under which each are produced in pneumatic two fluid atomizing scrubbers are discussed in relation to fine particle capture and air pollution control using wet scrubbers.

Experimental particle collection efficiencies related to type of atomization, liquid to gas ratio, liquid injection location, pressure drop and surface tension of scrubbant are included for laboratory and commercial scrubbers and compared with some theoretical efficiency expressions.

These data and the incorporation of diffusiophoresis, Stephan flow and thermophoresis could help make atomizing scrubbers more economical for fine particle control.

NOMENCLATURE FOR TERMS NOT OTHERWISE DEFINED

ACFM = actual cubic feet per minute of gas

C_o/C_i = ratio of concentration out to concentration in by weight

ΔP = pressure drop across Venturi, inches water

E = collection efficiency fraction by weight

exp = signifies e (natural log base) to the exponent indicated by the quantity in brackets after exp

fps = feet per second

gr = grain, 1/7000 of a pound

ID = inside diameter

L = liquid to gas ratio, gal/1000 SCFM

scfd = standard cubic feet of dry gas

scfm = standard cubic feet per minute at 70°F and 1 atmosphere

μ = microns or micro meters

$\bar{X}_{vs}$ = Sauter mean drop diameter in microns, the ratio of volume mean diameter cubed to surface area mean diameter squared

CONVERSION FACTORS

English to Metric Units

1scfm = 1.6 Nm^3/hr

1 gpm = 0.227 m^3/hr

1 ft^3 = 0.0283 m^3

1 gal = 3.785 ℓ

1 gal/1000 ft^3 = 0.134 ℓ/m^3

1 grain/ft^3 = 2.29 g/m^3

1 ft/sec = 0.3048 m/sec

1 in = 2.54 cm

1 pound = 454 grams

INTRODUCTION

It has been established (1) that pneumatic atomization can result in the production of either drop-type or cloud-type droplets. Drop-type atomization occurs when the scrubbing liquid is introduced into the atomizer as drops or sheets and the size of the resulting droplets can be predicted by the Nukiyama-Tanasawa equation (2) which has been presented by Calvert (3) for air-water systems near standard conditions of temperature and pressure:

$$\bar{X}_{vs} = \frac{16,400}{v} + 1.45\ (L)^{1.5} \qquad [1]$$

where v is the gas velocity in ft/sec.

The droplets formed by cloud-type atomization are much smaller than those formed by drop-type atomization and appear to have diameters of less than 10μ. In addition, these extremely small droplets bond together without coalescing and the clouds which result can be treated as a single system in a manner similar to the way atmospheric clouds are considered. This cloud behavior has been observed using glass-sided 600 cfm laboratory and 1500 cfm pilot plant atomizing fixed throat venturi scrubbers. The behavior in the laboratory wet scrubbers were also observed using stop-action open-shutter photographic techniques which provided a viewing time of 0.5 μsec and a 100 fold magnification (4).

Photographic stop-action inspection of the pneumatic atomization shows that essentially no atomization occurs when the velocity difference between the two fluid streams is less than 88 ft/sec. At velocity differences of about 120 ft/sec, a marked improvement occurs and, by the time the difference is 150 ft/sec, the liquid is essentially completely atomized.

If the liquid to be atomized is introduced into the gas stream from nozzles approximately 1 mm ID or larger, cloud-type atomization results. An equation has been developed for this (4) to indicate what minimum or critical differential velocity in ft/sec should be considered when the liquid is introduced through nozzles larger than 1 mm ID:

$$v_{min} = 1.7 \left[\left(\frac{8500}{d'} \right)^{1/2} + 15.3 \right] \qquad [2]$$

where d' is nozzle ID in mm.

EXPLANATION FOR EXISTENCE OF CLOUD-TYPE ATOMIZATION

The existence of cloud-type atomization can be resolved recognizing that pneumatic atomization is work required to break up the liquid fluid. The atomization work is required to overcome surface tension only as Lane (5) shows that viscous forces can be neglected except when viscosity is "very great". A stream of liquid such as water requires much less work to break it up than the same volume of water in the form of drops because the stream has a lower overall surface to volume ratio.

In one of the venturis studied, streams are 1.6 mm in diameter and at any moment of time have a length of 8.4 mm. The surface work holding the stream together is:

$$W_s = T\,A \qquad [3]$$

where: W_s = surface work, erg

T = surface tension, erg/cm^2

A = surface area, cm^2

Scrubbers that use spray nozzles often introduce the liquid as 0.5 mm diameter drops which are then pneumatically atomized. It would take 257 of these drops to produce the same volume as the stream. The surface area of these drops is 4.8 that of the stream, so atomization work for cloud-type atomization is 4.8 times less in this example. Atomization type in other scrubber arrangements could be appropriately accounted for.

EVIDENCE OF CLOUD-TYPE ATOMIZATION

Cloud Effective Diameter

One emperical study was performed (4) using a 600 cfm venturi to evaluate the effective diameters resulting from cloud-type atomization. In this study, emperical size, acceleration and drag data are used to relate cloud size and cloud drop Reynolds number (Re). These data were used with the equations:

$$Re = \frac{(v_a - v_p)\ \rho_a d_e}{\mu_a} \qquad [4]$$

$$C_o = \frac{4\rho_\ell a d_e}{3\rho_a (v_a - v_p)^2} \qquad [5]$$

where: C_o = coefficient of drag

d_e = effective diameter of the atomized cloud

ρ_a = density of the air

ρ_ℓ = density of the liquid

a = acceleration of the droplet clouds

$(v_a - v_p)$ = velocity difference between gas and clouds at point where a is determined

μ_a = viscosity of air

This work can be summarized by Figure 1 which shows that after the onset of complete atomization at a velocity difference of about 150 ft/sec, the cloud effective diameter increases with velocity difference. Note that the effective cloud diameter becomes very large compared with droplet size.

Diffusivity and Mass Distribution of Atomized Droplets

The series of studies by Behie and Beeckmans (6) produced data which

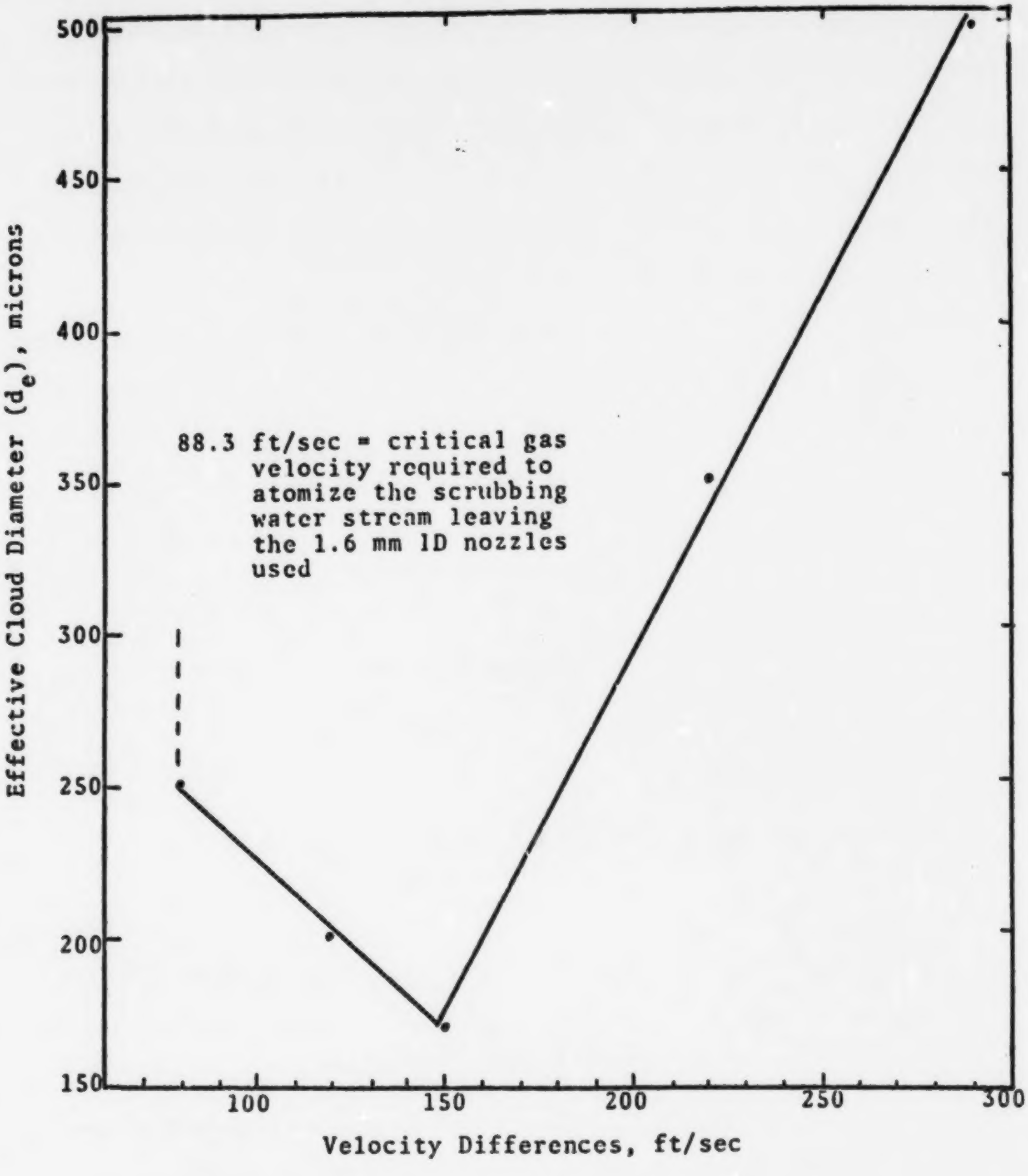

Figure 1: Effective diameter of atomized clouds for various Venturi throat velocities

"strongly supported the concepts of drop-type and cloud-type atomization...." However, they suggest that the apparent cloud dimensions might even be considerably larger, perhaps 1 or 2 cm. Their study evaluated nozzles larger and smaller than 1 mm at velocities up to 157 ft/sec. This study envisions the sluggish behavior of the micro droplets as the result of momentum diffusion resistance from the periphery of the jet.

The Behie studies show by diffusivity measurements that under cloud-type atomization conditions, the droplets are always small enough to follow the turbulent air fluctuations. They noted that the mass diffusion of cloud-type droplets in the plane perpendicular to gas flow was uniform in all directions and was Gaussian. Using the Ingebo (7) drag equation:

$$C_D = 27 \ \mathrm{Re}^{-0.84} \qquad [6]$$

and momentum transport equations, they obtained the following equation for droplet diffusivity D in a pneumatic atomization scrubber:

$$D = \sigma_z^2/2t \qquad [7]$$

where: σ_z^2 = variance in the plane perpendicular to gas flow
t = time

Under drop-type atomization conditions, the larger droplets formed had too much inertia and did not follow the turbulent air fluctuations resulting in low diffusivities, D_z, in the z direction (horizontal) and higher diffusivity, D_y in the y direction (vertical). These studies show that at low liquid to gas ratios, full eddy diffusivity of the air is related to the water to air concentration flux ratio.

Venturi Pressure Drop

A complete pressure drop vs. venturi throat gas velocity curve is given in Figure 2 for a 1500 cfm pilot plant scrubbing coal fly ash. Note that the point of inflection on this curve occurs at essentially the same velocity that results in complete atomization as shown in Figure 1. Utilization of available energy in atomization is poor (0.53% reported by Marshall (8) for drop-type atomization and 6.1% calculated for cloud-type atomization), but during the plateau shown on the curve in Figure 2, energy is being utilized to complete the atomization. On either side of this region, an increase in energy goes into creating system turbulence which is recorded as increased pressure drop. This 1500 cfm system is a fixed throat venturi and was operated so as to produce cloud-type atomization. The data are for before the throat injection of the scrubbing water.

FIGURE 2

VENTURI SCRUBBING OF COAL FLY ASH AFTER ELECTROSTATIC PRECIPITATOR

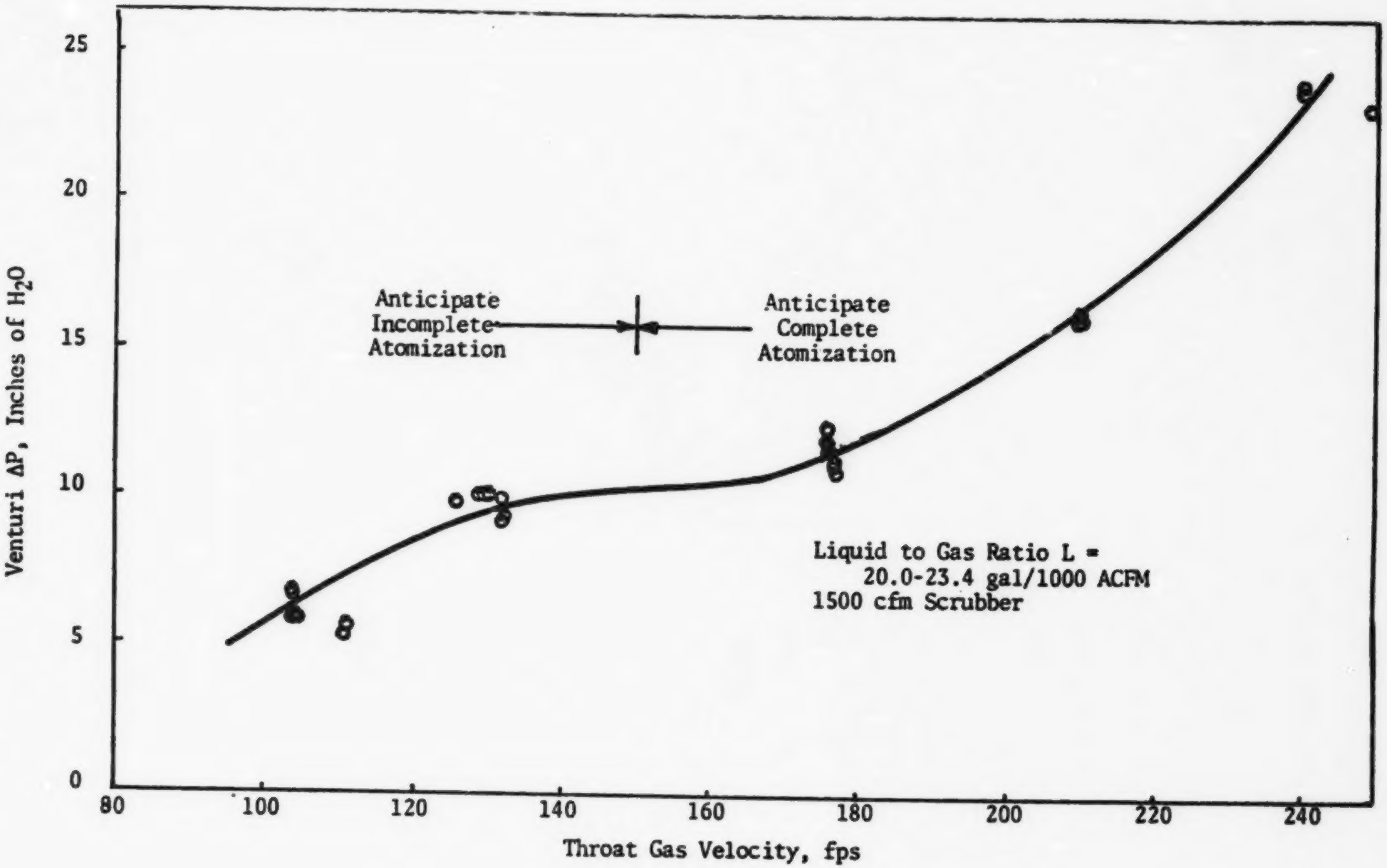

PARTICLE COLLECTION EFFICIENCY

It is recognized that wet scrubbers collect particles mainly by inertial impaction although smaller particles are also removed by diffusional mechanisms including diffusiophoresis, Stephan flow and thermophoresis. Systems are being installed by this investigator to obtain diffusional data, but at this time, the only significant data are related mainly to inertial impaction and the direct eddy diffusion aid to particle capture resulting when operating in the cloud-type atomization regime.

Collection Efficiency Equations

Many equations have been developed to predict particle capture. Calvert (3) presents data which for a venturi scrubber operating with a throat velocity of 200 ft/sec can be approximated as:

$$(1 - E) = C_o/C_i = 7.7 \exp(-0.656\ L) \qquad [8]$$

where: E = overall collection efficiency fraction by wt.

C_o = concentration of particulate matter into scrubber

C_i = concentration of particulate matter out of scrubber

L = liquid to gas ratio, gal/1000 ACFM

A series of tests on our 600 cfm laboratory venturi using coal fly ash with a mean diameter d_{50} of 9.1 and a standard deviation σ of 2.33 produced data that results in the equation:

$$(1 - E) = C_o/C_i = 8.3 \times 10^{-3} \exp(-0.220\ L) \qquad [9]$$

Equations 8 and 9 are the top two solid curves of Figure 3. Note that the data points used for the equations are indicated so do not extrapolate these lines.

FIGURE 3

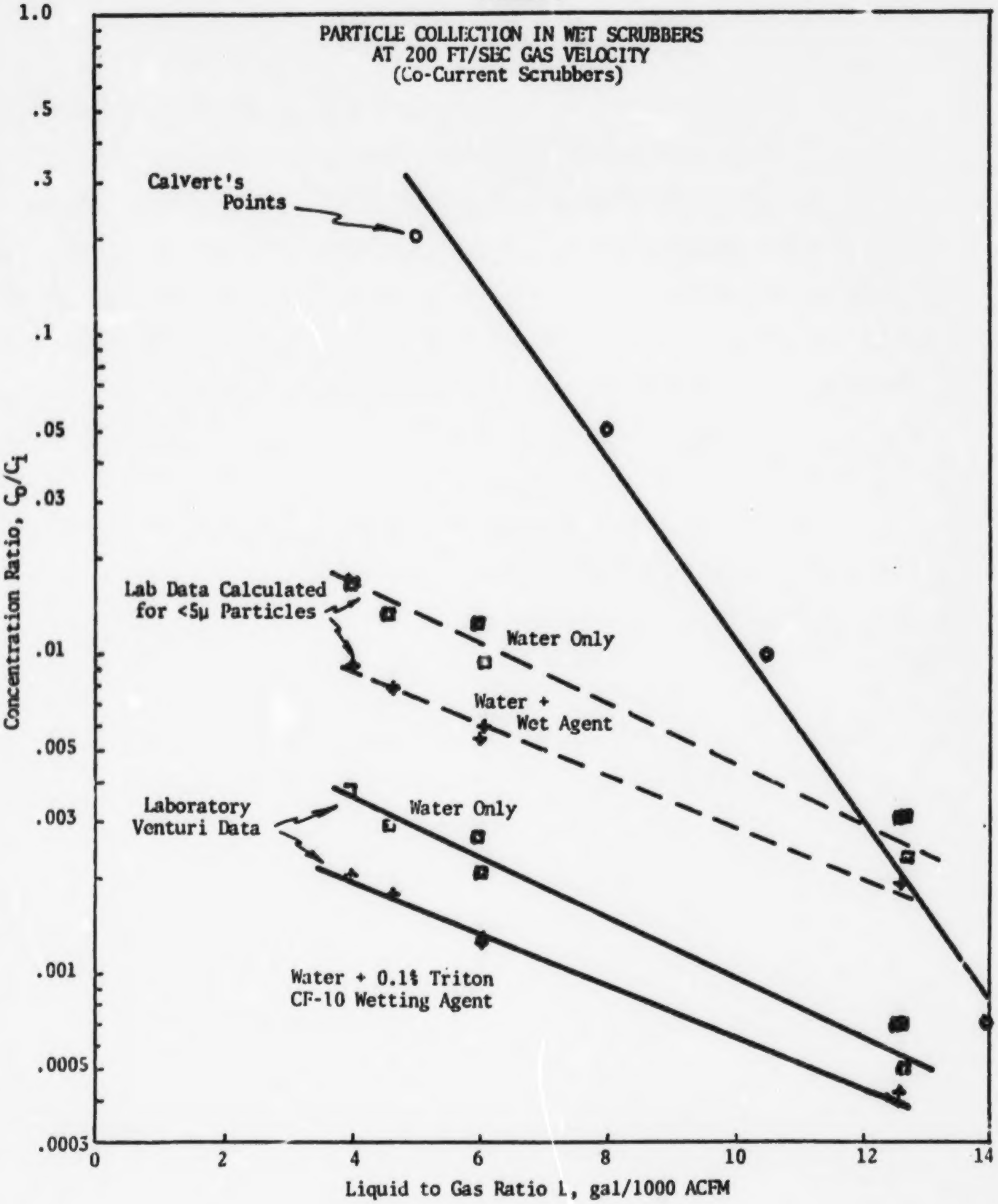
PARTICLE COLLECTION IN WET SCRUBBERS
AT 200 FT/SEC GAS VELOCITY
(Co-Current Scrubbers)
Calvert's Points
Lab Data Calculated for <5μ Particles
Water Only
Water + Wet Agent
Laboratory Venturi Data
Water Only
Water + 0.1% Triton CF-10 Wetting Agent
Concentration Ratio, C_o/C_i
Liquid to Gas Ratio L, gal/1000 ACFM
1.0
.5
.3
.1
.05
.03
.01
.005
.003
.001
.0005
.0003
0
2
4
6
8
10
12
14

Use of Wetting Agents in Scrubbers

Wetting agents or surfactants reduce the surface tension of the liquid and if properly used improve particle collection by not only making the atomization occur more easily but also by enhancing particle wettability. Several non-ionic, low foaming surfactants were studied and the optimum results were obtained using 0.1% by weight Rohm and Haus Triton CF-10 which reduced the water surface tension to about 10 dyne/cm at room temperature.

These data points are presented as the 3rd solid line in Figure 3 and the resulting equation is:

$$(1 - E) = C_o/C_i = 4.2 \times 10^{-3} \exp(-0.188\ L) \qquad [10]$$

Note that use of this wetting agent decreased outlet dust loadings by about 50% in these studies. Outlet dust loadings ranged from 0.001 to 0.0093 grains/ft^3 and inlet dust was 2.5 grains/ft^3.

Fine Particle Collection Equations

Enough data were available from this laboratory study to make it possible to express the results on the basis of less than 5 micron particles. On this basis, the fly ash into the scrubber would have a d_{50} of 3.1 and a σ of 1.55 and would amount to a concentration of 0.55 grains/ft^3. Assuming no particles greater than 5 microns passes through the scrubber, the measured outlet loadings can be used to establish a new ratio of C_o/C_i. These are plotted as the dashed lines in Figure 3 for the water and water with wetting agent runs.

Replotting these calculated points on log-log coordinates, as shown in Figure 4, not only fits our data better, but it also gives the relation needed to extrapolate these data. The resultant equations for collection

FIGURE 4

COLLECTION OF FINE PARTICLES (Less Than 5 Micron in Diameter)
USING A VENTURI SCRUBBER AT 200 FT/SEC

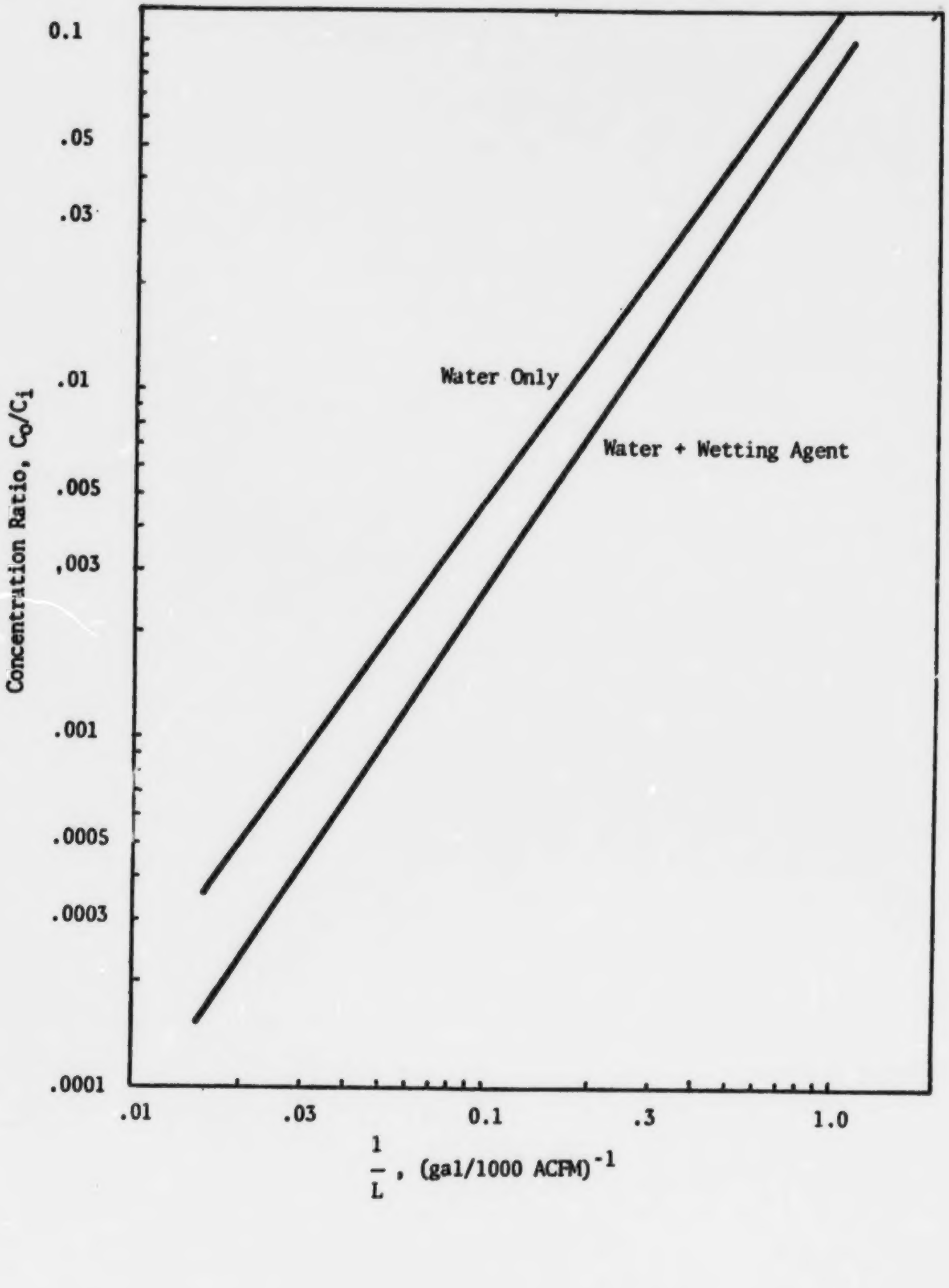

of less than 5 micron particles are:

$$(1 - E) = C_o/C_i = 0.115\ L^{-1.39} \quad \text{(for water)} \qquad [11]$$

$$(1 - E) = C_o/C_i = 0.084\ L^{-1.51} \quad \text{(for water + wetting agent)} \qquad [12]$$

Pressure Drop and Collection Efficiency

Pressure drop across a commercial scrubber is a much easier parameter to measure than liquid to gas ratio, so it would be beneficial to establish such a relationship. In turn, this could be used to relate collection efficiency if the scrubber is operated at non-scaling and non-plugging conditions—otherwise, one should stay with the equations using liquid to gas ratios as already given.

Pressure drop data were obtained from many fixed throat venturi scrubbers and it is observed that pressure drop (ΔP) is a function of throat gas velocity, throat cross-section area, gas density and liquid to gas ratio. In correlating data from systems including 600 cubic feet per minute (cfm) laboratory units, 1500 cfm pilot plant systems and commercial facilities as large as 300,000 cfm capacities the following equations were derived:

$$\Delta P = \frac{v_t^2\ \rho_g\ A^{0.133}}{507}\left(0.56 + 0.125\ L + 2.3 \times 10^{-3} L^2\right) \qquad [13]$$

$$\Delta P \cong \frac{v_t^2\ \rho_g\ A^{0.133}\ L^{0.78}}{1270} \qquad [14]$$

where: ΔP = venturi pressure drop, inches water gauge

L = liquid to gas ratio, gal/1000 ACFM

ρ_g = gas density downstream from venturi throat, lb/ft^3

v_t = throat velocity of gas, ft/sec

A = throat cross-section area, ft^2

Equation [13] is a more exact expression and a family of curves for a 1500 cfm scrubber ($A = 0.125\ ft^2$) calculated for various L are shown in Figure 5 along with the full curve from Figure 2. Equation [14] is an approximation but gives a more convenient relation between ΔP and L.

The data used for Equations [13] and [14] were obtained from units operated so as to produce cloud-type atomization and are for venturi scrubbers that have liquid injected before the throat. When the same amount of liquid is injected at the throat, data available so far indicate that the ΔP is somewhat higher (up to 10%).

Equation [14] combined with Equations [11] and [12] provide expressions for predicting collection efficiencies as a function of pressure drop in non-plugging venturi scrubbers for fine particles less than 5 microns in diameter at throat velocities of approximately 200 ft/sec:

$$(1 - E) \cong C_o/C_i = 53.7\ A^{0.145} \left(\frac{\rho_g}{\Delta P}\right)^{1.78} \quad \text{(for water)} \quad [15]$$

$$(1 - E) \cong C_o/C_i = 67.6\ A^{0.157} \left(\frac{\rho_g}{\Delta P}\right)^{1.93} \quad \text{(for water + wetting agent)} \quad [16]$$

FIGURE 5

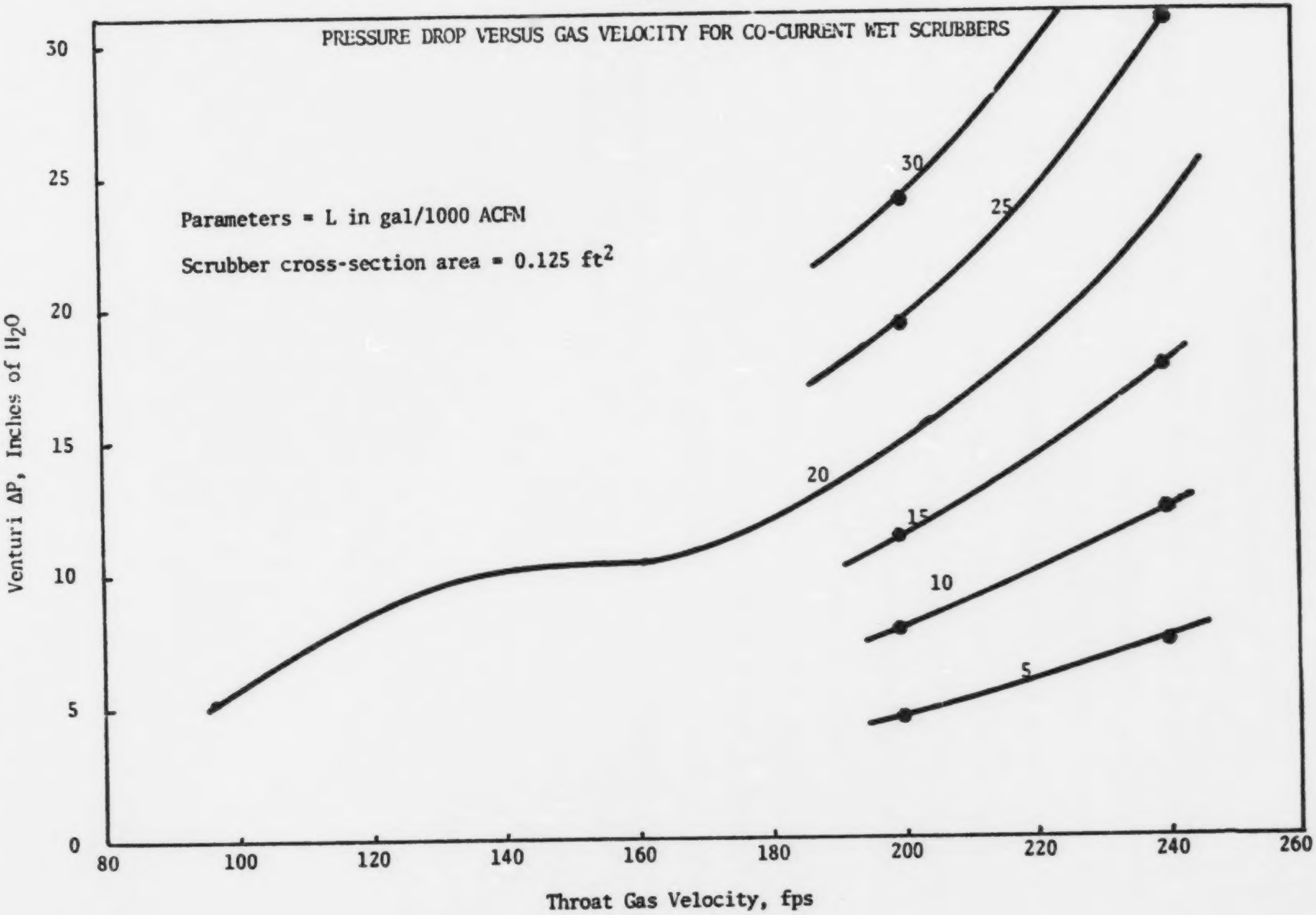

PRESSURE DROP VERSUS GAS VELOCITY FOR CO-CURRENT WET SCRUBBERS

Parameters = L in gal/1000 ACFM

Scrubber cross-section area = 0.125 ft^2

SUMMARY AND CONCLUSIONS

The presence of cloud-type atomization is shown by venturi scrubber drag correlation, by droplet mass diffusion in a pneumatic atomizer and by the presence of an inflection in venturi pressure drop vs. throat gas velocity. Particle scrubbers are normally operated at velocities of 150 ft/sec or greater, and if the liquid is introduced as a stream (i.e. spray nozzles, etc., are not used), the scrubber is probably operating in the cloud-type atomization regime.

Under these conditions, Equations [15] and [16] have been developed to relate collection efficiency for <5 micron particles and pressure drop for non-plugging venturi scrubbers at gas velocities of 200 ft/sec. Preliminary data, as shown in Figure 6, imply that collection efficiency is a function of pressure drop which needs only to be properly expressed as a function of gas velocity. If this is true, these collection efficiency equations would be:

$$(1 - E) = C_o/C_i \cong 3.45 \times 10^{-7} v_t^{3.56} A^{0.145} \left(\frac{\rho_g}{\Delta P}\right)^{1.78} \qquad [17]$$

(for water)

$$(1 - E) = C_o/C_i \cong 8.42 \times 10^{-8} v_t^{3.87} A^{0.157} \left(\frac{\rho_g}{\Delta P}\right)^{1.93} \qquad [18]$$

(for water + wetting agent)

FIGURE 6

FINE PARTICLE EMISSIONS OF <2 MICRON FLY ASH
FROM A 1500 CFM VENTURI SCRUBBER

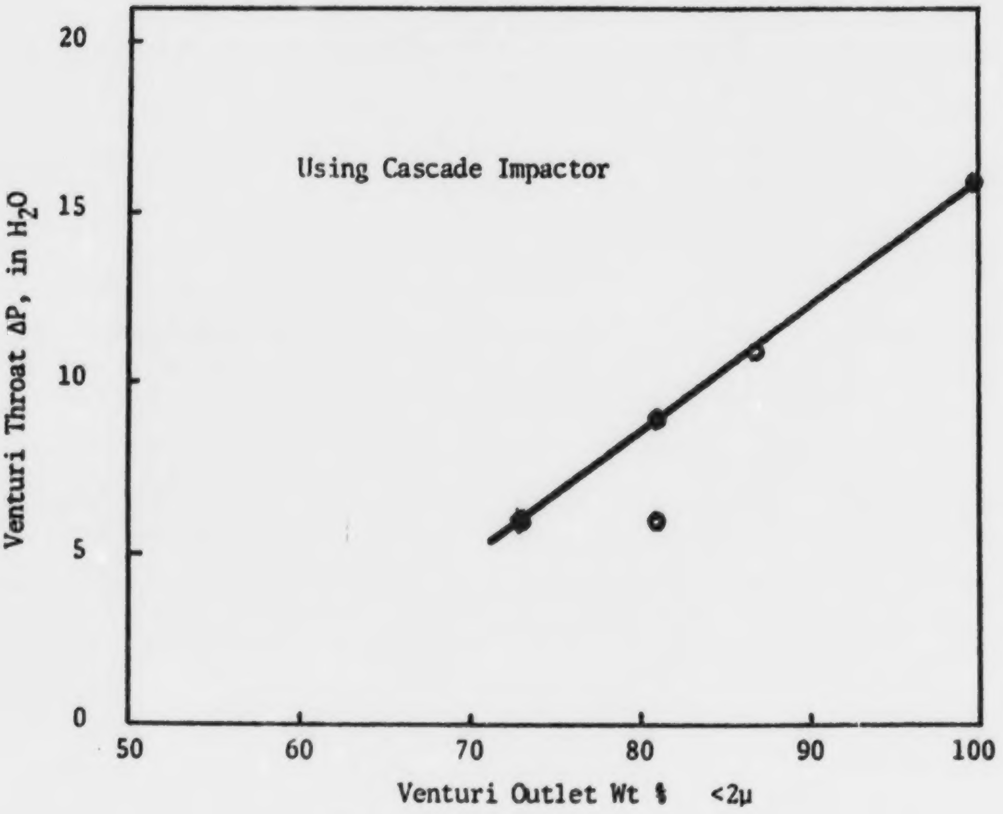

Conditions:

Outlet Dust Range Total =
0.0015-0.007 gr/scfd
Dust in Range =
0.032-0.42 gr/scfd
Efficiency Collection Range =
72-99.1%
L Range =
20.0-23.4 gal/1000 ACFM
Throat Velocity Range =
104-249 ft/sec

REFERENCES

(1) Hesketh, H.E., A.J. Engel and S. Calvert, "Atomization - A New Type for Better Gas Scrubbing", Atmospheric Environment, Vol. 4, No. 6, p 639 (1970).

(2) Nukiyama, S. and Y. Tanasawa, "An Experiment on the Atomization of Liquid by Means of an Air Stream", Trans. Soc. Mech. Engrg. (Japan), Vol. 4, p 86 (1938).

(3) Calvert, S., "Venturi and Other ATomizing Scrubbers Efficiency and Pressure Drop", Air Pollution (ed. by A.C. Stern), 2nd Ed., Vol. III, Ch. 46, Academic Press, NY (1968).

(4) Hesketh, H.E., "Atomization and Cloud Behavior in Venturi Scrubbing", JAPCA, Vol. 23, No. 7, p 600 (1973).

(5) Lane, W.R., "Shatter of Drops in Streams of Air", I&EC, Vol. 43, No. 6, p 1312 (1951).

(6) Behie, S.W. and J.M. Beeckmans, "Trajectory and Dispersion of Transverse Jets of Water in a Turbulent Air Stream", prepared for AIChE meeting, Tulsa, March 1974.

(7) Ingebo, R.D., NASA Tech. Note 3762 (1956).

(8) Marshall, W.R., Jr., "Atomization and Spray Drying", Chem. Eng. Progress Monograph Series, No. 2, Vol. 50 (1954).

(9) Bughdadi, S.M., "Effects of Surfactants on Venturi Scrubber Particle Collection Efficiency", M.S. Thesis, Southern Illinois University at Carbondale, School of Engineering and Technology, Carbondale, Ill. (March 1974).

Paper No. 20

REMOVAL OF CARBON BLACK FROM INDUSTRIAL GASES

by

Valery P. Kurkin

STATE RESEARCH INSTITUTE
OF INDUSTRIAL AND SANITARY GAS CLEANING

Moscow

REMOVAL OF CARBON BLACK FROM INDUSTRIAL GASES

by

V. P. Kurki

The removal of carbon black or soot from industrial gases has become very important. The development of such industries as tire production, printing and publishing, and the production of paint and varnish, demands an increased output of various industrial carbon blacks.

Industrial carbon black as the end product of the operation in which it produced must be removed from the gas and black mixture issuing from the soot burner. Also the effluent gases from carbon black production must be cleaned in order to prevent air pollution.

Carbon black is one of the most highly dispersed materials and its removal from the gas is quite difficult. Modern plants are equipped with various systems for removal of the black, which comprise devices for conditioning and cooling of the mixture of gas and black, removal of the black, and purification of the gas.

The removal of carbon black from gases is also important in acetylene production based on electric cracking of methane and in the thermal oxidative pyrolysis of methane. In recovering the final product--acetylene--from the gases, prior thorough filtering of the gases is required. Acetylene is used as the raw material in the synthesis of many products.

The output gases from the gasification of oil that are used as fuel in gas turbines and gas furnaces on steam boilers require prior removal of soot and ash.

The basic types of carbon black used in Soviet industry are: channel black, gas-furnace black, oil-furnace black, lampblack, semi-active and active carbon blacks (from liquid raw materials), and anthracene black (from mixtures of coal and coke-oven gases). They are classified according to the relative surface areas of their particles. Soviet active carbon blacks TM-70 and MT-100 have foreign counterparts HAF, ISAF, and CFR; TM-50 semi-active carbon black, oil-furnace black, and gas-furnace black are similar to FEF and GPF; and channel black is similar to CR.

I. Recovery of Lampblack and Oil-based Furnace Blacks

Lampblack and oil-based furnace blacks are produced by the injection of liquid raw materials into furnaces and their combustion. SG-type electrofilters are used for recovery of lampblack and oil-based furnace blacks after the mixture of gas and black is cooled in a scrubbing tower to a temperature of 180-230°C. Water evaporation not only lowers the temperature but also improves the collection efficiency of the electrofilter and reduces the risk of explosion.

Higher temperatures are undesirable because they lower the electrical resistance of the inter-electrode space and increase the danger of fire, which can deform the internal metal construction.

At lower temperatures, the carbon black is deposited on the electrodes along with moisture which leads to corrosion. SG-type electrofilters have a collection efficiency of up to 98-99% when the gas velocity does not exceed 0.5 - 0.6 m/sec.

The "dry" method of carbon black recovery consists of using cyclones and a filter of glass fiber fabric as bags or sleeves; all such installations operate under positive pressure up to 70 mm in the cyclones and up to 250 mm in the bags. Gases from a water spray cooler flow through 4 consecutively mounted cyclones of large diameter. The filter bags are sectioned and their regeneration takes place sequentially by blowing the purified gas back through them. Regeneration of the filter fabric requires 12,000-14,000 m^3/hr. of gas. The unit load of the filter fabric corresponds to a direct gas flow of about 0.35 m^3/m^2 min. The exit residual dust load is about 100 mg/m^3.

II. Removal of Carbon Black from Industrial Gases

1. Removal of carbon black from gas emitted from the decomposition of hydrocarbons in arc furnaces. This involves the following operations. First, the cracked gas goes to 3 cyclones (each 1200 mm in diameter) set in sequence and then to a common cyclone which represents the final stage of the dry part of the collection system. Each bunker has a steam jacket to heat the walls in order to prevent water vapor and organic compounds from condensing on them and thus to prevent the carbon black from adhering to the walls.

The residual content of carbon black after 4 cyclone stages is 4 g/m^3; thus the collection efficiency (filtration index) of dry filtration is about 78%.

The gas flows from the cyclones to a drain-type device with 3 trays, in which it undergoes additional filtering (to 50-100 mg/m^3). A very high index of filtration is obtained by condensation of steam, by which the black is washed out of the gas. Water is injected into the gas flue at the front end of the apparatus in order to prevent clogging of grids or spray nozzles by substances inclined to polymerization. The temperature of the gas is reduced to about 100°C, and it is preliminarily washed to remove polymerizing substances.

The final filtering of the gas to 1-5 mg/m^3 takes place in a turbulent washer with a gas velocity in the throat of the pipe of up to 110-120 m/sec and 100 mm water pressure differential.

2. Removal of carbon black in the thermal-oxidative pyrolysis of methane. In the production of acetylene by the thermal oxidative pyrolysis of methane, carbon black is a by-product. It is formed by the decomposition of acetylene.

Pyrolysis gases from the reactor are piped to a scrubber, where they are cooled from 90°C to 60°C, and then to an electrofilter where they undergo final cleaning. The input temperature of an SPM-8 electrofilter is kept constant automatically by varying the volume of water sent to the scrubber.

Partial removal of the black and resins takes place in the scrubber simultaneously. The cooled gases go to electrofilters for final purification. The SPM-8 electrofilter is a vertical steel single-section device of rectangular form. The gases are moistened and the carbon black, together with the resins, is removed by spray from fine injection nozzles located in the top of the electrofilter. Continuous water spray is under a pressure of 6 atm. A rotatable system fitted with sprayer nozzles can be placed in the lower part of the electrofilter in order to provide periodic washing (once in 8-10 days).

The content of carbon black in the gases coming from the electrofilter does not exceed 6 mg/m^3 and therefore the pyrolysis gases can be used industrially.

3. Removal of carbon black from synthesis gas from steam-oxygen gasification of residual oil (mazut) without pressure. The product of this process is the most effective raw material for production of ammonia, alcohol, and other organic chemicals. Since carbon black contaminates expensive catalysts, it must be removed from the gas before use. The carbon black content must not exceed 3-20 mg/m^3. The simplest way of filtering synthesis gas is the following: the output gas goes from the gas generator through a flue with a water-cooled jacket to a heat exchanger and to an air cooler, in which its temperature is lowered to 350-500°C and the black content is decreased to 1-5 mg/m^3.

From the air cooler the gas flows to the final filtering system, which consists of a spray apparatus and a venturi scrubber; in this system, the gas is cooled to 45-60°C and the final level of black content is achieved, i.e., less than 5 mg/m^3.

4. Thorough removal of carbon black from synthesis gas from oxygen gasification of residual oil under 15 atm pressure. Synthesis gas as produced by partial combustion and gasification of residual oil contains 6 g/m^3 of carbon black. The gas at 300°C flows from the exhaust-heat boiler to a cooler through which is dripped oil at 90°C, where the temperature of the gas is reduced to 140°C, and then the gas flows through two venturi tubes in sequence via an intermediate connecting separator and a scrubber with a spray of oil heated to 90°C.

The residual black (1-1.5 mg/m^3, maximum 3.5 mg/m^3) is collected in a venturi tube with a cold water spray. Light oil vapor is also condensed, together with water vapor. The oil is cooled in pipe water coolers during its circulation. The residual black content can be reduced to 1 mg/m^3. The scrubbing oil, which absorbs practically all the black, is burned in the boiler.

III. The Outlook for Scientific Research on the Collection of Carbon Black

Problems of collecting carbon black are pressing because of the continued growth in production of highly dispersed active carbon blacks.

Gas-cleaning equipment of the bag-filter type is being designed. The construction of such bag filters must satisfy the following requirements: it must have a large throughput capacity (100,000 m^3/hr) and high filtering efficiency; the dimensions of the equipment must fit the conditions of modern carbon black production; and the operating temperature of the equipment must be 350-400°C.

The problems of energy-technological uses of high-sulfur residual oil can be solved by gasification. From this point of view, high-temperature filtering of synthesis gas and its subsequent industrial use seem to be the most expedient.

The collection of carbon black in residual oil gasification is complicated by the pressure of the gas; filtration appears to be the most promising method of solving the problem.

The large amount of carbon black collected and its activity makes it necessary to control the material collected by gas cleaning. Such control is based on complete combustion of the carbon black and registration by automatic control devices to maintain continuous monitoring of the effluent.

This report presents the main problems which we face in our country in the collection of carbon black.

Paper No. 21

THE APPLICATION OF WET ELECTROSTATIC PRECIPITATORS FOR CONTROL OF FINE PARTICULATE MATTER

by

Even Bakke

UNITED STATES FILTER CORPORATION

Summit, New Jersey

Abstract

With the enforcement of much more stringent emission codes requiring the removal of condensable materials that form very small droplets in the sub-micron range, and with heavy emphasis on removal of solid particles smaller than 1 micron, the wet electrostatic precipitator has proven itself to be a highly efficient and economic alternative to high energy scrubbers. The recent development of a continuous sprayed, parallel plate, and horizontal flow wet electrostatic precipitator is described in detail.

The performance is not dependent upon the dust resistivity. The particle parameters that must be considered are the relative dielectric constant of the material and its size. The reentrainment loss is negligible and the cleaning (rapping) losses are non-existent. Particles with low dielectric constant, i.e., less than 10, have been shown both theoretically and experimentally to need a longer distance for collection. In a three field wet electrostatic precipitator, the removal efficiency of solid particles has been measured to exceed 99.5% even if 80% of the particles were less than 1 micron. Removal efficiencies higher than 95% have been measured on condensable hydrocarbons (tar fumes). The removal efficiency does not seem to change significantly with changes in the dust particle size distributions.

The Deutsch-Anderson equation for collection efficiency predictions and equipment sizing applies only for a limited range of operating parameters.

Introduction

The use of wet electrostatic precipitators for control of emission from industrial sources is almost as old as the use of the dry wire-tube, Cottrell type. However, until the mid sixties, its application was generally restricted to rather specialized applications such as on acid mist, coke oven off-gas, blast furnaces and detarring applications. The method of cleaning was in most cases intermittent and of the wetted wall type.

As a result of much more stringent local, state and federal emission codes, condensable materials forming small droplets or fumes are now being added to the total particulate loading. Hence, numerous applications have opened up for the wet electrostatic precipitator (WEP). In order to meet the codes, the energy consumption for scrubbers has increased exponentially. Also the removal of organic condensables which are very difficult to wet and form small droplets in the 0.1 to 2 micron range, requires scrubber pressure drops in the range from 40 to 60 inches of water gauge. Since the WEP is always operated at saturation temperature (100% relative humidity) it will remove organic materials with a condensation temperature higher or equal to the gas saturation temperature. It will also remove solid dust particles in the submicron range, and gaseous contaminants soluble in the spraying liquor. This removal is done with very low energy consumption; the pressure drop is usually less than 0.5 inches water gauge and the electric power input through the high voltage power supplies is quite modest, such as from 0.5 to 0.8 KW/1,000 ACFM.

The recent development of a continuously sprayed, parallel plate, frame electrode and horizontal flow design has provided industry with a realistic alternative to high energy scrubbers. The theory of operation, description of the design, range of applications with detailed discussion of the performance of the WEP on Horizontal Stud Soderberg pot line, the limitations of the method for performance prediction, the power consumption and its economics will be discussed below.

Theory of Operation

The corona generation, the charging and discharging processes in the wet electrostatic precipitator are, in general terms, similar to what takes place in a conventional dry electrostatic precipitator except for some important differences as described below.

Since the gas in the wet precipitator is always saturated with water vapor, the corona current and voltage relationship is somewhat different from the same relationship in the dry precipitator. With increasing amounts of water vapor, the sparkover voltage increases; i.e., the voltage at which the field breaks down, but the corona current at a given voltage is lower (1). When solid particles and droplets enter the electrostatic field, they will cause a local distortion of the electrostatic field between the electrode and the collecting plate. Some of the electric field lines intersect the particles and ions generated by the corona discharge will tend to travel along lines of maximum voltage gradient or along the field lines, and therefore, some of the ions will collide with the particles and the charge gradually builds up on the particles.

This process will continue until the charge on the particles is so high that it diverts the electric field lines away from the charged particles preventing new ions from colliding with the dust particle. When this state has been reached, the particles are said to be saturated with charge. Theory shows (1) that the saturation charge value and charging time is dependent upon electric field strength, size of the particle, the dielectric constant of the particle and the relative position of the particle in the field. This charging process is said to be field dependent and is the dominant process down to a particle size of 0.2 μm (2). For smaller particles, the so-called diffusion charging process is the dominant mechanism and is governed by the random thermal motion of the ions and is not limited to a saturation charge.

As soon as the charging process of the particle starts, the resulting electrostatic force will pull the particle towards the collecting plate. This force, together with the gravitational and the drag forces, and the gas flow distribution in the field, determine the particle trajectory and its point of collection.

In a dry electrostatic precipitator, the dust buildup on the collecting plate limits the maximum voltage at which the precipitator can operate. For dust layers with high resistivity (greater than 2×10^{10} ohm-cm) the voltage drop can be from 10 to 20 KV (2). This condition lowers the field strength in the space between the electrode and the dust deposit surface, and therefore results in a lower saturation charge which again gives a lower electrostatic force. If, on the other hand, the resistivity of the dust layer is lower than 10^7 ohm-cm (2), the electrostatic force holding the dust particle on the plates is low and reentrainment can become a serious problem during the electrode and plate cleaning (rapping) cycle and also during the steady operation, having the overall effect of lowering the precipitator collection efficiency.

For a continuously sprayed wet electrostatic precipitator, the abovementioned problems do not exist. The spray liquid drops form a film on the collecting plates which continuously washes off the dust that is being collected, and the resistivity of the water film is the governing factor in the dust discharging process and not the resistivity of the dust layer itself. Reentrainment problems are also non-existent, since the collected particles are instantaneously and continuously removed from the point of collection and are washed down as a light slurry. The exit loading is, therefore, much more stable and does not have the characteristic sharp increase as the dry electrostatic precipitator has during the collection plate and electrode rapping cycles.

Therefore, for a wet electrostatic precipitator, the operation is not influenced by the resistivity of the dust layer, and the major particle parameters to consider are their dielectric constant and size.

In order to get a better understanding of the effect of low dielectric constants on horizontal migration distance of the particle, a mathematical model of the particle collection mechanism was developed. The analysis was based upon a field charging process and a particle or droplet which had to traverse the whole net field spacing (one half of the plate to plate spacing). Particles of different sizes with dielectric constants of 2, 10 and 78 were investigated.

The unit consists of parallel collecting plates with a separation of 2r. The velocity profile between the plates is assumed to be flat (plug flow) and turbulent drag forces are neglected. Centered between two plates is an electrode frame with electrode spacing assumed sufficiently close to provide an approximately uniform electrostatic field near the plate surface. The field strength is approximately 70% of the field which would be produced by a solid discharge plate electrode (1), or

$$E = -0.70\ dv/dr \tag{1}$$

The current density under no-load condition will be (2)

$$J = i/A_c \tag{2}$$

The ionic space charge can be determined from the current density - electric field equation (2).

$$J = N_o e \mu_i \overline{E} \tag{3}$$

The saturation charge for a nonconductive particle is (2)

$$q_s = 12 \frac{\varepsilon}{\varepsilon+2} \pi \varepsilon_o a^2 E \tag{4}$$

The relative dielectric constant, ε, for a conducting particle approaches infinity and is equal to one for a perfect insulator.

The expression for the charge as a function of time is (2)

$$q_{(t)} = q_s \frac{t}{t+\tau} \tag{5}$$

where τ is a charging time constant or

$$\tau = 4\varepsilon_o / N_o e \mu \tag{6}$$

The particle size range examined is larger than 0.2 μm, so the diffusion charge can be omitted (3).

If we start with a particle entering the field halfway between two plates and without any charge, the force balance is divided into three different components:

x - axis, the direction of the electrostatic field (transverse to gas flow)

y - axis, the direction of the gravitation force (vertically down)

z - axis, the direction of the gas flow (horizontal and axial)

The force balance is then as follows:

$$\Sigma F_x = F_{qe} - F_x - F_{ix} = 0 \tag{7}$$

$$\Sigma F_y = F_g - F_{\eta_y} - F_{iy} = 0 \tag{8}$$

$$\Sigma F_z = F_{\eta_z} - F_{iz} = 0 \tag{9}$$

The electrostatic force can be expressed as

$$F_{qe} = qE \tag{10}$$

Substituting eqs. 1, 4 and 5 in eq. 10 gives

$$F_{qe} = 12 \frac{\varepsilon}{\varepsilon+2} \pi \varepsilon_o a^2 \frac{t}{t+\frac{4\varepsilon_o}{N_o e \mu}} \left(\frac{dv}{dr}\right)^2 0.49 \tag{11}$$

which shows the influence of the dielectric constant, the particle size and the field strength on the electrostatic force.

The gravitational force is

$$F_g = mg \tag{12}$$

The viscous force is, assuming Stoke's Law applies (laminar flow)

$$F_\eta = 6\pi a \eta w \tag{13}$$

and the inertia force can be expressed as

$$F_i = m\, dw/dt \tag{14}$$

If we assume a spherical particle with a radius "a" is moving in this field, it will be charged to carry an amount of q (coul) charges and the force balance in the transverse direction becomes after substituting eqs. 10, 13, and 14 in eq. 7:

$$qE - 6\pi a \eta w_x - m\, dw_x/dt = 0 \tag{15}$$

Substituting eq. 5 into eq. 15 gives

$$q_s \frac{t}{t+\tau} E - 6\pi a\eta w_x = m\frac{dw_x}{dt} \tag{16}$$

let

$$A = 6\pi a\eta/m \quad \text{and} \quad B = q_s E/m \tag{17}$$

Substituting this in eq. 16 and integrating gives

$$w_x = \frac{B}{A} - B\tau e^{-At}\int_0^T \frac{e^{-At}}{t+\tau}\, dt + C_1 e^{-At} \tag{18}$$

The term solution $\int \frac{e^{-At}}{t+\tau}\, dt$ cannot be integrated but using a series (by Jolly (4)):

$$\int \frac{e^{-ax}}{b+x}\, dx = e^{-ab}\left[\ln\ (b+x) + \sum_{n=1}^{\infty} \left[a(b+x)\right]^n/n\cdot n!\right]$$

Then by using this expression in eq. 18 and integrating it once more with the following initial conditions:

$$t = 0,\ w_x = w_{xo} = 0 \text{ and } s_x = s_{xo} = 0$$

the travel distance s_x becomes

$$s_x = \int_0^T w_x dt = \frac{B}{A}\ (t - \frac{1}{A}\ (1 - e^{-At}) + \tau e^{-A(t+\tau)}$$

$$\cdot\left[\ln \frac{t+\tau}{\tau} + \sum_{n=1}^{\infty} ((A(t+\tau))^n - (A\tau)^n)/n\cdot n!\right] - \tau \ln \frac{t+\tau}{\tau} \tag{19}$$

The migration distance is from 0 to 6 inches and the migration time, T, needed for the particle to be collected can then be found for s_x = 6 inches by a trial and error solution of eq. 19. The result is shown in Fig. 1 where the relationship between particle size and migration time is shown for a dielectric constant of 2, 10 and 78 respectively.

In order to obtain the horizontal distance needed for the particles to be collected, the force balance in the z direction must be considered, i.e., eq. 8. This expression becomes

$$6\pi a\eta\ (w_{gas} - w_z) = m\ dw_z/dt \tag{20}$$

where $(w_{gas} - w_z)$ is the relative velocity between the particle and the gas. Integrating eq. 20, using the constants given by eq. 17 gives

$$w_z = w_{gas}\ (1 - e^{-At}) + w_{zo}e^{-At} \tag{21}$$

where w_{zo} is the initial particle velocity along the z-axis. The horizontal travel distance becomes then

$$s_z = \int_0^T w_z dt = w_{gas}\ (t + \frac{1}{A}\ (e^{-At} - 1)) - \frac{1}{A}\, w_{zo}\ (e^{-At} - 1) \tag{22}$$

Then by using the travel time calculated from eq. 19, the horizontal traveling distance can be calculated as a function of particle (droplet) size and dielectric constant. This is shown in Fig. 2. With two 5 μm particles or condensed droplets, one with a dielectric constant of 2 (e.g. a condensed hydrocarbon droplet) and one with a dielectric constant of 78 (e.g. pure water droplet), for these two particles to migrate across a field spacing of 6 inches with an applied voltage of 50 kv and a gas velocity of 3 ft/sec, will take a horizontal distance of 7.2 ft. (2.2 m) and 3.9 ft. (1.2 m) respectively. Therefore, the low dielectric particle takes almost twice the horizontal distance before being collected and this analysis points to the fact that condensable hydrocarbons (tars) and other materials with a low dielectric constant will be much more difficult to collect than conductive particles, and this has been confirmed by measurements.

When considering the removal of condensable hydrocarbons (tar mist), it should be remembered that the dielectric constant for petroleum distillates are quite low, i.e. around 2. For example, hexane (C_6H_{14}) has a dielectric constant of 2 and a boiling point of 69° C., toluene (C_7H_8) has a dielectric constant of 2.15 and a boiling point of 110° C., and naphthalene ($C_{10}H_8$) has a dielectric constant of 2.54 and a boiling point of 218° C. Other organic liquids like phenol formaldehyde resin has a dielectric constant of 6.6. Pure water has a dielectric constant of 78.

The removal efficiency of the WEP on a given gas and dust stream is a function of six basic parameters:

Collection Area
Operating Voltage
Discharge Current
Liquid to Gas Ratio
Treatment Time
Local Average Velocity

The performance is often stated by the so-called migration velocity; the higher the migration velocity, the better the particulate removal efficiency or the smaller the WEP in terms of collection area needed to treat the gas flow. The relationship between migration velocity and WEP performance is given by the following equation, the so-called Deutsch-Anderson equation (1):

$$\omega = -Q/A \; 0.508 \; \ln(c_o/c_i) \qquad (23)$$

The efficiency of the unit is given by

$$\eta_e = (1-c_o/c_i) \quad 100 \qquad (24)$$

and when substituting eq. 23

$$\eta_e = (1-e^{(-Aw/0.508Q)}) \; 100 \qquad (25)$$

The migration velocity, ω is a performance parameter that does not in reality relate directly to the speed at which the particles migrate to the collecting plates. It is a "catch-all" which also includes all operating parameters not included in equation 23.

Description of the Wet Electrostatic Precipitator (WEP)

The wet electrostatic precipitator of the MikroPul design can be characterized as a continuously sprayed, horizontal flow, parallel plate, and solid discharge electrode type, and in terms of gaseous absorption it can be characterized as a combination of a co-current and cross flow scrubber. Figure 3 shows a cut-away view of the internal configuration.

In the application of a wet electrostatic precipitator, it is very important that the gas to be treated is saturated with water vapor to prevent that water inside the WEP evaporates which causes loss of washing water and dry zones on the internal members. The saturation of the gas can be done in a spray tower or scrubber upstream of the WEP, or it can be done in the inlet section of the WEP, or both.

In addition, it is also necessary to obtain a good and uniform velocity profile across the WEP, and the diffusion of the flow from the inlet duct velocity down to the WEP face velocity has to be performed in the inlet section. Furthermore, by spraying co-current into the inlet section, some of the coarser particles will be removed and the gas absorption process will be started. To accomplish this, sections of baffles and sprays are located in the inlet cone of the WEP.

After passing through the sections of transverse baffles, the dirty gas stream then enters into the first electrostatic field. Water sprays located above the electrostatic field sections introduce the proper amount of water droplets to the gas stream for washing of internal surfaces. The particulates and the water droplets in the electrostatic field pick up a charge and migrate to the collecting plates. The collected water droplets form a continuous downward flowing film over all the collecting plates and keep them clean. The water film and the collected particulates flow down the collecting plates into the troughs below which are sloped to a drain.

The transverse baffle gas distribution system combined with the extended electrode, located upstream and downstream of each field, insures complete gas flow uniformity from passage to passage, and collects particulates and droplets by impingement, and by electrostatic forces. Also the extended discharge electrode system improves the collection efficiency by increasing effective collection area. At the entry of a field, particles not captured by the transverse baffles are given an advance charge by the forward extended electrode before they come into proximity of the collecting plates. Thus charged, the particles start immediately to migrate toward the leading edge of the plates. It has been found that the downstream side of the baffles at the exit of a field collects a considerable amount of material. The very small charged particles escaping the parallel plate field are pulled into the wake of the baffles by the slight vacuum resulting from the turbulent dissipation of energy. Since the particles have an electrostatic charge, some of them will be collected on the back side of the baffles.

All baffles systems are arranged so that a walkway runs across the front and the back of each of the electrostatic fields. The discharge electrode frames are mounted on collar-type high voltage support insulators. Insulator compartments are heated and pressurized to prevent moisture and particulate leakage into the insulator compartment.

In any particulate and/or gaseous removal process where a liquid is used, it is important to remove the carry over liquid drops and mists before the outlet of the equipment. We have found that doing this electrostatically is highly efficient. Hence, the last section is operated dry, thereby establishing an electrostatic barrier which the liquid droplets cannot penetrate, and the mist collects on the front side of the baffles, and the downstream side is dry. However, some small dust particles can penetrate through and will collect on the downstream baffles. Therefore, this surface is washed intermittently to prevent buildup of particulates.

Range of Applications

During the past two years, many new applications have been piloted and units have been sold and installed following successful pilot plant work. The type of applications where the WEP should be used can be categorized as applications on gas streams containing relatively light dust loading of submicron particles and/or condensed organic materials forming a submicron fume. Ordinarily these applications would require very high pressure drop scrubbers in order to meet the current air pollution codes. Although the initial investment is higher for the WEP compared to a scrubber, the energy consumption and operating costs are only a small fraction of what would be needed to operate the scrubbers. The water treatment requirements would be the same as for scrubbers.

On some applications where the dust resistivity is either very high or very low, the WEP can also be applied successfully in competition with dry electrostatic precipitators.

MikroPul has installed WEP's on the following applications:

1) On Soderberg aluminum reduction cells (pot lines) both of the vertical and horizontal stud type cells, for simultaneous removal of aluminum oxides, solid and gaseous fluorides, tar mist (condensable hydrocarbons) and SO_2.

2) On carbon anode baking furnaces (ring furnaces) for removal of carbon particles, tar mists and SO_2.

3) On fiberglass resin application section and forming lines for removal of short broken glass fibers, phenolic resins and tars.

4) On molybdenum sulfate roasting, downstream of a scrubber for removing ammonium sulfite - sulfate aerosols which forms in the ammonia scrubbing process and SO_2.

WEP's are now being manufactured and installed on the following additional applications:

1) For upgrading of low pressure drop scrubbers on phosphate rock driers for removal of the submicron particles and SO_2.

2) On coke oven batteries when connected to a continuous shed or hood along the push side of the battery where the coke is pushed into the railroad car. Here the WEP will remove the fine carbon particles and the condensable hydrocarbons during the push cycle. In addition, the WEP will eliminate any emission caused by door leakage on the push side.

MikroPul has a very active pilot plant program and is now investigating several other new applications.

Detailed Description of an Application

The application of the WEP on horizontal stud Soderberg aluminum reduction cells (pot lines) will be discussed in order to compare the experimental results with commonly used theory and to give some detailed information of the level of performance of the WEP on very fine particulate matter and condensed hydrocarbon droplets (tar fumes) which are believed to be mostly of submicron size.

A 50,000 CFM prototype unit was installed at Reynolds Metals Company, Longview, Washington plant and started up in October of 1971 and has been in operation since. The precipitator was installed so that it could be evaluated when connected downstream of the existing cyclonic scrubbers and when connected directly to the duct from the forced draft fans, i.e., without presaturation before the WEP.

After showing excellent performance, four full size units were installed and have been in operation since May of 1973. Twenty-six more units are under construction which will complete the primary emission control system for the Longview North and South plants.

The Reynolds Metals Company specifications called for a maximum total outlet loading of 0.003 GR/SCF (6.9 mg/m^3) when the total inlet loading is 0.05 GR/SCF (114.4 mg/m^3) or less, and if the outlet loading is higher than 0.003 GR/SCF, the efficiency should stay higher than 95%. This efficiency would correspond to an overall migration velocity of 5.18 cm/sec. The loadings are defined as solids plus condensable hydrocarbons. The inlet loading of 0.05 GR/SCF is downstream of the scrubber which is the arrangement for the North Plant. For the South Plant, the scrubbers will be removed and the inlet loading will increase to 0.15 GR/SCF (340 mg/m^3) of solids and condensable hydrocarbons.

Figure 4 shows a schematic of the arrangement of equipment in the North Plant. The fans creating sufficient draft at the pots are connected to the manifold and the fan outlet ducts are connected to the inlet of the cyclonic scrubbers. In between potlines, two scrubber outlets were connected to one precipitator inlet giving a total flow of 100,000 ACFM through the WEP. At each end of the plant, one scrubber is connected with one WEP with a flow of 50,000 ACFM. The treated gas leaves the WEP through an outlet conversion piece and stack combination.

The high pH sodium based liquor is piped into the WEP and scrubbers as shown in Figure 4. The fresh liquor first passes through the WEP and discharges into a small receiving tank and is then pumped into the scrubber with a booster pump. From the scrubber, the liquor passes back to the clarifiers and the cryolite recovery plant. The liquid rate through each of the 100,000 CFM units is approximately 500 GPM.

The 100,000 CFM wet electrostatic precipitators have 28 passages and 3 electrically independent fields with four points of electrode suspension per field. The plates are 6 feet by 25 feet high. The specifications are summarized in Table I for the 100,000 CFM units installed in the North Plant.

Raemhild (5) performed an investigation to evaluate the cyclonic scrubbers in the North Plant. His results gave the scrubber inlet and outlet loadings of solids and condensables and are summarized in Table II. These are the average loadings based upon 11 tests performed in the fall of 1971. The scrubber inlet loading is the inlet loading to the WEP when no scrubber is used, i.e., in the South Plant, and the scrubber outlet loading is the inlet loading to the WEP's in the North Plant. The condensable scrubber outlet loading of 0.0069 GR/SCFD is low; higher values have been measured and found to be as high as 0.03 GR/SCFD. Raemhild also made particle size distribution measurements with an in-stack impactor. Figure 5 shows the particle size distributions

TABLE I

Summary of Specifications for the Wet Electrostatic Precipitators Installed at Reynolds Metals Company Plant at Longview, Washington

Gas Flow	100,000 SCFM
Inlet Temperature to Scrubbers	250° F.
Inlet Temperature to WEP	100-110° F.
Total Particulate Inlet Loading (solids and condensables, excluding water)	0.05 GR/SCF
No. of Electrostatic Fields	3
Liquor, Flow Rate at 60 PSI	500 GPM
Liquor pH in	7 - 10
Outlet Loading for an Inlet Loading of 0.05 GR/SCF or less	0.003 GR/SCF
Minimum Collection Efficiency for Outlet Loadings Greater than 0.003 GR/SCF	95%
Face Velocity	2.38 FT/SEC
Maximum Pressure Drop	1" W.G.
Treatment Time	10.1 SEC
Housing Material, Hot Rolled MS, Thickness	3/16"
Collection Plates, Hot Rolled MS, Thickness	10 GAUGE
Discharge Electrodes, Flatbars MS	1" x 1/8"
Piping Materials	PVC
Spray Nozzles, SS 316, Type	Full Cone
No. of Transformer Rectifiers	3
Rectifier Type	Silicon
Wave Form	Full
Minimum Output per T-R Set	60 KV, 1000 MA
Primary Voltage	480 V, 60 Hz

Manual and Automatic Voltage and Spark Rate Control for the scrubber inlet and outlet particulates. For the scrubber inlet, approximately 50% of the mass is smaller than 1 μm and for the outlet approximately 80% is smaller than 1 μm.

Reproduced from best available copy.

TABLE II

Reynolds Metals Company, North Plant,
Longview, Washington
Scrubber Inlet and Outlet Loadings (5)

	Avg.	Std. Dev.
Condensables In (GR/SCFD)	.0115	.0069
Solids In (GR/SCFD)	.0488	.0236
Total In (GR/SCFD)	.0603	.0254
Condensables Out (GR/SCFD)	.0069	.0035
Solids Out (GR/SCFD)	.0289	.0028
Total Out (GR/SCFD)	.0358	.0045

The 50,000 CFM prototype WEP removed approximately 95% of the hydrocarbons and 97% of the solids. The design improvements incorporated in the subsequent units gave a very significant improvement in solids removal efficiency. Even if the specific collection area was reduced from 315 SQ.FT./1000 ACFM for the prototype down to 295 SQ.FT./1000 ACFM for the new units, the solids removal efficiency increased to a value higher than 99.5%. The improvement was so significant that the plate area for the units in the South plant will not be increased even if the inlet loadings according to the specifications are three times higher (0.15 vs. 0.05 GR/SCF). The condensable removal efficiency did not change significantly probably because of the low dielectric constant of the tars and their small size. It has been observed that more tars collect in the third field than in the two upstream fields which tends to confirm the analysis presented above showing that low dielectric materials need a longer distance for collection than materials with larger values for ε ($\varepsilon > 10$). The HF outlet concentrations were found to be lower than needed by the codes and significantly improved when compared with the prototype.

Continuous vertical velocity profiles were made in the first 100,000 CFM unit with a hot-wire anemomoter measurement system in seven different gas passages across the unit, with two traverses at each passage. The measurements were made at the exit of the second field. When analyzing the 14 continuous vertical velocity profiles, the average velocity through the unit was found to be 2.37 FT/SEC with a standard deviation of 0.204 FT/SEC or 8.62% of the average value. True root mean square (RMS) measurements were made of the linearized hot wire voltage signals, and the level of turbulence, (i.e. the ratio of the RMS voltage to the mean D.C. voltage) was found to be higher in the central part of the WEP and varying from 0.56 to 0.83 and lower along the housing walls, varying from 0.23 to 0.29. Hence, the flow is highly turbulent even if the Reynolds number based upon the plate spacing is only 13,720 and the Reynolds number based upon the flow past the transverse baffles at the entry of the field is only 2,290. Point measurements were also made in the prototype. For one test, 30 point velocity measurements were made giving an average of 2.87 FT/SEC and a standard deviation of 1.03 FT/SEC or 35.7% of the average.

The gas distribution in the new units is judged to be very close to ideal flow conditions and is the major factor contributing to the improved performance.

Comparison of Analytical and Experimental Results

The Deutsch-Anderson expression, eq. 23, is commonly assumed to be valid for sizing calculations and performance predictions. However, several authors (6, 7) have pointed out that eqs. 23 and 25 are only valid over a limited range of operating parameters. Further, the development of the Deutsch-Anderson equation was based upon several simplifying and limiting assumptions (e.g., all particles have the same size, do not reentrain, are uniformly distributed over any cross section by turbulent diffusion forces, move independently, and are fully charged at the instant they enter the field).

In order to compare data from the potline application with theory, the measured collection efficiency was compared with predictions given by equation 25. Figure 6 shows the specific collection area in SQ. FT. per 1000 ACFM vs. collection efficiency in percent of solid particulates as measured on one of the 100,000 ACFM units at Reynolds Metals Company. The three groups of data at A/Q approximately equal 100, 200 and 300 represent data when one electrostatic field, two fields and three fields respectively are in operation. Two operating curves as calculated from eq. 25 are shown, i.e., for a migration velocity of 9 and 12 cm/sec. As it can be seen, the experimental points suggest a curve shown as the dotted line and this curve crosses over from the ω = 12 cm/sec line for A/Q approximately equal to 100 to the ω = 9 cm/sec curve for A/Q equal to 260 and greater. However, in a narrow range of A/Q the experimental points follow the respective theoretical lines quite well.

Another point that should be emphasized is the fact that the removal efficiency was always better when downstream fields were shut off, e.g., the first field in operation and the two fields downstream shut off. The data points with the downstream field shut off are marked with a "D" as shown in Fig. 6 and data points with upstream fields shut off are indicated with a "U". The reason for this difference in efficiency is obviously that charged particles are escaping a field in operation and they continue to migrate to some extent and are being collected in the downstream field even if it is not energized.

A third point that should be made about Fig. 6 is that the three collection efficiency data points when the cyclonic scrubber is by-passed and the particle size distribution of the incoming dust is much coarser (see the two particle size distribution curves in Fig. 5) are shown to fall nicely in with the operating points when the scrubber was in operation. This indicates that when the precipitator is operating with three field, an inlet dust loading with a smaller mean particle size distribution (0.22 um vs. 0.70 μm) does not reduce the collection efficiency.

Power Consumption and Economics

The power consumed to operate the wet electrostatic precipitators can be divided into 4 categories, (1) electrostatic power, (2) fan power, (3) insulator heating power, and (4) pump power.

The electrostatic power input is approximately 1.5 KW/1000 SQ. FT. of collection area. The pressure drop across the WEP is less than 0.5" W.G., and the net fan power is then 0.06 KW/1000 CFM. The insulator heating power is 6 KW per field, and if it is assumed that the WEP uses an L/G of 5 GPM/1000 CFM and a spray nozzle pressure of 50 PSIG, the net pump power would be 0.110 KW/1000 CFM. These values are summarized in Table III.

TABLE III

WEP Power Consumption (all net)

Electrostatic Power	1.5 KW/1000 SQ. FT.
Fan Power at .5" W.G.	0.06 KW/1000 CFM
Insulator Heating Power	6 KW/Field
Pump Power at 5 GPM/1000 CFM and 50 PSIG	0.11 KW/1000 CFM

If we consider a unit handling 100,000 CFM with a collection area of 300 SQ. FT./1000 CFM and having 3 fields, the total net power consumption is 80 KW.

Now, if we compare this with a Venturi scrubber, assuming it would have to operate with a pressure drop of approximately 50" W.G. and an L/G of 7 GPM/1000 CFM to give the same performance in terms of removal efficiencies, the total net power input is 615 KW. This would be more than 7 times higher power consumption when compared with the WEP power consumption.

The installed cost of a mild steel unit, with approximately 300 SQ. FT./1000 ACFM collecting area, flange to flange, would be between \$3.00 and \$4.00 per CFM. This cost also includes the power supplies. The annual operating cost is shown in Table IV assuming a cost of \$0.01/KWH for electric power. The annual operating cost of Venturi scrubbers is also shown. The installed cost of the Venturi scrubber, cyclonic absorber-separator and high pressure fan and motor was assumed to be \$1.20 per CFM. The fixed charges were assumed to be 15%.

TABLE IV

Annual Operating Cost, Flange to Flange, 100,000 CFM

	WEP	Venturi
Investment at 15%	\$52,500	\$18,000
Power Costs at \$0.01/KWH	7,500	54,000
Total Annual Cost	\$60,000	\$72,000

As it can be seen, the annual operating cost for a WEP is lower than for the Venturi scrubber even if the installed cost is much higher. The above analysis assumed that mild steel could be used, i.e., that a sufficient water treatment and neutralization plant is installed and that the maintenance costs were equal for the two alternatives.

Conclusions

The following conclusions can be drawn:

1. The performance and the collection efficiency of the wet electrostatic precipitator is not dependent upon the resistivity of the dust layer. The resistivity of the water film is the governing discharge parameter and the unit can handle very efficiently both high and low resistivity dusts. The reentrainment loss is negligible, the rapping loss is non-existent and the outlet loading is stable in magnitude.

2. The dielectric constant of the particle material and its size are the two most important particle parameters. Organic condensable materials which form a very fine aerosol usually have a low dielectric constant, i.e., less than 10 and as low as 2, and it was shown that from a theoretical standpoint, these particles will take almost twice the horizontal distance for collection when compared with particles with dielectric constants larger than 10. This finding has been confirmed by field observations which show that the last field has the heaviest buildup of condensable materials.

3. The wet electrostatic precipitator has been used with a high degree of success on applications where the solid particles are of sub-micron size and where condensable organic droplets also of sub-micron size have to be removed. On this type of application, the WEP competes favorably with the high energy scrubbers because of their very high energy requirements needed to give similar removal efficiencies. The wet electrostatic precipitator can also be applied in competition with dry electrostatic precipitator on dusts with either very high ($> 2 \times 10^{10}$ ohm-cm) or very low ($< 10^{7}$ ohm-cm) dust resistivities.

4. In a three field wet electrostatic precipitator, removal efficiencies higher than 99.5% on solid particulates with 80% less than 1 μm size has been measured consistently. Removal efficiencies of 95% and higher have been measured on tar mists (condensable hydrocarbons). The wet electrostatic precipitator is therefore a highly efficient device for removal of very fine particles both in the form of solid particles and condensable mist.

5. It has been shown that the Deutsch-Anderson equation for sizing the WEP can only be used over a relatively small range of operating parameters.

6. When operating with three electrically independent fields, the removal efficiency seems not to be influenced by a significant reduction in mean particle size of the incoming solid particulates.

Acknowledgement

The author expresses thanks to Mr. James Shen of the Research and Development Department of MikroPul for working out the details of the mathematical model, to Dr. David Rimberg for many valuable suggestions concerning the paper, and to Lorraine Simons for preparing the manuscript.

NOMENCLATURE

A = $6\pi a\eta/m$ = Constant
A_c = Collection Area
a = Particle Diameter
B = $q_s E/m$ = Constant
c_i = Particle Inlet Loading
c_o = Particle Outlet Loading
E = Electrostatic Field Strength
e = Electric Charge
F = Force
g = Gravitational Constant
i = Current
J = Current Density
$\ln$ = Natural Logarithm
m = Particle Mass
N_o = Number Density of Free Ions
Q = Gas Flow Rate
q = Charge
q_s = Saturation Charge
r = Net Field Spacing
s_x = Transverse Distance
s_z = Horizontal Distance
T = Migration Time for Collection
t = Time
v = Voltage
w = Velocity
w_{gas} = Gas Average Velocity
w_x = Transverse Particle Velocity
w_z = Horizontal Particle Velocity
x = Transverse Horizontal Distance
y = Vertical Distance
z = Horizontal Axial Distance

ε = Dielectric Constant
ε_o = Permittivity of Free Space
η = Viscosity of Gas
η_e = Collection Efficiency
μ_i = Carrier Mobility of the Gas
π = 3.14
τ = Charging Time Constant
ω = Migration Velocity Parameter

References

1. White, H.J. Industrial Electrostatic Precipitation, Addison-Wesley Publ. Co., Reading, Mass., 1963.

2. Oglesby, S. and Nichols, G.B. "A Manual of Electrostatic Precipitator Technology, Part I - Fundamentals", Contract CRA 22-69-73 for NAPCA, Cincinnati, Ohio.

3. Oglesby, S. and Nichols, G.B. "Electrostatic Precipitator Technology for Source Emission Control", AIChE Paper, No. 8E, 72nd National Meeting, St. Louis, Missouri, May 1972.

4. Jolly, L.B.W. Summation of Series.

5. Raemhild, G.A. "Collection of Aerosols from a Horizontal Spike Soderberg Aluminum Reduction Plant by a Wet Cyclonic Spray Scrubber as Related to Scrubber Operating Parameters", M.S. Thesis, University of Washington, 1972.

6. Penny, G.W. "Some Problems in the Application of the Deutsch Equation to Industrial Electrostatic Precipitators", Journal of the Air Pollution Control Association, Vol. 19, No. 8, August 1969.

7. Cooperman, P. "A New Theory of Precipitator Efficiency", Paper No. 69-4, Air Pollution Control Association Meeting, New York City, 1969.

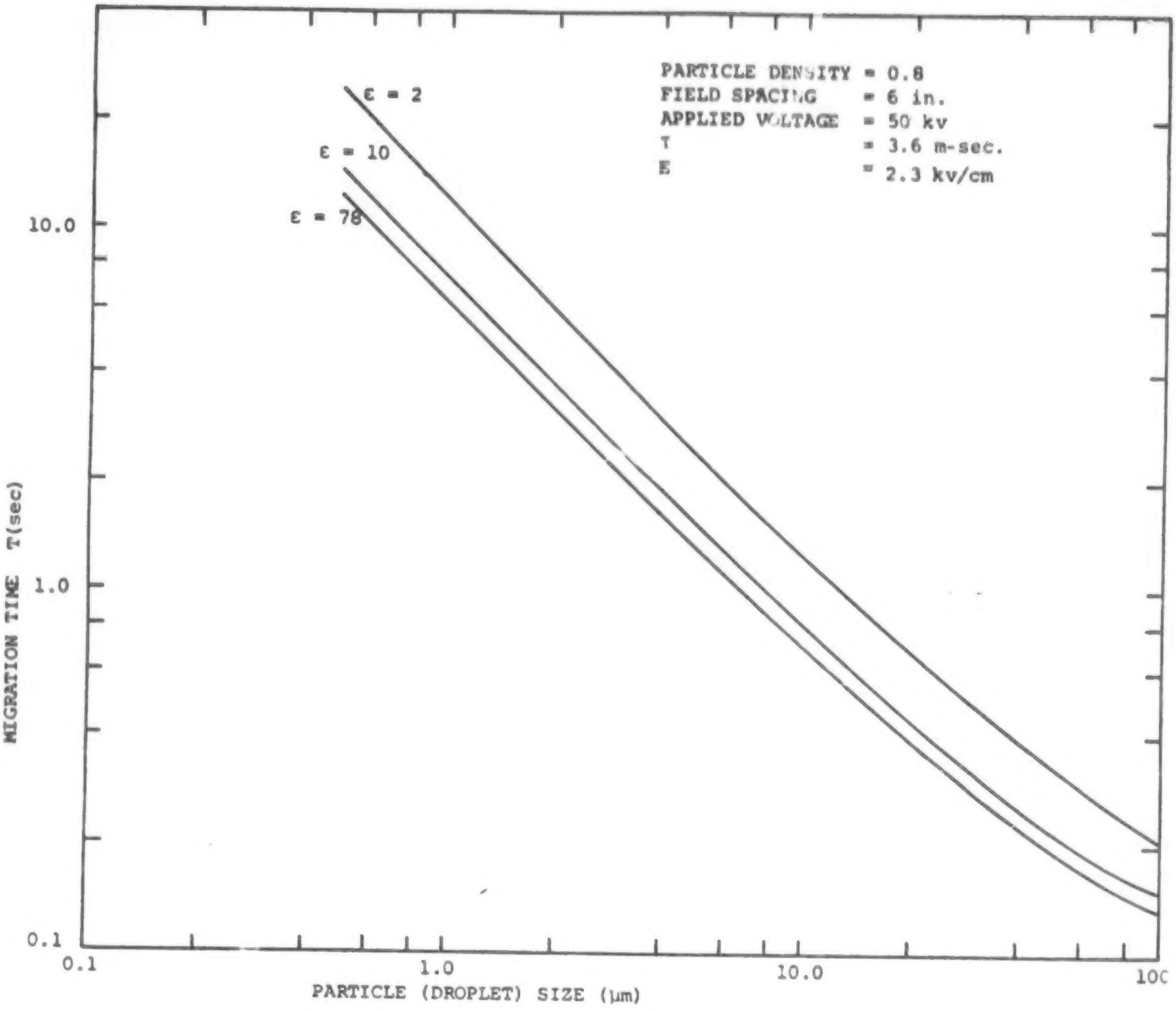

FIG. 1 PARTICLE SIZE VS. MIGRATION TIME FOR COLLECTIO

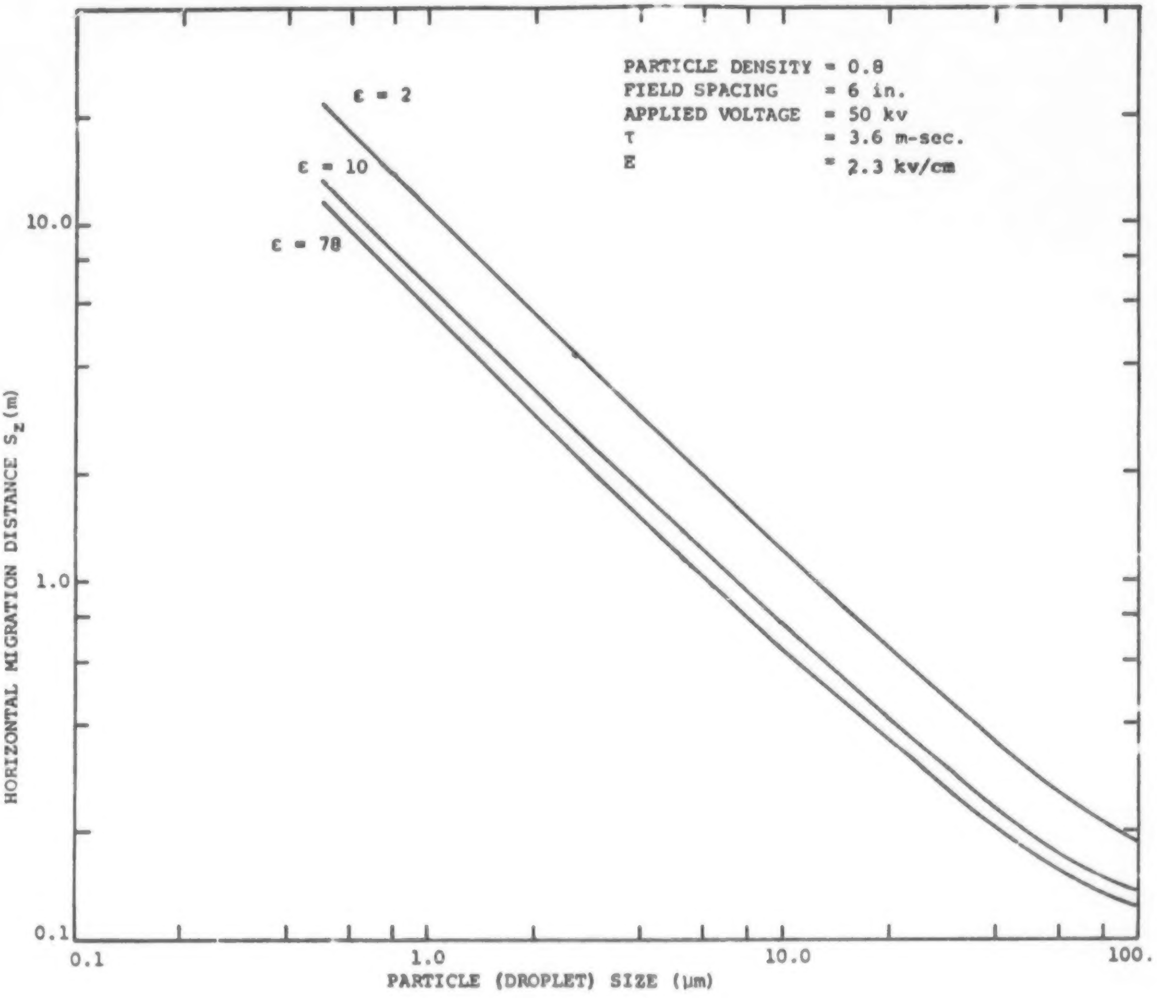

FIG. 2 PARTICLE SIZE VS. HORIZONTAL MIGRATION DISTANCE FOR COLLECTION

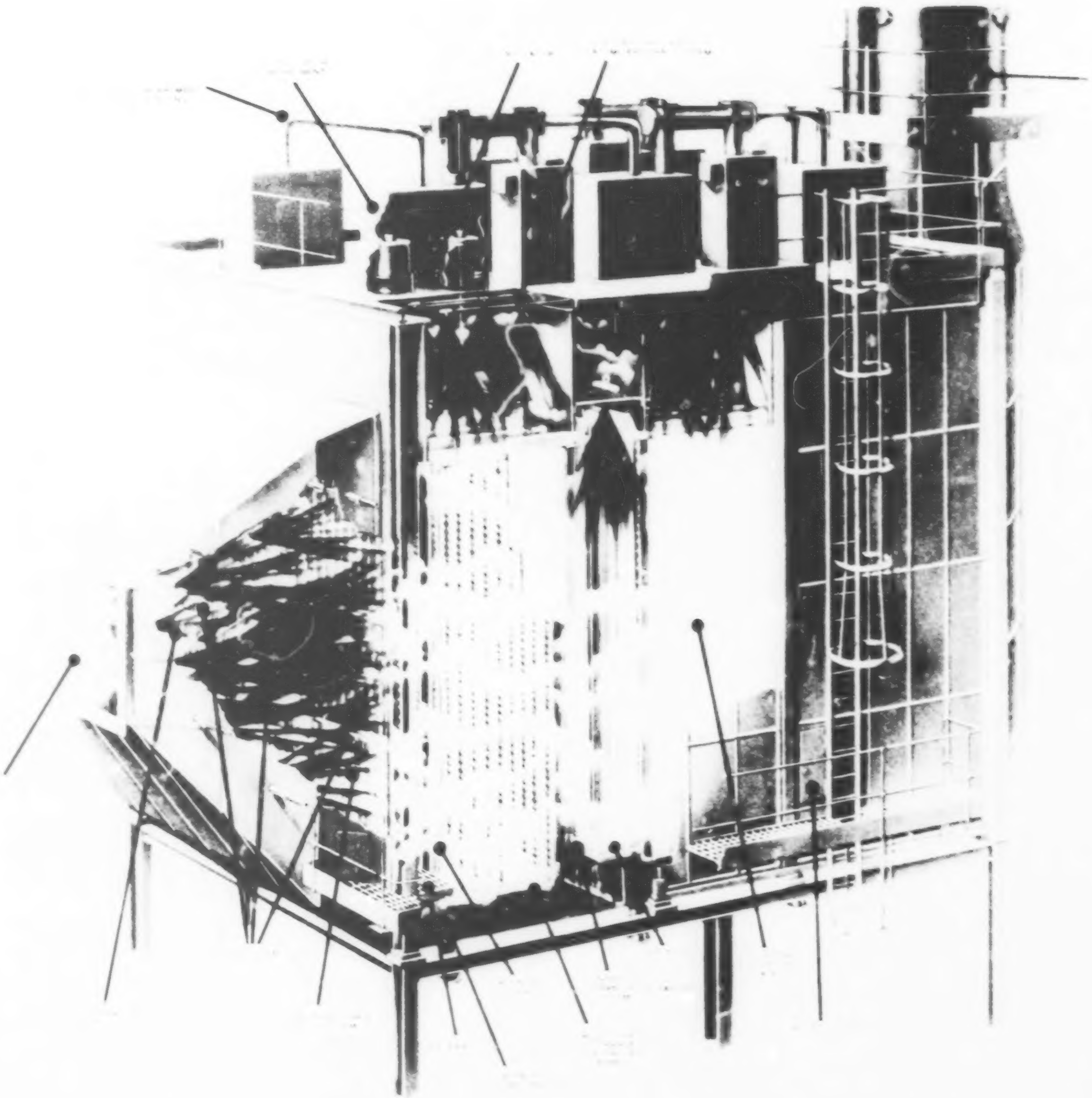

MIKROPUL ELEKTROFIL WET ELECTROSTATIC PRECIPITATOR

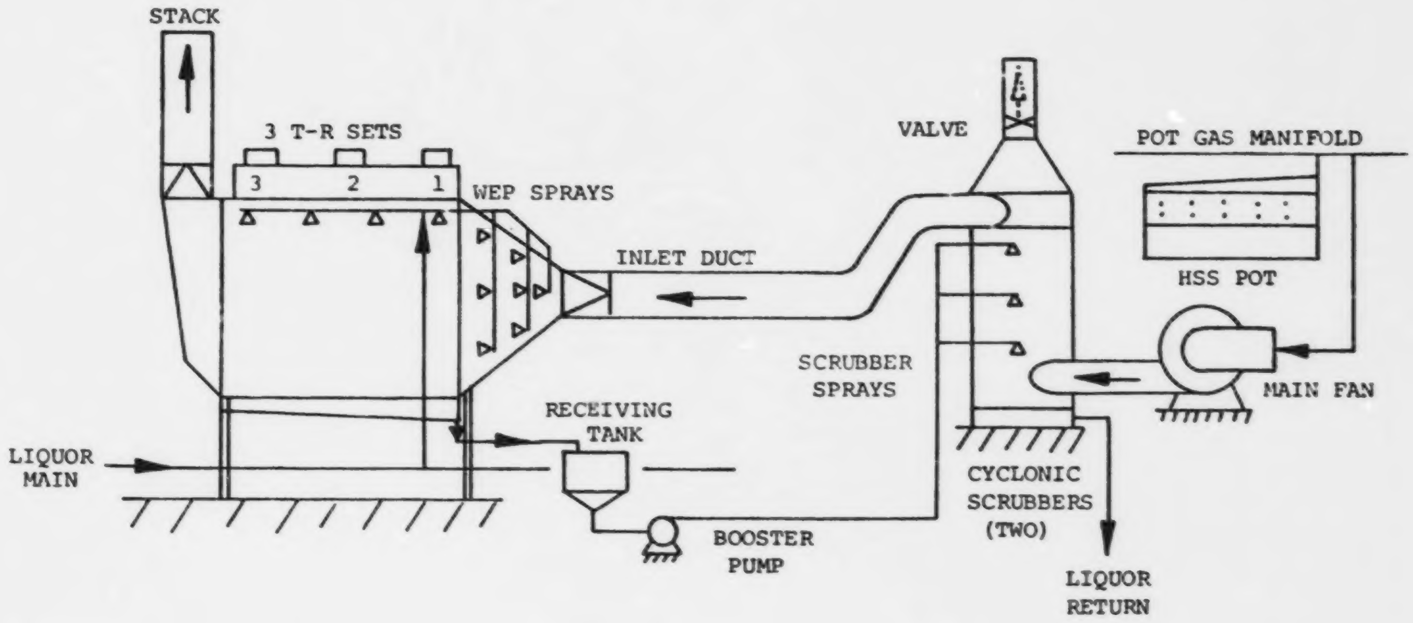
STACK
3 T-R SETS
3
2
1
WEP SPRAYS
INLET DUCT
VALVE
POT GAS MANIFOLD
HSS POT
MAIN FAN
SCRUBBER SPRAYS
RECEIVING TANK
LIQUOR MAIN
BOOSTER PUMP
CYCLONIC SCRUBBERS (TWO)
LIQUOR RETURN

FIG. 4 SCHEMATIC OF PRIMARY EMISSION CONTROL SYSTEM, REYNOLDS METALS, LONGVIEW, WASHINGTON

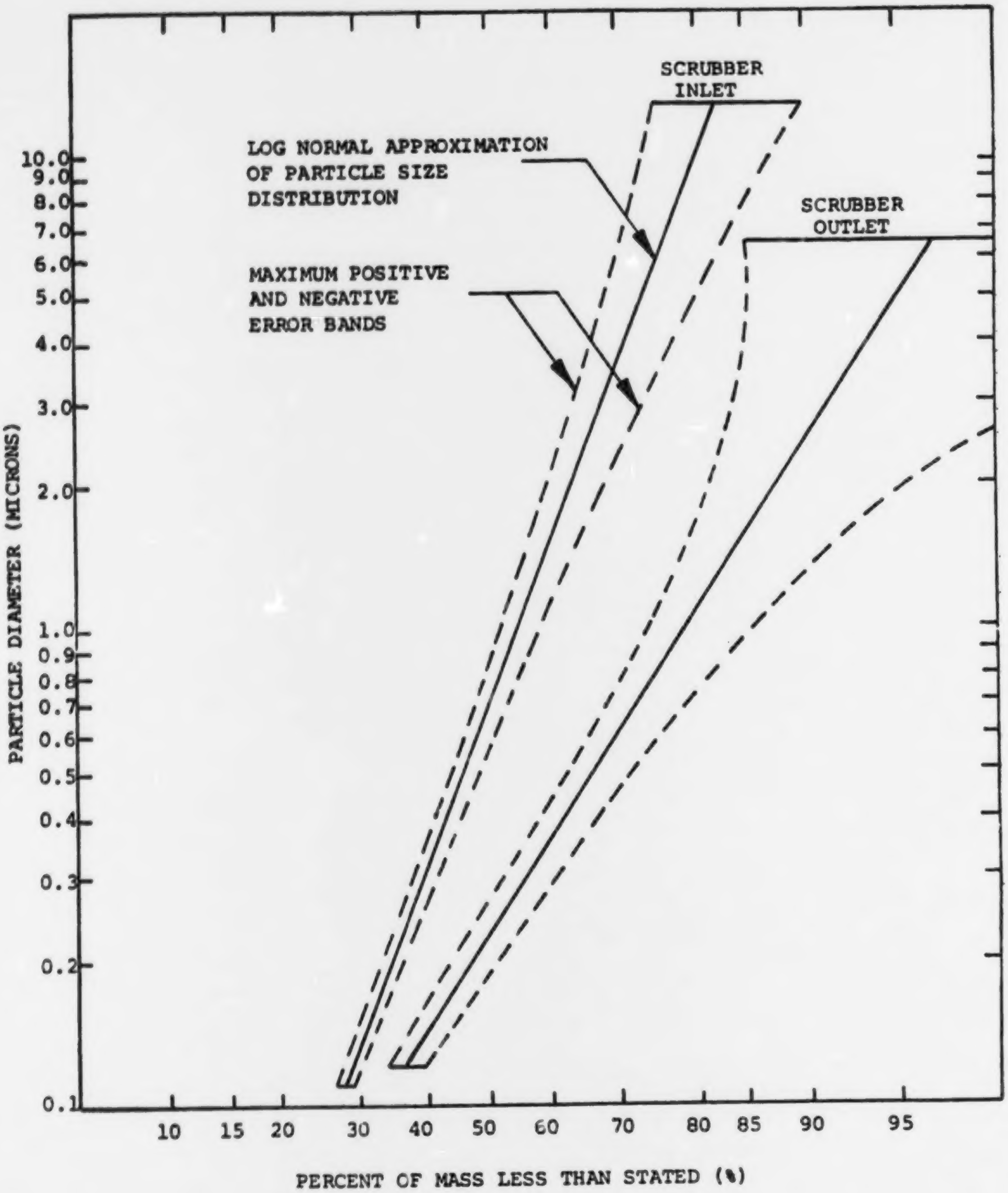

FIG. 5 SCRUBBER INLET AND OUTLET PARTICLE SIZE DISTRIBUTIONS
REYNOLDS METALS COMPANY, LONGVIEW WASHINGTON PLANT
BY RAEMHILD

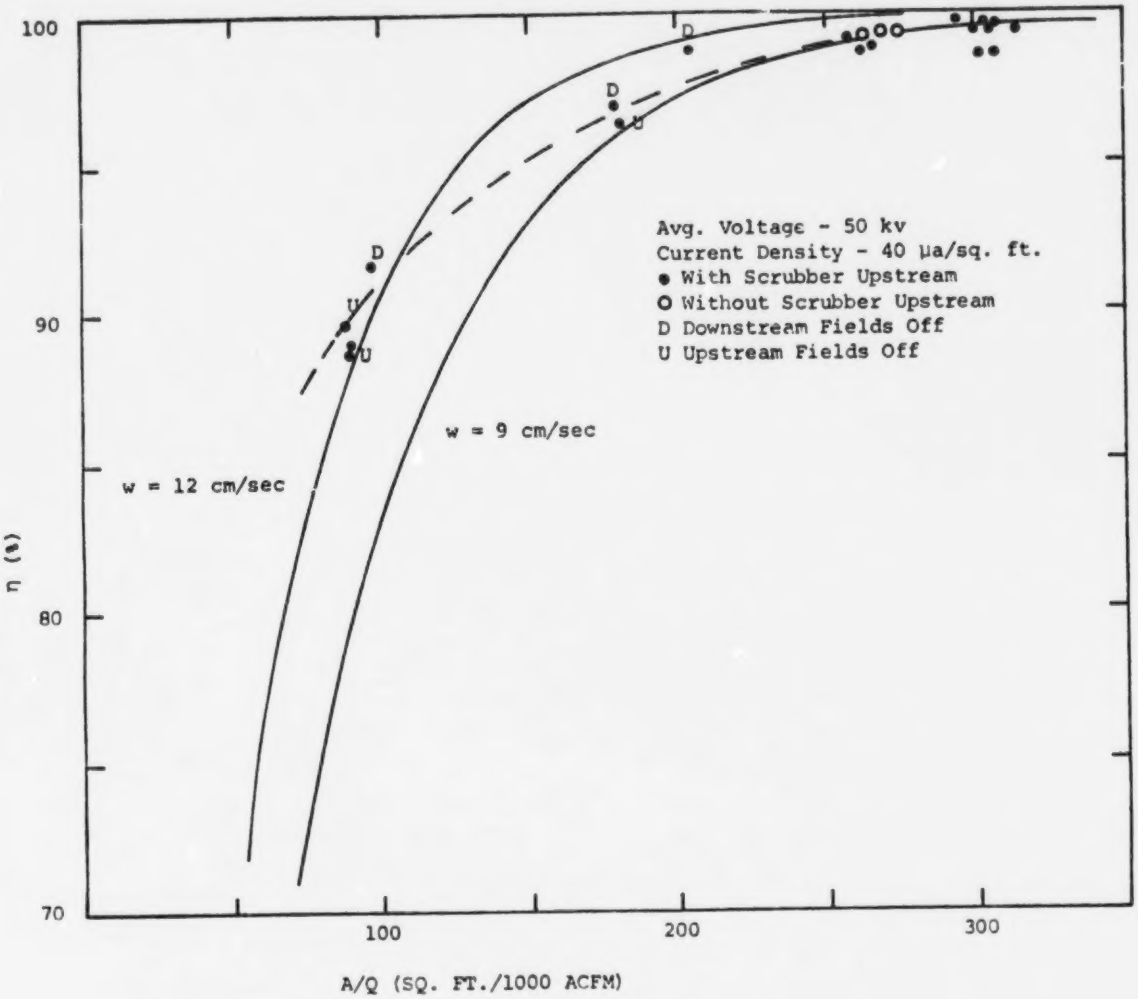

FIG. 6 SPECIFIC COLLECTION AREA VS. SOLIDS REMOVAL EFFICIENCY

Paper No. 22

THE INFLUENCE OF ASH CHEMISTRY ON THE VOLUME CONDUCTION IN FLY ASH

by

Roy E. Bickelhaupt

SOUTHERN RESEARCH INSTITUTE

Birmingham, Alabama

ABSTRACT

Research has been conducted to determine the influence of fly ash chemistry on resistivity at temperatures above 200°C. A large number of fly ashes having generally similar physical and structural character while possessing typical variations in ash chemistry were used. Resistivity as a function of temperature and transference experiments were performed.

It was determined that the quantity of electricity passed was proportional to a mass transfer and that lithium and sodium ions migrate. For a given iron concentration, the resistivity was inversely proportional to the combined lithium and sodium concentration. Also for a constant concentration of lithium and sodium, the resistivity was inversely proportional to the iron concentration.

It was concluded that the volume conduction process was controlled by an ionic mechanism in which lithium and sodium are the principal charge carriers. The effect of the iron concentration is presently being investigated.

THE INFLUENCE OF ASH CHEMISTRY ON THE VOLUME CONDUCTION IN FLY ASH

BY

ROY E. BICKELHAUPT
Southern Research Institute

INTRODUCTION

It is well known that one of the important considerations in the design of an electrostatic precipitator is the resistivity of the material to be collected.[1] Several of the preceding speakers at this symposium have emphasized this point. The literature[2] points out that a large number of factors control the magnitude of resistivity for fly ash produced from the combustion of coal.

In the absence of water vapor, ash resistivity is controlled largely by the chemistry, physical characteristics, and the temperature of the ash. The resistivity of fly ash without the influence of moisture is called volume resistivity. This property is of particular interest for precipitators functioning in the upper end of the operable temperature spectrum.

Moisture and other gases in the effluent can interact with the ash surface to provide an alternate conduction path. When measured resistivity is influenced by this process, the ash resistivity is termed surface resistivity. This effect is usually observed at lower operating temperatures due to the increased relative concentration of water vapor.

Precipitators for collecting fly ash normally operate after an air heater at a temperature where the ash resistivity is influenced by both surface and volume conduction. Research sponsored by the Environmental Protection Agency has been directed toward the identification of the factors affecting fly ash resistivity and the quantification of the relationship between resistivity and fly ash and flue gas chemistry. Knowledge pertaining to the conduction mechanisms and the chemical species involved will provide the approach by which resistivity may be predicted and altered.

This paper describes the first part of this investigation relating to volume conduction and illustrates the relationship between volume resistivity and ash chemistry. Additional research concerned with surface conduction phenomena is underway, but the results at this time are not conclusive.

BACKGROUND INFORMATION

Approximately twenty-five fly ash samples representing a reasonable cross-section of the ashes produced by coal-burning, steam-generating plants in the United States have been examined. The ashes have been physically, structurally, and chemically characterized. Two features of the characterization were especially noteworthy. First, a relatively large range in concentration for each element reported in chemical analysis occurs among the ashes. Table I shows the typical ranges found. Specific ashes possessed concentrations of certain elements outside the ranges shown. For example, isolated cases show greater amounts of Na_2O, CaO, and SO_3 with lesser amounts of SiO_2. With respect to this paper, the range of concentration of Na_2O and Fe_2O_3 should be noted. Second, the structural characterization revealed that

TABLE I

RANGES OF MAJOR CHEMICAL CONSTITUENTS REPORTED IN WEIGHT PERCENT AS OXIDES

Li_2O	0.01 - 0.07
Na_2O	0.13 - 2.66
K_2O	0.28 - 3.90
MgO	0.9 - 5.5
CaO	0.3 - 23.5
Fe_2O_3	3.9 - 23.7
Al_2O_3	17.9 - 31.0
SiO_2	40.2 - 61.0
TiO_2	0.8 - 2.3
P_2O_5	0.16 - 1.00
SO_3	0.07 - 1.83

all the ashes were principally amorphous. Three or four crystalline compounds could be identified, but the combined crystalline fraction was less than 10 to 15%.

Using a small group of these ashes selected with discrimination for chemical constitution, preliminary research was conducted regarding the volume resistivity-ash chemistry relationship. In particular, these ashes contained low, uniform concentrations of iron. The results[3] of this investigation will be published in the near future. The mode of research involved the measurement of resistivity and chemical transference on ash specimens which had been pressed and sintered into self-supporting discs. The primary conclusion from this research was that volume conduction in fly ash was controlled by an ionic mechanism having sodium ions as the principal charge carrier.

The present paper reiterates this point and treats another aspect of the volume resistivity-ash chemistry subject. Before examining the data reflecting ash resistivity as a function of ash chemistry, it would be of benefit to observe examples of the resistivity data. Figure 1 shows a group of curves relating resistivity to reciprocal absolute temperature. The curves form moreorless linear, parallel lines in compliance with an Arrehenius expression for resistivity. The similarity in the slope of the curves suggests that one conduction mechanism prevails in all the ashes. The three order of magnitude difference in resistivity between the upper and low curves indicates the pronouced effect

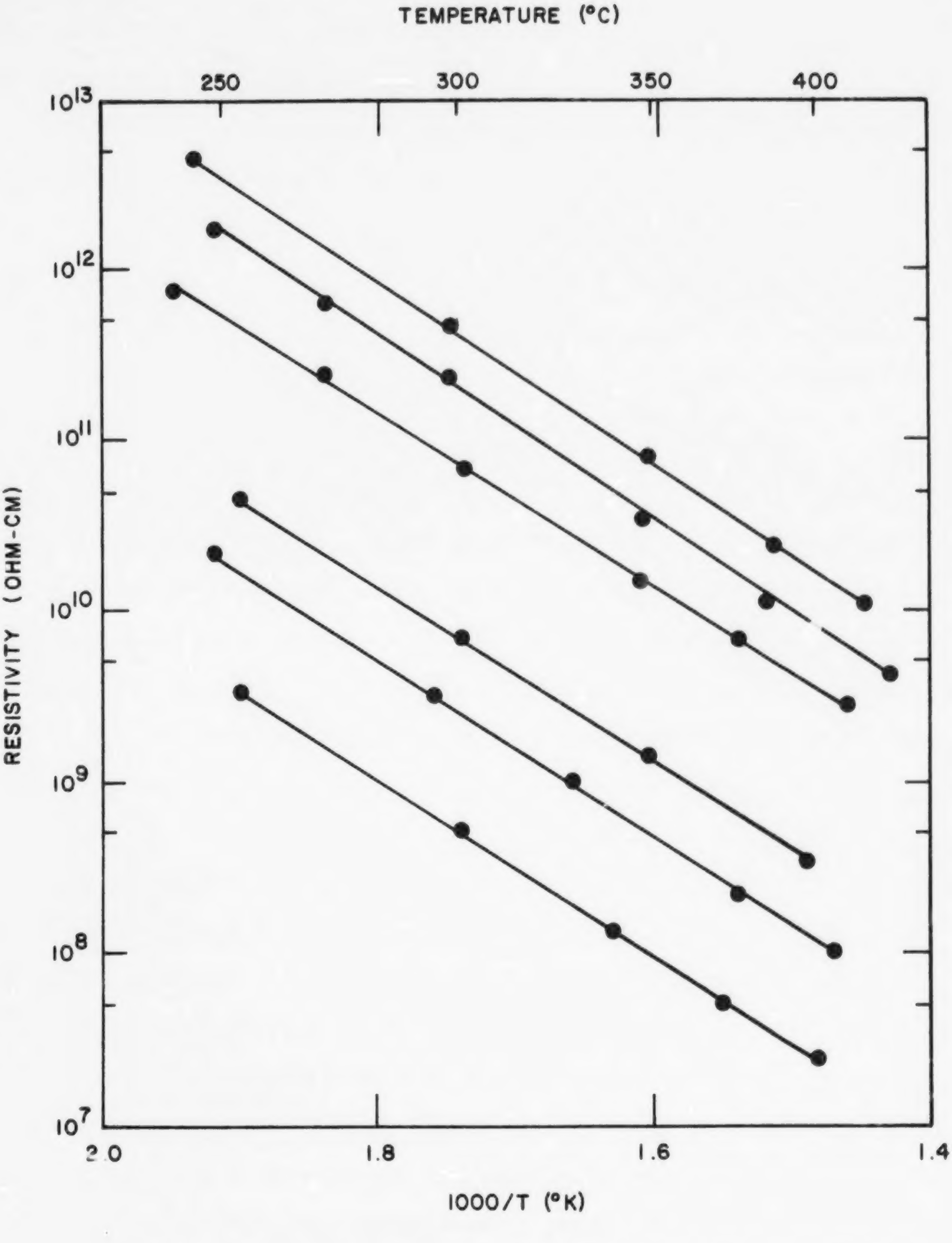

Figure 1. Resistivity (As Measured) vs Reciprocal Absolute Temperature, for Several Ashes Differing Principally in Na_2O Content

of ash chemistry. In the subsequent discussion, the values of resistivity used are those selected from the intersection of the resistivity-reciprocal temperature curve and the ordinate 1000/T = 1.6. These data were then empirically corrected to a constant porosity. The correction was established from the data for nine ash specimens for which resistivity was determined at two levels of porosity. Porosity was calculated from bulk and helium pycnometer density values. It is noteworthy that the correction used is similar to one which may be established from the data of Dalmon and Tidy.[4]

CORRELATION OF RESISTIVITY WITH CHARGE CARRIER CONCENTRATION

From the research detailed in reference 3 and synopzied above, it was concluded that an ionic volume conduction mechanism prevailed and that the principal charge carriers were lithium and sodium ions. Under these circumstances, the resistivity should be inversely proportional to the number of mobile charge carriers available.

Resistivities at a given temperature were plotted against the combined lithium and sodium concentrations of the respective ashes. Resistivity values corrected to 35% porosity were taken from plots of log resistivity versus 1/T for the temperature parameter value of 1000/K° = 1.6. The combined lithium and sodium concentrations, calculated from chemical analyses made on specific specimens used subsequently in the determination of resistivity, were expressed as molecular percentages. The molecular percentage was selected as a reasonable relative measure of the number of mobile carriers. The result of this approach is graphically illustrated in Figure 2.

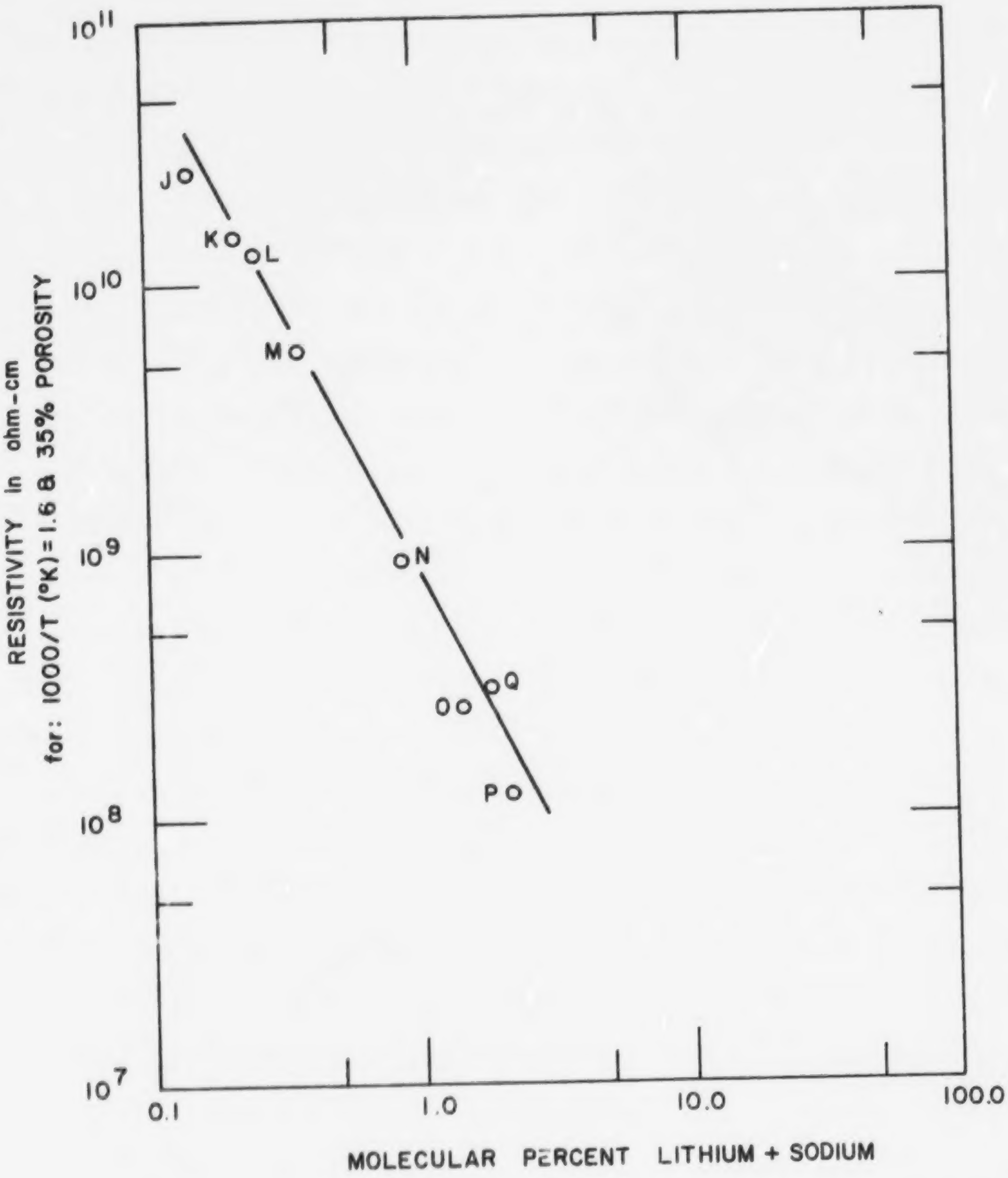

Figure 2. Resistivity vs Molecular Percent Lithium+Sodium for Western Ashes Differing Principally in Sodium Content

The constructed line is a least squares interpretation for eight data points obtained during the earliest part of the research. These data were obtained for a series of six ashes arbitrarily selected for minimal variation in overall chemistry and substantial differences in alkali metal content. These data points statistically had an excellent linear correlation coefficiency suggesting that the resistivity of the fly ash is indeed inversely proportional to the amount of lithium and sodium present. Furthermore, the slope of approximately two indicates the severity of the effect.

However, as more data were accumulated for ashes selected with no regard for overall chemistry, the previously indicated correlation seemed to deteriorate. After about twenty-five ashes had been examined, the situation shown in Figure 3 prevailed. All of the data points for Eastern ashes and a few for additional Western ashes were positioned below the established line. It was concluded that some other chemical species in addition to lithium and sodium had either a direct or indirect effect on the magnitude of resistivity. This effect was strong enough that by inspection of the resistivity data with reference to the total chemistry of the ashes it could noted that the higher iron contents were associated with lower resistivities.

To evaluate this observation, the resistivity data shown in Figure 3 were normalized to a constant percentage of lithium plus sodium using the coefficient of correlation indicated by the constructed line. These normalized data then represented the resistivity values expected if each ash contained the same molecular concentration of lithium plus sodium. The normalized data were then plotted against the molecular percentages of iron present in

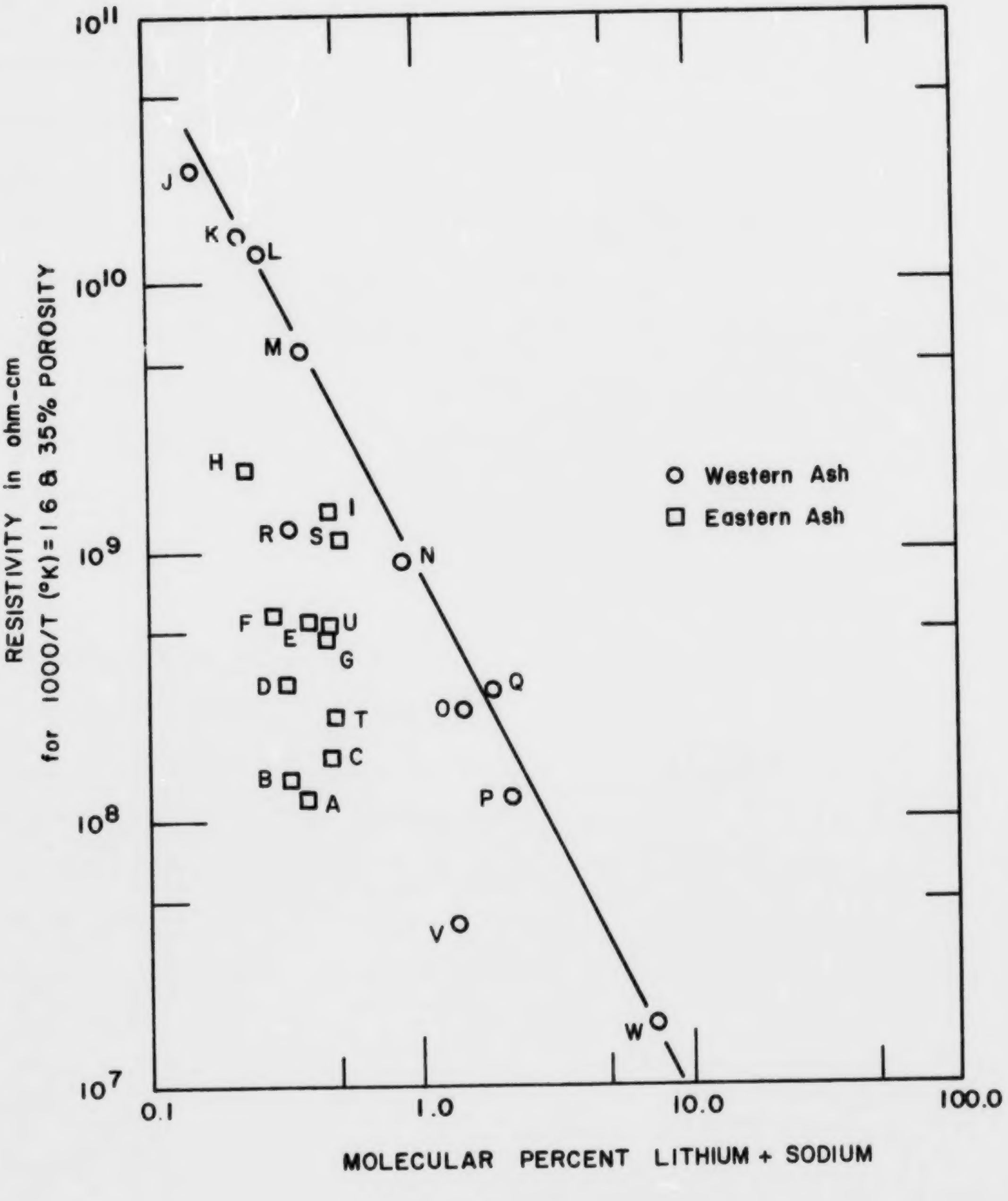

Figure 3. Resistivity vs Molecular Percent Lithium+Sodium for all Ashes Examined

the specific ashes. This is shown in Figure 4.

The correlation between resistivity and iron concentration shown in Figure 4 explains the data scatter in the previous figure where resistivity was plotted as a function of lithium plus sodium concentration. In Figure 3, the resistivity varied by two orders of magnitude at about 0.3 to 0.5 molecular percent sodium plus lithium. The fifteen data points plotted in this region represent the entire spectrum of iron concentrations for all the ashes examined in this laboratory. That no data points occurred above the constructed line in Figure 3 is not surprising. The data used to calculated this line came from ashes having a uniform iron concentration of the lowest level.

From the correlation shown in Figure 4, it becomes apparent that it is necessary to consider both the iron concentration and the sodium plus lithium concentration to define the volume resistivity of the fly ash. It can be seen that data point w does not conform well to the correlation. It should be noted that the ash used to obtain point w came from a pilot boiler and pilot precipitator, while all other ashes were taken from commercial, full scale equipment.

The Role of Iron

Since the effect of iron concentration on the magnitude of resistivity was apparently equivalent in severity to that of the combined sodium and lithium concentrations, research was conducted to define the role of iron. Two general hypothesis were advanced.

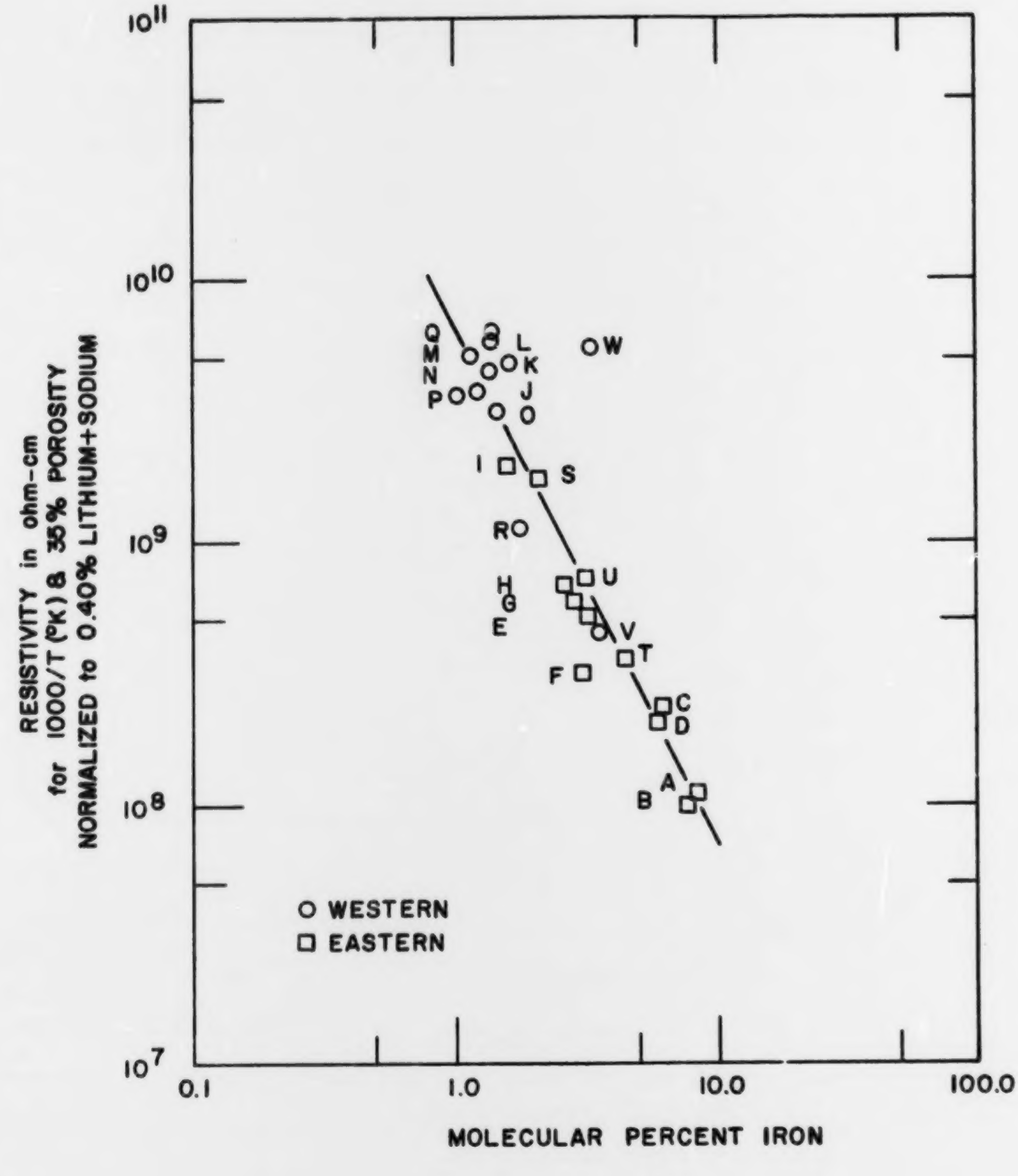

Figure 4. Resistivity Normalized to Constant Lithium+Sodium Concentration vs Molecular Percent Iron

On the one hand, the iron concentration may participate in the conduction process in a direct manner either by introducing an electronic component or an additional ionic carrier. From another viewpoint, the iron may perform in an indirect manner. It may affect the amorphous structure of the fly ash so that the effective concentration, the mobility, or the type of alkali metal serving as a charge carrier will be altered. Also, it could affect the heterogeneity of the ash so that the continuous conducting phase of the ash will possess an alkali metal concentration greater than that revealed by the average composition.

Four ashes containing a relatively uniform concentration of alkali metals but representing the total spectrum of iron concentrations encountered in this work were selected for additional experimentation.

Transference experiments were conducted on these four ashes to evaluate certain facets of the aforementioned hypotheses. For a description and discussion of the chemical transference experiments, one may consult reference 3. The type of experiment used and the character of the materials investigated precludes the extraction of unequivocal data. The data are meant to be used only for the qualitative understanding of the conduction process. The gravimetric data are representated in Figure 5. In this figure, the mass transferred out of the ash adjacent to the positive electrode toward the negative electrode is plotted against the quantity of electricity passed during the test. The lines labeled with the names of the alkali metals represent Faraday's Law. For example, if conduction were entirely ionic and potassium were the only charge carrier, one would expect a weight loss of about

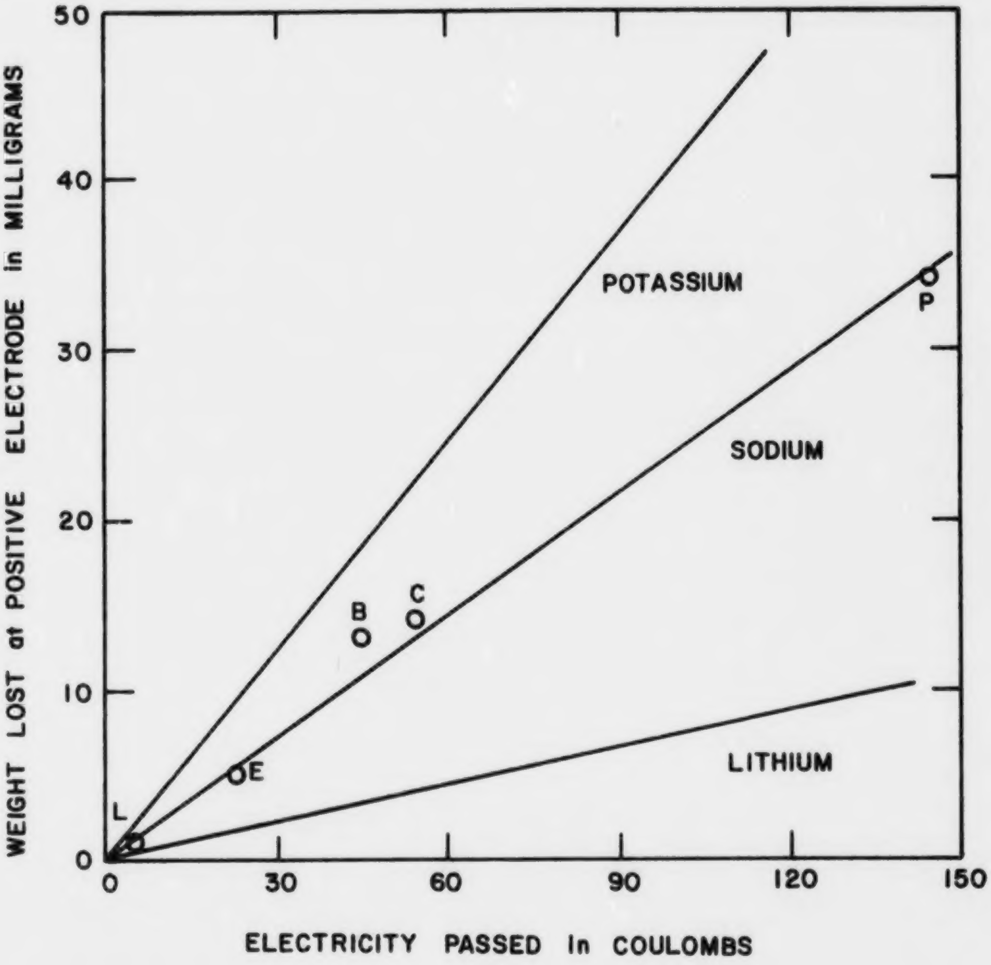

Figure 5. Gravimetric Data from Transference Experiments

50 mg for the passage of 120 coulombs of electricity. The open circles represent the experimental data points. These data strongly suggest that the electricity passed is accountable for by mass transfer and that sodium is the principal charge carrier. The only other way the data points could occur near the sodium line would be due to an averaging effect resulting from the migration of an element heavier than sodium coupled with the migration of a lighter element or an electronic contribution.

In Table II, the results of the chemical analyses for the transference experiments are given. The data show a trend similar to that experienced previously for transference tests on low iron specimens and that these data compliment or support the gravimetric data expressed in the Figure 5. For ashes containing from 5 to 22% weight percent iron, only the migration of sodium and lithium from the positive to the negative electrode can be detected. The small variations in potassium and iron concentrations are thought to be within the data error due to the technique of analysis and the selection of random samples. From this information, it was apparent that the iron does not act as an ionic carrier directly, and its presence in increased amounts does not induce the participation of potassium.

In carefully examining the data in Table II, it was observed that the percentage of lithium and sodium that had migrated, relative to the amounts initially present, increased with increasing iron concentration. An empirical parameter was devised to demonstrate this point. For a constant amount of electricity passed in each test, the percent increase in sodium and lithium

TABLE II

TRANSFERENCE EXPERIMENTS
CHEMICAL ANALYSES OF SPECIMENS
IN WEIGHT PERCENT

ASH	OXIDE	DISC CONTIGUOUS TO POSITIVE ELECTRODE	BASELINE COMPOSITION	DISC CONTIGUOUS TO NEGATIVE ELECTRODE
B	Li_2O	0.013	0.019	0.027
	Na_2O	-----	0.29	0.53
	K_2O	2.9	3.1	3.2
	Fe_2O_3	21.1	21.6	21.0
C	Li_2O	-----	0.024	0.041
	Na_2O	-----	0.45	0.80
	K_2O	-----	2.9	2.9
	Fe_2O_3	-----	16.8	16.6
E	Li_2O	0.03	0.04	0.05
	Na_2O	0.29	0.39	0.48
	K_2O	3.8	4.1	4.0
	Fe_2O_3	10.0	10.2	10.2
I	Li_2O	0.030	0.04	0.049
	Na_2O	0.40	0.48	0.56
	K_2O	3.9	3.9	4.0
	Fe_2O_3	4.8	4.9	4.9

content at the negative electrode over that contained initially by the ash was computed as "relative effectiveness". When this parameter was plotted against the iron concentrations of the four ashes studied, the result shown in Figure 6 was obtained. The increase in the relative effectiveness parameter with increasing iron concentration suggests that the role of iron is indirect in that it seemingly enhances the participation of lithium and sodium in the conduction process.

It is doubtful that the iron concentration affects the mobility of the subject alkali metals, for no appreciable deviation in experimental activation energy had been noted among all the tests run. However, it is conceivable that the iron concentration could influence the number of mobile charge carriers. Although one may use the total concentration of a particular ion species to graphically display data, it is highly probable that not every ion of the given type is free to migrate. It can be suggested that the role of iron is to in some way, possibly structurally or magnetically, alter the amorphous ash to allow the participation of a greater percentage of the total available sodium and lithium ions. Also in a manner unrelated to the amorphous structure, the iron concentration could induce additional heterogeneity so that the continuous phase that is responsible for conduction may contain a concentration of sodium and lithium that is greater than the average amount reported by chemical analyses.

The potential electronic contribution to the total conduction process due to iron was also considered. Although the uniformity of experimental activation energies among the ashes examined and

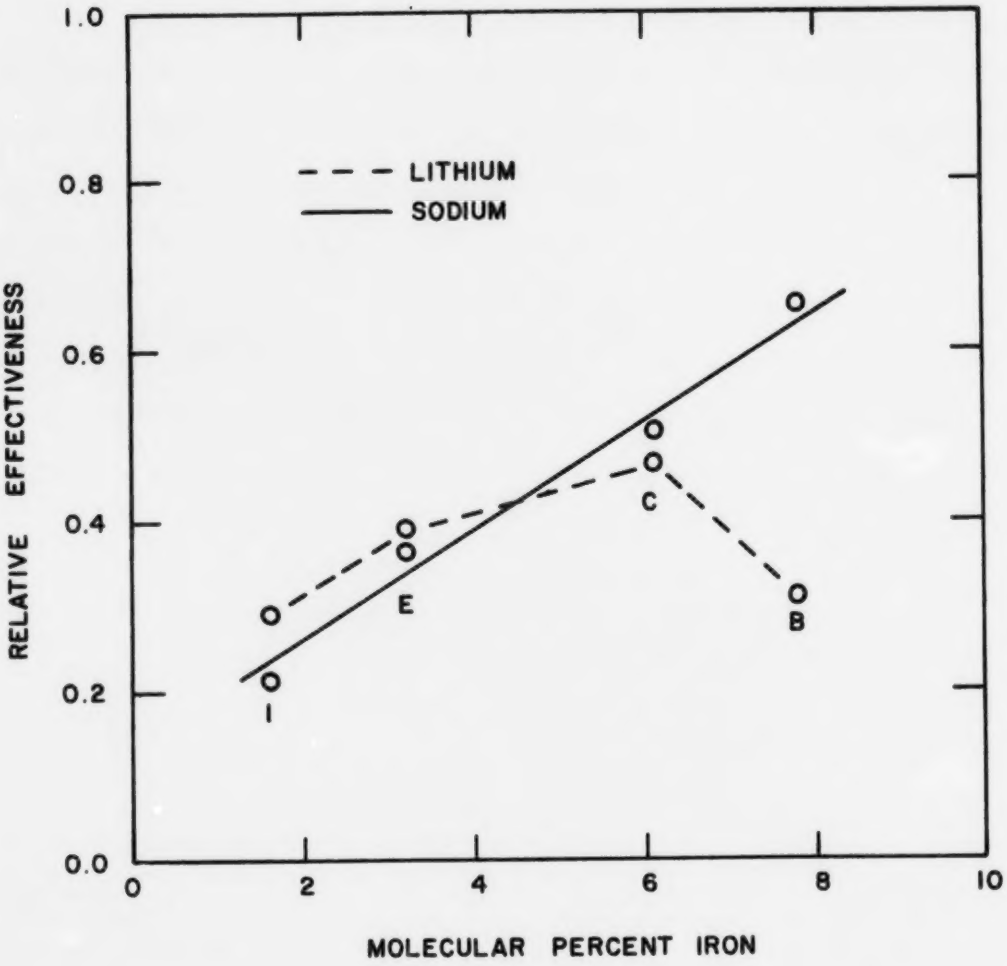

Figure 6. Relative Effectiveness of Lithium and Sodium as Charge Carriers as a Function of Iron Concentration

the pronouned effect of polarization demonstrated by current-time curves do not support an electronic contribution, two additional experiments were conducted. One ash was repeatedly put through a magnetic separator until half of the original iron concentration was eliminated and then formed into a test specimen. Since the resistivity of this specimen was almost identical to that of the one without the magnetic fraction removed, it would seem doubtful that the pronounced effect on resistivity due to iron was related to an electronic contribution. Also, a single experiment was conducted in which an ash specimen high in iron was used as a solid electrolyte in a galvanic cell.[5] The results were compared to that of the same cell with stabilized zirconia as an electrolyte. Only an ionic contribution to the conduction process was detected.

SUMMARY

From the characterization of a large number of fly ashes collected from commerical power stations in the U.S. and Canada, a collected layer of ash is visualized as an assemblage of more or less spherical, mainly amorphous particles accumulated to some degree of compaction. At temperatures where volume conduction predominates, it is concluded that the charge is carried through the layer by an ionic mechanism in which lithium and sodium are the principal carriers. An overall conduction process satisfying the required electrostatic balance was described in Reference 3. It is also concluded that the iron concentration of the ash in some unclear manner influences the number of lithium and sodium ions capable of mobility.

The conclusion that sodium ions were the principal charge carriers through the layer of collected ash was tested in a pragmatic manner in the laboratory and in the field. In the laboratory, a calculated quantity of sodium was introduced in the form of sodium carbonate to an ash sample of known chemical analysis prior to preparing pressed and sintered resistivity specimens. The addition of sodium produced a reduction in resistivity in excellent agreement with the reduction predicted by the data presented in this paper.

Sodium carbonate was also used to make predetermined additions of sodium to an ash of known chemical composition by adding the material to the coal feed of a commercial boiler. The objective in this case was to raise the Na_2O content of the ash from 0.2% to 2.0%. Both the insitu measurements made at the precipitator and resistivity measured made on ash returned to the laboratory showed a two order of magnitude decrease in resistivity which was the amount predicted for the addition selected.

From the ancillary tests described above, one can conclude that the effect of sodium can be quantified and that the effect is observed in commercial tests as well as in the laboratory.

REFERENCES

1. White, H. J., Industrial Electrostatic Precipitation, Addison-Wesley Publishing Company, Reading, Massachusetts (1963).

2a. White, H. J., "Chemical and Physical Particle Conductivity Factors in Electrical Precipitation", Chem. Engr. Progress 52, 244-248 (June 1956).

2b. Shale, C. C., Holden, J. H., and Fasching, G. E., "Electrical Resistivity of Fly Ash at Temperatures to 1500°F, RI7041, Bureau of Mines, U.S. Department of the Interior (1968).

2c. Maartmann, Sten, "The Effect of Gas Temperature and Dew Point on Dust Resistivity and Thus the Collecting Efficiency of Electrostatic Precipitators", Paper EN-34F, Second International Clean Air Congress of the International Union of Air Pollution Prevention Association, December 6-11, 1970, Washington, D. C., U.S.A.

2d. Dalmon, J., and Raask, E., "Resistivity of Particulate Coal Minerals", J. Inst. Fuel 46 (4) 201-205 (April 1972).

2e. Selle, S. J., Tufte, P. H., and Gronhovd, G. H., "A Study of the Electrical Resistivity of Fly Ashes from Low-Sulfur Western Coals Using Various Methods", Paper 72-107, presented at the 65th Annual Meeting of the Air Prevention Control Association, Miami Beach, Florida (June 18-22, 1972).

3. Bickelhaupt, R. E. "Electrical Volume Conduction in Fly Ash", J. Air Pol. Con. Assoc., (March 1974).

4. Dalmon, J. and Tidy, D., "A Comparison of Chemical Additives as Aid to the Electrostatic Precipitation of Fly Ash", Atmos. Environ. 6 (10) 721-734 (1972).

5. Kiukkola, K. and Wagner, C., "Measurements on Galvanic Cells Involving Solid Electrolytes", J. of the Electrochemical Soc. 104 (6) 379-387 (1957).

544a

SESSION 6

NEW CONCEPTS

Chairman: J. K. Burchard
U. S. Environmental Protection Agency
Research Triangle Park, N. C.

Paper No.

23 Basic Processes in Fine Particle Control

James R. Brock
University of Texas
Austin, Texas

24 Systems of Charged Particles and Electric Fields for Removing Sub-micron Particles

James R. Melcher and
K. S. Sachar
Massachusetts Institute of Technology
Cambridge, Massachusetts

25 Advances in the Sonic Agglomeration of Industrial Aerosol Emissions

David S. Scott
University of Toronto
Toronto, Ontario, Canada

Paper No. 23

BASIC PROCESSES IN FINE PARTICLE CONTROL

by

James R. Brock

UNIVERSITY OF TEXAS

Austin, Texas

ABSTRACT

Some of the fundamental physico-chemical processes available for fine particle control are analyzed briefly. These include primary processes such as impaction, diffusion, electrophoresis, thermophoresis, diffusiophoresis, etc., and secondary processes which alter the particle size distribution such as coagulation, condensation, and charging. New techniques for fine particle collection are possible utilizing coagulation and condensation in conjunction with the primary processes. Only a relatively small number of primary and secondary processes have been utilized up to the present time, so that it is likely that improvement can be obtained through additional investigation of fine particle control techniques.

BASIC PROCESSES IN FINE PARTICLE CONTROL

Introduction

The purpose of this paper is to indicate the very large number of possibilities which are open in the development of new fine particle collection methods. Present techniques for removing suspended particles from industrial gas streams are well known to be inefficient in removing fine particles—those particles with equivalent diameters less than the order of 1 μm.

Before discussing these basic collection processes, let us note some of the rationale for the control of fine particles and the inconsistency of total mass emission standards in achieving a certain mass of suspended particulate matter in the atmosphere.

It is well known that the fine particles in the size range of the order 0.1 -- 1.0 μm diameter have the maximum probability of reaching the lower lung where lung clearance mechanisms for such contaminants are believed to have the least efficiency. Such particles in the 'respirable range' are therefore most heavily implicated in laboratory and epidemiological studies which indicate adverse health effects of toxic and irritant particles (1). Particles in this same size range are also known to be responsible for much of the loss in visibility and solar insolation in urban areas (2).

Many governmental regulations limit particulate emissions according to the total mass rate of such emissions. Such regulations are designed to limit the total mass of suspended particulate matter in the atmosphere but are somewhat inconsistent inasmuch as they do not recognize another aspect of the nature of fine particles -- their relatively large residence time in the atmosphere. Table 1 illustrates the inadequacy of total mass emission standards by way of example. In this table are presented certain primary sources of particulate matter, their total mass emission rates for the U.S., the estimated mass median diameters of particles emitted from such sources, and the total mass of such aerosol from each source in the atmosphere at a given time. These last numbers are obtained from estimated mean residence times.

One can see from Table 1 (3) that even though the automobile has the lowest total mass emission rate, the mass of particulate matter in the atmosphere from the automobile is nearly an order of magnitude greater than a source whose total mass emissions are themselves an order of magnitude greater than the automobile.

TABLE 1

ATMOSPHERIC PARTICULATE MASS

	Primary Source	Mass Emission Rate, Tons/yr., U.S.	Mass Median Diameter, μm	Atmospheric Mass, tons
1.	Automobile	4×10^5	0.4	2×10^4
2.	Petroleum FCC Units	4.5×10^5	0.5	1.5×10^4
3.	Coal Fired Electric Utility, Pulverized	3×10^6	10	5×10^3
4.	Crushed Stone, Sand, Gravel	5×10^6	20	4×10^3

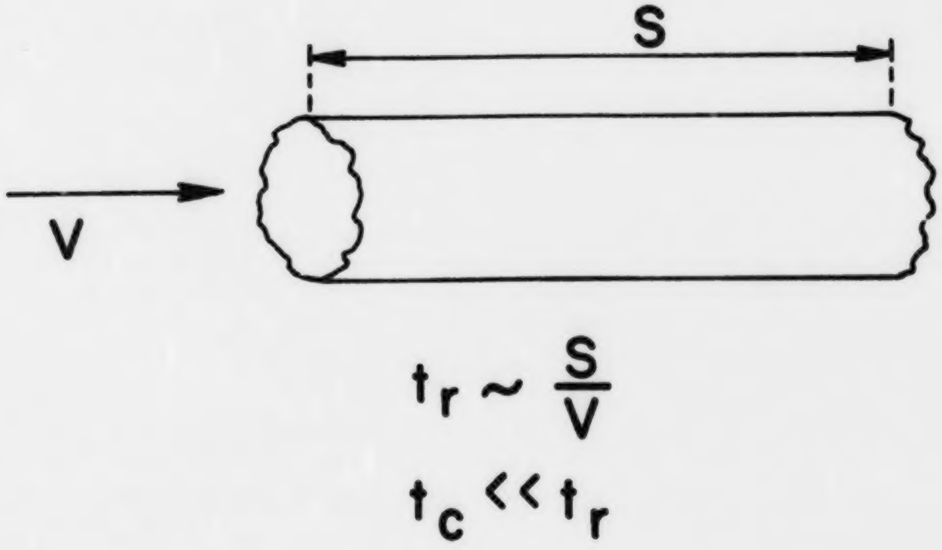
S
V
$t_r \sim \frac{S}{V}$
$t_c << t_r$

Figure 1.

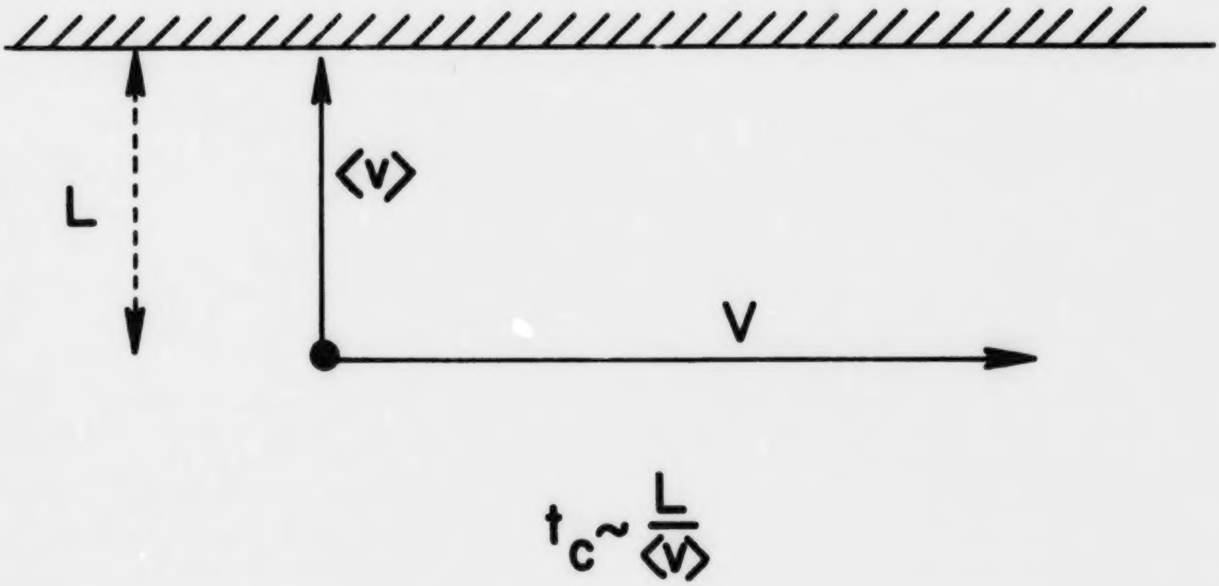
L
$\langle v \rangle$
V
$t_c \sim \frac{L}{\langle v \rangle}$

Figure 2.

Thus, control of fine particles is even more critical than that of larger particles if one seeks to limit mass of suspended particulate matter in the atmosphere over large areas.

In the discussion which follows the fundamental aspects of any particle control process are noted. Basic parameters for particle collection -- residence time and capture time -- are discussed. Examples of basic processes of particle collection are listed and some illustrations are given of their relation to particle size and their possible efficacy for fine particle control. Specific control devices will not be discussed nor will reentrainment phenomena be mentioned.

Processes for Fine Particle Control

Consider the basic processes of particle collection. Such collection involves the removal of the particles from the suspending gas, usually, but not always, by deposition on a surface, which could be, for example, the collection plate of an electrostatic precipitator, a water droplet as in a wet scrubber, and so forth. Of practical necessity, particle control processes are dynamic processes and one is therefore concerned with such variables as residence time of particles in a given device and the time necessary for collection of the particle. If V is the velocity of the particle-gas system through a given particle collection device and S is the distance in the direction of flow, then we can say that the residence time is of the order of S/V for the particles in the device. Clearly if one is to have an efficient collection method it is necessary that the time for capture of particles, t_c, be substantially less than this mean residence time for particles in the device. Figure 1 illustrates the concept of residence time and Figure 2 that of capture time, t_c.

The time for capture of particles in the device can be represented schematically as the ratio of some distance for collection, L, to an average speed of migration, <v>, owing to some external force acting on the particle. The distance L could be, for example, the distance an average particle must travel to some collection surface. In an electrostatic precipitator, this could be the order of the distance between collection plates or in the case of a wet scrubber, it could be the average distance between water drops. Therefore, L is a geometric parameter connected with the design of a particular collection device. The mean migration velocity <v>, however, is a function of the properties of the particle and the basic processes or forces of collection. For these reasons we will focus attention on <v> and consider how this migration velocity is related to particle size and the nature of the collection process. One can then easily imagine a large number of geometrical arrangements for carrying out particle collection.

One can classify the basic control processes as either primary or secondary. The primary control processes are those which directly produce a particle migration velocity. Examples are listed in Table 2 and include particle diffusion, sedimentation, electrophoresis, thermophoresis, diffusiophoresis, etc. This list is certainly not exhaustive. Secondary processes have the principal function of altering the particle size distribution so that the primary processes will be more efficient. Examples of secondary processes are coagulation or agglomeration, condensation of some molecular constituent on existing particles, evaporation wherein one seeks to evaporate the particle completely, and finally electrical charging.

We can examine a few of these primary processes in terms of their relative magnitudes and their dependence on particle size.

Figure 3 presents the migration velocity associated with centrifugation in fields of one and fifty times the gravitational acceleration. It is noteworthy that fine particles have small migration velocities even in relatively large centrifugal fields.

Figure 4 gives migration velocities associated with particle diffusion in a particle laden gas flowing through a one-inch diameter pipe. The migration velocity associated with Brownian diffusion, which arises from random molecular impacts on a particle, decreases rapidly with increasing particle size. Turbulent diffusion of particles produced by transport of particles by turbulent eddies is presented for comparison at a Reynolds number of 10^4. If Figures 3 and 4 are overlaid, one observes, regardless of the conditions, a definite minimum at $\sim$0.1 μm in the resultant value of <v>. Therefore, processes which depend on both diffusion and centrifugation (or impaction) will have a pronounced minimum in their effectiveness at about 0.1 μm diameter in particle size.

Figure 5 compares the process of thermophoresis with that of electrophoresis. The curve for electrophoresis, the movement of electrically charged particles in an electric field, represents the migration velocity for particles having approximately 50% of their saturation charge moving in an electric field of 4 kV/cm. One notes for electrophoresis again a minimum in <v> at the order of 0.1 μm diameter particle size, and a marked decrease with decreasing particle size of the magnitude of <v>. This is to be compared with the thermophoresis of sodium chloride particles to an 800 μm particle at a temperature difference between particle and gas of 100 degrees C. The term thermophoresis refers, of course, to the motion of a particle in a gas owing to a temperature gradient imposed on the suspending gas. It can be noted that the magnitude of <v> owing to thermophoresis decreases

TABLE 2

CONTROL PROCESSES

Primary	Secondary
Sedimentation	Coagulation
Impaction	Condensation
Interception	Evaporation
Diffusion	Charging
Image Force	
Phoresis:	
Electro- Magneto- Thermo- Diffusio- Photo-	

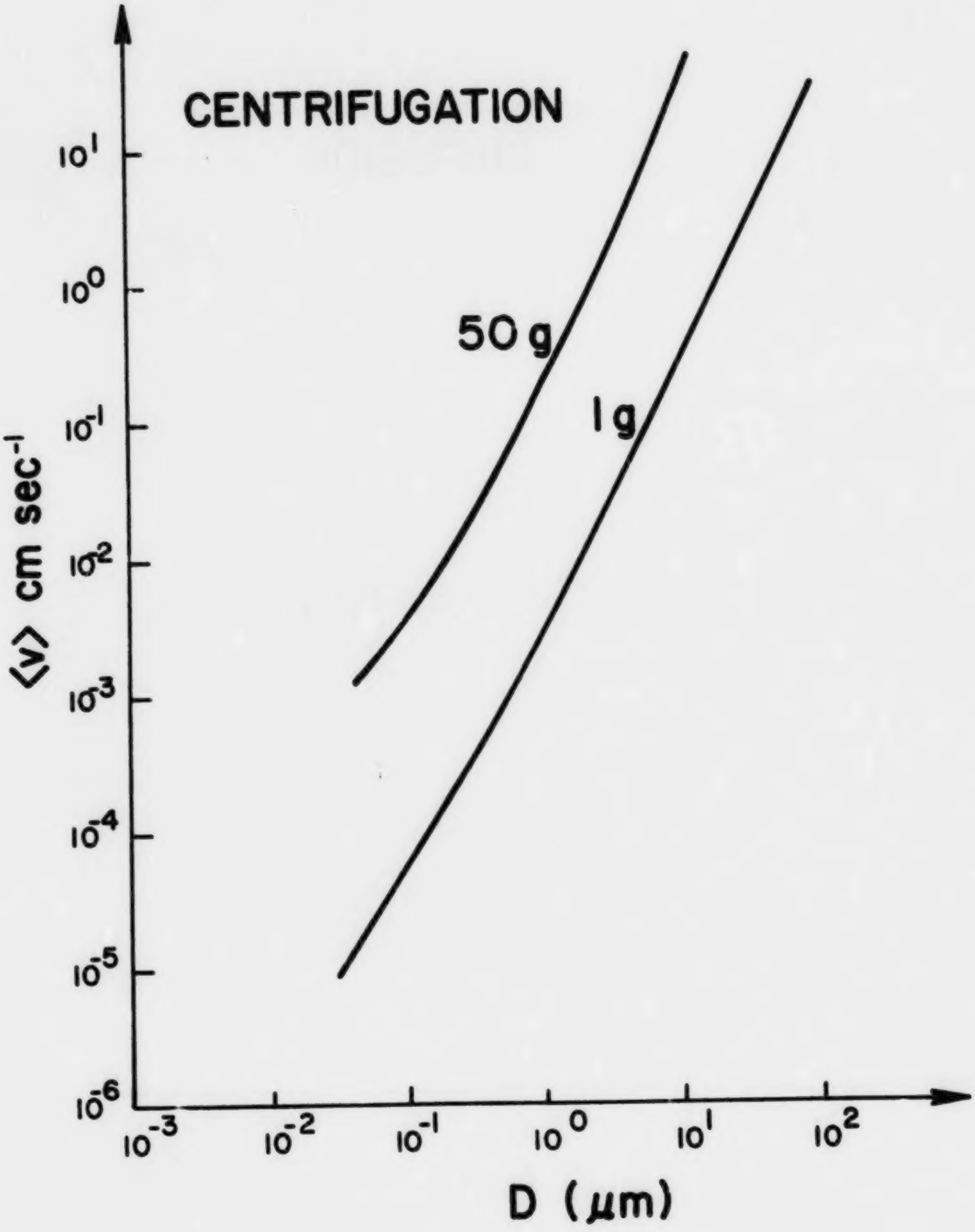
CENTRIFUGATION
50 g
1 g
⟨v⟩ cm sec⁻¹
10¹
10⁰
10⁻¹
10⁻²
10⁻³
10⁻⁴
10⁻⁵
10⁻⁶
10⁻³
10⁻²
10⁻¹
10⁰
10¹
10²
D (μm)

Figure 3.

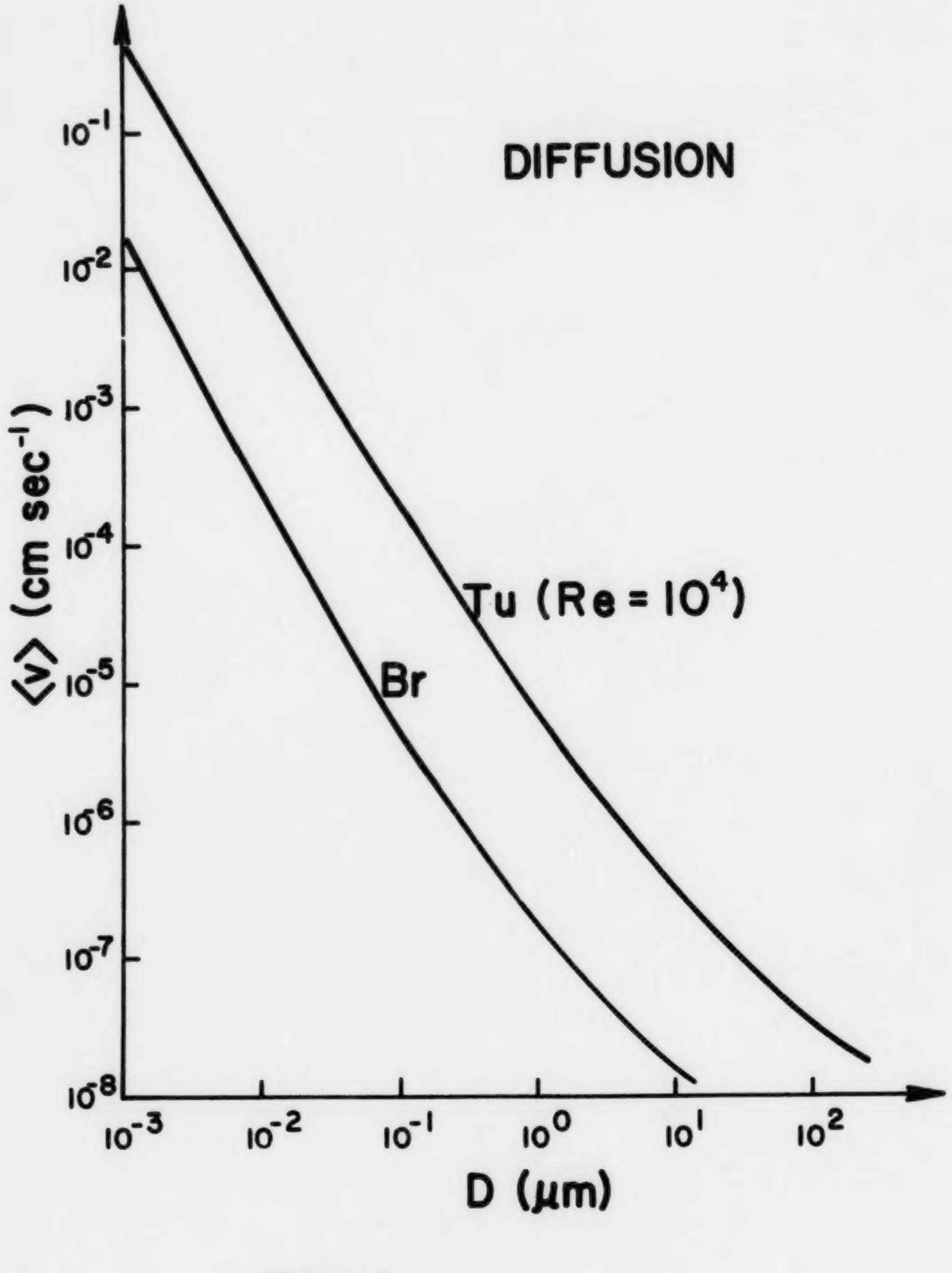
DIFFUSION
Tu (Re = 10^4)
Br
⟨v⟩ (cm sec^-1)
10^-1
10^-2
10^-3
10^-4
10^-5
10^-6
10^-7
10^-8
10^-3
10^-2
10^-1
10^0
10^1
10^2
D (μm)

Figure 4.

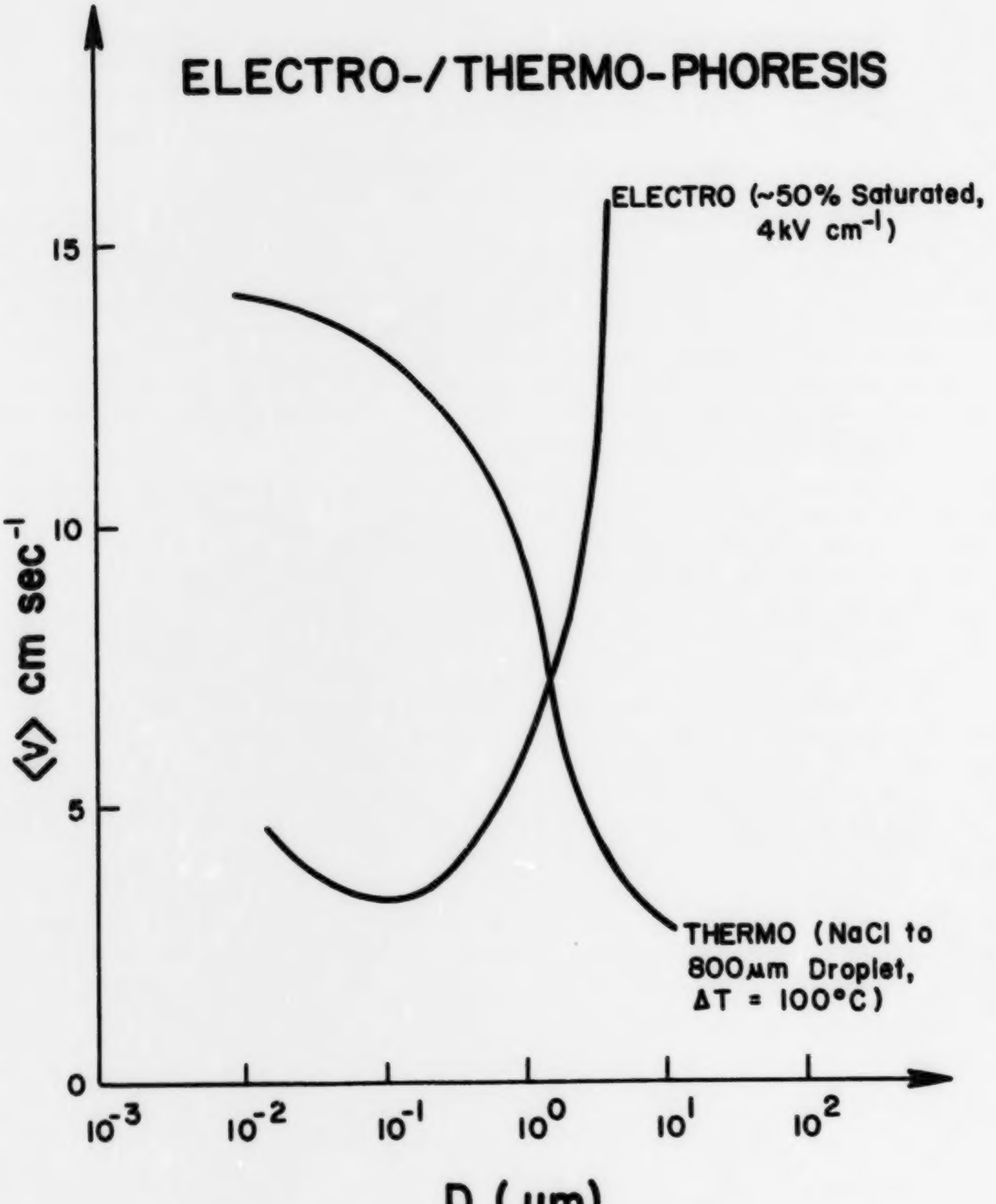
ELECTRO-/THERMO-PHORESIS
ELECTRO (~50% Saturated, 4kV cm⁻¹)
THERMO (NaCl to 800μm Droplet, ΔT = 100°C)
⟨v⟩ cm sec⁻¹
0
5
10
15
D (μm)
10⁻³
10⁻²
10⁻¹
10⁰
10¹
10²

Figure 5.

with increasing particle size, in contrast to the example of electrophoresis, and that indeed with this large imposed temperature gradient the magnitude of <v> owing to thermophoresis is comparable to that of electrophoresis.

Figure 6 compares the magnitudes of <v> for diffusiophoresis and thermophoresis to an 800 μm water drop suspended in air. Diffusiophoresis refers to the particle migration process induced by the presence of a concentration gradient in the suspending gas. The upper curve indicates <v> owing to diffusiophoresis, the positive sign indicating that the particle travels toward the drop. The lower curve indicates the thermophoretic velocity owing to the temperature gradient associated with the condensation process occurring on the water drop. This thermophoretic velocity is in the opposite direction from and much smaller than that owing to diffusiophoresis.

For these primary processes as well as those not listed here, the magnitude of <v> is critically dependent on particle size. Also in most cases, particularly in those presented in the preceding figures, those processes having large values of <v> for large particles have small values for small particles. One may refer in particular to the processes of centrifugation (impaction is implicit here) and electrophoresis, which form in part the basis for the important control process for large particles of electrostatic precipitation, wet scrubbing, and filtration. Hence, in general, by increasing particle size one can more efficiently utilize conventional particle collection processes for fine particle collection. This observation forms the motivation for the utilization of two of the secondary processes in Table 2 -- coagulation and condensation.

The desired effect from application of condensation or coagulation in control processes would be to increase the mean size of the particles in an aerosol. Both processes have the desired effect, but differ in the rate at which the increase occurs and in the nature of the alteration of the particle size distribution of the aerosol.

For the coagulation process one can write the equation describing the dynamics of change of the particle size distribution $n(r,t)$ where r is particle radius and t is the time (4):

$$\frac{\partial n(r,t)}{\partial t} = \tfrac{1}{2}\int_0^r b(r',r'')n(r')n(r'')dr' - n\int_0^\infty b(r,r')n(r')dr'$$

This relation for a spatially homogeneous system indicates that particles are contributed to the size class r by collisions between two particles of size less than r, as indicated by the

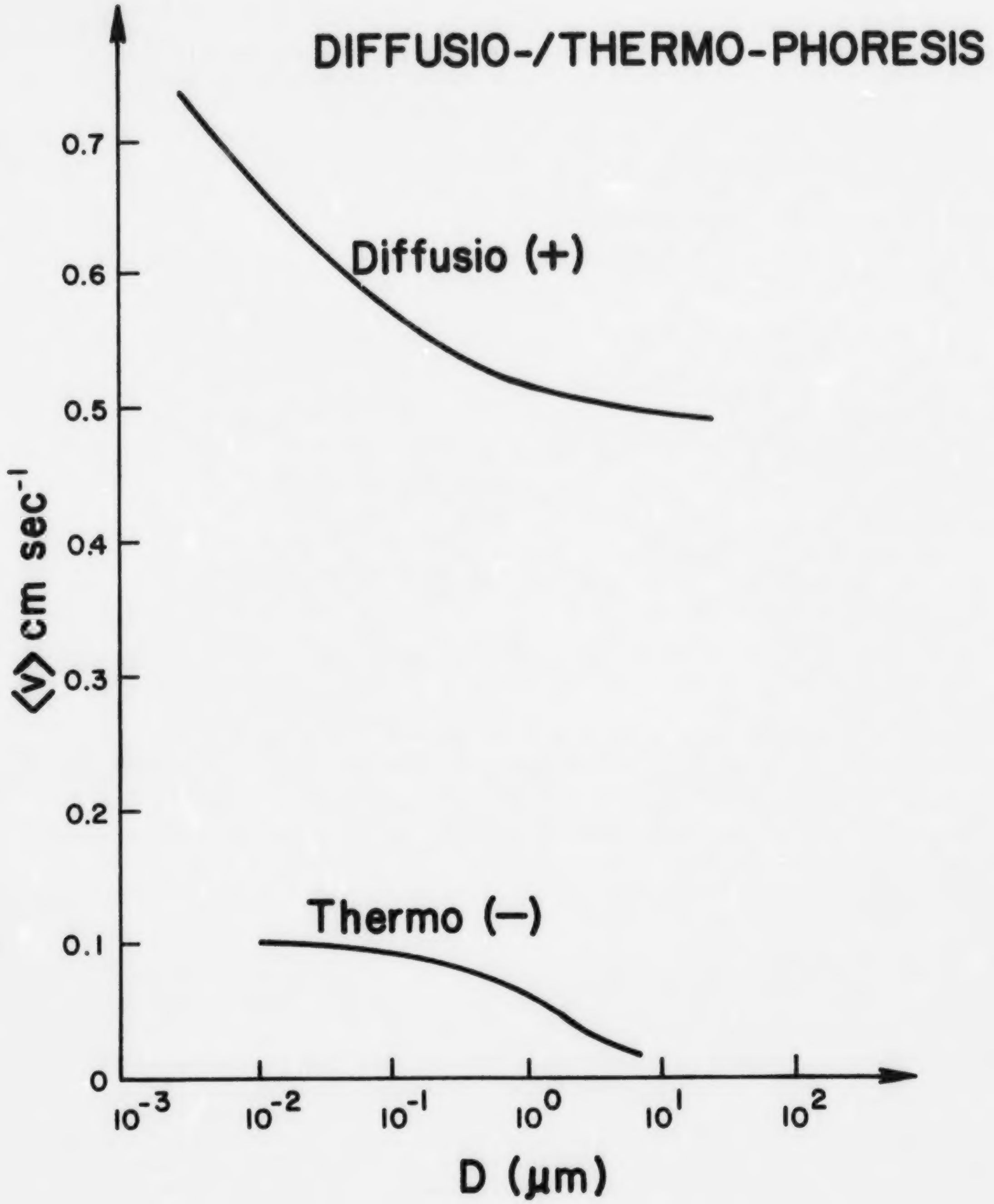
DIFFUSIO-/THERMO-PHORESIS
Diffusio (+)
Thermo (–)
⟨v⟩ cm sec^{-1}
0.7
0.6
0.5
0.4
0.3
0.2
0.1
0
10^{-3}
10^{-2}
10^{-1}
10^{0}
10^{1}
10^{2}
D (μm)

Figure 6.

first term on the right hand side of the equation, and that particles are lost from size class r by collision of a particle of that class with any other particle in the distribution. The mean size <r> of the particle size distribution will increase with time according to the approximate relation:

$$\langle r \rangle \sim (3\ \mu \bar{b} t / 4\pi\rho)^{1/2}$$

for a total mass concentration of particles μ, a mean collision frequency $\bar{b}$, and particle mass density ρ.

One has possible control over the magnitude of the mean collision frequency $\bar{b}$ appearing in this equations. One might also try to alter the initial mass concentration, μ, of particles by the addition of a large particle fraction. A possible defect in the utilization of coagulation for increasing the mean size of particles lies in the fact that usually coagulation acts to broaden the particle size distribution. That is,

$$\frac{\delta}{\langle r \rangle} \sim t^{\alpha}\ ,\ \alpha \geq 0$$

the standard deviation δ to the mean radius <r> is an increasing function of time in most situations. This increase in polydispersity owing to coagulation obviously presents problems in most collection processes inasmuch as we have seen that the primary collection processes will differ widely with particle size in their efficiency.

One can also write down a similar rate expression for the change with time of the particle size distribution owing to condensation of some molecular constituent on the particles:

$$\frac{\partial n(r,t)}{\partial t} = -\frac{\partial}{\partial r}\{\underline{a} f(r) n(r,t)\}$$

Here $\underline{a}$ is a parameter which depends on the supersaturation of the molecular constituent undergoing condensation, $f(r)$ is a function specifying the diffusional rate of condensing molecules to the particles and is dependent on such factors as the Reynolds and Knudsen numbers of gas dynamics. In contrast to coagulation, all condensation processes act to diminish the ratio of standard deviation to mean size for the particle size distribution. This statement holds for all particle sizes (4).

Conclusions

Up to the present, particle collection technology has employed only a relatively small number of the primary and secondary processes which we have listed in Table 2. However, even in this somewhat restricted list one can pose hundreds of possible combinations of primary and secondary processes to effect fine particle collection. Additional investigation of such possibilities should be encouraged as it seems probable that improvement can be obtained in fine particle collection efficiency.

Acknowledgment

Author wishes to acknowledge the support of the Chemistry and Physics Laboratory, National Environmental Research Center, Environmental Protection Agency.

REFERENCES

1. Friedlander, S. K., Environ. Sci. Tech., 7, 1115 (1973).

2. Kerker, M., "The Scattering of Light and Other Electromagnetic Radiation", Academic Press, N.Y. (1969).

3. Hidy, G. M. and Brock, J. R., "The Dynamics of Aerocolloidal Systems", Pergamon Press, Oxford, (1972).

4. Brock, J. R., Proceedings of the Faraday Society, (1973).

Paper No. 24

SYSTEMS OF CHARGED PARTICLES AND ELECTRIC FIELDS FOR REMOVING SUB-MICRON PARTICLES

by

J. R. Melcher
and
K. S. Sachar

MASSACHUSETTS INSTITUTE OF TECHNOLOGY

Cambridge, Massachusetts

ABSTRACT

Charged droplets, used as collection sites for charged particulate, result in a class of devices which combine the characteristics of a conventional scrubber and a conventional electrostatic precipitator. An overview will be given on the fundamental time constants governing the performance of these particulate control devices making use of charged drops or particles as collection sites. Experiments will be described that support the time constant picture of electrostatic agglomeration and self precipitation processes among particles in the sub-micron range, in the super-micron range, and finally among charged collection sites and the sub-micron particulate. A summary will be given of what are felt to be the over-riding issues in making electrically induced agglomeration processes a competitive approach to controlling sub-micron particulate.

I. Introduction

Electrostatic precipitators and wet-scrubbers have been the subjects of entire sessions in this symposium. Charged drop scrubbers, which are the subject of this paper, are a hybrid of these devices. Charged particles, typically exceeding 20 micron in diameter, are used as collection sites for oppositely charged submicron particles. Although we are also working on schemes that make use of solids as collection sites, in this discussion the large particles will be water drops. If compared to an electrostatic precipitator, the charged-drop scrubber replaces the electrodes with drops. If compared to a wet-scrubber, the effects of fine particle inertia, conventionally responsible for causing impaction, are replaced by an electric force of attraction.

No attempt is made here to trace the history of charged-droplet scrubbers since the pioneering efforts of Penney in the 1930's.(1,2) Rather, remarks are aimed at i) giving a fundamental view of the "bottleneck" issues that dominate in a wide range of seemingly different devices making use of electric fields induced by charge on systems of drops and sub-micron particles, and ii) to describe experiments that demonstrate the validity of this view. These experiments are designed to control and vary essential parameters so as to isolate and test the mechanisms governing scaling. In devices designed to achieve the highest possible collection efficiency it is by contrast desirable to incorporate other collection mechanisms such as those at work in the electrostatic precipitator and in the inertial impact scrubber.

We are fortunate to have as a participant in this symposium Dr. M. J. Pilat, who is in the forefront of those attempting to show the practical feasability of charged-drop scrubbers.

II. Critical Time-constants

If we key on gas residence-time in a control device as a major factor in determining its competitive position, then it is possible to characterize devices in terms of critical time-constants. For example, in a conventional precipitator, the critical time-constant is the time τ_p required for the charged submicron particles having mobility b to travel the distance s between electrodes in an imposed electric field E_s. This is true whether the device is in laminar flow or, as is typical of practical devices, in turbulent flow. In detail, the collection law in these devices are significantly different, but basically they are characterized by this same characteristic time τ_p. For a precipitator to be practical, τ_p must be short compared to the gas residence time.

The precipitation time τ_p, as well as three time constants essential to the performance of charged-drop scrubbers, are summarized in Fig. 1. For reference, nomenclature is presented in Table 1.

Table 1. Summary of nomenclature

$$\varepsilon_o \equiv 8.85 \times 10^{-12}$$

	number density	charge	mobility	radius
drop	N	Q	B	R
particulate	n	q	b	a

If a volume is filled with particles charged to the same polarity, then τ^* typifies the time required for these particles to self-precipitate on the walls. This time is based on the system parameters of particle number density n, particle charge q, and mobility b. Note that it does not involve the dimensions of the device. As a variation of this configuration, if a volume is filled with regions of positively charged particles and other regions of negatively charged particles, then τ^* typifies the time required for the oppositely charged particles to intermingle.

If, to prevent space-charge fields, positively and negatively charged particles are mixed, then τ^* (based on the density of one or the other of the species) is the time required for self-discharge and perhaps self-agglomeration of the particles.

The time required for collection of fine particles on oppositely charged drops is typically τ_d. This collection time is also based on the mobility of the fine particles, but the charge-density NQ of the drops rather than that of the particles (nq). The residence time of the gas must be at least of this order for the device to be practical.

For a system of charged drops, τ_R plays the role that τ^* does with respect to the particles. Thus, in a system of like-charged drops, τ_R is the self-precipitation time of the drops, while in a system of oppositely charged drops where there is no space-charge due to the drops, this same time-constant governs how long the drops will retain their charge before at least discharging each other and probably agglomerating.

A simple model that motivates the physical significance of τ^*, τ_d and τ_R in the role of inducing self-discharge and particle collection is shown in Fig. 2. The equation of motion for this two particle model, included in Fig. 2, is easily solved. Then, by recognizing the relation between initial interparticle spacing and particle densities, the three time constants are obtained as limiting cases. These three limits are summarized in Fig. 3.

The theory of Whipple and Chalmers$^{(2,3)}$ gives a detailed description of the collection of a continuum of charged particles on a charged drop in an ambient electric field and with a relative gas velocity. The diagram of Fig. 4 shows that there are 12 possible collection regimes, determined by the net drop charge Q, gas slip velocity w_o and ambient electric field E_o. The electrical current to the collection site associated with the collection of charged particles is either i_1^+ or i_2^+, depending on the regime. These currents depend on (Q,E_o). For example, in regimes (j), (k) and (ℓ), where the drops have charge $Q < -|Q_c|$ (Q_c the saturation charge $12\pi\varepsilon_o R^2 E_o$) the electrical current is $i_2^+ = -bnQ/\varepsilon_o$. Thus, the rate at which particles are collected is

$$\frac{dn}{dt} = -\frac{i_2^+}{\sigma} N = \frac{n}{(\varepsilon_o/bNQ)} \tag{1}$$

This equation makes it clear that the characteristic time constant for the collection of fine particles is τ_d. The details of the collection transient depend on the regime, but, so long as the drops are charged significantly the characteristic time is essentially τ_d. (It is useful to recognize that even if the drops have no net charge, but are polarized by the ambient electric field so that they collect particles over a hemisphere of their surface, τ_d is still the basic collection time provided that Q is interpreted as the charge on the collecting hemisphere.)

The alternative roles of τ^* and τ_R as self-precipitation times in systems of like charged particles or drops follows from the laws summarized in Fig. 5.

Consider now some possible configurations, all making use of fields induced by charges on fine particles and drops.

a) The volume of the control device is filled with oppositely charged particles only. Self-agglomeration proceeds at a rate characterized by τ^*, but leads to little increase in size with each agglomeration. Since the agglomerated particles must be recharged to achieve a significant increase in size, the process is generally too slow to be practical.

b) The volume is filled with fine particles charged to a single polarity. This is the space-charge precipitator(4), which can be regarded as a varient of the conventional precipitator. Hence, it is competition for the electrically augmented scrubber.

c) Drops charged to one polarity and fine particles charged to opposite polarity with drops dominating the volume charge density. Then the drops are lost from the collection volume in time τ_R. Because the mobility of the drops is generally much greater than that of the particles, $\tau_R << \tau_d$ and hence the drops have a residence time that is short compared to the time required to remove a significant fraction of particles. This means that charged drops must be resupplied to the volume many times during the gas residence time to achieve effective cleaning.

d) Drops are injected of opposite polarity and particles with opposite polarity. Then, there is no self-precipitation either of the drops or of the particles. However, the self-discharge among the drops occurs with time constant τ_R, and hence the drops are as effectively lost as collection sites as in case (c). Again, drops must be resupplied many times during one gas residence time to achieve effective cleaning.

e) Oppositely charged drops and particulate are injected with sufficient particle charge density to achieve space-charge neutrality. In this case, the drops are used efficiently, since they do not self-precipitate or self-discharge. Rather, the drops lose their charge by collecting particles. Such a configuration is possible only if the fine particles are very dense. Note that space charge neutrality means that $NQ = nq$ so that $\tau^* = \tau_d$. This means that the collection time is of the same order as would be obtained in a space-charge precipitator (particles injected without the drops). The difference is essentially in the space charge precipitator, the particles end up on the walls whereas in the charged drop scrubber, they are collected by the drops.

III. Theoretical Performance of a Controlled Experiment

The collection volume for a controlled experiment is shown schematically in Fig. 6. Monodisperse drops with acoustically controlled size (50 micron diameter) and electrically controlled charge are injected vertically at 10 m/sec at the top. Gas is injected horizontally at the top with intrained fine particle density n_{in} and removed at the bottom where the particle density is reduced to n_{out}. Momentum is transferred from the injected drops to the gas so that in the absence of drop charge, the drops form a fully developed jet by the time they reach the bottom of the central interaction region. The drops are found to slow to the gas velocity in about 1/3 of the device length. Mean gas and drop velocities in the center interaction region are 1.4m/sec. The collection volume is baffled so that the gas recirculates upward along the sides in a feedback loop that is driven by the drop jet ($c/d = 1$). This feedback loop insures that all of the gas is subject to drop cleaning the same number of times. Because $\tau_R << \tau_d$, the gas residence time is made much longer than the drop residence time. The gas typically circulates 50 times during one gas residence time.

The experiment is designed so that all of the configurations described in Section II can be tested. Here, remarks are confined to experiments aimed at configuration (c), with configuration (b) playing an inadvertant role. That is, electrically induced scrubbing is dominant in determining the one pass particle removal $\eta_{ab} \equiv n_b/n_a$ whereas self-precipitation is dominant in determining particle removal in the feedback sections represented by $\eta_{cd} \equiv n_d/n_c$.

The system equations representing conservation of particles in the mixing regions at the top and bottom are summarized in Fig. 6. It is assumed that the volume rate of gas flow through the device, F_v, is small compared to the recirculation volume rate of flow F_g. Thus, these system equations can be solved for the overall efficiency expression given in Fig. 7.

The laws used to determine the "one-pass" efficiency in the scrubber region, η_{ab}, and one pass efficiency η_{cd} in the space-charge precipitation feedback regions are summarized in Fig. 8. These expressions are based on the model of a fully developed turbulent flow in each of the regions. By defining the step- function $U_{-1}(E_w)$ as unity in the drop-scrubbing region where the electric field at the wall is positive (here the drops are positive and the particles are negative) and as zero in the feedback regions where E_w is negative, the same expressions pertain to either region. Of course in the feedback regions there are no drops, and hence $N = 0$ for these regions. In writing these expressions, it is assumed that the collection of particles on drops is described by i_2^+, defined with Eq. (1). Moreover, it is assumed that the respective regions are in a state of fully developed turbulent flow so that the simplified quasi-one-dimensional expressions apply.

With the further assumption that in the drop scrubbing region the charge density of the drops dominates, the one pass efficiencies summarized in Fig. 9 follow. Also included in the figure is the expression for the decay of drops in the interaction region. These expressions illustrate how the characteristic times discussed in Section II turn up in specific configurations. The one-pass self-precipitation of particles with position z measured from the location (c) in Fig. 6 upward is characterized by the length ℓ^* which will be recognized as $U\tau^*$. Similarly, in the interaction region, the drop density decays in number density as z increases from point (a) in Fig. 6 downward, with the characteristic length $\ell_R = U\tau_R$. The one pass scrubbing efficiency in this region, which has a total length ℓ, is determined by a combination of ℓ_R and a length ℓ_d which represents the rate of particle collection on the drops....$U\tau_d$.

As the drop charge is raised, both the time constant for particle collection, τ_d and that for drop self-precipitation, are decreased. Thus, it is expected that the one pass efficiency shows an optimum. In fact this optimum is characterized by the two charges Q_d and Q_R, and is obtained by making the drop charge $2Q_R$. The optimum efficiency and drop charge are summarized in Fig. 10.

IV. Experimental Observation

The experimental system is shown schematically in Fig. 11. Included are diagnostic components for accurately determining particle number density, mobility, volume rate of flow, drop size, charge and rate of injection. Not shown is the apparatus used to determine the feedback volume rate of flow found by making anemometer measurements in the feedback region.

The drop charge is induced by means of inducer bars next to the acoustically driven orifices. Because the rate of drop injection is controlled acoustically, measurement of the current carried by the drops as a function of the voltage on the inducer bars, V_{drop}, makes it possible to determine the drop charge, given the inducer bar voltage. This relation between drop charge and inducer bar voltage is shown in Fig. 12.

According to the self-precipitation model for the drops, the electrical current I intercepted by an electrode placed at the position z (measured from a in Fig. 6) in the interaction region is given by the relation summarized in Fig. 13. The drop charge is normalized to the charge Q_1 which characterized the system. At low values of drop charge, the current should increase linearly. But then, as Q is increased beyond Q_1, the self-precipitation should lead to a decrease in the drop current. Measurements, shown in Fig. 13, give this expected relation. Also, the peak in current as a function of V_{drop} (proportional to Q) shifts to the right as the measurement position z is increased.

The theoretically predicted performance of the device in removing particles is shown in Fig. 15. With the charge density used in the experiments, the self-precipitation of the particles is an important factor, in fact accounting for about 80% removal of the particles with the particles charged but the drops uncharged. Thus, with the inducer bar voltage $V_{drop} = 0$, $n_{out}/n_{in} \cong 0.2$. In the limit where the fine particles are very tenuous, n_{out}/n_{in} minimizes at about the same value of V_{drop}, but goes to unity as $V_{drop} \to 0$.

The experimentally observed removal is also given in Fig. 15. The observed removal peaks at 93%, as compared to the predicted peak of about 94%. Refinements to the theory include using as n_{in} the number density corrected for losses due to inertial impact (about 20%) in the entrance region. It is important to realize that there are no empirical inputs to the theory. Control over the hydrodynamics is the main difficulty in further refinements of the experiment. For example, the distance required to have a fully developed turbulent jet is a function of drop charge, and hence the flow structure varies somewhat with V_{drop}. This may account for the somewhat slower observed decrease in n_{out}/n_{in} with V_{drop} than would be theoretically expected. By far the most important confirmation is of the optimum in the efficiency curve as a function of drop charge. Both theory and experiment optimize in the range of an inducer bar voltage of 30 volts. Although not shown, efficiency measurements were made out to a value of V_{drop} exceeding 400 volts, with the observed efficiency found to continue to slowly degrade. Clearly, far more charge can be placed on the drops than is desirable.

With particles in the size range of 2 micron, the device functions efficiently as an inertial scrubber. In the size range of 0.6 micron used for these experiments it is clear that the electrically induced scrubbing can dominate inertial scrubbing.

This apparatus can also be used to test our understanding of the other configurations outlined in Section II. For example, oppositely charged drops can be injected either by making the inducer bars of opposite polarity so that they induce charges of opposite sign on the two rows of drops injected or by making V_{drop} a symmetric square-wave. The dual significance of the drop self-precipitation time or self-discharge time makes it clear that the limitations on particle removal efficiency should be very similar to those found here with drops of a single polarity.

V. Concluding Remarks

The experiments support the assumption made at the outset in this discussion that in the submicron range, the electrically induced impaction can easily dominate that due to inertia. So, when compared to the inertial impact scrubber, the electrically augmented device is indeed attractive. The fact that self-precipitation can make such an appreciable contribution to the removal efficiency supports the view that the charged drop scrubber is poor competition for the conventional precipitator. What we have emphasized here is that although the charged-drop scrubber appears closely related to the conventional precipitator, in fact it is subject to different limitations. The drops, unlike the electrodes of the conventional precipitator, are not fixed, either in charge or in mechanical position!

It is felt that in applications where the conventional precipitator is the competition, the charged-drop device is a poor contender. But, in applications where scrubber technology is appropriate, electrical augmentation of the scrubbing is attractive.

Finally, it should be remembered that our remarks have been confined to charged drops as collection sites. Fundamentally, it is difficult to make charged drop devices compete with the electrostatic precipitator because of limitations on the drop density resulting from the tendency of the drops to self-discharge or self-precipitate. Breakthroughs in residence time for efficient cleaning are possible by using dense systems of particle collection sites in an imposed electric field. Either the sites are continuously recharged by electrically induced collisions, or they function as sites through polarization in the imposed electric field. Such devices could outperform the electrostatic precipitator in terms of residence time, while providing new alternatives in solving problems such as the removal of high resistivity particles.

References

1. Penney, G. W., U.S. Patent 2,357,354, "Electrified Liquid Spray Dust Precipitators," (1944).
2. Melcher, J. R. and K. S. Sachar, "Charged Droplet Technology for Removal of Particulates from Industrial Gases," Final Report under Task No. 8, E.P.A. Contract #68,002-0018, (1971).
3. Whipple, F. J. W. and J. A. Chalmers, "On Wilson's Theory of the Collection of Charge by Falling Drops," Quart. J. of the Roy. Met. Soc., 70, (1944), pp. 103-119.
4. Hanson, D. N. and C. R. Wilke, "Electrostatic Precipitator Analysis," I & EC Process Design and Development, 8, #3 (1969), pp. 357-364.

Designation	Description	Schematic
$\tau_p \equiv \frac{s}{bE_s}$	Precipitation time for particle in conventional precipitator having electrode spacing s	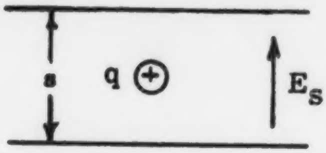
$\tau^* \equiv \frac{\varepsilon_o}{bqn}$	Particulate self-agglomeration or self-precipitation time.	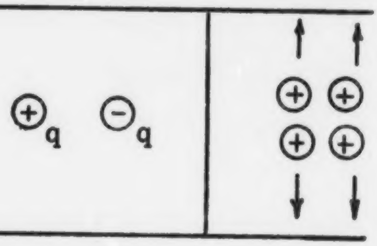
$\tau_d \equiv \frac{\varepsilon_o}{bQN}$	Particle-particulate collection time	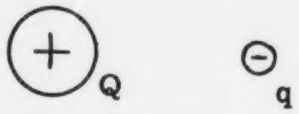
$\tau_R \equiv \frac{\varepsilon_o}{BQN}$	Drop discharge or self-precipitation time	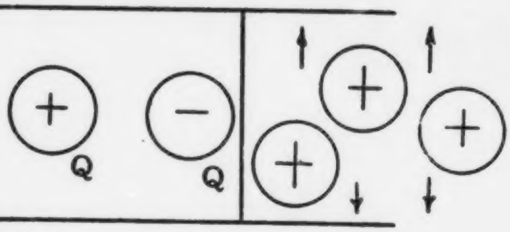

Fig. 1 Summary of time-constants governing performance of conventional electrostatic precipitator and a wide range of agglomeration devices.

Two-Particle Interactions

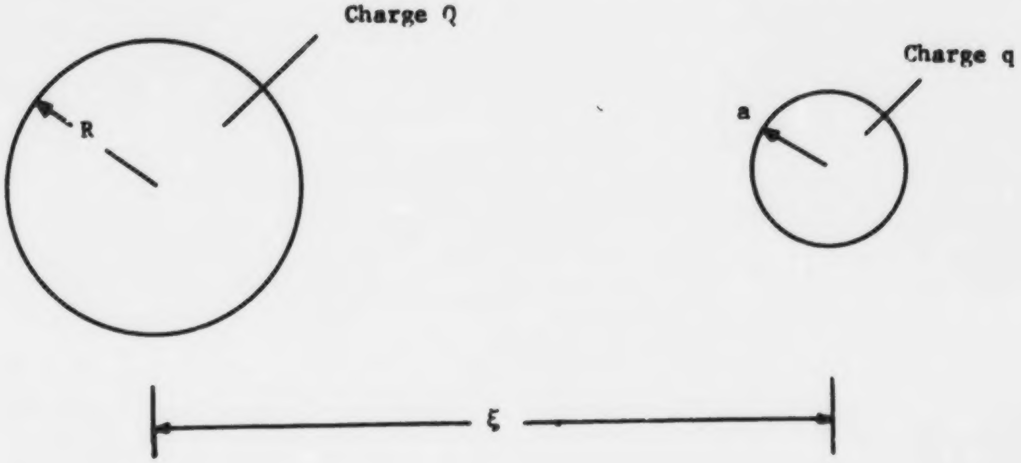
Charge Q
Charge q
R
a
ξ

$$\frac{d\xi}{dt} = -\frac{(qB + bQ)}{4\pi\varepsilon_o}\,\frac{1}{\xi^2}$$

$$b \equiv \frac{q}{6\pi\eta a} \;:\; B \equiv \frac{Q}{6\pi\eta R}$$

Fig. 2 Two-particle model for electrical interactions

Initial Spacing $\xi_o >> (R + a)$

$$\begin{tikzcd}
 & & \begin{bmatrix} Q \to q \\ B \to b \\ \xi_o^3 \to \frac{1}{n} \end{bmatrix} \arrow[r] & \tau = \frac{2}{3}\tau^* \\
\tau \arrow[r] & \frac{4\pi\varepsilon_o \xi_o{}^3}{3(qB + bQ)} \arrow[ur] \arrow[r] \arrow[dr] & \begin{bmatrix} bQ >> qB \\ (2\xi_o)^3 \to \frac{1}{N} \end{bmatrix} \arrow[r] & \tau = \frac{\pi}{6}\tau_d \\
 & & \begin{bmatrix} q \to Q \\ b \to B \\ \xi_o^3 \to \frac{1}{N} \end{bmatrix} \arrow[r] & \tau = \frac{2\pi}{3}\tau_R
\end{tikzcd}$$

Fig. 3 Limits of collection time for two particle model that give the three time constants when these are interpreted as self-discharge and drop-particle agglomeration times.

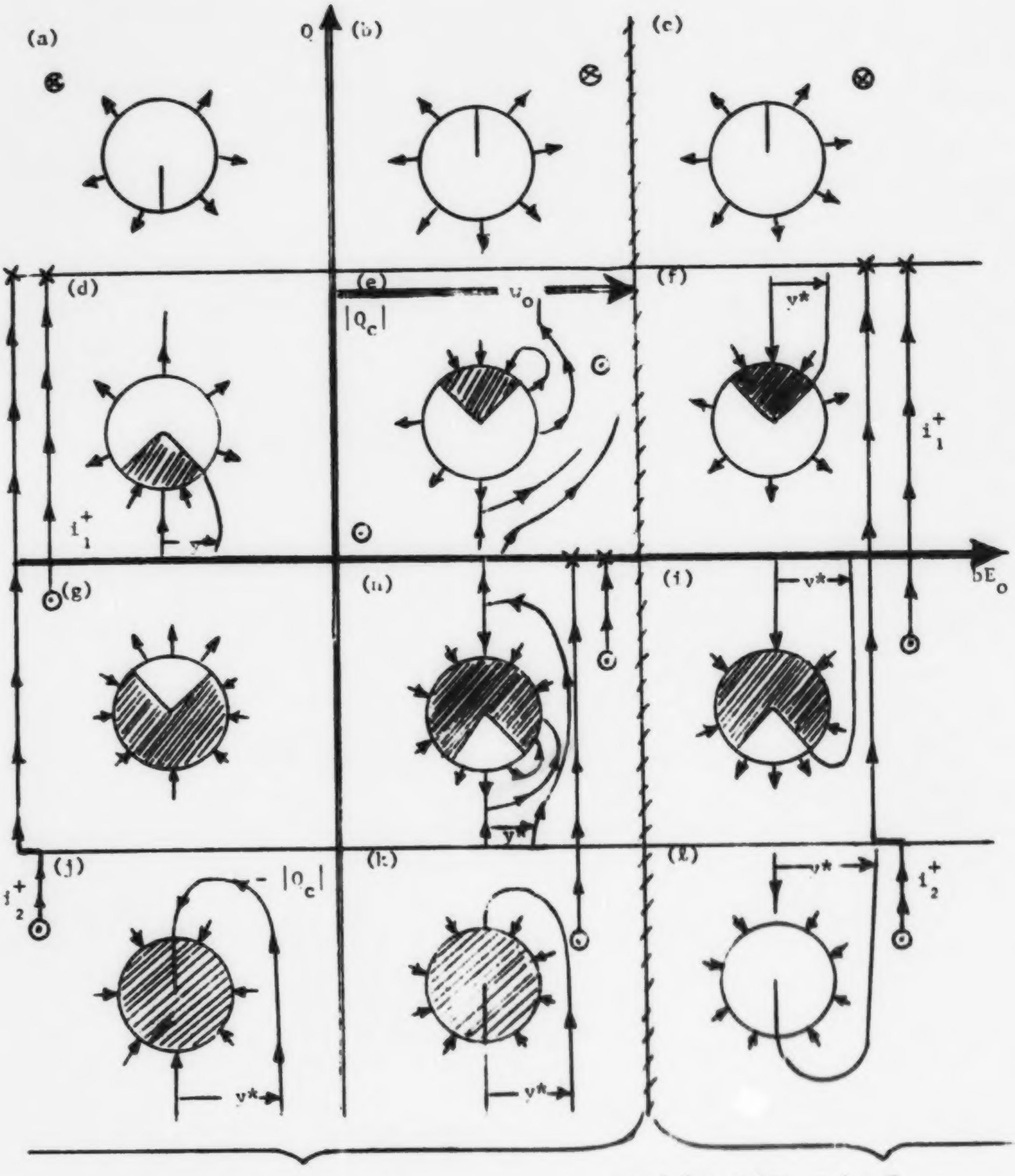

particles enter $z \to +\infty$ particles enter $z \to -\infty$

Fig. 4 Whipple and Chalmers model for collection of positively charged particles having mobility b on drop carrying charge Q in ambient electric field E_0 with relative gas velocity w_0. E_0 and w_0 are respectively defined as positive and negative in the z direction. With increasing gas velocity, the vertical line of demarcation indicated by w_0 moves to the right. Initial charges, indicated by ⊙, follow the trajectories shown until they reach a final value given by x. If there is no charging, the final and initial charges are identical, and are indicated by ⊗. The inserted diagrams show particle trajectories.

Self-Precipitation

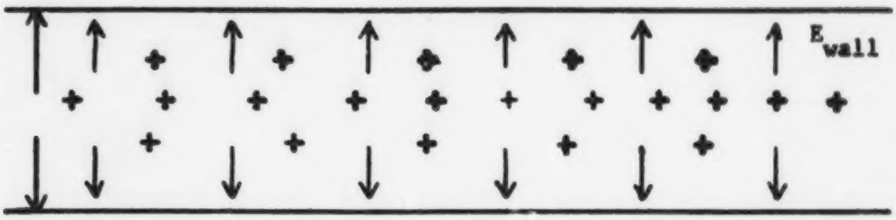

Gauss' Law: $E_w = \frac{nqs}{2\varepsilon_o}$

Conservation of Charge:

$$\frac{d}{dt}(nqs) = -2nqbE_{wall}$$

Together, for System of Charged Particles

$$\frac{dn}{dt} = -\frac{n}{\tau^*} \; ; \; \tau^* = \frac{\varepsilon_o}{nqb}$$

For System of Charged Drops:

$$\frac{dN}{dt} = -\frac{N}{\tau_R} \; ; \; \tau_R = \frac{\varepsilon_o}{NQB}$$

Fig. 5 Summary of simple model used to illustrate role of τ^* and τ_R as self-precipitation times for like-charged particles and like-charged drops respectively.

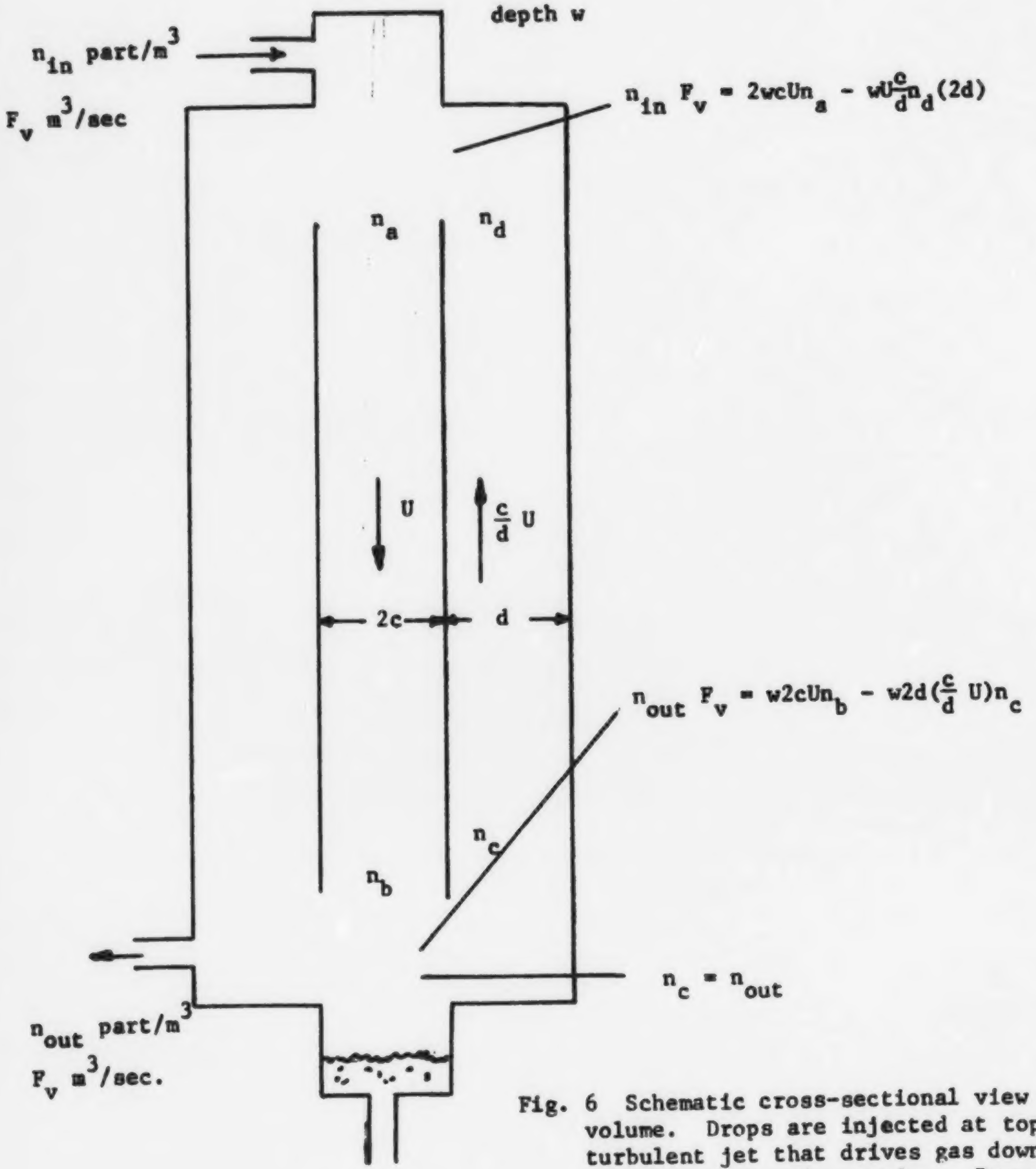
depth w
n_{in} part/m^3
F_v m^3/sec
$n_{in} F_v = 2wcUn_a - wU\frac{c}{d}n_d(2d)$
n_a
n_d
U
$\frac{c}{d}$ U
2c
d
$n_{out} F_v = w2cUn_b - w2d(\frac{c}{d} U)n_c$
n_c
n_b
$n_c = n_{out}$
n_{out} part/m^3
F_v m^3/sec.

Fig. 6 Schematic cross-sectional view of cleaning volume. Drops are injected at top to form turbulent jet that drives gas downward in the central interaction region. Drops are removed by impaction at the bottom, while the baffles provide a controlled recirculation of gas and particles. The equations describe the balance and mixing of gas streams at the inlet and outlet regions.

$$\frac{n_{out}}{n_{in}} = \frac{\eta_{ab}}{1 + \frac{F_g}{F_v}(1 - \eta_{ab}\eta_{cd})}$$

$$F_g \equiv 2cwU = 2dw(\frac{c}{d} U)$$

$$\eta_{ab} \equiv \frac{n_b}{n_a}$$

$$\eta_{cd} \equiv \frac{\eta_d}{\eta_c}$$

Fig. 7 Summary of equations which follow from those given in Fig. 6 in describing the system performance in terms of one-pass efficiencies η_{ab} and η_{cd}.

Drop Conservation

$$\frac{dN}{dZ} = - \frac{NQE_w}{6\pi\eta RUc} U_{-1} (E_w)$$

Drop Charge Conservation

$$\frac{dQ}{dZ} = - \frac{nqbQ}{\varepsilon_o U}$$

Particle Conservation

$$\frac{dn}{dZ} = - \frac{nbQN}{\varepsilon_o U} - \frac{bnE_w U_{-1}(-E_w)}{cU}$$

Gauss' Law

$$E_w = (NQ - nq) \frac{c}{\varepsilon_o}$$

Fig. 8 Summary of laws used to determine the one-pass collection of particles on drops in the interaction region and self-precipitation of particles in the feed-back regions. Model assumes a fully developed turbulent flow in each region.

Space Charge Precipitation

Particulate $\eta_{cd} = \frac{1}{1 + \frac{z}{\ell^*}}$; $\ell^* = \frac{\epsilon_o U}{bqn_c}$

Drops

$$\frac{N}{N_o} = \frac{1}{1 + \frac{z}{\ell_R}} \quad ; \quad \ell_R \equiv \frac{\epsilon_o U}{N_o QB}$$

$$\eta_{ab} = \left(1 + \frac{z}{\ell_R}\right)^{-\frac{\ell_R}{\ell_d}} \quad ; \quad \ell_d = \frac{\epsilon_o U}{N_o Qb}$$

Fig. 9 Summary of one-pass efficiencies and drop density distribution found using the model summarized in Fig. 8.

In Region $NQ >> nq$

Optimum

$$\eta_{ab} = [5]^{-(1/2)(\frac{Q_d}{Q_R})}$$

$$Q_d \equiv 6\pi\eta Rb$$

$$Q_R \equiv \sqrt{\frac{\varepsilon_o 6\pi U\eta R}{\ell N_o}}$$

$$Q_{opt} = 2Q_R$$

Fig. 10 Optimum one-pass efficiency of drop-particle scrubbing. For optimal collection, the drop charge should be $2Q_R$, and in that case the efficiency is the value of η_{ab} given.

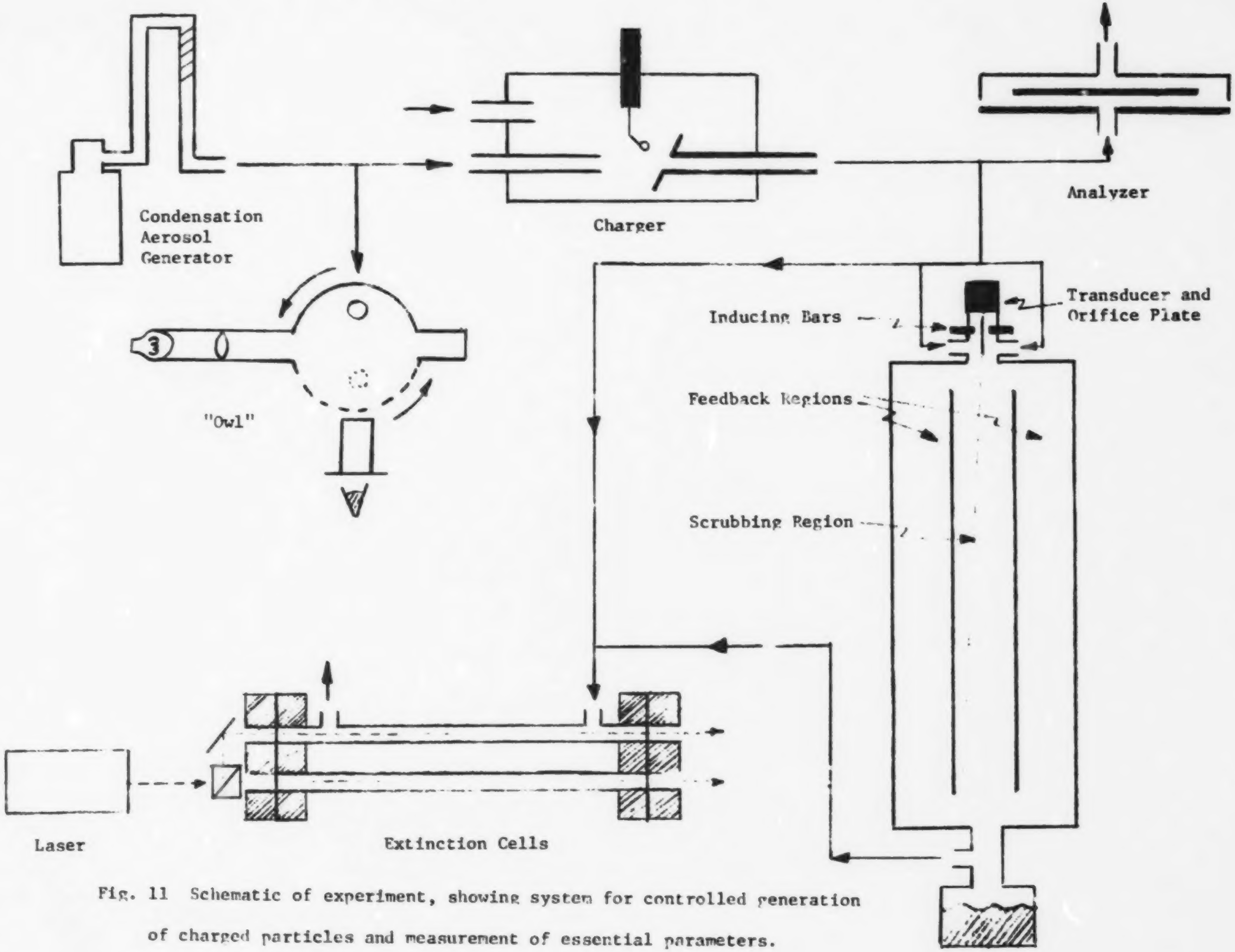
Condensation
Aerosol
Generator
Charger
Analyzer
"Owl"
Inducing Bars
Transducer and
Orifice Plate
Feedback Regions
Scrubbing Region
Laser
Extinction Cells

Fig. 11 Schematic of experiment, showing system for controlled generation of charged particles and measurement of essential parameters.

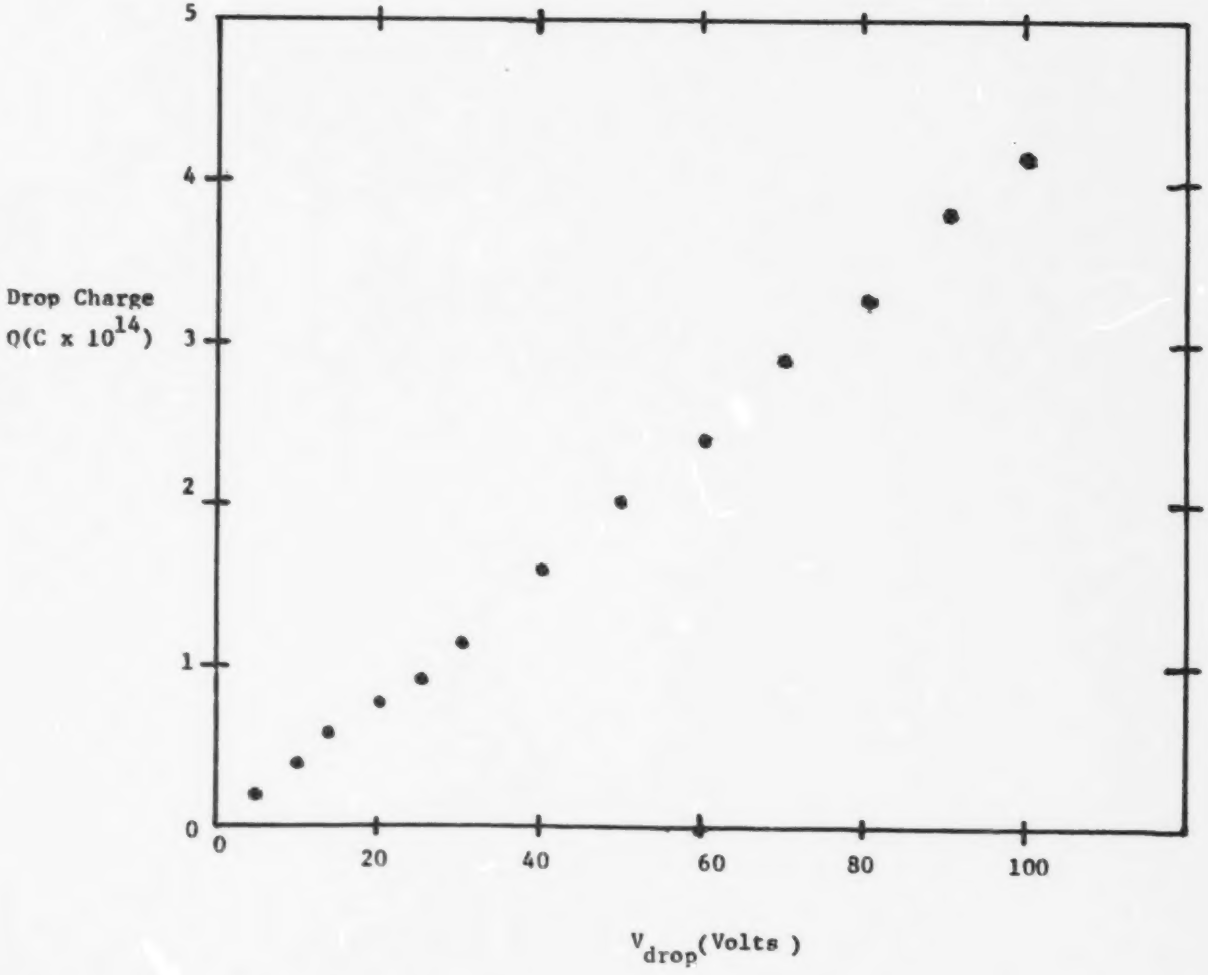

Fig. 12 Typical measured drop charge as a function of inducer bar voltage.

Drop Precipitation

$$I = C\,\frac{\underline{Q}}{1 + \underline{Q}^2}$$

$$\underline{Q} = \frac{Q}{Q_1}\;;\; Q_1 = \sqrt{\frac{\varepsilon_o U 6\pi\eta R}{N_o\, Z}}$$

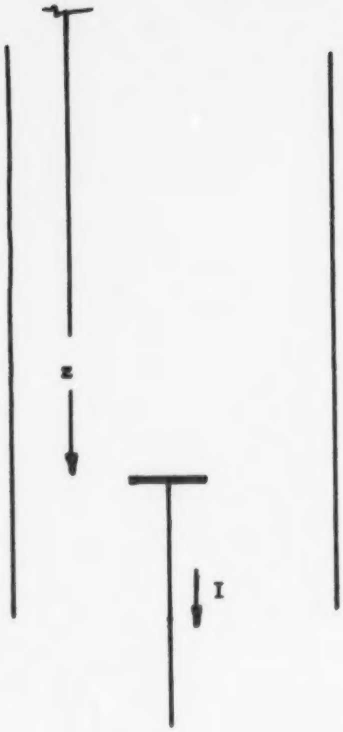

Fig. 13 Schematic of electrode used to intercept some of the drop current by impaction. Theory predicts the dependence on drop charge Q and electrode position z shown.

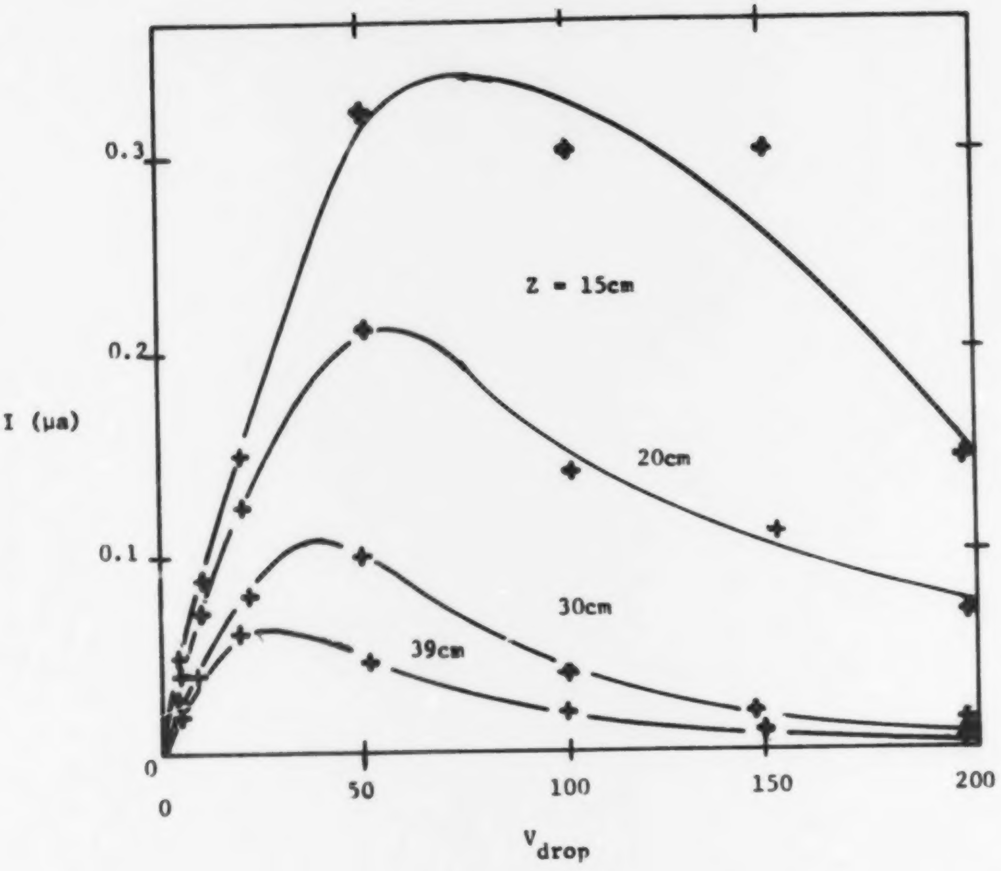

Fig. 14 Measured current as function of V_{drop}, which is proportional to Q at four different positions z.

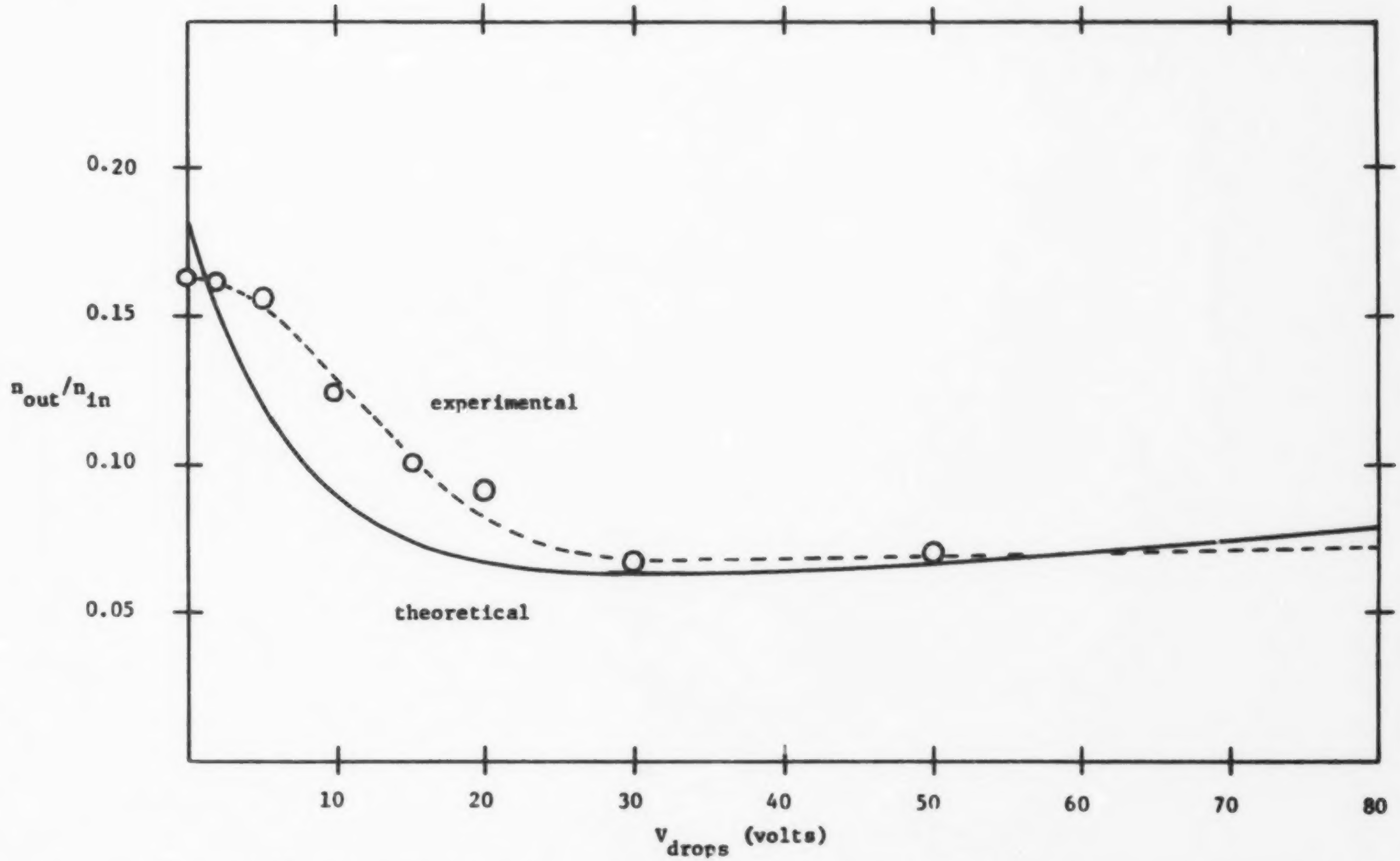

Fig. 15 Theoretical and observed overall efficiency of system. With the space charge used in the experiment, space-charge precipitation resulted in a removal of about 80% of the particles. Particle concentration that enters the interaction region is n_{in}, corrected for dilution and inertial impaction in the entrance region.

Paper No. 25

ADVANCES IN THE SONIC AGGLOMERATION OF INDUSTRIAL AEROSOL EMISSIONS

by

David S. Scott

UNIVERSITY OF TORONTO

Toronto, Ontario, Canada

ABSTRACT

The agglomeration of industrial aerosols by finite-amplitude sound is well known, although the process has enjoyed limited commercial application resulting primarily from high specific power requirements (and to some degree high capital costs). These limitations can be attacked by either more effective acoustic field configurations, and/or more efficient sound generation. The present paper outlines some of the results of recent studies carried out at the University of Toronto and the Ontario Research Foundation on both approaches to the solution.

A brief review of the first-order mechanisms of acoustic agglomeration is followed by an indication of the theoretical and practical advantages of progressive saw-tooth waves as compared with the conventional standing-wave configuration. The suitability of using a "resonant pulse-jet" to generate sound is discussed from the point of view of sound generation efficiency, waveforms, sound intensities and reliability. Estimates of annual operating costs (agglomeration plus subsequent collection) using a "pulse-jet" agglomerator are given. A very brief outline of the work of the Braxton Corporation on acoustic agglomeration is also presented.

INTRODUCTION

The phenomenon of acoustical enhanced aerosol agglomeration has been known for about four decades. For example, as early as 1935, Brandt[1] and his colleagues had studied acoustically enhanced agglomeration of tobacco smokes, ammonium chloride vapours, and paraffin oil fogs. Following the second world war, several American investigators, such as St. Clair[2] and Boucher[3], carried out laboratory and field studies. More recently, a number of Soviet scientists have conducted continuing and extensive research on the phenomenon. Of the many excellent Soviet scientists working in the area, probably the best known in the English-speaking world is Mednikov[4], whose well known monograph on the subject was published in English in 1965. Since the preceding is the barest outline of the substantial literature in this field, it is clear that I could not presume to present acoustic agglomeration as a "new concept", in spite of this paper finding itself placed in such a session. Nor could I claim to be capable of telling you about all the recent advances, or even the most significant recent advances, - as these could well have occurred in the Soviet Union. I will, however, discuss what we believe are some new approaches to sonic agglomeration which we have been following at Toronto. And while so doing, I will use this discussion as a vehicle to review the "motivation for", "a bit of how-it-works", and "certain other aspects" of the process.

The presence of finite-amplitude sound in an aerosol acts to increase the coagulation rate of that aerosol. Moreover, under fairly readily achieved conditions, this rate increase can be substantial. A finite-amplitude acoustic field can be said to exist when the acoustic mach number, ε , becomes non-negligible. This might be said to occur when $\varepsilon = 10^{-2}$, which corresponds approximately to a sound intensity level of 154 db under standard atmospheric conditions. Acoustically enhanced agglomeration is achieved by bringing about a manyfold increase in particle-particle contacts or, what is the same thing, particle-particle collision frequency. As such, it is a process by which a fine particle, high number density aerosol is changed into a coarse particle lower number density aerosol. As such, I believe we should think of acoustic agglomeration as a dust conditioning process. If the title of this paper had referred to "acoustic dust conditioning" , it would have better indicated where the process fits into a "systems approach" to air cleaning technology, but would have less well indicated "what it does".

I believe the advantages of acoustic dust conditioning fall into three primary categories:

(a) The process is especially suitable for high dust load ultrafine particulate matter.†

(b) In principle, there are no restrictions on resistivity, explosiveness, temperature, stickiness, or other aerosol characteristics which sometimes cause difficulties with conventional equipment.

(c) The process lends itself to installations which supplement existing equipment, thereby improving the overall process efficiency at a fraction of the cost of an entirely new system.

In view of the preceding technical advantages of the process, in my opinion, the limited commercial application of acoustic agglomeration has been due to high operating costs resulting from high specific power requirements and high capital costs.

The solution to the high power requirements would appear to fall into two general categories. First, we might seek more effective acoustic field configurations in order to bring about a greater increase in the coagulation rate for the same acoustic intensity. Secondly, we can direct attention to sound generation devices, in the hopes of bringing about an improvement in the efficiency of sound generation.

The solution to capital costs appears more difficult to subdivide. Rather, is probably best approached by noting that when we are seeking advances in either, the acoustic field configuration, or energy conversion efficiency of finite-amplitude sound generation, that we do so with an eye to capital cost implications. At least that has been our approach at Ontario Research Foundation, with the result that the remainder of this paper primarily subdivides into two headings; firstly, "Acoustic Field Configuration" and secondly, "Sound Generation". Capital cost implications will be discussed within these sections as we proceed and where appropriate.

ACOUSTIC FIELD CONFIGURATION

To date, the accepted acoustic configuration has been an essentially standing sinusoidal wave "tuned" to the aerosol being treated in order to maximize the particle-particle differential or "orthokinetic" motion. In my view, orthokinetic interactions may be regarded as the predominant "first order" mechanism responsible for agglomeration, and occur when two or more particles of different sizes, which are close together, are located with their line of centers substantially parallel to the gas vibration (i.e., orthogonal to a wave plane). Clearly, particles of different sizes vibrate with different amplitudes and phases. Hence, there is a differential motion established between such particles which increases their collision probability.

A simple way of looking at this process is to consider a particle sufficiently small that it moves with the gas and a particle so large that it is essentially unperturbed by the gas motion. In this case, the "largeness" or "smallness" of a particle should be defined in terms of the non-dimensional group $\omega\tau$, where ω is the acoustic frequency in radians per second, and τ is the particle dynamic relaxation time.* Corresponding to a very small particle $\omega\tau \to 0$, and corresponding to a large particle $\omega\tau \to \infty$.

However, the sinusoidal wave imposes limitations on the effectiveness of such interactions due, primarily, to the rather sharp transition from $E \to 0$ to $E \to 1$ which occurs over a particle radius change of order 10 as seen from Fig. 1.

These limitations are as follows:

(a) It is very important that the acoustic frequency be chosen to match the aerosol being treated, in order to "split" the particle size distribution at a point which maximizes the orthokinetic differential motion. This requires aerosol diagnostic and control equipment which can substantially add to capital costs.

(b) Even when the frequency is "tuned" such that $E \approx 0$ (essentially equivalent* to $\omega\tau \approx 1$) at the "mean" particle size, the frequency necessarily becomes "mistuned" as the size distribution evolves as a consequence of the acoustic treatment. In response to this difficulty, Mednikov[7] has proposed multiple stage agglomeration.

(c) Finally, and even if the optimum "tuning" could be achieved, each of the two sets of particles outside the set of particles for which $0.05 \lesssim E \lesssim 0.95$ experience little differential motion among themselves. Although this is probably the least significant limitation of standing sinusoidal acoustic fields, it could conceivably become important in aerosols exhibiting very broad size distributions.

In view of the preceding, we proposed the use of a series of progressive low-amplitude shocks (saw-tooth waves). We believe that, from the point of view of optimizing orthokinetic interactions, this alternate waveform exhibits two advantages over the standing sinusoidal waveform. These advantages can be illustrated by reference to Fig. 2, which gives the dynamic response of different size particles to the passage of a step velocity change in the bath gas, for the case of negligible particulate mass loading, that is $M \to 0^*$. The figure also assumes Stokes drag, which is, of course, inappropriate for the finer particulate sizes. Although this physical circumstance differs from that of a series of saw-tooth waves and finite particulate loading, and further deviates for the fine particulate sizes when Stokes drag law is inappropriate, the essential features with regard to optimizing the orthokinetic differential motion between different particle sizes are the same, and are better illustrated in this more simple case. The advantages of the progressive saw-tooth wave train are as follows:

(a) All particles initially experience a differential motion with respect to the gas as a consequence of the discontinuity in the gas velocity with the passage of each wavefront. But since the different size particles have different dynamic relaxation times, τ , all particles have a period during which they move differentially with respect to all others of different sizes. Considering Fig. 2, it is seen that at $t = t_1$, the set of particles of $r < 0.04$ μm are essentially moving with the gas, while the set of particles of $r > 1.0$ μm are essentially stationary. Later, at $t = t_2$, the set moving with the gas has increased to include all particles of $r < 0.2$ μm and the stationary set has decreased to include only those particles $r > 5$ μm . And so on. Thus, the passage of each saw-tooth wave "sweeps" the size distribution, in contrast to "splitting" the size distribution as occurs in the standing sinusoidal field.

(b) The second advantage of progressive saw-tooth waves follows directly from the first. That is, no "tuning" of the fundamental frequency is necessary. It is sufficient that the relaxation time of the largest particle be less than the inverse of the fundamental frequency. In practice, this requires only that f < 500 Hz.

(c) Thirdly, in the standing sinusoidal field and neglecting drifts, all particles remain in the same mean position with respect to the gas, and hence remain in the same mean position with respect to each other. Conversely, in a progressive saw-tooth wave train, different size particles change position with respect to the gas by different amounts and in accordance with their different relaxation times. As such, there is a systematic shifting of the relative position of different size particles with respect to each other, with each wave. Such a redistribution has no analog in the conventional standing field.

The preceding illustrate that by changing the waveform to a train of finite-amplitude progressive saw-tooth waves, the orthokinetic sub-mechanism of acoustic agglomeration can be expected to be optimized and, in addition, a new sub-mechanism has been introduced. The new sub-mech is the systematic redistribution of different size particles with respect to each other.

Before leaving the matter of the acoustic field con= figuration, we should note that there are several sub-mechanisms, notably acoustic drifts, self-centring processes, etc., and they cannot all be independently maximized in a single acoustic field. However, by introducing two mutually perpendicular fields, the first a progressive saw-tooth wave train as we have just discussed, and the second a standing sinusoidal field, it can be shown by qualitative arguments similar to the preceding that it is possible to optimize all the known sub-mechanisms which exist in conventional standing fields, while at the same time introducing several new sub-mechanisms, which do not exist in standing single acoustic fields. Very simply, in this system regions of concentrated aerosol are generated in the nodal/antinodal planes of the standing field (aerosol striations), and the shocks are run along these striations. Details of this more refined acoustic configuration are given by Scott.[8] Although this configuration holds certain process advantages, the primary current use appears to be in experimental isolation of the various sub-mechanisms of acoustic agglomeration. Early experimental results from such a facility at the University of Toronto (shown schematically in Fig. 3) indicate that (a) the aerosol striations are predominantly acoustic circulation induced, (b) the progressive saw-tooth wave does not break up the striations, and (c) for the same sound intensity the single progressive saw-tooth waveform brings about a greater coagulation rate increase than a single standing sinusoidal field. In these experiments, the sound pressure levels were up to 154 db in the standing field and 149 db in the progressive field. The basic frequency of the progressive field ranged between 500 - 2500 Hz. and for the standing field between 980 - 3155 Hz.

Returning to the matter of capital costs, and concentrating specifically on the single progressive saw-tooth wave train we note the following.

(a) Acoustic frequency tuning control requirements are eliminated.

(b) There is no need for special agglomeration chambers which involve adjustable lengths, in order to maintain an integral number of half wavelengths as the speed of sound through the aerosol changes with the loading and size distribution of the inlet dust.

(c) Taking the above to its logical conclusion, there is really no need for an agglomeration chamber at all. One simply looks for a convenient elbow in the flue gas line, and uses this point for the insertion of the sound horn.

SOUND GENERATION

In view of the discussion on waveforms, it is apparent that we would like a device which generated a waveform with the essential features of a progressive saw-tooth wave train, and accomplished this at a high energy conversion efficiency. We have investigated the use of a resonant pulse-jet (not dissimilar from a World War II V1 rocket engine) in both a (a) valved combustion chamber configuration and (b) a no-moving-part combustion chamber using aerodynamic valving. The advantages of this acoustic generator for sonic agglomeration appear to be as follows:

(a) Although the wave-form is rough, it contains the basic saw-tooth features for enhancing the particle-particle collision frequency.

(b) There is a direct conversion of fuel energy to acoustic energy which implies that this might be carried out with a relatively high overall efficiency.

(c) The capital costs of the equipment is very low.

Figures 4 and 5 show an overall view of the facility used to study the feasibility of a pulse-jet generated acoustic field at Ontario Research Foundation. The size of the facility points up the difficulty of scaling the pulse-jet to normal laboratory dimensions. To-date, a ZnO fume aerosol has been used exclusively. Figure 6 illustrates typical particle size distribution results prior to, and subsequent to, sonic treatment. The residence time in these cases was about 2 seconds. The no-moving-part pulse-jet appears to run indefinitely. Table 1 presents the range of values of the more important parameters involved in this study, as well as the indicated total annual loss for a typical installation including capital, maintenance and operating costs. These estimates were based upon using a cyclone as the ultimate collecting device.

In summary, the status of this program appears to be that both technical and commercial viability are indicated, in the sense that dusts can be agglomerated to a degree which would be useful in certain emission control installations and this can be accomplished with a cost range normally acceptable in such circumstances. Work from this point on will concentrate on three basic areas.

(a) Significant debugging and parameter optimization must be carried out.

(b) The coagulator must be viewed as a conditioner and optimization studies with cyclones, wet-scrubbers, and fabric filters must be conducted. It is speculated that sonic-coagulator/wet-scrubber combinations might hold the most promise.

(c) Work must be carried out on determining the most effective means of accomplishing ambient sound isolation, with particular emphasis on capital costs.

OTHER COMMERCIAL SCALE INSTALLATIONS

The only other sonic agglomerator development work in North America which I am aware of, and which is on the order of a commercial scale unit, is that which has been carried out by Braxton Corporation, Medfield, Massachusetts. This system, which is referred to by Braxton as their AVP (alternating velocity precipitator) uses the traditional standing-wave acoustic field and agglomeration chamber. From what little I know of the system, it appears to be an exceptionally well engineered unit. The system treats both particulate matter and noxious gases such as SO_2 and NO_x and, in most circumstances, utilizes the addition of a sodium carbonate "fine spray" solution to enhance the collection efficiency. It is my understanding that the Braxton system is capable of treating

15,000 acfm at 300° F. Residence times are in the order of 1/2 seconds and the sound intensity varies between 166 - 170 db at frequencies of 250 - 500 Hz. The installed capital costs for the unit are estimated at $4.00/acfm and I have no information on the power requirements. Undoubtedly, further information could be obtained from the Braxton Corporation.

FOOTNOTES

[*] The acoustic mach number, $\omega\tau$ product, mass loading ratio and other non-dimensional groups important in finite-amplitude acousto-aerosol interactions are discussed in Ref. 5 and 6.

[†] It should be noted, however, that there must necessarily be a lower limit on the dust loading for which the process is suitable. Typically, this lower limit can be expected about 1 grain/ft.^{3}, however, is somewhat dependent upon the mean particle size which is required after coagulation.

REFERENCES

1. Brandt, O. and Freund, H., "Uber die Aggregation von Aerosolenmittels Schallwellen", Z. Phys. 94 (5-6) pp. 348-355; (1935).
2. St. Clair, H.W., "Agglomeration of Smoke, Fog or Dust Particles by Sonic Waves", Indust. Eng. Chem. 41(11), pp. 2434-2438 (1949).
3. Boucher, R.M.G., "Acoustic Energy in Fog Dispersal Techniques", Ultrasonic News 4(1), pp. 11-19 (1960).

References (continued)

4. Mednikov, E.P., "Acoustic Coagulation and Precipitation of Aerosols", translation from Russian by Consultants Bureau, New York, 1965.
5. Davidson, George A., and Scott, David S., "Finite Amplitude Acoustic Phenomena in Aerosols from a Single Governing Equation", J. Acous. Soc. Amer., 54(5), pp. 1331-1342 (1973).
6. Davidson, George A., and Scott, David S., "Finite-Amplitude Waveforms in Aerosols", J. Aerosol Sc., 5(1), (1974).
7. Mednikov, E.P., "Method of Acoustic Coagulation of Aerosols USSR Patent 149399 (1962).
8. Scott, D.S., "Method of Coagulating Aerosols", U.S.A. Patent 3,771,286 (1973).

FIGURE CAPTIONS

Figure 1: Entrainment of particles by the gas motion, E , versus particle radius in μm , r , for several frequencies of sinusoidal waves. The particles are spherical and of 1 gm/cm^3 density. The gas is air at approximately STP.

Figure 2: Entrainment of particles by the gas motion, E , versus time, t , since the passage of a low amplitude step velocity change in the gas for several particle sizes. The particles are spherical and of 1 gm/cm^3 density. The gas is air at approximately STP.

Figure 3: Schematic of U. of T. striated-shock acousto-aerosol channel. The aerosol enters at upper right and exists at lower left. A progressive saw-tooth field is produced by the shock field generator and propagates down the channel to be absorbed in a relatively inefficient anechoic base of baffels and steel wool. The agglomeration chamber is 7.6 × 45.7 × 137.2 cm.

Figure 4: View of ORF pulse-jet agglomerator facility. (A) ZnO fuming chamber (B) Primary data readout station (C) Agglomeration chamber (D) Cyclone.

Figure 5: View of ORF pulse-jet agglomerator facility. (A) ZnO fuming chamber (D) Cyclone (E) Pulse-jet inserted in elbow (F) Fan (G) Baghouse.

Figure 6: Size distribution of treated and untreated ZnO aerosol, given in terms of cumulative percentage by particle mass versus particle aerodynamic diameter.

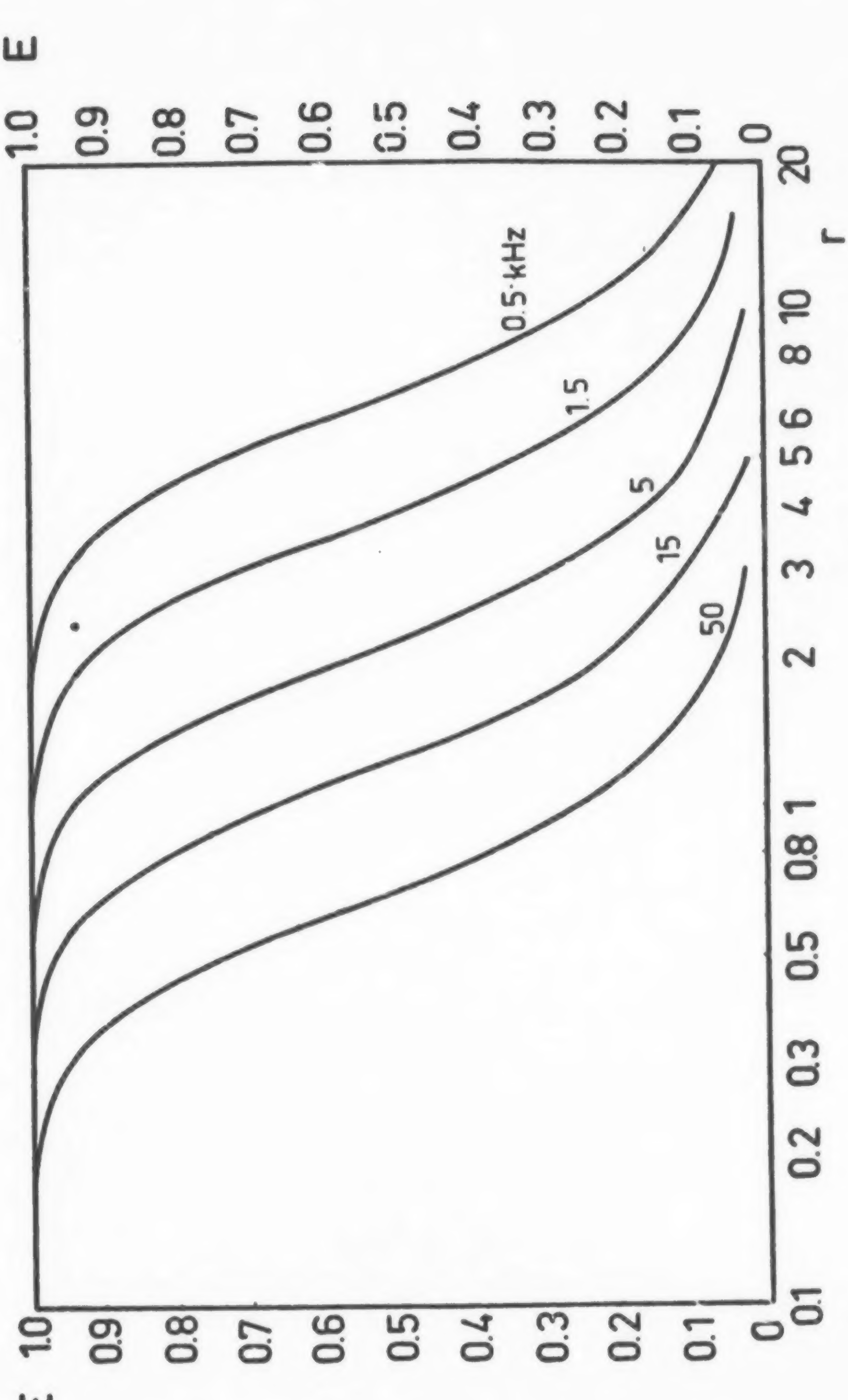
E
1.0
0.9
0.8
0.7
0.6
0.5
0.4
0.3
0.2
0.1
0
r
0.1
0.2
0.3
0.5
0.8
1
2
3
4
5
6
8
10
20
0.5·kHz
1.5
5
15
50

Figure 1.

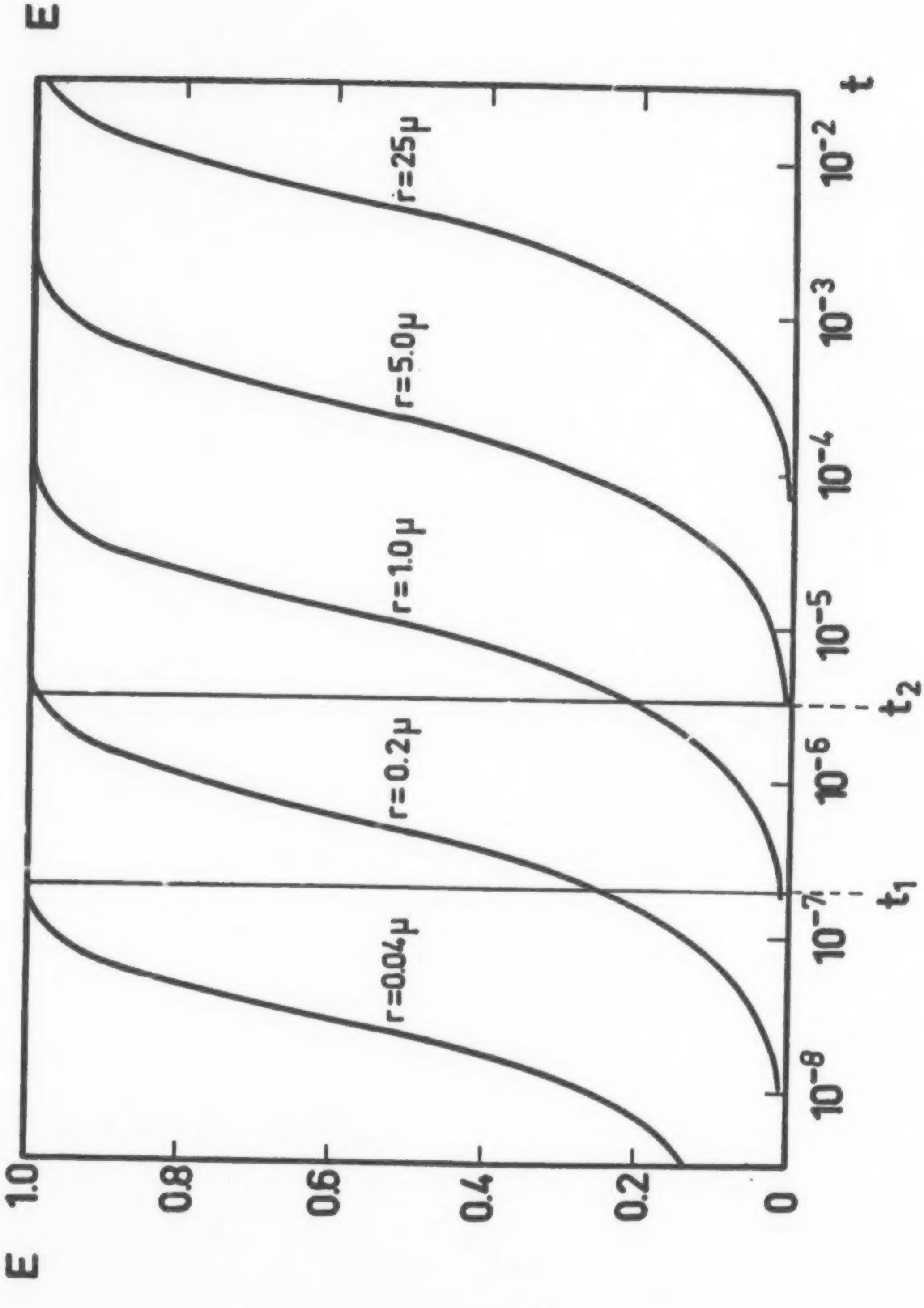
E
1.0
0.8
0.6
0.4
0.2
0
E
10^{-8}
10^{-7}
10^{-6}
10^{-5}
10^{-4}
10^{-3}
10^{-2}
t
t_1
t_2
r=0.04μ
r=0.2μ
r=1.0μ
r=5.0μ
r=25μ

Figure 2.

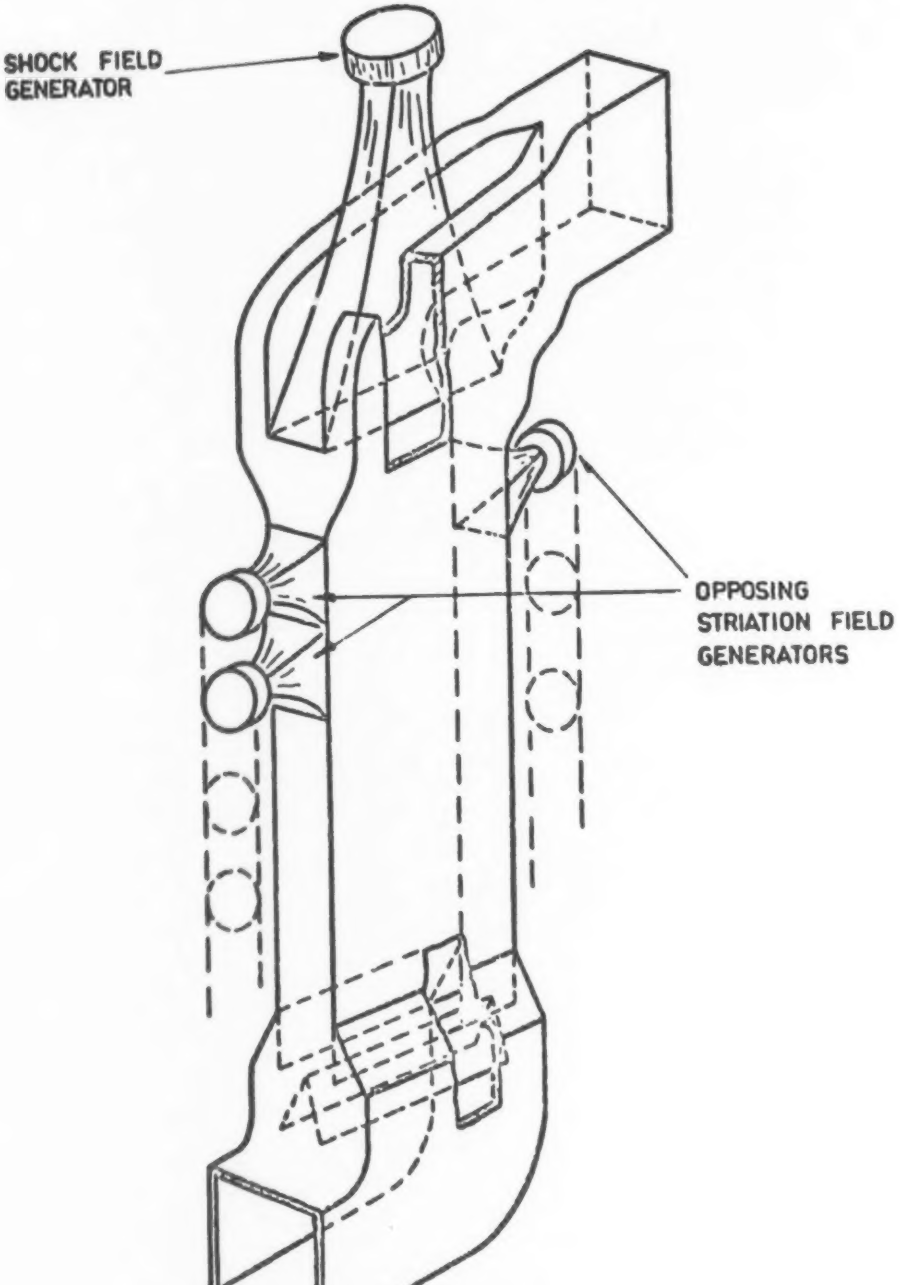
SHOCK FIELD GENERATOR
OPPOSING STRIATION FIELD GENERATORS

Figure 3.

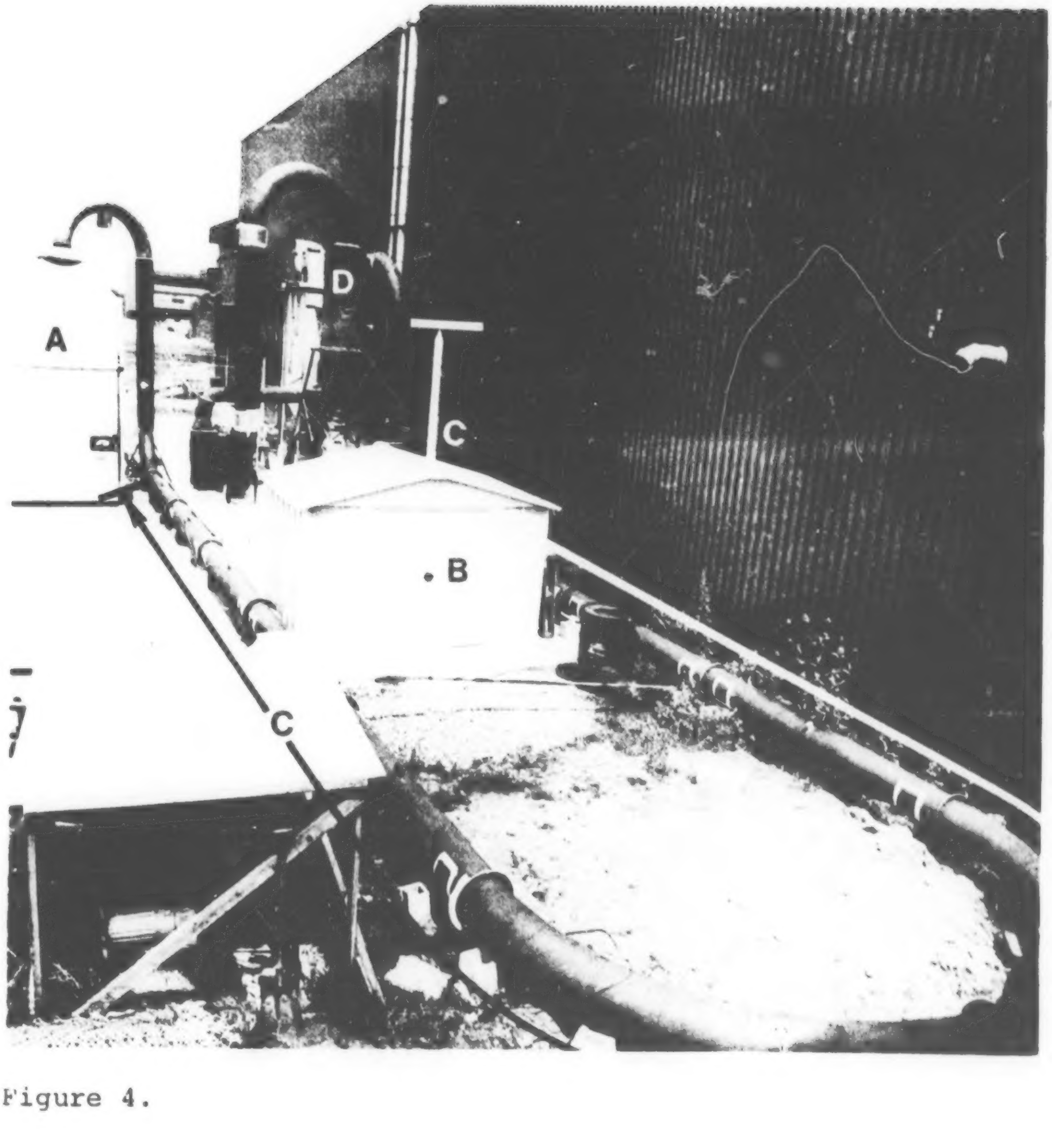

Figure 4.

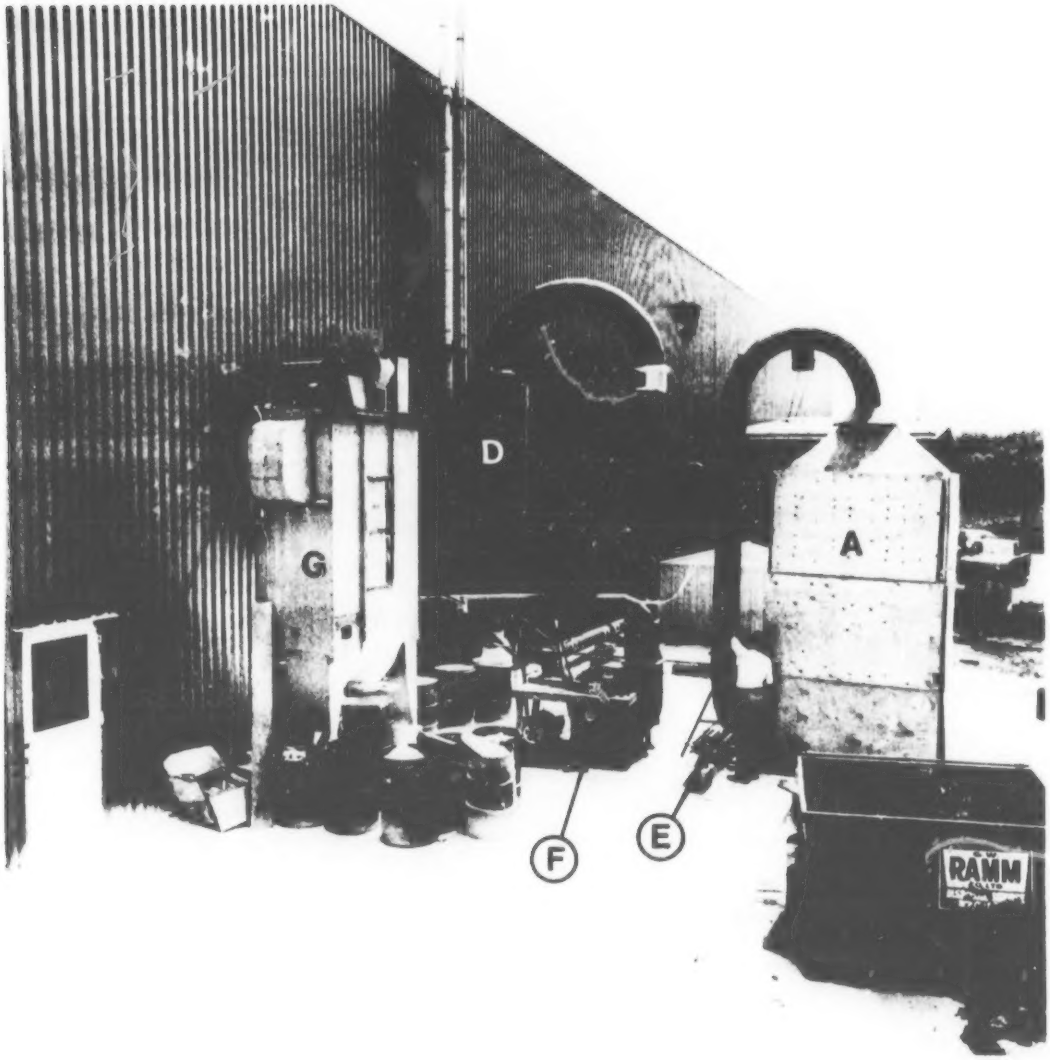

Figure 5.

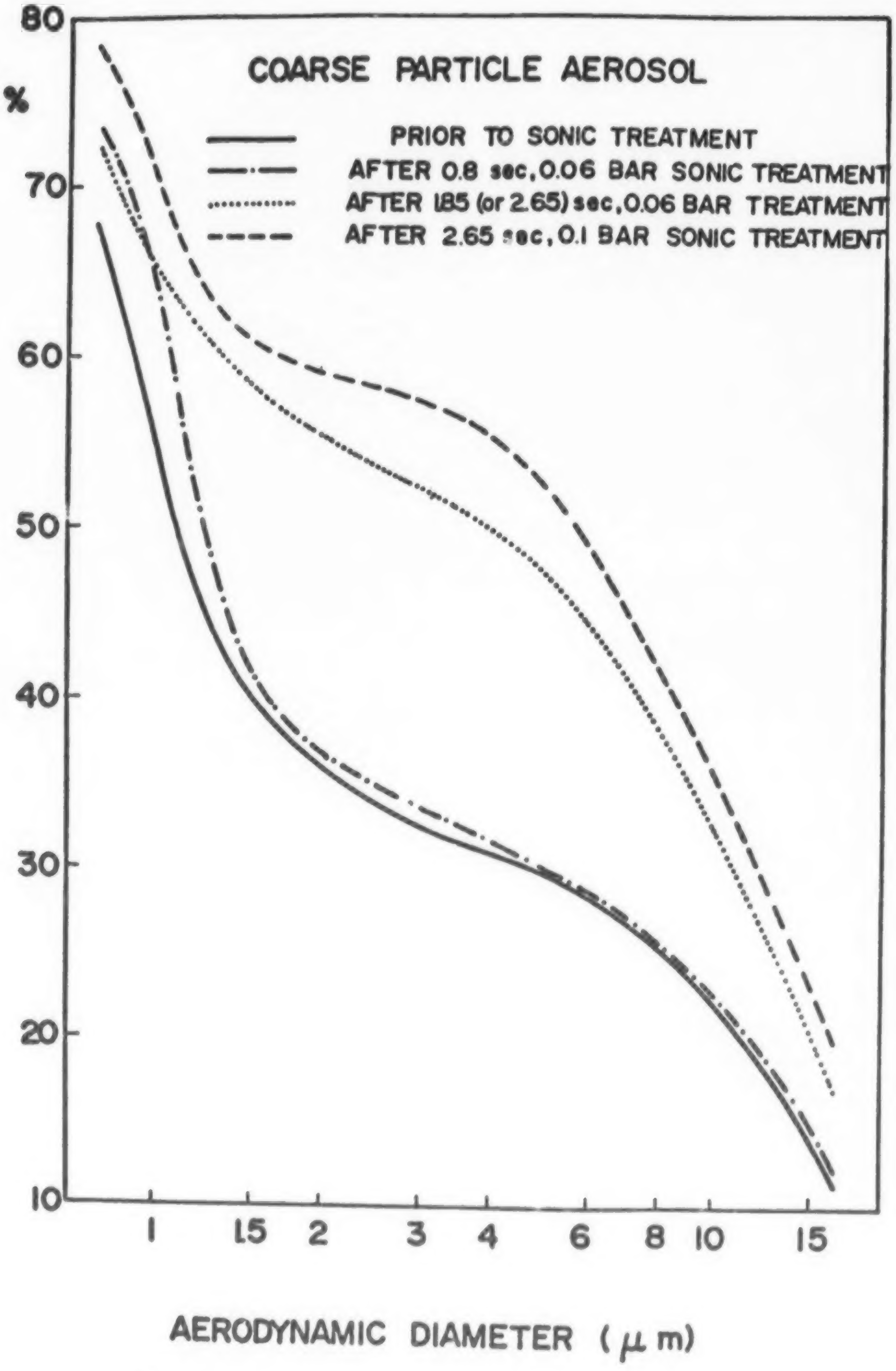
COARSE PARTICLE AEROSOL
PRIOR TO SONIC TREATMENT
AFTER 0.8 sec, 0.06 BAR SONIC TREATMENT
AFTER 1.85 (or 2.65) sec, 0.06 BAR TREATMENT
AFTER 2.65 sec, 0.1 BAR SONIC TREATMENT
%
80
70
60
50
40
30
20
10
1
1.5
2
3
4
6
8
10
15
AERODYNAMIC DIAMETER (μm)

Figure 6.

ENERGY CONVERSION (fuel to sound) EFFICIENCY	
Flap-valve unit	14 %
No-moving-part unit	7 %
Comparitive high-% siren	4 %

ACOUSTIC POWER AND INTENSITY	
Power	O(10 kwatts)
Intensity	O(160 db, ref 10^{-16} watts/cm^2)

AEROSOL	
Flow rate	75 m^3/min
Dust load	1-14 gms/m^3

TOTAL ANNUAL COSTS	
Agglomerator and collector	1.00-1.25 $/acfm.year
Comparitive equipment:	
Baghouse	0.71 $/acfm. year
Venturi scrubber	1.31 $/acfm. year
Electrostatic precipitator	2.04 $/acfm. year

TABLE 1
Summary ORF pulse-jet agglomerator results

SESSION 7

ADVANCES IN MEASUREMENT TECHNIQUES

Chairman: Elbert Tabor
U. S. Environmental Protection Agency
Research Triangle Park, N. C.

Paper No.

26 The Present Status of Particulate Mass Measurements

J. A. Dorsey and
D. B. Harris
U. S. Environmental Protection Agency
Research Triangle Park, N. C.

27 Plume Opacity Measurement

David S. Ensor
Meteorology Research, Inc.
Altadena, California

28 Instrumentation for Dispersion Analysis of Particulates in Industry

S. S. Yankovskiy and
Valery P. Kurkin
State Research Institute of
Industrial and Sanitary Gas Cleaning
Moscow
U.S.S.R.

29 Technology of Particulate Sampling From Reactive, Damp, and High-Temperature Gases

V. A. Anikeyev,
V. P. Bugayev,
V. A. Limanskiy,
Ye. N. Andrusenko, and
V. Yu. Padva
(presented by Valery P. Kurkin
State Research Institute of
Industrial and Sanitary Gas Cleaning)
Moscow
U.S.S.R.

SESSION 7 - Continued

Paper No.

30 Measurement of Particle Size Distributions at Emission Sources with Cascade Impactors

Michael J. Pilat
University of Washington
Seattle, Washington

31 The Chemical Composition of Fly Ash

David F. S. Natusch
University of Illinois
Urbana, Illinois

Paper No. 26

THE PRESENT STATUS OF PARTICULATE MASS MEASUREMENTS

by

J. A. Dorsey
and
D. B. Harris

U. S. ENVIRONMENTAL PROTECTION AGENCY

Research Triangle Park, N.C.

ABSTRACT

The manual and instrumental determination of particulate mass loading in process and control equipment in gas streams are discussed. These measurements remain among the most difficult required for air pollution stuides. Available manual methods, while costly and time consuming, are accurate at higher concentrations that have been reasonably well standardized. A significant lack of reproducibility exists at the low concentrations found after many control devices in work conducted thus far has failed to define the exact causes. A brief review of the principles available for instrumental measurements show that several approaches should be useful in research and development work. Of these, the adsorption of beta energy is the most general and has been shown to be applicable to control work. Several other techniques are promising at least for special situations. However, much work remains to be done before low costs, reliable particulate monitors are widely available.

Preceding page blank

Introduction

The majority of techniques presently available for the measurement of particulate mass were developed for the determination of concentrations that were in the range of 1.0 gr/NM^3 or greater and generally assumed the particulate size to be mostly 1 μm and larger. Not a great deal has been accomplished in evaluating the applicability of these approaches to the measurement of lower concentrations of particulate which have a large percentage by mass of submicron particles. The discussion of techniques that follows must, therefore, be considered with this in mind. Where data exists that is specifically applicable to the measurement of fine particulate, it will be pointed out.

In any discussion of particulate measurements it is necessary to consider the environment in which the measurements must be accomplished and what effect it will have on the validity of the data acquired. For particulate control system evaluations there are obviously two distinct environments; that of the stream entering the control device and; that of the stream leaving the device. For baghouses and electrostatic precipitators these regimes differ primarily in the amount and size distribution of the suspended particulate. For scrubbers, the exit regime may also differ drastically from the process stream being controlled in temperature, moisture content and composition of the suspended particulate. It is also quite possible that the two regimes have time dependent variations which are not influenced by the same parameters, that is, inlet particulate characteristics are process time dependent while the outlet particulate is most strongly dependent upon the control system operating characteristics.

As an attempt to mitigate against these factors, it has become standard practice to collect a time and spatially averaged sample through the techniques of traversing and isokinetic sampling. With this approach the duct or stack is divided into a number of equal areas, the sampling probe is moved in sequence to the center of each area and the probe velocity matched to the gas velocity at that point during acquisition of the sample. The procedures were developed many years ago and from the data available appear to be reasonably useful for steady state process streams with moderately efficient control devices. However, even under these circumstances, such sampling programs are very expensive and difficult to perform on large industrial equipment. It has been proposed that traversing and isokinetic sampling are unnecessary for fine particulate measurements and it would appear that the verification of these postulations could lead to significant reduction in the cost of fine particulate measurements. Unfortunately, the extent to which detailed sampling may be simplified is, for the most part, unknown and the areas where less complex approaches can be applied have not been investigated. It is, therefore, mandatory that the detailed techniques continue to be applied in spite of their cost.

Manual Sampling

A number of methods have been utilized for manual sampling in the United States with the most common being those published by the American Society of Mechanical Engineers (ASME, PTC 27), American Society for Testing Materials (ASTM, D-2928), Industrial Gas Cleaning Institute (IGCI Pub. No. 101) and Western Precipitating Company (Bulletin WP-50). All of these methods use dry filtration for collection of the particulate, and in general, were developed for "dusts" greater than 1 μm. There are many differences in the equipment specified in the methods and quite often several possible configurations are suggested without any comment as to the best or recommended system. Nevertheless, it is probably safe to assume that consistent results can be obtained by trained operators when the particulate concentrations are above 2 gm/NM^3 and are not primarily fine particles.

In 1961, investigators in what is now the Control Systems Laboratory, Office of Research and Development, EPA, devised a sampling train that incorporated features from a number of other methods. The basic concepts of this equipment were promulgated in 1971 as the official method for determining particulate emissions from fossil fuel fired steam generators, incinerators and cement plants. The equipment has a nominal flow rate of 25 lpm and uses dry filtration as do the previously mentioned methods but differs in that it specifies the filtration media and the minimum temperature of sampling and filtering. It is also unique in requiring velocity measurements to be made simultaneously with the sampling traverse and uses both instantaneous flow rate and integrated gas volume measurements. This train has been utilized successfully for sampling many processes and gives reproducible results down to approximately 0.5 gm/NM^3 with either dusts or fine particulate.

Recent data indicates that manual particulate measurements require improvement if they are to be useful for the very low concentrations normally found after high efficiency control devices. For example, while the coeffecient of variation at a 95 percent confidence level is about 24% at 2.0 gm/NM^3, it increases to 76% at 0.02 gm/NM^3, a concentration quite typical of the exit from control devices. The reasons for this rather drastic loss in reproducibility are not evident. Material handling losses, filter media penetration, adsorption of moisture and chemical reactions with the low mass, high surface area fine particulate sample have all been postulated as causes. However, the limited work conducted thusfar has not demonstrated a significant effect from any single parameter studied.

Instrumental Methods

The selection of particulate mass monitoring systems presents many problems because the characteristics of the particulate and gas stream have a profound effect on the system response. This situation makes the discussion of particulate monitoring difficult for it requires that each type of installation be specifically discussed in terms of the requirements necessary to perform the desired measurement accurately, reliably and at reasonable cost. Such a discussion of the specific effects of each measurement parameter for each possible monitoring application would require a comprehensive review and the following discussions will consider the generalized attributes of various analyzers and sampling equipment presently available.

There are a very limited number of techniques available for monitoring the mass concentration of particles in a process stream. A recent review of mass monitoring devices indicates that the only technique that has been reduced to practice is based on the attenuation of beta radiation by particulate collected on a filter media. The attenuation of energy is somewhat dependent upon the atomic number and atomic weight of the elements and the measurement is not strictly a function of mass. However, the data available for coal flyash, coal soot, cement dust and gypsum correlates to within 10% for a given sensor and the variation in the composition of particulate from a specific source is probably small enough in most cases to reduce the actual analysis error to 5% or less. There are also variations in sensor response introduced into the measurement by changes in filter media thickness, particulate deposition pattern on the filter and radiation source-detector geometry. These are all controllable variations which are fixed for a given sensor-source installation and can be kept small by proper calibration of the device.

There are commercially available beta attenuation sensors on the market. Several of these instruments operate at ambient temperatures and require gas stream cooling prior to filtration of the particulate.

The sensors have more than adequate sensitivity for most source concentrations and the cooling is normally accomplished by dilution in order to prevent liquid condensation. One recently available instrument filters at an elevated temperature and does not require cooling below 150°C (300°F). The overall measurement with all beta monitors is discontinuous in that the system goes through a repetitive sequence of filtration followed by analysis of the collected material. The time cycle is a function of particulate concentration, sample flow rate, dilution ratio and source-sensor properties. Information on the best combination of these variables for various process streams is lacking at present but it is reasonable to assume a 1 or 2 minute cycle can be achieved prior to any control equipment. After low temperature fabric filters and high efficiency dry electrostatic precipitators, adjustment of the sampling rate and dilution ratio should yield a cycle time of 2 to 4 minutes. Little is known about the operation of these devices after wet electrostatic precipitators, wet scrubbers or other high-moisture, low-particulate streams. Extremely high dilutions to prevent condensation could result in extended cycle times and require redesign of the sensing element geometry. Alternatively, filtration at even higher temperatures than presently available could produce a sensor which does not require any dilution and would be more suitable for these applications.

Both optical and electrical principles have also been applied to the analysis of particulate in process gases but only limited attempts have been made to correlate their response with particulate mass. Since these techniques are strongly influenced by many particle properties, it is virtually impossible to reach generalized conclusions concerning their applicability without acquiring extensive field data on the characteristics of various process streams.

Several particulate monitoring devices based on sensing the electrostatic charge on particles have been tested in process streams. In one system, the particles were passed through a corona discharge and the charge induced on them detected at a collector electrode located downstream. Several different design prototypes were constructed and measurements have been made on coal-fired boilers. No significant attempts to correlate the device response to particulate mass were made and the reports indicate that the responses were expected to correlate better with surface area. A second type of electrostatic device is based on the charge transfer developed between moving particles and a surface with which they are brought into contact. The response of this type of device is a function of the surface material, particulate composition and size, and gas flow rate through the sensor. In spite of these variables, several studies have shown a reasonably good correlation between instrument response and particulate mass in several different process streams. In each instance, calibrations were established for the specific source. These empirical calibrations varied considerably between the different sources. However, on a coal-fired boiler the correlation remained constant under conditions of full load, partial load and soot blowing which would indicate a low sensitivity to minor changes in particulate characteristics. All of the test data available has been obtained on effluent gases after particulate control devices and this would provide a partial answer to the unexpectedly good correlations since it is reasonable to assume that the mass size distribution of particles after a control device is fairly narrow. Devices based on this principle are available commercially and can reportedly be operated either with dilution or at elevated sensor temperatures. While the studies cited above indicate potential for use after all types of control equipment, there is no data available to define applicability to inlet gas streams where particulate properties may vary considerably.

No extensive correlations between mass and light transmission have been reported and the manufacturers of such instruments usually define the response of the sensor in terms of smoke density, percent transmittance or equivalent Ringelmann number. In one study, a reasonable correlation was found between mass and light transmission after an electrostatic precipitator on a coal-fired utility boiler under normal operating conditions. However, the same correlation did not hold under reduced load conditions and still a third response was noted when soot blowing was in progress. It appears that the complex nature of the interactions between particles and light will make this monitoring approach useful only for very homogeneous particulates: The application of the technique is improbable for general mass measurements.

The measurement of opacity has not been used in the evaluation of control equipment efficiency and does not appear to be applicable because of the complex interactions between particles and light energy mentioned earlier. The wide differences in particulate concentration and size distribution that exist between inlet and outlet of a control device would make the evaluation of efficiency based on light transmission data virtually impossible. However, the measurement of opacity after a control device is of importance in control equipment evaluations since there are often visible standards which must be met. Instruments are available for monitoring the opacity of effluent gases and they can be utilized to indicate the visual appearance of the plume provided the proper criteria have been considered in their design. In particular, the spectral response must be in the visible region and the sensor must be protected from stray light interference.

Sampling Systems

The techniques presently available for monitoring particulate mass require that a sample be extracted from the main gas stream and transported to the sensor. Normally, stainless steel nozzles and probes similar to those used in manual sampling systems are used to convey the sampled gases to the instrument. The use of this type of probe results in particulate losses by deposition and continuous monitoring, unlike manual sampling, cannot compensate for these losses. This may represent a major source of error in the measurement since probe depositions of 50% or more of the sampled particulate have not been uncommon in manual sampling. The losses are a function of many variables including particulate properties, nozzle design, probe diameter and length, and gas velocity in the transport system.

Conclusions

The measurement of particulate mass concentration, which was just beginning to achieve a reasonable level of technology for conventional sources, is now faced with a new set of problems related to fine particulate control systems. The existing manual methods are not capable of acquiring reproducible data at very low concentrations and have also become very expensive due to the long sampling times required to collect a weighable sample. The possibility of chemical reactions causing erroneous results has become very significant due to the much higher concentration of gaseous materials relative to the particulate mass. On the positive side, the requirements for traversing and isokinetic sampling can potentially be simplified--although studies must be conducted to demonstrate the validity of this--resulting in lower measurement costs.

The instrumental measurement of particulate may actually be easier to achieve for fine particulate than it has been for total particulate because the range of particle characteristics will undoubtedly be much smaller and this should increase the sensing principles which can be applied. As with manual methods, if the requirements for traversing and isokinetic sampling can be reduced, the installation of particulate monitors will be greatly simplified. The major effort required in the area of instrumental methods is the acquisition of field data that will define the applicability of available sensors to various process and control system streams.

Preceding page blank

Paper No. 27

PLUME OPACITY MEASUREMENT

by

David S. Ensor

METEOROLOGY RESEARCH, INC.

Altadena, California

Preceding page blank

ABSTRACT

The visual appearance of plumes has long been used as a means to regulate the emission of particulate matter from air pollution sources. The technical interperation of the visual effects of the plume in terms of other aerosal propenties such as size distribution, particle composition and concentration will be disucssed. The current approaches used to measure plume opacity will be covered including in-stack and remote sensing techniques. The physical limitations of present approaches as well as possible future developments will be covered.

Preceding page blank

I. INTRODUCTION

A. Objective

The visual appearance of smoke plumes has been used for regulation of air pollution sources for over 60 years. Opacity is defined in the Federal Register (1971) as

> "... the degree to which emissions reduce the transmission of light and obscure the view of an object in the background."

The generally accepted method for plume opacity measurement is a field observation by an individual who has been trained to "read" the plume under specified conditions of sun angle, wind direction, and distance from the stack. In the last few years, there has been increased interest in substituting or supplementing instrumentation for this "subjective" observation. It is the purpose of this paper to review the various instrumental concepts used to measure opacity.

B. Brief Review of Legal Aspects

The earliest air pollution law regulating smoke emissions in the United States was the 1881 Chicago smoke ordinance which deemed the emission of dense smoke a public nuisance (Nicholson, 1905). The nebulous legal definition of public nuisance or dense smoke in the regulation forced an inspector to make an arbitrary decision at the site as to the degree of public nuisance, a decision that could be easily challenged in court.

In 1898, Ringelmann reported a smoke chart devised to quantify the appearance of smoke. This chart consisted of standards constructed by drawing black ink lines of various widths on white paper to form a grid. When the charts are viewed from a distance of at least 50 ft, apparent shades of gray from white to black may be seen. The chart was simple and inexpensive and could be reproducibly constructed. The usefulness of this chart to quantify the public nuisance of dense smoke was quickly recognized, and the Ringelmann smoke chart was specified in regulations throughout the world. The first smoke ordinance in the United States utilizing the Ringelmann smoke chart was passed in Boston in 1910 (Kudlich, 1955). The constitutionality of smoke ordinances was upheld in the United States Supreme Court in the case of Northwestern Laundry versus City of Des Moines in 1916 (Edelman, 1970). The paper Ringelmann chart was used as a smoke standard in most large cities in the United States for the next 40 years.

The 1947 State of California enabling act, Health and Safety Code 24198 to 24341, allowed any county to form air pollution control districts. Section 24242 contained a provision extending the Ringelmann number evaluation to non-black smokes of "such opacity as to obscure an observer's view to degree equal to or greater than does smoke." This so-called "equivalent opacity" concept was first used in the Los Angeles County Air Pollution Control District Rule 50 in 1948. The use of equivalent opacity for source regulation is still a very controversial subject and was difficult initially to enforce.

The Los Angeles County Air Pollution Control District started a "plume reading school" to train smoke inspectors for qualification as legally recognized expert witnesses. The black smoke school was begun in 1950, and the qualification of trained smoke inspectors as expert witnesses for evaluation of smoke emissions without the paper Ringelmann chart was upheld in People versus International Steel in 1951. The white plume school was begun in 1954, and the "equivalent opacity" concept was legally recognized by the courts in People versus Plywood Manufacturers of California in 1955 primarily on the qualifications of the inspectors as expert witnesses (Edelman, 1970).

Smoke school field work consists of training inspectors with plumes of known opacity generated by a standard smoke source, as described by Weisburd (1962). The smoke source has a short stack about 15 ft high and 12 inches in diameter. A reference transmissometer is mounted near the top of the stack to measure the in-stack light transmittance. The Ringelmann number and opacity are related to the light transmittance as indicated in Table I.

Black smoke is generated by the incomplete combustion of benzene, and white smoke is usually generated by the injection of fuel oil into the manifold of a small air-cooled gasoline engine.

Table I

COMPARISON OF PLUME LIGHT ATTENUATION TERMS

Plume Transmittance (Percent)	Ringelmann Number (Black Plumes)	Plume Opacity (Percent) (Non-Black Plumes)
100	0	0
80	1	20
60	2	40
40	3	60
20	4	80
0	5	100

The training for witnessing white and black plumes is conducted separately. The inspectors are first familiarized with the reading techniques using plumes of known opacities. After the familiarization phase, the inspectors then evaluate plumes of unknown opacities to the nearest 5-percent opacity generated in random order in runs of 25 readings. For certification, an inspector must demonstrate a proficiency for plume evaluation within an absolute deviation of 7.5-percent opacity measured in the stack for at least two runs. Any reading in error by more than 15-percent opacity will void the run.

The training and subsequent field reading for enforcement purposes are usually performed according to the following rules:

1. The observer is at right angles to the plume.
2. The sun is at the back of the observer.
3. The plume is read at the point of greatest opacity.
4. The observer stands at approximately two stack heights but not more than a quarter of a mile from the stack.
5. The plume is viewed against a contrasting background.

The observation is shown diagrammatically in Fig. 1.

The Bay Area Air Pollution Control District adopted a similar "equivalent opacity" rule in its Regulation 2 in 1960. The Bay Area Air Pollution Control District, instead of using the defined relationship between the in-stack transmittance and plume opacity reported in Table I, considered the problem from a different aspect (Coons et al., 1965). A group of inspectors, trained with the paper Ringelmann chart, evaluated white and black plumes of unknown opacities generated with a standard smoke source. Their readings of plume opacity were then used to develop "calibration curves" relating the in-stack transmittance to the inspector plume opacity reading.

These calibration curves were used by the Bay Area Air Pollution Control District until recently when a new rule was approved reducing the Ringelmann limit from Number 2 to Number 1. Brennan (1971) reported that a new "calibration curve" had been developed by expert observers who had prior training with a smoke generator. This new calibration curve is said to be quite similar to the defined relationship in Table I.

The Texas Air Control Board Regulation I adopted in 1969 has a provision for the use of instrumental measurements of in-stack transmittance to supplement human observers (McKee, 1971). A simple smoke meter has been used in most of the industrial sources in Texas. The regulation specifies a minimum transmittance of 70 percent with standard graphs to correct the instrumental measurements for length of path and volumetric flow rate of the stack gases.

On December 23, 1971, the standards of performance for new stationary sources pursuant to Section 111 of the Clean Air Act as amended were promulgated. New (after August 17, 1971) steam generators, cement plants, incinerators, nitric acid plants, and sulfuric acid plants are regulated nationally to stringent limits of opacity. Also, the continuous monitoring of particulate matter in steam generators is required using "a photoelectric or other type smoke detector and recorder except where gaseous fuel is the only fuel burned."

II. INTERPRETATION OF OPACITY

A. Theory of the Smoke Plume Observation

The visual luminance contrast of an object against an extensive and uniformly appearing background is given by (Middleton, 1952)

$$C_o = \frac{B_o - B_b}{B_b} \qquad (1)$$

where B_o is the luminance of the object and B_b is the luminance of the background. Our sense of vision (in the absence of color effects) depends primarily on the perception by the eye of differences in luminance (light flux per unit area normal to the direction of observation divided by the solid angle subtended by the light source at the viewing surface, candles/m^2) between points in the field of view. For an ideally black object, the object luminance B_o is zero and the contrast equals -1.0. Contrasts greater than 10 are seldom measured for bright objects during periods of daylight.

If the visual contrast between the object and its background is less than the contrast threshold of the eye, the object will not be visually detectable. The contrast threshold is a function of the subtended angle of the object (size of the object and distance from the observer), the background luminance (eye adaptation luminance), the sharpness of the boundary of the object, and the presence of other interfering objects in the field of view. The contrast threshold for a 50-percent probability of visually detecting lighted targets was reported by Blackwell (1946) to be about 0.003 for daylight illumination and a subtended angle of the object greater than 30 minutes. The contrast threshold for black objects is usually 20 percent lower than for white objects.

The plume contrast is simply related to the light transmittance of the plume. The luminance of the plume is given by

$$B_p = B_a + B_b\,T \qquad (2)$$

where B_a is the plume air light (the light scattered by the plume to the observer), and $B_b T$ is the amount of light transmitted through the plume. B_b is the background luminance, and T is the fraction of background light transmitted through the plume. Often, the background luminance is the sky behind the plume. The plume contrast C_p can be obtained by substituting Eq. (2) for B_o in Eq. (1) as reported by Conner and Hodkinson, (1967)

$$C_p = \frac{B_a}{B_b} - (1 - T) \qquad (3)$$

$$\text{Plume contrast} = \frac{\text{Plume air light luminance}}{\text{Background luminance}} - \text{Plume opacity}$$

This equation illustrates the three main optical effects of plumes:

1. The plume contrast C_p indicates the visual appearance of the plume against its background (what a person sees).

2. The fractional plume opacity $(1-T)$ is an intrinsic property of the plume, which is independent of the illumination and the viewing angles, and indicates the fraction of background light transmitted through the plume.

3. The plume air light to background luminance ratio, B_a/B_b, indicates the magnitude of light scattered to the observer. This ratio is dependent upon the plume light scattering properties, the angle between the sun and the observer, and the background illumination.

Smoke inspectors are taught to associate a plume to background contrast with a given in-stack transmittance. The proper selection of a background is one which allows a consistent change in plume to background contrast with changes in the plume transmittance.

B. Relationship of Plume Transmittance to Mass Concentration

The plume transmittance is related to the diameter of the plume by

$$T = \exp[-b_{ext} L] \qquad (4)$$

where b_{ext} is the extinction coefficient and L is the diameter of the plume.

In a theoretical study reported by Ensor and Pilat (1971), the mass concentration is related to the extinction coefficient by

$$M = K \rho B_{ext} \qquad (5)$$

where K is a parameter which is a function of particle size distribution and refractive index, and ρ is the specific gravity of the particles. An example of these calculated results is shown in Fig. 2 for a refractive index of 1.50 and a log normal size distribution. One of the significant results of the calculations was the discovery that increasing polydispersity reduces the effects of size distribution variation on the parameter K.

C. Considerations in Developing Instruments for Opacity Measurement

The substitution of an instrument for the smoke inspector is a very desirable advance. The observer-determined opacity is an interpretation of the plume to background contrast to determine an opacity reading. Questions are always raised about the suitability of an instrument to measure the degree of public nuisance caused by the plume (Sim and Borgos, 1973). Fick (1973) has described in detail the many uncertainties caused by differences in-stack and exterior plume properties. Whatever instrumental approach is taken, the output will be subtly different than the legally recognized observation.

Texas Regulation I boldly specified a maximum in-stack light transmittance over a specified path length as the basis for the regulation. Thus, many of the objections of the use of instruments for compliance measurement were solved from a legal standpoint.

III. INSTRUMENTAL MEASUREMENTS

A. Stack-Mounted Sensors

1. Considerations in Application

Location of the sensor at the stack has the advantages of permanent installation and low cost and does not require constant attention. Stack sensors also are independent of ambient lighting conditions and are capable of continuous use. However, the engineering problems of measuring a hot, dirty, corrosive gas are often severe. The sensor electronics are also subject to vibrations and extremes in atmospheric temperatures.

2. Transmissometers

Stack transmissometers in the form of the "smoke meter" have been installed on smoke stacks for quite a number of years to warn operators of possible opacity violations. These instruments are very simple, consisting of a light source on one side of the stack and a detector on the opposite side of the stack as shown in Fig. 3. Various versions of these instruments have been used with hundreds of installations. However, these instruments vary widely in quality and price and many are considered to be qualitative rather than quantitative sensors.

The EPA is currently developing guidelines in the construction of stack transmissometers. The guidelines call for standardization of the wavelength response to a photopic or green, a restriction of the detector acceptance angle and collimation to less than 5 degrees, and minimum levels of reliability. The wavelength standardization is very important because the extinction is usually wavelength dependent. The function relationship between light extinction and wavelength depends on the particle size. The restriction of the acceptance angle of the transmissometer is important because the detection of scattered light may cause large increases in the apparent light transmittance. This is a subtle error because it is a function of the angle of the detector, projector, particle size, and, to a less appreciated extent, the light transmittance. The theoretical error in the extinction coefficient was computed by Ensor and Pilat (1971) for various size distributions, as shown in Fig. 4. The error is reported as the ratio R, the measured extinction coefficient divided by the real extinction coefficient.

The error in light transmittance from scattered light is also a function of the magnitude of the light transmittance as a consequence of Beer's law. This error is shown in Fig. 5 as a function of light transmittance and the parameter R.

Tomaides and Peterson (1973) reported experimental determinations of the errors in the measurement of fly ash transmittance. They compared the light transmittance measured with a transmissometer having a variable acceptance angle to a reference transmissometer.

The most advanced transmissometer is that developed by Irwin Sick. This instrument is sold in the United States by Lear Siegler, Inc. (Sims and Borgos, 1973). Other manufacturers have recently announced transmissometers which meet the EPA guidelines.

3. Integrating Nephelometer

A direct way to measure the extinction coefficient as defined by Beer's law, Eq. (4), is with the angular integrated nephelometer. An advantage of this approach is the inherent sensitivity of the instrument because the signal is directly proportional to the parameter of interest instead of a ratio as in the transmissometer. The extinction coefficient is used for correlations to mass concentration. The integrating nephelometer as reported by Charlson et al (1969) is proving to be an extremely useful instrument for measuring atmospheric visibility. (Samuels et al., 1973)

The instrument is almost as simple as a transmissometer without the problems of alignment and dirt buildup on optics. The optical arrangement is shown in Fig. 6. The instrument is a physical analog to the equation defining the scattering coefficient

$$b_{scat} = 2\pi \int_0^{\pi} I(\theta) \sin \theta d\theta$$

where $I(\theta)$ is the angular scattered light.

The light source is behind a diffuse filter which weighs the light as a cosine function. The detector at right angles to the light source looks past the light into a light trap. The scattered light as measured by the detector has a sine weighting by virtue of the perpendicular orientation to the cosine lamp. Thus, the progressive distance away from the detector in the scattering volume corresponds to a scattering angle of near forward to far backscattering. In addition, the scattering angles are weighed identically because the sample volume increases on the distance from the detector squared. This exactly balances the distance squared reduction in brightness of the scattered light.

Meteorology Research, Inc., is developing this concept into a useful stack monitoring device as described by Ensor and Bevan

(1973). Potential sources of error with this approach are light losses at the extremes of the integration "angular truncation" and light attenuation from the sample volume to the detector. The angular truncation errors from preliminary analysis are about ±15 percent and the error from light attenuation is less than 6 percent under most conditions. The instrument has been released in a production run of ten units after an extensive evaluation of the prototypes and is expected to be used on additional selected stacks.

The range of operation of the instrument is shown in Fig. 7. The stack instrument is two orders of magnitude less sensitive than the ambient instrument but has more than sufficient sensitivity for monitoring most sources.

It was decided to concentrate on an extractive method to solve the difficult sampling problems such as high humidity stacks and condensing materials. The flexibility gained with a sample probe and an out-of-stack sensor in many cases outweighs the uncertainties caused by line losses and representativeness of the sample.

B. Remote Methods

1. Implementation Considerations

Measurement of the exterior plume has the advantage of being more similar to the opacity observations than in-stack techniques because the plume near atmospheric temperature and dilution can be measured. All remote methods are affected by the ambient meteorological conditions and most are not usable at night. In addition, trained personnel must be used to operate many of the instruments.

2. Passive Methods

Passive methods utilize ambient lighting as a means of measurement and thus are not usable at night or under overcast conditions. Many of these methods are described in detail by Conner and Hodkinson (1967).

- Smoke Inspection Guide

For at least 60 years, smoke inspection guides utilizing tinted glass have been used to improve the accuracy of smoke reading. Modern guides for the evaluation of black smoke have been reported by Rose et al. (1958) and for white smoke by Conner et al. (1968). The guides allow the observer to compare the plume transmittance to the light transmittance of a reference filter that has light scattering and absorbing properties similar to many smoke plumes under similar atmospheric lighting conditions, rather than comparing plume transmittance with light reflected from a paper chart. However, the guides do not improve the accuracy of the observation over that of a trained observer sufficiently to be of general use.

- Sun Photometer

The sun photometer is a simple detector designed to measure the attenuation of the sun through the plume. Circumstances must be selected where the plume, sun, and observer are in the correct position. A sun photometer is currently being sold by Forney Engineering Company (1973) which is similar to a concept suggested by Conner and Hodkinson (1967).

- Contrasting Target Method

The brightness of a contrasting target viewed through the plume is measured either with a telephotometer or photographically. The points of measurement are shown in Fig. 8. The transmittance of the plume is given by

$$T = \frac{B_{sp} - B_{hp}}{B_s - B_h}$$

where B_{sp} is the brightness of the sky and plume, B_{hp} is the brightness of the hill and plume, B_s is the brightness of the sky, and B_h is the brightness of the hill. The ratio of the differences of brightness is used to cancel the plume air light. The target may be artificial, a handy hill, or nearby dark structure. When a telephometer is used to measure the brightness, the plume should be constant to allow time for the four measurements. When the plume and background target brightness is measured photographically, the optical density of the negatives at the point of interest is measured with a microdensitometer in a laboratory. The relative brightness is determined from the optical density with the use of a calibration curve determined for each roll by photographing a grey scale or a series of neutral density filters. This method is suitable for measurement of rapidly changing plume opacities.

3. Active Methods

These techniques are limited by the meteorological conditions but are not dependent on ambient lighting. A number of methods have been used for research, including external transmissometers, photometry of lights, and lidar (light detection and ranging). The lidar may have promise because it is a single-ended remote measurement technique. For this reason, extensive engineering efforts have been sponsored by the Edison Electric Institute and the EPA to develop plume lidar. These efforts are reported by Cook et al. (1972) and Bethke (1973).

The device consists of a pulsed or chopped laser light source, a telescope detector, and signal processing electronics as diagramed in Fig. 9. The return is quite similar to that diagramed in Fig. 10. There is a large backscatter signal from the plume followed by a light scattered from the atmosphere behind the plume. The light scattered beyond the plume is attenuated by the plume. The transmittance of the plume is related to the reduction in signal. The error, as reported by Cook et al. (1972), is less than 7.5 percent for transmittances greater than 0.8 and less than 12 percent for transmittances greater than 0.50. One of the goals of current plume lidar research is the development of an instrument with a price low enough for general use (Conner, 1973).

C. Future Development

1. Instrumentation

The instrumentation for smoke plume measurement is undergoing marked improvement in design in response to EPA guidelines and the demands of measurement of cleaner stacks. As regulations become more stringent, there will be a greater requirement for more sensitive detectors. If an invisible plume is required, an instrument must be made sensitive enough to be responsive to process upsets that may lead to visible emissions.

2. The Physics of Stack Aerosol

The new generation of opacity instruments as well as other source instrumentation will permit better measurements of source aerosol. These data will allow better understanding of the physics of the aerosol.

- Relationship of Plume Opacity to Mass Concentration, Size Distribution, and other Properties

In a number of research programs, the opacity to mass concentrations are being determined experimentally. This work is being done at the University of Washington under an EPA grant and under EPA contract.

- In-Stack Opacity vs. Exterior Opacity

One of the fundamental assumptions with the use of an in-stack monitor for compliance testing is that the monitor will correctly indicate the opacity seen by people outside. There have been some studies which indicate that for cool-fired power plants there is good correspondence between in-stack and out-of-stack opacity (Tomaides and Peterson, 1973). However, there is evidence that for other sources this may not be the case. For example, Kester (1972) reported that the exterior opacity of a hogged fuel boiler was related to the fuel moisture content rather than in-stack opacity.

• The Effect of Water Vapor on Opacity

The effect of water on plume opacity has been sidestepped by either exempting the plume from regulation or specifying an inspector to read the plume downwind of the source. With increased use of wet scrubbers, it will be imperative to understand this phenomenon. Yocom (1963) reported sample withdrawal from the stack and heating prior to measurement with a transmissometer. It appears that this approach has limited application. From experiments done with humidity conditioning of the inlet of an Integrating Nephelometer (Covent, Charlson, Ahlquist, 1972), ambient aerosols exhibit a large increase in scattering coefficient with increasing relative humidity. The relationship of scattering coefficient to relative humidity is a strong function of the composition of the material. The change in visual effects of a condensing and then evaporating plume should be similar to that determined for materials of similar composition.

• Relating Source Opacity to Downwind Visibility

The impact of point sources on the visibility of nearby regions is of great concern. The availability of improved opacity instruments and ambient aerosol and gaseous sensors in instrumented aircraft (Blumenthal, 1973) makes it possible to gather data that may allow linking of source opacity to ambient visibility. Predictions of this type have been reported by Ensor et al. (1973), and MRI is currently doing programs to gather this type of data for industrial clients.

IV. SUMMARY

The measurement of plume opacity still is dominated by the use of trained observers. The recent adoption of Regulation I in Texas as an alternative to the trained observers and the EPA specification of a "smoke meter" as a continuous monitor are stimulating the use of stack instrumentation. With the new proposed guidelines by EPA for opacity meters, instruments are being sold with known wavelength and acceptance angles. It is expected that the use of various kinds of instruments to measure opacity will become more accepted as scientific measurers.

The development of improved stack and exterior plume instruments of various kinds is expected to stimulate new research in plume aerosol physics.

V. ACKNOWLEDGMENTS

Much of the background information for this presentation was developed during graduate studies at the University of Washington Department of Civil Engineering. Support at that time was in the form of EPA Air Pollution Traineeships and Special Air Pollution Fellowships. Meteorology Research, Inc., internal research funds were used to write this paper.

VI. REFERENCES

Air Pollution Control Field Operations Manual, 1962, (M. F. Weisburd, ed.), P. H. S. Publ. 937.

Bethke, G. W., 1973: Development of range squared and off-gating modifications for a lidar system. December, EPA-650/2-73-040.

Blackwell, H. R., 1946: Contrast thresholds of the human eye. J. Opt. Soc. Amer., 36, 624-643.

Blumenthal, D. L., 1973: Measurement of physical and chemical plume parameters using an airborne monitoring system. Paper 73AP16, Pacific Northwest International Section Air Pollution Control Assoc., Seattle, Wash., November 28-30.

Brennan, T., 1971: Evaluation of visible plumes. Paper presented at 12th Conf. on Methods in Air Pollution and Industrial Hygiene Studies, Los Angeles, Calif., April 6-8.

Charlson, R. J., N. C. Ahlquist, H. Selvidge, and P. B. MacCready, Jr., 1969: Monitoring of atmospheric aerosol parameters with the integrating nephelometer. J. Air Poll. Control Assoc., 19, 937-942.

Conner, W. D. and J. R. Hodkinson, 1967: Optical Properties and Visual Effects of Smoke Stack Plumes. P. H. S. Publ. No. 999-AP-30.

Conner, W. D., C. F. Smith, and J. S. Nader, 1968: Development of a smoke guide for the evaluation of white plumes. J. Air Poll. Control Assoc., 18, 748-750.

Conner, W. D., 1973: Environmental Protection Agency personal communication.

Cook, C. S., G. W. Bethke, and W. D. Conner, 1972: Remote measurement of smoke plume transmittance using lidar. Appl. Optics, 11, 1742-1748.

Coons, J. D., H. A. James, H. C. Johnson, and M. S. Walker, 1965: Development, calibration and use of a plume evaluation training unit. J. Air Poll Control Assoc., 15, 199-203.

Covert, D. S., R. J. Charlson, and N. C. Ahlquist, 1972: A study of the relationship of chemical composition and humidity to light scattering by aerosols. J. Appl. Meteor., 11, 968-976.

Edelman, S., 1970: The Law of Air Pollution Control. Environmental Science Services Div., Stamford, Conn., 296 pp.

Ensor, D. S., and M. J. Pilat, 1971: Calculation of smoke plume opacity from particulate air pollutant properties. J. Air Poll. Control Assoc., 21, 496-501.

Ensor, D. S., and M. J. Pilat, 1971: The effects of particle size distribution of light extinction measurement. Amer. Ind. Hyg. J., 32, 287-292.

Ensor, D. S., and L. D. Bevan, 1973: Application of nephelometry to the monitoring of air pollution sources. Paper 73-AP-14 presented Annual Meeting Pacific Northwest International Section Air Pollution Control Assoc., November 28-30.

Ensor, D. S., L. E. Sparks, and M. J. Pilat, 1973: Light transmittance across smoke plumes downwind from point sources of aerosol emissions. Atmos. Environ., in press.

Environmental Protection Agency, 1971: Standards of performance for new stationary sources. Federal Register, 36, 247, December 23.

Fick, O. A., 1973: Compliance vs. control monitoring using optical, in-stack opacity monitors. Paper presented at Annual Meeting of Pacific Northwest International Section Air Pollution Control Assoc., Seattle, Wash., November 28-30.

Forney Engineering Co., 1973: Forney Opacity Meter. Product Information Bulletin, 3405 Wiley Post Road, P.O. Box 189, Addison, Texas 75001.

Kester, R. A., 1972: Hog-fuel boiler plume opacity related to operating parameters. Paper 72-AP-33 Air Pollution Control Assoc. Pacific Northwest Section, Eugene, Oregon, November 15.

Kudlick, R., 1955: Ringelmann smoke chart. U. S. Dept. of Interior, Bureau of Mines, Information Circular #7718.

Mckee, H. C., 1971: Instrumental method substitutes for visual estimation of equivalent opacity. J. Air Poll. Control Assoc., 21, 488-490.

Middleton, W. E. K., 1952: Vision Through the Atmosphere. University of Toronto Press, Toronto, Canada, 250 pp.

Nicholson, W., 1905: *Smoke Abatement,* Griffinan Co., London.

Rose, A. H., J. S. Nader, and P. A. Drinker, 1958: Development of an improved smoke inspection guide. *J. Air Poll. Control Assoc.*, *8,* 112-116.

Samuels, H. J., S. Twiss, and E. W. Wong, 1973: Visibility, light scattering and mass concentration of particulate matter. State of California Air Resources Board Report of the California Tri-City Aerosol Sampling Project, July.

Sem, G. J., and J. A. Borgos, 1973: State of the art: 1971, Instrumentation for measurement of particulate emissions from combustion sources, Vol. IV: Experiments and Final Report. TSI report to EPA Control Systems Laboratory, EPA-650/2-73-022.

Tomaides, M., and C. M. Peterson, 1973: Practical accuracy of the particulate emission opacity measurement. Paper presented at First International Conf. in Particle Technology, Chicago, Ill., August 21-24.

Yocom, J. E., 1963: Problems in judging plume opacity -- a simple device for measuring opacity of wet plumes. *J. Air Poll. Control* Assoc., 13, 36-39.

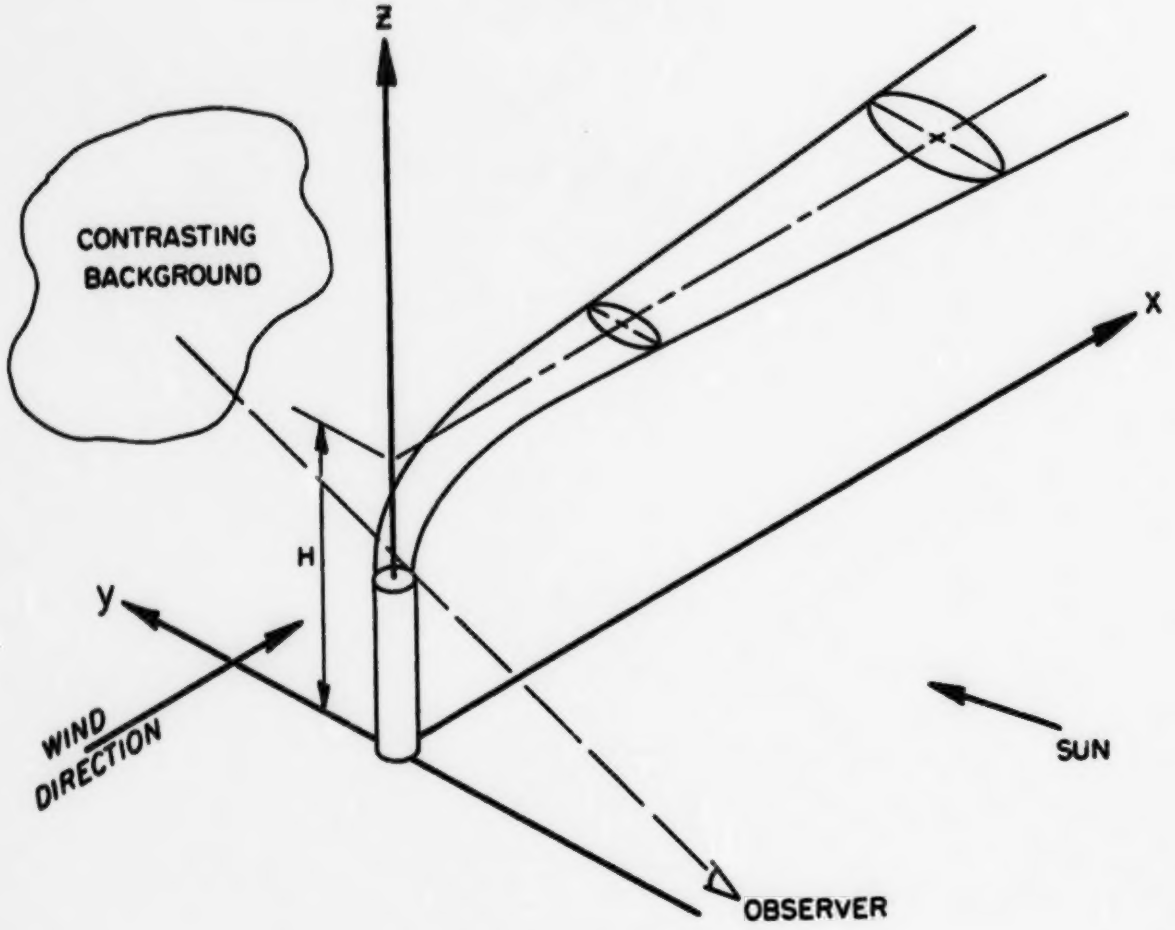
Z
CONTRASTING BACKGROUND
X
H
y
WIND DIRECTION
SUN
OBSERVER

Fig. 1. DIAGRAM OF PLUME OPACITY OBSERVATION

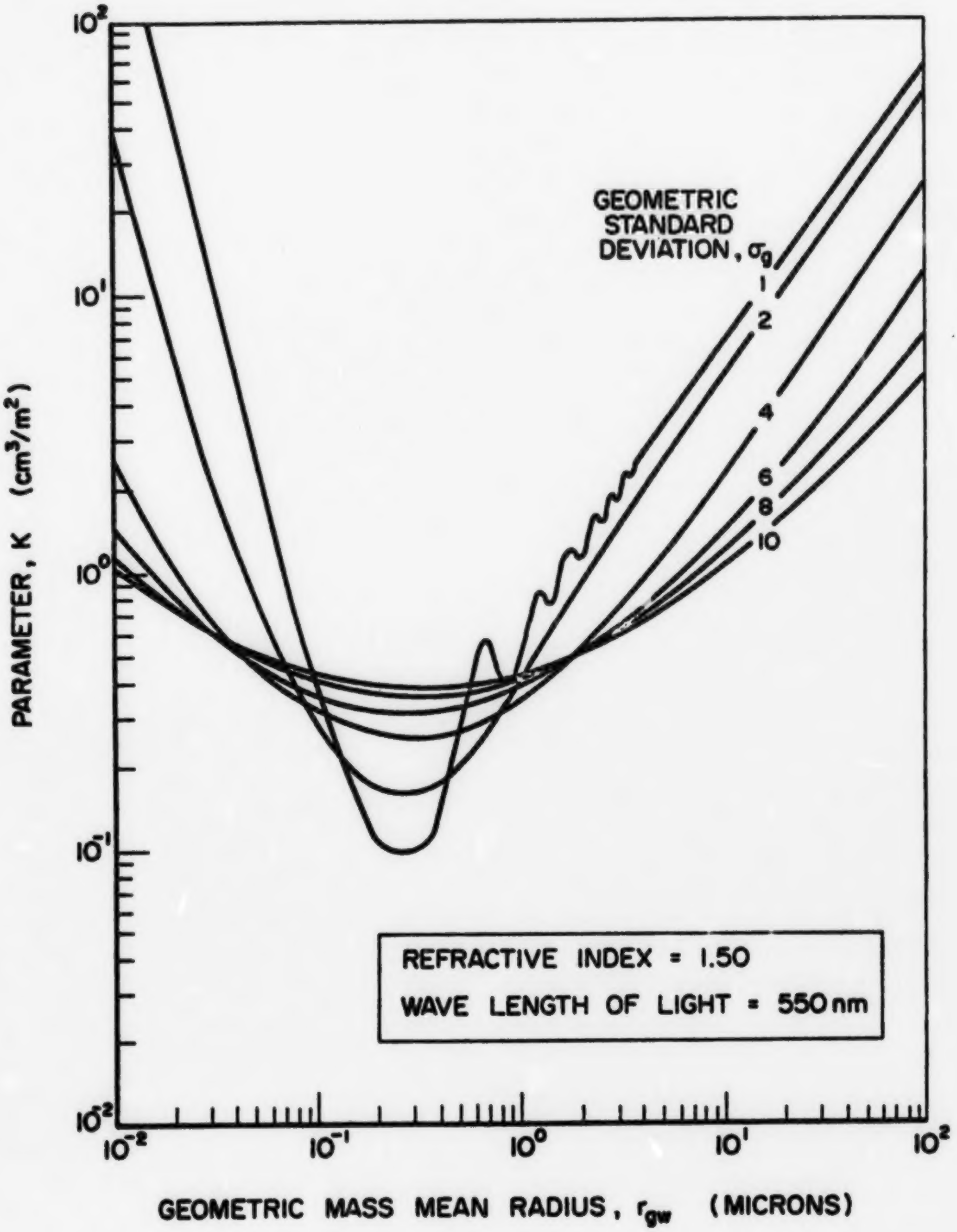

Fig. 2. THE PARAMETER AS A FUNCTION OF THE GEOMETRIC MASS MEAN RADIUS FOR A WHITE AEROSOL

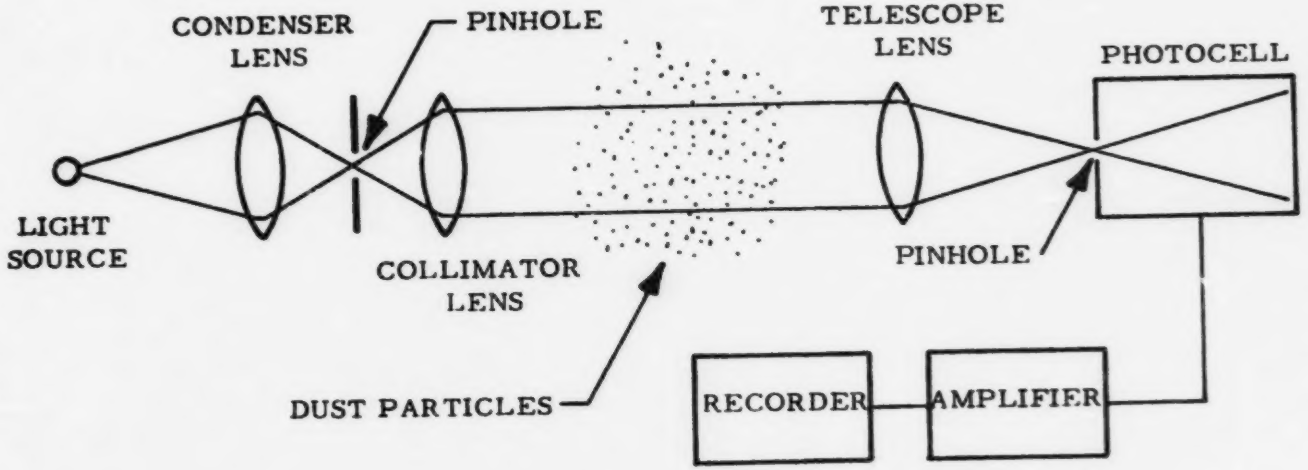
CONDENSER
LENS
PINHOLE
TELESCOPE
LENS
PHOTOCELL
LIGHT
SOURCE
COLLIMATOR
LENS
PINHOLE
DUST PARTICLES
RECORDER
AMPLIFIER

Fig. 3. DIAGRAM OF SIMPLE TRANSMISSOMETER

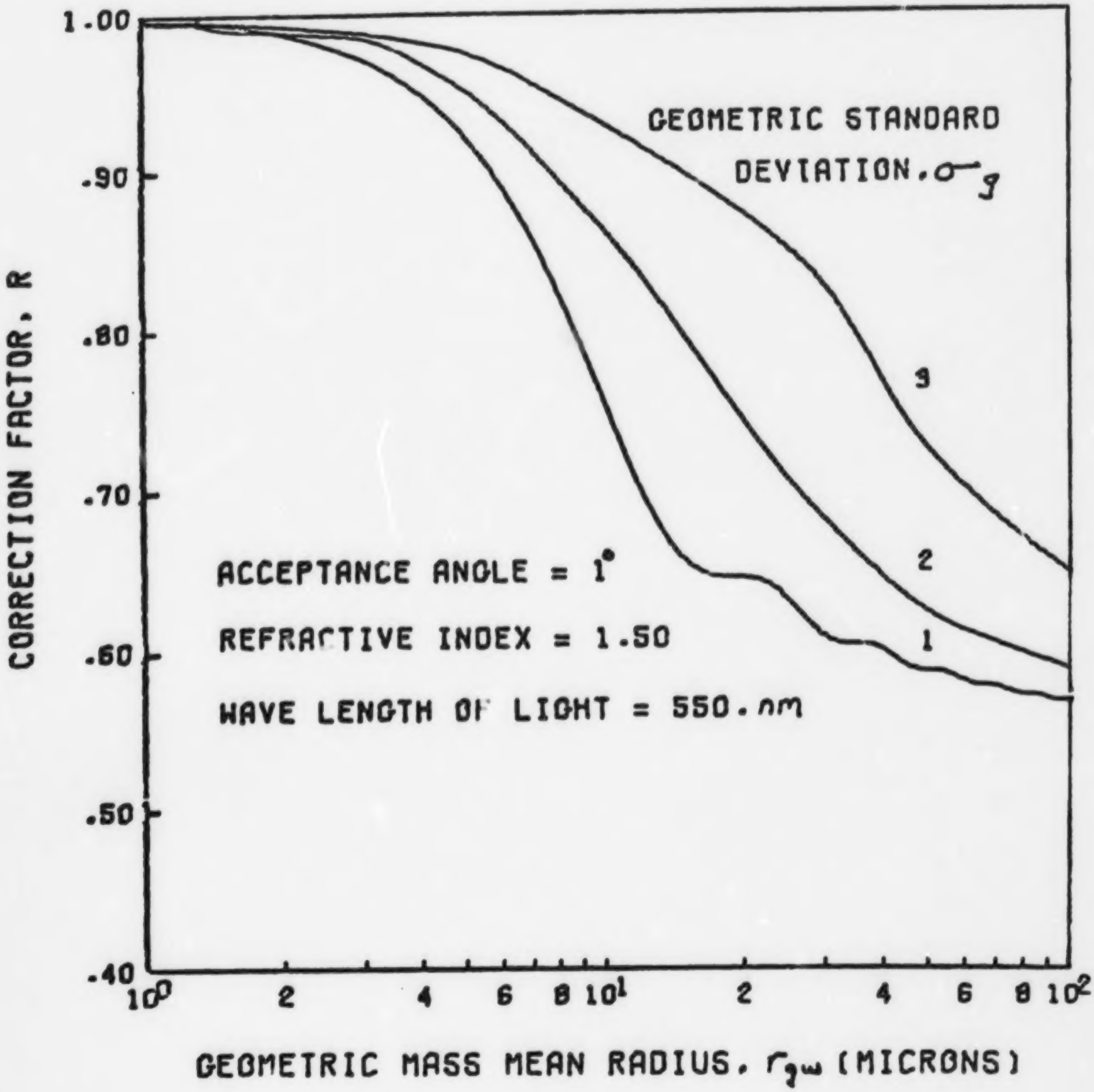

Fig. 4. THE EXTINCTION COEFFICIENT CORRECTION FACTOR, R, AS A FUNCTION GEOMETRIC MASS MEAN RADIUS

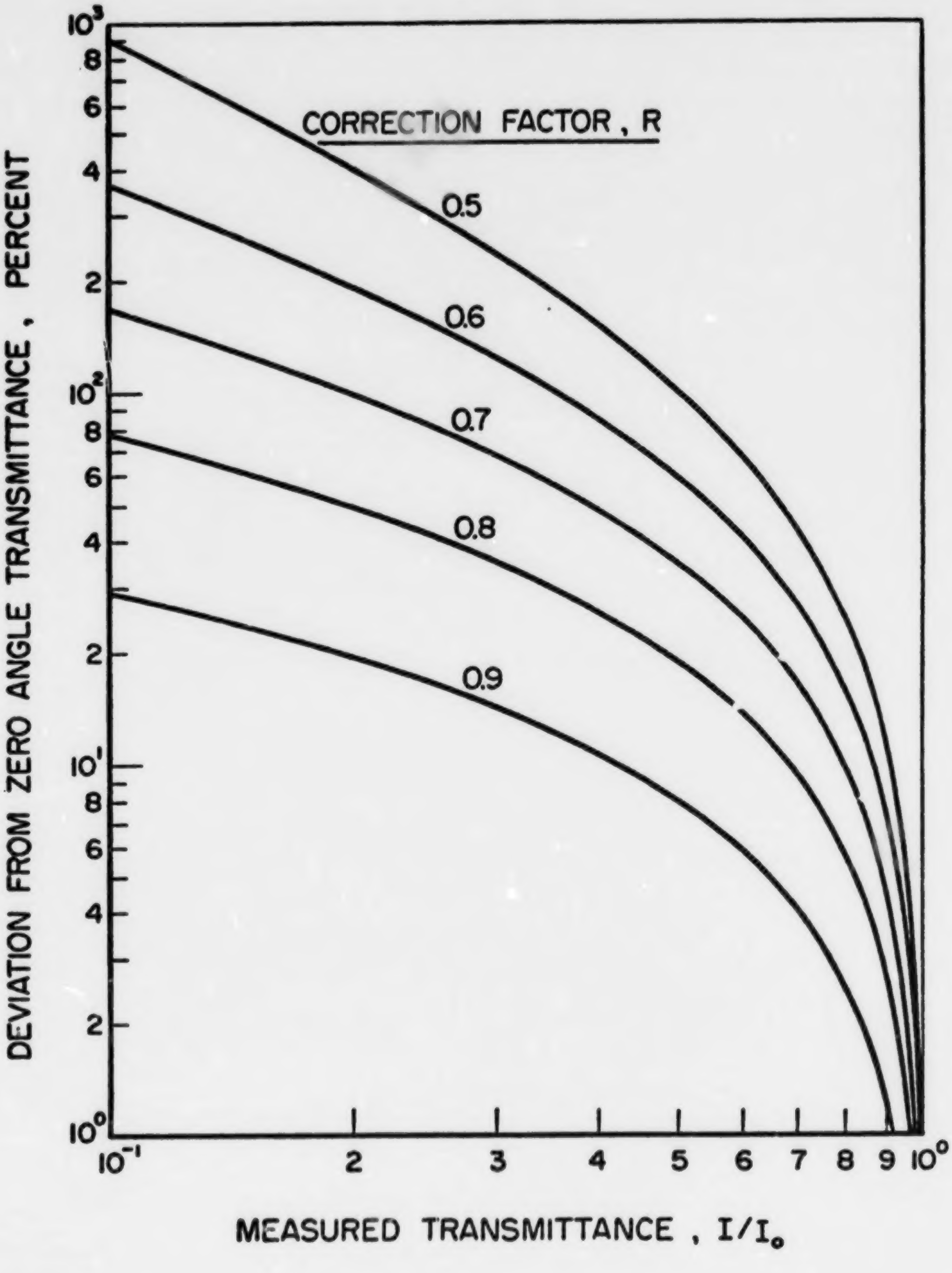

Fig. 5. ERROR IN MEASURED LIGHT TRANSMITTANCE

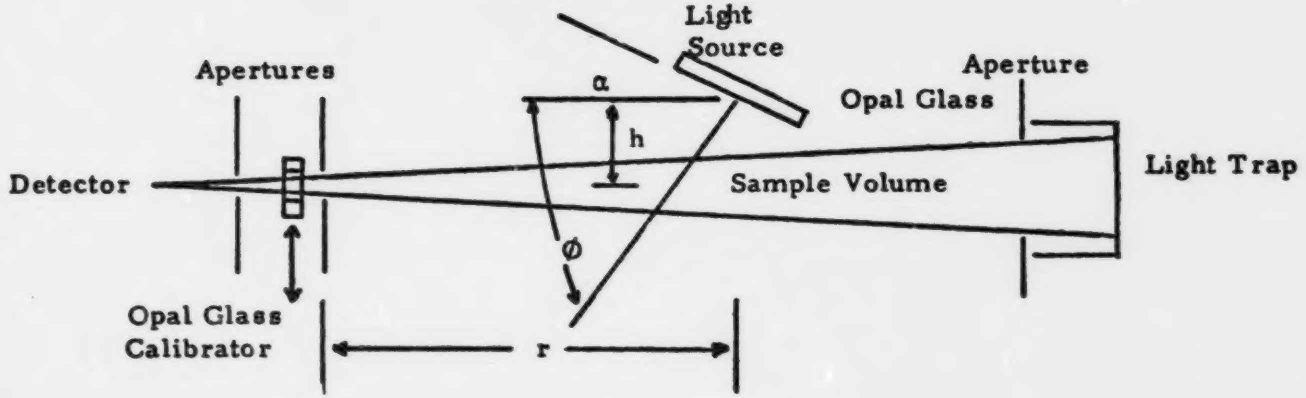
Light
Source
Apertures
Aperture
Opal Glass
α
h
Detector
Sample Volume
Light Trap
ϕ
Opal Glass
Calibrator
r

Fig. 6. DIAGRAM OF OPTICAL ASSEMBLY OF NEPHELOMETER FOR STACK MEASUREMENTS

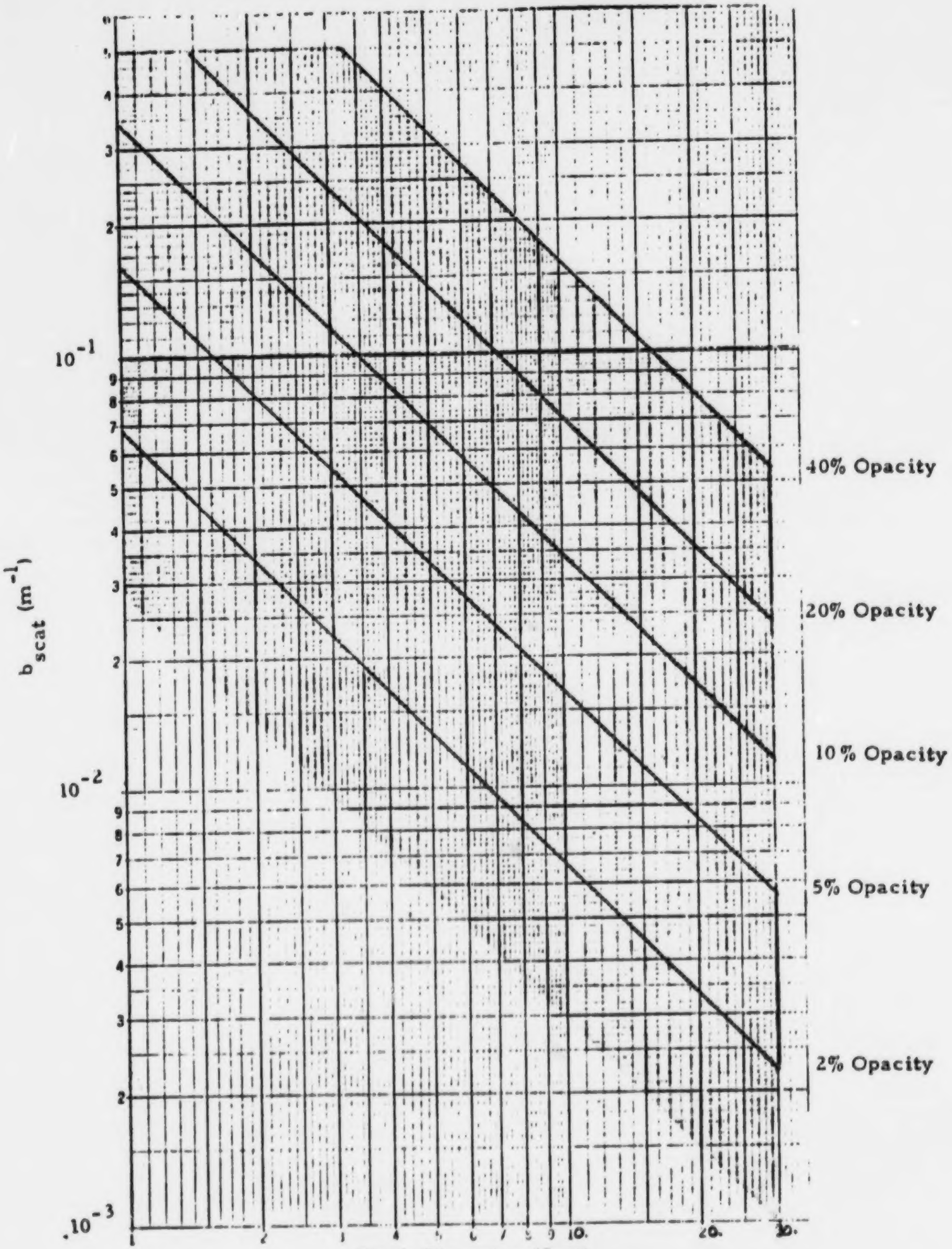

Fig. 7. RANGE OF OPERATION OF NEPHELOMETER FOR STACK MEASUREMENTS

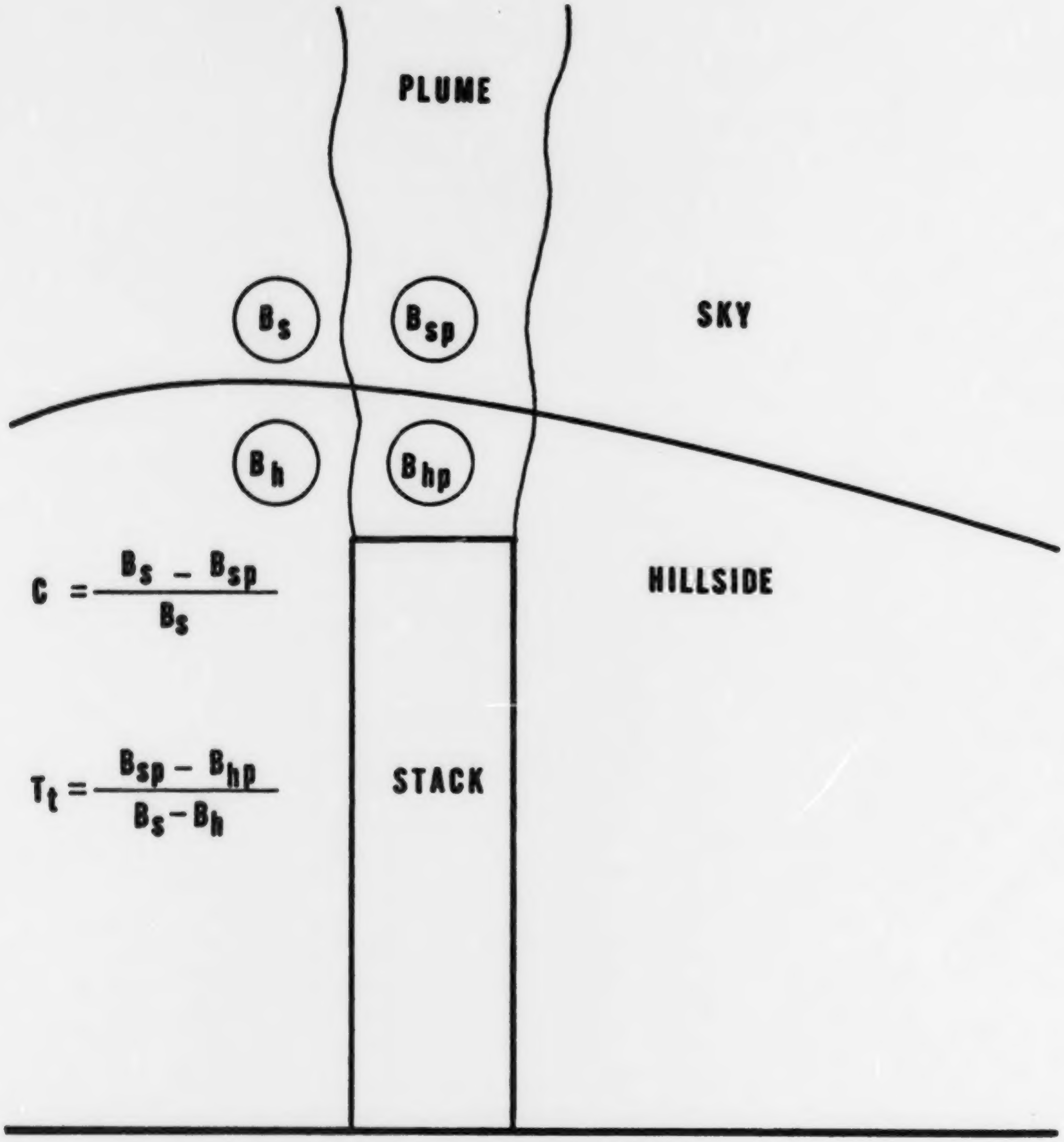
PLUME
SKY
HILLSIDE
STACK
B_s
B_{sp}
B_h
B_{hp}

$$C = \frac{B_s - B_{sp}}{B_s}$$

$$T_t = \frac{B_{sp} - B_{hp}}{B_s - B_h}$$

Fig. 8. BRIGHTNESS MEASUREMENT IN PLUME TO DETERMINE TRANSMITTANCE

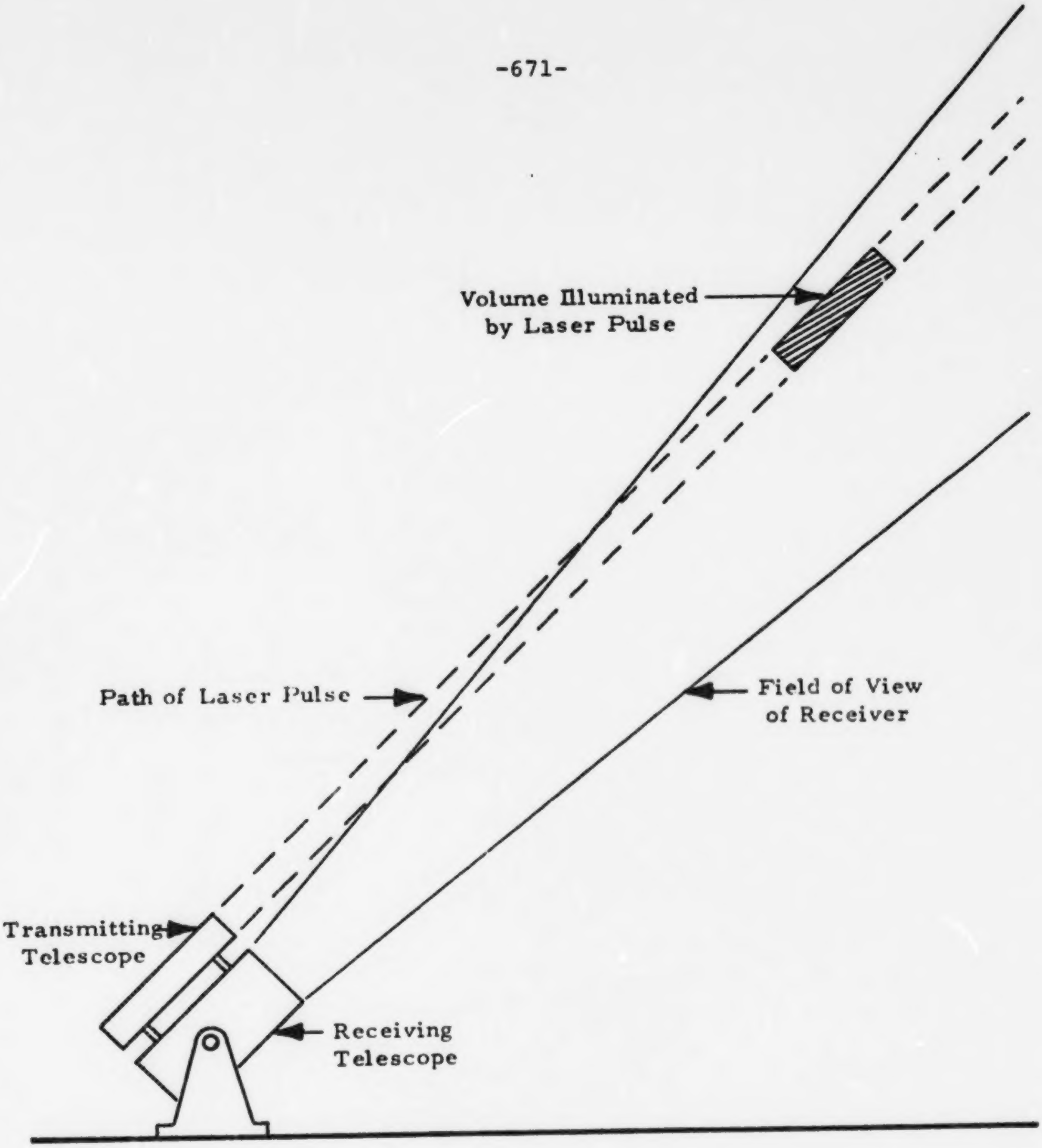
Volume Illuminated by Laser Pulse
Path of Laser Pulse
Field of View of Receiver
Transmitting Telescope
Receiving Telescope

Fig. 9. DIAGRAM OF TYPICAL LIDAR

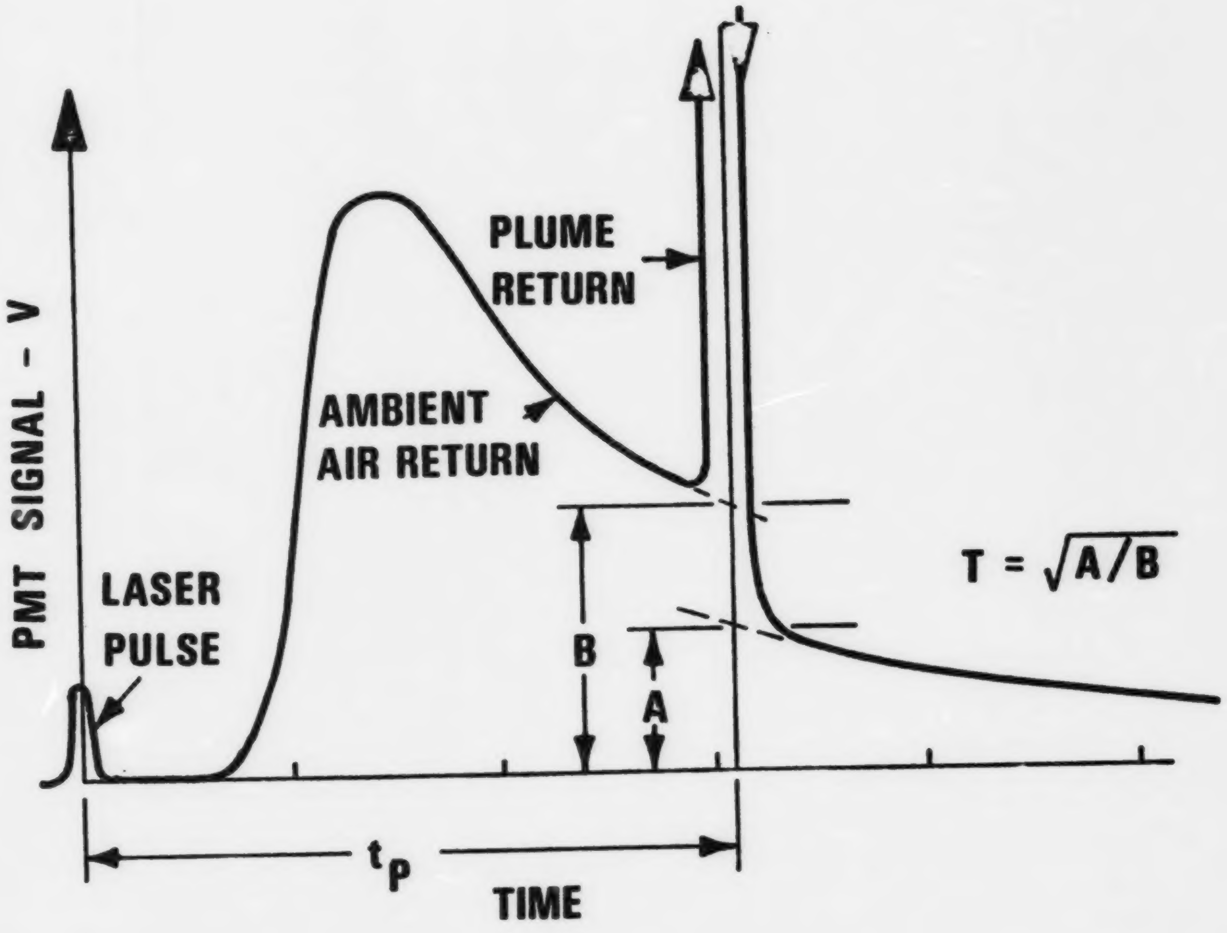
PMT SIGNAL - V
LASER PULSE
AMBIENT AIR RETURN
PLUME RETURN
B
A
$T = \sqrt{A/B}$
t_P
TIME

Fig. 10. DIAGRAM OF LIDAR RETURN

Paper No. 28

INSTRUMENTATION FOR DISPERSION ANALYSIS OF PARTICULATES IN INDUSTRY

by

S. S. Yankovskiy
and
Valery P. Kurkin

STATE RESEARCH INSTITUTE OF
INDUSTRIAL AND SANITARY GAS CLEANING

Moscow

Instrumentation for Dispersion Analysis of Particulates in Industry

S. S. Yankovskiy, V. P. Kurkin

Stokes diameter of particles must be calculated to evaluate fractional and general efficiencies of particle collection instruments like cyclons, filters, and scrubbers. The size of diameter may differ significantly from that determined by normal methods of dispersion analysis if agglomeration occurs in the gas stream. Measurement for purpose of determining instrument efficiency should, for that reason, be conducted directly inside of the gas stream.

Two types of instruments for dispersion analysis were developed in NIIOGAZ, small size eleven-stage impactor and cyclon separator. Both instruments analyze particles from 1 to 20-30 microns in size. Uniqueness of the developed impactor is its small dimensions which are of great importance in collection of samples from industrial scale gas streams. Entire body of the impactor is 125 mm long with a diameter equal to 40 mm. Impactor (Fig. 1) is made up of discs with perforations as nozzles for one level, and with lining for preceding level. In odd number levels, nozzles are located in central part of the disc and lining is located on the outer part. The opposite is true for even numbered discs. The first three levels have varied geometry but equal collection efficiency. Such design is more reliable for removal of large particles from the gas stream. Eleventh level of the impactor contains a filter for collection of very fine particles.

Two-phase lubricant or thin layer of nappy material is used as lining. It is placed in special depression of disc.

Both types of lining, patented, allow for good collection of dust particles, up to 30 mg. for one level. For use of two-phase lubricant gas temperature should not exceed 100°C and for use of nappy material 300°C.

Deposition of particles on each level has its own fractional efficiency curve. Usually it is a log-normal distribution curve. Fig. 2 shows that when the curves are drawn on log-probability paper, they become straight lines. The curves are described by two parameters; diameter, d_{50}, which has collection efficiency of 50% as its limit of separation and standard deviation σ fraction.

In plotting curve of dispersion composition for increases in individual levels, curve of fractional efficiency for each level usually is substituted by vertical line (for which σ fraction $= 0$) passing through d_{50}.

Last number is calculated with Stokes equation:

$$Stk_{50} = \frac{v\ d^2_{50}}{M\ D} = \frac{Q\ d^2_{50}}{M\ D^3} = \text{const} \qquad (1)$$

where:

Stk_{50} - Stokes diameter relating to d_{50}

v - gas velocity through nozzle

ρ - particle density

M - gas viscosity

D_n - nozzle diameter

Q - gas volume through the instrument

Nomogram (fig. 3) which is based on equation 1 allows to determine d_{50} as a fraction of the number of perforations, n and the size of perforation's diameter, D. Standard conditions are used in determination of d_{50}. Those are: $Q_{st} = 10$ l/min, $\rho_{st} = 1$ g/cm^3, $t_{st} = 20°C$. (temperature stability is related obviously to $M=M(+)=$ const)

Value d_{50} for standard conditions is most indicative in characterization of impactor levels. It can also be used when measurements are taken under conditions other than standard. Following correction is then applied. Standard value for d_{50} at that level is multiplied by $\alpha = d_{50}/d_{50}$ (standard).

$$d_{50} = \alpha \left(d_{50}\right)_{standard} \qquad (2)$$

Coefficient α is calculated from STK_{50} = const. According to equation J we have:

$$\alpha = \sqrt{\frac{Q_{st}\rho_{st}M}{Q\rho M_{st}}} = C\sqrt{\frac{M}{Q\rho}} \qquad (3)$$

Where: C - constant

Nomogram shown in fig. 4 is used to determine d_{50} for a known gas volume Q, density of particles ρ and gas temperature t. The nomogram allows to first find the size of coefficient α and then size of d_{50}.

Values of d_{50}, obtained with normal calibration of impactor under conditions which assure 100% retention of large particle on surface, (covered with thin oil layer) cannot directly relate to linings. The reason is that part of the particles which come into contact with lining may be carried away. Calibration method was developed in which two analogous levels are placed sequentially. An assumption was made that curves for fractional efficiency of levels and dispersion composition of particles in the instrument are log-normally distributed.

Two parameters (distribution limit d_{50}, standard deviation σ fraction) for the fractional efficiency curve are found with this method. The parameters are found by knowing two corresponding parameters (average geometric diameter d particle and standard deviation σ part) of dispersion composition at inlet to the instrument and from knowing efficiency values for first ψ_1 and second ψ_2 analogous levels of impactor. Nomograms constructed in generalized coordinates lg σ part./ lg σ fraction lg (d_{50}/d part.) / lg σ part. represents relationship between parameters of fractional efficiency and parameters of dispersion composition of particulates at the inlet and efficiency of two analogous levels of impactor.

Two curves, one with experimental value ψ_1 and other ψ_2, are drawn through tracing paper, placed on top of the nomogram, to calculate parameters d_{50} and σ fraction. X and Y coordinates at the point where two curves cross each other allow to calculate d_{50} and fraction providing d particle and σ particle for distribution by particle size at inlet to the instrument are known.

Results of measurements conducted at different levels of impactor are shown in Table 1. Values obtained in calibration, (d_{50})true and (σ fraction)true, characterize true curves of fractional efficiency of studied levels. Calculated values (d_{50})calculated and (fraction)calculated are also presented in the Table. Obtained data agrees with other presented in literature for normal calibration. Relationship between true and calculated d_{50} is also presented in the Table. For impactor under consideration, curves of fractional efficiency are slightly skewed and have a slightly different slope. To calculate particulate dispersion composition (d_{50})true should be used.

Cyclon separator consists of three sequentially connected cyclons with diameters 30,32,16 mm and filter at the outlet. Dimensions of the instrument are: 150 x 100 x 50mm. Rate of gas sampling is 10 ℓ/min. Increase in the amount of dust in the cyclons and on the filter is used for dispersion analysis.

Cyclon efficiency values are presented as two parameters of log-normal distribution. The parameters are average geometric diameter, dp, and distribution dispersion of particles $\lg\sigma p$. Both parameters are estimated by nomograms with equal value of efficiency curves on which amount of dispersion is shown on the ordinate and diameter of particles dp on the abscissa. Separate nomogram was constructed for each of the cyclons with gas flow rate equal to 10 ℓ/min. Fractional characteristics of cyclons were determined by calibration in laboratory with particles of known size, for purposes of nomogram development. Parameters of dispersion analysis are easily determined with nomograms.

Cyclons were investigated in great detail under experimental conditions.

Table 1

Comparison of Calculated and Experimental Characteristics of Impactors

No. of Levels	Diameter of Perforations	No. of Perforations	d_{50} Calculated Microns	d_{50} Experimental Microns	d_{50} exp/ d_{50} cal	σ exp
1	10	1	15	15	1	1.3
2	slit 5 x 30	-	15	15	1	1.3
3	8.5	1	12	12	1	1.3
4	3.5	8	8.5	8.5	1	1.3
5	5	1	5.5	5.5	1	1.4
6	2	6	3.2	4.0	1.25	1.5
7	1.4	8	2.3	3.2	1.4	1.6
8	1	8	1.4	2.1	1.5	1.7
9	1	5	1.0	1.6	1.6	1.8
10	0.8	4	0.65	1.1	1.6	1.8

Fractional characteristics of cyclons for particle concentration from 10 mg/m^3 to 40 g/m^3 remain the same. This was established by measuring particle dispersion by Stokes diameter at inlet and outlet of laboratory cyclons. Differences in cyclon efficiency observed by other authors are explained by phenomena of particle aggregation at inlet and in some cases their disaggregation in the cyclon. In determination of fractional cyclon efficiencies gas flow rates from 5 to 30 l/min were used. Gas velocity at inlet varied from 0.4 m/sec for cyclon with 50 mm diameter to 40 m/sec for cyclon with 16 mm diameter.

In all cases fractional efficiency curves were log-normally distributed. (fig. 6)

Analytically these lines are discribed by two parameters: distribution limit, d (particle) for which efficiency equals 50% and distribution dispersion, lgσ particle.

Changes in above parameters indicate changes in fractional efficiency for cyclons with varied geometry and varied operational systems. Stokes criteria function was used in evaluation of data on fractional efficiency of laboratory cyclons. Gas turbulence in cyclons, relationship ℓ cyclon/D cyclon. (ℓ-length, D-diameter) relationship F_{inlet}/F_{plane} (inlet cross-section/cross-section of cyclon body) were accounted for in evaluation.

Following empirical relation is used to calculate first of two parameters which characterize cyclon efficiency.

$$d_{50} = A\sqrt{\frac{M\ D_c}{\rho V_{in}\ Re^{0.38}\left(\ell/D_{cyclon}\right)^{0.27}}} \qquad (4)$$

Where:

M - gas viscosity

D_c - cyclon diameter

ρ - density of particles

Vin - velocity at inlet nozzle

Re - Reynolds number accounting for flow turbulence

A - constant, non-unit, for example equal to 6

Following empirical is used to calculate the second parameter lg   cyclon:

$$\lg \sigma_{cyclon} = B \left(\frac{d_{ex}}{D_{cyclon}} \right)^2 \qquad (5)$$

This parameter is determined by cyclon geometry and does not depend on aerodynamic parameters.

Equations 3 and 4 can be used in design of laboratory cyclons in making choices for geometric and system parameters which assure desired fractional characteristics.

Nomogram of equal efficiency values for cyclons with known fractional characteristics can be constructed with use of a single generalized nomogram, shown in fig. 7.

Coordinates lg (d particles/ d cyclon) and $\lg^2 \sigma$particle + $\lg^2 \sigma$cyclon. Following problems can be solved with this nomogram and with construction of individual nomograms for cyclons of known fractional characteristics:

a) When fractional characteristics for two different cyclons are known dispersion composition of particulates can be calculated with values of general efficiency.

b) When parameters of dispersion composition are fixed fractional characteristics of cyclon can be calculated with values of general efficiency for two different aerosols.

c) When fractional characteristics of cyclon are known with fixed dispersion composition general efficiency of cyclon can be determined.

Parametric representation of dispersion composition in industrial aerosols is advantageous in calculation and preliminary evaluation of efficiency of dust collectors. Log-normal distribution of dispersion composition is used most widely. It was determined in the past that aerosols of different origins characterized by same chemical composition are distributed log-normally.

It should be added that when fractional efficiency of apparatus and dispersion composition of aerosols at inlet is log-normal then dispersion composition of aerosols in the hopper and at the outlet of the collector is also log-normal. Kolmogorov criteria can be used to determine amount of deviation from log-normal distribution. According to this criteria size of maximum deviation, D, of two probability functions from each other is a measure of their deviation. D ranged from 3 to 5% for aerosols of log-normal dispersion composition in wide interval of dispersion values. (0.2 to 0.4) This was true for aerosols collected in cyclons and for those which passed through.

Errors resulting from approximation of dispersion composition are small when general efficiency of the collector is evaluated with curves of fractional efficiency and dispersion composition. (on probability scale). As an example: when D=3%, difference between calculated and true values of general efficiency in area close to 50% is about 1% and in area close to 95% is about 0.3%.

Measurements of dispersion composition were conducted for various aerosols in a number of industrial set-ups with a single cyclon separator and impactor. Table 2 shows some of the results. It can be observed that regardless whether the sample is taken at the inlet or outlet to the apparatus, aerosols of different origins, coagulated are log-normally distributed. This can be explained by the fact that during technological process (burning, drying, grinding, etc.) as well as during gas flow through pipes over-pulverization of aerosols occurs due to influence of gravity, inertia, turbulent diffusion of stream etc. The enumerated influences, none of which assures sharp separation of aerosols, should aid in normalization of distributions. Aerosols are also log-normally distributed by Stoke's diameter. The average diameter on distribution curve is skewed to an increase when dispersion distribution is retained or somewhat decreased.

For some aerosols measurements with impactor and cylindrical separator compared to results of dispersion analysis conducted in the laboratory with gonell instrument air separating deposition extracted from cyclon separator.

Results of measurements are presented in Table 3. Measurements of aerosols of magnesite, coal ash, and cement agree well for all three methods. For zinc oxide and dolomite significant changes were observed. For first three cases aerosols were larger than 10 microns and did not coagulate during flow through pipes. Fine oxide and dolomite coagulated which resulted in marked particle size increase.

TABLE 2

Results of Measurements of Dispersion Composition of Aerosols at Inlet and Outlet of Dust Collectors

Industrial Set-Up	Sampling Location	Aerosol Classification	Cyclon Separator		Impactor	
			Particle Microns	σ	Particle Microns	σ
Furnace for Aluminum Electrolysis	Inlet to Foam Apparatus	Electrolytic	35	2.3	30	2.1
"	Outlet to Foam Apparatus	"	4	1.9	5	2.1
Jet Mill	Cyclon Outlet	Hydrophobic Aerosols	32	2.2	28	2.3
Fire Kiln	Inlet to ESP	Dolomite	26	2.6	24	2.8
OJRES(?)	Outlet Foam	Fly Ash	10	3.8	12	3.5

TABLE 3

Comparison of Aerosol Dispersion Composition Measurement with Different Methods

Classification of Aerosol	Cyclon Separator		Impactor		Gonell Apparatus	
	Particle Microns	σ	Particle Microns	σ	Particle Microns	σ
Magnesite	14	2.3	12	2.1	15	2.1
Coal Ash	20	1.8	17	1.9	22	1.7
Cement	9	3.5	9	3.6	12	3.3
Zinc Oxide	3	2.3	2.6	2.1	15	2.7
Dolomite	4	1.6	3.4	1.8	13	1.7

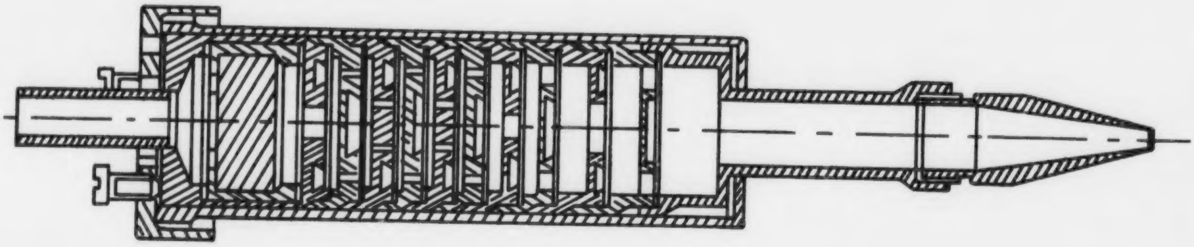

Figure 1. Eleven-stage impactor.

1. Body
2. Nozzle perforations
3. Lining (two-phase lubricant or nappy material)
4. Glass fiber filter
5. Outlet pipe
6. Inlet pipe with partition nozzle.

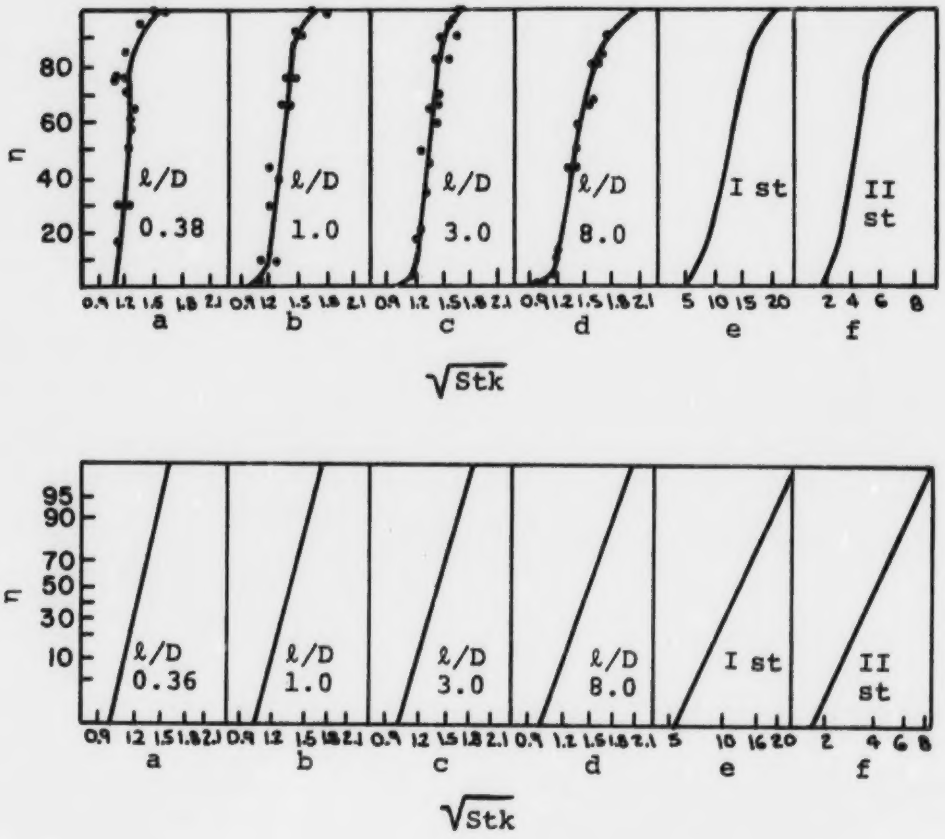

Figure 2. Experimental curves for fractional efficiency in different levels of impactors

a - d from: T. T. Mercer, R. G. Stafford, Ann. Occup. Hyg., 12, 1969

d - f from: W. E. Ranz, W. B. Wong, Ind. Eng. Chem., 44, 1952

Upper set - linear scales; lower set - log probability coordinates

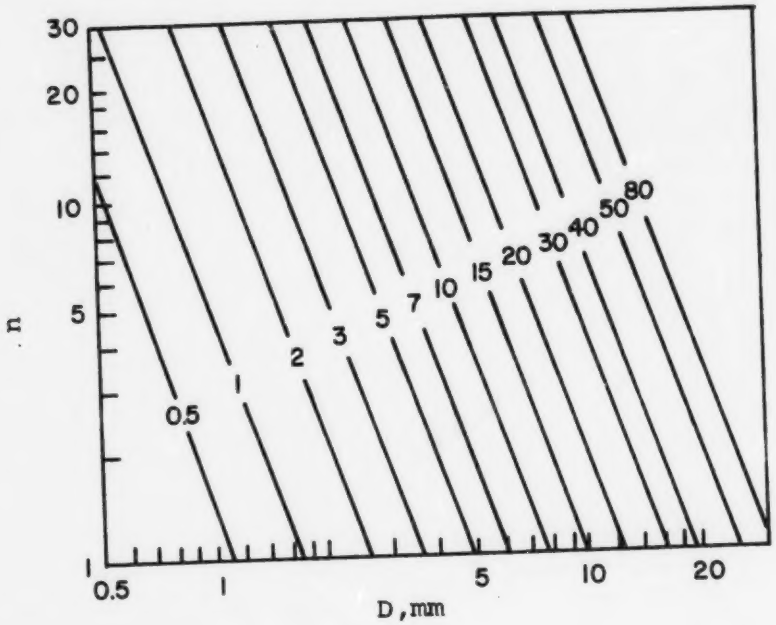

Figure 3. Nomogram for determination of d_{50} for various levels of impactor as it depends on nozzle diameter D_n and on number of perforations η with gas volume 10 l/min.

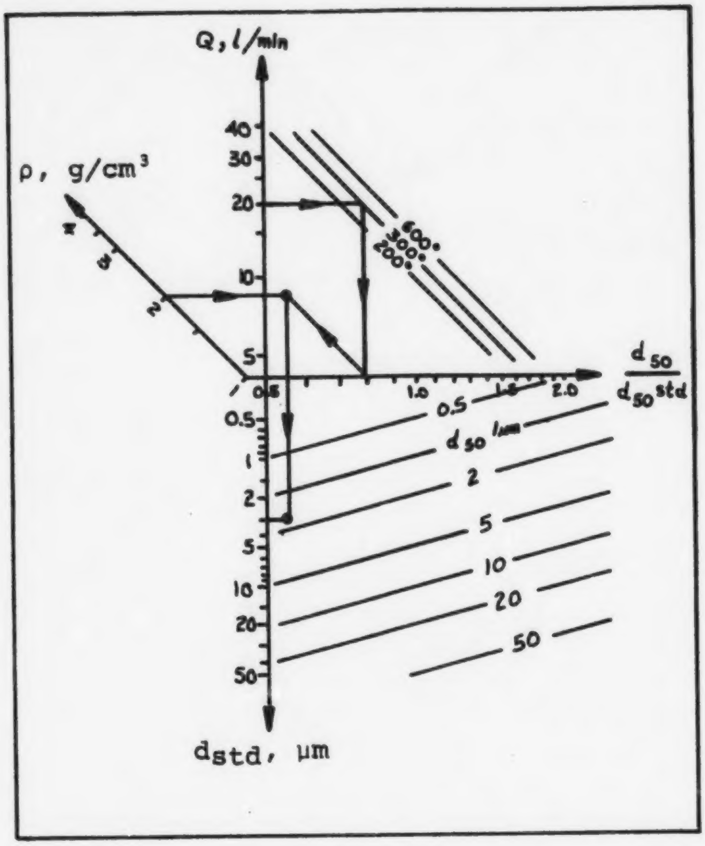
Q, l/min
40
30
20
10
5
ρ, g/cm³
1
2
3
4
600°
300°
200°
$\frac{d_{50}}{d_{50}std}$
0.5
1.0
1.5
2.0
0.5
1
2
5
10
20
50
d_{50}, μm
0.5
2
5
10
20
50
d_{std}, μm

Figure 4. Nomogram for determination of d_{50} for various levels of impactor with predetermined values of gas volume Q, particle density ρ, and gas temperature t.

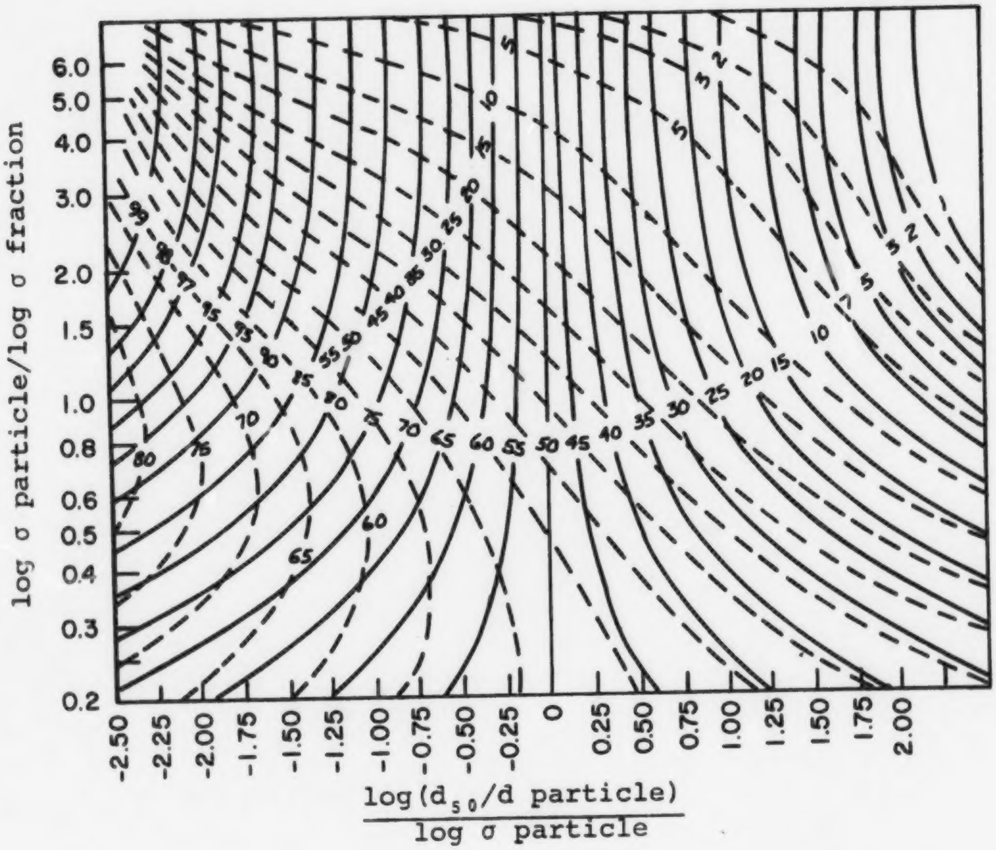

Figure 5. Curves for equal efficiency values for two analogous sequentially set up impactor levels.

―――――――― equal efficiency values, curves for first level

---------- equal efficiency values, curves for second level

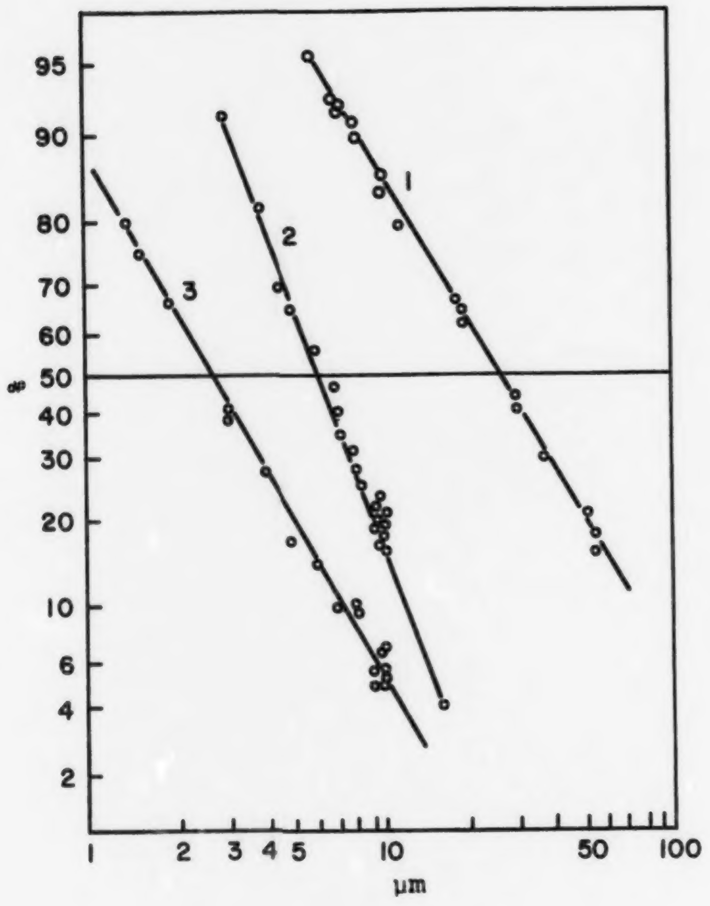

Figure 6. Curves of fractional efficiency for three cyclons which compose cyclon separator.

1. for first cyclon
2. for second cyclon
3. for third cyclon

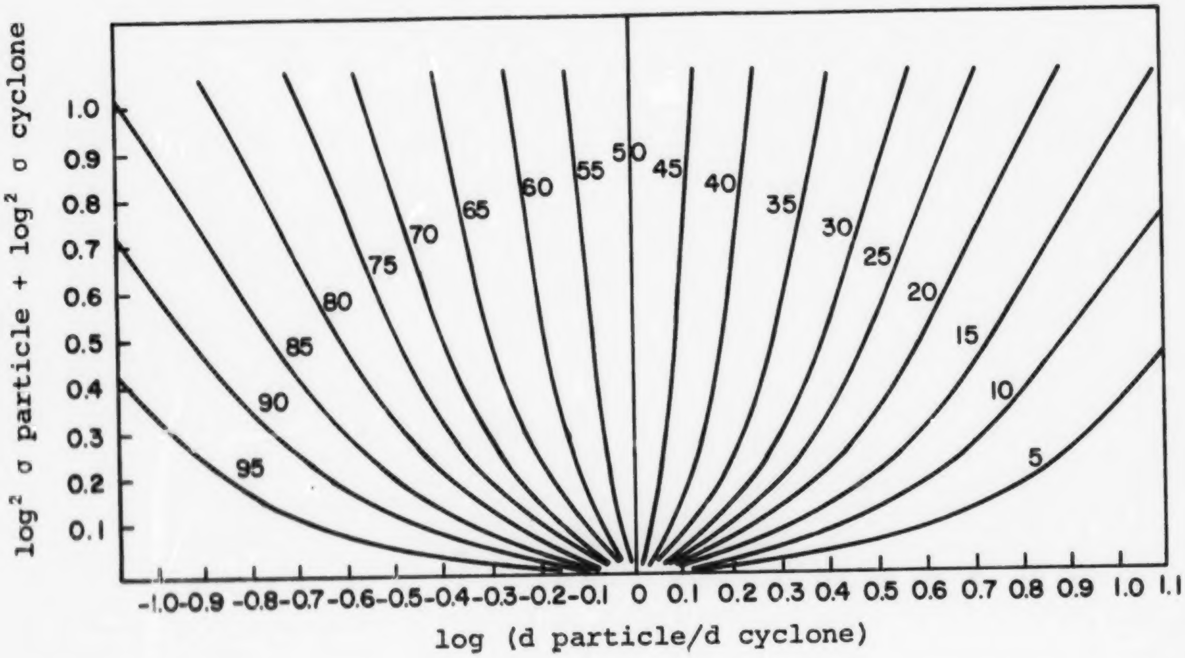

Figure 7. Generalized nomogram of equal values for cyclon efficiency.

Preceding page blank

Paper No. 29

TECHNOLOGY OF PARTICULATE SAMPLING FROM REACTIVE, DAMP, AND HIGH-TEMPERATURE GASES

by

V. A. Anikeyev,
V. P. Bugayev,
V. A. Limanskiy,
Ye. N. Andrusenko,
and
V. Yu. Padva

(Presented by Valery P. Kurkin,

STATE RESEARCH INSTITUTE OF
INDUSTRIAL AND SANITARY GAS CLEANING)

Moscow

Preceding page blank

Technology of Particulate Sampling from Reactive, Damp, and High-Temperature Gases

(Presented by V. P. Kurkin)
V. A. Anikeyev, V. P. Bugayev, V. A. Limanskiy,
Ye. N. Andrusenko, V. Yu. Padva

Aerosol sampling to obtain data like weight concentration, dispersivity and chemical compsotion of solid, liquid and gaseous phase is important in periodical efficiency inspection of the collector instruments in chemical, metallurgical and other branches of industry. The theoretical bases, classical sampling methods and instrumentation are described in literature. (1,2,3).

Sampling from damp, reactive and high temperature gases with the use of classical methods does not always give reliable results as was shown in the studies of Zaporozhe division of NIIOGAZ. This lack of reliability was explained by the presence of several reactive components in the gaseous phase, (H, HC, C_2, O_2, P_2O_3 and others) which reacted with elements of filtering materials, and also by the presence of liquid spray in the wet scrubber gases. One of the most difficult and complex problems during efficiency inspection of the collectors is calculation of particulates concentration in gas by weight. Automatic instruments for calculation of particulates concentration, which were developed recently, have had rather limited application for several reasons. The technology for particulates control in majority of cases uses instruments of intermittent functioning which require large number of servicing personnel.

In sampling for damp, high temperature and reactive gases, thermally and chemically stable designs and filtering materials were used in

Zaporozhe NIIOGAZ.

Improvement of the design of sampling instrumentation for intermittent functioning was also considered.

The use of the glass adapters filled with glass wool in sampling from wet scrubbers where the gas not only contains solid and liquid phases but also hydrogen fluoride in concentrations greater than 30 mg/nm^3 is not recommended.(2) The hydrogen fluoride reacts with the glass to form silico-fluorides. The original weight of the glass adapter decreases significantly. The resulting mistake, depending on the hydrogen fluoride concentration and time of sampling may reach tens of percent.

A number of synthetic fibers and a number of construction materials were experimented with in the laboratories and in the industry (3) for particulate sampling from electrolytic production of aluminum and from melting of fluoride flux in the furnaces. The model samples were subjected to hydrogen fluoride with concentration up to 700 mg/nm^3 and to the solutions of hydrofluoric acid (0.2 g/ℓ).

The recommendation was made to use stainless acid resistant steel and teflon sampling instruments with carbon or polyphene fibers in combination with porcelain clay wool.

To decrease the amount of time spent for sampling NIIOGAZ developed several cassette models of particulate sampling units. With these cassettes spray concentration up to 5 g/nm^3 and particulate concentration up to 10 g/nm^3 can be determined simultaneously or individually. The mist and particulate concentration is determined by weight.

Figure 1 shows a scheme of the aerosol sampling unit with manual control of filter exchange (Patent No. 380980, I. OIP 1/22). It is made up of the sampling nozzle 1, transport pipe 2, screw 3, turning socket 4, cassette 5 (with three filters), body 6, nut 7, which joins body 6 with hood 10, fingers 8, placed on the hinged disc 9, conical reductor 11, pipe 12, connecting pipe for gas outlet 13, handle for control of filter exchange 14, filters 15, and the sealing liner 16. The appropriately prepared filters are earlier placed in the cassettes. On the sampling location cassette is placed inside the sampler which is secured at the sampling point. The aerosol sample flows through one of the three filters. (gas does not flow into the other two at this time). When the earlier decided upon hydraulic resistence of the filter is reached, the cassette is moved with the fixed turn of the control handle. The dirty filter is exchanged for a clean one.

Other modifications of the aerosol sampling unit include different numbers of filters in the cassette and a different system of their exchange.

Three types of filters are used in the aerosol sampling unit. They are: for determination of particulates concentration, for determination of only spray concentration following wet scrubbers and for determination of total concentration of particulates and spray. The filters are porous teflon, metalloceramic, ceramic and other materials. Depending on the specific properties of the aerosols possibility exists that the filters can be used repeatedly. The filters are regenerated with acid or alkaline treatment. The regeneration procedure is determined experimentally for each specific case.

When the samples of damp gases are taken spray liquid also containing collected particulates separates on the surface of the sampling unit. The separated liquid flowing onto the surface of the sample unit is directed into the collector nozzle and on to the filter. In this way, the true concentration of the spray and the particulates is increased. This phenonenon is especially true for the vertical and sloped gas pipes with the uptake gas stream. The use of the gas collecting nozzle (Patent No. 393640 I. OIP 1/24) allows to exclude that increase from the measurements and allows highly reliable aerosol sampling for the determination of spray and particulate concentration. The separated spray liquid is removed from the surface surrounding the collector nozzle and in this way excludes possible (false) increase of true aerosol concentration. The aerosol sampling units are also fitted with such nozzles.

In sampling with the use of the cassettes, non-productive time loss is decreased by 25-30% in comparison to the sampling done with the singular filters in the conventional sampling units. The sampling instrumentation is constructed with non-corrosive materials which allows its use in sampling from damp, reactive gas with temperature range 0-250°C. The weight of the sampling unit is, depending on the modifications, from 3 to 4 kg, diameter 60-75 mm, length (with control handle) up to 1.5m. The dimensions allow for the sampling from the gas pipes with a diameter up to 2.5m.

The method developed for the internal sampling (Patent No. 326131, I. SOI v 17/02) allows for the determination of sulfur concentration in the gas stream with temperatures ranging from 550 to 500°C. The collected gas sample is filtered preliminarily in the adapters of molybdenum glass filled with porcelain clay wool. It is measured then under the gas stream conditions with a diaphragm. The elementary sulfur vapors condense in the storage and the second measurement of the gas sample is taken. The difference is indicative of the sulfur vapor concentration in the technological gases.

Concrete applications of the sampling units for the measurement of particulates concentration in gases, under raised pressures are looked at in the following examples.

1. Sampling from surfaces of reactors and regenerators of catalytic cracking installation and also following cyclon collectors in such installations.

Methods of external gas filtration are used. The sampling tube is introduced through the valve unit. (Fig. 2) The valve unit is constructed using standard fasteners with conventional inlet, 50-80 mm.

In sampling for reactor gases the valve unit has additional inlets for water vapor and drainage outlet for water. The use of the vapor is necessary for the control of salt compounds density before the sample is taken.

Depending on the concentration of particulates and the dispersion composition of the particulates.

a.) only laboratory cyclon with a hopper;

b.) laboratory cyclon and filtering adapter;

c.) only filtering adapter

are used.

The particulates have to be separated from the products of refining when the particulates from the reactors are sampled for. To accomplish that the samples and the residues of the products of refining and coke are washed and burned in the muffle furnace.

To take the gas samples following the cyclons, where stream velocities and particulates concentration are unevenly distributed, inside of the gas pipe devices are placed which equalize stream velocity and particulates concentration in the cross-section (gas line axis) before the gas sample is taken.

The measurements were conducted under the experimental as well as under the industrial conditions of catalytic cracking installations and butane dehydrogenation.

2. Taking of the samples following soot removal from gasification of sulfurous oils under pressures 2.5-2.0 atm.

With pressures higher than 2.5 atm. sampling with valve units becomes more complicated because special arrangements have to be made for inserting and removing the sampling tube.

Special units with intercepting rods were found to be more appropriate under those circumstances. (Fig. 3) The metal adapter for filtration is placed inside of the intercepting rod (internal filtration) or inside of the gas line (external filtration). All phases of the sampling (gas interception, purging of the sampling nozzle with inert gas, adapter installation, gas flow through the adapter.) are secured by different locations of the locking rod as it relates to the nozzle opening.

Each sampling unit contains a pneumatic drive of the intercepting drain, which allows for automatic change of the rod to different positions. The adapter is changed with the handle. The sampling time is determined by the particulates concentration. The units sample soot concentration in the gas stream from 2 mg/nm^3 to 10 mg/nm^3. The design studies and the preparation of the sampling unit models showed that the type with the intercepting rod can collect a sample automatically with pressures up to 100 atm.

3. With small concentration of particulates and temperatures reaching dew point (blast furnace gases P=2.5 atm., following passage through ESP) only internal filtration method of sampling is possible.

When particulates concentration reaches tens of mg/m^3 of gas glass adapters with glass wool are used. When the concentration of particulates is below 10 mg/m^3 gas is filtered through very thin cellulose fiber filters which were developed by Karpov Institute. The hydrophobic filter fibers eliminate the need for a long process of bringing the filter to constant weight. To determine the quantity of coarsely dispersed spray in the gas from the ESP, adapters which accumulate moisture are used. The spray settles in the adapters because of the gas celliding with the surface.

All sampling from the blast furnace is conducted with the use of the above described sampling units with valve interceptors.

REFERENCES

1. G. M. Gordon, T. L. Peysakhov, Inspection of Particulate Collectors, Moscow, 1961

2. V. P. Bugayev, V. A. Limanskiy, V. N. Sajonov, V. P. Klyushkin, Industrial and Sanitary Gas Cleaning, 1972, No. 4, 25-26.

3. I. Ya. Boyev, Ye. G. Levkov, V. A. Limanskiy, V. P. Bugayev, A. S. Levkova, Industrial Laboratory, 1972, No. 3 278-281.

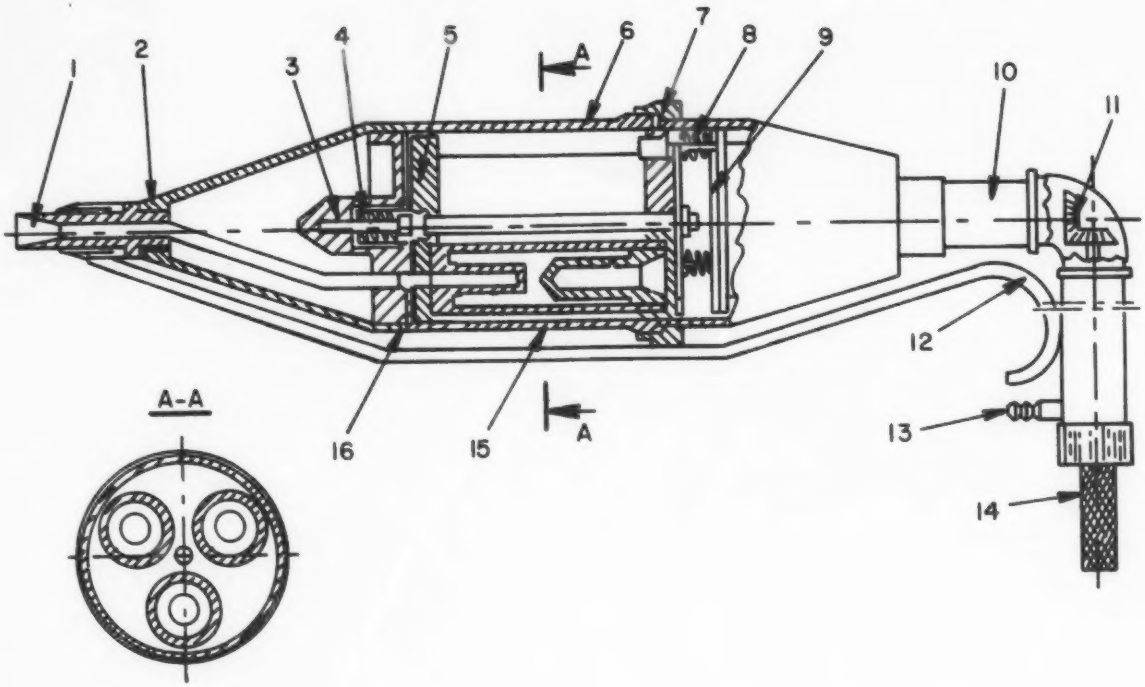
1
2
3
4
5
6
7
8
9
10
11
12
13
14
15
16
A
A
A-A

Figure 1. Sampling Unit.

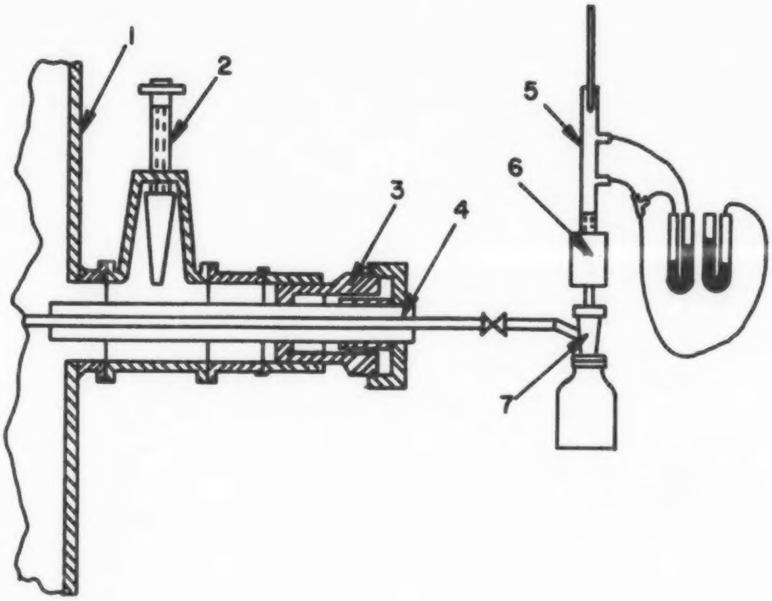

Figure 2.

1. regenerator
2. fastener
3. gasket packing
4. sampling tube
5. measurement diaphragm
6. metal adapter
7. cyclon with hopper

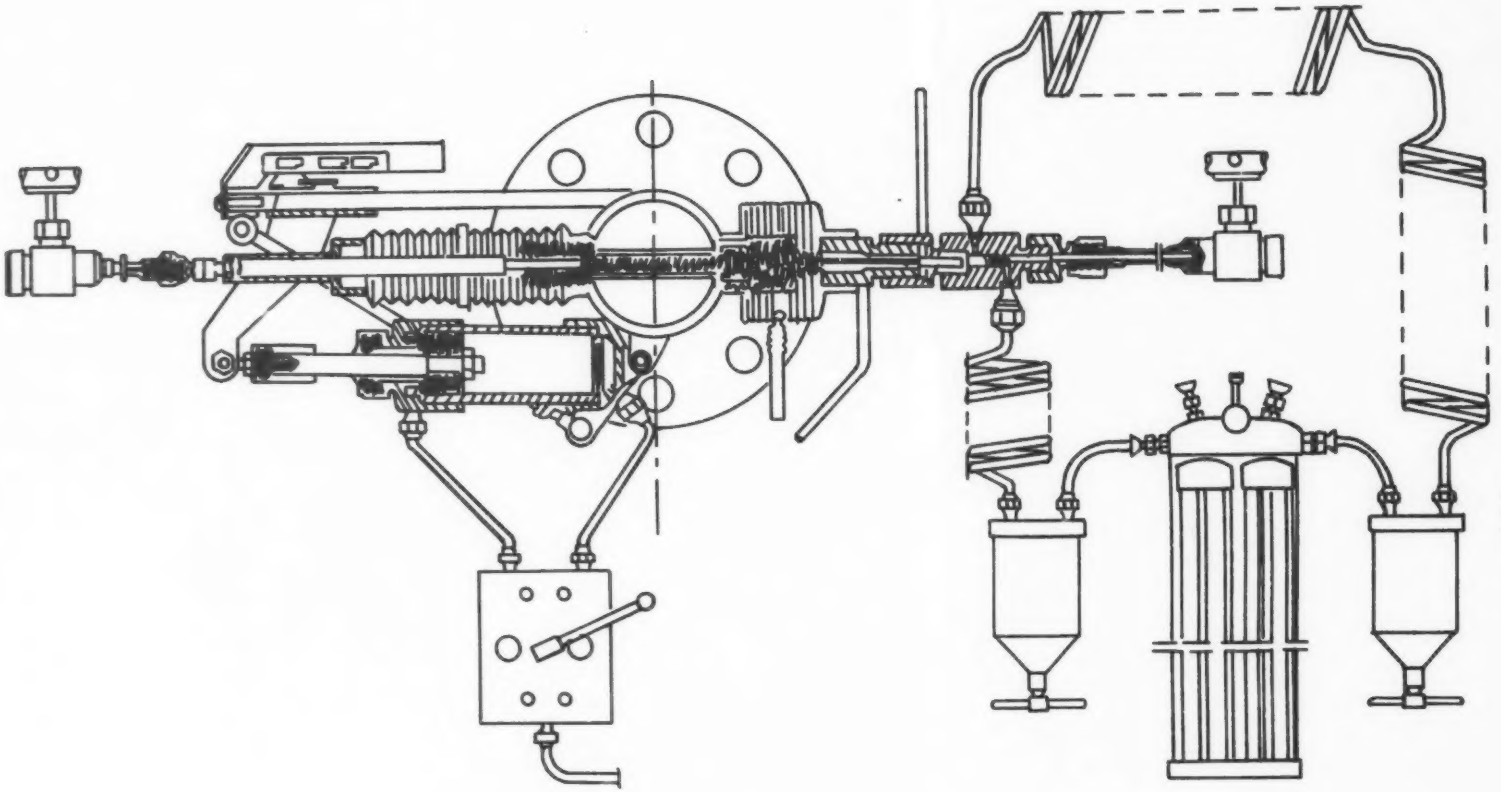

Figure 3. Schematic presentation of a set up for particulates sampling with increased pressure.

Paper No. 30

MEASUREMENT OF PARTICLE SIZE DISTRIBUTIONS AT EMISSION SOURCES WITH CASCADE IMPACTORS

by

Michael J. Pilat

UNIVERSITY OF WASHINGTON

Seattle, Washington

ABSTRACT

Cascade impactors can be used to measure the size distribution of particles in ducts and stacks at emission sources. The cascade impactor is usually inserted inside the duct or stack to enable isokinetic sampling, to minimize losses of particles to the sampling probe wall, and to reduce problems with water condensation. Traditionally, cascade impactors have provided particle size data in the 0.2 to 30 micron diameter general size range. Recently high pressure drop cascade impactors have been used to measure the particle size distribution down to about 0.02 microns diameter. Solutions to the problems of particle re-entrainment, sampling gases with entrained water droplets, and simultaneous sampling at the inlet and outlet of particulate control devices are discussed.

I. Introduction

Cascade impactors have been used for some 30 years to measure the size distribution of aerosol particles. May (1945) reported particle size data in the 1 to 20 micron diameter range measured with a 4-stage cascade impactor with rectangular jets. Since then many different types of cascade impactors have been developed, mainly for sizing aerosol particles in atmospheric and industrial hygiene studies.

First et al (1952) and Gussman and Gordon (1966) reported on the modification of a Casella impactor so that it could be used to sample particles in ducts and stacks. The Casella was modified such that the first impactor stage was located in the sampling probe elbow, thus preventing the loss of large particles to the elbow wall. Brink (1958, 1963) developed a five stage cascade impactor with single round jets to size mist droplets in the 0.3 to 3 micron diameter size range. The mist aerosol is sampled from the stack or duct into the Brink impactor located in a heated sampling box. In 1968 the need for size distribution data concerning particles in exhaust gas streams stimulated the development of the Mark I University of Washington Source Test Cascade Impactor. As reported by Pilat, Ensor and Bosch (1970), the Mark I UW impactor (has six stages with multiple round jets on each stage) had problems with the loss of particles onto the top of the first jet stage (particles too large to follow the gas stream lines through the jets) and with loss of particles to the walls between the stages. Based on the experience with the Mark I UW impactor, a Mark II model was developed. The Mark II UW impactor has a single jet first stage followed by six multi-jet stages and a 47 mm diameter filter holder. The sampling nozzle includes the single jet for the first stage and therefore, the problem of particle loss upon the top of the first multi-jet stage was eliminated.

The Mark III UW Cascade Impactor was developed in order to further reduce the loss of particles to the walls. The Mark III UW impactor has a single jet first stage followed by six multi-jet stages and a 47 mm filter holder as shown in Fig. 1. The particle collection plates have a hole in their centers for the gas to flow through and this center hole eliminates the need for the gas to flow around the outside edges of the plate. The various parts of the Mark III UW impactor are shown in the photo in Fig. 2. The annular particle collection plates have successfully solved the problem of particle loss to the cylindrical walls of the outer casing as the gas and aerosol particles have no contact with these walls. The only surfaces upon which the particles can be deposited (other than the tops of the particle collection plates) and become "lost" from the sample are the top and bottom of the jet stages and the bottom of the collection plates. By the proper selection of the gas sampling flow rates through the Mark III UW impactor the deposition of particles upon the jet stage tops and collection plate bottoms only seldom occurs (possibly due to rough handling of the impactor between the sampling location and the laboratory, to overloading the collection plate with too large a sample, or to very high electrostatic charges on the particles). However, at times the particles do bounce off the particle collection plates and deposit upon the bottom side of the jet stages. The problems with particle re-entrainment are covered in the discussion section of this paper.

Fig. 1 U.W. MARK III
SOURCE TEST CASCADE IMPACTOR
(CROSS SECTION)

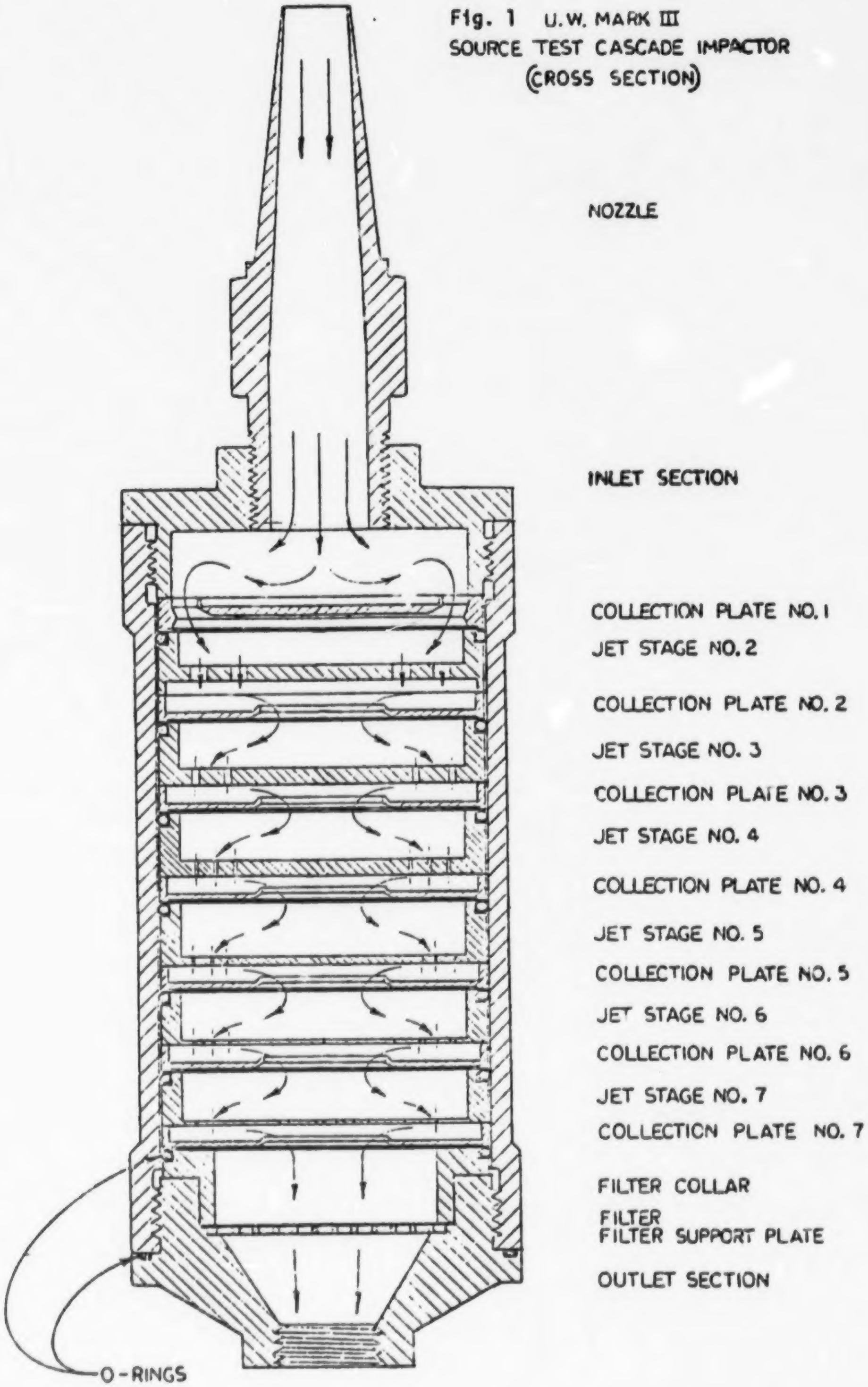
NOZZLE
INLET SECTION
COLLECTION PLATE NO. 1
JET STAGE NO. 2
COLLECTION PLATE NO. 2
JET STAGE NO. 3
COLLECTION PLATE NO. 3
JET STAGE NO. 4
COLLECTION PLATE NO. 4
JET STAGE NO. 5
COLLECTION PLATE NO. 5
JET STAGE NO. 6
COLLECTION PLATE NO. 6
JET STAGE NO. 7
COLLECTION PLATE NO. 7
FILTER COLLAR
FILTER
FILTER SUPPORT PLATE
OUTLET SECTION
O-RINGS

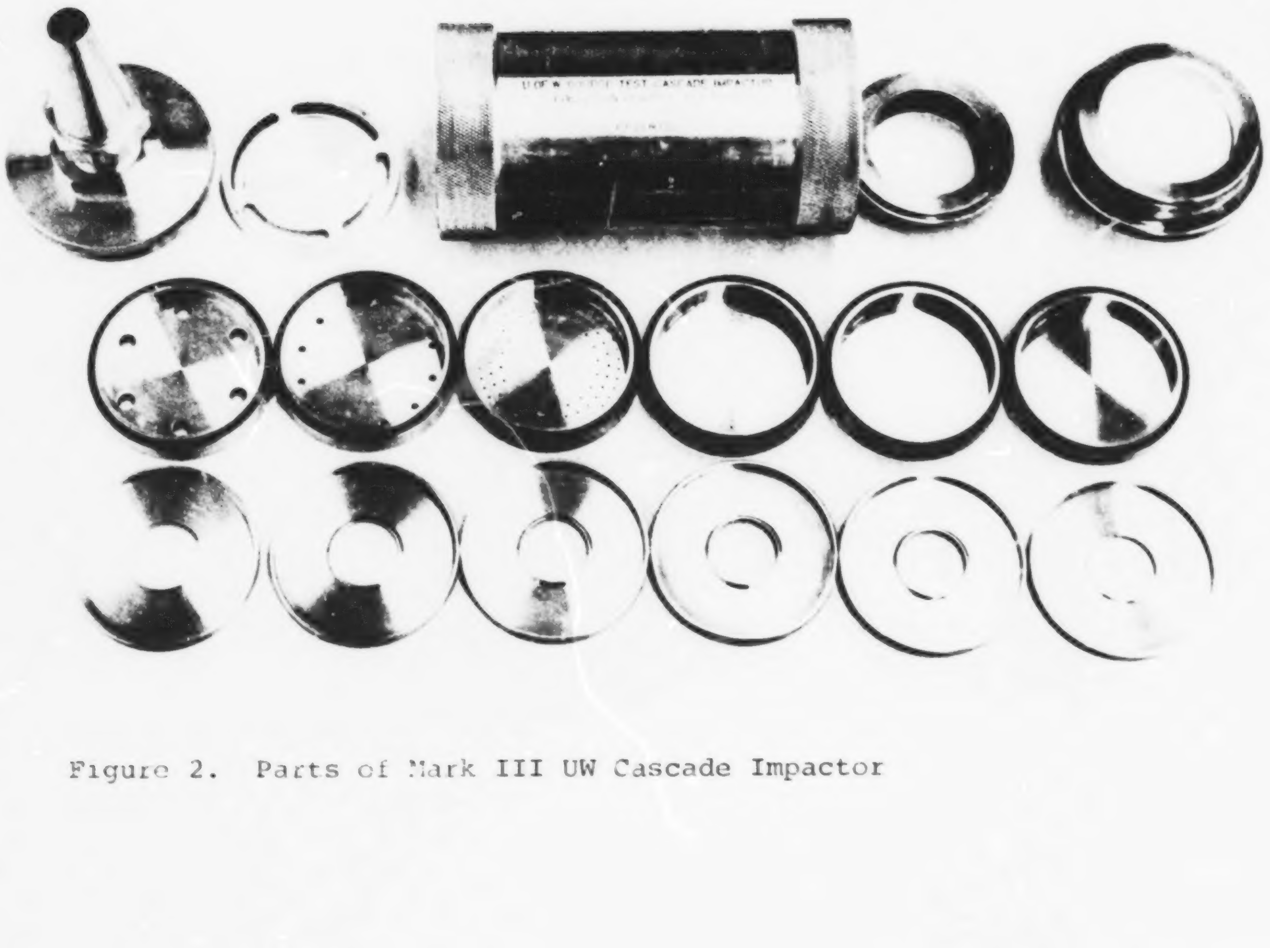

Figure 2. Parts of Mark III UW Cascade Impactor

Since the development of the UW Source Test Cascade Impactors, other cascade impactors have been also developed or adapted to stack sampling. Downs and Strom (1972) reported on the modification of a Brink Mist Sampler by adding a cyclone at the inlet, two additional jet stages and a filter at the outlet for use in sampling with the impactor inside the stack. Holland and Conway (1973) have reported on three in-stack sampling cascade impactors; the Andersen Stack Sampler, the TAG impactor, and the Mark III UW Source Test Cascade Impactor. Bird, McCain, and Harris (1973) reported on a comprehensive particle size measurement program involving the use of eleven different commercial and modified particle sizing devices at a coal-fired electric generating plant.

II. Calibration of UW Cascade Impactors

A. Theoretical

Based on a solution to the particle equation of motion the Stokes inertial parameter ψ is given as

$$\psi = \frac{C\rho_p d^2 V_j}{18\mu D_j} \qquad (1)$$

where C is the Cunningham correction factor ρ_p the density of the particles, d the particle diameter, V_j the velocity of the gas in the jet, μ the gas viscosity, and D_j the diameter of the gas jets in a given stage. The magnitude of the Stokes inertial parameter at the particle diameter that is collected with 50% efficiency by a given jet stage has been reported to range between 0.12 to 0.17 for circular jets (the square root of ψ_{50} ranges from 0.35 to 0.41). Note that these studies assumed impaction upon a flat plate and the particles upon impaction are collected (does not take into account particle bounce, particle re-entrainment, or particla impaction onto glass fiber filters).

Using equation (1) an equation can be developed which relates d_{50} to the cascade impactor design and operating parameters. Solving for the particle diameter in equation (1) gives

$$d = \left[\frac{18\mu D_j \psi}{C\rho_p V_j}\right]^{1/2} \qquad (2)$$

Substituting a value of 0.145 for ψ_{50} (corresponds to the square root of ψ_{50} of 0.38) provides the equation

$$d_{50} = \left[\frac{2.61\mu D_j}{C\rho_p V_j}\right]^{1/2} \qquad (3)$$

The velocity of the gas in each jet is calculated by

$$V_j = \frac{4Q}{\pi D_j^2 N} \qquad (4)$$

Where Q in the gas volumetric flow rate at stage conditions, N the number of jets on a given jet stage, and D_j is the jet diameter for that same stage. Substituting equation (4) for V_j in equation (3) gives

$$d_{50} = \left[\frac{2.05 \mu D_j^3 N}{C \rho_p Q}\right]^{1/2} \qquad (5)$$

Equation (5) can be used to calculate the d_{50} of any cascade impactor stage. The d_{50} magnitudes calculated for a certain set of stages for the UW Mark III impactor are presented in Fig. 3. Note that the gas flow rate Q is at the stack conditions (actual flow rate passing through the impactor).

B. Experimental Measurements

The experimental calibration of cascade impactor stages is sometimes desired in order to verify the impactor's sizing capabilities (even though its design may be based upon experimentally verified criteria). The UW Mark I Cascade Impactor was calibrated using monodisperse Dow latex spheres of 1.9 and 3.5 microns diameter as reported by Bosch, Pilat and Hrutfiord (1971). The quantity of particles collected on each collection plate was determined using an optical microscope and the stage collection efficiencies calculated from these quantities. The stage collection efficiencies and the square root of the Stokes number are plotted in Fig. 4 and show good agreement with the square root of ψ_{50} of 0.38 reported by Ranz and Wong (1952) for circular jet impactors.

It is recommended that photomicrographs of the particles sampled on the collection plates be periodically taken in order to illustrate the size, color, and shape of the particles being sampled. Please note that the size of the particles on a given collection plate should range from about the d_{50} of that stage to the d_{50} of the next upstream stage. For more detailed information on the interpretation of impactor data, please refer to Mercer (1965).

III. Sampling Procedure for UW Source Test Cascade Impactors

The entire particle size distribution measurement procedure includes three phases; pre-test preparation, source test sampling of the particulates, and analyses of the collected samples and recorded data. The pretest preparation includes cleaning the impactor, placing a thin layer of grease on the collection plates if solid particles are to be sampled, weighing the plates and filter (or weighing the insert foils placed on top of the plates). The source test involves first determining the gas velocity profile in the stack (measure the gas temperature and pressure drop profile with type S pitot tube) and then calculating the nozzle size for isokinetic sampling. The sampling train is set up as shown in Fig. 5 with the cascade impactor on a sampling probe (1/2 inch diameter stainless steel probe) followed by a 1/2 inch diameter Teflon lined flexible hose, four Greenburg-Smith impingers (first two with 100 ml of water, the third is dry, and the fourth has silica gel), a leakless vacuum pump, and a dry gas meter. Sometimes a 47 mm diameter glass fiber filter is placed downstream of the dry Greenburg-Smith impinger to collect particles condensed in the impingers. The UW Cascade Impactor is preheated to prevent conden-

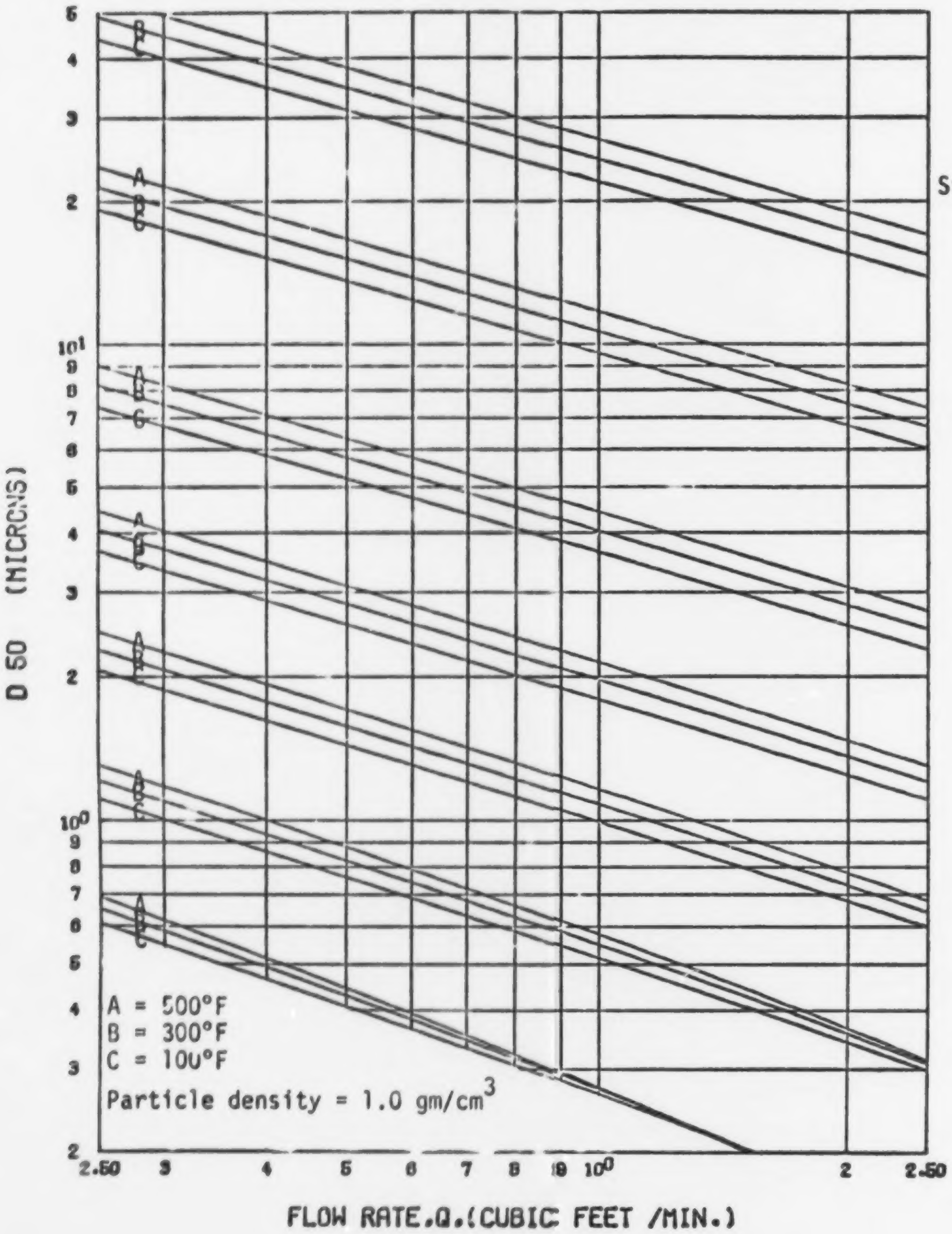

Stage	Jet Dia. (inches)	No. Jets
1	0.7180	1
2	0.2280	6
3	0.0960	12
4	0.0310	90
5	0.0200	110
6	0.0135	110
7	0.0100	90

Fig. 3 Calculated d_{50} of Mark III-F Stages

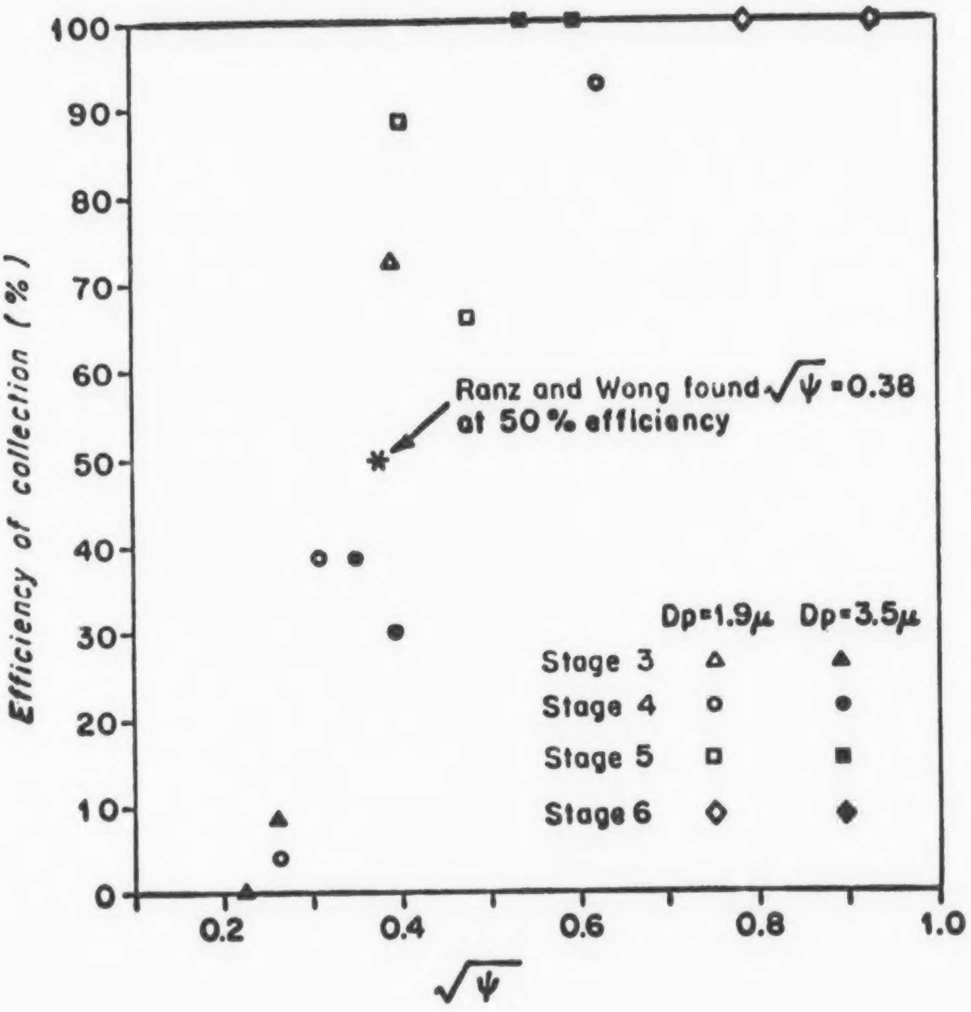

Fig. 4 Measured Particle Collection Efficiency versus Stokes Number for Mark I UW Cascade Impactor

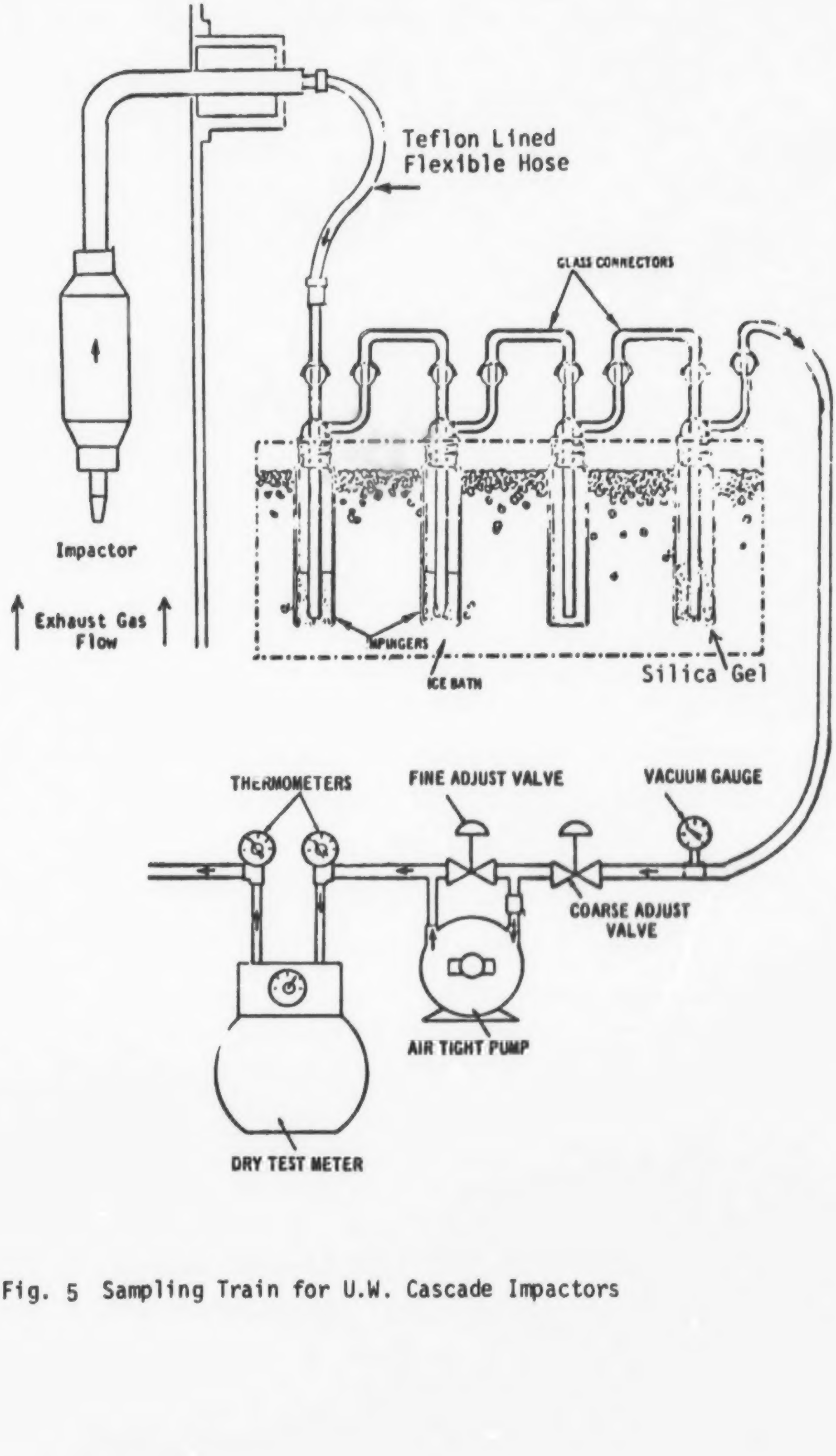
Teflon Lined
Flexible Hose
GLASS CONNECTORS
Impactor
Exhaust Gas
Flow
IMPINGERS
ICE BATH
Silica Gel
THERMOMETERS
FINE ADJUST VALVE
VACUUM GAUGE
COARSE ADJUST
VALVE
AIR TIGHT PUMP
DRY TEST METER

Fig. 5 Sampling Train for U.W. Cascade Impactors

sation problems by placing it into the stack with the nozzle faced downstream for about 10-15 minutes prior to sampling. After preheating the impactor, a particle sample is obtained by facing the impactor nozzle upstream and turning on the vacuum pump. The gas sampling rate is maintained at the constant isokinetic rate throughout the test (typical flow rates are in the 0.3 to 1.5 cfm range). As can be seen in Fig. 3 changing the gas sampling rate will also change the magnitude of the stage d_{50}s. The gas sampling time, temperature. volumetric readings from the dry gas meter, etc. are recorded on a data sheet. After obtaining the particle sample, the UW impactor is removed from the stack being careful not to hit the impactor or probe against the stack or sampling port (particles can fall off the collection plates if the impactor is bumped around too much). After removal from the stack, the impactor is disassembled and the particle collection plates are removed (preferably in a clean wind-free location) and weighed. In some cases (for example when sampling downstream of a wet scrubber) it may be necessary to dry the collected particles by heating in an oven and cooling to room temperature in a desiccator. The weights of the particles collected on the plates and in the filter are used to calculate the cumulative particle size distribution.

IV. Discussion

A. Particle Re-entrainment

The problem of the re-entrainment of particles impacting upon the collection plates of cascade impactors was reported many years ago by May (1945). May suggested that cascade impactors use low gas velocities in the jets and an adhesive (such as 3 parts castor oil to 1 part rosin) to reduce particle bounce and blow-off. By referring to equation (3)

$$d_{50} = \left[\frac{2.61\mu D_j}{C\rho_p V_j}\right]^{1/2} \qquad (3)$$

it can be seen that if the gas velocity in the jet V_j is restricted to lower magnitudes, then it is necessary to use small jet diameters D_j in order to obtain the lower magnitudes of the stage d_{50}s. To achieve sufficient gas volumetric sampling rates we have found it necessary to use many jets per stage (unfortunately the single large jet per stage impactors have excessive particle bounce and blow-off problems at the smaller particle d_{50}s).

The design of the UW Mark III Cascade Impactor includes considerations for reducing the particle blow-off caused by excessive gas velocities. Also adhesives such as Dow silicone high vacuum grease are used on the particle collection plates.

The magnitude of the apparent problems of particle blow-off is illustrated in Fig. 6 which presents particle size distributions simultaneously measured by four cascade impactors, as reported by Bird, McCain and Harris (1973). The measurements were made at a coal fuel power plant at the outlet of a mechanical collector and the inlet to the electrostatic precipitator. As is shown in Fig. 6 the peak in the particle size distribution is at about 4.5 microns diameter for the UW Mark III impactor (commercially

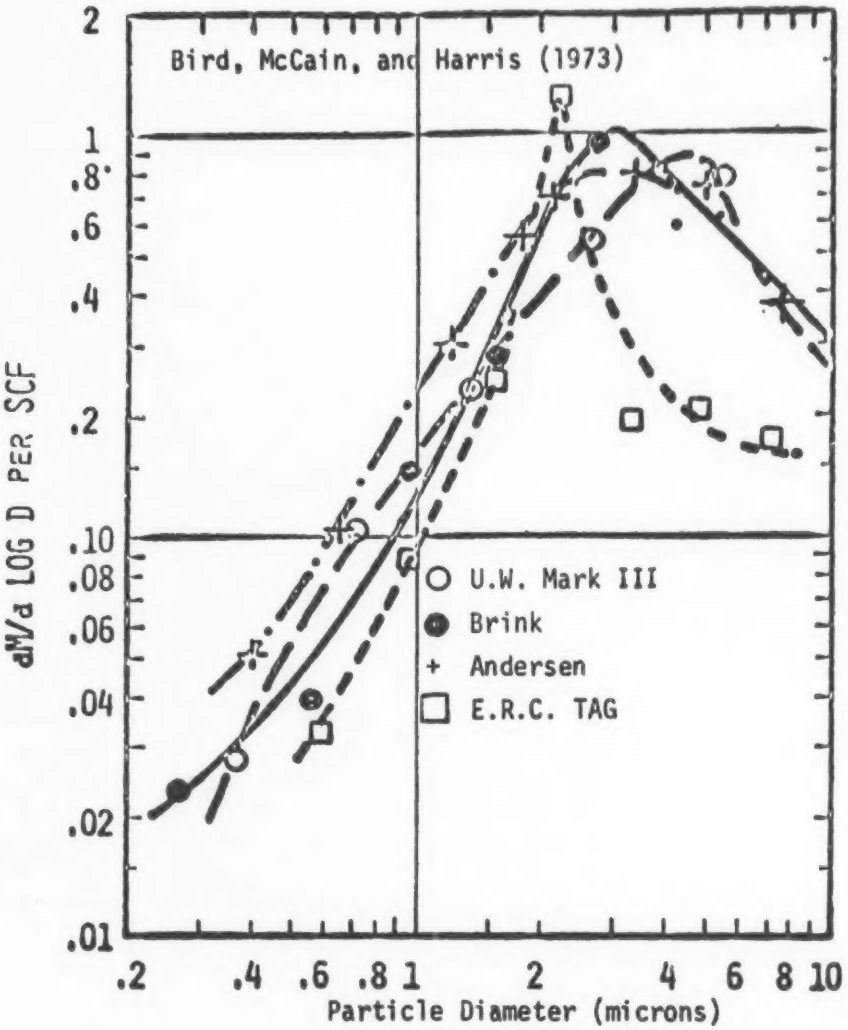

Fig. 6 Comparison of Simultaneous Cascade Impactor Size Distribution Measurements

available model as purchased from Pollution Control System Corp.), at about 3.0 microns diameter by the Brink impactor (specially modified for in-stack use with an additional stage, an internal filter holder, and one or two cyclone precollectors), at about 2.8 microns by an Andersen impactor (specially constructed prototype using glass fiber filter impaction substrates), and at about 2.3 microns diameter by an Environmental Research Corporation TAG (commercially available from ERC) with greased foils on the last four stages. It appears that the cascade impactors with the size distribution peaks at the lower sizes suffer from the problem of particles bouncing or blowing off and being collected on downstream plates or by the filter (and thus indicating a smaller size distribution than actually exists). It should be noted that only the UW Mark III and the ERC TAG impactors were commercially available models, whereas the other two were specially assembled for this EPA funded evaluation (this research project concerning the evaluation of cascade impactors for measuring the size distribution of particles at emission sources is being conducted by Southern Research Institute).

B. Simultaneous Sampling at the Inlet and Outlet of Particulate Control Equipment

For a single cascade impactor particle sample, the stack gas sampling time need only be as long as is necessary to obtain a weighable particle sample. Excessive sampling times can result in the overloading of the particle collection plates which can contribute to the particle re-entrainment problem. Note that a number of particle samples obtained with short sampling times (we have used as short as 4 minute sampling times) is superior to one sample of longer time, as reported by Kahnweld (1966). Of course, for characterizing the emissions from a process that is variable over small time periods, it is mandatory to use short sampling times.

When simultaneously sampling at the inlet and outlet of a particle collection device it is common to have the outlet concentration about 1 to 10% of the inlet particle concentration. Therefore, by sampling at the same gas volumetric flow rate with identical cascade impactors, the weight of particles collected on the outlet impactor plates is about 1 to 5% of the inlet impactor plates. This approximately one hundred-fold difference in the weight of the collected particles can result in overloading of the inlet impactor and insufficient particle sample weights with the outlet impactor.

There are a number of approaches to solving the simultaneous inlet-outlet sampling problem. One is to operate the inlet impactor at a lower gas sampling rate than the outlet impactor. However, this causes the impactor stage d_{50}s to be different between the inlet and outlet samples and can result in strange particle collection efficiency curves. A second approach is to use light weight foil inserts on the particle collection plates thus lowering the plate tare weight and increasing the weighing precision. Also using weighing balances with greater sensitivity (say to 0.010 milligrams) will enable accurate weighing of the outlet impactor plate samples (i.e., at about 0.5 milligrams particles per plate) with the inlet impactor plates not overloaded with particles (i.e., at about 50 milligrams particles per plate). A third approach is to use cascade impactors designed to operate at different gas sampling flow rates. The low sampling rate impactor would be used at the inlet and the high sampling rate impactor at the outlet.

The research and development of such a pair of cascade impactors is underway at the University of Washington (primarily for use with our research programs concerning the development of high efficiency particle collection systems). A fourth approach is to use a cyclone with a cascade impactor at the inlet of control equipment. A BCURA cyclone with a Mark III UW Impactor is shown in Fig. 7. The cyclone serves to prevent the impactor from becoming overloaded.

C. Sampling of Gases Containing Water Droplets

When sampling downstream of wet scrubbers it is possible to encounter water droplets in the gas stream. The presence of these water droplets is usually the result of inefficient (or the lack of) mist eliminators. As these water droplets usually contain particulate matter, it is actually not good practice to allow these water droplets to exhaust into the atmosphere (assuming that the objective is to reduce the particulate emissions). An in-stack cascade impactor will classify the water droplets into size fractions in a manner similar to any other aerosol particle. However, it is possible to flood the impactor when high water droplet concentration exists.

If the water droplet concentration is low, filters may be placed on the particle collection plates to absorb the water and thus prevent it from washing off the particles, seeping from plate to plate, and in general making a mess out of the impactor samples. The particle collection plates, the filters, and the collected particle and water sample can be weighed "wet" to provide information concerning the size distribution of the wet aerosol (particles plus water droplets).

With high water droplet concentrations and large diameter water droplets, it is very difficult to isokinetically sample the gases as the droplets flood the inlet particle collection plates. The use of a long heated inlet nozzle may serve to evaporate the water droplets sufficiently to prevent this flooding. However, in some cases it may be necessary to sample at right angles in order to obtain an indication of the size distribution and mass concentration of the smaller aerosol particles.

D. Use of UW Cascade Impactors to Measure In-Stack Particle Mass Concentration

The UW Cascade Impactors have been used to measure the particle mass concentrations at in-stack conditions. The sum of the particle weights collected by the plates and the filter divided by the volume of gas sampled provides the particle mass concentration. Simultaneous particle sampling with UW Cascade Impactors and in-stack alundum thimbles lined with glass fiber and followed by a 47 mm diameter glass fiber filter have shown good agreement in the particle mass concentration measurements. In Fig. 8 a plot of alundum thimble and UW Mark III Cascade Impactor mass concentration measurements made on particles emitted from a hog fuel boiler show a correlation coefficient of 0.94 between these measurements. However, it should be noted that to obtain the total particle mass concentration (in-stack particles plus condensible particles) it is necessary to add the weight of the residue from the probe and hose washings, the residue from the impinger solutions, and the particles collected by a filter located downstream of the third impinger in Fig. 5.

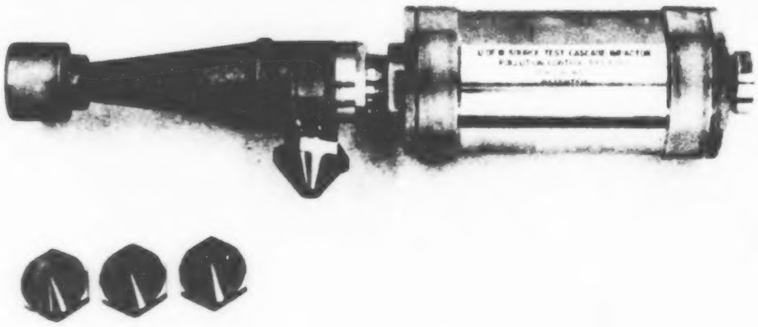

Figure 7. BCURA Cyclone at Inlet to Mark III UW Cascade Impactor

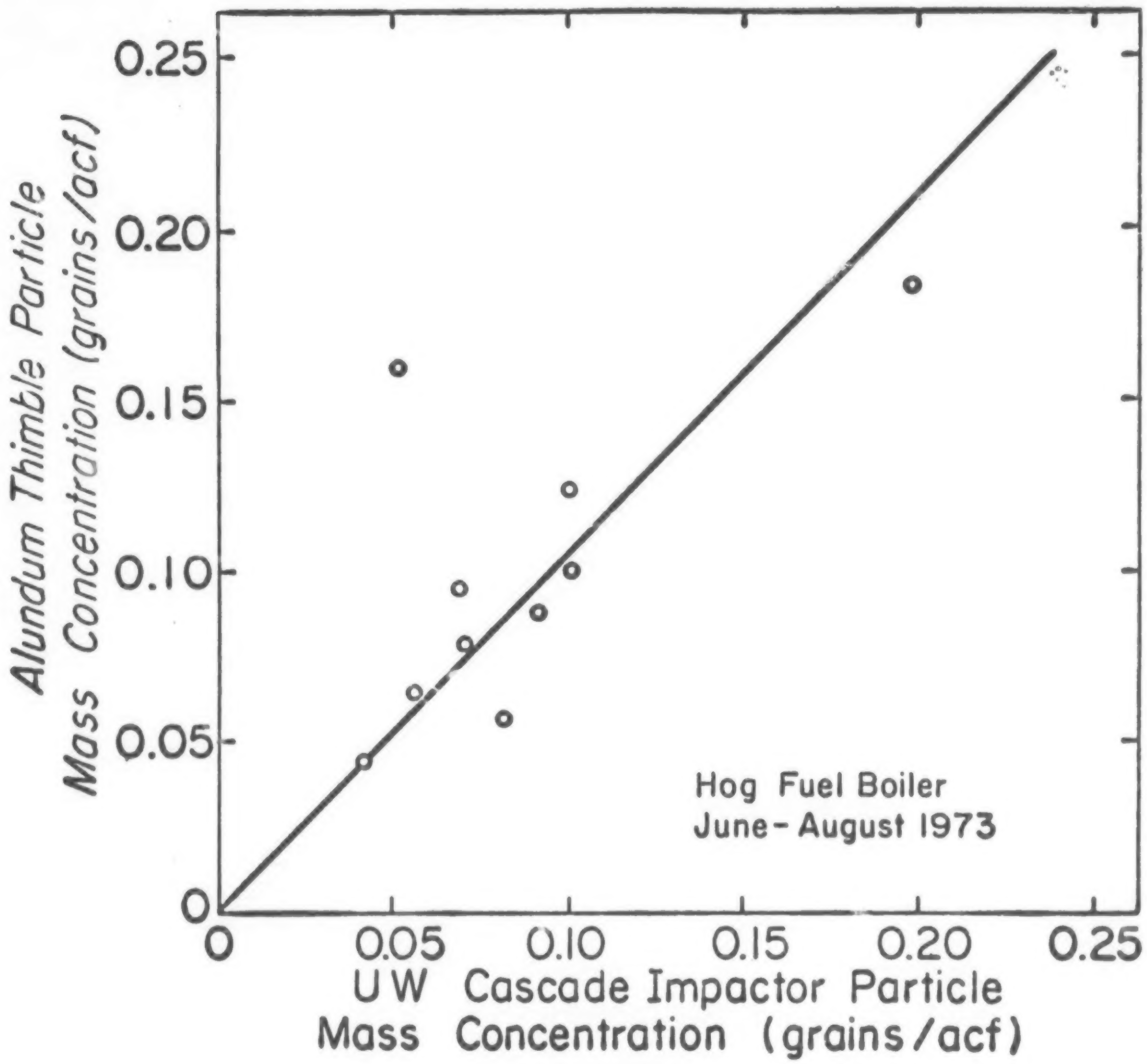

Fig. 8 Comparison of Particle Mass Concentrations Simultaneously Measured with Mark III UW Cascade Impactor and with Alundum Thimble Followed by Glass Fiber Filter

E. Variation in Measured Particle Size Distributions

The size distribution of particles emitted from different sources varies considerably. The size of particles emitted from non-continuous processes can change greatly. Hanna and Pilat (1972) reported that the measurements of particle emissions from the exhaust of a horizontal spike Soderberg aluminum reduction cell with a UW Mark II Cascade Impactor showed the particle mass mean diameter ranged from about 0.5 to 100 microns and the particle geometric standard deviation from about 5 to 1,000. However, the size distribution of particles emitted by a continuous process (such as a kraft recovery furnace) remains fairly constant as long as the operating conditions remain the same. But the size distribution of particles emitted by similar continuous processes are not necessarily similar.

Of course, there is considerably more size distribution data measured by the UW impactors than can be presented in this paper. For this additional information it is possible to refer to publications. The Mark I UW Cascade Impactors have been used to measure the particle size distributions at the UW coal-fired power plant, as reported by Pilat, Ensor, and Bosch (1970); at the exhaust of the number [illegible] kraft recovery furnace at the St. Regis Paper Co. pulp mill in Tacoma, as reported by Bosch, Pilat, and Hrutfiord (1971); and at the exhaust of a steam heated veneer drier at the U.S. Plywood-Champion Paper plant in Seattle, as reported by Larssen, Ensor, Sparks, and Pilat (1970). The UW Mark II Cascade Impactor has been used for sizing particles emitted from kraft recovery furnaces, as reported by Larssen, Ensor, and Pilat (1972); and for sizing the particles emitted from fluidized bed sewage sludge incinerators, as reported by Liao and Pilat (1972).

F. Measurement of Submicron Particle Size

Pilat (1973) reported on the use of cascade impactors to measure the size distribution of submicron particles down to about 0.02 microns diameter. Research concerning the development of the Mark IV UW Source Test Cascade Impactor for sizing these submicron particles has been underway since 1971. The Mark IV impactor utilizes low absolute gas pressures in the outlet jet stages to increase the Cunningham correction factor which, as shown in equation (3), can result in lower magnitudes of d_{50} for a given jet diameter (about 0.010 inch), gas velocity (less than Mach 1), particle density, and gas viscosity. The magnitude of the Cunningham Correction factors at low gas pressures using an equation reported by Davies (1945) is shown in Fig. 9. Laboratory and field tests have demonstrated that this approach will provide submicron particle size data. The major problems with this method appear to be the requirements for a good portable vacuum pump (light enough for stack sampling) and particle bounce at the high gas velocities.

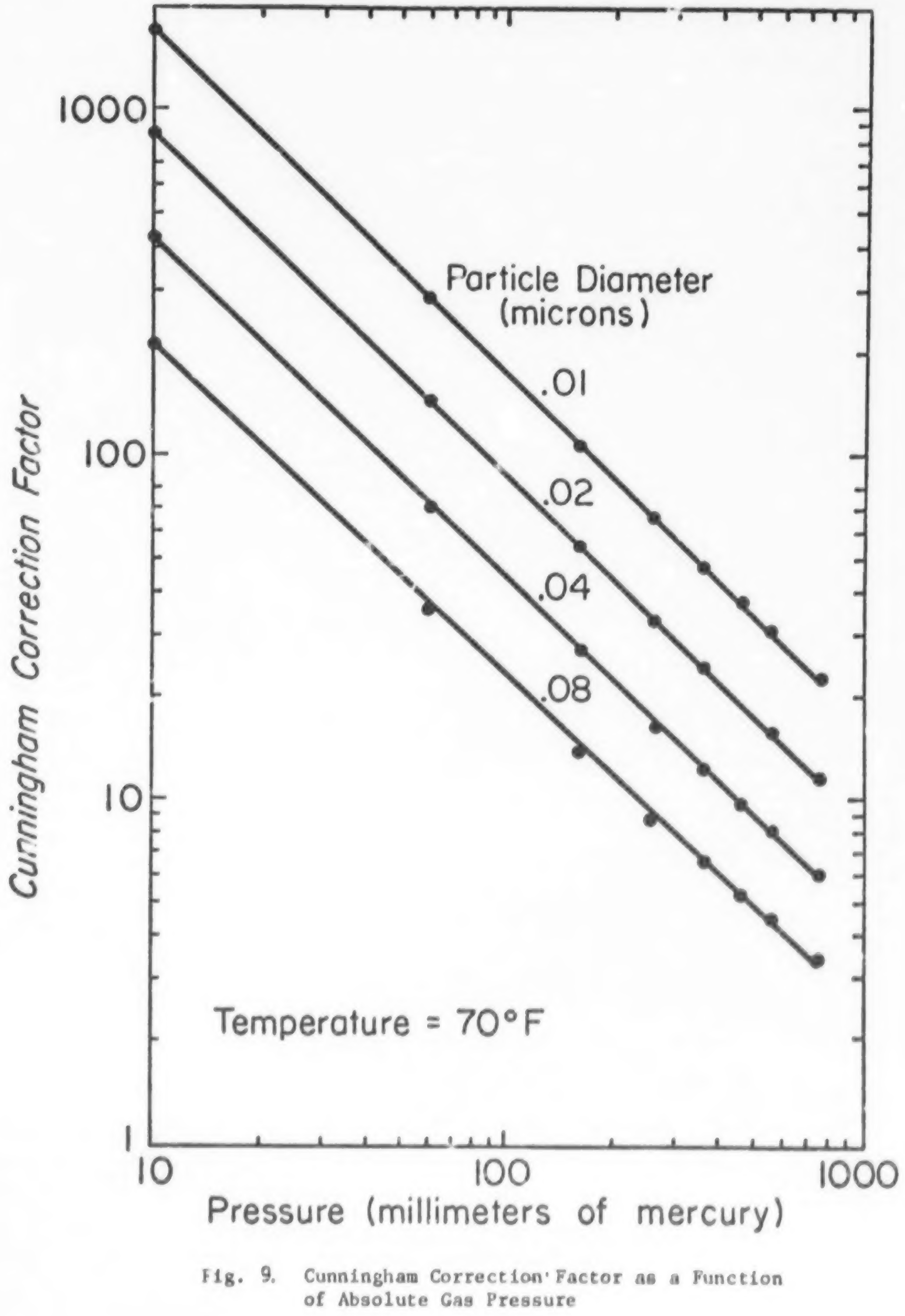

Fig. 9. Cunningham Correction Factor as a Function of Absolute Gas Pressure

References

Bird, A. N., J. D. McCain, and D. B. Harris (1973). "Particulate Sizing Techniques for Control Device Evaluation," Paper No. 73-282 presented at APCA Annual Meeting, Chicago, Ill.

Bosch, J. C., M. J. Pilat, and B. F. Hrutfiord (1971). "Size Distribution of Aerosols from a Kraft Mill Recovery Furnace," TAPPI 54 1871-1875.

Brink, J. A. (1958). "Cascade Impactors for Adiabatic Measurements," Ind. Engr. Chem. 50 645-648.

Brink, J. A. and W. F. Patton (1963). "New Equipment and Techniques for Sampling Chemical Process Gases," JAPCA 13 162-166.

Davies, C. N. (1945). "Definite Equations for the Fluid Resistance of Spheres," Proc. Phys. Soc. 57 259-270.

Downs, W. and S. S. Strom (1972). "New Particle Size Measuring Probe - Application to Aerosol Collector and Emissions Evaluations," J. Engr. Power (Transactions of ASME) 94 117-126.

First et al (1952). "Air Cleaning Studies Progress Report," NYO-1586, Harvard University.

Gussman, R. A. and D. Gordon (1966). "Notes on the Modification and Use of a Cascade Impactor for Sampling in Ducts," Am. Ind. Hyg. Ass. J. 27 252-255.

Hanna, T. R. and M. J. Pilat (1972). "Size Distribution of Particulates Emitted from a Horizontal Spike Soderberg Aluminum Reduction Cell," J. APCA 22 533-536.

Holland, W. D. and R. E. Conway (1973). "Three Multi-stage Stack Samplers," Chem. Engr. Progress 69 93-95.

Kahnweld, H. (1966). "Dust Measurements in Flowing Gases," Staub 26 20-22.

Larssen, S., D. S. Ensor, L. E. Sparks, and M. J. Pilat (1970). "Size Distribution of Particulate Emissions from a Veneer Drier," Presented at PNWIS-APCA, Spokane, WA.

Larssen, S., D. S. Ensor, and M. J. Pilat (1972). "Relationship of Plume Opacity to the Properties of Particulates Emitted from Kraft Recovery Furnaces," TAPPI 55 88-92.

Liao, P. B. and M. J. Pilat (1972). "Air Pollutant Emissions from Fluidized Bed Sewage Sludge Incinerators," Water and Sewage Works, 68-74.

May, K. R. (1945). "The Cascade Impactor: An Instrument for Sampling Coarse Aerosols," J. Sci. Instr. 22 187-195.

Mercer, T. T. (1965). "The Interpretation of Cascade Impactor Data," Amer. Ind. Hyg. Assoc. J. 26 236-241.

References - Cont.

Pilat, M. J., D. S. Ensor, and J. C. Bosch (1970). "Source Test Cascade Impactor," Atmos. Envir. 4 671-679.

Pilat, J. J. (1973). "Submicron Particle Sampling with Cascade Impactors," Paper No. 73-284, Presented at APCA Annual Meeting, Chicago, Ill.

Ranz, W. E. and J. B. Wong (1952). "Jet Impactors for Determining the Particle Size Distribution of Aerosols," A.M.A. Arch. Ind. Hyg. Occup. Med. 5 464-477.

Paper No. 31

THE CHEMICAL COMPOSITION OF FLY ASH

by

David F. S. Natusch

UNIVERSITY OF ILLINOIS

Urbana, Illinois

Preceding page blank

ABSTRACT

Almost all naturally occuring elements are represented in fly ashes and in airborne particulates derived from industrial processes. Special significance is, however, attached to toxic species containing elements such as As, Sb, Pb, Tl, Hg, Cd, Se, V, Ni, Cr, S, C and Be. In fly ash derived from coal combustion many of these elements are found to increase in concentration with decreasing particle size. This is possibly due to volatization of the element or one of its compounds followed by preferential adsorption or condensation onto the small particles. Evidence in support of this hypothesis is presented. The significance of toxic element dependence on particle size is discussed in terms of human respiratory intake, existing and potential control technology and emission inventories. Techniques for the sampling, size differentiation and chemical analysis of particles are briefly reviewed.

INTRODUCTION

From an engineering viewpoint the control of particulate emissions from stationary sources implies collection of as many particles as possible from the effluent gas stream. This is a good approach because, if successful, it ensures that all particles large and small, toxic and non-toxic, corrosive and non-corrosive will be prevented from reaching the atmosphere. Unfortunately many particles, especially those of sub-micrometer (μm) size, do reach the atmosphere and it is meaningful to find out what these particles are and what their environmental effects might be in order to make decisions about the need for their control and how this control might be achieved.

The intention of this paper is to show how a knowledge of the chemical and physical character of particulate matter is of fundamental importance in deciding which particles are most hazardous and how these hazards might be reduced. In short, it develops the thesis that control strategy should be more firmly based on an understanding of the chemical and physical nature of particulate material.

REASONS FOR PARTICULATE CONTROL

There are four major reasons why it is undesirable for particulates to reach the atmosphere. Not all have equal importance.

1. Soiling

Particles larger than about 5 μm can be seen by the naked eye and, as a consequence, give rise to visible soiling when they fall upon contrasting surfaces such as paint, clothing and the like. Their removal is therefore important for aesthetic reasons. However, current control technology is, in large part, capable of preventing emission of the large particles responsible for soiling. For example the mass median diameter of airborne particles in the San Francisco Bay area in 1960 was estimated to be 20μm[1] whereas today urban particulates commonly have a mass median diameter of about 1μm or less[2]. Prevention of soiling can thus no longer be considered as a major goal for control strategists.

2. Light Scattering

While the mass median diameter of U.S. urban aerosols has decreased over the last few decades, Table I shows that there has been no corresponding decrease in total mass[3]. Thus, the net effect has been to move the aerosol mass into smaller and smaller particles and promote the amount of material present in the size range 0.1 - 1.0 μm responsible for light scattering. It should be noted that light scattering is related primarily to particle size and number and is not effected by the chemical composition of a particle.

3. Atmospheric Interactions

A number of atmospheric reactions involving both natural and pollutant species are influenced catalytically by airborne particles. Many particles can also provide adsorption, condensation and nucleation surfaces for gaseous species (eg formation of water droplets). While such processes are not necessarily detrimental to the environment they do represent a significant environmental perturbation and, until more is known about them, they should be prevented where possible. The main point, however, is that these catalytic or reactivity effects depend upon the chemical nature of the particle.

4. Health Effects

The fourth, and in most instances the major, reason for particulate control involves both occupational and environmental health. Thus many sources emit particles which can produce adverse health effects when inhaled or when deposited on skin or sensitive tissues such as the membranes of the eye. In the great majority of cases (asbestos sapphires provide a notable exception) the toxicity of particulate matter resides in its content of more or less toxic organic and inorganic compounds. Consequently, the health effects of particulate matter are closely related to the chemical composition of the particles.

Collective consideration of these four adverse effects of particulate matter leads one directly to the conclusion that the need for control depends primarily on the chemical and physical character of the particles in question. In determining control strategy, therefore, it is clearly appropriate to consider the chemical composition of particulate emissions, their size distribution and the relationship between chemical composition and size distribution.

CHEMICAL COMPOSITION OF FLY ASH

The chemical composition and physical behavior of particles emitted to the atmosphere obviously depends upon the source or process of origin. Consideration of a variety of sources is, however, beyond the scope of this paper. The following remarks, therefore, apply to only one major particulate emission *viz* fly ash emitted from coal fired power generating plants. Such emissions are of major current concern (Table I) and, with the probable increase in coal usage in future, can be expected to remain so for some years to come.

Ideally, one would like to determine the actual chemical compounds present in fly ash both as major matrix constituents and at trace levels. However, while determination of elemental composition is relatively straightforward, actual compound identification is often difficult even for matrix species (> 1% by weight) and, in many cases, may be virtually impossible for species present at trace levels. In general, identification of trace organics can be achieved by sophisticated chromatographic-mass spectroscopic combinations[4] but speciation of trace inorganics (which include many highly toxic compounds) is still a matter for research. Consequently most data on fly ash composition is presented in terms of elemental abundance.

The matrix elements present in fly ash are normally Si, Fe, Al, C, Ca, Na and K. Relative concentrations vary widely depending primarily on the type of coal burned as shown by

Bickelhaupt[5] who also lists the probable compounds present. It should be stressed that these compounds are almost certainly not the only ones containing so called matrix elements. For example, substantial mass fractions of fly ash are ferromagnetic; an attribute which cannot be due to Fe_2O_3. It is also worth pointing out that fly ash is an extremely heterogeneous material so that the composition of individual particles may differ dramatically from the average composition of an integrated sample.

At the trace level (> 1μg/gm) almost every element in the periodic table is found in fly ash as shown by the mass spectrographic analysis in Table II[6]. Again, the actual concentrations found can vary considerably (by as much as 1000 times) depending on coal type so the values in Table II are representative only. Indeed the trace levels in this particular sample are relatively low.

DEPENDENCE OF ELEMENTAL COMPOSITION ON PARTICLE SIZE

Probably the most important single characteristic of a particle which determines both its ability to elude conventional control equipment and its atmospheric residence time is aerodynamic particle size. Consequently it is important not only to know the chemical composition of bulk fly ash but also to know how this composition depends on particle size. This dependence was therefore determined in a number of fly ash samples representing a variety of

U. S. coal types. The results are presented for a single power plant equipped with cyclonic precipitators and utilizing a Southern Indiana coal.

Two types of sample are represented:

(a) Fly ash retained in the precipitating system. This was collected in bulk and size differentiated in the laboratory using a Roller particle size analyzer.

(b) Fly ash emitted to the atmosphere. This was collected and size differentiated *in situ*. using an Anderson Stack Sampler. No backup filter was used so particles less than about 0.5 μm were not retained. The sampling point was about ten feet from the base of the stack where the temperature of the gas stream was approximately 350°F (~ 175°C).

Analyses were performed by spark source mass spectrometry, DC arc emission spectrometry, X-ray fluorescence spectrometry, atomic absorption spectrometry, differential pulse anodic stripping voltammetry and by colorimetry using the Weisz Ring Oven[7]. With the exception of carbon and sulphur, all elements were determined by at least two distinct techniques. Procedural details are given elsewhere[8].

The twenty five elements determined are classified roughly into three groups. In Table III are listed those elements which showed convincing dependences of concentration (μg/gm) on particle size in all samples analyzed. Table IV contains those elements which exhibited concentration trends in some, but not all, samples. Table V lists those elements which showed no evidence of particle size dependences. Multiple analyses indicated that the apparently random variations which are superimposed on the size dependences are probably due to poor sampling statistics. These variations have not been removed by averaging the raw data which is presented for a single set of size fractions analyzed by a single technique. The sulphur concentrations are considered to be only qualitative due to difficulties in obtaining a standard having a matrix composition and sulphur distribution similar to that of fly ash. It should be noted that quantitative comparison of results obtained for fly ash retained in the plant and that leaving is not justified since the two sample types represent material collected over quite different integrated time periods.

SURFACE DISTRIBUTION HYPOTHESIS

The results presented in Tables III-V show that many highly toxic elements are most concentrated (on a μg/gm basis) in the smallest particles emitted. The reasons for this size dependence are obviously important both in terms of environmental impact and potential counteractive control strategy.

One attractive explanation is that certain elements, or their compounds, are volatilized in the coal combustion zone and then either adsorb or condense (possibly via a nucleation process) onto the surface of entrained particles composed of non volatilizable materials. The mass deposited is thus greater, per unit weight, for small particles than for large. Three pieces of evidence are presented in support of this tentative hypothesis.

1. All the elements (with the exception of Ni and Cr) in Table III have boiling points comparable to or below the temperature of the coal combustion zone (1300-1600°C) so would be capable of volatilizing. (This is also true for Ba, Sr, and Rb which show similar size dependences in fly ash.)[9] The statement implies that metal compounds can be reduced to the element before volatilization; however, while reduction in the combustion zone is certainly feasible, such reduction is not necessary to the basic hypothesis. Indeed, neither Ni nor Cr could exist as stable elemental vapors (Table VI). It is suggested that these elements may have access to the gas phase as sulphides or, conceivably, as highly transient carbonyls whose formation has been postulated.[10] Mercury, of course, is known to volatilize as the element and is predicted to show a dependence of concentration on particle size for that fraction associated with fly ash.

2. Consideration of a simple volatilization-surface deposition model for a single particle containing an element, X, present both uniformly within the particle matrix and deposited additionally on the particle surface leads to a relationship of the form.

$$\bar{C}_X = \bar{C}_O + 6\bar{C}_S \cdot \rho^{-1} \ D^{-1} \qquad (1)$$

$\bar{C}_X$ is the total average concentration of X (μg/gm) in a size fraction with mean particle diameter D and density ρ. $\bar{C}_O$ and $\bar{C}_S$ are, respectively, the average concentration of X in the particle interior and deposited on the particle surface. Data from Table III for As, Ni, and Cd are plotted according to this relationship (1) in Figure 1. It can be seen that within the sampling and analytical errors, Equation (1) provides sufficient description of the particle size dependence to offer support for the proposed mechanism. Furthermore, although there are too few data points to establish firm statistical relationships, correlation between elements is indicated at the 95% confidence level suggesting that the same mechanism applies for all elements listed in Table III.

3. If, indeed, the proposed surface deposition hypothesis is correct, one would expect elemental concentrations to be higher on the particle surface than in its interior. This has been found. Fly ash particles were etched with a stream of argon ions so as to expose the particle interior and then subjected to X-ray spectrometric analysis under a scanning electron microscope[9]. Of the metals listed in Table III only Zn, Cr and Ni were present in sufficient concentrations for detection by this analytical technique, however, these elements were found to be present only on the particle exterior as predicted.

While the foregoing results do not constitute scientific proof of the volatilization-surface deposition hypothesis they do offer considerable supporting evidence[10]. In any event, it seems probable that the observed dependences of element concentration on particle size are due to a surface phenomenon.

If, in fact, the volatilization-surface deposition hypothesis is correct one would expect particle size dependences to be exhibited by any species capable of being volatilized by a high temperature combustion process and then retained in some fashion (eg adsorption, condensation, reaction) on a solid surface. Indeed, the process could well persist in the atmosphere. In this connection it is noteworthy that many species whose boiling points lie in the 100 - 400°C range are thermodynamically capable of existing in significant concentrations in the vapor phase at much lower temperatures once volatilized. For example, thermodynamic data[11] show that SeO_2 and As_2O_3 can exist in the vapor at 25°C up to concentrations as high as 80μg/m^3 of Se and 70μg/m^3 of As. The effect is even more pronounced for organic species. Consequently the exposure time of these vapors to particulate matter need not be limited to the period during which a molecule is at a temperature greater than its boiling point.

One might expect, therefore, to find many highly toxic organic species (eg the polyaromatic hydrocarbons) present at highest concentrations in the smallest fly ash particles. Indeed the size dependence should be very pronounced since τ_0 in Equation (1) should be small due to the low boiling points of organic compounds. No direct evidence in support of these suggestions exists although measurements of the dependence of hydrocarbon concentrations on particle size[12-14] in the Los Angeles aerosol do conform to Equation (1). Since organics present in fly ash may very well be responsible for health effects[15] their possible preponderance in small respirable particles emitted from stationary sources should be seriously investigated.

SIGNIFICANCE OF SIZE DEPENDENCES

Preferential concentration of certain species in the smallest emitted fly ash particles is of significance for the following reasons:

1. Control

The results in Table III show that existing control devices, whose efficiency falls off[16] below about 1μm, are least effective for collecting those particles containing the highest concentrations of undesirable species. Furthermore, existing control legislation, which specifies the total particulate mass which may be emitted, is least stringent for the most undesirable material. The data further indicate that estimates of toxic emissions which are based on analyses of fly ash retained in the plant, can be expected to be 10 to 20 times too low for many elements of interest.

2. Atmospheric Enrichment

The residence time of a particle in the atmosphere depends upon its effective aerodynamic size. Consequently, those elements which predominate in small particles can be expected to remain in the atmosphere longer than others which are not preferentially distributed with respect to size. One would therefore expect marked enrichment of the elements in Table III (and possibly some of those in Table IV) in urban aerosols when compared with crustal dusts. This is indeed found[17,18] in that the elements Zn, Ni, As, Cd, Sb, Pb, Se, S, Sn, Na, Cl and Br are enriched by at least 1000 times when normalized to Al. It should be noted that particles derived from any combustion source (eg. cement kilns, municipal incinerators, metal smelters and blast furnaces) should preferentially concentrate certain elements with decreasing particle size. The particular elements will vary with source depending on its operating temperature.

3. Health Effects

Probably the most important consequence of the observed elemental size dependences in fly ash is that many toxic elements, and probably organic species, are most concentrated in particles which will deposit in the human respiratory system[19,20]. The actual region of deposition depends markedly on particle size as illustrated in Figure 2. Furthermore, the potential health impact of toxic species present in retained particles depends upon the region of deposition[21]. Thus, particles deposited in the naso-pharyngeal and tracheobronchial regions of the respiratory tract are normally removed quite rapidly to the pharynx, often by cilial action,[22] and swallowed within a matter of hours. Consequently, extraction of toxic species from these particles takes place predominantly in the stomach where residence time is short. On the other hand, particles deposited in the pulmonary region may remain there for weeks or even years[23] in intimate contact with approximately 30 m^3 of alveolar membrane which separates the bloodstream from inhaled air.[19] The net result is that many species are extracted much more efficiently in the pulmonary region than in the stomach. For example only 5-15% of the lead present is extracted from particles in the stomach whereas in the lung the corresponding efficiency[24,25] is 60-80%.

The foregoing remarks make it clear that toxic species present in particles which can be deposited in the pulmonary region of the lung will have a much greater potential for producing adverse health effects than if the same particles were deposited earlier in the respiratory tract. Consequently those species having an equivalent mass median diameter of a micrometer or less constitute the greatest health hazard. The influence of preferential surface deposition of toxic species on small particles can be demonstrated quantitatively if the total particle mass emitted from a power plant, for example, is assumed to be log-normally distributed with respect to particle size. (This assumption is reasonable in many cases). Thus, the mass, M, in a given size fraction of mean particle diameter, D, is given by the normalized expression

$$\frac{dM}{d(\ln D)} = \frac{1}{\sqrt{2\pi}\,\ln\sigma_g} \cdot \exp\left[-1/2\,\frac{(\ln D/D_g)^2}{(\ln\sigma_g)^2}\right] \qquad (2)$$

where σ_g is the geometric standard deviation of the size distribution and D_g is its equivalent mass median diameter.

If all chemical species were equally distributed in concentration (in μg/gm) and showed no particle size dependence then all would have the same mass median diameter, D_g. However, if some species are subject to surface deposition according to Equation (1) then the mass distribution of a species, X, is obtained by combining Equations (1) and (2) to give[21].

$$\frac{dM_X}{d(\ln D)} = \frac{1}{\sqrt{2\pi}\,\ln\sigma_g}\left\{\bar{C}_0 \cdot \exp\left[-1/2\;\frac{(\ln D/D_g)^2}{(\ln\sigma_g)^2}\right]\right.$$

$$\left. + \bar{C}_S \exp\left[1/2\;\ln^2\sigma_g\right] \cdot \exp\left[-\;\frac{(\ln D/D_g + \ln^2\sigma_g)^2}{2(\ln\sigma_g)^2}\right]\right\} \qquad (3)$$

Here D_g and σ_g refer to the distribution of the substrate particles as in Equation (2) and $\bar{C}_0$ and $\bar{C}_S$ are as defined for Equation (2). Equation (3) is not normalized.

Extraction of an explicit expression for the mass median diameter of X, $D_g(x)$ from Equation (3) is tedious, however, in the case where $\bar{C}_0 << \bar{C}_S$ (ie most of X is present on the surface as expected for an organic species) it can readily be shown that[26]

$$\ln D_g(X) = \ln D_g - \ln^2\sigma_g \qquad (4)$$

This equation (3) demonstrates the profound effect of surface deposition of a species X in reducing its effective mass median diameter even though that of the substrate particles is unaltered. For example[21] if the total mass distribution emitted has $D_g = 2.7$ μm and $\sigma_g = 2.9$ μm the data for Zn in Table III, when incorporated into Equation (3), show that Zn has a mass median diameter of approximately 1 μm. Similarly, an organic species distributed such that $\bar{C}_0 << \bar{C}_S$ would have a mass median diameter < 0.1 μm.

POSSIBLE PROTOCOL FOR DETERMINING PARTICULATE TOXICITY

Just because a toxic species may be present in particles emitted to the atmosphere does not necessarily imply that this species will have an adverse health effect when inhaled. Before this can be established the following factors must be considered.

(a) The mass distribution of the species, X, emitted.

(b) The contribution of this distribution to that inhaled. (From the standpoint of environmental health the inhalable distribution is an essentially stable urban aerosol. Occupational health considerations will involve a more localized distribution).

(c) The particle size deposition profile in the respiratory tract.

(d) The efficiency of transport of X from particle to target organ or molecule as a function of particle size. This factor can be subdivided in terms of

(i) Particle clearance rate

(ii) Extraction rate of X

(iii) Elimination rate of X

(iv) Rate of transport of X to target

(e) The effective toxicity of X at a target site.

At first sight quantitative evaluation of (a) through (e) seems a formidable and barely worthwhile task. However, such a protocol can be greatly simplified by recognizing that the data required for (d) and (e) can be determined directly by bioassay in which the appropriate particle size distribution of all X is presented for inhalation. (Determination of the toxicity of fly ash to bacteria or tissue cultures has little merit in this context). (a) can be determined experimentally and recent work[27] has shown that step (b) can be mathematically modelled surprisingly well for contributions to an urban aerosol.

As an example of the utility of this type of approach consider the case of an urban aerosol for which D_g and σ_g have been experimentally determined for the total mass, and for Fe, Zn, Pb, and the carcinogen Benzo-a-pyrene.[28,29] (Table VII). Assuming a log-normal distribution of these species (a bimodal distribution with two log-normal components is more realistic) the deposition efficiency, E, in Figure 2 can be incorporated into Equation 2 such that

$$\left[\frac{dM}{d(\log D)}\right]_{\text{deposited}} = 2{\cdot}303\ E \left[\frac{dM}{d(\ln D)}\right]_{\text{inhaled}} \qquad (5)$$

Equation (5), with appropriate experimental parameters from Table VII, thus describes the retention of inhaled species in each respiratory region and has been used to generate Figures 3, 4, 5 6 and 7 which show the retention of total aerosol mass, Fe, Zn, Pb and Benzo-a-pyrene. The fractions of inhaled mass retained in each region are presented in Table VIII.

It is possible to go one stage further and include (d) (i), (ii) and (iii) in the case of lead whose efficiency of extraction into the blood stream is 60-80% in the pulmonary region and 5-15% in the stomach.[24,25] Assuming mean values of

70% and 10% the data in Table VIII show that 22% of the total inhaled lead enters the bloodstream by absorption through pulmonary membranes while only 2.3% enters from the stomach. Based on these figures an average adult inhaling 20 m^3 of air per day containing 2μg/m^3 of lead (a typical urban aerosol loading) would absorb 10 μg of lead per day. Absorption from food and water amounts to about 30 μg per day.[23,30] Recent Pb isotope labelling studies[31] indicate that approximately 30% of the daily lead intake comes from inhaled aerosols; a figure which is considered to be in excellent agreement with that estimated using the partial protocol.

Obviously considerable information is required before such a protocol could be used to assess the effective toxicity of a given source emission. However, it is clear that this procedure can easily include the collective influence of a variety of both known and unknown toxic species and their synergisms. Insofar as it provides at least a semiquantitative basis for establishing the environmental health significance of chemical species present inurban aerosols and emission sources its importance in terms of source control strategy is clear.

CHEMISTRY AND CONTROL PROCESSES

The foregoing sections have presented information relating to the chemical composition of fly ash, the possible processes which establish trace element distribution, and the significance of this distribution in terms of control, environmental perturbation, and health. They have illustrated the suggestion that more emphasis should be placed on controlling undesirable particles and less on controlling particles *per se*. However a knowledge of the chemistry of particles and of particle production can assist not only in delineating the least desirable particle fractions but also in indicating possible new methodology for control. The following examples illustrate how such a principle might be realized in practice. It should be strongly stressed that the examples are primarily illustrative and do not, at this time, constitute practical propositions.

1. Preliminary studies have shown that substantial fractions of most coal flyashes are ferromagnetic and that even higher proportions of many toxic species are associated with this magnetic fraction. In view of the recent advances made in magnetic collection the possibility of employing magnetic collection for preferential collection of toxic particulates is viable.[34] Before such a process could be considered, however, the relationships of toxic species to the ferromagnetic fraction must be established.

2. If many toxic species are, indeed, preferentially concentrated in small particles by surface deposition it may be possible to provide an alternative surface for deposition. For example entrainment of activated carbon particles and fly ash through cadmium vapor produces highly preferential association of Cd with the large, easily collected, carbon particles[32].

Carbon may have an additional advantage in that recent work[33] has indicated it to be extremely active in catalyzing the formation of solid sulphate from gaseous SO_2. Certainly adsorption of volatile organics is entirely feasible. Alternatively, injection of magnetic Fe_3O_4 particles may provide a suitable surface for preferential deposition. In essence such a procedure would take advantage of the volatilization--deposition of toxic species to increase their effective mass median diameter to a range which can be more efficiently collected by existing, or future, control equipment.

3. A similar preconditioning process can be envisaged for increasing the resistivity of certain fly ashes to a level at which more efficient electrostatic collection can be achieved. In principle, at least, modification of combustion chemistry or subsequent chemical conditioning could be employed to reduce the surface concentrations of Na and Li which appear to be responsible for electrical conduction in fly ash.

PROTOCOL FOR CHEMICAL CHARACTERIZATION

In none of the examples cited above is sufficient basic information available to assess even their potential feasibility. This amply demonstrates the need for a deeper chemical understanding of fly ash and its production. Although a number of independent studies have been, and are being, conducted the tremendous variability of fly ashes makes it very difficult to correlate results. It is considered vitally important, therefore, that a coherent investigational protocol be developed for the chemical and physical characterization of a single fly ash sample. Having established parameters of major interest these can then be effectively and efficiently investigated in other samples.

Such a protocol, which is being followed in our laboratory, is presented in the form of an experimental matrix, in Table IX. The fly ash is physically separated into fractions on the basis of aerodynamic particle size, ferromagnetism, particle density and solubility all of which differentiate material having different chemical composition, physical properties and practical significance. Each fraction is then processed to obtain, where possible, the parameters listed. Completion of such a matrix is clearly a major undertaking. However it is considered that this type of approach provides the most efficient and coherent method for obtaining basic data relating to existing and potential control methods for the most environmentally significant fractions of coal fly ash.

CONCLUSION

Particulate control processes have improved considerably over the last few decades to the stage where further improvement necessitates consideration of more and more subtle parameters. On the one hand it is appropriate to assess the justifications for more stringent control very seriously; on the other it is necessary to seek ways of improving collection, of reducing costs, and of accomodating to new processes and fuels resulting from a changing energy production profile. In all cases practical considerations require a much better understanding of of the chemistry of particulates from their production to their eventual removal to an environmental sink.

REFERENCES

1. W.R. Crouse, G.D. Aase, H.C. Johnson, J.D. Coons and J.E. Yocom, J. Air Pollution Control Assoc. 10, 285 (1960).

2. R.E. Lee and S. Goranson, Environ. Sci. Technol., 6, 1019 (1972).

3. W. J. Moroz and V. Withstandly, paper presented to 66th Annual A.I.Ch.E. Meeting, Philadelphia, November 1973.

4. R.C. Las, R.S. Thomas, H. Oja and L. Dubois, Anal. Chem., 45, 909 (1973).

5. R.E. Bickelhaupt, paper presented to US-USSR Working Group Symposium on Control of Fine Particulate Emissions from Industrial Sources, San Francisco, January 1974. (Included in these Proceedings)

6. R. Brown, M.L. Jacobs and H.E. Taylor, American Laboratory, 29, (November 1972).

7. H.H. Weisz, "Microanalysis by the Ring Oven Technique", Pergamon Press, N.Y., 1961.

8. R.L. Davison, D.F.S. Natusch, J.R. Wallace and C.A. Evans, Environ. Sci. Technol. (in press).

9. Sparks, Oak Ridge National Laboratory (personal communication).

10. D.F.S. Natusch, J.R. Wallace and C.A. Evans, SCIENCE, 183, 202 (1974).

11. Handbook of Chemistry and Physics, 44th ed., The Chemical Rubber Publishing Co., Cleveland, Ohio pp. 2430-2445 (1963).

12. P.K. Mueller, R.W. Mosely, L.B. Price, J. Colloid Interface Sci., 39, 235 (1972).

13. S.L. Heisler, S.K. Friedlander, R.B. Husar, Atmos. Environ., 7, 633 (1973).

14. R.B. Husar, and K.T. Whitky, Environ. Sci. Technol. 7, 241 (1973).

15. H.R. Menck, J.T. Casagrande and B.E. Henderson, SCIENCE, 183, 210 (1974).

16. G.B. Nichols, paper presented to US-USSR Working Group Symposium on Control of Fine Particulate Emissions from Industrial Sources, San Francisco, January 1974 (Included in these Proceedings)

17. G.E. Gordon and W.H. Zoller, paper presented to Oak Ridge Trace Elements Conference, Oak Ridge, Tennessee, August 1973.

18. K.A. Rahn, M. Demuynck, R. Dams and J. Degraeve, Proc. Third International Clean Air Congress, Dusseldorf, Germany, 1973, C81.

19. T.F. Hatch and P. Gross, "Pulmonary Deposition and Retention of Inhaled Aerosols," Academic Press, N.Y., 1964.

20. U.S. Dept. of H.E.W., National Air Pollution Control Board, Pub. No. A849, "Air Quality Criteria for Particulate Matter," Washington D.C., January 1969.

21. D.F.S. Natusch and J.R. Wallace, SCIENCE (in press).

22. H.A. Schroeder, Environment, 13, 18 (1971).

23. P.E. Morrow, Ind. Hyg. Assoc. J., 25, 213 (1965).

24. L. Dautreband, "Microaerosols," Academic Press, N.Y., 1962.

25. C.C. Patterson, Arch. Environ. Health, 11, 344 (1965).

26. S.S. Butcher and R.J. Charlson, "An Introduction to Air Chemistry," Academic Press, N.Y. 1972 (Chapter 9).

27. S.K. Friedlander, Proc. Third International Clean Air Congress, Dusseldorf, Germany, 1973, C78.

28. R.E. Lee, SCIENCE, 178, 567 (1972).

29. M. Kertesz-Saringer, E. Meszaros and T. Varkonyi, Atmos. Environ., 5, 429 (1971).

30. G. Nagelschmidt, E.S. Nelson, E.J. King, D. Atygalle and M. Yoganathan, A.M.A. Arch. Ind. Health, 16, 188 (1957).

31. G. Wetherill, M. Rabinowitz and J. Kopple, SCIENCE (in press).

32. D.F.S. Natusch, Unpublished results.

33. T. Novakov, Lawrence Berkeley Laboratory, personal comcunication.

34. Chemical and Engineering News, Jan. 28th (1974) page 21.

ACKNOWLEDGEMENTS

The assistance of Dr. C. A. Evans, Materials Research Laboratory, University of Illinois, Mr. J. Kuhn, Illinois State Geological Survey, and Mr. R. Fry, Environmental Analytical Laboratory, University of Illinois, in performing some of the analyses reported herein is gratefully acknowledged. Stimulating discussions with Professor G.E. Gordon, Dr. W. Fulkerson, Dr. T. Novakov, Dr. C.A. Evans and with the author's research group are also acknowledged.

The original work reported was supported in part by N.S.F. grants GI 31605 and GH 33634.

TABLE 1

NATIONWIDE ESTIMATES OF PARTICULATE EMISSIONS 1940 - 1970

(10^6 tons/year)

Source Category	1940	1950	1960	1968	1969	1970
Fuel combustion in stationary sources	9.6	9.0	7.6	6.5	6.4	6.8
Transportation	0.4	0.4	0.5	0.8	0.7	0.7
Solid waste disposal	0.4	0.6	1.0	1.4	1.4	1.4
Industrial process losses	8.8	10.8	11.9	13.8	14.3	13.3
Agricultural burning	1.6	1.8	2.1	2.4	2.4	2.4
Miscellaneous	6.4	3.3	2.1	1.7	2.1	1.0
Total	27.1	25.9	25.3	26.6	27.3	25.6
Total controllable[a]	20.7	22.6	23.2	24.9	25.2	24.6

[a] Miscellaneous sources not included

Reference: Nationwide Inventory of Air Pollutant Emission Trends 1940 - 1970 U.S. E.P.A.

TABLE II

Typical trace element analysis of fly ash, concentration, in μg/gm.

Element	Conc.	Element	Conc.	Element	Conc.
Thorium	40	Lanthanum	40	Copper	200
Uranium	30	Barium	2400	Nickel	50
Bismuth	0.50	Cesium	20	Cobalt	7.0
Lead	60	Iodine	0.20	Iron	Major
Thallium	0.8	Tellurium	0.20	Manganese	400
Mercury	<0.01	Antimony	4.5	Chromium	110
Tungsten	6.0	Tin	60	Vanadium	50
Tantalum	0.50	Cadmium	0.70	Titanium	1600
Hafnium	9.0	Silver	0.50	Scandium	3.7
Lutetium	0.50	Molybdenum	36	Calcium	Major
Ytterbium	5.5	Niobium	60	Potassium	7000
Thulium	3.0	Zirconium	300	Chlorine	420
Erbium	3.4	Yttrium	100	Sulfur	Major
Holmium	1.2	Strontium	2000	Phosphorus	8000
Dysprosium	7.0	Rudidium	140	Silicon	Major
Terbium	2.3	Bromine	0.70	Aluminum	Major
Gadolinium	13	Selenium	0.30	Magnesium	Major
Europium	3.0	Arsenic	22	Sodium	Major
Samarium	11	Germanium	2.4	Fluorine	150
Neodymium	55	Gallium	20	Boron	230
Praseodymium	38	Zinc	260	Beryllium	8.0
Cerium	100			Lithium	42

TABLE III
Elements showing pronounced Concentration trends

Particle diameter (μm)	Pb	Tl	Sb	Cd	Se	As	Ni	Cr	Zn	S	Mass fraction (%)
	μg/g									(wt%)	
A. Fly ash retained in the plant											
Sieved fractions											
>74	140	7	1.5	<10	<12	180	100	100	500	----	66.30
44-74	160	9	7	<10	<20	500	140	90	411	1.3	22.89
Aerodynamically sized fractions											
>40	90	5	8	<10	<15	120	300	70	730	<0.01	2.50
30-40	300	5	9	<10	<15	160	130	140	570	0.01	3.54
20-30	430	9	8	<10	<15	200	160	150	480	----	3.25
15-20	520	12	19	<10	<30	300	200	170	720	----	0.80
10-15	430	15	12	<10	<30	400	210	170	770	4.4	0.31
5-10	820	20	25	<10	<50	800	230	160	1100	7.8	0.33
<5	980	45	31	< 10	< 50	370	260	130	1400	----	.08
Analytical method	b	b	b	b	b	b	d	d	b	c	
B. Airborne fly ash											
>11.3	1100	29	17	13	13	680	460	740	8100	8.3	
7.3-11.3	1200	40	27	15	11	800	400	290	9000	---	
4.7-7.3	1500	62	34	18	16	1000	440	460	6600	7.9	
3.3-4.7	1550	67	34	22	16	900	540	470	3800	---	
2.1-3.3	1500	65	37	26	19	1200	900	1500	15000	25.0	
1.1-2.1	1600	76	53	35	59	1700	1600	3300	13000	---	
0.65-1.1	--	--	--	--	--	--	--	--	--	48.8	
Analytical method	a	b	b	a	a	a	a	a	b	c	

(a) Atomic Absorption Spectrometry

(b) Spark Source Mass Spectrometry

(c) X-ray Fluorescence Spectrometry

(d) DC Arc Emission Spectrometry

TABLE IV

Elements showing limited concentration trends

Particle diameter (um)	Fe (wt %)	Mn (µg/g)	Si (wt %)	Mg (wt %)	C (wt %)	Be (µg/g)	Al (wt %)
A. Precipated at base of stack							
Sieved fractions							
>74	--	700	--	--	--	12	--
44-74	18	600	18	.39	--	12	9.4
Aerodynamically sized fractions							
>40	50	150	3.0	.02	.12	7.5	1.3
30-40	18	630	14	.31	.21	18	6.9
20-30	--	270	--	--	.63	21	--
15-20	--	210	--	--	2.5	22	--
10-15	6.6	160	19	.16	6.6	22	9.8
5-10	8.6	210	26	.39	5.5	24	13
<5	--	180	--	--	--	24	--
Analytical method	c	d	c	c	e	d	c
B. Airborne material							
>11.3	13	150	34	.89	.66	34	19.7
7.3-11.3	--	210	--	--	.70	40	--
4.7-7.3	12	230	27	.95	.62	32	16.2
3.3-4.7	--	200	--	--	.57	55	--
2.06-3.3	17	240	35	1.4	.81	43	21.0
1.06-2.06	--	470	--	--	.61	60	--
.65-1.06	15	--	23	.19	--	--	9.8
Analytical method	c	d	c	c	e	d	c

(a) Atomic Absorption

(b) Spark Source Mass Spectrometry

(c) X-ray Fluorescence Spectrometry

(d) DC Arc Emission Spectrometry

(e) Oxygen Fusion

TABLE V

Showing no concentration trends

Particle diameter (µm)	Bi (µg/g)	Sn (µg/g)	Cu (µg/g)	Co (µg/g)	V (µg/g)	Ti (wt %)	Ca (wt %)	K (wt %)
				A. Fly ash retained in plant				
Sieved fractions								
>74	>2	>2	120	28	150	--	--	--
44-74	>2	>2	260	27	260	.61	5.4	1.2
Aerodynamically sized								
>40	>2	>2	220	75	250	.01	2.5	2.54
30-40	>2	>2	120	76	190	.64	6.3	6.26
20-30	>2	>2	160	55	340	--	--	--
15-20	>2	>2	220	50	320	--	4.5	4.46
10-15	>2	>2	220	55	320	.66	4.0	4.04
5-10	>2	>2	390	46	330	1.09	--	--
>5	>2	>2	490	54	320	--	--	--
				B. Airborne material				
>11.3	>1.7	7	270	60	150	1.12	4.9	4.9
7.3-11.3	>3.5	11	390	85	240	--	--	--
4.7-7.3	>4.0	18	380	90	420	.92	4.2	4.2
3.3-4.7	>4.8	19	--	95	230	--	--	--
2.06-3.3	>4.5	16	330	90	310	1.59	5.0	5.0
1.06-2.06	>4.4	18	300	130	480	--	--	
.65-1.06	--	--	--	--	--	1.08	2.6	2.6
Analytical method	b	b	b	d	b	c	c	c

(b) Spark Source Mass Spectrometry

(c) X-ray Fluorescence Spectrometry

(d) DC Arc Emission Spectrometry

TABLE VI

Boiling points of possible inorganic species evolved during coal combustion

Species boiling or subliming ≤ 1550°C	Species boiling or subliming > 1550°C
As, As_2O_5, As_2O_3, As_2S_3	Al, Al_2O_3
Ba	Be, BeO
Bi	Bi_2O_3
Ca	C
Cd, CdO, CdS	CaO
$Cr(CO)_6$, $CrCl_3$, CrS(1550)	Co, CoO, CoS
K	Cr, Cr_2O_3
Mg	Cu, CuO
$Ni(CO)_4$	Fe, Fe_2O_3, Fe_3O_4, FeO
Pb	MgO, MgS
Rb	Mn, MnO, MnO_2
S	Ni, NiO
Se, SeO_2, SeO_3	Si, SiO_2
Sb, Sb_2S_3, Sb_2O_3(1550)	Sn, SnO_2
SnS	Ti, TiO_2, TiO
Sr	U, UO_2
Zn, ZnS	
Tl, Tl_2O, Tl_2O_3	

TABLE VII

Typical Size Parameters of Urban Aercsol Components

Species	Mass Median Diameter (μm)	Deviation	Reference	Comment
Total mass	.6	7.0	28	Year Average for 6 Eastern U.S. Cities
Fe	2.7	2.9	28	" "
Pb	.56	4.1	28	" "
Zn	1.03	2.06	28	Year Average for Chicago
Ba	1.95	3.54	28	Denver Quarterly Average
Noncarbonate Carbon	.6	-	12	Los Angeles Photo-Chemical Smog, 90% < .6 μm
Benzo-a-pyrene	.15	-	29	Budapest
SO_4^{-}	.45	7.8	21	Week Average for Cincinnati

TABLE VIII

Percent Deposition of Inhaled Aerosols.
Size distribution parameters are listed
in Table I.

Species	Nasopharyngeal %	Tracheobronchial %	Pulmonary %
Total mass	23	6	30
Fe	48	7	22
Pb	17	6	32
Benzo-a-pyrene	5	7	39

Separation Procedure	Bulk	Aerodynamic Sizes	Magnetic Separation	Density Separation	Solubility Separation	
Particle Density						
Particle Morphology						
Particle Size Distribution						
B.E.T. Surface Area						
Resistivity						
Magnetic Susceptibility						
Matrix Elements						
Matrix Compounds						
Trace Elements						
Trace Compounds						
Volatilizable Organics						
Extractable Organics						
Reversible Adsorption						
Irreversible Adsorption						
Surface Characterization						
D.T.A.						
Anions						
Natural and Biological Extraction						

TABLE IX
Investigational Matrix
for particles

Figure Captions

Figure 1.	Dependence of the average concentrations of As, Ni and Cd on airborne particle size in coal fly ash.
Figure 2.	Respiratory deposition profiles for inhaled particles[20].
Figure 3.	Respiratory deposition efficiency of particle mass a typical urban aerosol.
Figure 4.	Respiratory deposition efficiency of iron in an urban aerosol.
Figure 5.	Respiratory deposition efficiency of zinc in an urban aerosol.
Figure 6.	Respiratory deposition efficiency of lead in an urban aerosol.
Figure 7.	Respiratory deposition efficiency of benzo-a-pyrene in an urban aerosol. (A typical value of $\sigma_g = 3.0$ was assumed since no experimental values were available).

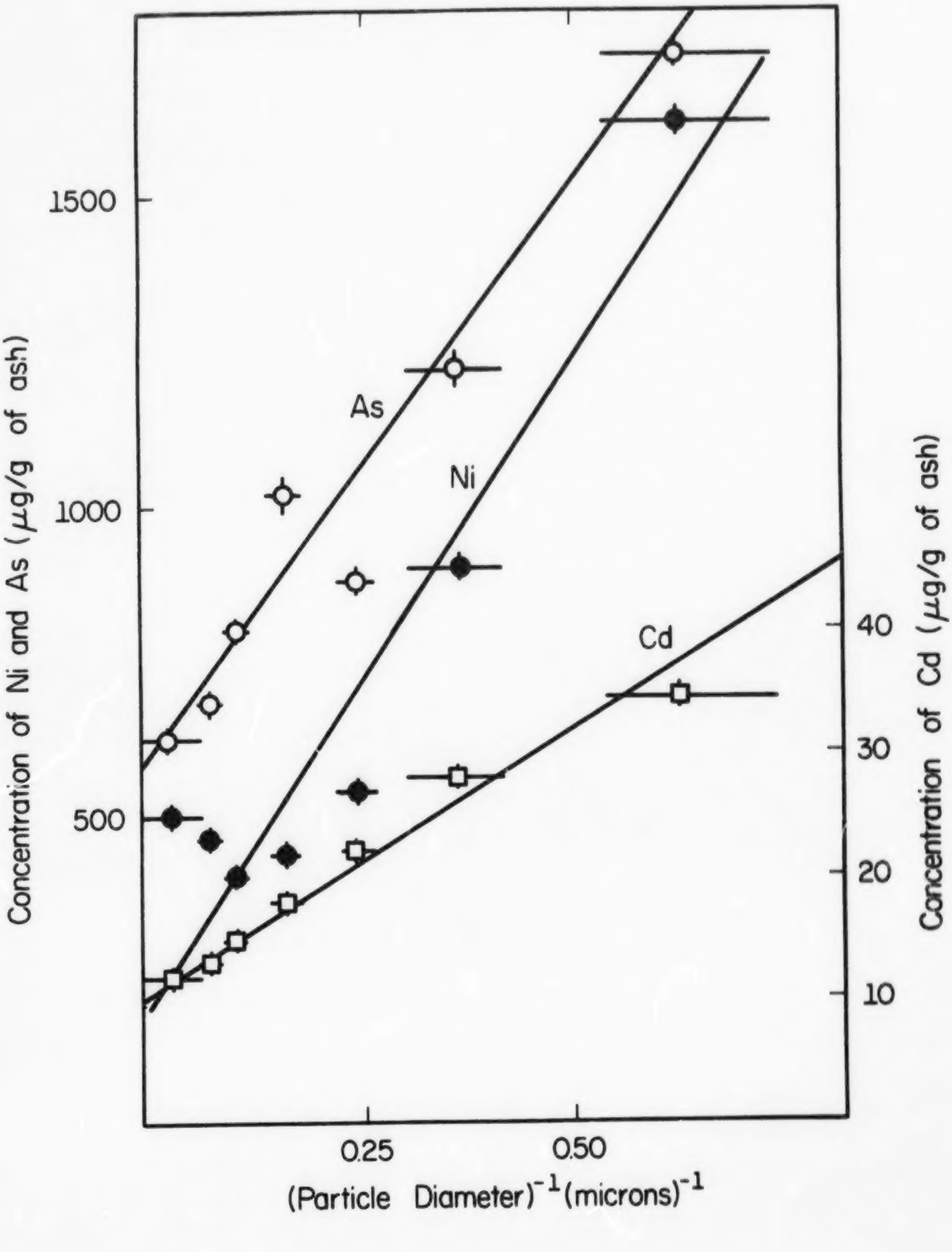

Concentration of Ni and As (μg/g of ash)
1500
1000
500
As
Ni
Cd
Concentration of Cd (μg/g of ash)
40
30
20
10
0.25
0.50
(Particle Diameter)⁻¹(microns)⁻¹

Figure 1.

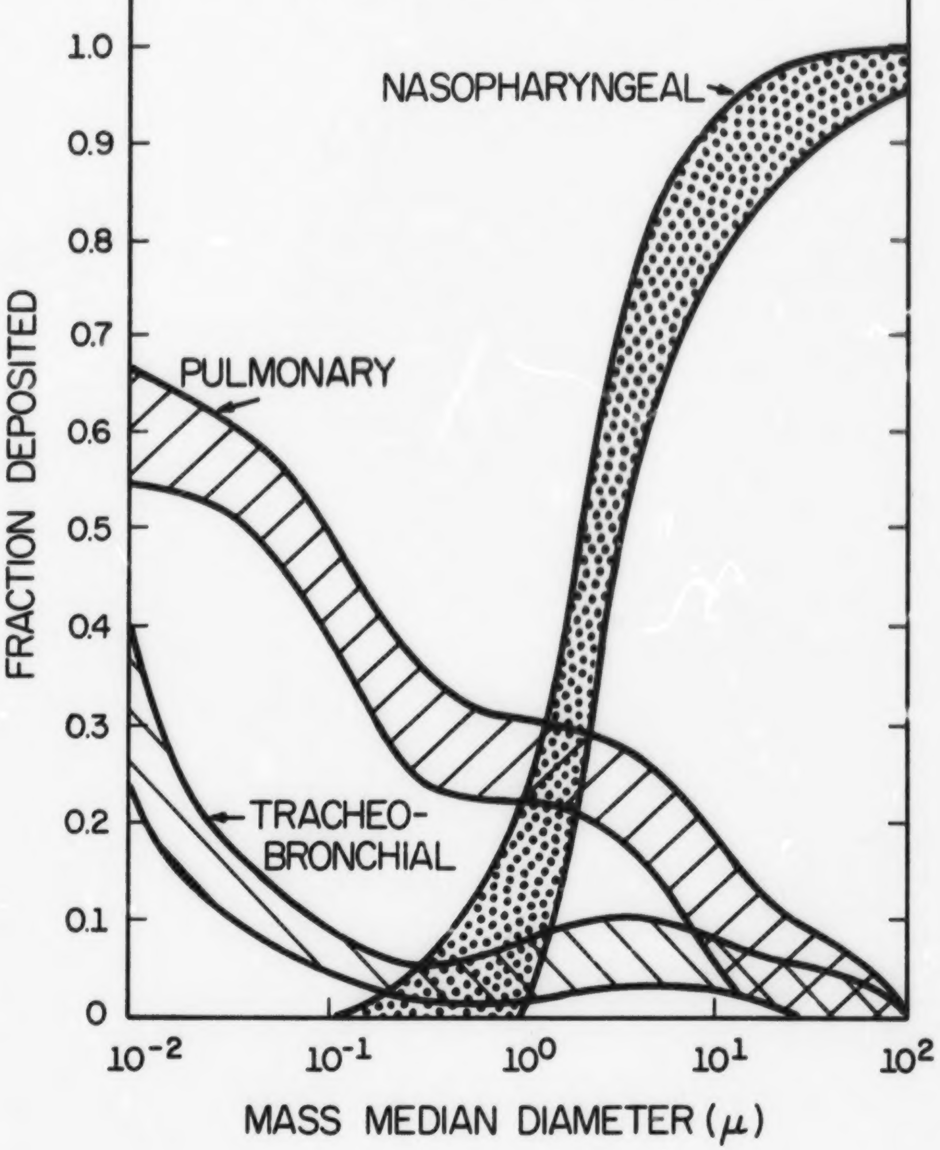
1.0
0.9
0.8
0.7
0.6
0.5
0.4
0.3
0.2
0.1
0
FRACTION DEPOSITED
NASOPHARYNGEAL
PULMONARY
TRACHEO-
BRONCHIAL
10^{-2}
10^{-1}
10^{0}
10^{1}
10^{2}
MASS MEDIAN DIAMETER (μ)

Figure 2.

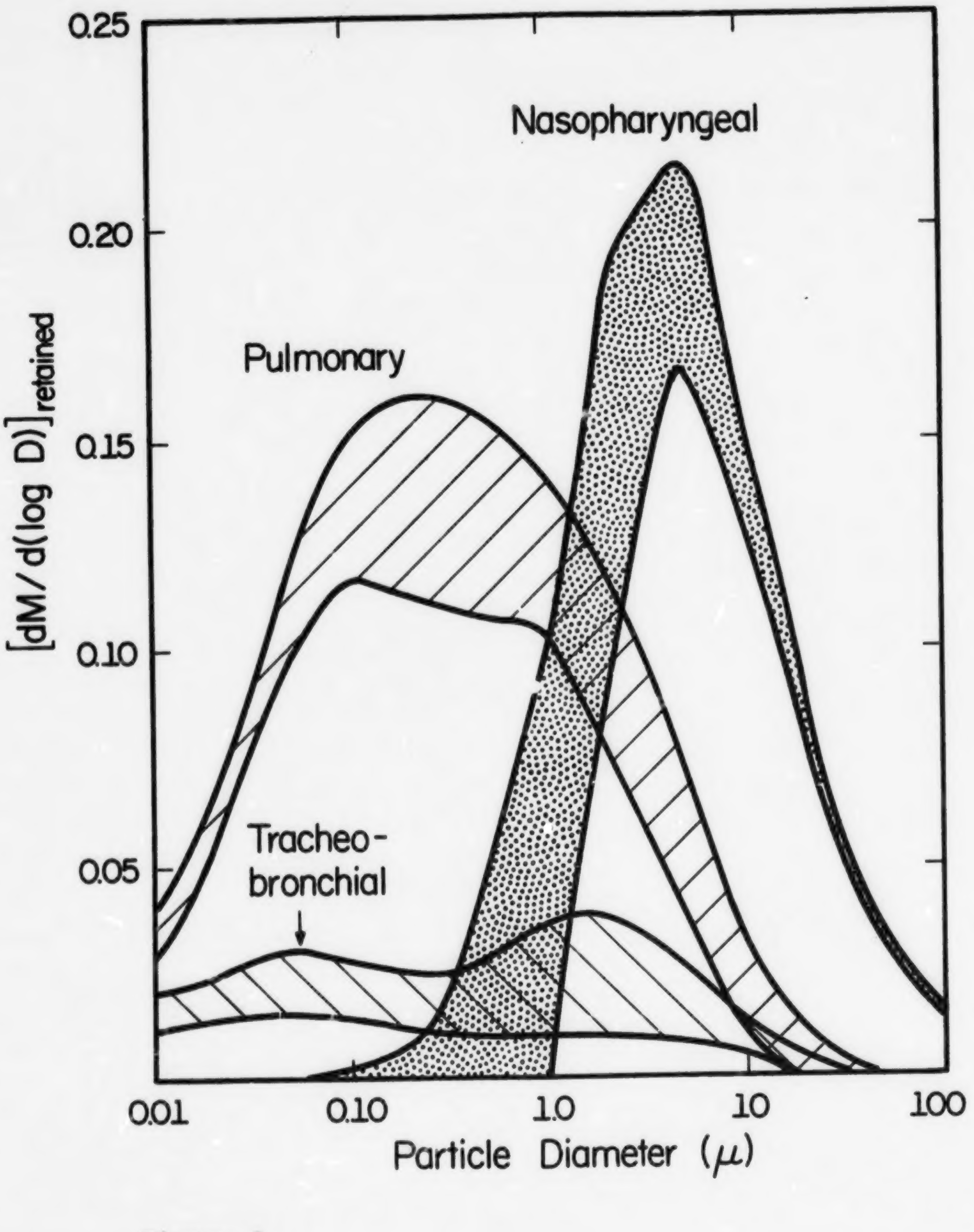
0.25
0.20
0.15
0.10
0.05
[dM/d(log D)]$_{retained}$
Nasopharyngeal
Pulmonary
Tracheo-
bronchial
0.01
0.10
1.0
10
100
Particle Diameter (μ)

Figure 3.

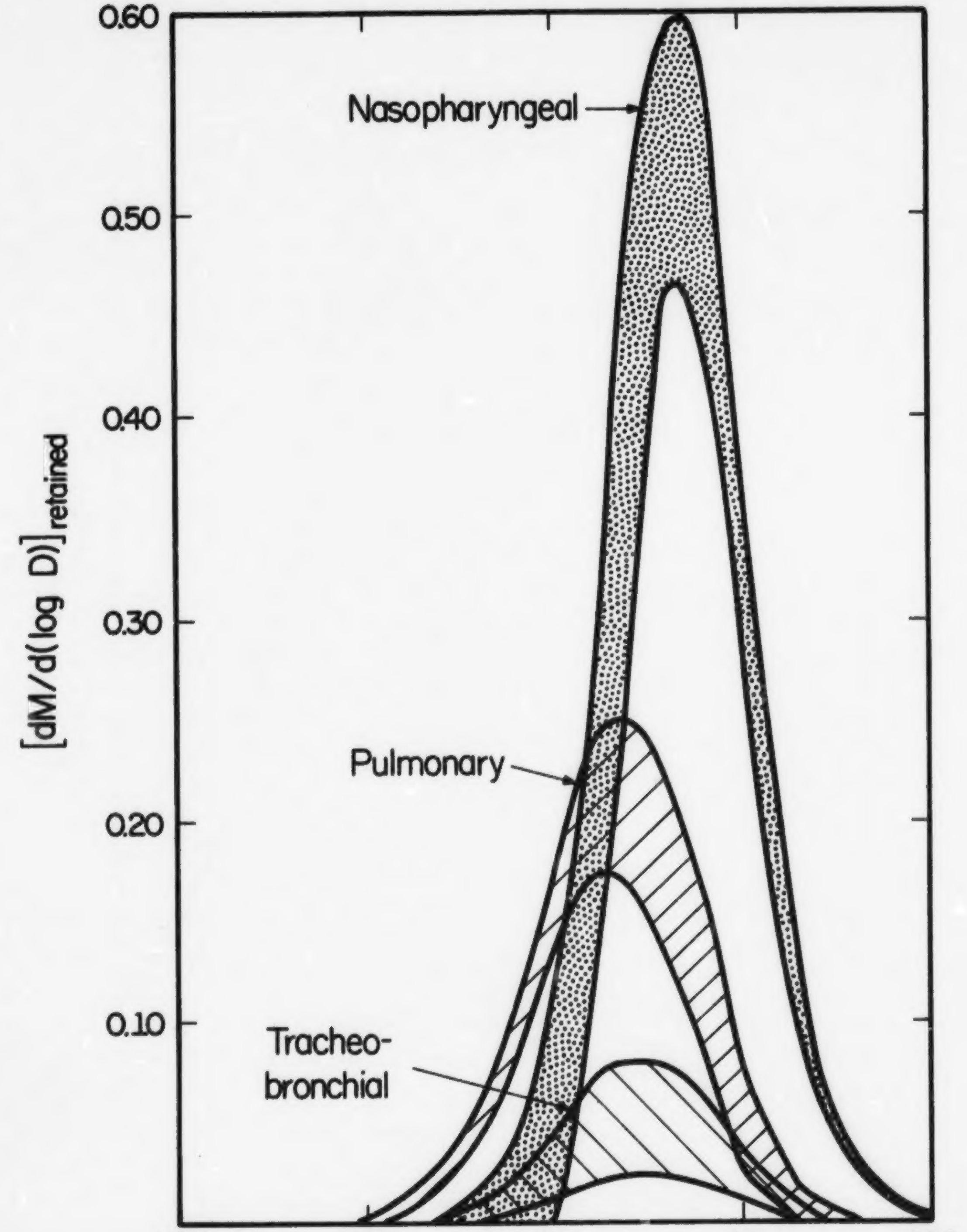
0.60
0.50
0.40
0.30
0.20
0.10
[dM/d(log D)]retained
Nasopharyngeal
Pulmonary
Tracheo-
bronchial
0.01
0.10
1.0
10
100
Particle Diameter (μ)

Figure 4.

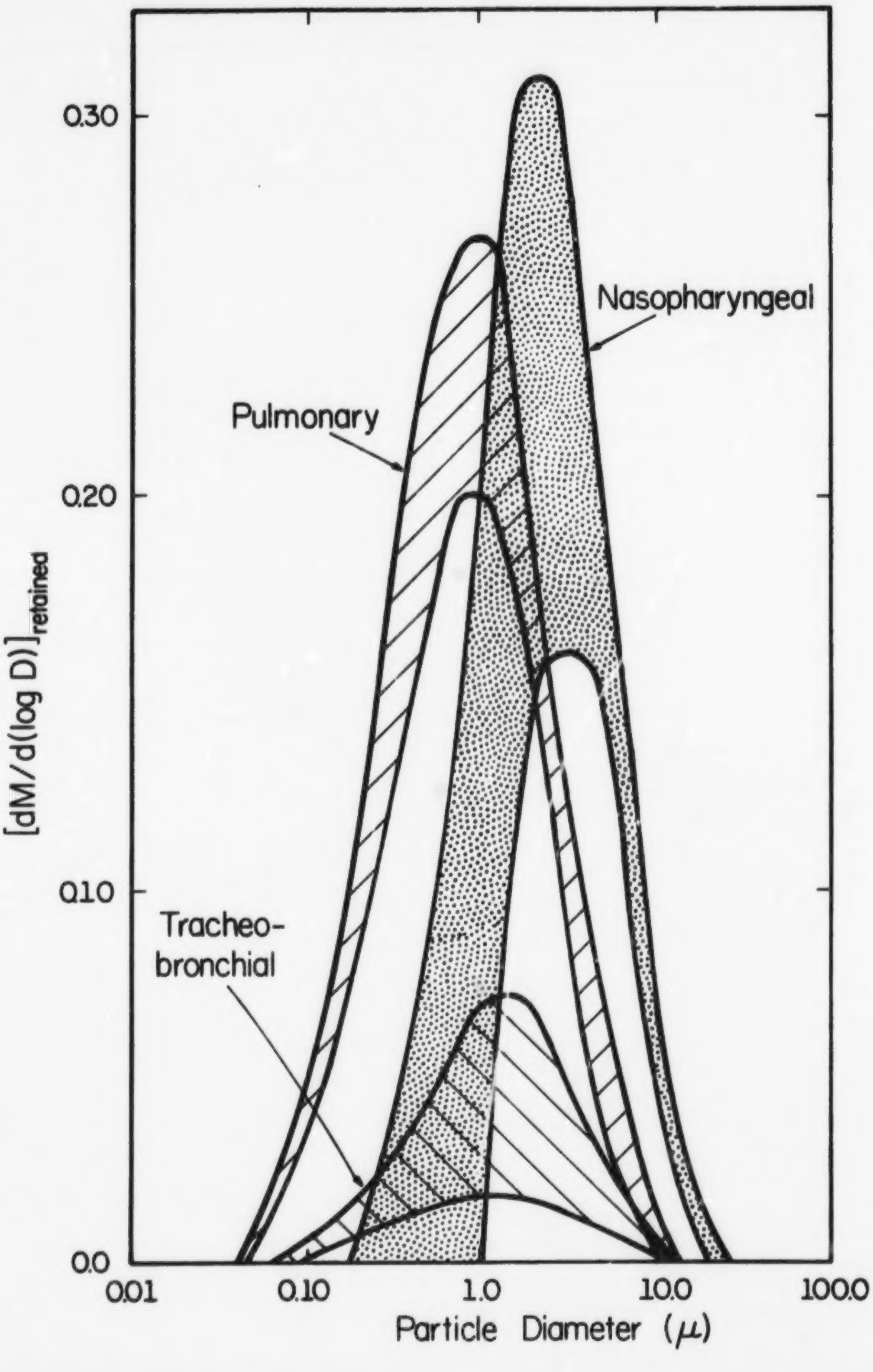
0.30
0.20
0.10
0.0
[dM/d(log D)]$_{retained}$
0.01
0.10
1.0
10.0
100.0
Particle Diameter (μ)
Nasopharyngeal
Pulmonary
Tracheo-
bronchial

Figure 5.

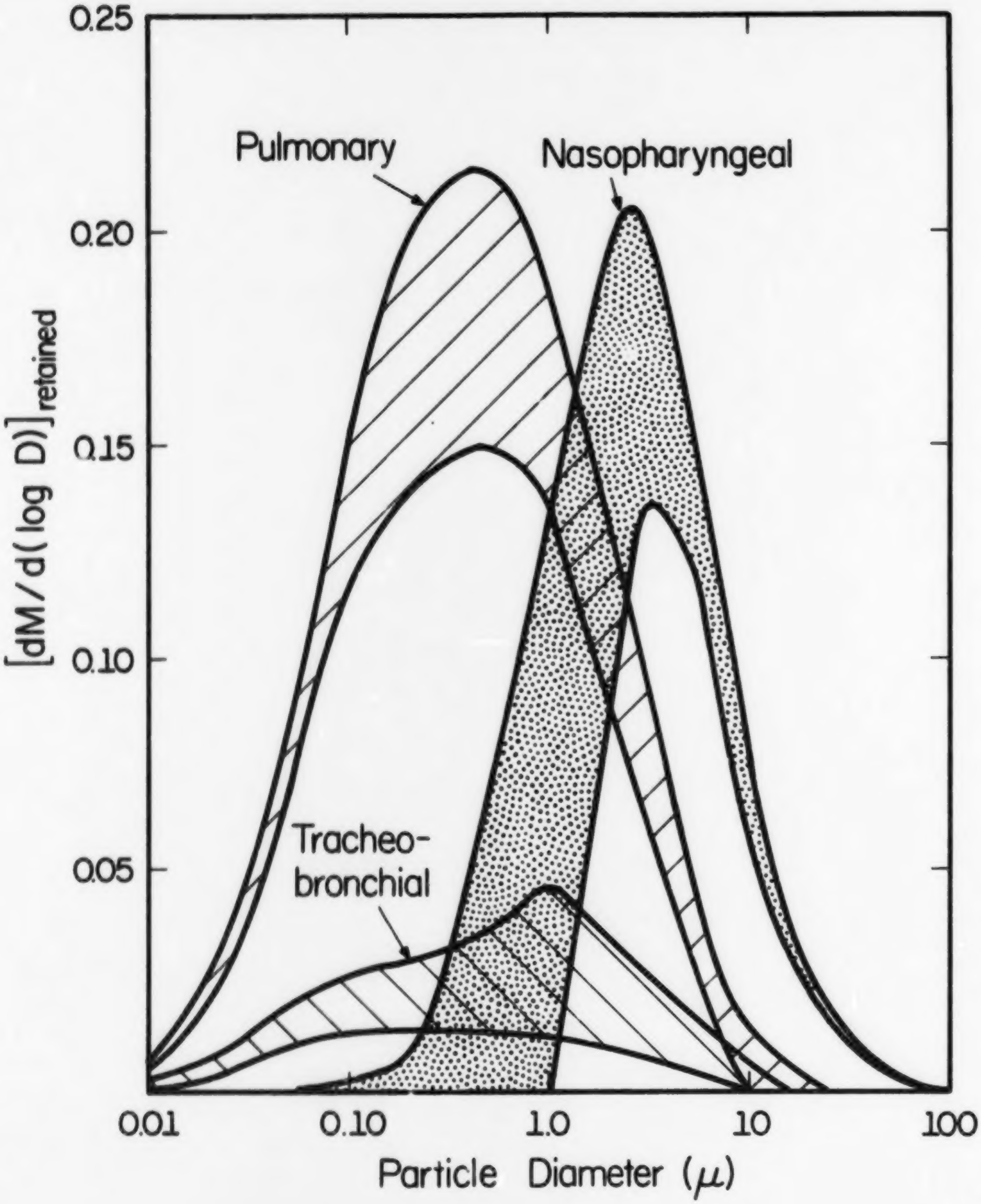
[dM/d(log D)]$_{retained}$
0.25
0.20
0.15
0.10
0.05
0.01
0.10
1.0
10
100
Particle Diameter (μ)
Pulmonary
Nasopharyngeal
Tracheo-bronchial

Figure 6.

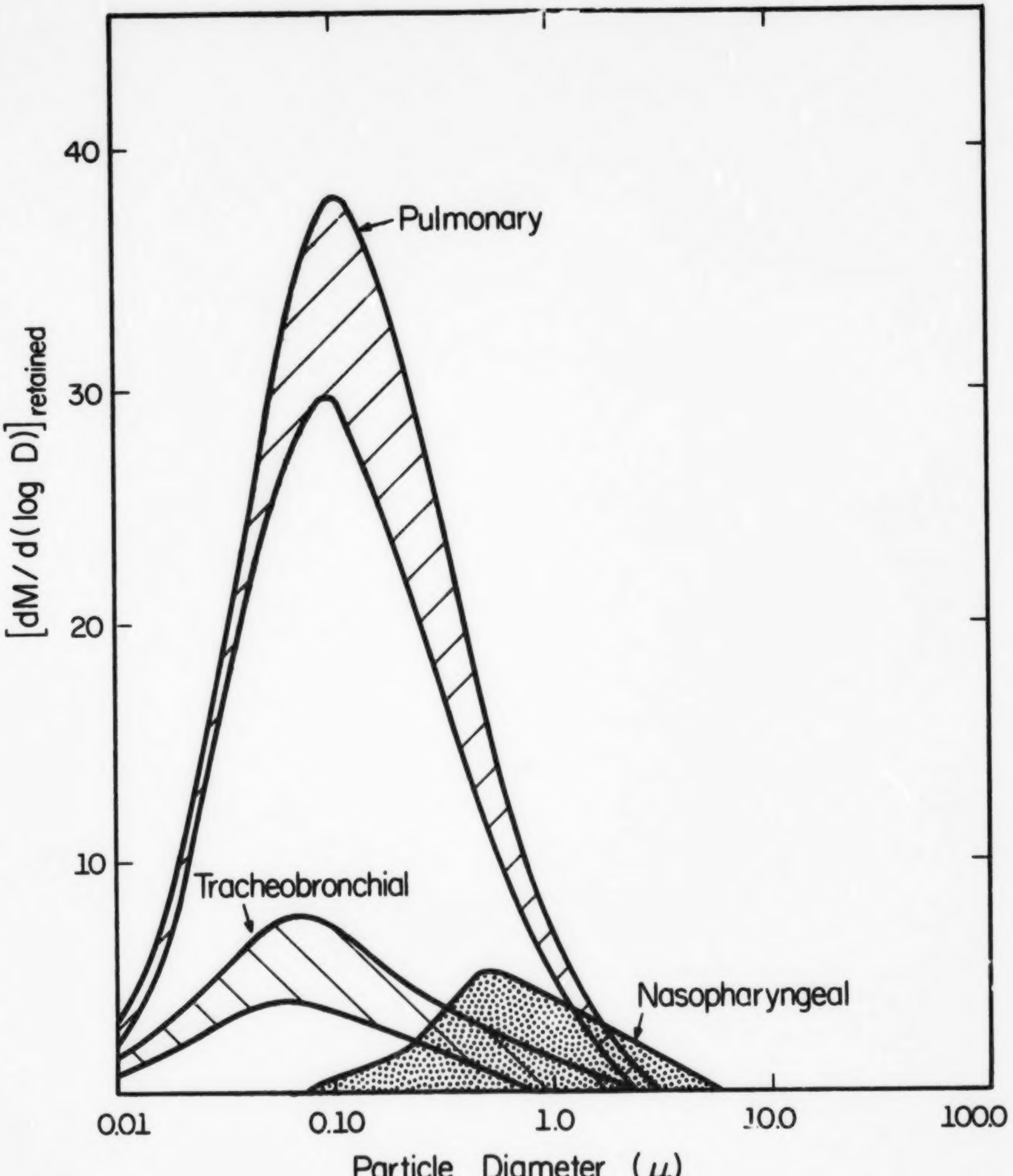
40
30
20
10
[dM/d(log D)]$_{retained}$
Pulmonary
Tracheobronchial
Nasopharyngeal
0.01
0.10
1.0
10.0
100.0
Particle Diameter (μ)

Figure 7.